NEUROPATHOGENESIS OF AFRICAN TRYPANOSOMIASIS:

The use of a mouse model system to elucidate likely mechanisms of the disease process and to design potential therapeutic strategies in man.

Jean Rodgers
B.Sc.(Hons.)

A thesis submitted to the University of Glasgow Veterinary School for the degree of Doctor of Philosophy

UNIVERSITY
of
GLASGOW

Department of Veterinary Clinical Studies
University of Glasgow Veterinary School

May 2003

"Keep away from people who try to belittle your ambitions.

Small people always do that, but the really great ones make you feel that you too,

can become great."

Mark Twain

Summary

Human African trypanosomiasis (HAT), also known as sleeping sickness, is prevalent in sub-Saharan Africa. The illness results from infection with the protozoan parasites *Trypanosoma brucei (T.b.) gambiense* in West and Central Africa and *T.b.rhodesiense* in East and Central Africa and is spread through the bite of the insect vector of the parasite, the tsetse fly. Both forms of the disease are invariably fatal if not diagnosed and drug treated.

During the acute-stage of the infection the trypanosomes spread from the site of the tsetse fly bite, via the lymphatics and bloodstream to invade most of the organs and tissues of the body. As the disease progresses the parasites enter the brain tissue and become established within the CNS and a neuroinflammatory reaction develops. Treatment of the infection once it has reached the CNS-stage is problematic since few trypanocidal drugs can cross the blood-brain barrier (BBB) to clear the parasites that are sequestered in the brain. The only drug commonly available to treat this stage of the disease is the arsenical derivative melarsoprol but its use is associated with the development of a post-treatment reactive encephalopathy (PTRE) that can in itself prove fatal. The PTRE is characterised by a severe meningoencephalitic reaction with the presence of reactive astrocytes, macrophages, T-cells, B-cells and plasma cells. The pathogenesis of this adverse reaction remains unclear.

Since brain tissue can only be obtained from post-mortem cases of HAT, there is a paucity of information regarding the early changes that occur within the CNS following infection and during the development of the PTRE. Therefore, a well-established and highly reproducible murine model, which closely mimics the human disease, was used in the current investigation to elucidate the kinetics of cellular reactivity and the expression of cytokines and chemokines following trypanosome-infection and induction of the PTRE. The mode of action of the ornithine decarboxylase inhibitor, eflornithine, a typanostatic drug used in the treatment of trypanosome infections, was also examined in the possible prevention and amelioration of the severe meningoencephalitic reaction. In addition, the role of the neuropeptide Substance P (SP) in the modulation of the inflammatory response associated with the disease was investigated.

The study of the kinetics of cellular reactivity within the CNS found that the astrocyte activation could be detected by 14-days post-infection. This initial cellular activation was

associated with an influx $CD4^+$ and $CD8^+$ cells. These cells were first detected in the meninges and ventricles but spread throughout the brain tissue as the disease progressed. $CD4^+$ cells were consistently detected in higher numbers than $CD8^+$ cells and in general preceded the appearance of $CD8^+$ cells. Macrophages were also detected in rising numbers as the severity of the CNS reaction increased and B-cells were identified in the later stages. Following the induction of the PTRE, the population of both T-cell subsets increased significantly although $CD4^+$ cells remained predominant. An expansion in the B-cell population was also found and numerous plasma cells were identified. No further increase in the macrophage population was detected.

The investigation of cytokine and chemokine transcription clearly demonstrated variations in the expression levels of IL-1α, IL-6, TNF-α, MCP-1, MIP-1α and RANTES within the CNS. Elevated levels of IL-6, TNF-α, MCP-1, MIP-1α and RANTES were found 7-days following trypanosome infection and, with the exception of RANTES, continued to rise as the reaction progressed. Initially, IL-1α transcription was reduced after infection but this too increased with time. IL-1α, IL-6, TNF-α and MIP-1α transcription dropped while RANTES expression increased in the late-stage of the CNS reaction. Immediately following the induction of the PTRE a further rise in the transcription of IL-1α, IL-6, TNF-α, MCP-1 and MIP-1α was detected and RANTES levels were reduced at this stage. IL-1α and IL-6 expression continued to rise as the PTRE developed but TNF-α, MCP-1 and MIP-1α levels dropped. This was accompanied by a rise in RANTES expression.

In the current study, the ability of SP to influence the development of the CNS inflammatory reaction, associated with trypanosome infection, was demonstrated in experiments blocking the NK1, NK2 and NK3 receptors, with specific antagonists, in normal and NK1 receptor knockout mice. When the action of SP was inhibited by administration of the NK1 receptor a less severe neuroinflammatory response was found. Therefore, SP was shown to exert a pro-inflammatory effect, via interaction with the NK1 receptor, within the CNS following trypanosome infection and induction of the PTRE.

The elucidation of the kinetics of cellular reactivity and cytokine and chemokine expression patterns, taken together with a role for the neuropeptide SP, has allowed the following hypothesis regarding the pathogenesis of the CNS reaction to be developed. The CNS inflammatory response begins to generate very quickly after the initial infection and before trypanosomes can be detected within the brain. Astrocytes are the primary cell type to display signs of cellular reactivity. The factor that instigates this response remains

unclear and could be either parasite derived or a mediator synthesised in the periphery in response to the infection out-with the CNS. Once activated the astrocytes could be responsible for the production of an array of cytokines and chemokines including IL-6, TNF-α, MCP-1 and RANTES. The presence of these inflammatory mediators augments the neuroinflammatory reaction, leading to the recruitment of inflammatory cells, including $CD4^+$ cells, $CD8^+$ cells and macrophages, to the CNS, and stimulates further cellular activation. The neuropeptide Substance P may also be integrally involved in the generation of the reaction acting in a pro-inflammatory manner through signalling via the NK1 receptor. This receptor is expressed on many of the cell types present in the reaction. Once the trypanosomes enter the CNS all of the constituents required to propagate the immune response are present within the brain and could initiate clonal expansion and further activation of the T-cell population. As the inflammation progresses the $CD4^+$ cells become the predominant cell type in the reaction and may supersede the astrocytes in controlling the generation of the response. B-cells enter the brain in increasing numbers as the reaction matures and the population expands following the induction of the PTRE. The B-cells entering the brain proliferate, probably in response to parasite antigen, and may be induced to differentiate into antibody-producing plasma cells under the direction of the $CD4^+$ cells and the cytokines, such as IL-6, that are present in the local environment. Ultimately, this cascade of events would result in the development of the extremely severe meningoencephalitis that is characteristic of the PTRE.

The investigation of action of eflornithine in the prevention and amelioration of the CNS inflammatory reaction confirmed that eflornithine treatment could reduced the severity of the neuroinflammatory reaction when administered prior to the development of the CNS response, and resulted in a dramatic reduction in the degree in inflammation when given to mice exhibiting an established PTRE. In both cases a reduction in the level of astrocyte activation was also found. When eflornithine was used to prevent the development of the CNS reaction a significant reduction in the transcription of IL-1α and IL-6 was detected together with lowered expression of MIP-1α and RANTES. No alterations in the levels of TNF-α or MCP-1 were apparent. No changes were found in the expression of the cytokines and chemokines studied when eflornithine was used to resolve an established PTRE. Therefore the mechanisms employed by the drug, in the prevention and amelioration of the CNS inflammation, are divergent. The pathway used by eflornithine to prevent the development of the inflammatory reaction would appear to involve inhibition of the expression of the pro-inflammatory cytokines IL-1α and IL-6. The mechanism resulting in the resolution of the meningoencephalitis remains a matter of conjecture. In

this study eflornithine resistant trypanosomes were used in the infections to isolate the anti-inflammatory effects of the drug treatment from those that arise due to the clearance of the parasites. Therefore, the value of eflornithine treatment as an anti-inflammatory agent, even in cases where trypanosome resistance to the drug is suspected was demonstrated.

The identification of the key cellular and functional events resulting in the neuroinflammatory reaction associated with trypanosome infection have allowed a further degree of understanding regarding the mechanisms involved in the development of the CNS inflammation in human disease. Without the existence of the murine model the above conclusions could not have been reached. Furthermore, it is now possible to consider application of the potential novel therapeutic approaches indicated by this study, to prevent and ameliorate the development of the CNS inflammatory reaction, in the management of this devastating disease condition in man.

List of Contents

Title Page i

Quotation ii

Summary iii

List of Contents vii

List of Tables xvi

List of Figures xix

List of Publications and Presentations xxii

Author's Declaration xxiii

Acknowledgements xxiv

Dedication xxv

Abbreviations xxvi

Quotation xxix

CHAPTER 1 1

INTRODUCTION 1

1.1. Aetiology of African trypanosomiasis 2

1.1.1. History of the disease 4

1.1.2. Trypanosome taxonomy 5

1.1.3. Transmission of infection 7

1.1.4. Scale and economic considerations of trypanosomiasis 9

1.1.5. Parasite biology 10

1.2. Trypanosomiasis in man 13

1.2.1. Clinical picture 13

1.2.2. Pathogenesis 13

1.2.2.1. Haemo-lymphatic manifestations 14

1.2.2.2. Specific organ damage 15

1.2.2.2.1. Central nervous system manifestations 16

1.2.3. Diagnosis 18

1.2.4. Current treatment strategies 19
1.2.4.1. Chemotherapy of early-stage infections 19
1.2.4.2. Chemotherapy of CNS-stage infections 20
1.2.4.3. Adverse reactions to melarsoprol treatment 20
1.2.5. Alternative chemotherapeutic approaches 21
1.2.5.1. Eflornithine 21
1.2.5.2. Nifurtimox 22
1.2.5.3. Megazol 23
1.3. Aims and objectives 23
1.4. Rationale 24
1.4.1. Neuropathogenesis and the mouse model 24
1.4.2. Migration of leucocytes across the blood-brain barrier 24
1.4.3. Modulation of CNS pathology 25
1.4.4. The role of substance P 25
1.5. Brief methodology 26
CHAPTER 2 27
GENERAL MATERIALS AND METHODS 27
2.1. Introduction 28
2.2. Murine model of human African trypanosomiasis 28
2.2.1. Trypanosomes 28
2.2.1.1. *Trypanosoma brucei brucei* GVR 35/C1.6 28
2.2.2. Animals and infection regimens 29
2.2.2.1. Donor animals 29
2.2.2.2. Mouse model experimental design 29
2.2.2.2.1. Acute infection 31
2.2.2.2.2. Early CNS-stage 31
2.2.2.2.3. Late CNS-stage 31
2.2.2.2.4. Post-treatment reactive encephalopathy 32
2.2.3. Tissue Harvesting 32
2.2.3.1. Sample preparation for histological assessment 33
2.2.3.2. Sample preparation for RT-PCR analyses 33
2.3. Neuropathological assessment 34
2.4. Immunocytochemistry 34
2.4.1. Immunocytochemistry staining procedure 36
2.4.1.1. Detection of horseradish peroxidase labels 39

2.4.1.2. Detection of alkaline phosphatase labels....41
2.5. Ribonucleic acid purification and quantification....41
2.5.1. Sample handling strategy....41
2.5.2. Sample preparation....42
2.5.3. RNA extraction....42
2.5.4. RNA quantification....44
2.6. Reverse-Transcriptase Polymerase-Chain Reaction....44
2.6.1. Reverse-transcription....44
2.6.2. PCR background information....45
2.6.3. PCR cycling parameters....46
2.6.4. Amplification pattern....48
2.6.5. Performance of the RT-PCR....48
2.6.6. PCR controls....50
2.6.7. Analysis of RT-PCR products....50
2.6.8. Relative quantification of results....52
2.7. Statistical analyses....53

CHAPTER 3....62

TRYPANOSOME-INDUCED CELLULAR IMMUNE REACTIVITY WITHIN THE CNS....62

3.1. Introduction....63
3.1.1. The inflammatory response....63
3.1.1.1. Innate immunity....64
3.1.1.1.1. Monocytes / macrophages....64
3.1.1.2. Acquired immunity....66
3.1.1.2.1. T-lymphocytes....66
3.1.1.2.1.1. $CD4^+$ T-cells....66
3.1.1.2.1.2. $CD8^+$ T-cells....68
3.1.1.2.2. B-lymphocytes....69
3.1.2. The CNS and 'immuno-privilege'....70
3.1.2.1. The blood-brain barrier....70
3.1.2.1.1. The microvascular endothelial cell barrier....71
3.1.2.1.2. The choroid plexus epithelial cell barrier....71
3.1.2.1.3. 'Gaps' in the barrier....72
3.1.2.2. Immune surveillance within the CNS....72
3.1.2.2.1. Macrophages in the CNS....73
3.1.2.2.2. T-cells in the CNS....73
3.1.2.2.3. B-cells in the CNS....74

3.1.2.2.4. Lymphatic drainage in the CNS 74
3.1.2.3. CNS cells with immune roles 74
3.1.2.3.1. BBB endothelial cells 75
3.1.2.3.2. Microglia 75
3.1.2.3.2.1. Microglial morphology 76
3.1.2.3.2.2. Microglia in the normal CNS 76
3.1.2.3.2.3. Microglial response to injury or infection 77
3.1.2.3.3. Astrocytes 77
3.1.2.3.3.1. Astrocyte morphology 78
3.1.2.3.3.2. Astrocytic responses to injury 79
3.1.2.3.3.3. Astrocytes as immunocompetent cells 80
3.1.3. CNS inflammation in disease states 81
3.1.3.1. Trypanosome-induced CNS inflammation 82
3.2. Materials and methods 85
3.2.1. Animals, infections and treatments 85
3.2.2. Sample preparation and staining 85
3.2.2.1. Paraffin sections 86
3.2.2.1.1. Neuropathology grading scale 86
3.2.2.2. Frozen sections 86
3.2.2.2.1. Quantification of $CD4^+$ and $CD8^+$ cell infiltration 87
3.2.3. Statistical analyses 87
3.2.3.1. Grading of neuropathological response 88
3.2.3.2. Assessing T-cell infiltration 88
3.3. Results 89
3.3.1. Assessment of the severity of the neuropathological response 89
3.3.1.1. Acute and early-stage CNS infections 90
3.3.1.2. Late-stage CNS infections and the PTRE 90
3.3.2. Inflammatory cell infiltration and astrocyte activation 91
3.3.2.1. T-lymphocyte infiltration 91
3.3.2.1.1. Comparison of $CD4^+$ and $CD8^+$ cell infiltration 91
3.3.2.1.2. Pattern of $CD4^+$ cell infiltration 95
3.3.2.1.3. Pattern of $CD8^+$ cell infiltration 99
3.3.2.2. Macrophage infiltration 103
3.3.2.3. B-lymphocyte infiltration 103
3.3.2.4. Astrocyte activation 104
3.4. Discussion 137

CHAPTER 4 148

CYTOKINE AND CHEMOKINE RESPONSES IN A TRYPANOSOME-INDUCED CNS INFLAMMATORY REACTION 148

4.1. Introduction 149

4.1.1. What are cytokines and chemokines? 149

4.1.1.1. Cytokines 149

4.1.1.1.1. Control of cytokine production and action 150

4.1.1.1.2. Cytokine function 151

4.1.1.1.2.1. Th1 and Th2 cytokines 151

4.1.1.2. Chemokines 152

4.1.1.2.1. Chemokine families 152

4.1.1.2.2. How are chemokines chemotactic? 153

4.1.1.2.3. Chemokine receptors 155

4.1.2. Cytokines and chemokines in the CNS 155

4.1.2.1. Interleukin-1 156

4.1.2.2. Interleukin-6 159

4.1.2.3. Tumour necrosis factor-α 160

4.1.2.4. RANTES 163

4.1.2.5. Monocyte chemoattractant protein-1 164

4.1.2.6. Macrophage Inflammatory Protein-1α 166

4.1.3. CNS cytokines and chemokines; helpful or harmful? 167

4.1.4. Cytokines and chemokines in trypanosomiasis 170

4.1.4.1. Trypanosome-derived lymphocyte triggering factor 172

4.1.4.2. Cytokines and differential susceptibility to trypanosomiasis 173

4.2. Materials and methods 176

4.2.1. Animals, infections and treatments 176

4.2.2. RT-PCR analyses 177

4.2.3. Immunocytochemistry 177

4.2.3.1. Fixation of cryostat sections 177

4.2.3.2. Antigen retrieval techniques 179

4.2.3.2.1. Proteolytic enzyme digestion 180

4.2.3.2.2. Wet-heat antigen retrieval 181

4.2.3.2.2.1. Citrate buffer antigen retrieval protocol 181

4.2.3.2.2.2. Sertoc tissue unmasking fluid (STUF) 182

4.2.3.3. Tissue permeablisation 182

4.2.4. In situ techniques 183

4.2.4.1. *In-situ* hybridisation 183

4.2.4.1.1 ISH of murine CNS sections 184

4.2.4.1.1.1 ISH control sections 187
4.2.4.1.2. Visualising the digoxigenin reporter molecule 187
4.2.4.2. *In-situ* reverse-transcriptase polymerase chain reaction 189
4.2.4.2.1. Direct IS-RT-PCR 189
4.2.4.2.2. Indirect IS-RT-PCR 192
4.2.5. Statistical analyses 193
4.3. Results 194
4.3.1. Kinetics of cytokine and chemokine expression 194
4.3.1.1. Observational differences and trends in cytokine expression 194
4.3.1.2. Statistical analyses of RT-PCR results 196
4.3.2. Immunocytochemistry 199
4.3.3. In-situ techniques 200
4.3.3.1. *In-situ* hybridisation 200
4.3.3.2. IS-RT-PCR 200
4.4. Discussion 216

CHAPTER 5 226

THE ACTION OF EFLORNITHINE IN TRYPANOSOME-INDUCED CNS INFLAMMATION 226

5.1. Introduction 227
5.1.1. Polyamines and eflornithine 227
5.1.2. Eflornithine as an anti-cancer agent 227
5.1.3. Eflornithine in non-cancer related conditions 229
5.1.4. Eflornithine in brain injury 229
5.1.5. Cosmetic applications for eflornithine 230
5.1.5.1. Benefits of a commercially viable eflornithine application 231
5.1.6. Eflornithine treatment of African trypanosomiasis 232
5.1.6.1. Polyamines and ODC in African trypanosomes 232
5.1.6.2. Eflornithine studies in experimental infections 233
5.1.6.2.1. Innate resistance to eflornithine treatment 234
5.1.6.3. Eflornithine trials in human trypanosome infections 236
5.1.7. Additional pharmacological actions of eflornithine 238
5.2. Materials and methods 240
5.2.1. Parasites 240
5.2.2. Animals infection and treatments 242
5.2.2.1. Prevention of the CNS inflammatory response 242
5.2.2.2. Amelioration of an established meningoencephalitis 242
5.2.2.3. Control animals 244

5.2.3. Neuropathological assessment....244
5.2.3.1.Astrocyte activation....244
5.2.4. RT-PCR analyses....245
5.2.5. Statistical analyses....245
5.3. Results....247
5.3.1. Assessment of the severity of the meningoencephalitis....247
5.3.1.1. Prevention of the neuroinflammatory response....247
5.3.1.2. Amelioration of an established meningoencephalitis....248
5.3.2. The effect of eflornithine on cytokine expression....249
5.3.2.1. Prevention of the neuroinflammatory response....249
5.3.2.1.1. Statistical analysis....251
5.3.2.2. Amelioration of an existing meningoencephalitis....252
5.3.2.2.1. Statistical analysis....253
5.4. Discussion....288
5.4.1. Eflornithine in the prevention of CNS inflammation....288
5.4.2. Eflornithine in the amelioration of CNS inflammation....290
5.4.3. Potential mechanism of action of eflornithine....292
CHAPTER 6....296
SUBSTANCE P AND HUMAN AFRICAN TRYPANOSOMIASIS....296
6.1. Introduction....297
6.1. Introduction....297
6.1.1. Background....297
6.1.1.1. What is substance P?....297
6.1.1.2. Tachykinin nomenclature....297
6.1.2. Substance P biosynthesis....298
6.1.2.1. Preprotachykinin A gene....298
6.1.2.2. Post-translational processing....298
6.1.3. Tachykinin receptors....299
6.1.4. Substance P and the NK1 receptor in nervous tissues....300
6.1.4.1. Distribution in the CNS....300
6.1.4.2. SP and NK1 receptors in spinal cord....301
6.1.4.3. SP and NK1 receptors in astrocytes....303
6.1.5. SP and NK1 receptors in peripheral tissues....305
6.1.5.1. The cardiovascular system....305
6.1.5.2. The respiratory system....306
6.1.5.3. The gastrointestinal system....307

6.1.6. NK1 receptors and SP in inflammatory cells 308
6.1.6.1. Monocytes 308
6.1.6.2. Polymorphonuclear leucocytes 309
6.1.6.3. Lymphocytes 310
6.1.7. Substance P and trypanosomiasis 311
6.2. Materials and methods 313
6.2.1. Administration of the NK1 receptor antagonist 313
6.2.1.1. RP-67,580 and RP-68,651 313
6.2.1.2. Animals, infections and treatments 313
6.2.1.2.1. Experiments 1, 2 & 3 313
6.2.1.2.2. Experiment 4 314
6.2.2. Use of NK1 receptor knockout mice 314
6.2.2.1. Generation of the knockout animals 314
6.2.2.2. Animals, infections and treatments 315
6.2.2.2.1. Neuroinflammation in NK1 knockout animals 316
6.2.2.2.1.1. Experiment 1 316
6.2.2.2.1.2. Experiment 2 316
6.2.2.2.1.3. Experiment 3 316
6.2.2.2.1.4. Experiment 4 317
6.2.2.2.2. NK2 and NK3 receptor antagonists 317
6.2.2.2.2.1. Experiment 5 317
6.2.2.3. Clinical Assessment 318
6.2.3. Histopathology 318
6.2.3.1. Assessing the inflammatory reaction 318
6.2.3.2. Assessing astrocyte activation 320
6.2.4. Statistical analyses 320
6.3. Results 322
6.3.1. The effect of the NK1 receptor antagonist 322
6.3.1.1. Severity of the meningoencephalitis 322
6.3.1.2. Astrocyte activation 323
6.3.2. The effect of genetic ablation of the NK1 receptor 324
6.3.2.1. Severity of the meningoencephalitis 324
6.3.2.2. Astrocyte activation 325
6.3.2.3. Severity of the clinical response 325
6.3.3. The effect of NK2 and NK3 receptor antagonists 326
6.3.3.1. Severity of the meningoencephalitis 326
6.3.3.2. Severity of the clinical response 328

6.4. Discussion 345
6.4.1. Neuropathology 345
6.4.1.1. Astrocytosis 349
6.4.2. Clinical Response 350
6.4.3. Influence of the photoperiod 352
6.4.4. SP and human African trypanosomiasis 353

CHAPTER 7 355

GENERAL DISCUSSION AND CONCLUSIONS 355

7.1. Development of CNS inflammation 356
7.2. Substance P in the CNS response 360
7.3 . Mechanism of action of eflornithine 362
7.4. Future investigations 363
7.5. Conclusions 364

APPENDIX 1 367

20x SSC (Salt Sodium Citrate) 368
2M sodium acetate pH4.0 368
0.1M citrate buffer 368
0.2M phosphate buffer 369
4% paraformaldehyde 369
Bouin's fixative 369
Denaturing Solution 369
DEPC water 370
LANA's fixative 370
Phosphate Buffered Saline (PBS) for ICC 371
PCR loading buffer 371
TBE electrophoresis buffer (x10 stock solution) 371

REFERENCE LIST 372

List of Tables

CHAPTER 1
INTRODUCTION

Table 1.1. Trypanosome species and susceptible hosts..... 3

CHAPTER 2
GENERAL MATERIALS AND METHODS

Table 2.1. Neuropathological grading scale..... 35

Table 2.2. Antibodies employed for immunohistochemical analyses..... 38

Table 2.3. Oligonulceotide primer sequences..... 51

CHAPTER 3
TRYPANOSOME INDUCED CELLULAR IMMUNE REACTIVITY WITHIN THE CNS

Table 3.1. The effect of treatment regimen on the severity of the neuroinflammatory response..... 105

Table 3.2. Comparison of CD4 and CD8 cell infiltration of the meninges, corpus callosum, external capsule, caudate putamen and cerebral cortex following trypanosome infection and subcurative drug treatment..... 106

Table 3.3. Comparison of CD4 and CD8 cell infiltration of the meninges following trypanosome infection and subcurative drug treatment..... 107

Table 3.4. Comparison of CD4 and CD8 cell infiltration of the corpus callosum following trypanosome infection and subcurative drug treatment..... 108

Table 3.5. Comparison of CD4 and CD8 cell infiltration of the external capsule following trypanosome infection and subcurative drug treatment..... 109

Table 3.6. Comparison of CD4 and CD8 cell infiltration of the caudate putamen following trypanosome infection and subcurative drug treatment..... 110

Table 3.7. Comparison of CD4 and CD8 cell infiltration of the cerebral cortex following trypanosome infection and subcurative drug treatment..... 111

Table 3.8. Comparison of CD4 cell infiltration in the meninges at various time-points following trypanosome infection and subcurative drug treatment..... 112

Table 3.9. Comparison of CD4 cell infiltration in the corpus callosum at various time-points following trypanosome infection and subcurative drug treatment..... 113

Table 3.10. Comparison of CD4 cell infiltration in the external capsule at various time-points following trypanosome infection and subcurative drug treatment..... 114

Table 3.11. Comparison of CD4 cell infiltration in the caudate putamen at various time-points following trypanosome infection and subcurative drug treatment..... 115

Table 3.12. Comparison of CD4 cell infiltration in the cerebral cortex at various time-points following trypanosome infection and subcurative drug treatment..... 116

Table 3.13. Comparison of CD4 cell infiltration of different brain areas 14 days following trypanosome infection..... 117

Table 3.14. Comparison of CD4 cell infiltration of different brain areas 21 days following trypanosome infection..... 118

Table 3.15. Comparison of CD4 cell infiltration of different brain areas 28 days following trypanosome infection..... 119

Table 3.16. Comparison of CD4 cell infiltration of different brain areas 7 days following the induction of the late-stage CNS response..... 120

Table 3.17. Comparison of CD4 cell infiltration of different brain areas 14 days following the induction of the late-stage CNS response..... 121

Table 3.18. Comparison of CD4 cell infiltration of different brain areas 7 days following the induction of the PTRE..... 122

Table 3.19. Comparison of CD4 cell infiltration of different brain areas 14 days following the induction of the PTRE..... 123

Table 3.20 Comparison of CD8 cell infiltration in the meninges at various time-points following trypanosome infection and subcurative drug treatment..... 124

Table 3.21. Comparison of CD8 cell infiltration in the corpus callosum at various time-points following trypanosome infection and subcurative drug treatment..... 125

Table 3.22. Comparison of CD8 cell infiltration in the external capsule at various time-points following trypanosome infection and subcurative drug treatment..... 126

Table 3.23. Comparison of CD8 cell infiltration in the caudate putamen at various time-points following trypanosome infection and subcurative drug treatment..... 127

Table 3.24. Comparison of CD8 cell infiltration in the cerebral cortex at various time-points following trypanosome infection and subcurative drug treatment..... 128

Table 3.25. Comparison of CD8 cell infiltration of different brain areas 14 days following trypanosome infection..... 129

Table 3.26. Comparison of CD8 cell infiltration of different brain areas 21 days following trypanosome infection..... 130

Table 3.27. Comparison of CD8 cell infiltration of different brain areas 28 days following trypanosome infection..... 131

Table 3.28. Comparison of CD8 cell infiltration of different brain areas 7 days following the induction of the late-stage CNS response..... 132

Table 3.29. Comparison of CD8 cell infiltration of different brain areas 14 days following the induction of the late-stage CNS response..... 133

Table 3.30. Comparison of CD8 cell infiltration of different brain areas 7 days following the induction of the PTRE..... 134

Table 3.31. Comparison of CD8 cell infiltration of different brain areas 14 days following the induction of the PTRE..... 135

CHAPTER 4
CYTOKINE AND CHEMOKINE RESPONSES IN A TRYPANOSOME-INDUCED CNS INFLAMMATORY REACTION

Table 4.1. Antibodies employed for immunohistochemical analyses of cytokines..... 178

Table 4.2. Assessment of differential cytokine and chemokine expression in the mouse brain following trypanosome infection and subcurative drug treatment..... 202

CHAPTER 5
THE ACTION OF EFLORNITHINE IN TRYPANOSOME-INDUCED CNS INFLAMMATION

Table 5.1. The effect of eflornithine on the development of a CNS inflammatory reaction..... 256

Table 5.2. The effect of eflornithine on an established meningoencephalitis..... 257

Table 5.3. Assessment of differential cytokine and chemokine expression in the brain of trypanosome-infected mice in the presence and absence of eflornithine treatment..... 258

Table 5.4. Assessment of the effect of eflornithine on differential cytokine and chemokine expression in the brain of trypansome-infected mice with an established meningoencephalitis..... 259

CHAPTER 6
SUBSTANCE P AND HUMAN AFRICAN TRYPANOSOMIASIS

Table 6.1. Parameters defining the visual assessment scale for the clinical grading scores..... 319

Table 6.2. Assessment of the neuropathological response score to trypanosome-infection in the presence or absence of SP antagonist treatment..... 335

Table 6.3. Assessment of the astrocytic response to trypanosome-infection in the presence or absence of SP antagonist treatment..... 336

Table 6.4. Assessment of the neuropathological response score to trypanosome-infection in $NK^{+/+}$ and $NK^{-/-}$ animals..... 337

Table 6.5. Assessment of the astrocytic response to trypanosome-infection in $NK^{+/+}$ and $NK^{-/-}$ animals..... 338

Table 6.6. Assessment of the clinical response score to trypanosome-infection in $NK^{+/+}$ and $NK^{-/-}$ animals..... 339

Table 6.7. Neuroinflammatory response scores of $NK^{+/+}$ mice following treatment with specific NK receptor antagonists..... 340

Table 6.8. Neuroinflammatory response scores of $NK^{-/-}$ mice following treatment with specific NK receptor antagonists..... 341

Table 6.9. Assessment of the neuropathological response scores following treatment with selective NK receptor antagonists..... 342

Table 6.10. Comparison of clinical responses between $NK^{+/+}$ and $NK^{-/-}$ mice..... 343

Table 6.11. Assessment of clinical response following treatment with specific NK receptor anatgonists..... 344

List of Figures

CHAPTER 1
INTRODUCTION

Figure 1.1. Trypanosome classification..... 6

Figure 1.2. Life-cycle of trypanosome parasites in man and its vector the tsetse fly..... 8

Figure 1.3. Schematic representation of the morphology of the trypomastigote form of *Trypanosoma brucei spp*..... 11

CHAPTER 2
GENERAL MATERIALS AND METHODS

Figure 2.1. Schematic representation of the treatment regimens comprising the murine model of human African trypanosomiasis..... 30

Figure 2.2. Schematic representation of the immunocytochemistry technique..... 37

Figure 2.3. The polymerase chain reaction..... 47

Figure 2.4. TNF-α banding pattern resulting from increasing amplification cycles..... 54

Figure 2.5. IL-1α banding pattern resulting from increasing amplification cycles..... 55

Figure 2.6. IL-6 banding pattern resulting from increasing amplification cycles..... 56

Figure 2.7. MIP-1α banding pattern resulting from increasing amplification cycles..... 57

Figure 2.8. MCP-1 banding pattern resulting from increasing amplification cycles..... 58

Figure 2.9. RANTES banding pattern resulting from increasing amplification cycles..... 59

Figure 2.10. β-actin banding pattern resulting from increasing amplification cycles..... 60

Figure 2.11. Grading scale used to score intensity of PCR amplicons..... 61

CHAPTER 3
TRYPANOSOME INDUCED CELLULAR IMMUNE REACTIVITY WITHIN THE CNS

Figure 3.1. CNS inflammatory response to trypanosome-infection and subcurative drug treatment..... 136

CHAPTER 4
CYTOKINE AND CHEMOKINE RESPONSES IN A TRYPANOSOME-INDUCED CNS INFLAMMATORY REACTION

Figure 4.1. Classification of chemokine families according to structure..... 154

Figure 4.2. Schematic representation of the procedure used in the direct *in-situ* reverse-transcriptase polymerase chain reaction..... 192

Figure 4.3. β-actin check gel for groups of animals used to investigate the time-course of cytokine and chemokine expression in trypanosome-infection..... 203

Figure 4.4. IL-1α transcription pattern through the various stages trypanosome-infection..... 204

Figure 4.5. IL-6 transcription pattern through the various stages trypanosome-infection..... 205

Figure 4.6. TNF-α transcription pattern through the various stages trypanosome-infection..... 206

Figure 4.7. MCP-1 transcription pattern through the various stages trypanosome infection..... 207

Figure 4.8. MIP-1α transcription pattern through the various stages trypanosome infection..... 208

Figure 4.9. RANTES transcription pattern through the various stages trypanosome-infection..... 209

Figure 4.10. Summary statistics for IL-1α..... 210

Figure 4.11. Summary statistics for IL-6..... 211

Figure 4.12. Summary statistics for TNF-α..... 212

Figure 4.13. Summary statistics for MCP-1..... 213

Figure 4.14. Summary statistics for MIP-1α..... 214

Figure 4.15. Summary statistics for RANTES..... 215

CHAPTER 5
THE ACTION OF EFLORNITHINE IN TRYPANOSOME-INDUCED CNS INFLAMMATION

Figure 5.1. Production of eflornithine resistant *T.b.brucei* GVR 35/C1.3 DFMO 5.1..... 241

Figure 5.2. Schematic representation of the treatment schedules utilised to determine the effects of eflornithine treatment..... 243

Figure 5.3. Prevention of CNS inflammation by eflornithine treatment..... 260

Figure 5.4. Amelioration of an established meningoencephalitis by eflornithine treatment..... 261

Figure 5.5. β-actin check gel for groups of animals used to study the development of a CNS inflammatory reaction..... 262

Figure 5.6. The effect of eflornithine treatment on IL-1α expression in the development of a CNS inflammatory reaction..... 263

Figure 5.7. The effect of eflornithine treatment on IL-6 expression in the development of a CNS inflammatory reaction..... 264

Figure 5.8. The effect of eflornithine treatment on TNF-α expression in the development of a CNS inflammatory reaction..... 265

Figure 5.9. The effect of eflornithine treatment on MCP-1 expression in the development of a CNS inflammatory reaction..... 266

Figure 5.10. The effect of eflornithine treatment on MIP-1α expression in the development of a CNS inflammatory reaction..... 267

Figure 5.11. The effect of eflornithine treatment on RANTES expression in the development of a CNS inflammatory reaction..... 268

Figure 5.12. Summary statistics for IL-1α..... 269

Figure 5.13. Summary statistics for IL-6..... 270
Figure 5.14. Summary statistics for TNF-α..... 271
Figure 5.15. Summary statistics for MCP-1..... 272
Figure 5.16. Summary statistics for MIP-1α..... 273
Figure 5.17. Summary statistics for RANTES..... 274
Figure 5.18. β-actin check gel for groups of animals used to study the effect of eflornithine in the amelioration of a meningoencephalitis..... 275
Figure 5.19. The effect of eflornithine treatment on the expression of IL-1α in the amelioration of a meningoencephalitic reaction..... 276
Figure 5.20. The effect of eflornithine treatment on the expression of IL-6 in the amelioration of a meningoencephalitic reaction..... 277
Figure 5.21. The effect of eflornithine treatment on the expression of TNF-α in the amelioration of a meningoencephalitic reaction..... 278
Figure 5.22. The effect of eflornithine treatment on the expression of MCP-1 in the amelioration of a meningoencephalitic reaction..... 279
Figure 5.23. The effect of eflornithine treatment on the expression of MIP-1α in the amelioration of a meningoencephalitic reaction..... 280
Figure 5.24. The effect of eflornithine treatment on the expression of RANTES in the amelioration of a meningoencephalitic reaction..... 281
Figure 5.25. Summary statistics for IL-1α..... 282
Figure 5.26. Summary statistics for IL-6..... 283
Figure 5.27. Summary statistics for TNF-α..... 284
Figure 5.28. Summary statistics for MCP-1..... 285
Figure 5.29. Summary statistics for MIP-1α..... 286
Figure 5.30. Summary statistics for RANTES..... 287

CHAPTER 6
SUBSTANCE P AND HUMAN AFRICAN TRYPANOSOMIASIS

Figure 6.1. The effect of RP-67,580 treatment on the severity of the neuroinflammatory response..... 330
Figure 6.2. The effect of RP-67,580 treatment on astrocyte activation..... 331
Figure 6.3. The neuroinflammatory reaction in NK1 receptor knockout and wild-type mice..... 332
Figure 6.4. The astrocytic reaction in NK1 receptor knockout and wild-type mice..... 333
Figure 6.5. The effect of treatment with NK2 and NK3 receptor antagonists on the severity of the neuroinflammatory reaction in nk1 receptor knockout and wild-type mice..... 334

CHAPTER 7
GENERAL DISCUSSION AND CONCLUSIONS

Figure 7.1. Schematic representation of possible inflammatory mechanisms involved in the generation of the post-treatment reactive encephalopathy (PTRE)..... 357

List of Publications and Presentations

Publications from thesis

Kennedy,P.G.E., Rodgers,J., Jennings,F.W., Murray,M., Leeman,S.E., and Burke,J.M. (1997) A substance P antagonist, RP-67,580, ameliorates a mouse meningoencephalitic response to Trypanosoma brucei brucei. *Proceedings of the National Academy of Sciences of the USA* **94**, 4167-4170.

In press publications

Kennedy,P.G.E., Rodgers,J., Bradley,B., Hunt,S.P., Gettinby,G., Leeman,S.E., De Felipe,C., and Murray,M. (2003) Clinical and neuroinflammatory responses to meningoencephalitis in substance P receptor knockout mice. *Brain*

Related publications

Eckersall,P.D., Gow,J.W., McComb,C., Bradley,B., Rodgers,J., Murray,M., and Kennedy,P.G.E. (2001) Cytokines and the acute phase response in post-treatment reactive encephalopathy of Trypanosoma brucei brucei infected mice. *Parasitology International* **50**, 15-26.

Eckersall,P.D., Rodgers,J., Murray,M., and Kennedy,P.G.E. (1999) Haptoglobin, the acute phase response and natural human immunity to trypanosomes [letter]. *Parasitology Today* **15** , 251-252.

Jennings,F.W., Rodgers,J., Bradley,B., Gettinby,G., Kennedy,P.G.E., and Murray,M. (2002) Human African trypanosomiasis: potential therapeutic benefits of an alternative suramin and melarsoprol regimen. *Parasitology International* **51**, 381-388.

Kennedy,P.G.E., Murray,M., Jennings,F., and Rodgers,J. (2002) Sleeping sickness: new drugs from old? *Lancet* **359**, 1695-1696.

Related publications prior to thesis

Gichuki,C.W., Jennings,F.W., Kennedy,P.G.E., Sommer,I.U., Murray,M., Rodgers,J., and Burke,J.M. (1997) The effect of azathioprine on the neuropathology associated with experimental murine African trypanosomiasis. *Neurological Infections and Epidemiology* **2** , 53-61.

Jennings,F.W., Gichuki,C.W., Kennedy,P.G., Rodgers,J., Hunter,C.A., Murray,M., and Burke,J.M. (1997) The role of the polyamine inhibitor eflornithine in the neuropathogenesis of experimental murine African trypanosomiasis. *Neuropathology and Applied Neurobiology* **23**, 225-234.

Oral Presentations

Rodgers, J., Kennedy, P.G.E., Jennings, F.W., Bradley, B., Eckersall, P.D., Williams, A., Murray, Max. Management of the neuropathology of African trypanosomosis. *17th International Conference of the World Association for the Advancement of Veterinary Parasitology.* Copenhagen, August 1999.

Rodgers, J., Kennedy, P.G.E., Jennings, F.W., Bradley, B., Eckersall, P.D., Williams, A., Murray, Max. Novel chemotherapeutic regimens to control the post-treatment reactive encephalopathy associated with African trypanosomiasis. *Fifty and Forward Jubilee Celebrations.* Glasgow University Veterinary School, September, 1999.

Poster presentations

Rodgers, J., Murray, Max, Bradley, B., Kennedy, P.G.E. Kinetics of CD4 and CD8 cell infiltration associated with the meningoencephalitis induced in a murine model of African trypanosomiasis. *The British Society for Parasitology.* Warwick, April 1999 P03.

Author's Declaration

The work presented in this thesis is original and has been carried out by the author, except where collaboration with others is acknowledged.

Jean Rodgers

Acknowledgements

The research culminating in this thesis stemmed from a fortuitously successful grant application prepared by Prof. Peter Kennedy, Prof. Max Murray and I. The original concepts leading to this proposal were the result of a team effort to further the trypanosomiasis research within the Department. The idea of investigating the actions of Substance P in the development of the CNS response was inspired through discussion between Prof. Susan Leeman of Boston University School of Medicine and Prof. Peter Kennedy. Without this funding, none of the work comprising this thesis would have been possible. I am therefore forever grateful to the Sir Jules Thorn Charitable Trust for providing the means to carryout the investigations.

The ultimate completion of this thesis is the result of support and encouragement from numerous people both directly involved with the project and out-with the scientific field. I would like to thank all of these people, especially the non-scientists, my friends and family for believing in me when even I began to doubt.

To Max and Peter, for agreeing to act as my Supervisors during the course of this study, I extend my warm thanks and appreciation. Peter's unremitting enthusiasm for trypanosome research and Max's constant positive and encouraging attitude to the project and to the preparation of this thesis have helped to motivate me to complete the task.

The world of Statistics has always remained foreign to me despite several years of study as an undergraduate. As such, I would like to express my deep gratitude to Prof. George Gettinby who has managed to succeed where all others have failed. I now appreciate the value of correctly analysed data in the interpretation of scientific material and no longer find the whole area daunting to approach. His cheerful disposition and encouragement when 'the end' seemed distant have helped tremendously. I will always remember, on frequent occasions, being told; "it (the PhD) will change your life". (I hope it's for the better George!)

Special thanks go to Barbara Bradley who, through even the most difficult periods, did not lose faith that this thesis would be completed. Her constant support, and technical assistance with the animal model, grading of pathology sections and the drudgery of RT-PCR reactions too numerous to count are sincerely appreciated. Not to mention the endless provision of tea, coffee and tasty morsels. I am deeply indebted to you Barbara.

My thanks also go to Dr. Frank Jennings. Without the availability of the murine model of human African trypanosomiasis this research would not have been possible. Frank's Irish charm and wit have brought many a smile to my face over the past few years.

Finally, I would like to take this opportunity to thank my colleagues in the Department of Veterinary Clinical Studies for giving me the time and the space to produce this tome, particularly in the later stages of its preparation, and the Faculty of Veterinary Medicine for allowing me to undertake this period of study.

Dedication

To Steven and our 'Petite bébé' with love.

Their motivational skills remain unsurpassed!

Abbreviations

± ---------- Plus or minus

µl ---------- Microlitres

µM ---------- Micromolar

µm---------- Microns

^{0}C---------- Degrees centigrade

ADC ---------- AIDS dementia complex

ANOVA---------- Analysis of variance

BBB---------- Blood-brain barrier

bp---------- Basepairs

BSA---------- Bovine serum albumen

cDNA---------- Complementary deoxyribonucleic acid

cm ---------- Centimetre

CNS---------- Central nervous system

CSF ---------- Cerebro spinal fluid

DAB ---------- diaminobenzidene

DALY'S---------- Disability of adjusted life years lost

DEPC---------- Diethyl pyrocarbonate

DFMO---------- DL-α-difluoromethylornithine

DMSO---------- Dimethylsulphoxide

DNA ---------- Deoxyribonucleic acid

DNase ---------- Deoxyribonuclease

dNTPs ---------- Deoxynucleoside triphosphates

EDTA---------- ethylene diamine tetra acetic acid

g ---------- Grams

GFAP ---------- Glial fibrillary acidic protein

GLM ---------- General linear model

GPI---------- Glycophosoinositol

GSH---------- Reduced glutathione

GS-SG---------- Oxidised glutathione

H&E ---------- Haematoxylin and eosin

H_2O ---------- Water

HAT ---------- Human African trypanosomiasis

HIV ---------- Human immunodeficiency virus

i.p. ---------- intraperitoneal

ICAM ---------- intercellular adhesion molecule

ICC ---------- Immunocytochemistry

IFN ---------- Interferon

Ig ---------- Immunoglobin

IL ---------- Interleukin

ISG ---------- Invariant surface glycoprotien

ISH ---------- *in situ* hybridisation

IS-RT-PCR ---------- *In situ* reverse transcriptase polymerase chain reaction

kb ---------- Kilobases

kDa ---------- Kilodaltons

kg ---------- Kilograms

LPS ---------- lipopolysaccharide

M ---------- Molar

MCP ---------- Monocyte chemoattractant protein

mg ---------- Milligrams

MHC ---------- Major histocompatability

MIP ---------- Macrophage inflammatory protein

ml ---------- Millilitres

mM ---------- Millimolar

mRNA ---------- messenger ribonucleic acid

MS ---------- Multiple sclerosis

MSF ---------- Médecins Sans Frontièrs

NADPH ---------- Nicotinamide adenine dinucleotide phosphate

ng ---------- Nanograms

$NK1^{-/-}$ ---------- NK1 receptor knockout

$NK1^{+/+}$ ---------- NK1 receptor wild-type

nm ---------- Nanometres

OD ---------- Optical density

ODC ---------- Ornithine decarboxylase

PBGS ---------- Phophate buffered glucose saline

PBS ---------- Phosphate buffered saline

PCR ---------- Polymerase chain reaction

PTRE ---------- Post-treatment reactive encephalopathy

RANTES ---------- Regulated on activation, normal T-cell expressed and secreted

RNA ---------- Ribonucleic acid

RNase ---------- Ribonuclease

RT-PCR ---------- Reverse transcriptase-polymerase chain reaction

SE ---------- standard error

SP ---------- Substance P

$T(S_2)$ ---------- Trypansothione disulphide

$T(SH)_2$ ---------- Dihydrotrypanothione

T.b.brucei ---------- *Trypanosoma brucei brucei*

T.b.gambiense ---------- *Trypanosoma brucei gambiense*

T.b.rhodesiense ---------- *Trypanosoma brucei rhodesiense*

TBE ---------- Tris borate EDTA

TBS ---------- Tris buffered saline

Tc ---------- T-cytotoxic

TCR ---------- T-cell receptor

Th ---------- T-helper

TNF ---------- Tumour necrosis factor

Tris ---------- Tris (hydroxymethyl) methylamine

VCAM ---------- Vascular cell adhesion molecule

VSG ---------- Variant surface glycoprotein

WHO ---------- World Health Organisation

"If we knew what we were doing, it would not be called research, would it?"

Albert Einstein

CHAPTER 1

INTRODUCTION

1.1. Aetiology of African trypanosomiasis

Tsetse-transmitted trypanosomiasis affects both man and animals in Africa. The organisms responsible for causing the disease are protozoan parasites belonging to the genus *Trypanosoma*. Although there are numerous individual species of trypanosome that can affect many different hosts, species including, *Trypanosoma brucei, T.congolense, T.vivax* and *T.simiae* are responsible for the bulk of the disease. Two sub-species of *T.brucei* namely *T.brucei gambiense* and *T.b.rhodesiense* are the causative agents of sleeping sickness in man while *T.congolense, T.vivax, T.simiae* and *T.b.brucei* result in infections in domestic ruminants and wild-life (Murray and Njogu, 1989). The main pathogenic species together with their hosts are listed in Table 1.1 (Hoare, 1970; Molyneux, Pentreath, and Doua, 1996).

The occurrence of trypanosomiasis is episodic and during the first decade of the last century sleeping sickness outbreaks devastated Central and East Africa resulting in the death of 750,000 people and in the depopulation of several trypanosome endemic areas. At the same time the presence of trypanosomes in Africa has precluded livestock rearing over vast areas of the continent and epidemics of the disease remain common to date (Kuzoe, 1993). Trypanosome infection of African wild-life, as well as certain breeds of cattle and small ruminants, by and large, produces a protracted infection with long periods where the animals appear aparasitaemic and remain in generally good health. This endurance of the infection is known as trypanotolerance. In contrast, trypanosomiasis in most domestic livestock generally results in a high degree of morbidity and mortality and in some instances death can occur within 2-3 weeks of infections (Morrison, Murray, and McIntyre, 1981; Murray, Trail, Davis, and Black, 1984; Murray and Njogu, 1989). This suggests that wild animals are the original and natural hosts for these pathogenic trypanosomes and as such may act as the reservoirs of infection from which man and domestic livestock acquire the disease (Hoare, 1972a; Murray and Trail, 1987). In a recent study by Welburn and colleagues 18% of the domestic cattle in the Tororo district of Uganda were found to be infected with *T.b.rhodesiense* indicating that domestic animals present a significant public health risk by providing a livestock reservoir of human infective trypanosomes (Welburn, Picozzi, Fevre, Coleman *et al.*, 2001). Furthermore, large scale restocking of domestic live-stock in the previously disease-free Soroti district of Uganda, with animals purchased from trypanosomiasis endemic areas, has resulted in the introduction and establishment of trypanosomiaisis in this region (Fevre, Coleman, Odiit, Magona *et al.*, 2001). These

Parasite	Possible Hosts	Alternative disease name
T.congolense	cattle, sheep, goats, equidae, dogs, antelope	Not applicable
T.vivax	cattle, sheep, goats, equidae, dogs, antelope	Souma
T.b.brucei	all domestic mammals, antelope	Nagana
T.b.gambiense	man, pigs, cattle, dogs[a]	Sleeping sickness
T.b.rhodesiense	man, cattle, goats, dogs, antelope	Sleeping sickness
T.suis	pigs, warthogs, bush-pigs	Not applicable
T.simiae	pigs, warthogs, cattle, equidae, camels	Not applicable
T.evansi	cattle, equidae, camels, dogs	Surra
T.equiperdum	equidae	Dourine

Table 1.1. Trypanosome species and susceptible hosts The main species of trypanosomes are listed together with animals in which they can cause infections. [a] Although animals infected with *T.b.gambiense* have been found their significance as reservoirs of human infective parasites remains unclear.

findings indicate the central role of live-stock farming in the spread and maintenance of human trypanosome infections.

1.1.1. History of the disease

The genus *Trypanosoma* was named over 150 years ago by Gruby, in 1843 following the isolation of *Trypanosoma sanguinis* parasites from frogs. Very little progress was made in the field during the ensuing years until Griffith Evans, a veterinarian working in India in 1880, showed that Surra, a disease of cattle and horses, was associated with the presence of trypanosomes in the blood of the infected animals. The parasite responsible for these infections came to bear Evans' name and is now known as *Trypanosoma evansi* (Hoare, 1972c; Vickerman, 1997). The discovery that trypanosomes could be serious pathogens proved pivotal in the elucidation of further conditions affecting both man and animals that result from trypanosome infection.

Sleeping sickness in man and nagana in cattle and horses had been recognised in Africa for many centuries but it was not until 1895 that David Bruce and his wife Mary, while investigating the deaths of numerous cattle in Zululand, identified a trypanosome as the causative agent of nagana. They also demonstrated that the infection was transmitted by the bite of the tsetse fly and that wild animals could act as reservoir hosts for the parasites (Bruce, 1895; Bruce, 1897). Following this Plimmer and Bradford isolated a trypanosome from the blood of a dog experimentally infected with 'nagana' and sent to England, and named the parasite *Trypanosoma brucei* in Bruce's honour (Plimmer and Bradford, 1895). Acknowledgement for identification of trypanosomes as the aetiological agents of sleeping sickness however cannot be so easily credited. The subject remains controversial as trypanosomes were isolated from the blood of sleeping sickness patients by both Aldo Castellani and David Bruce in 1903. Whether Castellani made the connection between the presence of the parasites and the disease condition in man before Bruce produced his findings remains a subject of debate.

These discoveries began a cascade of events leading to the detection of many of the important trypanosome species that cause disease in man and animals (Table 1.1). In 1902 Dutton isolated trypanosomes from humans in West Africa and named them *T.gambiense*. These were similar parasites to those isolated by Bruce, in 1903, who deemed them the infectious agent responsible for the development of sleeping sickness. Although it is now recognised that these parasites are two different subspecies of *T.brucei*, the technology

available to Dutton and Bruce at this time did not allow this distinction to be made. To reconcile the differences between the disease patterns resulting from infection with the individual trypanosomes it was believed that *T.b.gambiense* infection represented the early stages of the disease, known as 'trypanosome fever', while the acute disease resulting from *T.b.rhodesiense* infection was the late stage of the condition and called 'sleeping sickness'. A few years later in 1910 the causative agent of the acute form of the disease was 're-discovered' by Stephens and Fantham who erroneously described a morphological difference between this parasite and *T.gambiense*. This 'new' species was named *T.rhodesiense* (Hoare, 1972c). Since this time *T.gambiense* and *T.rhodesiense* have been shown to be morphologically indistinguishable from the *T.brucei* parasite originally isolated from cattle suffering from nagana. These three trypanosomes have therefore become classified as sub-species of *T.brucei* and are now termed *Trypanosoma brucei gambiense, T.b.rhodesiense* and *T.b.brucei*. Trypanosomes infecting domestic animals and livestock were also discovered during the early 20th century. These include; *T. equiperdum* in 1901, *T. congolense* in 1904, *T. vivax* and *T. suis* in 1905 and *T. simiae* in 1911 (Hoare, 1972c).

1.1.2. Trypanosome taxonomy

Trypanosomes are protozoan parasites (Fig.1.1) belonging to the phylum Sarcomastigophora, subphylum Mastigophora, class Zoomastigophora, order Kinetoplastida, suborder Trypanosomatina and family Trypanosomatidae. This family divides into eight genera with trypanosome parasites belonging to the *Trypanosoma* genus. The genus has two sections, the Stercoraria and the Salivaria. This division indicates the media, faecal or salivary respectively, in which the parasites complete their developmental cycle in their insect vector. The Stercoraria is formed by three subgenera; *Megatrypanum, Herpetosoma* and *Schizotrypanum*. Most African trypanosomes of any economic importance, with the exception of *Trypanosoma (Megatrypanum) theileri* which is Stercorarian, belong to the Salivaria which further divides into four subgenera; the *Duttonella* group which includes *Trypanosoma (Duttonella) vivax* and *Trypanosoma (Dutonella) uniforme*, the *Nannomonas* group which includes *Trypanosoma (Nannomonas) congolense* and *Trypanosoma (Nannomonas) simiae*. The *Trypanozoon* group is the largest of the subgenera and includes three separate species of trypanosome; *Trypanosoma (Trypanozoon) equiperdum, Trypanosoma (Trypanozoon) evansi* and *Trypanosoma (Trypanozoon) brucei*. The species *Trypanosoma brucei* consists of three individual subspecies; *Trypanosoma brucei brucei (T.b.brucei), T.b.rhodesiense* and *T.b.gambiense*.

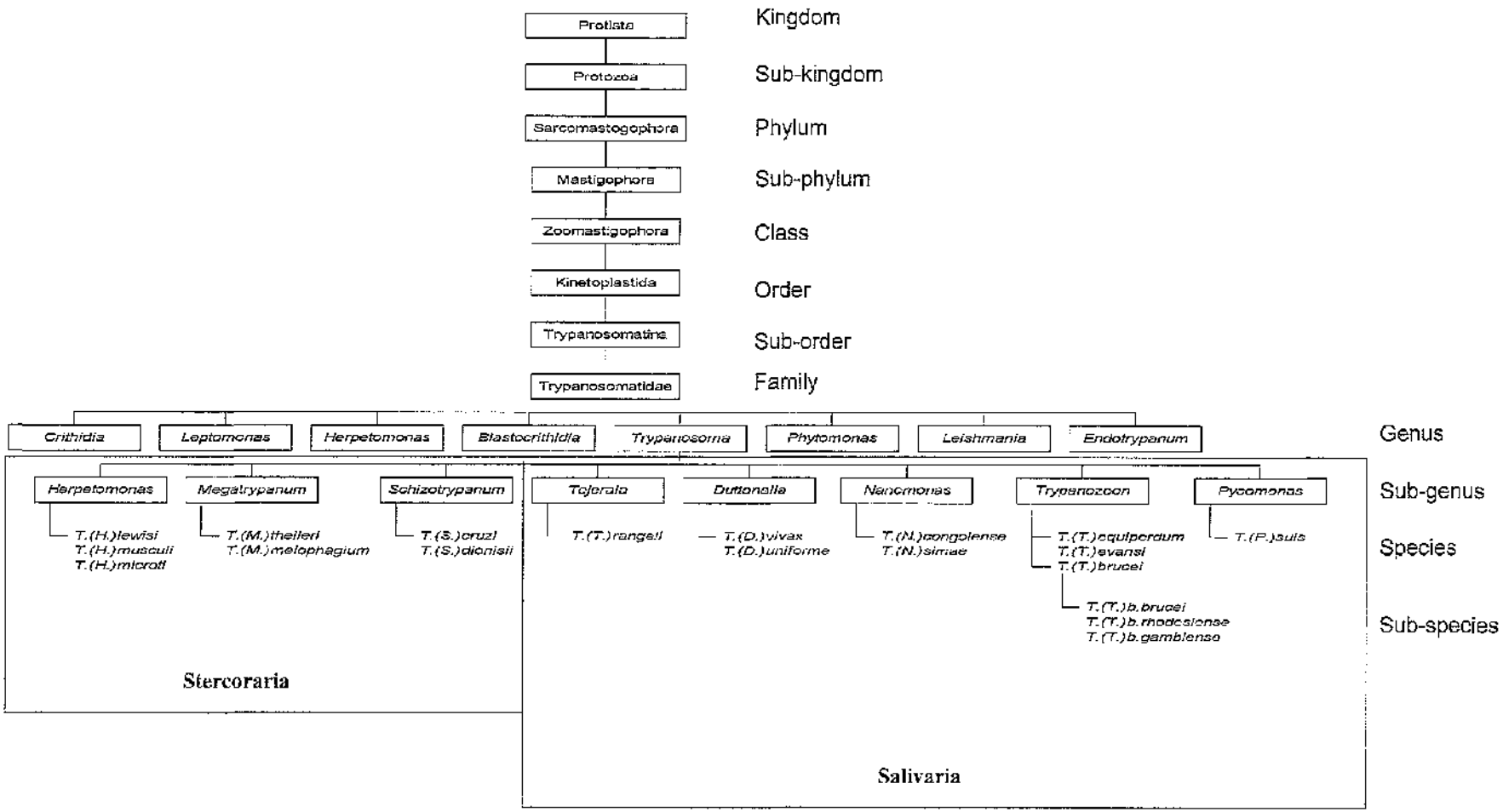

Fig 1.1. Trypanosome Classification

T.b.rhodesiense and *T.b.gambiense* are pathogenic to man and result in East African and West African trypanosomiasis respectively. The forth subgenus is the *Pycomonas* group which includes just one species, *Trypanosoma (Pycomonas) suis*. The trypanosome taxonomy as described here was detailed in a doctoral thesis by de Atouguia (de Atouguia, 1998).

1.1.3. Transmission of infection

In 1909 the tsetse fly was confirmed as the biological vector of the trypanosomes by Kleine who demonstrated that the parasites undergo a cyclical developmental process within the fly (Kleine, 1909). Before this time the transmission of the disease by the fly was widely thought to be purely mechanical in nature with the insect playing no role in the life cycle of the parasite.

Blood-sucking flies of the genus *Glossina* are responsible for the transmission of the disease. There are at least 23 species of tsetse fly and a number of sub-species. However, only a few are of importance in the transmission of sleeping sickness (Molyneux *et al.*, 1996). The different species of fly have different ecological requirements and therefore separate species are responsible for the transmission of East and West African sleeping sickness. In general, *Glossina morsitans, G. pallipides*, and *G. swynnertoni* transmit East African disease whereas *G. palpalis, G. tachinoides* and *G. fuscipes* are responsible for the transmission of West African disease.

Under normal circumstances, in a trypanosomiasis endemic area, between 2 and 10% of tsetse flies are infected with trypanosomes. Flies become infected, by ingesting the trypomastigote form of the parasite, during a blood meal (Fig.1.2). Once the fly has become infected with the parasite it remains infective for life. Following ingestion the trypomastigotes travel to the anterior mid-gut of the fly where they undergo morphological and physiological changes. The parasites change their energy source from glucose to proline and switch from aerobic to anaerobic respiration. In the mid-gut of the fly the parasites loose their variant surface antigenic coat and begin to multiply. The newly produced parasites have a long slender shape and move quickly to the salivary glands. Once in the glands they differentiate first into epimastigotes and then after further division they develop into the short and stumpy infective metacyclic form of the parasite. Transmission occurs during the infected tsetse fly's next feed when the metacyclics are

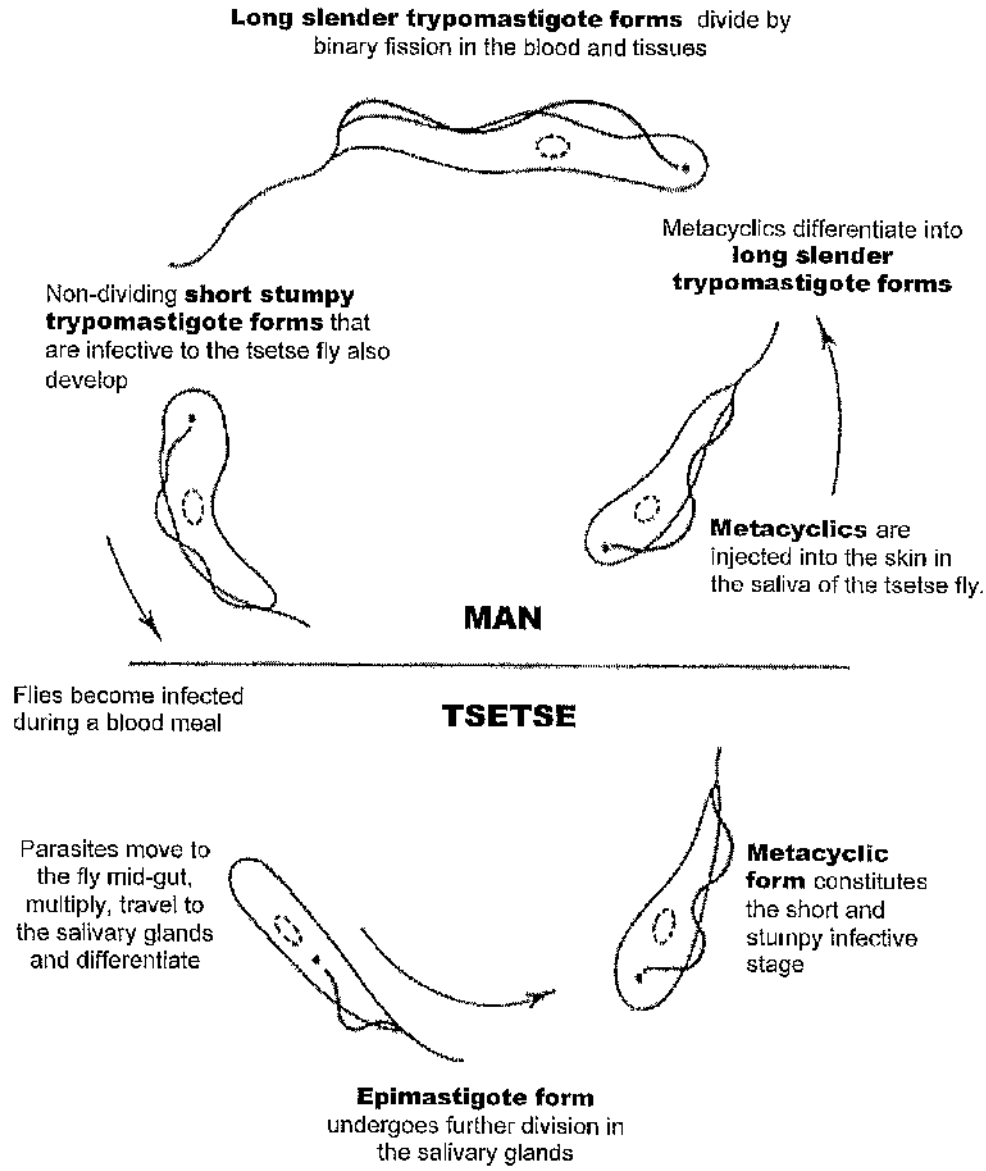

Figure 1.2. Life-cycle of trypanosome parasites in man and its vector the tsetse fly

introduced directly into the host in the saliva of the fly (de Atouguia and Kennedy, 2000; Wakelin, 1996).

1.1.4. Scale and economic considerations of trypanosomiasis

Trypanosomiasis of man and both wild and domestic animals remains a major socio-economic problem in sub-Saharan Africa. The disease is prevalent between the latitudes 14° North and 29° South, an area covering some 10 million square kilometres and including 36 African countries. This sector corresponds with the region infested by the tsetse fly and current estimates suggest that approximately 60 million people are at risk of infection. Although the disease is often regarded as a problem of the past there has been an upsurgence in the number of diagnosed infections with around 300,000 new cases each year (WHO, 1998). In recent years over 100,000 new cases have been detected in the Democratic Republic of Congo with one quarter of these infections presenting in 1997 alone (Welburn, Fevre, and Coleman, 1999). Of the 60 million people at risk, WHO estimates that less than 4 million are under medical surveillance and only 10% of new infections are actually diagnosed (WHO, 1998). The problem is being exacerbated by war, civil unrest, population and livestock movements together with a deteriorating infrastructure all of which result in the breakdown of systematic medical surveillance and lead to increased mortality rates.

In human terms trypanosomiasis is a significant contributor to the global burden of parasitic diseases. This is calculated as the disability of adjusted life years lost (DALY'S) as a result of the infection. DALY'S combine the healthy life years lost through premature mortality and those lost due to disability. When expressed in these terms the most burdensome parasitic disease is malaria which results in 315.1 x 10^5 DALY'S followed by schistosomiasis which results in 34.9 x 10^5 DALY's. Trypanosomiasis is responsible for 17.8 x 10^5 DALY'S and is the third most important parasitic disease adversely effecting human health (Molyneux *et al.*, 1996).

In financial terms, trypanosomiasis results in the loss of millions of dollars annually through the death of livestock, reduction in milk and meat production as well as lowering fertility rates. Using geographic information systems to spatially link a biophysical herd simulation model with an economic surplus model, the financial costs of trypanosomiasis in livestock has recently been estimated to be in the region of $1340 million dollars

annually. This figure does not include the losses sustained though indirect livestock benefits such as manure and traction (Kristjanson, Swallow, Rowlands, Kruska *et al.*, 1999). In the same study the potential benefits of improved trypanosomiasis control were estimated to be around $700 million per annum in terms of meat and milk production alone.

1.1.5. Parasite biology

Trypanosoma brucei spp. are unicellular, eukaryotic, protozoan parasites (Fig.1.3). They form elongated, spindle shaped cells that vary in length from 12-42μm with tapering anterior and blunt posterior ends. A characteristic feature of African trypanosomes is the presence of a free flagellum. The flagellum arises from the basal body, near the flagellar pocket, at the posterior end of the cell, and is attached along the entire length of the parasite. In the epimastigote form of the parasite (Fig.1.2) the kinetoplast and flagellum are situated anterior to the nucleus. When the flagellum beats it draws up the cell membrane or pellicle to form an undulating membrane. This combination of flagellum and undulating membrane facilitates the parasite's motility (Hoare, 1972b). The flagellar pocket is secluded from the environment to help prevent exposure of its antigenic sites to the host immune system. It is however a critical structure in the endo- and exocytosis of macromolecules and contains specialised receptors for the absorption of host-derived growth factors and nutrients (Hill, Hutchings, Russell, and Donelson, 1999).

The parasite has a single mitochondrion that contains a specialised organelle called the kinetoplast. The kinetoplast consists of a network of approximately 10,000 interlinked minicircles and around 50 maxicircles of DNA. The maxicircles are highly conserved and encode components of the mitochondrial respiratory chain and mitochondrial ribosomal RNAs. The RNA transcribed from the maxicircle genes is edited during its maturation with the help of small guide RNAs that are transcribed from the minicircles. These small RNA molecules serve as a template for editing the maxicircle transcripts by guiding the insertion and deletion of uridine nucleotides (Simpson and Shaw, 1989).

The trypanosome nucleus is located centrally in the cell. The parasites are regarded as diploid with a haploid DNA content of around 4×10^4 base pairs that probably encodes not more than 8000 genes. The nuclear organisation differs from that of higher eukaryotes in that the chromatin does not condense during metaphase of mitosis hence an accurate definition of ploidy is difficult to assess. However, by employing pulse-field gel electro-

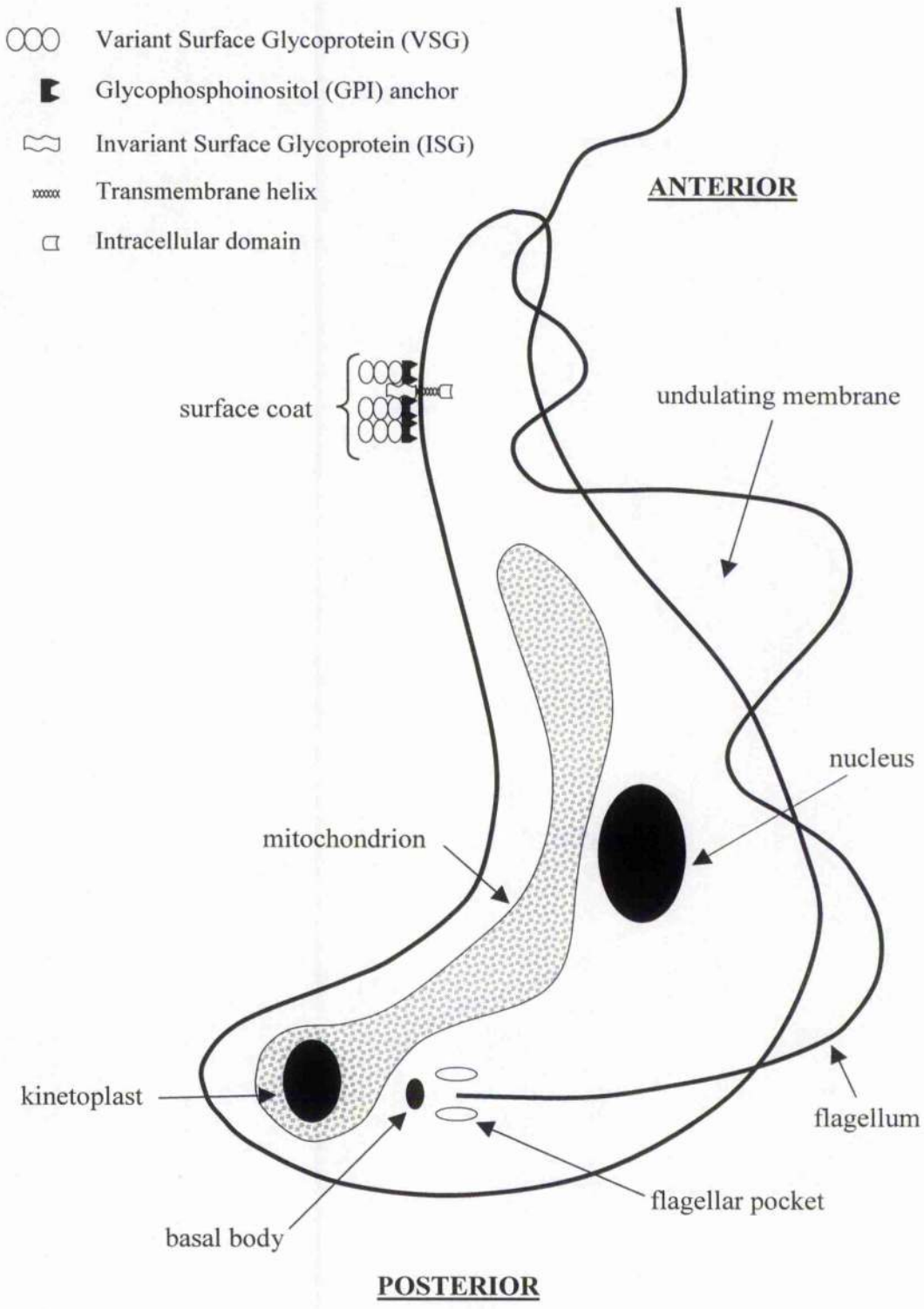

Figure 1.3. Schematic representation of the morphology of the trypomastigote form of *Trypanosoma brucei spp.*

phoresis it appears that the nucleus of African trypanosomes contains at least 120 chromosomal associated DNA molecules that can be divided into two groups depending on their size. There are around 20 DNA molecules that range from 200 kilobases (kb) to 5700kb and at least 100 'minichromosomal' DNAs of 50-150kb. With the exception of one report on the tyrosine transfer RNA gene no other introns have been demonstrated in the trypanosome genome (Schneider, McNally, and Agabian, 1993).

An electron dense coat covers the outer surface of the trypanosome in the mammalian host. This layer is approximately 15nm thick and is composed of variable surface glycoprotein (VSG) molecules and invariant surface glycoprotein (ISG) molecules. A glycophosphoinositol (GPI) anchor attaches the VSG molecules to the surface of the plasma membrane whereas the ISG molecules are fixed via a transmembrane helix and a short intracellular domain. Approximately 10 million copies of a single VSG species cover the surface of the parasite. These VSG molecules out number the ISG molecules by about 100 fold. Although the trypanosome can express over a thousand different VSG genes only one form of the molecule is present on the coat at any one time. This conservative method of antigenic variation allows the parasite to evade the immune system of the host by continually altering its major surface antigen. As parasites expressing one form of VSG are destroyed by the host a small proportion of the surviving trypanosomes, expressing a different VSG, continue to multiple producing successive waves of parasitaemia. If the parasites expressed more than one VSG at a time they would ultimately reduce the length of time that they could escape from the host's defences. Each trypanosome has around 1000 different VSG genes located on the minichromosomal DNA elements.

Approximately 6% of the total parasite genome is devoted to antigenic variation via the production of VSG molecules. Each VSG molecule is about 65kDa in size and consists of a polypeptide chain of around 500 amino acids. The molecule can be divided into specific regions. The N-terminal domain contains a short signal sequence as well as a highly variable region where the amino acid sequence shows little homology with other VSG molecules. The C-terminal of the molecule shows considerable sequence homology between VSGs, however, as the molecules are densely packed only the variable N-terminal of the molecule is exposed to the host and the constant regions are effectively concealed. The complete molecules form cylindrical structures that are attached to the cell surface at a 90° angle by the GPI anchor. Both the polypeptide back bone of the molecule and the GPI anchor carry carbohydrate side chains, however, as with the constant C-terminal portion of the VSG these molecules are effectively shielded from exposure to the environment and are not readily accessible for interaction with the host antibodies (Wakelin, 1996).

1.2. Trypanosomiasis in man

1.2.1. Clinical picture

Human African trypanosomiasis (HAT) results from infection with either *T.b.gambiense* in West and Central Africa or *T.b.rhodesiense* in East and Central Africa. West African sleeping sickness is a chronic disease with a duration of months to years whereas East African sleeping sickness follows an acute course with a duration of 3 to 9 months before death ensues. Both forms of trypanosomiasis are invariably fatal without chemotherapeutic intervention. Clinical manifestations of sleeping sickness are not pathognomic and can vary greatly from one individual to another. After initial infection the trypanosomes are localised to a non-suppurative lesion or chancre that develops at the site of the infected tsetse bite. The chancre disappears spontaneously 2 to 3 weeks after infection. This is followed by a systemic phase when the parasites invade the lymph and blood. Clinically the patient experiences febrile episodes with headaches and enlarged lymph nodes may be present at this stage. An erythomatous skin rash may also appear. From here the parasites invade a variety of tissues including spleen, liver and heart and ultimately enter the central nervous system (CNS). In Rhodesian sleeping sickness CNS involvement occurs early after infection, usually within 3 to 4 weeks of the tsetse bite, and there is no clear distinction between early and late stage disease. In Gambian sleeping sickness, CNS invasion can be delayed until years after infection and asymptomatic carriers occur frequently. Early signs of neurological involvement include, irritability, lack of concentration, personality changes and alterations in sleep patterns. However, these symptoms are not diagnostic of CNS involvement as they are occasionally found before any changes can be detected in the cerebrospinal fluid (CSF). As the disease progresses, further neurological symptoms become apparent including seizures and muscle fasciculations. There is a general wasting and increased sleep disturbance with the patient becoming more difficult to rouse. This leads to coma and death in untreated patients (de Atouguia and Kennedy, 2000).

1.2.2. Pathogenesis

Although the clinical and pathological features of HAT are well documented the pathogenesis of the disease remains to be fully elucidated and much of the information with regard to this topic has been extrapolated from animal models and experimental

animal infections. Trypanosome infection in man results in numerous progressive pathological changes that encompass most of the organs and the systems of the body. After initial restriction to the chancre, the trypanosomes spread throughout the haemo-lymphatic system and alterations in haematology and immunology are frequently encountered. Widespread dissemination of the parasites throughout the body tissues then occurs with trypanosomes invading the major organs including the heart, liver, spleen and CNS where they evoke inflammatory reactions and tissue damage.

1.2.2.1. Haemo-lymphatic manifestations

Following infection many changes are found in the haematological constituents of the affected individual including anaemia, thromobocytopenia, fluctuations in leucocyte numbers, macroglobulinaemia and lipaemia (Molyneux *et al.*, 1996). The anaemia associated with HAT is more severe in cases of the Rhodesian form of the disease and may be absent or only mild in Gambian sleeping sickness (Greenwood and Whittle, 1980). The anaemia results from a combination of factors such as impaired erythropoesis and haemodilution. However, the major cause of the severe anaemia appears to be erythrophagocytosis. During infection, many of the red blood cells become coated in immune complexes. These erythrocytes are subsequently phagocytosed by macrophages in the spleen, liver and lymph-nodes leading to a reduction in the pool of circulating red cells (de Atouguia and Kennedy, 2000; Jenkins and Facer, 1985; Molyneux *et al.*, 1996; Murray and Dexter, 1988). In animals, the spleen has been shown to be the site of red cell phagocytosis during mild anaemia while the liver plays the major role in cases of severe anaemia (Jenkins and Facer, 1985). Haemolytic factors liberated directly by the trypanosomes may also contribute to the destruction of red blood cells (Jenkins and Facer, 1985; Molyneux *et al.*, 1996; Murray and Dexter, 1988). Furthermore, as the disease advances the production of new erythrocytes by the bone marrow is significantly reduced due to a lack of incorporation of iron into the red cell precursors (Jenkins and Facer, 1985; Murray and Dexter, 1988). In addition, the plasma volume increases as the disease progresses producing a haemodilution effect (Jenkins and Facer, 1985). The body therefore fails to compensate for this decrease in red cell number and increase in total plasma volume and a severe anaemia develops.

Thrombocytopenia commonly develops in both forms of sleeping sickness. Again this may be mild in the Gambian form of the disease and probably results from an enhancement of the reticuloendothelial system. In Rhodesian sleeping sickness the thrombocytopenia is

often more pronounced and can be associated with disseminated intravascular coagulation (Greenwood and Whittle, 1980). The coagulopathy consists of thrombosis, haemorrhage, multiple petechiae, and tissue necrosis. This is accompanied by fibrinolysis and fibrinogen and fibrin degradation products are elevated. In addition decreases in platelet cell numbers are found in patients with either form of sleeping sickness (Greenwood and Whittle, 1980; Molyneux *et al.*, 1996).

Pronounced immunological changes also occur following trypanosome infection resulting in fluctuations in the numbers of circulating leucocytes and antibody levels. In the acute stage of the disease there is a dramatic plasma cell response in the lymph-nodes and spleen. This plasma cell response is accompanied by a rise in the levels of circulating immunoglobins and produces a marked alteration in the ratio of plasma albumin to globulin levels. This macroglobulinaemia is common to both *T.b.rhodesiense* and *T.b.gambiense* infections and reflects the non-specific polyclonal B-cell activation that occurs at this stage of the infection. During the initial parasitaemia, IgM is the major immunoglobin produced but as the disease progresses this switches to IgG although IgM levels remain elevated. However, it appears that little of the IgM produced by sleeping sickness patients is specific for trypanosome antigens. Moreover, affinity for autoantigens such as aggregated IgG and double stranded DNA, as well as other tissue components has been reported (de Atouguia and Kennedy, 2000; Greenwood and Whittle, 1980; Hunter and Kennedy, 1992). During the polyclonal response the splenic B-cells become unresponsive to mitogens such as LPS, later in infection this immunosuppressive interference extends to the T-cell population (Bancroft and Askonas, 1985; Murray, 1974). The mechanisms involved in this depletion of T-cell and B-cell responses remain unclear. Several hypotheses have been suggested including; saturation of the leucocyte cell surface receptors due to the continual changing of the parasite antigenic coat, or the transformation of the B-cells by a mitogenic effect of the trypanosome leaving the population unable to respond to alternative antigens (Murray, 1974).

1.2.2.2. Specific organ damage

Cellular degradation occurs in most of the organs of patients affected by sleeping sickness (Murray, 1974). However, as post-mortem information is only available from patients who have died of the advanced stage of the disease many of the details regarding the progress of the infection have been obtained from animal models. In early infections, lymphadenopathy is commonly found and the glands show lymphocyte, plasma cell and

macrophage production (Ormerod, 1970). In some instances, especially those involving Gambian disease, the cervical lymph nodes in the neck can become easily visible. This is referred to as 'Winterbottom's sign' (Apted, 1970). In advanced cases, fibrosis of the lymph nodes occurs and they become small and hard and morular or Mott cells can be detected in the glands at this stage. Mott cells are large plasma cells with a characteristically vacuolated cytoplasm and pycnotic nucleus. The cytoplasmic vacuoles, or Russell bodies, are dilated cisternae of the endoplasmic reticulum and are filled with non-secreted, mutated immunoglobin that cannot be degraded from the endoplasmic reticulum (Maggioni, Carelli, Cabibbo, Fagioli *et al.*, 1998).

Following trypanosome infection the spleen also increases in size and develops a firm texture. This organ shows few indications of fibrosis until the advanced stages of the disease are reached. Changes similar to those initiated in the lymph nodes are seen in the Malpighian corpuscles and numerous plasma cells can be found (Ormerod, 1970).

The inflammatory processes triggered by trypanosome infection result in a general increase in perivascular cellularity, characterised by the presence of monocytes, lymphocytes and plasma cells. However, it appears that polymorphonuclear lymphocytes have little input in the immune response generated in sleeping sickness (Ormerod, 1970). In contrast large numbers of polymorphonuclear lymphocytes have been found associated with the sites of tissue lesions in dogs experimentally infected with *T.b.brucei* (Morrison, Murray, and Sayer, 1997). The perivascular reaction is associated with tissue oedema and haemorrhage (Molyneux *et al.*, 1996). In *T.b.rhodesiense* infections cardiac reactions are prominent and a myocarditis develops rapidly which quickly spreads to all layers of the heart including the valves and conduction pathways (Molyneux *et al.*, 1996). Numerous plasma cells are present in the inflammatory infiltrate amongst which are Mott cells. Fibrosis and myocytolysis can also be seen in the cardiac tissue lesions as the disease advances.

1.2.2.2.1. Central nervous system manifestations

The data regarding the progressive changes that occur in the brain following trypanosome infection are limited to material obtained from patients that have died during the advanced stages of the disease. Therefore a substantial portion of the neuropathogenesis information has been gained from experimental animal models of the infection. The CNS is affected in both forms of sleeping sickness, although the changes become more apparent in the chronic Gambian form of the disease since infection with *T.b.rhodesiense* can cause fatal cardiac involvement before the CNS reaction becomes pronounced. It is likely that

changes to the meninges and brain begin early in the infection and it has been suggested that the severe headaches that accompany the early stages of the diseases result from this CNS involvement (Ormerod, 1970).

The mechanisms employed by the parasites to enter the CNS and the kinetics of this invasion have yet to be fully elucidated. However since the choroid plexus shows injury fairly quickly after infection this seems a feasible route to allow the parasite to gain access to the CNS. From here the parasites can enter the cerebrospinal fluid (CSF) and subsequently penetrate the brain via the subarachnoid and Virchow-Robin spaces (Molyneux *et al.*, 1996; Pentreath, Baugh, and Lavin, 1994). Further evidence to substantiate this hypothesis is available since large numbers of trypanosomes have been found, soon after infection, in the choroid plexus of dogs experimentally infected with *T.b.brucei* (Morrison, Murray, Whitelaw, and Sayer, 1983). Moreover, in experimental rodent infections the parasites localise to areas of the CNS where the BBB is weak such as the choroid plexus, the trigeminal and dorsal root ganglia and the circumventricular organs including the pineal gland and median eminence (Bentivoglio, Grassi-Zucconi, Olsson, and Kristensson, 1994). However, human studies have shown only a minor involvement of the choroid plexus in the overall inflammatory reaction (Adams, Haller, Boa, Doua *et al.*, 1986). Investigations in a rodent model employing *T.b.brucei* have suggested that progressive damage to the BBB occurs as the disease advances (Pentreath *et al.*, 1994; Philip, Dascombe, Fraser, and Pentreath, 1994). Therefore the route of entry of trypanosomes to the CNS remains to be elucidated definitively.

Pathologically the neuroinflammatory changes resulting from trypanosome infection are characterised by an influx of inflammatory cells including macrophages, T-cell, B-cells and many plasma cells eventually progressing to a severe meningoencephalitis. In many cases the inflammation results in a thickening of the leptomeninges which become adherent to the dura mater (Ormerod, 1970). This phenomenon has been reported in both the ventral and basal regions of the brain (Cegielski and Durack, 1997). The meningitis is accompanied by severe perivascular cuffing of the blood vessels with inflammatory cells infiltrating the parenchyma (Adams and Graham, 1998). The inflammatory infiltrate is composed of lymphocytes, macrophages and plasma cells. In addition, Mott cells are frequently encountered. A pronounced astrocytosis and diffuse microglial hyperplasia are also significant features of the neuroinflammatory reaction (Adams *et al.*, 1986). In some cases the lesion can take the form of a severe haemorrhagic leukencephalopathy (Adams *et al.*, 1986). Despite the severity of this reaction there appears to be little damage to the neuronal elements of the brain and these are, in general, spared from harm. However in

some fatal cases of sleeping sickness, perivascular demyelination has been reported in the subcortical white matter (Cegielski and Durack, 1997).

1.2.3. Diagnosis

Clinical diagnosis of early stage human African trypanosomiasis (HAT) is difficult since many of the initial symptoms are commonly found in a plethora of other infectious diseases endemic to the area. Due to the intermittent bouts of fever interspersed with periods when the patient feels well, it is not unusual for malaria or bacterial infections to be diagnosed and anti-malarial or antibiotic drugs administered. This treatment regimen reduces the fever and frequently results in the delay of an accurate diagnosis until the trypanosomiasis has progressed and signs of CNS involvement become apparent.

As there are no pathognomic clinical manifestations in HAT laboratory confirmation of infection is essential. Definitive diagnosis is dependent on the direct demonstration of trypanosome parasites in the chancre, blood smears, lymph node aspirates or CSF. This is usually carried out by examination of either wet smears or Giemsa-stained thick or thin peripheral blood smears. However, direct demonstration of the parasite can be difficult as the parasitaemia is cyclical and often extremely low therefore time consuming repeated examinations are often required. If the parasites are detected, a lumbar puncture is essential. Since there is a high probability of CNS involvement if the CSF shows increased IgM levels or a raised leucocyte count, this test allows the clinician to determine the stage of the infection and prescribe the appropriate form of chemotherapy.

Several trypanosome concentration techniques are available such as the micro-haematocrit centrifugation technique (Woo, 1970), the quantitative buffy coat method (Bailey and Smith, 1992; Bailey and Smith, 1994), the miniature anion exchange technique and the double centrifugation technique. Although these methods improve the detection rates many infections remain undiagnosed. Indirect methods, such as the subinnoculation of blood into susceptible laboratory animals or the kit for *in vitro* isolation (KIVI), can be more sensitive than microscopic examination of samples. However these tests are expensive and there is a significant time delay before they yield results (McNamara, Bailey, Smith, Wakhooli *et al.*, 1995; Truc, Bailey, Doua, Laveissiere *et al.*, 1994).

Alternative approaches, based on the detection of host antibody responses to the trypanosome antigens have emerged. The most useful are the immunofluorescent antibody test (IFAT) (WHO, 1976), the enzyme linked immunosorbant assay (ELISA) (Lejon,

Buscher, Magnus, Moons *et al.*, 1998; WHO, 1976) and the card agglutination trypanosomiasis test (CATT) (Truc *et al.*, 1994). However major problems still remain since the presence of anti-trypanosomal antibodies does not distinguish between past and active infections. Assays for the detection of circulating trypanosome antigens have been developed to circumvent these problems. Sandwich antibody antigen capture ELISA based tests are the most common format and their use in both human (Liu, Cattand, Gardiner, and Pearson, 1989; Nantulya, Doua, and Molisho, 1992) and animal (Liu, Pearson, Sayer, Gould *et al.*, 1988; Nantulya, Lindqvist, Stevenson, and Mwangi, 1992) diagnostics has been described. Unfortunately, generation of false positive and false negative results is not uncommon when trypanosome antigen based tests are employed.

1.2.4. Current treatment strategies

The successful chemotherapy of HAT is precarious due to dwindling supplies of an extremely limited array of useful drugs and further hampered by the development of drug resistance by the parasite (Ross and Sutherland, 1997). Whereas new compounds that can be delivered orally have been developed for the treatment of many parasitic diseases, the treatment of HAT still relies on highly toxic drugs, developed before 1950, that must be administered parenterally in repeated doses.

1.2.4.1. Chemotherapy of early-stage infections

Trypanosomiasis is considered to be in the early-stage when parasites can be detected in the blood and no trypanosomes or high leucocyte or protein levels are present in the cerebrospinal fluid (CSF). The current treatment regimens employed for early-stage chemotherapy are as follows: only two drugs are recommended for the treatment of trypanosomiasis if the disease is diagnosed during the early stage, before the parasites have progressed into the central nervous system. These drugs are pentamidine and suramin. Pentamidine (Pentacarinate®) is only used in the treatment of *T.b.gambiense* infections as *T.b.rhodesiense* has shown primary resistance to pentamidine therapy. It is administered as a course of 7 to 10 intramuscular injections, given once daily or every second day (WHO, 1998).

Suramin is effective against both *T.b.gambiense* and *T.b.rhodesiense*. However its use, for the time being, is generally restricted to the treatment of east African trypanosomiasis. Suramin is administered as an intravenous injection. The course usually comprises a test

dose, to check the patient's tolerance of the drug, followed by a series of 5 injections given at 5 to 7 day intervals.

Treatment of early-stage infections with the above regimens is usually successful although the patient may experience adverse reactions to the drugs that can occasionally be fatal (WHO, 1998).

1.2.4.2. Chemotherapy of CNS-stage infections

If the infection has progressed to the CNS, as indicated by the presence of trypanosomes or elevated leucocyte or protein levels in the CSF, the only commonly available drug of use is the trivalent arsenical melarsoprol (Mel B®). This drug is not soluble in water and is therefore produced as a 3.6% solution in propylene glycol. Treatment schedules for melarsoprol differ but generally consist of a series of daily intravenous injections administered over a 3 to 4 day period followed by a 7-day interval. This regimen is repeated 3 to 4 times using increasing doses of melarsoprol on each successive round of treatment. Melarsoprol treatment is generally preceded by two injections of either pentamidine or suramin to clear the trypanosomes from the bloodstream (WHO, 1998).

1.2.4.3. Adverse reactions to melarsoprol treatment

Unfortunately, melarsoprol therapy can result in several serious side effects. Myocardial damage and polyneuropathies occasionally appear. Due to the noxious nature of the propylene glycol solvent, severe venous damage occurs frequently in melarsoprol regimens. This tissue damage can be so severe that it necessitates amputation of the affected limbs. Great skill is therefore required to administer the drug whilst causing the least tissue damage over the protracted course of the therapy.

The most serious adverse reaction to melarsoprol therapy is the development of the post-treatment reactive encephalopathy (PTRE). This occurs in 5-10% of melarsoprol treated individuals. In up to 50% of affected patients the condition deteriorates to a deep coma followed by death (Adams *et al.*, 1986). The basis of this adverse reaction is unknown, although several hypotheses exist. These include; parasite persistence as a consequence of subcurative drug treatment (Hunter and Kennedy, 1992; Jennings, McNeil, Ndung'u, and Murray, 1989), the release of parasite antigen within the CNS as a result of chemotherapy (Pepin and Milord, 1991), the toxic nature of the arsenical drug (Hurst, 1959), immune

complex deposition (Lambert, Berney, and Kazyumba, 1981) and autoimmunity (Poltera, 1980).

The onset of the PTRE is shown clinically by fever, tremors, slurring of speech and convulsions. Pathologically, the PTRE is characterised by a severe meningoencephalitis with the influx of lymphocytes, macrophages and plasma cells and an intense astrocytosis. Occasionally the PTRE can take the form of an acute haemorrhagic leucoencephalopathy (Adams *et al.*, 1986). The kinetics of the inflammatory cell infiltration into the CNS and the breakdown of the proportions of individual cell types involved in the development and control of the meningoencephalitis have yet to be fully determined.

1.2.5. Alternative chemotherapeutic approaches

At present, up to 20% of diagnosed patients are failing to respond to melarsoprol therapy as a consequence of parasite resistance to the drug (Barrett, 1999). Hence, the search for an alternative therapeutic regimen for the treatment of this disease is of paramount importance.

1.2.5.1. Eflornithine

Since the introduction of melarsoprol in 1949, the only new drug registered for the treatment of late-stage HAT is eflornithine also known as DL-α-difluoromethylornithine (DFMO). Eflornithine is a potent irreversible inhibitor of ornithine decarboxylase (ODC), the key enzyme in the production of the polyamines putrescine, spermine and spermidine which are required by all dividing cells. Since the concentration of ODC is elevated in most tumours and pre-malignant lesions, eflornithine was originally developed as an anti-cancer drug. It was first used, although unregistered, to treat HAT by van Nieuwenhove in 1981 (Van Nieuwenhove, Schechter, Declercq, Bone *et al.*, 1985). Since eflornithine crosses the blood-brain barrier it can be used to treat late-stage disease. In fact the positive effects produced by eflornithine treatment of comatose sleeping sickness patients were so dramatic that it was nicknamed 'the resurrection drug'. In addition, it was shown that eflornithine therapy could also produce a dramatic clinical improvement in late-stage sleeping sickness patients even when the patient's immune system had become damaged by the disease and remained only partially functional. In these patients the treatment failed to resolve the infection however, the general sense of well being of the individual was nevertheless improved. These findings led to speculation that eflornithine has previously

unrecognised pharmacological actions within the inflamed brain over and above the inhibition of ODC.

Senior scientists employed by the Merrell Dow Research Institute, the initial producers of eflornithine, pursued extensive clinical trials on eflornithine therapy of trypanosomiasis and eflornithine was registered by the US Food and Drug Administration (FDA) for the treatment of *T.b.gambiense* sleeping sickness in 1990 (Sjoerdsma and Schechter, 1999). There is limited information available on eflornithine monotherapy of East African sleeping sickness, although the existing data indicate that *T.b.rhodesiense* is not susceptible to the action of eflornithine (Iten, Matovu, Brun, and Kaminsky, 1995). On the other hand there is some evidence to suggest that eflornithine therapy, in combination with other trypanocidal drugs, may be effective in the treatment of late-stage *T.b.rhodesiense*-infections (Taelman, Clerinx, Bogaerts, and Vervoort, 1996) and in *T.b.gambiense*-infections where the parasites are refractory to melarsoprol therapy (Simarro and Asumu, 1996; Van Nieuwenhove *et al.*, 1985).

After dissolution of Merrell Dow, eflornithine production was discontinued and the drug became virtually unavailable. Recently WHO and Hoechst Marion Roussel inc. signed a new Licensing Agreement that grants WHO reference right to the license to produce eflornithine. This will allow the necessary technology to be transferred to a third party within the private sector who will manufacture the drug. Although this third party has not yet been identified it is envisaged that funds will be secured to guarantee the production of eflornithine until 2005 (WHO, 2000).

1.2.5.2. Nifurtimox

Since the mid-1970's nifurtimox (Lampit®) has been used to treat Chagas' disease, the Latin American form of trypanosomiasis caused by infection with *Trypanosoma cruzi*. The drug is not well tolerated and can produce serious side effects ranging from gastro-intestinal upset to neurological reactions. However, a few clinical trials have been carried out in patients with melarsoprol refractory *T.b.gambiense*-infections. The efficacy of the treatment varied substantially in these trials. A relapse rate of 63% was seen in patients given 12-17 mg/kg nifurtimox daily for a period of 60 days (Pepin, Milord, Mpia, Meurice *et al.*, 1989). This high failure rate was reduced to 36% by raising the dosage of nifurtimox to between 24-37 mg/kg daily for a 30 day period, but this higher dose rate produced significant toxicity in the patients and severe neurological reactions were not uncommon (Pepin, Milord, Meurice, Ethier *et al.*, 1992).

The possibility of nifurtimox treatment has not been abandoned completely as more promising results were seen recently in the Democratic Republic of Congo. Here a regimen comprising a combination of melarsoprol and nifurtimox was employed and further trials are planned using this composite approach (WHO, 2001a)

1.2.5.3. Megazol

Megazol is a 5-nitroimidazole derivative that has shown *in vitro* trypanocidal activity against *T. brucei* (de Atouguia, 1998) although the mode of action remains unclear. The drug is absorbed into the cells mainly by passive diffusion through the cell membrane however use of the P2 transporter has also been suggested as the drug possess the prerequisite motif for binding to the molecule (Denise and Barrett, 2001). In mouse models, megazol monotherapy is only effective against early-stage trypanosome infections and does not cure CNS-stage disease. However, if megazol is administered in combination with suramin or melarsoprol CNS-stage infections can be successfully resolved (Enanga, Keita, Chauviere, Dumas *et al.*, 1998; Jennings, Chauviere, Viode, and Murray, 1996).

Despite the promising results with combination therapy the use of megazol to treat human African trypanosomiasis has been largely abandoned due to the fact that the drug produces a positive result in the Ames' test and its use could therefore produce mutagenic effects. However, given the serious nature of the disease and the lack of effective drugs to treat the condition, flexibility in the licensing of 'new' drugs for use in the treatment of late-stage trypanosomiasis seems to be required.

1.3. Aims and objectives

In view of the possible therapeutic implications for trypanosomiasis and other CNS inflammatory conditions such as multiple sclerosis (MS), Alzheimer's disease, AIDS dementia complex and cerebral malaria *inter alia*, an investigation of the key events leading to the CNS inflammatory lesion will be pursued in this thesis. In addition, the mechanisms of action of eflornithine and the role of the neuropeptide substance P in the control of the immune response within the CNS will be elucidated. This will significantly enhance our knowledge of CNS inflammatory responses and may prove important in the search for more efficacious treatment regimens for a variety of immune-mediated CNS conditions.

The investigation has four main objectives:

- To define the kinetics of cytokine production in the central nervous system (CNS) during a meningitis and subsequent encephalitis.
- To detemine the temporal and spatial transmigration of leucocytes into the CNS following trypanosome infection and the development of the PTRE.
- To investigate the modulatory effects of the drug eflornithine on cytokine production and inflammatory cell recruitment into the CNS.
- To study the role of the neuropeptide Substance P in the generation of the neuroinflammatory reaction induced by subcurative drug treatment of trypanosome-infected mice.

1.4. Rationale

1.4.1. Neuropathogenesis and the mouse model

During late-stage human African trypanosomiasis (HAT), parasites invade the CNS leading to the development of neurological disease. Following chemotherapy there is often a post-treatment inflammatory reaction in the CNS that augments the ongoing pathology and can be fatal. Pathologically the CNS lesions are characterised by a meningitis and subsequent encephalitis, with lymphocytes, plasma cells and macrophages infiltrating the meninges and perivascular spaces, and a reactive astrocytosis. A mouse model that simulates all phases of the CNS pathology, in particular the severe meningoencephalitis found in patients that exhibit the post-treatment reactive encephalopathy (PTRE) will be used to elucidate the mechanisms culminating in this inflammatory reaction. This model is described in greater detail in Chapter 2 of this thesis.

1.4.2. Migration of leucocytes across the blood-brain barrier

Leucocytes interact with and traverse the blood-brain barrier to enter the parenchyma in a multi-step process occurring in an ordered sequential fashion. The release of mediators

controls the expression of an ensemble of adhesion molecules that are reciprocally expressed on endothelial cells and leucocytes. The local release of chemoattractant cytokines, termed chemokines, is also thought to be a prerequisite for leucocyte recruitment into the CNS. Most data have been derived from studies on non-CNS derived tissue and do not, therefore, address the unique situation within the brain. The time course of cytokine and chemokine expression within the CNS will therefore be investigated in this study.

1.4.3. Modulation of CNS pathology

Eflornithine, a specific inhibitor of ornithine decarboxylase, the main regulatory enzyme for the *de novo* synthesis of polyamines, has been used effectively in the treatment of both human and animal trypanosomiasis. An intriguing aspect associated with the use of this drug is the rapid clinical improvement that it induces in comatose patients, even when it has failed to eliminate the infection prompting investigators to call it the 'resurrection drug'. This led to speculation that eflornithine may have important pharmacological effects besides its trypanostatic action. Using an eflornithine-resistant trypanosome stabilate, we have demonstrated previously that treatment of infected animals with eflornithine both prevents and ameliorates the meningoencephalitis associated with the PTRE (Jennings, Gichuki, Kennedy, Rodgers *et al.*, 1997). These findings indicate an important previously unrecognised action of eflornithine in controlling the CNS pathology of the disease. It is possible that eflornithine is achieving this anti-inflammatory effect by inhibition of cytokine production within the CNS. This could block the cascade of events that lead to the formation of the inflammatory lesion and the ultimate transmigration of leucocytes across the blood-brain barrier. These possibilities will be investigated in this thesis.

1.4.4. The role of substance P

The neurotransmitter substance P (SP) is an 11 amino-acid neuropeptide that is widely distributed in the central nervous system and peripheral tissues. Recent evidence shows that SP may also be involved in a wide range of inflammatory reactions from rheumatoid arthritis (Anichini, Lepori, Maddali Bongi, Maresca *et al.*, 1997) to multiple sclerosis (Barker and Larner, 1992). A role for SP in the pathogenesis of cerebral malaria has also been suggested as sera from *Plasmodium falciparum*-infected patients has been shown to induce the production of SP by human brain micro-vascular endothelial cells *in vitro*

(Chiwakata, Hort, Hemmer, and Dietrich, 1996). The development of potent, highly specific, non-peptide SP antagonists provides a new opportunity to investigate the possible involvement of SP in sleeping sickness. The mechanism by which SP may modulate inflammation and its site of action in the inflamed brain remain to be elucidated. This will be investigated through the use of NK1, NK2 and NK3 receptor antagonists, to block the action of SP by inhibiting receptor stimulation. In addition, NK1 receptor knockout mice will be employed. These animals are phenotypically normal but express no NK1 receptors at any sites throughout the body effectively blocking the action of SP.

1.5. Brief methodology

Our *Trypanosoma brucei brucei* mouse model will be used to induce meningoencephalitic responses with varying degrees of severity. Long-term experience of this model within the Department provides familiarity in handling and maintaining trypanosome infections and in the consistent induction of the desired degrees of inflammation. The techniques of immunocytochemistry and *in-situ* reverse transcriptase polymerase chain reaction will be employed to determine which cell types express cytokines and chemokines within the inflamed brain. Also, using these techniques, we will discover when the expression of these molecules is up-regulated during the infection. The reverse transcriptase polymerase chain reaction (RT-PCR) technique will be used to elucidate the kinetics of cytokine production in relation to the developing inflammatory reaction. Immunocytochemistry, using antibodies against $CD4^+$ and $CD8^+$ lymphocytes, B-cells and macrophages will be employed to follow the transmigration of these cells into the CNS. This will allow a comparison between the production of cytokines and chemokines and the appearance of leucocytes within the CNS. These parameters will also be investigated in infected animals treated with eflornithine in an effort to elucidate its mechanism of action. In addition, the CNS inflammatory response in mice treated with specific SP receptor antagonists and the neuroinflammatory reaction in transgenic mice that have no functional NK1 receptors will be examined.

CHAPTER 2

GENERAL MATERIALS AND METHODS

2.1. Introduction

In this Chapter the techniques that are used repeatedly throughout this thesis will be described. Any modification made to these methods for their application in specific situations, or procedures that are only employed for investigations in a single area of study will be detailed in the Materials and Methods section of the relevant Chapter.

2.2. Murine model of human African trypanosomiasis

The experimental animal model described below provides a valuable resource to investigate each stage analogous with trypanosome-infection in human patients, from the initial acute period to the development of the post-treatment reactive encephalopathy (PTRE) that can occur following melarsoprol administration. The use of this murine model to study the neuropathogenesis associated with trypanosome infections and to develop alternative drug strategies for the treatment of the disease is now well documented (Atouguia, Jennings, and Murray, 1995; Gichuki, Jennings, Kennedy, Sommer *et al.*, 1997; Jennings, 1993; Jennings *et al.*, 1997; Kennedy, 1999; Kennedy, Rodgers, Jennings, Murray *et al.*, 1997). This experimental murine model will be used throughout the following investigations as a means to further analyse the CNS inflammatory reaction and to elucidate the mode of action of the trypanostatic drug, eflornithine.

2.2.1. Trypanosomes

The trypanosome stabilates used in this study were developed in the Department of Veterinary Parasitology, University of Glasgow, under the auspices of Dr. Frank Jennings.

2.2.1.1. *Trypanosoma brucei brucei* GVR 35/C1.6

In 1966 *T.b.brucei* parasites were isolated from an infected wildebeest in the Serengeti National Park (Serengeti/66/SVRP/10) and subsequently transferred to the London School of Tropical Medicine and Hygiene. In 1977, a clone of this *T.b.brucei* stabilate (*T.brucei* LUMP 1001) was obtained by Dr. Frank Jennings, at Glasgow University. A new clone was grown from this stabilate by passage through sub-lethally irradiated mice. The

resulting parasites were designated GVR 35/C1 and maintained in liquid nitrogen. New working clones were prepared from this reserve stabilate as necessary. The current study employs parasites of the *T.b.brucei* stabilate GVR 35/C1.6.

2.2.2. Animals and infection regimens

Female CD1 mice weighing 28-35g were purchased from Charles River Breeding Laboratories. These mice were allowed to acclimatise to the animal house facilities at Garscube Parasitology Animal Unit for a period lasting at least two weeks before any experimental procedures were carried out. Throughout all treatment regimens the animals were housed in standard caging and provided with food pellets and water *ad libitum*.

2.2.2.1. Donor animals

To generate the quantity of parasites required to infect the number of mice necessary for each experiment, a small group of donor animals was inoculated with *Trypanosoma brucei brucei* GVR35/C1.6 prepared directly from the frozen stabilate. Each mouse was injected intraperitoneally (i.p.) with a total volume of 0.1ml phosphate buffered glucose saline (PBGS) pH8.0 [A1] containing $4x10^4$ trypanosomes. The level of parasitaemia in these mice was monitored by microscopic examination of fresh blood smears prepared from tail snips. When the parasitaemia reached the first parasitaemic peak (antilog 8.1) (Herbert & Lumsden, 1976) the mice were terminally anaesthetised and the blood collected by cardiac puncture. This blood was diluted in PBGS until an infective dose of approximately $2x10^4$ trypanosomes was contained in a volume of 0.1ml. This concentration equates to approximately two trypanosomes per microscopy field when examined at a magnification of 400 fold. The resulting solution was subsequently used to infect the experimental animals.

2.2.2.2. Mouse model experimental design

The standard experimental regimens that comprise the mouse model of HAT are outlined in Figure 2.1. The model is made up of three separate treatment schedules that allow us to simulate closely each of the four different stages of infection found in the human patient namely; acute infection, early CNS-stage, late CNS-stage and the PTRE.

[A1] The formulation for this solution is described in Appendix 1

Treatment Schedule 1

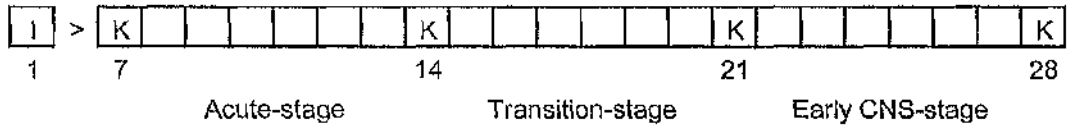

Treatment Schedule 2

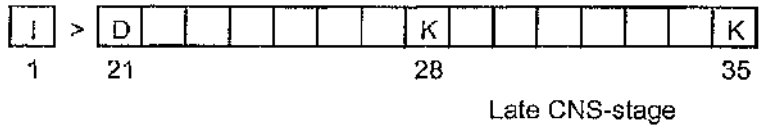

Treatment Schedule 3

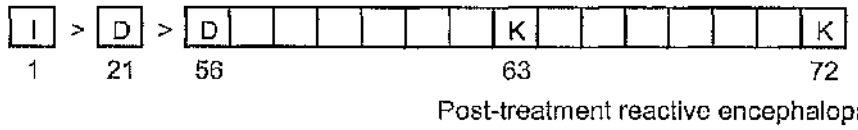

Figure 2.1. Schematic representation of the treatment regimens comprising the murine model of human African trypanosomiasis. In this model all mice will be infected (I) with $2x10^4$ *T.b.brucei* parasites of the cloned stabilate GVR35/C1.6. Animals will be administered diminazene aceturate (D) as indicated. The number of days post-infection and the stage of HAT simulated are detailed below the treatment regimens and the mice were killed (K) on the days indicated.

In all investigations control groups of uninfected mice that receive drug regimens identical to those given to the infected animals are included in the experimental design.

2.2.2.2.1. Acute infection

To mirror the acute-stage of trypanosome infection animals are injected with 0.1ml PBGS containing an infective dose of $2x10^4$ trypanosomes prepared and administered as described above. Following infection the parasites remain confined to the peripheral systems for approximately 14 days with no CNS involvement. Therefore animals killed at 7 and 14 days post-infection simulate the acute stage of HAT and show no obvious signs of CNS inflammation.

2.2.2.2.2. Early CNS-stage

If the disease is allowed to progress naturally the parasites invade the CNS between day 14 and day 21 after infection and the mice can survive for a period of approximately 30-days. Day 21 through to day 28 after infection mirror the early CNS stage of the disease and animals killed at these time points show only a very mild CNS-inflammatory reaction. This is characterised by a slight rise in the level of astrocyte activation and the presence of a few inflammatory cells in the meninges.

2.2.2.2.3. Late CNS-stage

The late-stage CNS condition can be induced in the mice by treating infected animals at day 21 post-infection, or later, with the trypanocidal drug diminazene aceturate. Diminazene aceturate is available as a commercial preparation from Hoechst AG under the trade name Berenil®. The compound is dissolved at a concentration of 9mg/ml in pyrogen free water and administered to the mice at a dose rate of 0.1ml/10g bodyweight i.p. As there is 445mg of diminazene aceturate per gram of Berenil® this results in a final dose of 40mg/kg bodyweight of the active principle. Although this is approximately ten times the recommended dose, the treatment is subcurative when it is administered on or after day 21 post-infection. Since the diminazene aceturate does not cross the blood-brain barrier (BBB) efficiently the trypanosomes out-with the CNS are killed and the mice become aparasitaemic, however, the parasites established within the CNS remain viable and the animals relapse to parasitaemia approximately 4 to 6 weeks after the initial drug treatment. If the mice are killed at 7 or 14 days following the trypanocidal therapy the neuropathology resembles that found in human patients that have died during late-stage CNS disease. The

neuroinflammatory response in these animals shows a moderate meningitis with lymphocytes and macrophages infiltrating the meninges and perivascular spaces. The inflammatory cell infiltration is accompanied by a diffuse astrocytosis. It is possible to manipulate the severity of the CNS inflammation in these animals by altering the timing of the trypanocidal treatment. When the diminazene aceturate treatment is delayed beyond day 21 post-infection a corresponding increase the degree of the inflammatory reaction is seen in the CNS of the infected mice. In addition to meningitis and astrocytosis, animals given diminazene aceturate at a delayed date exhibit a mild encephalitis with inflammatory cells present in the parenchyma.

2.2.2.2.4. Post-treatment reactive encephalopathy

The inflammatory pattern found in cases of the post-treatment reactive encephalopathy (PTRE) can be simulated by subcuratively treating the *T.b.brucei*-infected mice with diminazene aceturate on day 21 post-infection as before. This treatment clears the peripheral systems of trypanosomes, however the aparasiteamia is transitory and the animals eventually relapse. When relapse occurs, usually between 4 and 6 weeks following the initial diminazene aceturate treatment, the mice are given a second trypanocidal treatment. This exacerbates the CNS pathology and animals killed 7 and 14-days after the second diminazene aceturate treatment exhibit an extremely severe inflammatory response within the CNS that closely resembles the pathology found in human patients who have died of the PTRE. The meningoencephalitis generated in these mice is distinguished by the presence of numerous lymphocytes, plasma cells and macrophages in the brain parenchyma, meninges and perivascular spaces. A marked astrocytosis is also associated with this neuroinflammatory reaction.

2.2.3. Tissue Harvesting

At the scheduled termination points of the experiment the mice were killed and the brains extracted for subsequent analysis. Tissue was prepared for histological assessment, including both grading of the severity of the neuroinflammatory reaction and immunocytochemistry. In addition material was extracted for RT-PCR analyses, to assess the levels of cytokine transcription. To carry out this procedure the mice were deeply anaesthetised with fluorothane and exsanguinated by cardiac puncture. To remove any residual blood from the brain tissue the animals were perfused via the left ventricle of the heart with approximately 150ml of physiological saline. Following perfusion the brains

were carefully removed from the skull and prepared for further analyses. To help prevent artefacts the brains were not dissected and divided among the different analysis techniques, instead a whole brain was used for each of the subsequent examinations.

2.2.3.1. Sample preparation for histological assessment

The tissue required to determine the severity of the inflammatory reaction induced by each treatment regimen was fixed in 4% neutral buffered formalin before processing to paraffin blocks. From these blocks, brain sections each of 3μm thickness, were prepared. One section from each block was stained with haematoxylin and eosin (H&E) to assess the severity of the inflammatory reaction. Additional sections were stained using immunocytochemistry techniques to determine the degree of astrocytosis. The processing procedure required for the preparation of paraffin embedded tissue damages certain cell surface markers therefore samples were also taken for the preparation of frozen sections. To prevent the tissue from developing ice crystal artefact during the freezing procedure the brains were placed into PBS containing 30% sucrose and stored overnight at 4^0C. Following cryoprotection, the blocks were embedded in OCT, snap frozen in liquid nitrogen and stored at -70^0C until required. A cryostat as used to prepare 10μm thick sections from these frozen blocks. The sections were air dried, fixed in cold acetone for 10 minutes and stored at -20^0C until required for staining.

2.2.3.2. Sample preparation for RT-PCR analyses

Following dissection the brain samples required for RT-PCR analyses were homogenised in 5ml of denaturing solution[AI] by gentle trituration through a 20 gauge hypodermic needle. Once homogenised the samples were aliquoted into diethyl pyrocrbonate (DEPC) treated 1.5ml eppendorf tubes and stored at -20^0C until required. The precautions necessary for handling tissues for subsequent RNA extraction, including the significance of DEPC treatment, are discussed in more detail in Chapter 2, section 2.5 'Ribonucleic acid purification and quantification'.

[AI] The formulation for this solution is described in Appendix I

2.3. Neuropathological assessment

Formalin fixed paraffin sections were stained with the standard histological H&E staining method. This is a popular staining method due to its simplicity and its ability to clearly demonstrate a wide variety of different tissue structures in an array of tissue types. Essentially the haematoxylin component stains the cell nuclei blue, with good intra-nuclear detail. The eosin constituent of the technique stains the cell cytoplasm and most of the connective tissue in varying shades and intensities of pink, orange and red. Brain sections stained in this manner were used to assess the degree of severity of the CNS inflammatory reaction following trypanosome infection and induction of the PTRE.

The sections were examined under light microscopy using a magnification of 200 fold. The severity of the meningitis, the occurrence and extent of perivascular cuffing and the degree of inflammatory cell infiltration of the brain parenchyma were utilised to compile a standardised grading scale to define the severity of the CNS inflammatory reaction. The criteria defining each neuropathological grade are described in Table 2.1. In this scale a score of 0 was assigned to sections showing a normal histopathology with no infiltration of inflammatory cells. Mice displaying signs of a mild meningitis with a few inflammatory cells present in the meninges but no perivascular cuffing were graded as 1, while animals with a moderate meningitis and cuffing of some of the vessels were assigned grade 2. As the response worsened the severity of the meningitis increased further and perivascular cuffs became prominent, there was also mild infiltration of the neuropil by some inflammatory cells. Animals displaying this level of inflammation were assigned a neuropathological score of 3. A grading score of 4 was reserved for animals displaying severe meningitis, prominent perivascular cuffs and a severe encephalitis with the presence of many inflammatory cells in the neuropil. Each section was graded independently by two assessors in a blinded fashion.

2.4. Immunocytochemistry

Immunocytochemistry (ICC) is an established staining technique employed in routine diagnostic histopathology to demonstrate specific cellular or tissue components in tissue sections through the use of antigen-antibody interactions. The method relies on the availability of antibodies that will specifically bind with a particular tissue antigen of interest and their subsequent visualisation. The method can be used in a number of different formats and can be adapted for light microscopy, fluorescent microscopy and

	0	1	2	3	4
Meningitis	None	Mild	Moderate	Severe	Severe
Perivascular cuffing	None	None	Mild cuffing of some vessels	Prominent cuffing of some vessels	Prominent cuffing of most vessels
Encephalitis as defined by cellular activity in the neuropil	None	None	None	Moderate	Severe

Table 2.1. Neuropathological grading scale. This table details the criteria that define the neuropathological grading score associated with specific levels of the CNS inflammatory reaction. The severity scores are given horizontally along the top of the table; the parameters defining the specific score are shown vertically.

electron microscopy (Polak and Van Noorden, 1986). This study will employ ICC to stain specific cellular markers in both paraffin and frozen sections.

2.4.1. Immunocytochemistry staining procedure

A similar fundamental protocol was employed in ICC throughout this study a schematic representation of the complete protocol is shown in Figure 2.2. Details of the antibodies used together with their optimal concentrations and their suitability for use on paraffin or frozen sections are given in Table 2.2.

In cases where paraffin embedded material was used the tissue sections were dewaxed and rehydrated before the staining procedure was performed. The wax was removed from the sections by placing the slides into 3 changes of xylene, each lasting for 5 minutes. Since xylene is not miscible with water the slides were then rehydrated by cycling them through graded alcohols at concentrations of 100%, 90% and 70% ethanol. Again, the slides were allowed to remain in each concentration of ethanol for a 5 minute period. From here the slides were placed into running tap water for 5 minutes to complete the rehydration process.

Both frozen and paraffin embedded tissue sections contain endogenous peroxidase enzymes that can produce false positive results at the end of the staining procedure. To quench this activity the sections were placed into 0.5% hydrogen peroxide (H_2O_2) in phosphate buffered saline [A1] (PBS) for 30 minutes and then rinsed in running tap water (Van Noorden, 1986). This step is only required if peroxidase is to be employed as the enzyme label at the end of the procedure and can be omitted if alkaline phosphatase is to be used. The slides were then wiped carefully with paper towel allowing a 3mm gap around the sections and placed into the humidity chamber. Certain tissues including collagen and reticulin, or areas of high inflammation or necrosis, show an apparent affinity for the immunoglobins used in the ICC staining sequence. To overcome this non-specific reaction approximately 300µl of 5% bovine serum albumen (BSA) in PBS was placed over the section and allowed to react for 30 minutes at room temperature. The antibodies present in the BSA 'block' sites on the tissue section that could interact non-specifically with immunoglobins, perhaps through the Fc portion of the molecule. This step in the process substantially reduces background staining resulting from non-specific binding.

[A1] The formulation for this solution is detailed in appendix 1

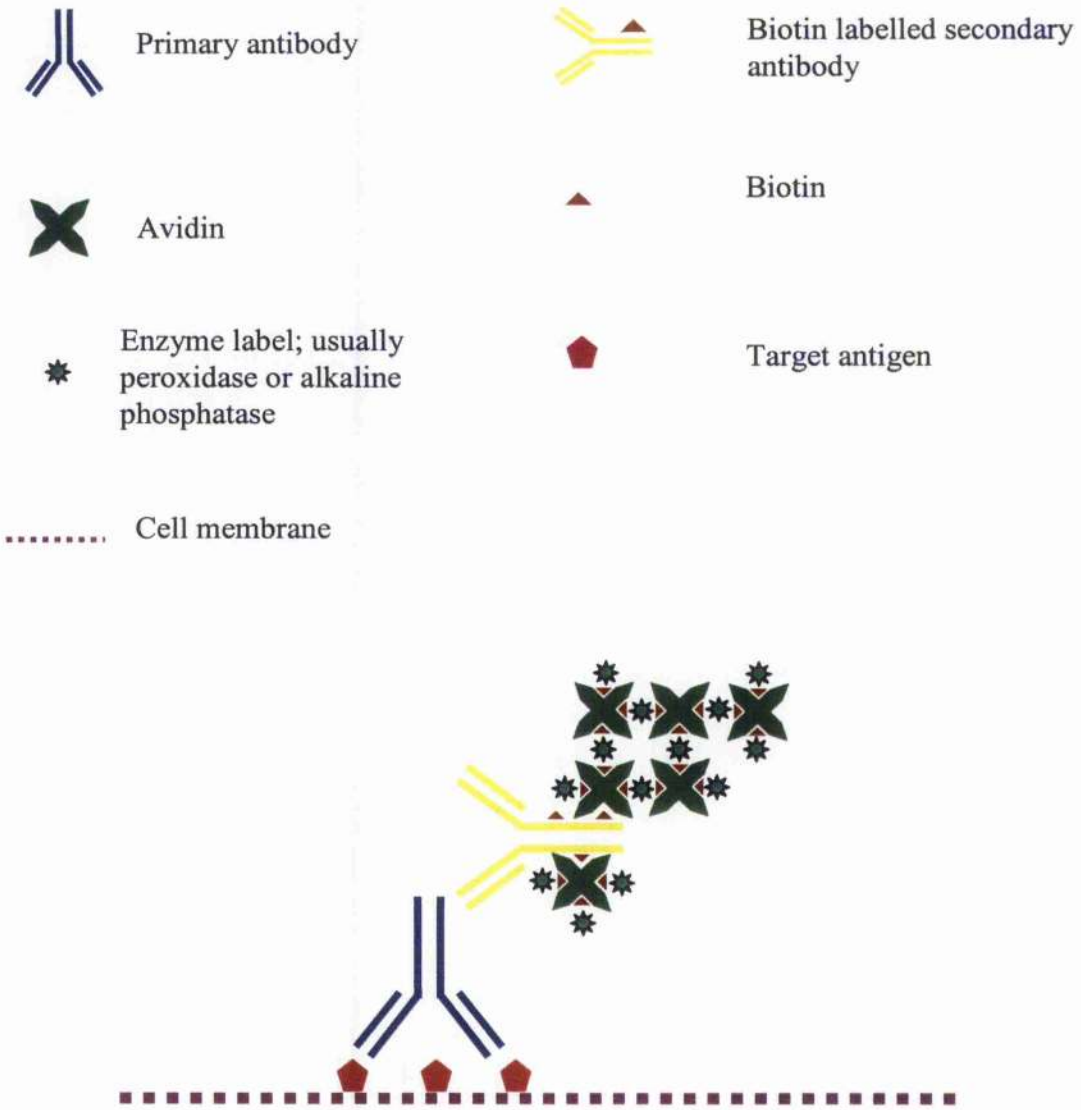

Figure 2.2. Schematic representation of the immunohistochemistry technique.

The primary antibody binds with the antigen target in the tissue section. A secondary, biotinylated antibody, that binds to the primary immunoglobin molecule, is then added. Finally, the ABC -enzyme complex binds to the biotin label on the secondary antibody. The enzyme label subsequently determines the areas of antibody binding to the section through the use of a substrate solution that produces a coloured reaction product.

Primary Antibody	Target cell	Host Species	Source	Section Type	Dilution	Secondary antibody
B220	B-cells	Rat	Serotec	Paraffin/Frozen	1:1000	Rabbit anti-Rat IgG
CD3	T-cells	Rat	DAKO	Paraffin	1:20	Rabbit anti-Rat IgG
CD4	T-helper cells	Rat	Pharmingen	Frozen	1:40	Rabbit anti-Rat IgG
CD8	T-cytotoxic cells	Rat	Pharmingen	Frozen	1:40	Rabbit anti-Rat IgG
F4/80	Macrophages	Rat	Serotec	Paraffin/Frozen	1:40	Rabbit anti-Rat IgG
FA11	Microglia/Macrophages	Rat	Gifted	Frozen	1:20	Rabbit anti-Rat IgG
GFAP	Astrocytes	Rabbit	DAKO	Paraffin	1:500	Goat anti-Rabbit IgG

Table 2.2. Antibodies employed for immunohistochemical analyses. The listed antibodies were used to demonstrate particular cell types or markers in tissue sections. The antibody specificities are given together with the source of the reagent. Antibodies listed as 'gifted' were kindly donated by Dr. Alun Williams, Department of Pathology, University of Glasgow Veterinary School. Optimal dilutions for use of the primary antibody are detailed together with the optimal tissue processing procedure. All secondary antibodies were biotinylated, used at a dilution of 1:200 and purchased from Vector® Laboratories, Peterborough, UK.

During this blocking period the primary antibody was prepared by making the appropriate dilution in 2% BSA in PBS. Depending on the surface area to be covered, 100-200µl of diluted antibody solution was allowed for each section. After 30 minutes the blocker was drained from the section and the excess fluid wiped from the slides as before. The primary antibody was then applied to the sections using a glass pipette. To allow an even spread of the solution across the section the tip of the pipette was held roughly 5cm above the section and the antibody applied in a drop-wise manner. The sections were then transferred to 4^0C overnight or incubated for 60-90 minutes at room temperature.

Following this incubation the sections were washed for 10 minutes in PBS to remove the primary antibody. This washing procedure was then repeated twice more using fresh PBS. During the washing steps the biotinylated secondary antibody was diluted to the appropriate concentration in 2% BSA in PBS and applied as previously described after the final wash. The secondary antibody was allowed to react with the section for 60-90 minutes at room temperature. While the sections were incubating the ABC (Avidin Biotin Complex) reagent was prepared by making a 1:50 dilution of reagents A and B in PBS (*i.e.* 1µl A + 1µl B + 48µl PBS). Either an ABC-peroxidase kit or an ABC-alkaline phosphatase kit (Vecastain® Elite® ABC kit, Vecatastain® ABC-AP kit, Vector Laboratories Inc., Peterborough, UK.) was employed at this step in the procedure. To form the mature ABC reagent, the mixture was allowed to complex for 45 minutes at room temperature. Again 100-200µl of reagent were allowed for each section.

After incubation with the secondary antibody the sections were washed in 3 changes of PBS, each wash lasting for 10 minutes as before. The ABC reagent was applied to the sections following the wash procedure and incubated at room temperature for 60 minutes. The sections were then washed in 3 changes PBS before carrying out the visualisation procedure.

2.4.1.1. Detection of horseradish peroxidase labels

Diaminobenzidene tetrahydrochloride (Sigma-Aldrich) is employed to visualise the location of peroxidase enzyme labels in tissue sections (Van Noorden, 1986). DAB is a suspected carcinogen, therefore precautions must be taken to prevent contamination of the laboratory and personnel. Double gloves should be worn at all times during procedures involving the use of DAB and the chemical should only be handled in a fume cupboard. The DAB was purchased in powder form as a 5g vial. A stock solution of DAB was

prepared from this vial to avoid the inhalation risks associated with repeated weighing of the powder form of the chemical. To aid dissolution of the powder, 5ml of dimethyl formamide were initially added to the contents of the vial. Following this, 0.05M tris-buffered saline (TBS) pH7.4[A1] was gradually added to the mixture to a total volume of 50ml. The original container does not hold a 50ml volume, therefore, when approximately 30ml of TBS had been added the solution was decanted carefully into a 50ml measuring cylinder and the remaining buffer added. To allow the powder to dissolve completely the mixture was left overnight on a magnetic stirrer in the fume cupboard. The stock solution was divided into 1ml aliquots and stored at -20^0C until required.

The final substrate solution was prepared by placing 225ml 0.05M TBS and 25ml 0.1M imidazole in 0.05M TBS into a 300ml staining dish. The presence of the imidazole helps to intensify the colour of the DAB reaction (Van Noorden, 1986). The 1ml aliquot of DAB and 125µl of 30% H_2O_2 were added to the solution immediately before use giving final concentration of 0.4mg/ml and 0.015% respectively. Following the final washes the sections were placed into this substrate solution for 5 minutes and allowed to react. In this procedure it is the H_2O_2 that is the substrate for the peroxidase enzyme rather that the DAB itself. In the presence of an electron donor such as DAB, the peroxidase enzyme will reduce the H_2O_2 to water and atomic oxygen and oxidise the DAB producing an insoluble brown end product that can be detected on the section when examined under the microscope. After 5 minutes in this solution the sections were carefully removed and allowed to rinse in running tap water for 5 minutes. The sections were then counter-stained with haematoxylin, dehydrated through graded alcohols and cleared through 3 changes of xylene. Finally, glass coverslips were mounted onto the sections using Histomount mounting media.

It is necessary to decontaminate the fume cupboard and inactivate the remaining DAB solution before discarding it to the drain. This was carried out by swabbing the work area with a weak solution of sodium hypochlorite solution. As the hypochlorite solution is corrosive and will corrode the metal casing of the fume cupboard it was necessary to repeat this swabbing procedure using tap water. Approximately 20ml of sodium hypochlorite was then added to the DAB solution and the solution left to stand for around 60 minutes to allow complete decativation of the DAB. After this time the inactivated DAB disposed of to the fume cupboard drain followed by 20ml of diluted hypochlorite solution and copious amounts of water. The staining dish used to hold the DAB solution was left to steep in

[A1] The formulation of this solution is detailed in appendix 1

detergent overnight and thoroughly rinsed before being placed into the general glass washing facilities.

2.4.1.2. Detection of alkaline phosphatase labels

A commercially produced Vector® Red substrate kit (Vector® Red Alkaline Phosphatase Substrate Kit I, Vector Laboratories Inc. Peterborough, UK) was used to detected alkaline phospahtase labelled ABC reagents. This substrate kit produces an intense red reaction product in the presence of alkaline phosphatase. The product is insoluble in alcohol and xylene and can therefore be permanently mounted in histomount. The substrate solution was prepared according to the manufacturer's instructions. Two drops of reagent 1 were added to 5ml of 100mM Tris-HCl, pH8.2-8.5[A1] and mixed thoroughly. This was followed by 2 drops of reagent 2 and then 2 drops of reagent 3. The solution was mixed thoroughly following each addition of reagent. In addition, 5µl of 1M levamisole was added to the substrate solution giving final concentration of 10mM. This inhibits any endogenous alkaline phosphatase activity but does not affect the calf intestine alkaline phosphatase used as the reporter on the ABC reagent (Van Noorden, 1986).

Following the final washing steps the substrate solution was applied to the sections and allowed to react for 20-30 minutes. Since the solution shows some light sensitivity the incubation was carried out in the dark. The slides were washed in PBS, counter-stained with haematoxylin, dehydrated through graded alcohols, cleared in xylene and permanently mounted using histomount.

2.5. Ribonucleic acid purification and quantification

2.5.1. Sample handling strategy

Ribonucleic acid (RNA) is an extremely labile molecule that can be easily degraded during experimental manipulations. Therefore, several precautions were taken when handling samples for subsequent RNA extraction. Ribonuclease (RNase), an enzyme that is present on the surface of the skin, is the major factor contributing to this unwanted breakdown of

[A1] The formulation of this solution is detailed in appendix 1

RNA. To prevent contamination of equipment or samples with RNase, the following procedures were observed;

- disposable gloves were worn at all times throughout procedures involving RNA manipulation.

- all micro-centrifuge tubes were submerged in a 0.1% di-ethyl-pyro-carbonate (DEPC) solution, to denature any RNase that may be present, for at least two hours at room temperature followed by autoclaving

- commercially available RNase free disposable filter tips were used during pipetting stages

- samples were immediately placed into denaturing solution[A1], this contains guanidium thiocyanate which lyses the cells and denatures any RNase

- samples and solutions were kept at 4^0C prior to long-term storage of the samples at -20^0C.

2.5.2. Sample preparation

The messenger RNA (mRNA) profiles of various cytokines, chemokines and adhesion molecules, within the murine CNS following various treatment regimens, were investigated. At sacrifice the animals were perfused with approximately 150ml of sterile 0.9% saline by cardiac perfusion via the left ventricle, to remove any peripheral blood from the brain tissue. Each brain was carefully dissected from the skull and homogenised in 5ml of denaturing solution by several triturations through a sterile 20-gauge needle. The resulting homogenate was aliquoted into DEPC-treated 1.5ml micro-centrifuge tubes and stored at -20^0C until required.

2.5.3. RNA extraction

Total RNA was extracted from brain tissue using a modified acid guanidium-thiocyanate phenol chloroform (AGPC) method (Chomczynski and Sacchi, 1987). The RNA was extracted from a total of 1ml of whole brain tissue / denaturing solution homogenate. Two

[A1] The formulation for this solution is describe in Appendix 1

500µl aliquots of the homogenate were placed into 1.5ml micro-centrifuge tubes. 50µl of 2M sodium acetate, pH 4.0[A1], 500µl of 0.1M citrate buffer saturated phenol (pH 4.3) (Sigma) and 100µl of chloroform : isoamyl-alcohol (49:1) were added sequentially to each tube. Chloroform used in conjunction with phenol improves the efficiency of the nucleic acid extraction. Chloroform helps both to denature the protein and to remove lipid. Also, because of its high density, chloroform assists in the separation of the organic and aqueous portions of the mixture. Isoamyl-alcohol is added to the solution to help to prevent foaming of the mixture. The acid pH is an important factor in the success of this method as RNA remains water soluble in a solution containing 4M guanidium-thiocyanate at pH 4. Under these acid conditions most proteins and fragments of DNA separate into the organic phase of the mixture. This acidic environment is maintained by the presence of the sodium acetate pH 4 and the citrate buffer pH 4.3 used to saturate the phenol (Ausubel, Brent, Kingston, Moore, Seidman, and Smith, 1987)

After vortexing thoroughly the samples were incubated on ice for 15 minutes. Following this incubation the tubes were centrifuged at 12,000g for 20 minutes at 4^0C to separate the aqueous and organic phases. The aqueous upper phase, containing the RNA, was then transferred to fresh 1.5ml micro-centrifuge tubes. The flocculent interphase and lower organic phase containing the proteinaceous material was discarded. The RNA was initially precipitated from the solution by the addition of 1ml of cold isopropanol and subsequent incubation at -70^0C for 1 hour. The samples were then centrifuged as before, the supernatant was discarded and the resulting pellet resuspended in 150µl of denaturing solution. At this point the RNA-denaturing solution mixture resulting from the two original 500µl aliquots were amalgamated into a single tube and precipitated with 2 volumes of cold ethanol. Following another incubation at -70^0C for 1 hour the samples were centrifuged at 12,000g for 20 minutes at 4^0C as previously described. After centrifugation the pellet was resuspended in 1ml of 70% ethanol. The sample was then centrifuged as before and the 70% ethanol wash procedure repeated. Following this final wash step the ethanol was carefully discarded and the tube covered with perforated parafilm. The sample was allowed to stand at room temperature for approximately 1 hour to permit the evaporation of any residual ethanol. However, the newly extracted RNA was not allowed to dry out completely as this greatly decreases its solubility. When the pellet appeared 'dry' the RNA was dissolved in 60µl of DEPC-treated sterile water. If necessary the sample was incubated at 55^0C for 20-30 minutes to aid dissolution of the RNA. The sample was then stored at -20^0C until required.

2.5.4. RNA quantification

The concentration of the extracted RNA was calculated by measuring the optical density of a 1 in 100 dilution of the original sample. This was prepared by the addition of 1µl of the sample to 99µl of sterile water. The sample was placed in a quartz microcuvette and the optical density assessed. The spectrophotometer was zeroed using water as a blank. The optical density of the sample was then measured at both 260nm (OD_{260}) and 280nm (OD_{280}) wavelengths. The purity of the RNA sample was evaluated by calculating the OD_{260}/OD_{280} ratio. Pure RNA yields a ratio of 2.0 therefore a ratio of 1.7 or higher was considered to be of an acceptable purity to allow further analyses. The concentration of the RNA, expressed in µg/ml, was calculated by multiplying the OD_{260} by 40 and correcting for the dilution factor. This information was used to prepare a 1µg/µl RNA solution by dilution of the original sample with DEPC water as appropriate.

2.6. Reverse-Transcriptase Polymerase-Chain Reaction

The reverse-transcriptase polymerase-chain reaction (RT-PCR) procedure combines the technique of 'reverse-transcription' with the amplification of specific DNA sequences via the 'polymerase-chain reaction' (PCR). The expression of genes within tissues can be followed using this procedure since it allows the production of individual mRNAs to be detected in a sensitive and specific manner under virtually all conditions.

2.6.1. Reverse-transcription

Under normal circumstances in the cell when a gene is expressed, DNA is transcribed into RNA and the RNA is translated into protein. Reverse transcriptase, an enzyme that is present in retroviruses, facilitates the synthesis of a complementary DNA (cDNA) molecule from an RNA template, the 'reverse' of the process found in the normal cell cycle.

Before an extracted RNA sample can be amplified by PCR it has to be transcribed into a cDNA molecule. This step is carried out by the reverse-transcriptase enzyme described above and requires the presence of the RNA sample, dNTPs, and primers. Reverse-transcriptase is a RNA-dependent DNA polymerase that recognises single stranded RNA

as a template. The enzyme elongates primers bound to the template by incorporation of dNTPs to synthesise the new cDNA strand. The primers can be of a specific sequence that will anneal to a particular region of the RNA molecule, oligo(dT) that will anneal to the 3'-poly-adenylated tail of mRNA or random primers. Random primers are short oligonucleotides, typical hexamers, which anneal randomly to the RNA molecule providing multiple sites to 'prime' the start of the reverse transcription process. This non-specific priming reaction results in the conversion of the entire population of RNA into cDNA. The resulting cDNA can then be amplified with any specific PCR primers of interest allowing numerous different assays to be performed from only one reverse transcriptase reaction. If a specific primer is used the cDNA generated will only be of use in one particular PCR analysis.

2.6.2. PCR background information

The PCR technique was invented by Mullis and colleagues at the Cetus Corporation (Mullis and Faloona, 1987) although the principles behind the procedure had been described over a decade earlier (Kleppe, Ohtsuka, Kleppe, Molineux *et al.*, 1971; Panet and Khorana, 1974). PCR allows the rapid *in vitro* amplification of specific DNA sequences through the use of primers that bind specifically to individual sequences on a DNA molecule and the subsequent extension of those primers to form new molecules of DNA that are complementary to the original strand. Amplifying the number of copies of a specific DNA species of interest allows the molecule to be easily detected or purified for use in further studies.

The theoretical basis of PCR is represented schematically in Figure 2.3. The template or sample DNA must be free from chemicals that would inhibit the reaction such as detergent, EDTA or phenol and the integrity of the molecule must be intact over the length of the sequence to be amplified with no nicks or breaks in the sequence.

The main requirements for the PCR are; dNTPs, the DNA polymerase enzyme, specific primers, a DNA template (*i.e.* the sample under test) and a reaction buffer containing magnesium ions. The dNTPs provide both the energy and the nucleosides for the production of the new DNA molecule and are supplied in excess. This allows the synthesis step to be repeated as necessary without the exhaustion of the dNTPs limiting the amplification reaction. A DNA-dependent DNA polymerase enzyme carries out the synthesis of the new DNA molecule. In PCR the most commonly used DNA polymerase

is *Taq* polymerase, isolated from the bacteria *Thermus aquaticus*. These bacteria are extreme thermophiles and thrive in high temperature environments. The enzyme therefore has the advantage of being heat stable and its activity is not reduced by the temperature cycling procedures necessary during the PCR. The magnesium ion concentration in the reaction buffer affects the performance of the *Taq* polymerase. In the absence of free magnesium ions the enzyme is inactive and conversely excess magnesium reduces the fidelity of the *Taq* polymerase. The optimum magnesium concentration should therefore be determined for each PCR reaction. The primers are generally designed as oligonucleotides ranging from 18-30 bases in length. Two different primers are used in each individual PCR reaction and again these are provided in excess. The nucleotide sequences of the primers are complementary to specific regions on each strand of the DNA molecule, one primer per strand, lying at a known distance apart. Each primer directs the synthesis of the new cDNA molecule, in the 5' to 3' direction, by the DNA polymerase enzyme. The end result is the *de novo* synthesis of the DNA flanked by the two primers.

2.6.3. PCR cycling parameters

To perform the PCR reaction a master mix, containing the components described above, together with the DNA sample must be subjected to a number of optimised temperature cycles. Each step in the cycle requires a minimum amount of time to be effective, however too long a period at each stage is not only a waste of time but also can be deleterious to the overall PCR. These cycles comprise a denaturation step, an annealing stage and an extension stage. Each of the steps in the reaction is critical to the success of the technique. During the denaturation period the sample is heated to 94^0C, this results in the separation of the double stranded DNA in the sample into single stranded DNA (ssDNA) molecules. Following this denaturation the primers can anneal to the ssDNA. The optimal temperature for this step varies with the G-C content of the primers used. Primers with a low G-C content (<50%) may require relatively low annealing temperatures of 55^0C or below whereas primers with a high G-C content will require a higher annealing temperature. Once the primers have attached to the template the new strand of DNA can be synthesised. This is carried out during the extension segment of the cycle. The prime temperature for this step in the reaction, when employing *Taq* polymerase, is 72^0C. This is close to the optimal temperature for the enzyme (75^0C) but is not so hot that the primers become detached from the template DNA.

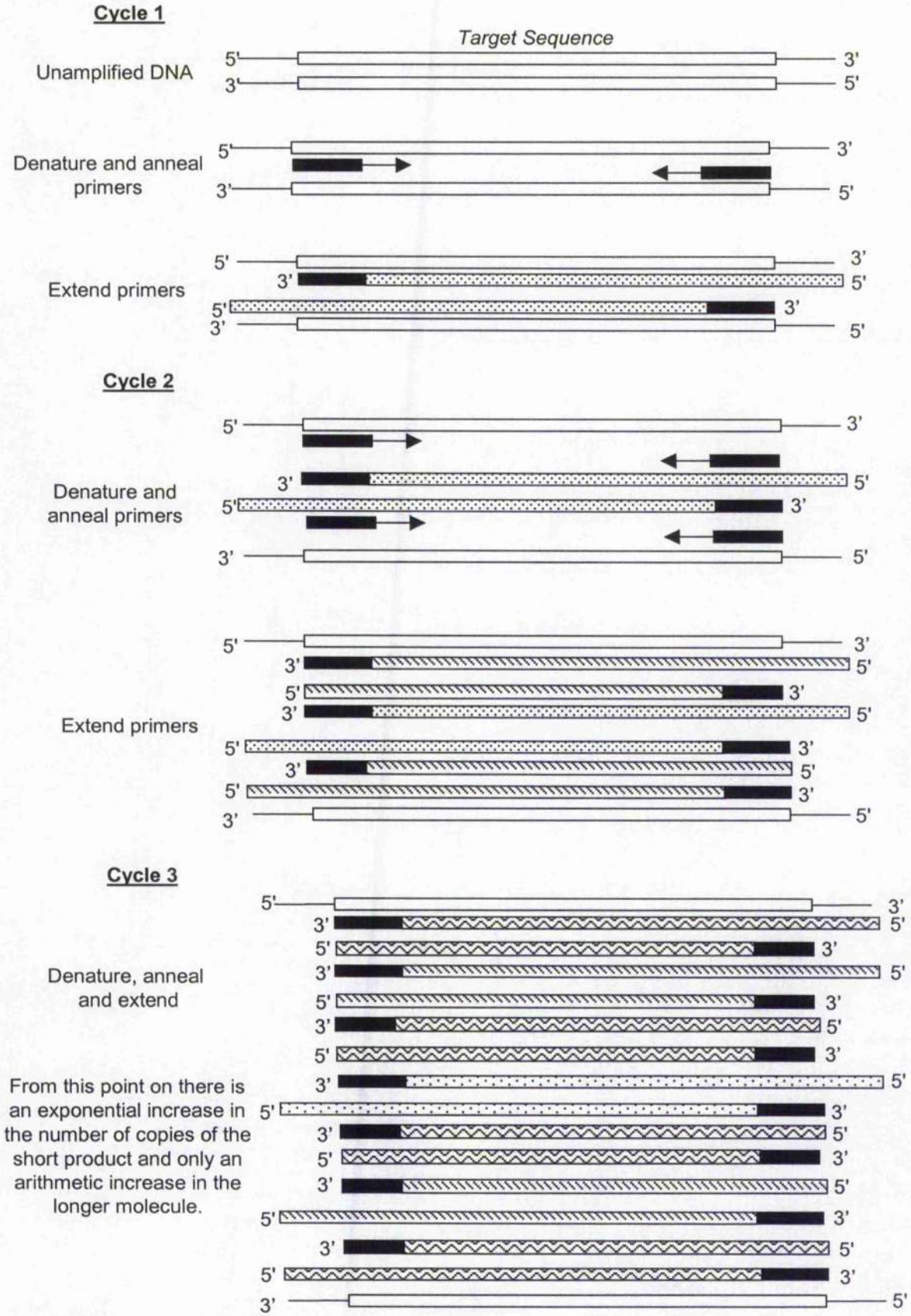

Figure 2.3. The polymerase chain reaction.

A schematic representation of the amplification pattern that occurs during the polymerase chain reaction resulting in the accumulation of a double stranded DNA molecule of a discrete size.

Many PCR protocols include lengthened initial denaturation and final extension periods. The increased initial denaturation stage ensures that there is no secondary structure in the DNA molecule and ensures the complete separation of the two strands. Whereas the lengthened extension step attempts to produce final PCR products that are as complete as possible, with no bases missing from the ends.

2.6.4. Amplification pattern

During the initial round of synthesis the new DNA molecules produced are of intermediate length and like the parental strands can hybridise to the primers (Figure 2.3). These intermediate length molecules accumulate at an arithmetic rate during the subsequent cycles of denaturation, annealing to the primers and synthesis of new DNA. However, when these new molecules of DNA are used as the templates in the subsequent rounds of the PCR the DNA produced is of a discrete size. The formation of this discrete product occurs because the starting point for the synthesis of each of the new DNA strands has been determined by position of the primer on the original DNA and therefore no template exists beyond the 5' end of the primer. The amount of the discrete product synthesised doubles with each subsequent round of cycling and accumulates exponentially. A PCR comprising of 30 cycles should therefore result in a 270 million fold amplification of the target DNA (Ausubel *et al.*, 1987).

2.6.5. Performance of the RT-PCR

By using RT-PCR the expression of various cytokines, chemokines and receptor molecules including; TNF-α, IL-1α, IL-6, MIP-1α, MCP-1, and RANTES was investigated in the murine CNS following diverse treatment regimens.

The cDNA template to be used in the subsequent PCR was synthesised by reverse transcription of 5μg of total RNA prepared from each brain sample. The reaction was performed in a 50μl reaction total volume containing 1x 1st strand buffer (50mM Tris/HCl, pH 8.3; 75mM KCl; 3mM $MgCl_2$) (Gibco BRL), 10mM dithiothreitol (DTT), 1.25mM deoxynucleoside triphosphates (dNTPs) (Hybaid), 25U RNase inhibitor (Hybaid), 100U Moloney-murine leukemia virus reverse-transcriptase (M-MLV-RT) (Gibco BRL) and 1μg random primers (Gibco BRL).

To carry out the reverse transcriptase reaction a 5µg aliquot (5µl of a 5µg/µl stock solution) of total RNA was placed into a 200µl thin walled PCR tube and heated to 65^0C for 5mins on the PCR thermo-cycler. This procedure helps to remove any secondary structure present in the RNA molecule and aids the subsequent reverse transcription reaction. To prevent the RNA from refolding the tube was immediately transferred to ice and 45µl of the reverse transcriptase master mix, as detailed above, was added to the sample. The tube was then returned to the thermo-cycler and incubated for 30mins at 37^0C followed by a 60 minute incubation at 42^0C. After this the temperature was raised to 94^0C for 5mins to denature the M-MLV enzyme and stop the reaction. The cDNA was then stored at -20^0C until required for PCR analyses.

The PCR reaction was performed in a 50µl total reaction volume containing; 1x reaction buffer (20mM Tris/HCl, pH 8.55; 16mM $(NH_4)_2SO_4$; 1.5mM $MgCl_2$) (Hybaid-AGS), 0.5µg 3'primer, 0.5µg 5'primer , 2 units *Taq* polymerase and 2.5µl of cDNA sample from the reverse-transcriptase reaction. No additional dNTPs were required in the reaction mix as these were already present in the cDNA aliquot. All PCR primers were commercially synthesised by MWG-biotech Ltd. The sequences and expected product sizes are detailed in Table 2.3. Each primer pair was designed so that the 5' and 3' primers would anneal to different exons in the target mRNA. This type of primer design allows the amplification of mRNA to be easily distinguished from possible amplification of contaminating DNA. The PCR products from amplification of DNA would contain the sequence information corresponding to the intron segment of the gene. Since this information is omitted from the mRNA molecule any products resulting from DNA amplification would be significantly larger those resulting from mRNA amplification.

The samples were placed in a Perkin Elmer thermo-cycler and heated to 94^0C for 5 mins as an initial denaturation step. The PCR was performed by denaturing the samples for 15 seconds at 94^0C, allowing the primers to anneal for 30 seconds at 60^0C and an extension step of 90 seconds at 72^0C to synthesise the new DNA strand. The samples were subjected to 35 cycles* of this heating and cooling procedure followed by a lengthened final extension step of 10 mins at 72^0C to allow completion of the synthesis reaction. On culmination of the thermo-cycling procedure the samples were removed from the PCR block and maintained at 4^0C until the products were analysed.

* Actin PCR was repeated for 30 cycles only

2.6.6. PCR controls

Before the RT-PCR technique can be used to investigate the expression of any genes the integrity of the cDNA produced must be checked. To do this each sample was analysed for the presence of the housekeeping gene, β-actin. Housekeeping genes are expressed by all tissues at all times at low levels and should yield positive PCR results in all samples. They can therefore be used to determine whether the sample is of sufficient quality to under go the PCR. A negative β-actin PCR would indicate that the initial RNA was not adequately extracted and should not be used in subsequent PCR analyses.

Due to the highly sensitive nature of the PCR the inclusion of negative and positive controls is essential to the technique. In each PCR experiment one known positive sample and one negative control, that contains all the components of the PCR reaction with the exception of the template DNA, were included with the test samples. These controls demonstrate respectively that the PCR is functioning satisfactorily and that no contamination of the samples by extraneous material has occurred.

2.6.7. Analysis of RT-PCR products

The RT-PCR products are double stranded DNA molecules of a discrete length defined by the position of the primers. These molecules can be separated according to their size by electrophoresis through a 2% agarose gel. As DNA molecules have a slight overall negative charge they migrate through the agarose towards the positive electrode. The rate of passage through the agarose is primarily determined by their molecular weight with the smaller molecules travelling more quickly through the gel than the larger heavier molecules. The products can be visualised in the gel by the addition of ethidium bromide, a dye that intercalates between the DNA strands and fluoresces under ultraviolet illumination. The ethidium bromide can be added to the molten gel at a final concentration of 1μg/ml or the gel can be stained following the electrophoresis by the addition of the ethidium bromide to the buffer. Ethidium bromide is a known carcinogen therefore great care was taken when preparing the working solution. To avoid having to weigh the powder 100mg vials of the dye were purchased and 10ml of distilled H_2O added to give a 10mg/ml working solution.

To allow the size of the PCR products to be calculated a 100bp DNA molecular weight ladder (Gibco BRL) was added to the first lane in each gel. This ladder comprises 15

Primer target	Nucleic acid sequence	Band Size
3' β-actin*	CTC TTT GAT GTC ACG CAC GAT TTC	540bp
5' β-actin*	GTG GGC CGC TCT AGG CAC CAA	
3' IL-1α*	AGG TCG GTC TCA CTA CCT GTG ATG AGT TTT GG	491bp
5' IL-1α*	AAG ATG TCC AAC TTC ACC TTC AAG GAG AGC CG	
3' IL-6*	CAC TAG GTT TGC CGA GTA GAT CTC	638bp
5' IL-6*	ATG AAG TTC CTC TCT GCA AGA GAC	
3' TNF-α*	GTA TGA GAT AGC AAA TCG GCT GAC GGT GTG GG	354bp
5' TNF-α*	TTC TGT CTA CTG AAC TTC GGG GTG ATC GGT CC	
3' MIP-1α*	TCA GGC AAT CAG TTC CAG GTC AGT GAT GTA TTC	279bp
5' MIP-1α*	ATG AAG GTC TCC ACC ACT GCC	
3' RANTES#	ACT TCT TCT CTG GGT TGG CAC	222bp
5' RANTES#	GCT GCC CTC ACC ATC ATC CTC	
3' MCP-1#	GTC ACA CTG GTC ACT CCT AC	519bp
5' MCP-1#	AGA GAG CCA GAC GGA GGA AG	

Table 2.3. Oligonucleotide primers sequences. The nucleotide sequence of the oligonucleotide primers used in the RT-PCR analyses performed in these investigations are detailed together with the expected product sizes. *Primers synthesised from commercially prepared Clonetech primer sequences. #Primer sequence taken from Godiska, Chantry, Dietsch, and Gray, 1995.

blunt-ended fragments of DNA ranging from 100bp to 1500bp in length, rising in increments of 100bp with an additional fragment at 2072bp. The 600bp band in this ladder appears more brightly stained than the other fragments and provides a source of internal orientation if incomplete separation of the larger bands or loss of the smaller markers occurs. The commercial ladder was diluted 1 in 10 with PCR loading buffer[A1] and NaCl added to a final concentration of 20mM before use. The prepared ladder was aliquoted into 50µl volumes and stored at -20^{0}C. A 5µl aliquot of this working solution was used on each gel.

The gels were prepared by melting the required amount of agarose (2g/100ml) in tris-borate-electophoresis buffer (TBE)[A1] in the microwave with constant supervision to prevent the solution from boiling over. The ethidium bromide was added to the gel and the molten agarose poured into a horizontal gel bed fitted with a medium toothed comb to form the sample wells and allowed to cool. Once solidified the comb was removed from the gel and the electrophoresis tank filled with TBE until the gel was covered. The samples were added to the wells and electrophoresed through the gel at 70 volts with a constant current of 0.35 amps. The rate of diffusion through the gel was monitored by the inclusion of 5µl of PCR loading buffer with each 15µl sample of PCR product before loading on to the gel. The electrophoresis was stopped once the dye front had travelled approximately 8cm through the agarose and the gel examined using an ultraviolent transilluminator. The gel was photographed as a permanent record and the size and comparative brightness of the bands noted.

2.6.8. Relative quantification of results

Theoretically, due to the exponential nature of the PCR there is a linear relationship between the number of cycles performed and the logarithm of the number of molecules produced. However in practice several factors including competitive reactions, substrate exhaustion and inactivation of the polymerase enzyme, result in a decrease in efficiency of the amplification. Therefore, as the number of cycles increases the efficiency of the reaction decreases eventually producing a plateau effect. If the PCR products are to be analysed in a semi-quantitative fashion the reaction must be terminated during the exponential phase of the amplification. To ensure that this was case, PCR was performed and terminated after 20, 25, 30, 35, 40 and 45 cycles for each of the primer sets with the exclusion of β-actin. For this primer pair the number of cycles ranged between 15 and 40.

[A1] The formulation for this solution is describe in Appendix 1

These preliminary reactions showed that the PCRs, with the exception of β-actin, were still in the exponential phase of the amplification after 35 cycles and had not reached the plateau stage (Figures 2.4 to 2.9). Therefore these PCRs were terminated following 35 rounds of amplification to permit the results to be assessed in a semi-quantitative manner. β-actin, however, reached the plateau stage earlier than the other primer pairs and this PCR was therefore performed with only 30 reaction cycles (Figure 2.10).

As each PCR was terminated during the exponential phase of amplificaton and since all the RT-PCR analyses were performed on a standard amount of both RNA starting material and resultant cDNA the results can be interpreted in a semi-quantitative manner. This experimental design allows comparisons to be made between the relative amounts of a specific PCR product by grading the brightness of the resulting PCR band on the agarose gel. The scale used to grade the intensity of the PCR bands is shown in Figure 2.11. This can be equated to the relative amount of target present in the original sample. However, these comparisons only apply within primer sets and cannot be made between different primers.

2.7. Statistical analyses

The data generated during these investigations was analysed using proprietary statistical analysis software. A range of descriptive hypothesis testing and estimation methods was used. Both parametric and non-parametric tests were employed depending on whether the response variables were measured on an interval or ordinal scale respectively. The analyses required depended on the experimental design and nature of data set generated. Therefore, the statistical tests are described in detail in each chapter of this thesis as appropriate. All statistical analyses undertaken in this investigation were performed with advice from Prof. George Gettinby, Department of Statistics and Modelling Science, University of Strathclyde, Glasgow.

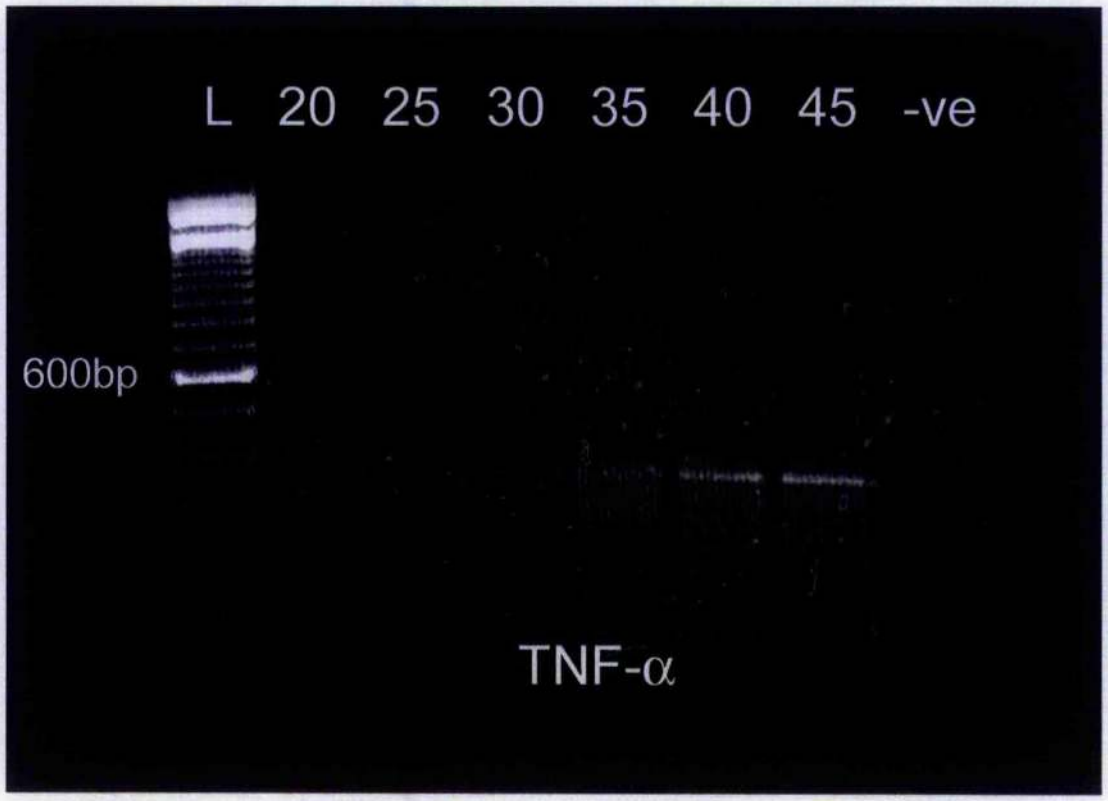

Figure 2.4. TNF-α banding pattern resulting from increasing amplification cycles. Photograph of an ethidium bromide stained, 2% agarose gel showing the TNF-α reaction products following increasing numbers of PCR amplification cycles. A 100bp ladder has been included to assess the size of the resultant PCR bands (lane 1). PCR amplification was performed for 20 (lane 2), 25 (lane 3), 30 (lane 4), 35 (lane 5), 40 (lane 6) and 45 (lane 7) cycles. A negative control (-ve) (lane 8) comprising the PCR master mix and water in place of the cDNA template is shown following 45 cycles of the PCR reaction (lane 9). The increasing intensity of the resultant bands demonstrate that the PCR is in the exponential phase of of the reaction following 35 cycles of amplification.

Figure 2.5. IL-1α banding pattern resulting from increasing amplification cycles. Photograph of an ethidium bromide stained, 2% agarose gel showing the IL-1α reaction products following increasing numbers of PCR amplification cycles. A 100bp ladder has been included to assess the size of the resultant PCR bands (lane 1). PCR amplification was performed for 20 (lane 2), 25 (lane 3), 30 (lane 4), 35 (lane 5), 40 (lane 6) and 45 (lane 7) cycles. A negative control (-ve) (lane 8) comprising the PCR master mix and water inplace of the cDNA template is shown following 45 cycles of the PCR reaction (lane 9). The increasing intensity of the resultant bands demonstrate that the PCR is in the exponention phase of the reaction following 35 cycles of amplification.

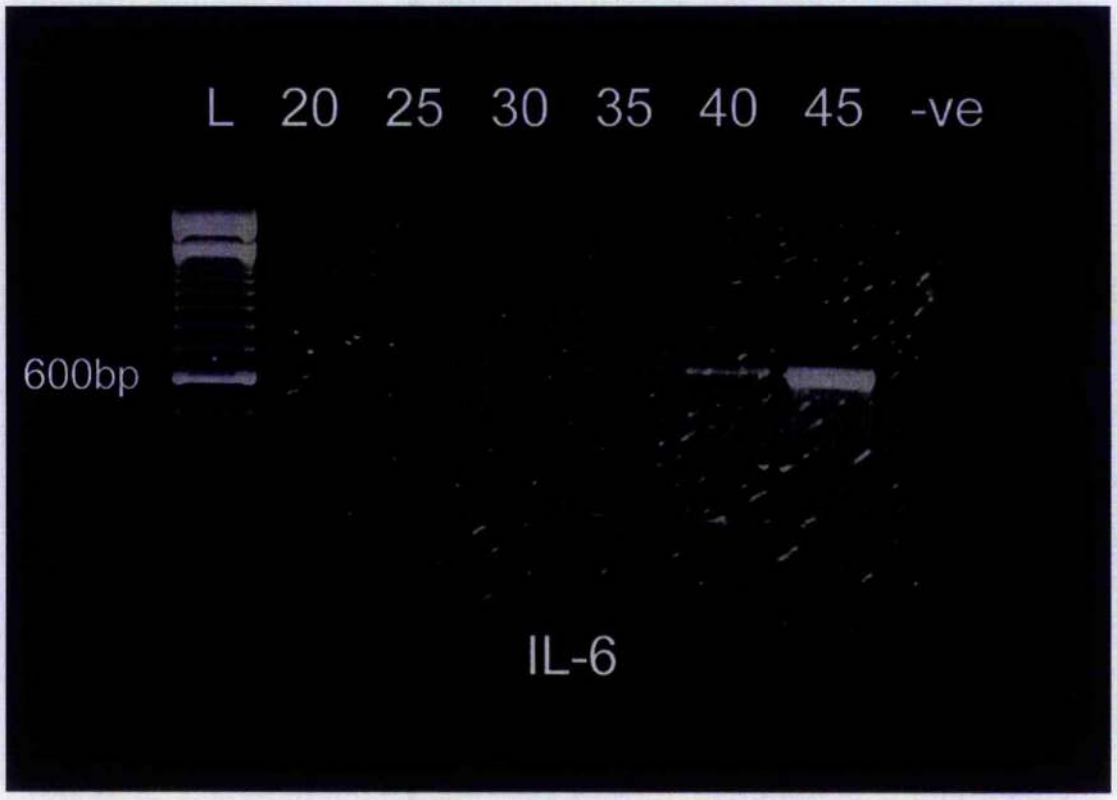

Figure 2.6. IL-6 banding pattern resulting from increasing amplification cycles. Photograph of an ethidium bromide stained, 2% agarose gel showing the IL-6 reaction products following increasing numbers of PCR amplification cycles. A 100bp ladder has been included to assess the size of the resultant PCR bands (lane 1). PCR amplification was performed for 20 (lane 2), 25 (lane 3), 30 (lane 4), 35 (lane 5), 40 (lane 6) and 45 (lane 7) cycles. A negative control (-ve) (lane 8) comprising the PCR master mix and water inplace of the cDNA template is shown following 45 cycles of the PCR reaction (lane 9). The increasing intensity of the resultant bands demonstrate that the PCR is in the exponention phase of the reaction following 35 cycles of amplification.

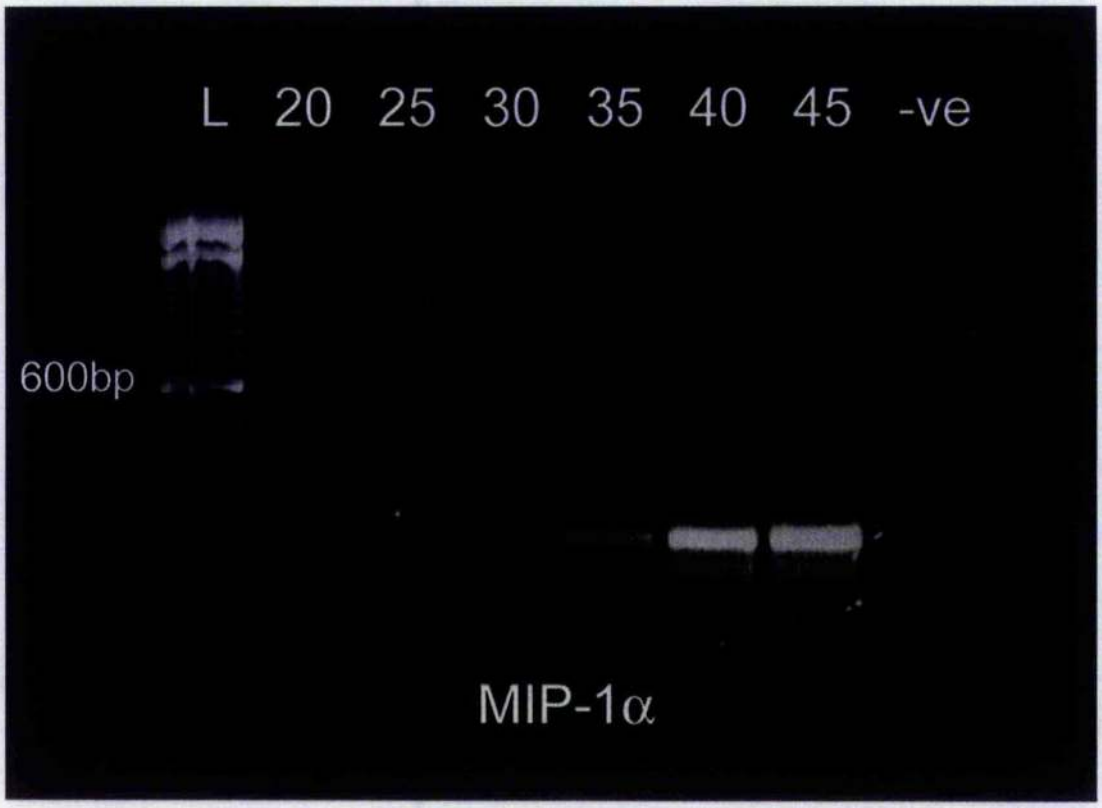

Figure 2.7. MIP-1α banding pattern resulting from increasing amplification cycles. Photograph of an ethidium bromide stained, 2% agarose gel showing the MIP-1α reaction products following increasing numbers of PCR amplification cycles. A 100bp ladder has been included to assess the size of the resultant PCR bands (lane 1). PCR amplification was performed for 20 (lane 2), 25 (lane 3), 30 (lane 4), 35 (lane 5), 40 (lane 6) and 45 (lane 7) cycles. A negative control (-ve) (lane 8) comprising the PCR master mix and water inplace of the cDNA template is shown following 45 cycles of the PCR reaction (lane 9). The increasing intensity of the resultant bands demonstrate that the PCR is in the exponention phase of the reaction following 35 cycles of amplification.

Figure 2.8. MCP-1 banding pattern resulting from increasing amplification cycles. Photograph of an ethidium bromide stained, 2% agarose gel showing the MCP-1 reaction products following increasing numbers of PCR amplification cycles. A 100bp ladder has been included to assess the size of the resultant PCR bands (lane 1). PCR amplification was performed for 20 (lane 2), 25 (lane 3), 30 (lane 4), 35 (lane 5), 40 (lane 6) and 45 (lane 7) cycles. A negative control (-ve) (lane 8) comprising the PCR master mix and water inplace of the cDNA template is shown following 45 cycles of the PCR reaction (lane 9). The increasing intensity of the resultant bands demonstrate that the PCR is in the exponention phase of the reaction following 35 cycles of amplification.

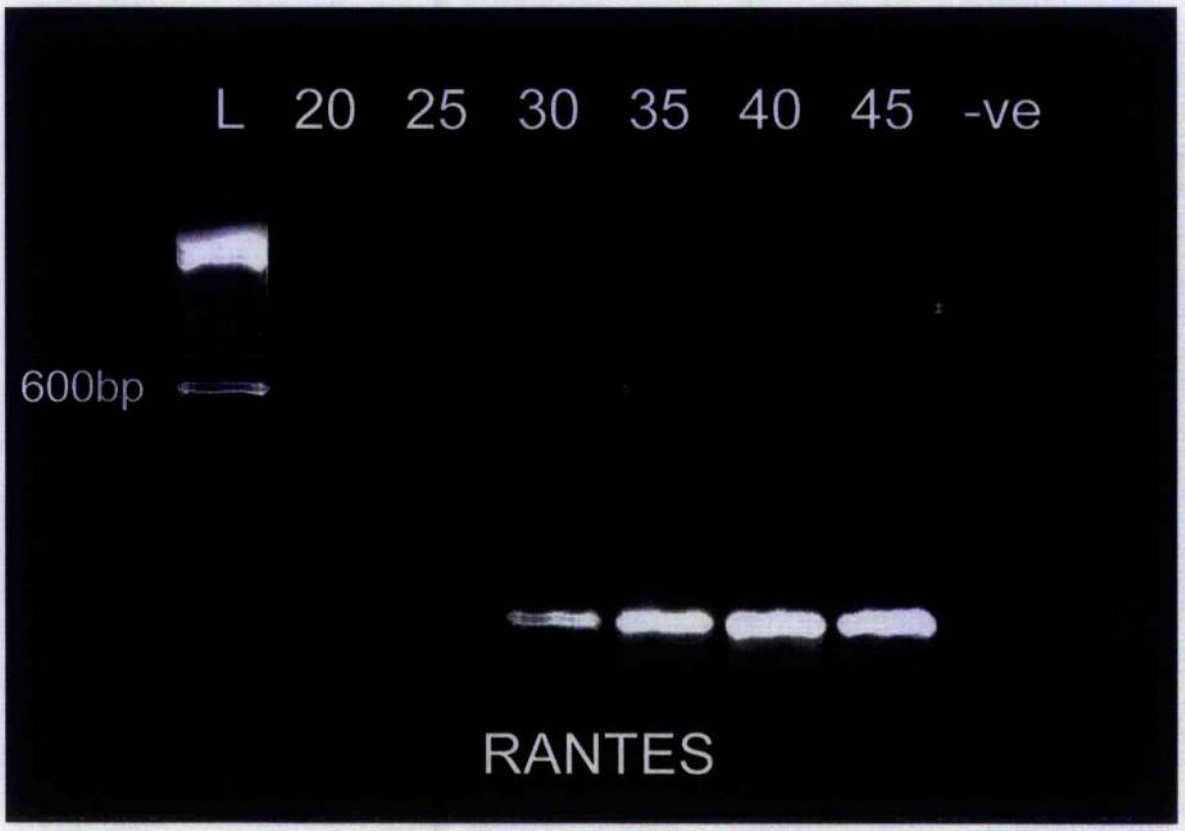

Figure 2.9. RANTES banding pattern resulting from increasing amplification cycles. Photograph of an ethidium bromide stained, 2% agarose gel showing the RANTES reaction products following increasing numbers of PCR amplification cycles. A 100bp ladder has been included to assess the size of the resultant PCR bands (lane 1). PCR amplification was performed for 20 (lane 2), 25 (lane 3), 30 (lane 4), 35 (lane 5), 40 (lane 6) and 45 (lane 7) cycles. A negative control (-ve) (lane 8) comprising the PCR master mix and water inplace of the cDNA template is shown following 45 cycles of the PCR reaction (lane 9). The increasing intensity of the resultant bands demonstrate that the PCR is in the exponention phase of the reaction following 35 cycles of amplification.

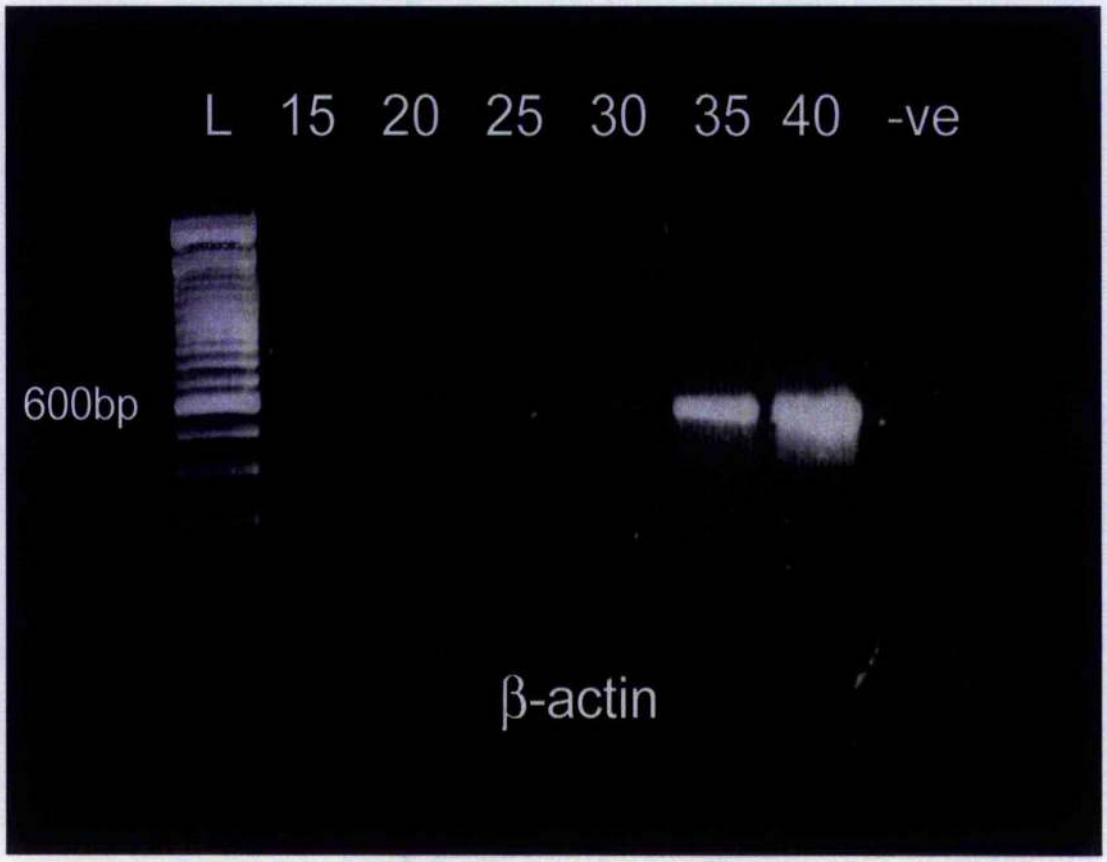

Figure 2.10. β-actin banding pattern resulting from increasing amplification cycles. Photograph of an ethidium bromide stained, 2% agarose gel showing the β-actin reaction products following increasing numbers of PCR amplification cycles. A 100bp ladder has been included to assess the size of the resultant PCR bands (lane 1). PCR amplification was performed for 15 (lane 2), 20 (lane 3), 25 (lane 4), 30 (lane 5), 35 (lane 6) and 40 (lane 7) cycles. A negative control (-ve) (lane 8) comprising the PCR master mix and water in place of the cDNA template is shown following 40 cycles of the PCR reaction. The increasing intensity of the resultant bands demonstrate that the PCR is in the exponential phase of of the reaction following 30 cycles of amplification.

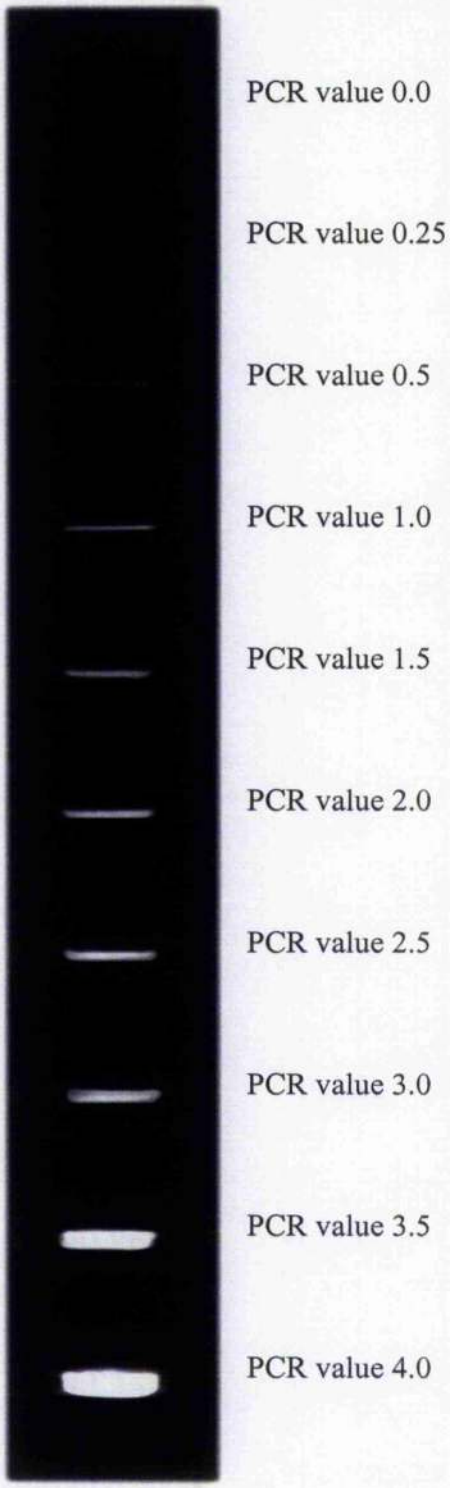

Figure 2.11. Grading scale used to score intensity of PCR amplicon.

The banding pattern illustrated above is a composite figure prepared from a variety of PCR products, visualised on a 2% agarose gel stained with ethidium bromide. The figure illustrates the scoring system of 0 to 4, employed in grading the intensity of the amplicons resulting from the PCR analyses used in this investigation.

CHAPTER 3

TRYPANOSOME-INDUCED CELLULAR IMMUNE REACTIVITY WITHIN THE CNS

3.1. Introduction

During the late-stage of human African trypanosomiasis, the presence of the parasites in the brain induces an inflammatory reaction within the CNS. This inflammatory reaction can be exacerbated by subcurative chemotherapy resulting in an extremely severe meningoencephalitis, known as the post-treatment reactive encephalopathy (PTRE). This reaction is characterised by the presence of macrophages, T-cells, B-cells and plasma cells within the meninges, perivascular spaces and brain parenchyma. The pathogenesis of this response remains unknown. Before the mechanisms and kinetics resulting in this inflammatory cell infiltration of the CNS can be investigated an appreciation of the complexity of the immune response is vital. Therefore, the evolution of an inflammatory reaction within the brain and the infiltration of the CNS by inflammatory cells will be discussed. In addition, the information currently available regarding the cellular components identified in the CNS following trypanosome infection and the development of the PTRE will be detailed.

3.1.1. The inflammatory response

Human beings and other complex organisms respond to tissue injury, infection and neoplastic change through the process of inflammation. The primary function of this reaction is to protect the integrity of the organism and maintain the complex internal balance on which life depends. The immune response has been well characterised in the peripheral tissues and relies heavily on the trafficking of leucocytes, the most common and widely recognised component of the immune system, into the affected tissues and the subsequent initiation of appropriate effector mechanisms.

There are various cell types which belong to the leucocyte category, including, phagocytic cells such as monocytes / macrophages and polymorphonuclear granulocytes. These cells generally use a non-specific recognition system that allows them to bind to a variety of microbial products before internalising and destroying them. Consequently, they constitute the basis of the innate immune system and hold infections in check until the body can mount a specific or acquired immune response against the pathogen or foreign material. In addition, some of these cells can act as antigen-presenting cells (APC's) and are responsible for presenting antigens to a second group of leucocytes, known as lymphocytes, which includes both T-cells and B-cells. This antigen presentation process initiates the specific immune reaction and primes the lymphocytes to recognise particular

antigenic molecules in a highly specific manner. Although these separate groups of leucocytes have been identified, there is a constant interplay between the sets with each cell type interacting with and controlling the actions of the other cell types. This results in a complex milieu of responses all designed to protect the organism from harm.

3.1.1.1. Innate immunity

The innate or natural immune response is controlled by various factors that are present in an organism from birth. The response is relatively non-specific and operates against a wide range of substances. No prior exposure to a pathogen is necessary to stimulate the innate immune response and the cells are immediately available to combat the unfamiliar substance. Therefore, this type of immune reaction forms the basis of an organism's first line of defence against disease and foreign particles. The key cell types involved in innate immunity are; the monocytes / macrophages, the polymorphonuclear granulocytes including, neutrophils, eosinophils, basophils and mast cells; and the natural killer cells. As polymorphonuclear granulocytes and natural killer do not play a major role in the CNS inflammatory response to trypanosome infection these will not be described further.

3.1.1.1.1. Monocytes / macrophages

Blood monocytes are produced from myeloid progenitor cells in the bone marrow and constitute a circulating pool of cells within the blood stream. The blood monocytes migrate through the blood-vessel walls into various organs and tissues and there differentiate into macrophages. Since blood monocytes are more easily obtained than macrophages many studies have been carried out utilising this cell type and their responses extrapolated to macrophages. Human blood monocytes are approximately 10-18μm in diameter and contain a horseshoe shaped nucleus. In addition the cells often hold faint azurophilic granules and many intracytoplasmic lysosomes. These lysosomes contain various enzymes, including, peroxidase and acid hyaluronidases that are important in the killing of microorganisms following their phagocytosis (Roitt, Brostoff, and Male, 2001).

To help them recognise and adhere to invading microorganisms monocytes / macrophages have a variety of cell surface receptors. One of the principle stimulators of the innate immune system is lipopolysaccharide (LPS). LPS forms a component of the cell wall of many bacteria and is therefore a good target for a non-specific defence mechanism. Monocytes / macrophages express CD14 on their cell surface, this receptor binds LPS, in

conjunction with the serum protein, lipopolysaccharide-binding-protein, triggering an inflammatory reaction. Mannosyl-fucosyl receptors (MFR) are also present on monocytes / macrophages. These recognise and bind to sugars that are commonly found on the surface of microorganisms. In the body, pathogens can become coated with specific antibody and complement components. This renders the pathogen more attractive to phagocytic cells and allows them to be killed more readily. The attachment of the phagocytic cells to the coated pathogen is facilitated by the presence of three distinct receptors for the Fc portion of the IgG and a receptor for the C3b component of complement on the monocyte / macrophage cell surface. The three isoforms of the Fc_γ receptors in humans are $Fc_\gamma RI$ (CD64), $Fc_\gamma RII$ (CD32) and $Fc_\gamma RIII$ (CD16); they have high, medium and low affinities, respectively, for the Fc portion of IgG. The equivalent murine homologues to these Fc_γ receptors are $Fc_\gamma RIIa$, $Fc_\gamma RIIb/1$ and $Fc_\gamma RIIIlo$. If any of these cell surface receptors are activated the monocyte / macrophage extends its cell membrane into pseudopodia that surround the bound microorganism forming a phagosome. Lysosomes then fuse with the phagosome to form a phagolysosome, and the infectious agent is killed (Janeway and Travers, 1996; Roitt *et al.*, 2001).

Monocytes / macrophages also have specialised cell surface receptors that bind IgE, these are known as $Fc_\varepsilon R1$. However, the binding of IgE does not activate the cell and this process only occurs when the attached IgE is cross-linked by binding to a multivalent antigen. Stimulation of the receptors in this manner results in the externalisation of the cytoplasmic vesicles and the killing of the pathogen in the external matrix.

Adhesion molecules, including, leucocyte function antigen (LFA) can also be found on the surface of monocytes /macrophages. These are important in the transmigration of the cells from the vasculature into specific organs. In addition monocytes / macrophages express receptors for a variety of cytokines and can therefore be 'activated' by T-cell derived mediators leading to increased phagocytosis and microbicidal activity (Janeway and Travers, 1996; Roitt *et al.*, 2001).

A number of monocytes / macrophages express major histocompatability (MHC) antigens, these are necessary for the presentation of antigen to specific sets of lymphocytes. Professional APC's form a varied population of leucocytes. These cells can process antigens and display peptide fragments on their cell surface in conjunction with surface molecules to initiate lymphocyte activation.

3.1.1.2. Acquired immunity

Acquired immunity is a more specialised form of immune response than innate immunity and is only present in vertebrates. The main difference between innate and acquired immunity is the ability of lymphocytes to recognise particular antigens in a specific manner. This is made possible through the presence of cell surface receptors on the lymphocytes that recognise discrete parts of an antigen. These parts are known as antigenic determinant groups or epitopes. An acquired immune response results as a consequence of an encounter with a foreign substance displaying these epitopes. This triggers a chain of events which lead to a specific reaction against that particular component. Therefore, as the name suggests, acquired immunity develops only after the organism has encountered a specific antigen and in some cases can confer a life-long protective immunity to re-infection with the same pathogen. Although the acquired immune response appears in many ways superior to innate immunity the reaction is in fact highly dependent on the cells of the innate immune system and could not operate if they were not present. The two main cell types associated with the acquired immune response are the T-lymphocytes or T-cells, including $CD4^+$ and $CD8^+$ cell subsets, and the B-lymphocytes or B-cells. Both cell types have cell surface receptors that allow them to recognise specific antigen. However, the functions of the T-cells and B-cells are dissimilar.

3.1.1.2.1. T-lymphocytes

T-cells are derived from bone marrow stem cells and their progenitors migrate to the thymus early in the development process. Here the immature T-cells or thymocytes proliferate intensely and differentiate into mature T-cells. In mice, only around 2% of the thymocytes generated reach maturity and the remainder die, mainly through apoptosis, within the thymus. This massive cell death is a necessary step in the development of the mature T-cells as they undergo intense screening for MHC restriction and self-tolerance before they can be exported to the periphery. As the thymocytes mature they pass through distinct phases. Each stage in this process is marked by the expression of distinctive cell surface molecules.

3.1.1.2.1.1. $CD4^+$ T-cells

T-cells that carry the CD4 surface marker mainly perform functions that 'help' or 'induce' an immune reaction and are therefore known as T-helper (Th) cells. These Th-cells can be

further divided into at least two additional subgroups, Th1 and Th2. The subgroups can be distinguished by the array of cytokines that they produce. Th1 cells are particularly important for the eradication of intracellular pathogens including bacteria, parasites, yeast and viruses and will react to antigen only if it is presented in conjunction with MHC class II molecules. They typically express the cytokines IL-2, IFN-γ and lymphotoxin which can activate further cytokine production by macrophages and stimulate microbicidal activity as well as inducing opsinization and complement fixation. In addition a Th1 response can result in the activation of NK-cells and CD8 T-cells (Lee, Kum, Cockram, Teoh *et al.*, 1989; Mosmann and Sad, 1996). Th2 cells produce cytokines that induce B-cell proliferation, antibody production and eosinophil and mast cell activation. The cytokines expressed by the Th2 cells including IL-4, IL-5, IL-6 and IL-10. Consequently, Th2 cells primarily mediate functions associated with protecting the organism from free-living pathogens. Hence Th1 cells are predominantly associated with cell-mediated immunity while Th2 cells induce strong antibody and allergic responses. Not only do these Th1 and Th2 cell subset induce different effector pathways they also tend to hamper the development of the opposite cell type. Therefore, Th1 cells tend to inhibit the actions of Th2 cells and Th2 cells tend to inhibit the actions of Th1 cells. For example IL-10 production by Th2 cells inhibits IFNγ production by Th1 cells and prevents subsequent macrophage activation while IFNγ production by Th1 cells inhibits the proliferation of Th2 cells (Janeway and Travers, 1996).

However, this demarcation of cytokine production is not comprehensive since some Th-cells express cytokine profiles that overlap both Th1 and Th2 cell subsets. These cells are known as Th0 cells and can produce both the Th1 cytokine IFNγ and the Th2 cytokine IL-4. Th0 cells are thought to be in a less differentiated state that Th1 or Th2 cells and appear to occur when certain polarising signals are not present following T-cell activation. Th0 cells can potentially develop into either Th1 or Th2 cell phenotypes and are therefore considered to be an intermediate stage in T-cell maturation (Janeway and Travers, 1996). The factors that determine whether a proliferating T-cell will become a Th1 or a Th2 cell are not fully understood. However, it appears many inter-locking factors including the type of co-stimulatory signal resulting in the initial proliferation, the nature of the MHC:peptide complex stimulating the response as well as the presence of various cytokines in the vicinity of the T-cell all have an effect in the final outcome of the differentiation (Janeway and Travers, 1996; Roitt *et al.*, 2001).

3.1.1.2.1.2. $CD8^+$ T-cells

T-cells that express the CD8 cell surface marker are predominantly cytotoxic in function and are therefore known as T-cytotoxic (Tc) cells. There are no sub-divisions in this class of T-cell and naïve $CD8^+$ T-cells can differentiate only into cytotoxic cells. The $CD8^+$ cells perform a crucial role in the elimination of intracellular pathogens such as viruses and certain bacteria. Once inside the cells these pathogens are not accessible to antibodies and can therefore only be destroyed by killing the infected cell.

When activated Tc-cells recognise pathogen derived peptides, in conjunction with MHC class I molecules, they inducing the cell to enter apoptosis resulting in the death of the infected cell. Following induction of the apoptotic pathway the Tc-cell disengages from the target cell and can recycle to kill multiple infected cells. The principle method through which Tc-cells function involves the release of perforin and enzymes that induce apoptosis in the target cell. Tc-cells do not require the target cell to be coated with immunoglobin and will only kill a target cell if it can recognise the antigen specified by its T-cell receptor (TCR), presented on MHC class I molecules. Once dead the cellular debris attracts mononuclear cells that rapidly clear the cell fragments by phagocytosis. Tc-cells and NK-cells act in a complementary fashion. NK-cells survey the body to ensure all cells display MHC class I molecules and Tc-cells check the antigen tag associated with the MHC molecule. This double-checking process is of great importance in the body's defence against certain viruses that have evolved mechanisms of avoiding detection by Tc-cells. These viruses reduce the cellular expression of MHC class I molecules to try and prevent their antigens from being displayed to the immune cells. However, this lack of MHC class I expression leaves the infected cells open to attack by NK-cells (Roitt *et al.*, 2001).

Alternative mechanisms for inducing apoptosis in their target cells are also employed by Tc-cells. Tc-cells can signal to their target cells via membrane bound receptors belonging to the TNF group of molecules. These receptors include, Fas (CD95) and the TNF type 1 receptor (TNFR-1) (CD120a). Another member of this TNF receptor family is the CD40 molecule necessary for induction of expression of the co-stimulatory molecules B7.1 and B7.2 on B-cells. Mature Tc-cells and some activated $CD4^+$ cells express the ligand for Fas (FasL). Both Fas and TNFR-1 have 'death' domains attached to the cytoplasmic region of the molecule that are involved in the recruitment of caspases. Caspase enzymes have an extensive remit and are involved in intracellular signalling, cell cycle control, DNA integrity and repair and intracellular adhesion. If the Fas receptor is bound to the FasL this induces a conformational change in the Fas receptor that subsequently recruits and

activates caspases 8 and 10. The actions of these enzymes then lead to apoptosis of the target cell (Roitt *et al.*, 2001).

3.1.1.2.2. B-lymphocytes

Many human diseases result from infection with pathogens that multiple either in the extracellular spaces of the body or survive as intracellular forms that spread by moving from cell to cell through the extracellular fluids. One of the main mechanisms employed by the host immune system to prevent the proliferation of these pathogens is the production of specific antibodies that bind to the antigens displayed by the infective agent. Coating of the pathogens with antibody facilitates their destruction by phagocytes and NK-cells. Intracellular pathogens can become covered in antibody while moving between cells. These bound antibodies can prevent the pathogen from entering the new host cell and are therefore said to 'neutralise' the pathogen. The antibodies responsible for protecting the host in this fashion are produced by the B-lymphocytes or B-cells (Janeway and Travers, 1996; Roitt *et al.*, 2001).

Like T-cells, B-cells develop in the bone marrow. However, in contrast to T-cells the B-cells also mature in the bone marrow before entering the bloodstream and migrating to the peripheral lymphoid organs. The naïve mature B-cells can only survive in the periphery for a few weeks before they are killed by entering apoptosis. However, if these B-cells encounter the antigen specified by their cell surface immunoglobin they become activated, proliferate and differentiate into plasma cells or memory B-cells (Roitt *et al.*, 2001).

B-cells comprise approximately 5-15% of the circulating lymphocyte population and can be defined by the presence of cell surface IgM and IgD. The antigen binding sites of all the immunoglobin molecules expressed on the surface of individual B-cells are identical. Therefore, a particular B-cell will only react with one distinct antigen and will ultimately produce only that antibody. However, many forms of antibody are expressed within the B-cell population. The B-cell surface antibody is associated with additional molecules that consist of disulphide bonded heterodimers of Igα and Igβ. This complex of the surface antibody with Igα (CD79a) and Igβ (CD79b) molecules forms the B-cell antigen receptor complex (BCR). The Igα and Igβ molecules are thought to couple the surface antibody with the intracellular signalling pathways and are involved in the activation of the B-cell. In addition, the surface antibody helps to deliver bound antigen to the interior of the B-cell where it is processed and returned to the cell surface in conjunction with MHC class II molecules for presentation to either naïve or primed T-cells.

In general, naïve B-cells do not become activated following an encounter with antigen alone and require accessory signals to complete the transition from naïve to activated, differentiated cells. These accessory signals can be generated by either armed $CD4^+$ cells or directly by certain microbial constituents. Therefore, B-cells are said to be activated either by a T-cell dependent antigen or by a T-cell independent antigen.

3.1.2. The CNS and 'immuno-privilege'

Initial microscopic investigations of brain tissue rarely showed the presence of any inflammatory cells even following grafting of allogenic tissue into the brain (Hickey, Hsu, and Kimura, 1991). This initiated the belief that the brain was devoid of immune protection and instigated the concept of 'immune privilege' (Shrikant and Benveniste, 1996; Streit and Kincaid-Colton, 1995).

The principal role of leucocytes is to defend the organism against disease. However, the potent substances that they secrete during an inflammatory reaction are also capable of destroying or harming neighbouring host cells. If these 'bystander effects' were to occur within brain tissue the resulting tissue damage could be extremely injurious to the organism. The inflammatory response is therefore a double-edged sword; it is vital to the survival of the organism but its effects could also be devastating if unrestrained. Consequently, the passage of leucocytes from the vasculature to the CNS must be rigorously controlled. Therefore, the CNS is separated from the rest of the body, including the immune system, by the blood-brain barrier (BBB). The concept of such a barrier was developed in the early 19^{th} century following observations by Edwin Goldmann that dye molecules, when injected into the cerebrospinal fluid (CSF) of small animals, readily stained the brain tissue but were unable to enter the blood stream to stain the peripheral organs (Goldstein and Betz, 1986). It is now known that this barrier controls the trafficking of most items, including, nutrients and leucocytes, as well as the exchange of inflammatory mediators and antibodies, between the circulation and the CNS (Lassmann, Zimprich, Rossler, and Vass, 1991).

3.1.2.1. The blood-brain barrier

Physically the BBB takes two different forms. The first occurs in the endothelium of the microvessels supplying the brain while the second is located in the choroid plexus epithelium found within the brain ventricles (Tuomanen, 1996). In contrast to the

permissive vessels of the peripheral system, which are fenestrated and show active trans-membrane pinocytosis, the endothelial cells of the cerebral vessels and the epithelial cells of the choroid plexus are 'joined' continuously by tight junctions that prevent the passage of even small molecules such as dyes and antibiotics into the brain tissue. The barrier arising form these modifications is so formidable that specialised transport systems have developed to provide the brain with essential nutrients such as glucose, iron and the amino acids required to support the tissue behind the barrier (Tuomanen, 1996). These transport systems are highly complex and allow the capillary to strictly control the entry and exit of substances to and from the CNS. Some of these transporters facilitate osmotic diffusion while others are active transport mechanisms that require an energy source to enable movement of the compound across the barrier (Goldstein and Betz, 1986).

3.1.2.1.1. The microvascular endothelial cell barrier

The most extensive site of the BBB can be found in the brain microvessels. As previously stated the presence of extremely strong tight junctions between the endothelial cells of the vessels and the lack of continuous channels or gaps through the endothelium distinguishes this membrane from that found in the peripheral microvasculature. In addition the endothelium of CNS microvessels is almost completely surrounded by astrocyte foot processes. These glial processes were originally thought to constitute the barrier since the astrocytes are intimately associated with the endothelial cells (Compston, 1993). However, it is now known that tight junctions are not present between the astrocytic cells (Tuomanen, 1996) and that the endothelial cells alone establish the barrier. In addition, the processes of microglia also contact the brain endothelial cells (Prat, Biernacki, Wosik, and Antel, 2001). The exact role of the astrocytes and microglia in relation to the brain microvascular endothelial cells remains incompletely understood (Goldstein and Betz, 1986). However, the function of the tight junctions is known to be influenced by these neuroglial cells (Prat *et al.*, 2001) and the permeability of the barrier is increased by up to 15 fold if the endothelial cells become disengaged from the basement matrix (Tuomanen, 1996).

3.1.2.1.2. The choroid plexus epithelial cell barrier

The choroid plexus is a highly localised structure found only within the ventricles of the brain. Under light microscopy it appears as a network of highly branched fronds consisting of capillaries and surrounded by a single layer of epithelial cells. These epithelial cells form a polarised epithelium similar to that found in the kidney. The choroid

plexus is responsible for the production of CSF that performs a number of essential functions such as supplying the specialised chemical micro-environment of nutrients required by the brain tissue. In addition, the CSF provides a certain degree of buoyancy to the brain that effectively reduces the true weight of the tissue by up to 30 fold (Spector and Johanson, 1989). Although tight junctions join the cells of the choroid plexus epithelium, the barrier exhibits a lower electrical resistance than that formed by the endothelial cells of the brain microvessels. This allows the passage of some blood components across the BBB that are required to form the CSF but this permissiveness also leaves the area more exposed to breach by invading organisms (Zhang and Tuomanen, 1999).

3.1.2.1.3. 'Gaps' in the barrier

The endothelial cells in the CNS form a continuous barrier throughout the majority of the brain microvessels. However, in several small regions of the brain the barrier is incomplete and gaps or channels traverse the endothelium enabling substances in the blood to enter the CNS. Most of these areas are situated close to the ventricle and are therefore known collectively as the circumventricular organs (Risau, 1994). Areas that show the presence of this 'leaky' barrier include the pituitary gland, the pineal gland and the median eminence of the hypothalamus. It is thought that the pathways through the endothelium are necessary in these areas to allow the passage of circulating hormones that must reach the neurons in the brain and complete the feedback loop that controls the regulation of their secretion (Goldstein and Betz, 1986). In addition, the subfornical organ, the organum vasculosum lamina terminalis and the area prostrema show the presence of endothelial cells that are fenestrated and do not form tight junctions (Risau, 1994).

3.1.2.2. Immune surveillance within the CNS

As previously stated the CNS has long been considered as an immuno-privileged organ due to its innate lack of cells belonging to the peripheral immune system. The BBB not only interferes with the passage of these cells into the CNS tissue but also controls the exchange of immunological mediators such as cytokines and antibodies between the circulation and the CNS. However, under defined circumstances the CNS can mount a highly effective immune reaction against invading pathogens or foreign material. Therefore intensive research has been carried out in order to characterise the events that allow the passage of immune cells into the CNS for purposes of immune surveillance and immunological defence (Lassmann *et al.*, 1991).

3.1.2.2.1. Macrophages in the CNS

The BBB is not impermeable to all cells. In fact it has been shown that there is a constant, slow, movement of monocytes into the brain parenchyma which differentiate into microglia, pericytes or macrophages within the brain (Flugel and Bradl, 2001; Matyszak, 1998). In the case of microglia, it seems that most of these cells arrive before birth with only a very slow repopulation occurring. However, the resident perivascular cells and macrophages are continuously replenished from peripheral sources (Hickey, 2001). The ultimate fate of these cells is still a subject of some debate. It remains unclear whether perivascular cells and macrophages can leave the CNS, carrying antigens for presentation to peripheral immune cells in the spleen and lymph nodes, and thereby prime the cells to antigens sequestered behind the BBB (Hickey, 2001). This would provide a method to continuously and effectively monitor the CNS for foreign material. However, experiments that directly introduced particulate antigen, which would be taken up by these macrophages, into the CNS have failed to induce an immune response to these antigens (Hickey, 2001).

3.1.2.2.2. T-cells in the CNS

It is also apparent that although resting T-cells are excluded from the CNS, activated cells can cross the BBB irrespective of their antigen specificity. The ability of activated T-cells to enter the CNS was demonstrated in animals given intravenous injections of activated T-cells that were later detected within the brain tissue. This phenomenon explains the development of experimental allergic encephalomyelitis (EAE) following intravenous injection of activated myelin basic protein (MBP) specific T-cells into healthy recipient animals but not following the injection of resting T-cells (Wekerle, Linington, Lassmann, and Meyermann, 1986). The results also suggest that under normal circumstances, in the healthy brain, the endothelial cells must express the prerequisite molecules to allow this passage to take place.

The exact mechanisms that permit cell traffic through the BBB have yet to be elucidated. However, it is thought that the expression of cellular adhesion molecules plays an important role in the process. It is known that in the normal brain the endothelial cells of the BBB express only low levels of these cellular adhesion molecules. This paucity of adhesion molecules may reflect the relatively low numbers of T-cells present in the healthy brain when compared with other body organs (Hickey, 2001). A role for these circulating T-cells in the maintenance of the healthy CNS has also been suggested since, when

activated, these cells can produce a variety of neurotrophic substances that could enhance the repair of CNS tissue (Hickey, 2001). As yet, the fate of T-cells entering the CNS, which do not encounter their specified antigen, remains unclear. Whether these cells recirculate to the periphery or are killed by the induction of apoptosis or by some other mechanism inherent to the CNS is unknown at present (Hickey, 2001).

3.1.2.2.3. B-cells in the CNS

The ability of B-cells to enter the CNS appears to follow similar criteria to the influx of T-cells since B-cells are known to be present in many pathological processes. It has also been shown that if antigen, to which an animal has previously been sensitised, is deposited behind the intact BBB, B-cells and plasma cells accumulate at the site of antigen introduction. This suggests that B-memory cells in the peripheral lymph nodes are activated by restimulation with the antigen and migrate through the tissues in search of further antigen. When they encounter the antigen in the brain the B-cells remain at that site, proliferate and develop into antibody secreting-plasma cells (Hickey, 2001).

3.1.2.2.4. Lymphatic drainage in the CNS

The ability of certain antigens to stimulate peripheral immune cells even though they are introduced behind the BBB raises questions with regard to lymphatic drainage in the CNS. Although there are no anatomically defined lymphatics in the CNS it would appear that the CSF partially accomplishes the role of the lymph within the brain. As the CSF travels through the brain tissue and Virchow-Robins spaces it penetrates areas beneath the cribiform plate and along the cranial and spinal nerve roots where anatomically recognisable lymphatics are present. It is therefore feasible that the CSF can carry potential antigenic substances form the brain tissue to the lymphatic system and thereby facilitate in the immune surveillance of the CNS (Hickey, 2001).

3.1.2.3. CNS cells with immune roles

To compensate for the relative lack of immune system cells within the CNS, several endogenous types of cell have the potential to perform immune functions. Amongst these the cerebral endothelial cells of the BBB are capable of performing immune roles. In addition, the glial cells of the brain also possess immune capabilities. When the glial cells were first discovered during the 1800's they were thought to belong to a single category of cell and to serve only as the 'glue' between the neurons and the spinal cord. However, by

the early 20th century three individual types of glial cell had been identified, the astrocyte, the oligodendrocyte and the microglia. By the 1970's it had become apparent that the astrocytes played a major role in the immune response within the CNS. However, it was a further ten years before the immune functions of the microglial cells were demonstrated definitively (Streit and Kincaid-Colton, 1995).

3.1.2.3.1. BBB endothelial cells

The endothelial cell constituents of the BBB may contribute to the instigation and control of inflammatory reactions in the brain. Cerebral endothelia cells can be induced to express the adhesion molecules and co-stimulatory molecules, MHC class II and B7.1 or B7.2, respectively, required to initiate a T-cell response. However their exact function in this scenario remains unclear since, in tissue culture, the endothelial cells fail to promote T-cell proliferation and the T-cells enter a state of anergy. This non-responsive condition can be overcome by supplementing the cultures with IL-2 which subsequently restores the proliferative response in the T-cells (Antel and Prat, 2000).

3.1.2.3.2. Microglia

In a similar manner to peripheral tissues the CNS has a resident population of specialised macrophage cells that appear to phagocytose pathogens and present antigen in a similar fashion to their systemic counterparts. These specialised macrophages are the microglial cells and they comprise between 5-20% of the glia within the CNS and are more numerous in the grey rather than the white matter (Nakajima and Kohsaka, 2001). The cells were first identified in the late 19th century by Nissl who named them 'rod cells' and proposed that they had a capacity for migration and phagocytosis. The idea of these cells being residents within the CNS was proposed by Rio-Hortega in the early 1900's who differentiated the microglia from other glial cell types and suggested that the cells were derived from the mononuclear-phagocyte lineage (Barron, 1995; Male and Rezaie, 2001). However, it was not until 1985, with the discovery of monoclonal antibodies which distinguished reliably between microglia and astrocytes in tissue sections, and the development of pure microglial cell cultures that the attributes of this cell type were demonstrated definitively (Streit and Kincaid-Colton, 1995). In a similar fashion, the derivation of the microglial cells also remained controversial for the majority of the 20th century. However, as more specific antibodies became available it was shown that microglia react with those that recognise patterns exclusively found on cells of the immune

system. In addition, certain antibodies demonstrated that the microglia were related to the macrophage cell type.

3.1.2.3.2.1. Microglial morphology

Microglia are the smallest of the three glia cell types. When examined under light microscopy they have an oval or elliptical nucleus with little or no visible cytoplasm. In their resting state, the cells are highly ramified with many short spiny projections (Barron, 1995). However, when the brain is injured or affected by disease these ramified microglia retract their cellular processes and migrate to the site of injury or infection. Their cell bodies also enlarge and the cells become proliferative. The specific conformation of the newly activated microglial cell is usually dependent on the structure or the brain region in which the response is taking place. If space is available the cells may assume a bushy conformation. In contrast, if the microglia are required along thin neuronal projections they may adopt a more rod-like appearance. When the injury or infection in the CNS is resolved the microglia can revert to their original ramified resting state. However, a further change in the cellular morphology of the activated microglia can occur. In response to cell death within the brain, activated microglia can adopt a phagocytic conformation to facilitate the removal of the resulting cell debris. The ultimate fate of these phagocytic microglia remains unclear (Streit and Kincaid-Colton, 1995).

3.1.2.3.2.2. Microglia in the normal CNS

Microglia develop from bone marrow derived-macrophage precursor cells that invade the brain during embryonic development and early post-natal life. The presence of microglia within the CNS is critical for the normal growth of the embryo. During this early stage of development the microglial cells phagocytose the cell debris that appears naturally through apoptosis, resorption and remodelling of the developing brain (Nakajima and Kohsaka, 2001). When this developmental process is complete the requirement to degrade large quantities of surplus cellular material decreases and the microglia cells transform into the ramified or resting forms commonly found in the mature CNS (Barron, 1995).

Although little is know about the functions of microglia in the normal mature CNS their branched structure is thought to allow the microglial cells to monitor the health status of surrounding cells. Interestingly microglial processes abut both astrocytes and neurons but do not connect with other microglial cells (Streit and Kincaid-Colton, 1995). It has also been suggested, from evidence derived from microglial cell cultures, that these cells

produce low levels of growth factors such as fibroblast and nerve growth factor that may facilitate the survival of mature glia and neurons (Streit and Kincaid-Colton, 1995).

3.1.2.3.2.3. Microglial response to injury or infection

Resting or ramified microglia show a down regulated phenotype with minimal expression of the cell surface antigens commonly found on macrophage type cells. However, as stated above, these cells undergo a dramatic conformational change following CNS injury or infection. This response occurs almost immediately, within minutes of the microglia detecting disruptive changes in the CNS microenvironment (Streit and Kincaid-Colton, 1995). In addition to the structural alterations, the cells show enhanced or novel expression of a variety of macrophage differentiation markers and effector properties (Aloisi, 2001). These include expression of complement receptor 3 and MHC class I and MHC class II molecules (Nakajima and Kohsaka, 2001). The co-stimulatory molecule B7.2 is expressed constitutively by microglial cells and B7.1 expression can be induced under inflammatory conditions (Antel and Prat, 2000). In addition, microglia have been shown to express a further co-stimulatory molecule, CD40, in multiple sclerosis (MS) and experimental allergic encephalomyelitis (EAE) brain lesions and the expression of this molecule can be induced by stimulation of microglia in culture by LPS or IFN-γ (Aloisi, 2001). Furthermore, activated microglia in MS lesions have also been shown to express the adhesion molecule ICAM-1 (Aloisi, Ria, Penna, and Adorini, 1998). The presence of these adhesion and co-stimulatory molecules indicates that microglial cells are equipped to play a major role in antigen presentation and T-cell activation within the CNS in addition to their phagocytic functions.

3.1.2.3.3. Astrocytes

Astrocytes are the most abundant glial cell type within the brain comprising between 20-25% of its total volume and in some areas they constitute up to 50% of the brain tissue. Furthermore, astrocytes are ten fold more numerous that neurons in the mammalian CNS (Montgomery, 1994). Once thought to play a purely structural role within the CNS, astrocytes have now been shown to fulfil numerous and diverse functions. As well as providing support for neurons during development, astrocytes help to maintain the CNS microenvironment. In addition, astrocyte can release a range of neuronal growth factors and have been shown to stimulate unspecialised cells to differentiate into neurons (Svendsen, 2002). Astrocytes, as previously mentioned, also help to preserve the integrity

of the BBB. Furthermore, these cells can modulate immune reactions within the CNS (Eng, Yu, and Lee, 1992; Montgomery, 1994; Svendsen, 2002).

3.1.2.3.3.1. Astrocyte morphology

As the name suggests, astrocytes are stellate shaped cells that are found distributed throughout the brain and spinal cord. The major identifying ultrastructural feature of astrocytes is the presence of intermediate filaments composed mainly of glial fibrillary acidic protein (GFAP). GFAP is by and large specific for astrocytic cells and has therefore proved invaluable as a cellular marker in the study of this cell type both *in vivo* and *in vitro*. GFAP plays a structural role within the cell and is thought to be important in the formation of the cellular processes since astrocytes prevented from manufacturing this protein could no longer produce the cellular branches in response to neurons in cell culture (Eng *et al.*, 1992)

There appears to be two sub-populations of astrocyte although the classification for these cells remains equivocal. One system defines the two groups as protoplasmic and fibrous, while the second uses the terms type 1 and type 2 astrocytes. In general type 1 cells are proposed to be analogous with protoplasmic astrocytes and type 2 cells are thought to be comparable with fibrous astrocytes. The two sub-populations of astrocyte are believed to develop from specific progenitor cells. While the progenitor cells for type 1 astrocytes are thought to be committed to the astrocyte lineage, type 2 cells are believed to develop from bipotential O-2A progenitor cells that can generate either oligodendrocytes or astrocytes (Montgomery, 1994).

Although astrocytes are distributed throughout the CNS, type 1 cells are most commonly found in the white matter while type 2 cells predominate in the grey matter. When the cells are stained with haematoxylin and eosin for examination under light microscopy, type 1 astrocytes appear as pale staining cells with oval to round nuclei and little discernable cytoplasm. In comparison, type 2 astrocytes typically display more lobate nuclei. It can be difficult to distinguish astrocytes from small neurons in tissue sections. However, neurons have distinct nucleoli, whereas, the nucleoli of astrocytes are frequently unapparent.

Astrocytes have intimate associations with other constituents of the CNS. Astrocyte processes surround neuronal cell bodies as well as the nodes of Ranvier of myelinated axons. These astrocytic processes also form the dense network of fibres known as the glial limitans and completely encircle blood vessels within the CNS. The relevance of these

intimate connections may lie in the presence of gap junctions in the astrocyte cell membrane. Gap junctions are constructed of hollow transmembrane proteins, termed connexons, which join with similar proteins on an adjacent cell and allow the exchange of small molecules such as ions, oligosaccharides, amino acids, nucleotides and certain trophic factors, between the cells. These connections can be made from astrocyte to astrocyte, astrocyte to ependymal cell or astrocyte to oligodendrocyte. However, the formation of gap junctions in the CNS is not restricted to the astrocyte population as they also exist between oligodendrocytes and between ependymal cells (Montgomery, 1994).

The astrocyte processes, particularly those surrounding blood vessels, also show the presence of numerous orthogonal assemblies. These structures can only be viewed in freeze-fracture preparations and again may play a role in the transport of molecules between the astrocyte and the blood or CSF. In addition, these structures could be important in cellular adhesion processes. It appears that the interaction between astrocytes and cerebral endothelial cells is significant in the formation of the orthogonal arrays since fibroblasts, smooth muscle cells and non-cerebral endothelial cells fail to induce the formation of the orthogonal arrays in astrocytes *in vitro* (Montgomery, 1994).

3.1.2.3.3.2. Astrocytic responses to injury

Astrocytes respond vigorously to trauma or infection in a reaction commonly referred to as astrocyte activation, astrocytosis or astrogliosis. This is characterised by an increase in detectable astrocyte cell number at the site of insult. The augmentation of the demonstrable astrocyte population is thought to arise by migration of astrocytes from areas distal to the site of injury, proliferation of the neighbouring cells and phenotypic changes in the local astrocyte population. The phenotypic changes are complex and involve the *de novo* expression and upregulation of a variety of molecules including the production of GFAP. In addition to the increase in cell number, activated astrocytes also appear to be larger and have numerous, intricate cytoplasmic processes compared with quiescent or resting cells. Astrocytosis can occur extremely rapidly following insult and has been detected within 24 hours of infection with neurotropic viruses (Mucke and Eddleston, 1993).

The dramatic response of astrocytes to injury can be either beneficial or detrimental depending on the circumstances. Astrocytosis can result in the production of growth factors and neurotrophins that promote neuronal survival and ablation of the astrocyte population has been shown to result in substantial neurodegeneration in the injured brain.

However, astocytosis can also lead to the formation of dense gliotic scars that are thought to have disadvantageous characteristics since they can prevent the extension of axons through the resulting astrocytic mass (Dong and Benveniste, 2001).

3.1.2.3.3.3. Astrocytes as immunocompetent cells

As stated earlier, astrocytes are found dispersed throughout the CNS and their foot processes are in close apposition with the endothelial cells of the BBB. They are therefore ideally situated to influence the entry of inflammatory cells into the CNS and subsequently manipulate their activity in the brain. However, to control this process astrocytes would be required to express the prerequisite battery of adhesion and co-stimulatory molecules.

Astrocytes were the first CNS cell type shown to be capable of expressing the MHC class II molecules required for antigen presentation to T-helper cells (Wong, Bartlett, Clark-Lewis, Battye *et al.*, 1984). In these *in vitro* experiments, Wong and colleagues demonstrated that supplementing astrocyte cultures with the cytokine IFN-γ induced the expression of MHC class II molecules by the cells. In contrast, TNF-α did not induce MHC class II expression when added to the astrocytes. When TNF-α was administered in conjunction with IFN-γ the expression of MHC class II molecules by the astrocytes was enhanced. These cytokines are commonly found in CNS inflammatory conditions, including, MS, HIV-associated dementia and in the brains of animals with EAE (Dong and Benveniste, 2001). Nevertheless, the expression of MHC class II molecules by astrocytes *in vivo* remains a controversial topic. Although intrathecal injection of IFN-γ does result in MHC class II expression by astrocytes, the presence of the molecules in disease states is equivocal with some researchers detecting their expression while others were unable to demonstrate MHC class II positive astrocytes (Shrikant and Benveniste, 1996).

Astrocytes have been shown to express adhesion molecules such as ICAM-1 and VCAM-1 when stimulated with a variety of cytokines, including TNF-α, IL-1β and IFN-γ, as well as LPS and viral proteins (Shrikant and Benveniste, 1996). It appears, however, that human astrocytes do not express the costimulatory molecules B7.1 or B7.2 either constitutively or following stimulation with IFN-γ. Contradictory findings have been generated with regard to the expression of these molecules by murine astrocytes in both *in vivo* and *in vitro* models. Some investigators report the constitutive expression of one or other of the molecules with up regulation or *de novo* expression following stimulation with IFN-γ or under disease conditions, while others could not detect the molecules either following IFN-

γ stimulation or in CNS inflammatory states (Dong and Benveniste, 2001). The expression of another costimulatory molecule, CD40, by astrocytes also remains controversial. Again some authors fail to detect CD40 expression in astrocyte cultures following IFN-γ stimulation, while others did observe the presence of the molecule (Aloisi *et al.*, 1998; Dong and Benveniste, 2001). In contrast to B7.1 and B7.2 it appears that human foetal astrocytes constitutively express CD40 which is upregulated following stimulation with TNF-α, IL-β, IFN-γ or LPS. However, the data taken from *in vivo* studies suggest that CD40 expression is confined to the microglial / macrophage population and does not occur on astrocytes (Dong and Benveniste, 2001).

At the present time, no definitive conclusions regarding the ability of astrocytes to present antigen to either activated or naïve T-cells can be drawn from the data available. If astrocytes cannot express the costimulatory molecules required to induce T-cells to proliferate and develop effector functions then, due to their ability to express MHC class II molecules it is possible that these cells induce a state of anergy in the T-cell population and effectively dampen immune reactions within the inflamed CNS.

3.1.3. CNS inflammation in disease states

Despite the 'immuno-priveledged' status of the brain many immune-mediated diseases of the CNS are now recognised that encompass a wide range of disease aetiologies. These conditions include those of a viral nature such as herpes simplex virus, polio, varicella zoster virus and HIV; many and varied bacterial agents; transmissible spongiform encephalopathies (TSE's); and fungal infections (Adams and Graham, 1998). In addition to the plethora of pathological agents that can cause CNS inflammatory reactions there are diseases associated with ageing such as Alzheimer's disease, Pick's disease and vascular dementia. There is also a diverse group of conditions known as the inflammatory demyelinating diseases of the CNS and perhaps the most well-known and commonly occurring inflammatory condition affecting the brain, multiple sclerosis (MS), belongs to this family of diseases (Bright and Sriram, 2001; Keegan and Noseworthy, 2002).

Over and above this array of CNS inflammatory conditions there are a wide range of parasitic infections that can produce severe immune responses within the CNS. These parasitic infections include *Plasmodium* spp., *Toxoplasma gondii,* as well as *Trypanosoma* spp. infections.

3.1.3.1. Trypanosome-induced CNS inflammation

It has been known for many years that chronic trypanosome infection leads to CNS invasion by the parasite and results in an inflammatory reaction within the brain. At present the mechanisms and pathways used by the trypanosomes to gain entry and become established within the CNS remain unclear. In animal models, parasites have been localised in the choroid plexus, circumventricular organs and peripheral ganglia, areas, as previously mentioned, where the BBB is weak (Schultzberg, Ambatsis, Samuelsson, Kristensson *et al.*, 1988). However, this has yet to be definitively established as the route of parasite invasion into the CNS since investigations employing rodent models suggest that the BBB becomes progressively damaged as the disease advances (Pentreath *et al.*, 1994; Philip *et al.*, 1994). In a rat model of trypanosome infection, fluorescent dye injected into the carotid artery could be detected in several brain areas, including, the thalamus and hypothalamus, by day 35 post-infection with *T.b.brucei*, indicating impairment of the BBB. By 40 days post-infection, this BBB damage had become extensive and the dye could be found throughout both the grey and the white matter of the cortex (Philip *et al.*, 1994). These studies suggest strongly that infection with trypanosome parasites has a direct effect on the function of the BBB that could ultimately leave the CNS vulnerable to insult and injury. In contrast to these findings it has been shown that the invasion of the CNS by trypanosome parasites does not necessarily result in an indiscriminate loss of tight junctions in the BBB (Mulenga, Mhlanga, Kristensson, and Robertson, 2001). The integrity of the tight junctions following trypanosome infection in rats was determined by demonstration of two tight junction proteins; occludin and zonula occludens 1, in brain sections using immunofluorescent histochemistry.

In humans, the CNS inflammatory reaction resulting from trypanosome infection develops as the disease progresses. Unfortunately, this reaction can be exacerbated by chemotherapy, and in 5-10% of treated patients leads to the generation of the post-treatment reactive encephalopathy (PTRE). The CNS inflammatory cell infiltrate is comprised of macrophages, T and B-lymphocytes and plasma cells. The inflammatory reaction is also associated with a widespread astrocytosis and diffuse microglial hyperplasia (Adams and Graham, 1998; Adams *et al.*, 1986; Molyneux *et al.*, 1996). The PTRE is characterised by an increase in the severity of this CNS inflammatory reaction and in some instances can take the form of an acute haemorrhagic leucoencephalopathy (Adams *et al.*, 1986).

Comparable CNS inflammatory reactions have been reported in primate models of the disease (Schmidt, 1983). Infiltration of the brain cerebral vessels by lymphocytes, plasma cells and macrophages has been described following *T.b.rhodesiense*-infections in vervet monkeys. Proliferation of the microglial cells in immediate proximity to the inflammatory infiltrates was also detected. However, a fully developed meningoencephalitis, with the presence of inflammatory cells in the neuropil was only identified in one out of 20 experimental animals. This author also found an equivalent degree of inflammation, in two additional monkeys during a separate series of experiments, following unsuccessful drug treatment of the trypanosome infection (Schmidt, 1983). The development of this meningoencephalitic reaction, resulting from ineffectual trypanocidal therapy has been noted in additional investigations (Poltera, Sayer, Brighouse, Bovell *et al.*, 1985). In this study moderate to severe perivascular cuffing, microglial activation and the presence of plasma cells in the neuropil were demonstrated following subcurative diminazene aceturate treatment of *T.b.rhodesiense*-infections in vervet monkeys.

A CNS inflammatory reaction has been reported in experimental infections of goats (Whitelaw, Moulton, Morrison, and Murray, 1985), cattle and dogs (Morrison *et al.*, 1983) following trypanosome infection. Again the main cell types constituting the inflammatory infiltrate were found to be lymphocytes, plasma cells and macrophages although differences in the distribution of the resulting lesions were present. The CNS inflammatory reaction observed in dogs was mainly confined to the choroid plexus and meninges, whereas, cattle and goats exhibited infiltration of the brain parenchyma by the inflammatory cells. However, since these dogs had received no trypanocidal therapy it is possible that a similar inflammatory pattern to that seen in the vervet monkey was present and subcurative treatment may have exacerbated the response producing a meningoencephalitis.

A similar pattern of cellular infiltration has also been described in rodent models of trypanosomiasis. *T.b.rhodesiense*-infection of NMRI-outbred mice has been shown to produce a chronic infection with the animals surviving for up to 9 weeks. A mild inflammatory infiltrate was detected in the brain connective tissue in animals killed 7 days after infection and the severity of the reaction increased as the disease progressed with a meningoencephalitis present in animals killed 4 weeks after infection (Fink and Schmidt, 1979). The inflammatory cells consisted of lymphocytes, plasma cells and macrophages. The study also found that the pattern of inflammatory cell infiltration in the CNS closely mirrored the invasion of the brain tissues by the parasites. In *T.b.brucei*-infections of OF1-outbred mice inflammatory changes were detected in the choroid plexus and meninges

from approximately 4 weeks after infection and in advanced cases perivascular cuffing was observed in meningeal and cerebral vessels. Again the cells comprising this infiltrate were lymphocytes, plasma cells and macrophages (Poltera, 1980). An analogous pattern of inflammatory changes was also present when this strain of mouse was infected with *T.b.gambiense* although this produced a more chronic infection, in some cases lasting for a 22 month period (Poltera, Hochmann, and Lambert, 1982).

It appears that the severity of the inflammatory response can be exacerbated in the murine CNS by subcurative drug treatment of the infection in the same manner as previously described in the vervet monkey and goat (Hunter and Kennedy, 1992; Jennings *et al.*, 1989). When NIH-inbred mice were infected with *T.b.brucei* a few inflammatory cells were found in the choroids plexus by 29 days post-infection. No significant perivascular cuffing was detected at this stage. However, if these mice were treated with a subcurative dose of diminazene aceturate on day 21 post-infection and then sacrificed at day 29 post-infection, encephalitic lesions and large perivascular cuffs consisting mainly of lymphocytes and macrophages were observed. The severity of this reaction was further increased by a second subcurative drug treatment following relapse of the mice to parasitaemia (Hunter, Jennings, Adams, Murray *et al.*, 1992). Despite the severity of the inflammatory response induced in the CNS, several of the studies described above make note of the relative lack of neuronal damage that results from the inflammatory cell infiltration of the brain parenchyma (Fink and Schmidt, 1979; Morrison *et al.*, 1983) .

Although the basic cellular components of the reaction are known, the kinetics of the inflammatory cell invasion and an assessment of the specific cell types involved have yet to be performed. Another common feature described in these animal models is the increased severity of the CNS inflammation observed following subcurative drug treatment. This is analogous to the situation found in human patients who develop the PTRE. Therefore, this study aims to map the course of events that result in the generation of the inflammatory reaction and to evaluate the level of CNS infiltration by $CD4^+$ and $CD8^+$ T-cell sub-sets, macrophages and B-lymphocytes. A time-course of the appearance of the inflammatory cells in the CNS together with the areas of the brain infiltrated by the cells will be determined following infection and induction of the PTRE.

3.2. Materials and methods

The main aim of the following investigation was to determine the kinetics of the infiltration, and subsequent distribution, of immune system cells within the CNS following trypanosome infection. Each stage of the CNS inflammatory response, from the initial mild inflammation through to the severe meningoencephalitis characteristic of the post-treatment reactive encephalopathy, was examined using the mouse model of human African trypanosomiasis previously described in Chapter 2.

3.2.1. Animals, infections and treatments

Female CD-1 mice (Charles River Breeding Laboratories) weighing 28-35g were infected with $2x10^4$ *T.b.brucei* parasites of cloned stabilate GVR/C1.6 as previously described. The complete mouse model is explained in detail in Chapter 2 of this thesis and mice were induced to simulate each stage of the response. To mirror acute stage infections the mice were killed at 7 and 14 days after infection, while animals killed on days 21 and 28 post-infection imitated the early CNS-stage of the disease. Further mice were treated on day 21 after infection with a subcurative dose of diminazene aceturate (40mg/kg i.p.) to induce a more severe CNS response. Groups of these drug treated animals were killed at 7 and 14 days following the diminazene aceturate treatment. The CNS reaction induced in these mice simulates the neuroinflammatory response found in patients with late-CNS stage infections. Additional mice were subcuratively drug treated and then allowed to relapse to parasitaemia before receiving a second diminazene aceturate treatment. These mice were killed at 7 and 14 days following the second subcurative trypanocidal drug treatment and mirror the pathological reaction found in human patients who have died from the PTRE.

The complete experiment was performed in duplicate. On both occasions, each of the levels of inflammation was induced in a separate group of mice. Each of the individual experimental groups was comprised of six animals in total.

3.2.2. Sample preparation and staining

At scheduled points during the experimental procedures mice were killed by cardiac perfusion with sterile saline while under terminal anaesthesia. The brains were then dissected and either placed into 5% neutral buffered formalin for processing to paraffin or

30% sucrose in PBS for cryoprotection before snap freezing for cryostat sectioning (See Chapter 2).

3.2.2.1. Paraffin sections

To allow the severity of the immune reaction within the CNS to be assessed, paraffin sections of 3μm thickness were stained using the standard histological haematoxylin and eosin (H&E) staining method. The severity of the neuropathological response was graded, as described in Chapter 2, in sections prepared from each animal. To investigate the degree of astrocyte activation and lymphocyte infiltration additional sections were prepared from a representative portion of the blocks and stained using the immunocytochemistry (ICC) procedure again described in Chapter 2. The reagents utilised on these paraffin sections were anti-glial fibrillary acidic protein (GFAP) (DAKO), anti-B220 (Serotec) and anti-CD3 (DAKO) (Table 2.2). These antibodies will specifically react with GFAP, the intermediate filament protein of astrocytes; the high molecular weight, 220kD fragment, of the CD45 antigen expressed by B-cells; and the CD3 cell surface marker commonly found on all T-cells respectively. The timing of the appearance of these cells and their distribution throughout the brain was investigated.

3.2.2.1.1. Neuropathology grading scale

Haematoxylin and eosin stained paraffin embedded sections were used to assess the severity of the inflammatory reaction induced in the CNS at each of the different stages of the animal model. The severity of the response was graded on a scale of 0-4 where 0 indicates a normal pathology with no signs of inflammatory changes and 4 signifies a severe meningoencephalitic response with the presence of inflammatory cells in the neuropil. This scale is described in detail in Chapter 2 and the inflammatory criteria are listed in Table 2.1 of this thesis. The severity of the reaction in each section was graded independently by two assessors in a blinded fashion. The sections were examined at a magnification of 200 fold and the criteria described in the grading scale (Table 2.1) considered before a neuropathology score was assigned.

3.2.2.2. Frozen sections

Sections were prepared at a thickness of 10μm from cryoprotected snap frozen mouse brains. The sections were air dried and fixed for 10 minutes in cold acetone before storage

at -20^0C until required for ICC staining. Using frozen sections it was possible to quantify the levels of T-helper and T-cytotoxic cells infiltrating the CNS as the reaction developed. The reagents used to determine the degree of infiltration of the brain by the T-cell sub-sets were anti-$CD4^+$ and anti-$CD8^+$ monoclonal antibodies (Pharmingen). The anti-$CD4^+$ antibody binds specifically to the $CD4^+$ cell surface marker found on T-helper cells while the anti-$CD8^+$ antibody specifically reacts with the $CD8^+$ cell surface marker found on T-cytotoxic cells. The progress of macrophage infiltration into the CNS was also examined using ICC of frozen sections. In this instance the antibody employed was F4/80 (Serotec). This recognises a 160kD plasma membrane component found on mature macrophages. The timing of the infiltration and the areas of the brain invaded by the inflammatory cells were monitored at each stage throughout the development of the neuroinflammatory response. Further details on this technique and the antibodies employed are described in Chapter 2 and Table 2.2.

3.2.2.2.1. Quantification of $CD4^+$ and $CD8^+$ cell infiltration

The number of positively stained $CD4^+$ and $CD8^+$ cells was counted at a 200-fold magnification under light microscopy. To standardise the area of the brain assessed a 100 square grid, fitted into the eyepiece of the microscope, was used. Cell numbers were determined by counting the total number of stained cells in 5 separate areas of the meninges, one area of the corpus callosum, and two areas of the external capsule, caudate putamen and cerebral cortex. The average of the cell counts for each area was then calculated and the cell counts were converted and expressed as the number of cells per mm^2 of tissue. The cellular infiltration of these particular brain areas was assessed as they form representative, idenitifiable, regions within the area of the CNS investigated. In addition, inflammatory changes are known to occur in these discrete regions, and, although not assessed individually, these regions form the basic composition of the sections used for grading the severity of the neuroinflammation as described in Chapter 2, Table 2.1.

3.2.3. Statistical analyses

All statistical tests were undertaken using the proprietary statistical software package, Minitab version 13, and P-values of less than 0.05 were considered significant. Means and standard errors (S.E.) are shown as summary statistics.

3.2.3.1. Grading of neuropathological response

Comparisons were made between groups of animals to assess the differences in the level of CNS inflammation following induction of a CNS inflammatory response by trypanosome infection and sub-curative diminazene accturate treatment. The severity of the reaction was analysed in mice killed at 7-day intervals after infection until day 28 post-infection. In addition the neuropathological reaction was measured in mice killed at 7 and 14 days following a single subcurative diminazene aceturate treatment and 7 and 14 days following a second diminazene aceturate treatment. The neuropathological scores for the individual mice were based on the average of two independent assessor scores. A Wilcoxon signed rank test was employed to ensure that the independent gradings were assigned in a uniform manner and were not biased by the individual assessor. Analyses were possible using parametric statistical tests. Comparisons across experiments were performed using general linear model procedures and the randomised block analyses of variance.

3.2.3.2. Assessing T-cell infiltration

The pattern of $CD4^+$ and $CD8^+$ cell infiltration into five separate brain areas was assessed in the groups of mice outlined above. To permit parametric tests to be employed in the analyses, the resulting data were transformed and the natural logarithm of the data set, as suggested by the Box-Cox test, was used in subsequent analyses. Differences between the treatment groups for each of the brain areas studied were identified using a one-factor analysis of variance technique followed by Tukey's procedure to obtain individual p-values for each of the pairwise comparisons and their associated 95% confidence intervals. Differences between the brain areas for each of the treatment groups were similarly identified, however, in this case two-factor analysis of variances were used to take account of measurements from the same mice for each area assessed. All analyses were carried out using general linear model procedures.

3.3. Results

3.3.1. Assessment of the severity of the neuropathological response

Histopathological examination of brain sections prepared from animals killed at various points during the mouse model of human African trypanosomiasis showed inflammatory cell infiltration beginning in the meninges and ventricles. The severity of this inflammation worsened as the disease progressed. Perivascular cuffing of the cerebral vessels was commonly found and the infection culminated with the development of a severe meningoencephalitis. The inflammatory cells present throughout were mainly composed of lymphocytes and macrophages. Plasma cells became common as the inflammation developed, however neutrophils were rarely present in the infiltrate (Fig. 3.1).

Two individual assessors independently graded the severity of the neuropathological response of mice to the trypanosome infection using the grading scale described in Table 2.1. The results of a Wilcoxon signed rank test demonstrated that there was no evidence of a difference between the neuropathology grades measured by the individual assessors and that the grading scale had been applied uniformly. Therefore it was possible to use an average of the two grades in all subsequent analyses. A summary of these results can be found in Table 3.1.

Analyses of the neuropathological response data using general linear model procedures showed that there was no significant difference ($p=0.235$) between the results gained from each individual experiment. The analyses also determined that there was a significant difference ($p<0.001$) in the severity of the inflammatory reactions induced by the individual treatment regimens. To determine where the individual difference lay, one way analysis of variance procedures were performed and individual p-values and confidence intervals determined using Tukey's pair wise comparisons multiple range test. A summary of the results of the statistical analysis is detailed in Table 3.1.

3.3.1.1. Acute and early-stage CNS infections

Brain sections, prepared from *T.b.brucei*-infected mice, killed at 7 and 14 days post-infection, to mimic the acute stages of trypanosome infection, and 21 and 28 days post-infection to imitate the early-stage CNS infection, were examined under light microscopy. No gross inflammatory changes were seen in animals at 7 days post-infection and these mice showed a neuropathology grade of 0.375 $\pm$ 0.072 (mean $\pm$ S.E.). By 14 days after infection a few animals displayed a slight increase in the cellularity in the meninges and ventricles and this returned only a very minor increase in the pathology score (0.417 $\pm$ 0.077). This increase was not statistically significant (p=1.000). The degree of neuroinflammation found in animals killed at 7 and 14 days post-infection was not significantly increased (p=0.3411, p=0.201 respectively) from neuropathological grading scores of the uninfected control animals (0.033 $\pm$ 0.023).

The severity of the neuroinflammation seen in animals killed at 21 days post-infection (1.021 $\pm$ 0.129) was significantly higher than the response found in mice killed at the earlier, 7 and 14-day time points (p=0.003, p=0.006 respectively). By 28 days post-infection the severity of the inflammatory response (1.477 $\pm$ 0.186) was again significantly more severe that that seen in animals killed at 7 and 14 days after infection (p<0.0001). The severity of the response in these animals was also increased compared to that found in mice 21 days following infection. However, this increase was not significant (p=0.122). The neuropathological grading score attributed to animals killed at both 21 and 28-days post-infection was significantly (p<0.0001) higher than that assigned to the uninfected control mice.

The neuroinflammatory response occurring during the acute and early-CNS stages of the infection were significantly (p<0.0001) less severe than the reaction seen following the induction of the late-CNS stage of the disease and the PTRE.

3.3.1.2. Late-stage CNS infections and the PTRE

Sections were appraised from animals killed at 7 and 14 days following a single subcurative diminazene aceturate treatment to simulate the situation found in late-stage CNS infections and 7 and 14 days after a second diminazene aceturate treatment to mirror the reaction found in the PTRE.

Mice killed at 7 days following a single diminazene accturate treatment showed a neuropathology score of 2.833 ± 0.117 while the response in those animals killed after 14 days was 2.886 ± 0.123. The severity of the reaction found in animals killed at 7 and 14 days following a second diminazene aceturate treatment was 3.281 ± 0.010 and 3.375 ± 0.189 respectively. Although higher than those found in mice receiving only one trypanocidal drug treatment this increase was not considered significant. However, the severity of the neuropathological response in all groups of animals mirroring either the late-CNS stage of infection or the PTRE were significantly ($p<0.0001$) higher than those measured in the acute and early-CNS stage infections or uninfected mice.

3.3.2. Inflammatory cell infiltration and astrocyte activation

3.3.2.1. T-lymphocyte infiltration

The presence of helper ($CD4^+$) and cytotoxic ($CD8^+$) T-lymphocytes within the brain of trypanosome-infected and subcuratively treated mice was investigated in a quantitative manner. The cellular infiltration pattern in the meninges, corpus callosum, external capsule, caudate putamen and cerebral cortex was assessed and analysed using the statistical methods outlined previously (Chapter 3, materials and methods). All cell counts are expressed as the number of cells per mm^2 of tissue. Summary data comparing $CD4^+$ and $CD8^+$ cell infiltration is detailed in Tables 3.2-3.7 while summary data outlining the temporal and spatial pattern of either $CD4^+$ or $CD8^+$ cell infiltration is given in Tables 3.8-3.31.

3.3.2.1.1. Comparison of $CD4^+$ and $CD8^+$ cell infiltration

When the cell counts assessed in five brain areas; meninges, corpus callosum, external capsule, caudate putamen and cerebral cortex, were combined (Table 3.2), no T-cells were detected in uninfected mice (data not shown) or in animals killed at 7 days post-infection. Small numbers of both $CD4^+$ [0.1.420 ± 1.170 (mean ± S.E.)] and $CD8^+$ (0.700 ± 0.490) T-cells were found infiltrating the CNS by 14 days post-infection. Although the number of $CD8^+$ cells was lower than $CD4^+$ cells the difference between the cell counts was not significant at this point in the infection ($p=0.685$). By day 21 post-infection the numbers of both $CD4^+$ (8.790 ± 1.950) and $CD8^+$ (0.938 ± 0.938) cells had increased with the $CD4^+$ cell count remaining higher than that of the $CD8^+$ cell count, the difference between the

two cell counts at this stage in the infection was significant (p=0.040). On day 28 following infection a mean of 25.540 ± 5.660 $CD4^+$ cells were detected while a significantly (p=0.031) lower number of $CD8^+$ cells was found (6.110 ± 2.080). Following exacerbation of the CNS reaction by administration of a single diminazene aceturate treatment the population of both T-cell subsets increased. In animals killed 7 days following the diminazene aceturate treatment 255.800 ± 76.900 $CD4^+$ cells were detected in the brain areas studied and 31.100 $CD8^+$ cells were found. No standard error was calculated for this group of mice as only one animal provided a $CD8^+$ cell count for all the brain areas investigated at this time-point in the infection and subsequently no significant difference was detected (p=0.164). By 14 days after the administration of the drug 335.700 ± 48.500 $CD4^+$ cells and 91.400 ± 2.950 $CD8^+$ cells were detected. The number of $CD4^+$ cells found in animals killed following this treatment regimen was significantly higher than the number of $CD8^+$ cells detected (p<0.0001). To mirror the neuropathological reaction found in the PTRE, the severity of the CNS response was further increased by the administration of a second diminazene aceturate treatment. The numbers of $CD4^+$ (293.600 ± 14.800) and $CD8^+$ (60.240 ± 5.400) cells detected in mice killed 7 days after the drug treatment remained similar to those found in animals at 14 days following a single diminazene aceturate treatment. By 14 days after administration of the second dose of diminazene aceturate the cell numbers had increased with 457.400 ± 74.100 $CD4^+$ cells found and 105.300 ± 27.800 $CD8^+$ cells detected. The infiltration of $CD4^+$ cells at both 7 and 14 days following the induction of the PTRE was significantly higher than the level of $CD8^+$ cell infiltration (p=0.0001, p=0.042 respectively).

When the infiltration pattern of $CD4^+$ and $CD8^+$ cells into the meninges was examined a similar situation to that seen in the whole brain was found (Table 3.3). No T-cells were detected before day 14 post-infection at which point 1.370 ± 1.210 $CD4^+$ cells and 0.700 ± 0.490 $CD8^+$ cells were found. Although the number of $CD8^+$ cells was smaller than $CD4^+$ cells this was not significantly lower at this time-point in the infection (p=0.693). By day 21 post-infection an increased presence of both cell types was detected and the difference between the numbers of $CD4^+$ (7.330 ± 1.970) and $CD8^+$ cells (0.938 ± 0.938) showed borderline significance (p=0.051). On day 28 post-infection a significant (p=0.045) difference between the number of infiltrating $CD4^+$ cells (18.330 ± 6.140) and $CD8^+$ cells (4.440 ± 1.290) was detected. Animals killed 7 days after exacerbation of the reaction showed a mean $CD4^+$ cell infiltration of 110.300 ± 58.200 while a lower, but not significantly reduced (p=0.085), number $CD8^+$ cells were detected (17.080 ± 7.720). By 14 days after the drug treatment a highly significant difference (p<0.0001) was found between the numbers of cells present from the $CD4^+$ (193.300 ± 27.500) cell and $CD8^+$

(39.950 ± 2.870) cell subsets. This highly significant difference ($p<0.0001$) in infiltration pattern was also found in mice killed 7 days following the induction of the PTRE when 180.380 ± 6.780 $CD4^+$ cells and 32.690 ± 4.790 $CD8^+$ cells were detected. A further increase in the level of $CD4^+$ (238.400 ± 52.800) and $CD8^+$ (36.400 ± 10.100) cell infiltration was by 14 days after the second diminazene aceturate treatment with the number of $CD4^+$ cells remaining significantly ($p=0.026$) higher than the number of $CD8^+$ cells.

No T-cell infiltration of the corpus callosum was detected until day 14 post-infection. At this time only a very small population of $CD4^+$ cells were found (0.050 ± 0.050) and no $CD8^+$ cells were present (Table 3.4). By day 21 post-infection a slight increase in $CD4^+$ cell (0.333 ± 0.220) infiltration was seen and $CD8^+$ cells (0.167 ± 0.167) were detected. The difference in cell numbers between these two T-cell subsets was not significant on either day 14 or day 21 post-infection ($p=0.347$, $p=0.5484$ respectively). On day 28 post-infection the number of $CD4^+$ cells (1.875 ± 0.402) found was significantly ($p=0.041$) higher than that of $CD8^+$ cells (0.417 ± 0.300). When the animals were treated with a single diminazene aceturate an increase in the infiltration of the corpus callosum by both T-cell subsets was detected. By 7 days following the drug treatment the number of $CD4^+$ cells had risen to 28.250 ± 4.250 and the number of $CD8^+$ cells had increased to 7.630 ± 2.620. The difference in T-cell subset population was not significant ($p=0.068$) at this time. However by 14 days after the administration of the drug the number of $CD4^+$ cells (48.410 ± 7.800) was significantly ($p=0.008$) higher than the number of $CD8^+$ cells (22.020 ± 3.790) detected. Mice killed 7 days after the induction of the PTRE showed a further increase in $CD4^+$ cell (54.300 ± 11.700) and $CD8^+$ cell (11.740 ± 1.690) infiltration with $CD4^+$ cell numbers remaining significantly ($p=0.002$) higher than $CD8^+$ cell numbers. By 14 days after the administration of the second diminazene aceturate treatment the number of $CD4^+$ cells had risen to 63.900 ± 12.300. The $CD8^+$ cell count at this point was 27.540 ± 7.110 and was not considered to be significantly ($p=0.120$) lower than that of the $CD4^+$ cells.

When the T-cell infiltration of the external capsule was examined no cellular infiltration was detected until 21 days post-infection (Table 3.5). At this time the cell count for both $CD4^+$ and $CD8^+$ cells was 0.833 ± 0.833. By 28 days post-infection both the $CD4^+$ (4.583 ± 0.417) and the $CD8^+$ (1.250 ± 0.722) cell count had increased. The difference in infiltration levels between these T-cell subsets showed a borderline level of significance ($p=0.052$) at this time. On exacerbation of the CNS response a further increase in $CD4^+$ (48.520 ± 3.120) and $CD8^+$ (12.287 ± 0.000) cell numbers was detected and the difference

in these two populations was again of marginal significance (p=0.053). By 14 days after receiving a single diminazene aceturate treatment the level of $CD4^+$ (61.880 ± 8.520) cell infiltration was significantly (p=0.002) higher than that of the $CD8^+$ (23.630 ± 3.210) T-cell subset. When the animals were treated with a second dose of diminazene aceturate, to induce an extremely severe meningoencephalitis, the infiltration pattern similar to that found 7 days following a single diminazene aceturate treatment was seen with 40.160 ± 5.460 $CD4^+$ cells and 12.030 ± 1.180 $CD8^+$ cells detected. By 14 days after induction of the PTRE the $CD4^+$ cell population had raised to 69.380 ± 1.250 while the $CD8^+$ cell number was 25.00 ± 5.00. The $CD4^+$ cell count, remained significantly higher than the $CD8^+$ cell count, at both time-points following the administration of the second diminazene aceturate dose (p=0.0004, p=0.035 respectively).

Only very few T-cells were found to in the caudate putamen during the acute and early CNS stage of trypanosome infection (Table 3.6). No T-cells were detected until day 21 post-infection when 0.250 ± 0.250 cells of each cell subset, $CD4^+$ and $CD8^+$, were found. On day 28 post-infection a slight increase in the number of $CD4^+$ (0.750 ± 0.520) cells was seen but no $CD8^+$ cells were detected at this time. The difference between $CD4^+$ and $CD8^+$ cell infiltration was not significant at either 21 or 28 days post-infection (p=1.000, p=0.830 respectively). Following a single diminazene aceturate treatment the number of $CD4^+$ cells found in the caudate putamen increased to 19.780 ± 6.340 and 3.094 ± 0.281 $CD8^+$ cells were detected. The levels of $CD4^+$ (19.130 ± 9.340) and $CD8^+$ (3.710 ± 1.440) cell numbers remained similar in mice killed at 14 days after administration of the drug. At both time-points after exacerbation of the CNS response the $CD4^+$ cell count was significantly higher than the $CD8^+$ cell count (p=0.039, p=0.033 respectively). Seven days following the induction of the PTRE by administration of a second diminazene aceturate treatment 13.310 ± 1.130 $CD4^+$ cells and 2.453 ± 0.736 $CD8^+$ cells were detected. Again the $CD4^+$ population was significantly (p=0.003) greater in number than that of the $CD8^+$ cells. By 14 days after the drug treatment $CD4^+$ (24.310 ± 9.060) cell numbers were no longer significantly (p=0.331) higher than $CD8^+$ (10.440 ± 6.060) cell counts.

The infiltration of the cerebral cortex by $CD4^+$ and $CD8^+$ cells was also assessed (Table 3.7). A very occasional $CD4^+$ cell (0.042 ± 0.042) was detected in the cortex on day 21 post-infection. No $CD8^+$ cells were found at this time. The difference between these two populations was not significant (0.374) on day 21 post-infection. Neither $CD4^+$ nor $CD8^+$ cells were detected on day 28 post-infection. On exacerbation of the CNS response an increase in the detection of both $CD4^+$ (6.750 ± 0.000) and $CD8^+$ (2.250 ± 0.000) was found and this rise continued on day 14 after the administration of the drug with 12.790 ±

3.950 $CD4^+$ cells and 3.100 ± 0.816 $CD8^+$ cells found at this time. The number of $CD4^+$ cells counted in the cortex of these mice was significantly (p=0.013) higher than the number of $CD8^+$ cells present. When a severe meningoencephalitis was induced in the mice the number of $CD4^+$ (4.430 ± 1.600) was not significantly (p=0.098) higher than the number of $CD8^+$ (1.328 ± 0.465) cells by 7 days after administration of the second dose of diminazene aceturate. However, if the mice were killed at 14 days after receiving the drug a significantly (p= 0.011) higher level of $CD4^+$ (16.340 ± 1.220) cell infiltration compared with $CD8^+$ (5.969 ± 0.469) cell infiltration was detected in the cortex of the animals.

3.3.2.1.2. Pattern of $CD4^+$ cell infiltration

Following trypanosome infection a few $CD4^+$ cells (1.370 ± 1.120) were detected in the meninges 14 days after infection (Table 3.8). The number of $CD4^+$ cells increased as the infection progressed through days 21 and 28 post-infection (7.330 ± 1.970, 18.330 ± 6.140 respectively). This increased number of cells was not considered significantly higher than found at early time-points in the infection. Seven days following the exacerbation of CNS reaction the $CD4^+$ cell (110.300 ± 58.200) number showed a further increase. The infiltration of the meninges by $CD4^+$ cells at this time was significantly more substantial than that found during the acute and early-CNS stages of the reaction (p<0.0001, p<0.0001, p=0.0001 and p=0.0003 respectively). The $CD4^+$ cell (193.300 ± 27.500) count increased further in mice killed 14 days following the administration of a single diminazene aceturate treatment. This was again significantly higher than the infiltration levels encountered in the animals killed before diminazene aceturate administration (p<0.0001, p<0.0001, p<0.0001, p=0.0001) but was not considered significantly different to the cell count assessed in mice killed 7 days after the drug treatment (p=0.990). In animals killed 7 days after the induction of the PTRE, 180.380 ± 6.780 $CD4^+$ cells were detected in the meninges. This was significantly higher than the cell count detected in the acute and early CNS-stages of the infection (p<0.0001, p<0.0001, p=0.0001 and p=0.0004) but was not changed significantly from animals in which the late-CNS stage of the disease had been induced (p=0.993, p=1.000). By 14 days after the administration of the second diminazene aceturate treatment the $CD4^+$ cell count had increased to 283.400 ± 25.800. Although this was considered significantly higher than the infiltration seen in animals at 7, 14, 21 and 28 days post-infection (p<0.0001, p<0.0001, p< 0.0001, and p=0.0001) the increase cell count was not significantly higher than that resulting from the induction of the late-stage CNS reaction or that found 7 days following the induction of the PTRE (p=0.999, p=0.901, p=0.929).

A similar overall pattern of $CD4^+$cell infiltration was found in the corpus callosum (Table 3.9). However in this area of the brain, $CD4^+$ cell counts (1.875 $\pm$ 0.402) from animals killed at 28 days post-infection were significantly higher than those found in mice at earlier time-points in the infection (p=0.0002, p=0.0004, p=0.016). This difference was not apparent in the meninges. Following the induction of the late-CNS stage of the infection and the PTRE an increased $CD4^+$ cell count was found. The infiltration level of the corpus callosum by $CD4^+$ cells at each of these times was significantly higher than that encountered in the acute and early-CNS stages of the disease (p<0.0001 in each case). Although an increase in $CD4^+$ cell infiltration was found in animals with the PTRE compared to those with late-CNS stage infections, this rise in cell number was not considered significant.

When $CD4^+$ cell infiltration of the external capsule was investigated an analogous pattern to that found in the corpus callosum was seen (Table 3.10). Again animals killed on day 28 post-infection showed a significantly higher $CD4^+$ cell (4.583 $\pm$ 0.417) infiltration than that seen in the mice killed at the earlier time-points (0.0001, p<0.0001, p=0.0005). Following induction of the late-stage CNS response and the PTRE the number of $CD4^+$ cells infiltrationg the corpus callosum increased significantly compared with all animals killed during the acute and early-stage CNS infections (p<0.0001 in each case). No significant changes were apparent between any of the groups of mice killed during the late-CNS stage of the infection or the PTRE.

An investigation of the $CD4^+$ cell infiltration of the caudate putamen (Table 3.11) showed a pattern similar to that found in the meninges where no significant changes were detected between groups of animals killed during the acute and early-CNS stage of the disease. Mice killed 7 days after administration of a single diminazene aceturate treatment displayed increased levels of $CD4^+$ cells in the caudate putamen which were significantly higher than the cell count found during the acute and early-CNS stage of the infection (p<0.0001, p<0.0001, p=0.0001, p=0.0003). The cell count found at 14 days after the drug treatment remained significantly higher than that measured in the earlier groups (p<0.0001, p<0.0001, p<0.0001, p=0.0001). When the PTRE was induced, by treating relapsed mice with a second dose of diminazene aceturate, $CD4^+$ cell counts in animals killed at 7 (p<0.0001, p<0.0001, p=0.0001, p=0.0004) and 14 (p<0.0001, p<0.0001, p<0.0001, p=0.0001) days after the drug treatment remained significantly higher than that seen during the acute and early-CNS stages of the disease. Again no significant differences were detected between the $CD4^+$ cell counts in the caudate putamen from any group of animals following the induction of the late-CNS stage of the infection or the PTRE.

This pattern was again followed in the $CD4^+$ cell infiltration of the cerebral cortex (Table 3.12). Only a very occasional $CD4^+$ cell was detected during the acute and early-CNS infections and no significant differences were found between these groups. Seven days after exacerbation of the CNS reaction, by administration of a subcurative diminazene aceturate dose, the $CD4^+$ cell (6.750 ± 0.000) number was significantly higher than that seen in all groups of animals killed previously ($p<0.0001$, $p<0.0001$, $p=0.0002$, $p=0.0001$). The $CD4^+$ cell (12.790 ± 3.950) count increased in animals killed at 14 days after administration of the drug and remained significantly higher than that found during the acute and early-CNS stages of the infection ($p<0.0001$ in all cases). In mice killed 7 days following the induction of the PTRE the $CD4^+$ cell (4.430 ± 1.600) remained significantly higher than that seen in the acute and early-CNS stage mice ($p=0.0002$, $p=0.0002$, $p=0.001$, $p=0.0007$) but was reduced compared to that found in animals at 14 days after induction of the late-CNS stage reaction. The reduction in $CD4^+$ cell infiltration showed a borderline significance level ($p=0.052$) when compared to this group of late-CNS stage animals. By 14 days after the induction of the PTRE the $CD4^+$ (16.340 ± 1.220) cell infiltration had again increased and was significantly higher than that seen in groups of mice killed during the acute and early CNS-stage of the infection ($p<0.0001$ in each case). In addition, the $CD4^+$ cell count seen in the cerebral cortex at this time was shown to be significantly higher than that found in animals killed at 7 days following the induction of the PTRE ($p=0.017$).

Differences in the infiltration pattern of $CD4^+$ cells between each brain area, following the various treatment regimens, were also examined. No $CD4^+$ cells were detected in any of the areas at 7 days post-infection. At 14 days post infection (Table 3.13) a few cells were apparent in the meninges and corpus callosum but no significant differences between the $CD4^+$ cell population infiltrating each area were found at this time. In animals killed on day 21 post-infection (Table 3.14) the $CD4^+$ cell (7.330 ± 1.970) count in the meninges was significantly higher than that found in the corpus callosum (0.333 ± 0.220), external capsule (0.833 ± 0.833), caudate putamen (0.250 ± 0.250) and cerebral cortex (0.042 ± 0.042) with p-values of 0.002, 0.003, 0.001, 0.001 respectively. At day 28 post-infection (Table 3.15) this significant increase in $CD4^+$ population in the meninges (18.330 ± 6.140) compared with the remaining brain areas was still apparent ($p=0.002$, $p=0.028$, $p=0.0003$, $p=0.0001$). The level of $CD4^+$ cells in the cerebral cortex (0.000 ± 0.000) at this time was significantly lower that seen in the corpus callosum (1.875 ± 0.402) and the external capsule (4.583 ± 0.417) ($p=0.046$, $p=0.003$ respectively). In addition, the external capsule showed a significantly ($p=0.018$) higher $CD4^+$ count than that found in the caudate putamen (0.750 ± 0.520).

Following the exacerbation of the CNS response, to mirror the late-stage CNS disease, $CD4^+$ cells were detected in all brain areas. The number of $CD4^+$ cell found in the meninges (110.300 ± 58.200) 7 days after the induction of the reaction (Table 3.16) was significantly higher than that seen in the corpus callosum (28.250 ± 4.250), caudate putamen (19.780 ± 6.340) and cerebral cortex (6.750 ± 0.000) (p=0.037, p=0.018, p=0.004 respectively). No significant difference (p=0.138) was detected between the $CD4^+$ count in the meninges and the external capsule (48.520 ± 3.120) at this time. By 14 days after the administration of a single diminazene aceturate treatment (Table 3.17) the meninges (193.3000 ± 27.500) showed a significantly higher $CD4^+$ cell level than the corpus callosum (48.410 ± 7.800), external capsule (61.880 ± 8.520), caudate putamen (19.310 ± 9.340) and cerebral cortex (12.790 ± 3.950) with p-values of 0.0005, 0.003, <0.0001 and <0.0001 respectively. The number of $CD4^+$ cells found in the corpus callosum and external capsule was significantly higher than that found in the caudate putamen (p=0.002, p=0.0003 respectively) and cerebral cortex (p=0.004, p=0.0001 respectively).

Seven days following the induction of the PTRE (Table 3.18), the $CD4^+$ population in the meninges (180.380 ± 6.780) was significantly higher than the number of $CD4^+$ cells found in the corpus callosum (54.300 ± 11.700), external capsule (40.160 ± 5.460), caudate putamen (13.310 ± 1.130) or cerebral cortex (4.430 ± 1.600) (p=0.022, p=0.003, p=0.0001, p<0.0001 respectively). The $CD4^+$ population in the corpus callosum was not significantly different to that seen in the external capsule (p=0.842), but was significantly higher than that found in the caudate putamen (p=0.016) and the cerebral cortex (p=0.0002). This situation was also apparent in the external capsule, which showed a higher $CD4^+$ cell infiltration of borderline significance than the caudate putamen (p=0.056) and a significantly higher $CD4^+$ count than that seen in the cerebral cortex (p=0.0005). The presence of $CD4^+$ cells in the caudate putamen was found to be significantly greater than the $CD4^+$ infiltration seen in the cerebral cortex (p=0.044) at this time. By 14 days after the induction of the severe meningoencephalitis (Table 3.19) the $CD4^+$ population in the meninges (138.400 ± 52.800) remained significantly higher than in the corpus callosum (63.900 ± 12.300), external capsule (69.380 ± 1.250), caudate putamen (24.310 ± 9.060) and cerebral cortex (16.340 ± 1.220) (p=0.009, p=0.013, p=0.001, p=0.0009 respectively). In addition, the infiltration level found in the corpus callosum and the external capsule was higher than that seen in the caudate putamen (p=0.040, p=0.029 respectively and the cerebral cortex (p=0.016, p=0.012 respectively).

3.3.2.1.3. Pattern of $CD8^+$ cell infiltration

Following trypanosome infection a few $CD8^+$ cells (0.700 ± 0.490) were detected in the meninges at 14 days after the infection (Table 3.20). The number of $CD8^+$ cells in the meninges increased on days 21 (0.938 ± 0.938) and 28 (4.440 ± 1.290) post-infection as the infection progressed. On day 28 post-infection the level of $CD8^+$ infiltration was significantly higher than that seen at either 7 days post-infection ($p=0.0008$) or 14 days post-infection ($p=0.013$) but was not increased significantly compared with animals killed at day 21 post-infection ($p=0.142$). When the late-CNS stage of the infection was induced by a subcurative diminazene aceturate treatment a further increase in $CD8^+$ cell (17.080 ± 7.720) infiltration was found. This was significantly higher than the level seen in animals at 7 ($p<0.0001$), 14 ($p<0.0001$) or 21 ($p=0.0003$) days post-infection, not significantly altered compared with animals killed on day 28 post-infection ($p=0.070$). By 14 days after the drug treatment the $CD8^+$ cell (38.950 ± 2.870) number was significantly higher than that found in all groups of mice killed during the acute and early-CNS stage of the disease ($p0.0001$, $p<0.0001$, $p<0.0001$, $p=0.0001$) but was not altered compared to mice killed 7 days after exacerbation of the CNS reaction ($p=0.090$). Following the induction of the PTRE by administration of a second dose of diminazene aceturate, animals killed 7 days following the drug treatment showed a $CD8^+$ cell count of 32.690 ± 4.790. This count was again significantly higher than that witnessed in the acute and early-CNS stage infections ($p<0.0001$, $p<0.0001$, $p<0.0001$, $p=0.0003$). By 14 days after the induction of the PTRE the $CD8^+$ level (36.400 ± 10.100) remained significantly elevated compared with animals killed on days 7, 14, 21 and 28 post-infection ($p<0.0001$, $p<0.0001$, $p<0.0001$, $p=0.0001$). No significant changes in the $CD8^+$ cell infiltration in the meninges were detected between groups of animals killed following the induction of the late-stage CNS response or the PTRE.

Infiltration of the corpus callosum by $CD8^+$ cells was not detected until day 21 post-infection when a small number of cells was counted (0.167 ± 0.167) (Table 3.21). This increased slightly on day 28 post-infection (0.417 ± 0.300). No significant alterations in the $CD8^+$ cell population were detected in any of the groups of mice killed during the acute or early-CNS stage of the infections. A rise in the level of $CD8^+$ cell (7.630 ± 2.620) infiltration was found in animals killed 7 days after exacerbation of the CNS response. The $CD8^+$ cell count measured in these mice was significantly higher than that seen in any of the groups killed during the acute or early-CNS stage of the infection ($p<0.0001$ in all cases). A further increase in $CD8^+$ cell (22.020 ± 3.790) count was found in animals killed

14 days after the administration of a single diminazene aceturate treatment. The $CD8^+$ population in the corpus callosum of these mice was significantly higher than in animals killed at 7, 14, 21, and 28 days post-infection ($p<0.0001$ in all cases) and that found in mice killed at 7 days after the induction of the late-CNS stage response ($p=0.005$). The $CD8^+$ cell (11.740 ± 1.690) count in animals killed 7 days following the induction of the PTRE was not significantly different to that found in either group of mice exhibiting the late-CNS stage of the infection ($p=0.636$, $p=0.072$ respectively) but was significantly higher than the acute and early-CNS stage groups ($p<0.0001$ in all cases). By 14 days after the induction of the PTRE the $CD8^+$ cell (27.540 ± 7.11) count was significantly raised compared with mice killed at 7, 14, 21, and 28 days post-infection ($p<0.0001$ in all cases) as well as mice killed at 7 days after administration of a single diminazene aceturate treatment ($p=0.003$) and mice killed 7 days after the induction of the PTRE ($p=0.037$).

When the $CD8^+$ cell infiltration pattern of the external capsule was examined no cells were detected until day 21 post-infection when a few $CD8^+$ cells (0.833 ± 0.833) were counted (Table 3.22). The number of $CD8^+$ cells (1.250 ± 0.722) detected increased slightly by day 28 post-infection. No statistically significant changes were found in the $CD8^+$ cell numbers between groups of mice killed during the acute of early-CNS stage of the infection. A further rise in the $CD8^+$ cell (12.287 ± 0.000) population was seen in mice killed 7 days following the exacerbation of the CNS reaction. The cell count seen in these animals was significantly higher that that found in mice killed during the acute and early-CNS stage of the disease ($p<0.0001$, $p<0.0001$, $p=0.0006$, $p=0.002$). The $CD8^+$ cell (23.630 ± 3.210) count in animals killed 14 days after administration of the diminazene aceturate dose was also significantly higher than that seen in non-diminazene aceturate treated animals ($p<0.0001$ in all cases). In addition, the $CD8^+$ cell counts in mice killed at 7 (12.030 ± 1.180) and 14 (25.000 ± 5.000) days following the induction of the PTRE were significantly higher than those found in mice during the acute and early-CNS stage of the infection ($p<0.0001$ in all cases). No significant changes were detected in the level of $CD8^+$ cell infiltration between any of the groups of animals exhibiting the late-CNS stage of the disease and the PTRE.

Only the very occasional $CD8^+$ cell (0.250 ± 0.250; day 21 post-infection) was detected in the caudate putamen during the acute and early-CNS stage of trypanosome infection (Table 3.23). A slight increase in the number of $CD8^+$ cells (3.094 ± 0.281) was seen 7 days after the administration of a single diminazene aceturate dose. The $CD8^+$population in these animals was significantly higher than that found in mice killed at 7 ($p=0.008$), 14 ($p=0.008$) and 28 ($p=0.017$) days post-infection. The increase was of borderline

significance (p=0.052) when compared to mice killed at day 21 post-infection. By 14 days after the exacerbation of the CNS response the $CD8^+$ cell (3.170 $\pm$ 1.440) count was significantly higher than that seen in any of the non-diminazene aceturate treated mice (p=0.0005, p=0.0005, p=0.012, p=0.003). The level of $CD8^+$ cell (2.453 $\pm$ 0.736) infiltration found in mice killed 7 days following the induction of the PTRE remained significantly higher than that seen in animals killed at 7 (p=0.0006), 14 (p=0.0006), and 28 (p=0.019) days post-infection but was not significantly altered from the population found at 21 (p=0.069) days post-infection. By 14 days after the administration of a second diminazene aceturate treatment the $CD8^+$ cell (10.440 $\pm$ 6.060) count was again significantly greater than that found in all groups of animals killed during the acute or earl-CNS stage of the infection (p<0.0001, p<0.0001, p=0.0003, p=0.0001). The $CD8^+$ cell populations found in all the groups of mice killed following either a single or double dose of diminazene aceturate were not significantly different to each other.

No $CD8^+$ cells were detected in the cerebral cortex of mice killed during the acute or early-CNS stage of trypanosome infection (Table 3.24). By 7 days after the induction of the late-CNS stage of the disease a few $CD8^+$ cells (2.250 $\pm$ 0.000) were found. This cell population was significantly higher than in any of the earlier groups of mice (p=0.006, p=0.006, p=0.009, p=0.009). In animals killed at 14 days after the administration of a single diminazene aceturate treatment the $CD8^+$ cell (3.100 $\pm$ 0.816) remained significantly greater than that found during the acute or early-CNS stage of the disease (p<0.0001 in all cases). Seven days following the induction of the PTRE the $CD8^+$ cell (1.328 $\pm$ 0.465) remained significantly higher than that found in mice killed at 7, 14, 21 or 28 days post-infection (p=0.002, p=0.002, p=0.008, p=0.008). This increased presence of $CD8^+$ cells (5.969 $\pm$ 0.469) was also seen in mice killed at 14 days after treatment with a second dose of diminazene aceturate and the infiltration level of the cerebral cortex was significantly higher than that seen in mice during the acute or early-CNS stage of the infection (p<0.0001 in all cases). Furthermore, the $CD8^+$ population found in mice 14 days after the induction of the PTRE was significantly greater than that seen in mice killed at 7 days following the second diminazene aceturate treatment (p=0.0006). No additional differences were detected in $CD8^+$ cell infiltration between any other groups of mice killed following the induction of the late-CNS stage of the infection or the PTRE.

In addition to examining the $CD8^+$ cell infiltration in individual brain areas following each treatment regimen, differences in the $CD8^+$ population between each brain area studied were investigated. No $CD8^+$ cells were found in any of the brain areas monitored at 7 days post-infection. By 14 days after the infection a few $CD8^+$ cells were detected in the

meninges (0.700 ± 0.490) (Table, 3.25). However, the presence of these cells was not considered to be a significant increase in population compared with the remaining brain areas. On day 21 post-infection $CD8^+$ cells were found in the meninges (0.938 ± 0.938), the corpus callosum (0.167 ± 0.167) and the external capsule (0.833 ± 0.833) (Table 3.26). $CD8^+$ cells were not seen in the cerebral cortex in this group of mice. No significant alterations to the $CD8^+$ cell population were detected between the various areas of the brain studied at this time. On day 28 post-infection 4.440 ± 1.260 $CD8^+$ cells were found in the meninges (Table 3.27). This was significantly higher than that seen in the corpus callosum (0.417 ± 0.300), caudate putamen (0.000 ± 0.000) or cerebral cortex (0.000 ± 0.000) with p-values of 0.008, 0.002 and 0.002 respectively. The raised level of $CD8^+$ cell infiltration seenin external capsule (1.250 ± 0.722) was of borderline significance (p=0.050) to that found in the meninges.

Following exacerbation of the CNS reaction by administration of a single diminazene aceturate treatment, $CD8^+$ cells were found in the meninges (17.080 ± 7.720), corpus callosum (7.630 ± 2.620), external capsule (12.287 ± 0.000), caudate putamen (3.094 ± 0.281) and cerebral cortex (2.250 ± 0.000) 7 days after administration of the drug (Table 3.28). No significant differences were detected in the $CD8^+$ cell infiltration between the various brain areas following this regimen. In mice killed 14 days after the induction of the late-CNS stage response the number of $CD8^+$ cells in the meninges (38.950 ± 2.870) was significantly higher than the number of $CD8^+$ cells in the caudate putamen (3.710 ± 1.440) and cerebral cortex (3.100 ± 0.816) ($p<0.0001$ in both cases) (Table 3.29). differences were apparent between the $CD8^+$ cell population found in the meninges and that found in either the corpus callosum (22.020 ± 3.790) or external capsule (23.630 ± 3.210) (p=0.203, p=0.334 respectively). The number of $CD8^+$ cells seen in the corpus callosum and external capsule was significantly higher than the $CD8^+$ cell infiltration of either the caudate putamen (p=0.0001, $p<0.0001$ respectively and cerebral cortex (p=0.0001, $p<0.0001$ respectively). No difference in $CD8^+$ cell infiltration was apparent between the population found in the caudate putamen and the cerebral cortex (P=0.999).

In animals killed 7 days following the induction of the PTRE the number of $CD8^+$ cells infiltrating the meninges (32.690 ± 4.790) was significantly higher that that seen in the corpus callosum (11.740 ± 1.690), external capsule (12.030 ± 1.180), caudate putamen (2.453 ± 0.736) and cerebral cortex (1.328 ± 0.456) (p=0.007, p=0.009, $p<0.0001$, $p<0.0001$ respectively) (Table 3.30). The $CD8^+$ population in the corpus callosum and external capsule was also significantly higher than seen in the caudate putamen (p=0.0005, p=0.0004 respectively) and the cerebral cortex (p=0.0001, $p<0.0001$ respectively). No

significant difference in the infiltration of $CD8^+$ cells was found between the caudate putamen and the cerebral cortex (p=0.493). When mice were killed 14 days after administration of a second diminazene aceturate treatment the number of $CD8^+$ cells found in the meninges (36.400 ± 10.100) remained significantly (p=0.035) higher than that found in the cerebral cortex (5.969 ± 0.469). No further significant differences were found between the $CD8^+$ cell infiltration in the corpus callosum (27.540 ± 7.110), external capsule (25.000 ± 5.000), and caudate putamen (10.440 ± 6.060) at this stage in the disease (Table 3.31).

3.3.2.2. Macrophage infiltration

A small number of macrophages were detected within in the meninges and blood vessels of uninfected animals and those killed at 7 days post-infection. As the neuroinflammatory response progressed, the number of macrophages infiltrating the brain increased. By day 28 post-infection these cells were found in the corpus callosum and an occassional macrophage was seen in the caudate putamen. No macrophages were detected in the cerebral cortex during the acute or early-CNS stages of the infection. If the CNS reaction was exacerbated by the administration of a single diminazene aceturate treatment numerous macrophages could be seen in the meninges, perivascular cuffs, corpus callosum and external capsule. Positively stained cells were also detected in the caudate putamen and cerebral cortex at this stage. If a second dose of diminazene aceturate was given to the infected animals to induce a severe meningoencephalitis no further increase in macrophage infiltration was found and the numbers of these cells remained largely stable despite the increase in the severity of the CNS reaction induced by this treatment regimen. The absolute number of macrophages within the inflammatory infiltrate was not assessed.

3.3.2.3. B-lymphocyte infiltration

The presence of B-lymphocytes within the CNS was examined in a qualitative manner and was not quantified. No B-lymphocytes were detected in the brains of uninfected or *T.b.brucei*-infected mice during the acute or early CNS-stage of the infection. Following induction of the late-CNS stage of the disease by diminazene aceturate treatment, a few B-cells could be found infiltrating the meninges and in the perivascular cuffs. The presence of the B-cells increased with the severity of the CNS reaction and larger numbers of these cells were found following the administration of a second diminazene aceturate treatment to further augment the neuroinflammatory response. Furthermore, as the CNS

inflammatory response developed, increasing numbers of plasma cells were found in the inflammatory cell infiltrate. The majority of the B-cells and plasma cells remained confined to the meninges, perivascular cuffs and the ventricles. Only a small proportion of the B-cell population was detected infiltrating the brain parenchyma.

3.3.2.4. Astrocyte activation

Astrocyte activation, as characterised by an increase in; the production of glial fibrillary acidic protein (GFAP), the degree and complexity of cellular stellation, and in the numbers of GFAP positive cells was detected in the brains of mice rapidly following trypanosome infection (Figure 3.1, GFAP positive cells show brown staining pattern). Initial signs of astrocyte activation were seen in animals by 14 days after infection. At this point astrocytes in the hippocampus and surrounding the ventricles displayed an increased level of GFAP compared to uninfected mice. As the severity of the neuroinflammation increased the degree of astrocyte activation was also found to increase. The astrocytes stained more intensely for GFAP, increased in size and number and developed longer and more complex cellular processes. Following sub-curative drug treatment activated astrocytes were seen in the hippocampus and diffusing throughout the brain. Intense GFAP staining was detected around blood vessels and delimiting the ventricles and meninges. A further increase in the astrogliosis was found following the induction of the PTRE and reactive cells were widespread throughout the brain tissue. At this point the cells were large, displayed numerous highly complex cellular processes and stained intensely for GFAP. Although the astrocyte activation was diffuse, the population within the hippocampus appeared greater in number and stained more intensely for GFAP that the reactive cells found in the cerebral cortex and caudate putamen (Figure 3.1).

	7DPI	14DPI	21DPI	28DPI	7DPD	14DPD	7DPDD	14DPDD	UIC
14DPI	p=1.000 (-0.455, 0.539)								
21DPI	p=0.003 (0.149, 1.143)	p=0.006 (0.107, 1.101)							
28DPI	p<0.0001 (0.590, 1.606)	p<0.0001 (0.548, 1.565)	p=0.122 (-0.056, 0.961)						
7DPD	p<0.0001 (1.961, 2.955)	p<0.0001 (1.919, 2.914)	p<0.0001 (1.315, 2.309)	p<0.0001 (0.852, 1.869)					
14DPD	p<0.0001 (1.999, 3.016)	p<0.0001 (1.957, 2.974)	p<0.0001 (1.353, 2.369)	p<0.0001 (0.890, 1.928)	p=1.000 (-0.459, 0.557)				
7DPDD	p<0.0001 (2.350, 3.462)	p<0.0001 (2.309, 3.420)	p<0.0001 (1.705, 2.816)	p<0.0001 (1.242, 2.374)	p=0.219 (-0.108, 1.004)	p=0.390 (-0.167, 0.965)			
14DPDD	p<0.0001 2.444, 3.556)	p<0.0001 (2.403, 3.514)	p<0.0001 (1.798, 2.910)	p<0.0001 (1.336, 2.468)	p=0.063 (-0.014, 1.097)	p=0.141 (-0.073, 1.059)	p=0.999 (-0.515, 0.703)		
UIC	p=0.341 (-0.816, 0.127)	p=0.201 (-0.858, 0.085)	p<0.0001 (-1.462, -0.519)	p<0.0001 (-1.926, -0.959)	p<0.0001 (-3.275, -2.331)	p<0.0001 (-3.335, -2.369)	p<0.0001 (-3.784, -2.718)	p<0.0001 (-3.878, -2.812)	
Mean ± SE	0.375 ± 0.072	0.417 ± 0.077	1.021 ± 0.129	1.477 ± 0.186	2.833 ± 0.117	2.886 ± 0.123	3.281 ± 0.099	3.375 ± 0.189	0.033 ± 0.023
Number	12	12	12	11	12	11	8	8	15

Table 3.1. The effect of treatment regimen on the severity of the neuroinflammatory response

The neuropathological response scores were measured in nine groups of mice housed under different treatment regimens. These groups comprised: mice infected with *T.b.brucei* GVR35/C1.6 and killed at 7 (7DPI), 14 (14DPI), 21 (21DPI) and 28 (28DPI) days post-infection; infected mice treated on day 21 post-infection with diminazene aceturate (40mg/kg i.p.) to exacerbate the CNS response and killed 7 (7DPD) and 14 (14DPD) post-drug treatment; infected mice treated with diminazene aceturate on day 21 post-infection, re-treated with the drug following relapse to parasitaemia and killed 7 (7DPDD) and 14 (14DPDD) after administration of the second drug treatment; and uninfected control (UIC) animals. The mean score and standard error, together with the number of animals, are shown for each group. The figures in the body of the table demonstrate the comparisons in terms of statistical significance, between the groups shown in the row and column headings. The 95% confidence intervals for the differences between the means are given with the p-values. Figures detailed in red highlight groups showing significant differences.

	Assessment of T-cell infiltration of the meninges, corpus callosum, external capsule, caudate putamen and cerebral cortex							
	7DPI	14DPI	21DPI	28DPI	7DPD	14DPD	7DPDD	14DPDD
CD4 count	0.000 ± 0.000 (*n*=5)	1.420 ± 1.170 (*n*=5)	8.790 ± 1.950 (*n*=3)	25.540 ± 5.660 (*n*=3)	255.800 ± 76.900 (*n*=2)	335.700 ± 48.500 (*n*=5)	293.600 ± 14.800 (*n*=3)	457.400 ± 74.100 (*n*=2)
CD8 count	0.000 ± 0.000 (*n*=5)	0.700 ± 0.490 (*n*=5)	0.938 ± 0.938 (*n*=2)	6.110 ± 2.080 (*n*=3)	31.100 ± NA (*n*=1)	91.400 ± 2.950 (*n*=5)	60.240 ± 5.400 (*n*=4)	105.300 ± 27.800 (*n*=2)
p-value	p=1.000	p=0.685 (-1.173, 0.181)	p=0.040 (-3.363, -0.149)	p=0.031 (-1.376, -0.009)	p=0.164 (-8.827, 4.762)	p<0.0001 (-1.567, -0.950)	p=0.0001 (-1.888, -1.274)	p=0.042 (-2.834, -0.134)

Table 3.2. Comparison of CD4 and CD8 cell infiltration of the meninges, corpus callosum, external capsule, caudate putamen and cerebral cortex following trypanosome infection and subcurative drug treatment

Mice were infected with *T.b.brucei* GVR/C1.6 and the CD4 and CD8 cell infiltration of the brain was assessed in the meninges, corpus callosum, external capsule, caudate putamen and cerebral cortex at 7 (7DPI), 14 (14DPI), 21 (21DPI) and 28 (28DPI) days post-infection; 7 and 14 days after exacerbation of the CNS reaction by administration of a single diminazene aceturate treatment (7DPD, 14DPD); and 7 and 14 days following the induction of the PTRE by administration of a second diminazene aceturate treatment (7DPDD, 14DPDD). The data in the body of the table details the mean cell count ± standard error and the number (*n*) of animals per group. The p-values and 95% confidence intervals for differences are based on analysis using the logarithmic transformation [log(x + 1)] of the cell counts. Figures detailed in red highlight groups showing significant differences. NA; not applicable.

	Assessment of T-cell infiltration of the meninges							
	7DPI	14DPI	21DPI	28DPI	7DPD	14DPD	7DPDD	14DPDD
CD4 count	0.000 ± 0.000 (*n*=5)	1.370 ± 1.120 (*n*=5)	7.330 ± 1.970 (*n*=3)	18.330 ± 6.140 (*n*=3)	110.300 ± 58.200 (*n*=3)	193.300 ± 27.500 (*n*=5)	180.380 ± 6.780 (*n*=4)	238.400 ± 52.800 (*n*=2)
CD8 count	0.000 ± 0.000 (*n*=5)	0.700 ± 0.490 (*n*=5)	0.938 ± 0.938 (*n*=2)	4.440 ± 1.290 (*n*=3)	17.080 ± 7.720 (*n*=3)	38.950 ± 2.870 (*n*=5)	32.690 ± 4.790 (*n*=4)	36.400 ± 10.100 (*n*=2)
p-value	p=1.000	p=0.693 (-1.152, 0.805)	p=0.051 (-3.088, 0.006)	p=0.045 (-2.428, -0.044)	p=0.085 (-3.644, 0.365)	p<0.0001 (-1.883, -1.232)	p<0.0001 (-2.105, -1.325)	p=0.026 (-3.493, -0.607)

Table 3.3. Comparison of CD4 and CD8 cell infiltration in the meninges following trypanosome infection and subcurative drug treatment

Mice were infected with *T.b.brucei* GVR/C1.6 and the CD4 and CD8 cell infiltration of the meninges was assessed at 7 (7DPI), 14 (14DPI), 21 (21DPI) and 28 (28DPI) days post-infection; 7 and 14 days after exacerbation of the CNS reaction by administration of a single diminazene aceturate treatment (7DPD, 14DPD); and 7 and 14 days following the induction of the PTRE by administration of a second diminazene aceturate treatment (7DPDD, 14DPDD). The data in the body of the table details the mean cell count ± standard error and the number (*n*) of animals per group. The p-values and 95% confidence intervals for differences are based on analysis using the logarithmic transformation [log(x + 1)] of the cell counts. Figures detailed in red highlight groups showing significant differences, figures detailed in blue show groups with differences of borderline significance.

	Assessment of T-cell infiltration of the corpus callosum							
	7DPI	14DPI	21DPI	28DPI	7DPD	14DPD	7DPDD	14DPDD
CD4 count	0.000 ± 0.000 (*n*=5)	0.050 ± 0.050 (*n*=5)	0.333 ± 0.220 (*n*=3)	1.875 ± 0.402 (*n*=3)	28.250 ± 4.250 (*n*=2)	48.410 ± 7.800 (*n*=5)	54.300 ± 11.700 (*n*=3)	63.900 ± 12.300 (*n*=2)
CD8 count	0.000 ± 0.000 (*n*=5)	0.000 ± 0.000 (*n*=5)	0.167 ± 0.167 (*n*=3)	0.417 ± 0.300 (*n*=3)	7.630 ± 2.620 (*n*=2)	22.020 ± 3.790 (*n*=5)	11.740 ± 1.690 (*n*=4)	27.540 ± 7.110 (*n*=2)
p-value	p=1.000	p=0.347 (-0.148, 0.058)	p=0.584 (-0.713, 0.461)	p=0.041 (-1.416, -0.046)	p=0.068 (-2.751, 0.233)	p=0.008 (-1.286, -1.260)	p=0.002 (-2.101, -0.792)	p=0.120 (-2.207, 0.532)

Table 3.4. Comparison of CD4 and CD8 cell infiltration in the corpus callosum following trypanosome infection and subcurative drug treatment

Mice were infected with *T.b.brucei* GVR/C1.6 and the CD4 and CD8 cell infiltration of the corpus callosum was assessed at 7 (7DPI), 14 (14DPI), 21 (21DPI) and 28 (28DPI) days post-infection; 7 and 14 days after exacerbation of the CNS reaction by administration of a single diminazene aceturate treatment (7DPD, 14DPD); and 7 and 14 days following the induction of the PTRE by administration of a second diminazene aceturate treatment (7DPDD, 14DPDD). The data in the body of the table details the mean cell count ± standard error and the number (*n*) of animals per group. The p-values and 95% confidence intervals for differences are based on analysis using the logarithmic transformation [log(x + 1)] of the cell counts. Figures detailed in red highlight groups showing significant differences.

	Assessment of T-cell infiltration of the external capsule							
	7DPI	14DPI	21DPI	28DPI	7DPD	14DPD	7DPDD	14DPDD
CD4 count	0.000 ± 0.000 (*n*=5)	0.000 ± 0.000 (*n*=5)	0.833 ± 0.833 (*n*=3)	4.583 ± 0.417 (*n*=3)	48.520 ± 3.120 (*n*=2)	61.880 ± 8.520 (*n*=5)	40.160 ± 5.460 (*n*=4)	69.380 ± 1.250 (*n*=2)
CD8 count	0.000 ± 0.000 (*n*=5)	0.000 ± 0.000 (*n*=5)	0.833 ± 0.833 (*n*=3)	1.250 ± 0.722 (*n*=3)	12.287 ± NA (*n*=1)	23.630 ± 3.210 (*n*=5)	12.030 ± 1.180 (*n*=4)	25.000 ± 5.000 (*n*=2)
p-value	p=1.000	p=1.000	p=1.000 (-1.640, 1.640)	p=0.052 (-2.067, 0.015)	p=0.053 (-2.703, 0.076)	p=0.002 (-1.402, -0.447)	p=0.0004 (-1.531, -0.745)	p=0.035 (-1.856, -0.173)

Table 3.5. Comparison of CD4 and CD8 cell infiltration in the external capsule following trypanosome infection and subcurative drug treatment

Mice were infected with *T.b.brucei* GVR/C1.6 and the CD4 and CD8 cell infiltration of the external capsule was assessed at 7 (7DPI), 14 (14DPI), 21 (21DPI) and 28 (28DPI) days post-infection; 7 and 14 days after exacerbation of the CNS reaction by administration of a single diminazene aceturate treatment (7DPD, 14DPD); and 7 and 14 days following the induction of the PTRE by administration of a second diminazene aceturate treatment (7DPDD, 14DPDD). The data in the body of the table details the mean cell count ± standard error and the number (*n*) of animals per group. The p-values and 95% confidence intervals for differences are based on analysis using the logarithmic transformation [log(x + 1)] of the cell counts. Figures detailed in red highlight groups showing significant differences, figures detailed in blue show groups with differences of borderline significance. NA; not applicable.

	Assessment of T-cell infiltration of the caudate putamen							
	7DPI	14DPI	21DPI	28DPI	7DPD	14DPD	7DPDD	14DPDD
CD4 count	0.000 ± 0.000 (*n*=5)	0.000 ± 0.000 (*n*=5)	0.250 ± 0.250 (*n*=3)	0.750 ± 0.520 (*n*=3)	19.780 ± 6.340 (*n*=2)	19.310 ± 9.340 (*n*=5)	13.310 ± 1.130 (*n*=3)	24.310 ± 9.060 (*n*=2)
CD8 count	0.000 ± 0.000 (*n*=5)	0.000 ± 0.000 (*n*=5)	0.250 ± 0.250 (*n*=3)	0.000 ± 0.000 (*n*=3)	3.094 ± 0.281 (*n*=2)	3.710 ± 1.440 (*n*=5)	2.453 ± 0.736 (*n*=4)	10.440 ± 6.060 (*n*=2)
p-value	p=1.000	p=1.000	p=1.000 (-0.732, 0.732)	p=0.183 (-1.288, 0.344)	p=0.039 (-2.967, -0.189)	p=0.033 (-2.456, -0.134)	p=0.003 (-2.198, -0.780)	p=0.331 (-3.899, 2.117)

Table 3.6. Comparison of CD4 and CD8 cell infiltration in the caudate putamen following trypanosome infection and subcurative drug treatment

Mice were infected with *T.b.brucei* GVR/C1.6 and the CD4 and CD8 cell infiltration of the caudate putamen was assessed at 7 (7DPI), 14 (14DPI), 21 (21DPI) and 28 (28DPI) days post-infection; 7 and 14 days after exacerbation of the CNS reaction by administration of a single diminazene aceturate treatment (7DPD, 14DPD); and 7 and 14 days following the induction of the PTRE by administration of a second diminazene aceturate treatment (7DPDD, 14DPDD). The data in the body of the table details the mean cell count ± standard error and the number (*n*) of animals per group. The p-values and 95% confidence intervals for differences are based on analysis using the logarithmic transformation [log(x + 1)] of the cell counts. Figures detailed in red highlight groups showing significant differences.

	Assessment of T-cell infiltration of the cerebral cortex							
	7DPI	14DPI	21DPI	28DPI	7DPD	14DPD	7DPDD	14DPDD
CD4 count	0.000 ± 0.000 (*n*=5)	0.000 ± 0.000 (*n*=5)	0.042 ± 0.042 (*n*=3)	0.000 ± 0.000 (*n*=3)	6.750 ± 0.000 (*n*=2)	12.790 ± 3.950 (*n*=5)	4.430 ± 1.600 (*n*=3)	16.340 ± 1.220 (*n*=2)
CD8 count	0.000 ± 0.000 (*n*=5)	0.000 ± 0.000 (*n*=5)	0.000 ± 0.000 (*n*=3)	0.000 ± 0.000 (*n*=3)	2.250 ± NA (*n*=1)	3.100 ± 0.816 (*n*=5)	1.328 ± 0.465 (*n*=4)	5.969 ± 0.469 (*n*=2)
p-value	p=1.000	p=1.000	p=0.374 (-0.148, 0.069)	p=1.000	#	p=0.013 (-1.945, -0.303)	p=0.098 (-1.759, 0.207)	p=0.011 (-1.331, 0.492)

Table 3.7. Comparison of CD4 and CD8 cell infiltration in the cerebral cortex following trypanosome infection and subcurative drug treatment

Mice were infected with *T.b.brucei* GVR/C1.6 and the CD4 and CD8 cell infiltration of the cerebral cortex was assessed at 7 (7DPI), 14 (14DPI), 21 (21DPI) and 28 (28DPI) days post-infection; 7 and 14 days after exacerbation of the CNS reaction by administration of a single diminazene aceturate treatment (7DPD, 14DPD); and 7 and 14 days following the induction of the PTRE by administration of a second diminazene aceturate treatment (7DPDD, 14DPDD). The data in the body of the table details the mean cell count ± standard error and the number (*n*) of animals per group. The p-values and 95% confidence intervals for differences are based on analysis using the logarithmic transformation [log(x + 1)] of the cell counts. Figures detailed in red highlight groups showing significant differences. #; too few data points to calculate standard error and p-value. NA; not applicable.

	CD4 cell count in meninges							
	7DPI	14DPI	21DPI	28DPI	7DPD	14DPD	7DPDD	14DPDD
14DPI	p=1.000 (-0.526, 1.625)							
21DPI	p=0.999 (0.812, 3.326)	p=0.999 (0.249, 2.763)						
28DPI	p=0.861 (1.601, 4.116)	p=0.861 (1.039, 3.553)	p=0.994 (-0.616, 2.195)					
7DPD	p<0.0001 (3.121, 5.636)	p<0.0001 (2.558, 5.073)	p=0.0001 (0.904, 3.715)	p=0.0003 (0.114, 2.925)				
14DPD	p<0.0001 (4.147, 6.325)	p<0.0001 (3.584, 5.762)	p<0.0001 (1.909, 4.424)	p=0.0001 (1.119, 3.634)	p=0.990 (-0.399, 2.115)			
7DPDD	p<0.0001 (4.044, 6.353)	p<0.0001 (3.481, 5.790)	p=0.0001 (1.815, 4.444)	p=0.0004 (1.025, 3.655)	p=0.993 (-0.495, 2.135)	p=1.000 (-1.192, 1.118)		
14DPDD	p<0.0001 (4.192, 7.073)	p<0.0001 (3.629, 6.511)	p<0.0001 (1.992, 5.136)	p=0.0001 (1.203, 4.346)	p=0.999 (0.317, 2.826)	p=0.901 (-1.043, 1.838)	p=0.929 (-1.056, 1.926)	
Mean ± SE	0.000 ± 0.000	1.370 ± 1.120	7.330 ± 1.970	18.330 ± 6.140	110.300 ± 58.200	193.300 ± 27.500	180.380 ± 6.780	283.400 ± 52.800
Number	5	5	3	3	3	5	4	2

Table 3.8. Comparison of CD4 cell infiltration in the meninges at various time-points following trypanosome infection and subcurative drug treatment

Mice were infected with *T.b.brucei* GVR/C1.6 and the CD4 cell infiltration of the meninges was assessed at 7 (7DPI), 14 (14DPI), 21 (21DPI) and 28 (28DPI) days post-infection; 7 and 14 days after exacerbation of the CNS reaction by administration of a single diminazene aceturate treatment (7DPD, 14DPD); and 7 and 14 days following the induction of the PTRE by administration of a second diminazene aceturate treatment (7DPDD, 14DPDD). The figures in the body of the table demonstrate the comparisons, in terms of statistical significance, between the groups shown in the row and column headings. The 95% confidence intervals for differences between the group means, based on analysis using the logarithmic transformation [log(x + 1)] of the cell counts, together with the p-values are detailed. The mean cell count ± standard error and the number of animals per group are also shown. Figures detailed in red highlight groups showing significant differences.

	CD4 cell count in the corpus callosum							
	7DPI	14DPI	21DPI	28DPI	7DPD	14DPD	7DPDD	14DPDD
14DPI	p=1.000 (-0.474, 0.564)							
21DPI	p=0.814 (-0.338, 0.860)	p=0.917 (-0.383, 0.815)						
28DPI	p=0.0002 (0.438, 1.636)	p=0.0004 (0.393, 1.591)	p=0.016 (0.106, 1.446)					
7DPD	p<0.0001 (2.679, 4.052)	p<0.0001 (2.634, 4.007)	p<0.0001 (2.355, 3.852)	p<0.0001 (1.580, 3.077)				
14DPD	p<0.0001 (3.336, 4.373)	p<0.0001 (3.291,4.329)	p<0.0001 (2.995, 4.193)	p<0.0001 (2.219, 3.417)	p=0.291 (-0.197, 1.176)			
7DPDD	p<0.0001 (3.364, 4.562)	p<0.0001 (3.319, 4.518)	p<0.0001 (3.032, 4.372)	p<0.0001 (2.256, 3.596)	p=0.182 (-0.151, 1.347)	p=0.998 (-0.491, 0.708)		
14DPDD	p<0.0001 (3.469, 4.842)	p<0.0001 (3.424, 4.797)	p<0.0001 (3.145, 4.643)	p<0.0001 (2.369, 3.867)	p=0.064 (-0.030, 1.610)	p=0.810 (-0.386, 0.987)	p=0.986 (-0.557, 0.941)	
Mean ± SE	0.000 ± 0.000	0.050 ± 0.050	0.333 ± 0.220	1.875 ± 0.402	28.250 ± 4.250	48.410 ± 7.800	54.300 ± 11.700	63.900 ± 12.300
Number	5	5	3	3	2	5	3	2

Table 3.9. Comparison of CD4 cell infiltration in the corpus callosum at various time-points following trypanosome infection and subcurative drug treatment

Mice were infected with *T.b.brucei* GVR/C1.6 and the CD4 cell infiltration of the corpus callosum was assessed at 7 (7DPI), 14 (14DPI), 21 (21DPI) and 28 (28DPI) days post-infection; 7 and 14 days after exacerbation of the CNS reaction by administration of a single diminazene aceturate treatment (7DPD, 14DPD); and 7 and 14 days following the induction of the PTRE by administration of a second diminazene aceturate treatment (7DPDD, 14DPDD). The figures in the body of the table demonstrate the comparisons, in terms of statistical significance, between the groups shown in the row and column headings. The 95% confidence intervals for differences between the group means, based on analysis using the logarithmic transformation [log(x + 1)] of the cell counts, together with the p-values are detailed. The mean cell count ± standard error and the number of animals per group are also shown. Figures detailed in red highlight groups showing significant differences.

	CD4 cell count in the external capsule							
	7DPI	14DPI	21DPI	28DPI	7DPD	14DPD	7DPDD	14DPDD
14DPI	p=1.000 (-0.623, 0.623)							
21DPI	p=0.537 (-0.301, 1.137)	p=0.537 (-0.301, 1.136)						
28DPI	p<0.0001 (0.995, 2.431)	p<0.0001 (0.995, 2.433)	p=0.0005 (0.493, 2.100)					
7DPD	p<0.0001 (3.077, 4.724)	p<0.0001 (3.077, 4.724)	p<0.0001 (2.584, 4.381)	p<0.0001 (1.288, 3.085)				
14DPD	p<0.0001 (3.472, 4.717)	p<0.0001 (3.472, 4.717)	p<0.0001 (2.958, 4.396)	p<0.0001 (1.662, 3.100)	p=0.992 (-0.629, 1.018)			
7DPDD	p<0.0001 (3.032, 4.353)	p<0.0001 (3.032, 4.353)	p<0.0001 (2.523, 4.026)	p<0.0001 (1.227, 2.730)	p=0.990 (-1.061, 0.644)	p=0.479 (-1.063, 0.258)		
14DPDD	p<0.0001 (3.430, 5.077)	p<0.0001 (3.430, 5.077)	p<0.0001 (2.938, 4.735)	p<0.0001 (1.641, 3.438)	p=0.922 (-0.631, 1.338)	p=0.998 (-0.665, 0.983)	p=0.386 (-0.291, 1.414)	
Mean ± SE	0.000 ± 0.000	0.000 ± 0.000	0.833 ± 0.833	4.583 ± 0.417	48.520 ± 3.120	61.880 ± 8.520	40.160 ± 5.460	69.380 ± 1.250
Number	5	5	3	3	2	5	4	2

Table 3.10. Comparison of CD4 cell infiltration in the external capsule at various time-points following trypanosome infection and subcurative drug treatment

Mice were infected with *T.b.brucei* GVR/C1.6 and the CD4 cell infiltration of the external capsule was assessed at 7 (7DPI), 14 (14DPI), 21 (21DPI) and 28 (28DPI) days post-infection; 7 and 14 days after exacerbation of the CNS reaction by administration of a single diminazene aceturate treatment (7DPD, 14DPD); and 7 and 14 days following the induction of the PTRE by administration of a second diminazene aceturate treatment (7DPDD, 14DPDD). The figures in the body of the table demonstrate the comparisons, in terms of statistical significance, between the groups shown in the row and column headings. The 95% confidence intervals for differences between the group means, based on analysis using the logarithmic transformation [log(x + 1)] of the cell counts, together with the p-values are detailed. The mean cell count ± standard error and the number of animals per group are also shown. Figures detailed in red highlight groups showing significant differences

	CD4 cell count in the caudate putamen							
	7DPI	14DPI	21DPI	28DPI	7DPD	14DPD	7DPDD	14DPDD
14DPI	p=1.000 (-1.009, 1.009)							
21DPI	p=0.999 (-0.979, 1.352)	p=0.999 (-0.979, 1.352)						
28DPI	p=0.861 (-0.693, 1.638)	p=0.861 (-0.693, 1.638)	p=0.994 (-1.017, 1.589)					
7DPD	p<0.0001 (1.650, 4.320)	p<0.0001 (1.650, 4.320)	p=0.0001 (1.342, 4.255)	p=0.0003 (1.056, 3.970)				
14DPD	p<0.0001 (1.652, 3.671)	p<0.0001 (1.652, 3.671)	p<0.0001 (1.310, 3.640)	p=0.0001 (1.024, 3.355)	p=0.990 (-1.659, 1.012)			
7DPDD	p<0.0001 (1.489, 3.820)	p<0.0001 (1.489, 3.820)	p=0.0001 (1.165, 3.771)	p=0.0004 (0.879, 3.485)	p=0.993 (-1.787, 1.126)	p=1.000 (-1.172, 1.158)		
14DPDD	p<0.0001 (1.828, 4.498)	p<0.0001 (1.828, 4.498)	p<0.0001 (1.519, 4.433)	p=0.0001 (1.234, 4.147)	p=0.999 (-1.418, 1.773)	p=0.901 (-0.834, 1.836)	p=0.929 (-0.949, 1.965)	
Mean ± SE	0.000 ± 0.000	0.000 ± 0.000	0.250 ± 0.250	0.750 ± 0.520	19.780 ± 6.340	19.310 ± 9.340	13.310 ± 1.130	24.310 ± 9.060
Number	5	5	3	3	2	5	3	2

Table 3.11. Comparison of CD4 cell infiltration in the caudate putamen at various time-points following trypanosome infection and subcurative drug treatment

Mice were infected with *T.b.brucei* GVR/C1.6 and the CD4 cell infiltration of the caudate putamen was assessed at 7 (7DPI), 14 (14DPI), 21 (21DPI) and 28 (28DPI) days post-infection; 7 and 14 days after exacerbation of the CNS reaction by administration of a single diminazene aceturate treatment (7DPD, 14DPD); and 7 and 14 days following the induction of the PTRE by administration of a second diminazene aceturate treatment (7DPDD, 14DPDD). The figures in the body of the table demonstrate the comparisons, in terms of statistical significance, between the groups shown in the row and column headings. The 95% confidence intervals for differences between the group means, based on analysis using the logarithmic transformation [log(x + 1)] of the cell counts, together with the p-values are detailed. The mean cell count ± standard error and the number of animals per group are also shown. Figures detailed in red highlight groups showing significant differences.

	CD4 cell count in the cerebral cortex							
	7DPI	14DPI	21DPI	28DPI	7DPD	14DPD	7DPDD	14DPDD
14DPI	p=1.000 (-0.771, 0.771)							
21DPI	p=1.000 (-0.851, 0.929)	p=1.000 (-0.851, 0.929)						
28DPI	p=1.000 (-0.891, 0.891)	p=1.000 (-0.891, 0.891)	p=1.000 (-1.035, 0.957)					
7DPD	p<0.0001 (1.027, 3.068)	p<0.0001 (1.027, 3.068)	p=0.0002 (0.895, 3.122)	p=0.0001 (0.944, 3.161)				
14DPD	p<0.0001 (1.683, 3.226)	p<0.0001 (1.683, 3.226)	p<0.0001 (1.525, 3.306)	p<0.0001 (1.564, 3.345)	p=0.870 (-0.613, 1.427)			
7DPDD	p=0.0002 (0.679, 2.459)	p=0.0002 (0.679, 2.459)	p=0.001 (0.534, 2.526)	p=0.0007 (0.573, 2.565)	p=0.824 (-1.592, 0.635)	p=0.052 (-1.776, 0.005)		
14DPDD	p<0.0001 (1.830, 3.871)	p<0.0001 (1.830, 3.871)	p<0.0001 (1.698, 3.925)	p<0.0001 (1.738, 3.964)	p=0.381 (-0.416, 2.023)	p=0.885 (-0.624, 1.416)	p=0.017 (0.168, 2.395)	
Mean ± SE	0.000 ± 0.000	0.000 ± 0.000	0.042 ± 0.042	0.000 ± 0.000	6.750 ± 0.000	12.790 ± 3.950	4.430 ± 1.600	16.340 ± 1.220
Number	5	5	3	3	2	5	3	2

Table 3.12. Comparison of CD4 cell infiltration in the cerebral cortex at various time-points following trypanosome infection and subcurative drug treatment

Mice were infected with *T.b.brucei* GVR/C1.6 and the CD4 cell infiltration of the cerebral cortex was assessed at 7 (7DPI), 14 (14DPI), 21 (21DPI) and 28 (28DPI) days post-infection; 7 and 14 days after exacerbation of the CNS reaction by administration of a single diminazene aceturate treatment (7DPD, 14DPD); and 7 and 14 days following the induction of the PTRE by administration of a second diminazene aceturate treatment (7DPDD, 14DPDD). The figures in the body of the table demonstrate the comparisons, in terms of statistical significance, between the groups shown in the row and column headings. The 95% confidence intervals for differences between the group means, based on analysis using the logarithmic transformation [log(x + 1)] of the cell counts, together with the p-values are detailed. The mean cell count ± standard error and the number of animals per group are also shown. Figures detailed in red highlight groups showing significant differences, figures detailed in blue show groups with differences of borderline significance.

	CD4$^+$ cell infiltration at 14 days post-infection				
	Meninges	Corpus callosum	External capsule	Caudate putamen	Cerebral cortex
Corpus callosum	p=0.147 (-1.160, 0.125)				
External capsule	p=0.101 (-1.205, 0.079)	p=0.999 (-0.686, 0.597)			
Caudate putamen	p=0.101 (-1.205, 0.079)	p=0.999 (-0.686, 0.597)	p=1.000 (-0.642, 0.642)		
Cerebral cortex	p=0.101 (-1.205, 0.079)	p=0.999 (-0.686, 0.597)	p=1.000 (-0.642, 0.642)	p=1.000 (-0.642, 0.642)	
Mean $\pm$ SE	1.370 $\pm$ 1.120	0.050 $\pm$ 0.050	0.000 $\pm$ 0.000	0.000 $\pm$ 0.000	0.000 $\pm$ 0.000
Number	5	5	5	5	5

Table 3.13. Comparison of CD4$^+$ cell infiltration of different brain areas 14 days following trypanosome infection

Mice were infected with *T.b.brucei* GVR/C1.6 and killed 14 days later. The number of CD4$^+$ cells infiltrating the meninges, corpus callosum, external capsule and cerebral cortex was assessed and expressed as the number of cells per mm^2 of tissue. The figures in the body of the table demonstrate the comparisons, in terms of statistical significance, between the brain areas shown in the row and column headings. The p-values and 95% confidence intervals for differences are based on analysis using the logarithmic transformation [log(x + 1)] of the cell counts. The mean cell count $\pm$ the standard error and the number of animals per group are also shown.

	$CD4^+$ cell infiltration at 21 days post-infection				
	Meninges	Corpus callosum	External capsule	Caudate putamen	Cerebral cortex
Corpus callosum	p=0.002 (-2.815, -0.808)				
External capsule	p=0.003 (-2.658, -0.644)	p=0.981 (-0.850, 1.164)			
Caudate putamen	p=0.001 (-2.890, -0.875)	p=0.999 (-1.081, 0.933)	p=0.926 (-1.238, 0.776)		
Cerebral cortex	p=0.001 (-3.037, -1.023)	p=0.935 (-1.229, 0.786)	p=0.699 (-1.385, 0.629)	p=0.984 (-1.154, 0.859)	
Mean ± SE	7.330 ± 1.970	0.333 ± 0.220	0.833 ± 0.833	0.250 ± 0.250	0.042 ± 0.042
Number	3	3	3	3	3

Table 3.14. Comparison of $CD4^+$ cell infiltration of different brain areas 21 days following trypanosome infection

Mice were infected with *T.b.brucei* GVR/C1.6 and killed 21 days later. The number of $CD4^+$ cells infiltrating the meninges, corpus callosum, external capsule and cerebral cortex was assessed and expressed as the number of cells per mm^2 of tissue. The figures in the body of the table demonstrate the comparisons, in terms of statistical significance, between the brain areas shown in the row and column headings The p-values and 95% confidence intervals for differences are based on analysis using the logarithmic transformation [log(x + 1)] of the cell counts. The mean cell count ± the standard error and the number of animals per group are also shown. Figures detailed in red highlight groups showing significant differences.

	CD4$^+$ cell infiltration at 28 days post-infection				
	Meninges	Corpus callosum	External capsule	Caudate putamen	Cerebral cortex
Corpus callosum	p=0.002 (-2.839, -0.804)				
External capsule	p=0.028 (-2.162, -0.127)	p=0.237 (-0.340, 1.695)			
Caudate putamen	p=0.0003 (-3.404, -1.369)	p=0.379 (-1.582, 0.453)	p=0.018 (-2.259, -0.224)		
Cerebral cortex	p=0.0001 (-3.876, -1.841)	p=0.046 (-2.054, -0.019)	p=0.003 (-2.731, -0.696)	p=0.533 (-1.490, 0.545)	
Mean ± SE	18.330 ± 6.140	1.875 ± 0.402	4.583 ± 0.417	0.750 ± 0.520	0.000 ± 0.000
Number	3	3	3	3	3

Table 3.15. Comparison of CD4$^+$ cell infiltration of different brain areas 28 days following trypanosome infection

Mice were infected with *T.b.brucei* GVR/C1.6 and killed 28 days later. The number of CD4$^+$ cells infiltrating the meninges, corpus callosum, external capsule and cerebral cortex was assessed and expressed as the number of cells per mm^2 of tissue. The figures in the body of the table demonstrate the comparisons, in terms of statistical significance, between the brain areas shown in the row and column headings. The p-values and 95% confidence intervals for differences are based on analysis using the logarithmic transformation [log(x + 1)] of the cell counts. The mean cell count ± the standard error and the number of animals per group are also shown. Figures detailed in red highlight groups showing significant differences.

	$CD4^+$ cell infiltration at 7 days after induction of late-stage CNS response				
	Meninges	Corpus callosum	External capsule	Caudate putamen	Cerebral cortex
Corpus callosum	p=0.037 (-2.979, -0.129)				
External capsule	p=0.138 (-2.444, 0.406)	p=0.532 (-0.890, 1.960)			
Caudate putamen	p=0.018 (-3.359, -0.509)	p=0.761 (-1.805, 1.045)	p=0.184 (-2.340, 0.509)		
Cerebral cortex	p=0.004 (-4.297, -1.447)	p=0.064 (-2.743, 0.108)	p=0.020 (-3.278, -0.428)	p=0.173 (-2.362, 0.488)	
Mean ± SE	110.300 ± 58.200	28.250 ± 4.250	48.520 ± 3.120	19.780 ± 6.340	6.750 ± 0.000
Number	3	2	2	2	2

Table 3.16. Comparison of $CD4^+$ cell infiltration of different brain areas 7 days following the induction of the late-stage CNS response

Mice were infected with *T.b.brucei* GVR/C1.6, treated with diminazene aceturate (40mg/kg i.p.) on day 21 post-infection and killed 7 days later. The number of $CD4^+$ cells infiltrating the meninges, corpus callosum, external capsule and cerebral cortex was assessed and expressed as the number of cells per mm^2 of tissue. The figures in the body of the table demonstrate the comparisons, in terms of statistical significance, between the brain areas shown in the row and column headings. The p-values and 95% confidence intervals for differences are based on analysis using the logarithmic transformation [log(x + 1)] of the cell counts. The mean cell count ± the standard error and the number of animals per group are also shown. Figures detailed in red highlight groups showing significant differences.

	CD4$^+$ cell infiltration at 14 days after induction of late-stage CNS response				
	Meninges	Corpus callosum	External capsule	Caudate putamen	Cerebral cortex
Corpus callosum	p=0.0005 (-2.158, -0.605)				
External capsule	p=0.003 (-1.918, -0.364)	p=0.874 (-0.536, 1.017)			
Caudate putamen	p<0.0001 (-3.351, -1.798)	p=0.002 (-1.969, -0.416)	p=0.0003 (-2.210, -0.657)		
Cerebral cortex	p<0.0001 (-3.557, -2.004)	p=0.004 (-2.176, -0.623)	p=0.0001 (-2.416, -0.864)	p=0.922 (-0.983, 0.569)	
Mean ± SE	193.300 ± 27.500	48.410 ± 7.800	61.880 ± 8.520	19.310 ± 9.340	12.790 ± 3.950
Number	5	5	5	5	5

Table 3.17. Comparison of CD4$^+$ cell infiltration of different brain areas 14 days following the induction of the late-stage CNS response

Mice were infected with *T.b.brucei* GVR/C1.6, treated with diminazene aceturate (40mg/kg i.p.) on day 21 post-infection and killed 14 days later. The number of CD4$^+$ cells infiltrating the meninges, corpus callosum, external capsule and cerebral cortex was assessed and expressed as the number of cells per mm^2 of tissue. The figures in the body of the table demonstrate the comparisons, in terms of statistical significance, between the brain areas shown in the row and column headings. The p-values and 95% confidence intervals for differences are based on analysis using the logarithmic transformation [log(x + 1)] of the cell counts. The mean cell count ± the standard error and the number of animals per group are also shown. Figures detailed in red highlight groups showing significant differences.

	$CD4^+$ cell infiltration at 7 days after induction of the PTRE				
	Meninges	Corpus callosum	External capsule	Caudate putamen	Cerebral cortex
Corpus callosum	p=0.022 (-2.221, -0.172)				
External capsule	p=0.003 (-2.423, -0.790)	p=0.842 (-1.334, 0.715)			
Caudate putamen	p=0.0001 (-3.530, -1.481)	p=0.016 (-2.367, -0.250)	p=0.056 (-2.024, 0.026)		
Cerebral cortex	p<0.0001 (-4.615, -2.566)	p=0.0002 (-3.452, -1.336)	p=0.0005 (-3.109, -1.060)	p=0.044 (-2.144, -0.027)	
Mean ± SE	180.380 ± 6.780	54.300 ± 11.700	40.160 ± 5.460	13.310 ± 1.130	4.430 ± 1.600
Number	4	3	4	3	3

Table 3.18. Comparison of $CD4^+$ cell infiltration of different brain areas 7 days following the induction of the PTRE

Mice were infected with *T.b.brucei* GVR/C1.6 and treated with diminazene aceturate (40mg/kg i.p.) on day 21 post-infection. On relapse to parasitaemia the mice were given a second dose of diminazene aceturate to induce a severe meningoencephalitis similar to that seen in patients that have died from the PTRE. The animals were killed 7 days following administration of the drug. The number of $CD4^+$ cells infiltrating the meninges, corpus callosum, external capsule and cerebral cortex was assessed and expressed as the number of cells per mm^2 of tissue. The figures in the body of the table demonstrate the comparisons, in terms of statistical significance, between the brain areas shown in the row and column headings. The p-values and 95% confidence intervals for differences are based on analysis using the logarithmic transformation [log(x + 1)] of the cell counts. The mean cell count ± the standard error and the number of animals per group are also shown. Figures detailed in red highlight groups showing significant differences, figures detailed in blue show groups with differences of borderline significance.

	$CD4^+$ cell infiltration at 14 days after induction of the PTRE				
	Meninges	Corpus callosum	External capsule	Caudate putamen	Cerebral cortex
Corpus callosum	p=0.009 (-2.408, -0.548)				
External capsule	p=0.013 (-2.309, 0.449)	p=0.986 (-0.831, 1.029)			
Caudate putamen	p=0.001 (-3.400, -1.540)	p=0.040 (-1.922, -0.062)	p=0.029 (-2.021, -0.161)		
Cerebral cortex	p=0.0009 (-3.712, -1.852)	p=0.016 (-2.234, -0.374)	p=0.012 (-2.333, -0.473)	p=0.614 (-1.242, 0.618)	
Mean ± SE	138.400 ± 52.800	63.900 ± 12.300	69.380 ± 1.250	24.310 ± 9.060	16.340 ± 1.220
Number	2	2	2	2	2

Table 3.19. Comparison of $CD4^+$ cell infiltration of different brain areas 14 days following induction of the PTRE

Mice were infected with *T.b.brucei* GVR/C1.6 and treated with diminazene aceturate (40mg/kg i.p.) on day 21 post-infection. On relapse to parasitaemia the mice were given a second dose of diminazene aceturate to induce a severe meningoencephalitis similar to that seen in patients that have died from the PTRE. The animals were killed 14 days following administration of the drug. The number of $CD4^+$ cells infiltrating the meninges, corpus callosum, external capsule and cerebral cortex was assessed and expressed as the number of cells per mm^2 of tissue. The figures in the body of the table demonstrate the comparisons, in terms of statistical significance, between the brain areas shown in the row and column headings. The p-values and 95% confidence intervals for differences are based on analysis using the logarithmic transformation [log(x + 1)] of the cell counts. The mean cell count ± the standard error and the number of animals per group are also shown. Figures detailed in red highlight groups showing significant differences.

	CD8 cell count in meninges							
	7DPI	14DPI	21DPI	28DPI	7DPD	14DPD	7DPDD	14DPDD
14DPI	p=0.825 (-0.511, 1.290)							
21DPI	p=0.806 (-0.663, 1.719)	p=0.999 (-1.052, 1.330)						
28DPI	p=0.0008 (0.583, 2.663)	p=0.013 (0.194, 2.273)	p=0.142 (-0.205, 2.394)					
7DPD	p<0.0001 (1.689, 3.769)	p<0.0001 (1.300, 3.379)	p=0.0003 (0.901, 3.501)	p=0.070 (-0.056, 2.268)				
14DPD	p<0.0001 (2.777, 4.579)	p<0.0001 (2.389, 4.190)	p<0.0001 (1.959, 4.341)	p=0.0001 (1.016, 3.095)	p=0.090 (-0.090, 1.989)			
7DPDD	p<0.0001 (2.528, 4.438)	p<0.0001 (2.139, 4.049)	p<0.0001 (1.722, 4.188)	p=0.0003 (0.773, 2.948)	p=0.326 (-0.333, 1.842)	p=0.997 (-1.150, 0.760)		
14DPDD	p<0.0001 (2.392, 4.774)	p<0.0001 (2.003, 4.385)	p<0.0001 (1.631,4.479)	p=0.001 (0.660, 3.260)	p=0.389 (-0.444, 2.154)	p=1.000 (-1.287, 1.096)	p=1.000 (-1.133, 1.333)	
Mean ± SE	0.000 ± 0.000	0.700 ± 0.490	0.938 ± 0.938	4.440 ± 1.290	17.080 ± 7.720	38.950 ± 2.870	32.690 ± 4.790	36.400 ± 10.100
Number	5	5	2	3	3	5	4	2

Table 3.20. Comparison of CD8 cell infiltration in the meninges at various time-points following trypanosome infection and subcurative drug treatment

Mice were infected with *T.b.brucei* GVR/C1.6 and the CD8 cell infiltration of the meninges was assessed at 7 (7DPI), 14 (14DPI), 21 (21DPI) and 28 (28DPI) days post-infection; 7 and 14 days after exacerbation of the CNS reaction by administration of a single diminazene aceturate treatment (7DPD, 14DPD); and 7 and 14 days following the induction of the PTRE by administration of a second diminazene aceturate treatment (7DPDD, 14DPDD). The figures in the body of the table demonstrate the comparisons, in terms of statistical significance, between the groups shown in the row and column headings. The 95% confidence intervals for differences between the group means, based on analysis using the logarithmic transformation [log(x + 1)] of the cell counts, together with the p-values are detailed. The mean cell count ± standard error and the number of animals per group are also shown. Figures detailed in red highlight groups showing significant differences.

	CD8 cell count in the corpus callosum							
	7DPI	14DPI	21DPI	28DPI	7DPD	14DPD	7DPDD	14DPDD
14DPI	p=1.000 (-0.563, 0.563)							
21DPI	p=0.996 (-0.514, 0.785)	p=0.996 (-0.514, 0.785)						
28DPI	p=0.759 (-0.344, 0.955)	p=0.759 (-0.344, 0.955)	p=0.992 (-0.556, 0.897)					
7DPD	p<0.0001 (1.362, 2.850)	p<0.0001 (1.362, 2.850)	p<0.0001 (1.159, 2.783)	p<0.0001 (0.989, 2.613)				
14DPD	p<0.0001 (2.519, 3.644)	p<0.0001 (2.519, 3.644)	p<0.0001 (2.297, 3.596)	p<0.0001 (2.126, 3.425)	p=0.005 (0.231, 1.729)			
7DPDD	p<0.0001 (1.919, 3.113)	p<0.0001 (1.919, 3.113)	p<0.0001 (1.702, 3.061)	p<0.0001 (1.532, 2.890)	p=0.636 (-0.359, 1.181)	p=0.072 (-1.162, 0.032)		
14DPDD	p<0.0001 (2.575, 4.063)	p<0.0001 (2.575, 4.063)	p<0.0001 (2.372, 3.996)	p<0.0001 (2.202, 3.826)	p=0.003 (0.324, 2.102)	p=0.956 (-0.506, 0.982)	p=0.037 (0.032, 1.573)	
Mean ± SE	0.000 ± 0.000	0.000 ± 0.000	0.167 ± 0.167	0.417 ± 0.300	7.630 ± 2.620	22.020 ± 3.790	11.740 ± 1.690	27.540 ± 7.11
Number	5	5	3	3	2	5	4	2

Table 3.21. Comparison of CD8 cell infiltration in the corpus callosum at various time-points following trypanosome infection and subcurative drug treatment

Mice were infected with *T.b.brucei* GVR/C1.6 and the CD8 cell infiltration of the corpus callosum was assessed at 7 (7DPI), 14 (14DPI), 21 (21DPI) and 28 (28DPI) days post-infection; 7 and 14 days after exacerbation of the CNS reaction by administration of a single diminazene aceturate treatment (7DPD, 14DPD); and 7 and 14 days following the induction of the PTRE by administration of a second diminazene aceturate treatment (7DPDD, 14DPDD). The figures in the body of the table demonstrate the comparisons, in terms of statistical significance, between the groups shown in the row and column headings. The 95% confidence intervals for differences between the group means, based on analysis using the logarithmic transformation [log(x + 1)] of the cell counts, together with the p-values are detailed. The mean cell count ± standard error and the number of animals per group are also shown. Figures detailed in red highlight groups showing significant differences.

	CD8 cell count in the external capsule							
	7DPI	14DPI	21DPI	28DPI	7DPD	14DPD	7DPDD	14DPDD
14DPI	p=1.000 (-0.736, 0.736)							
21DPI	p=0.712 (-0.432, 1.267)	p=0.712 (-0.432, 1.267)						
28DPI	p=0.169 (-0.162, 1.537)	p=0.169 (-0.162, 1.537)	p=0.975 (-0.679, 1.220)					
7DPD	p<0.0001 (1.313, 3.861)	p<0.0001 (1.313, 3.861)	p=0.0006 (0.826, 3.512)	p=0.002 (0.556, 3.242)				
14DPD	p<0.0001 (2.435, 3.906)	p<0.0001 (2.435, 3.906)	p<0.0001 (1.903, 3.602)	p<0.0001 (1.633, 3.332)	p=0.776 (-0.691, 1.857)			
7DPDD	p<0.0001 (1.774, 3.334)	p<0.0001 (1.774, 3.334)	p<0.0001 (1.248, 3.025)	p<0.0001 (0.978, 2.754)	p=1.000 (-1.333, 1.267)	p=0.191 (-1.396, 0.164)		
14DPDD	p<0.0001 (2.266, 4.212)	p<0.0001 (2.266, 4.212)	p<0.0001 (1.760, 3.883)	p<0.0001 (1.489, 3.613)	p=0.775 (-0.772, 2.077)	p=1.000 (-0.904, 1.042)	p=0.343 (-0.322, 1.693)	
Mean ± SE	0.000 ± 0.000	0.000 ± 0.000	0.833 ± 0.833	1.250 ± 0.722	12.287 ± NA	23.630 ± 3.210	12.030 ± 1.180	25.000 ± 5.000
Number	5	5	3	3	1	5	4	2

Table 3.22. Comparison of CD8 cell infiltration in the external capsule at various time-points following trypanosome infection and subcurative drug treatment

Mice were infected with *T.b.brucei* GVR/C1.6 and the CD8 cell infiltration of the external capsule was assessed at 7 (7DPI), 14 (14DPI), 21 (21DPI) and 28 (28DPI) days post-infection; 7 and 14 days after exacerbation of the CNS reaction by administration of a single diminazene aceturate treatment (7DPD, 14DPD); and 7 and 14 days following the induction of the PTRE by administration of a second diminazene aceturate treatment (7DPDD, 14DPDD). The figures in the body of the table demonstrate the comparisons, in terms of statistical significance, between the groups shown in the row and column headings. The 95% confidence intervals for differences between the group means, based on analysis using the logarithmic transformation [log(x + 1)] of the cell counts, together with the p-values are detailed. The mean cell count ± standard error and the number of animals per group are also shown. Figures detailed in red highlight groups showing significant differences. NA; not applicable.

	CD8 cell count in the caudate putamen							
	7DPI	14DPI	21DPI	28DPI	7DPD	14DPD	7DPDD	14DPDD
14DPI	p=1.000 (-0.849, 0.849)							
21DPI	p=0.998 (-0.794, 1.167)	p=0.998 (-0.794, 1.167)						
28DPI	p=1.000 (-0.980, 0.980)	p=1.000 (-0.980, 0.980)	p=0.999 (-1.283, 0.909)					
7DPD	p=0.008 (0.284, 2.530)	p=0.008 (0.284, 2.530)	p=0.052 (-0.005, 2.446)	p=0.017 (0.182, 2.633)				
14DPD	p=0.0005 (0.518, 2.216)	p=0.0005 (0.518, 2.216)	p=0.012 (0.200, 2.161)	p=0.003 (0.386, 2.347)	p=1.000 (-1.164, 1.083)			
7DPDD	p=0.006 (0.265, 2.066)	p=0.006 (0.265, 2.066)	p=0.069 (-0.047, 2.004)	p=0.019 (0.139, 2.191)	p=0.996 (-1.405, 0.921)	p=0.994 (-1.102, 0.699)		
14DPDD	p<0.0001 (1.149, 3.395)	p<0.0001 (1.149, 3.395)	p=0.0003 (0.860, 3.311)	p=0.0001 (0.046, 3.498)	p=0.413 (-0.478, 2.207)	p=0.176 (-0.218, 2.029)	p=0.069 (-0.056, 2.269)	
Mean ± SE	0.000 ± 0.000	0.000 ± 0.000	0.250 ± 0.250	0.000 ± 0.000	3.094 ± 0.281	3.170 ± 1.440	2.453 ± 0.736	10.440 ± 6.060
Number	5	5	3	3	2	5	4	2

Table 3.23. Comparison of CD8 cell infiltration in the caudate putamen at various time-points following trypanosome infection and subcurative drug treatment

Mice were infected with *T.b.brucei* GVR/C1.6 and the CD8 cell infiltration of the caudate putamen was assessed at 7 (7DPI), 14 (14DPI), 21 (21DPI) and 28 (28DPI) days post-infection; 7 and 14 days after exacerbation of the CNS reaction by administration of a single diminazene aceturate treatment (7DPD, 14DPD); and 7 and 14 days following the induction of the PTRE by administration of a second diminazene aceturate treatment (7DPDD, 14DPDD). The figures in the body of the table demonstrate the comparisons, in terms of statistical significance, between the groups shown in the row and column headings. The 95% confidence intervals for differences between the group means, based on analysis using the logarithmic transformation [log(x + 1)] of the cell counts, together with the p-values are detailed. The mean cell count ± standard error and the number of animals per group are also shown. Figures detailed in red highlight groups showing significant differences, figures detailed in blue show groups with differences of borderline significance.

	CD8 cell count in the cerebral cortex							
	7DPI	14DPI	21DPI	28DPI	7DPD	14DPD	7DPDD	14DPDD
14DPI	p=1.000 (-0.523, 0.523)							
21DPI	p=1.000 (-0.603, 0.603)	p=1.000 (-0.603, 0.603)						
28DPI	p=1.000 (-0.603, 0.603)	p=1.000 (-0.603, 0.603)	p=1.000 (-0.675, 0.675)					
7DPD	p=0.006 (0.274, 2.084)	p=0.006 (0.274, 2.084)	p=0.009 (0.225, 2.133)	p=0.009 (0.225, 2.133)				
14DPD	p<0.0001 (0.808, 1.853)	p<0.0001 (0.808, 1.853)	p<0.0001 (0.727, 1.934)	p<0.0001 (0.727, 1.934)	p=0.999 (-0.753, 1.057)			
7DPDD	p=0.002 (0.239, 1.348)	p=0.002 (0.239, 1.348)	p=0.008 (0.162, 1.424)	p=0.008 (0.162, 1.424)	p=0.844 (-1.309, 0.538)	p=0.061 (-1.092, 0.017)		
14DPDD	p<0.0001 (1.248, 2.631)	p<0.0001 (1.248, 2.631)	p<0.0001 (1.185, 2.693)	p<0.0001 (1.185, 2.693)	p=0.237 (-0.251, 1.773)	p=0.110 (-0.083, 1.299)	p=0.0006 (0.430, 1.861)	
Mean ± SE	0.000 ± 0.000	0.000 ± 0.000	0.000 ± 0.000	0.000 ± 0.000	2.250 ± NA	3.100 ± 0.816	1.328 ± 0.465	5.969 ± 0.469
Number	5	5	3	3	1	5	4	2

Table 3.24. Comparison of CD8 cell infiltration in the cerebral cortex at various time-points following trypanosome infection and subcurative drug treatment

Mice were infected with *T.b.brucei* GVR/C1.6 and the CD8 cell infiltration of the cerebral cortex was assessed at 7 (7DPI), 14 (14DPI), 21 (21DPI) and 28 (28DPI) days post-infection; 7 and 14 days after exacerbation of the CNS reaction by administration of a single diminazene aceturate treatment (7DPD, 14DPD); and 7 and 14 days following the induction of the PTRE by administration of a second diminazene aceturate treatment (7DPDD, 14DPDD). The figures in the body of the table demonstrate the comparisons, in terms of statistical significance, between the groups shown in the row and column headings. The 95% confidence intervals for differences between the group means, based on analysis using the logarithmic transformation [log(x + 1)] of the cell counts, together with the p-values are detailed. The mean cell count ± standard error and the number of animals per group are also shown. Figures detailed in red highlight groups showing significant differences. NA; not applicable.

	CD8$^+$ cell infiltration at 14 days post-infection				
	Meninges	Corpus callosum	External capsule	Caudate putamen	Cerebral cortex
Corpus callosum	p=0.160 (-0.882, 0.103)				
External capsule	p=0.160 (-0.882, 0.103)	p=1.000 (-0.492, 0.492)			
Caudate putamen	p=0.160 (-0.882, 0.103)	p=1.000 (-0.492, 0.492)	p=1.000 (-0.492, 0.492)		
Cerebral cortex	p=0.160 (-0.882, 0.103)	p=1.000 (-0.492, 0.492)	p=1.000 (-0.492, 0.492)	p=1.000 (-0.492, 0.492)	
Mean ± SE	0.700 ± 0.490	0.000 ± 0.000	0.000 ± 0.000	0.000 ± 0.000	0.000 ± 0.000
Number	5	5	5	5	5

Table 3.25. Comparison of CD8$^+$ cell infiltration of different brain areas 14 days following trypanosome infection

Mice were infected with *T.b.brucei* GVR/C1.6 and killed 14 days later. The number of CD8$^+$ cells infiltrating the meninges, corpus callosum, external capsule and cerebral cortex was assessed and expressed as the number of cells per mm^2 of tissue. The figures in the body of the table demonstrate the comparisons, in terms of statistical significance, between the brain areas shown in the row and column headings. The p-values and 95% confidence intervals for differences are based on analysis using the logarithmic transformation [log(x + 1)] of the cell counts. The mean cell count ± the standard error and the number of animals per group are also shown.

	CD8$^+$ cell infiltration at 21 days post-infection				
	Meninges	Corpus callosum	External capsule	Caudate putamen	Cerebral cortex
Corpus callosum	p=0.519 (-1.837, 0.682)				
External capsule	p=0.910 (-1.555, 0.964)	p=0.881 (-0.817, 1.382)			
Caudate putamen	p=0.595 (-1.786, 0.733)	p=0.999 (-1.048, 1.151)	p=0.937 (-1.330, 0.868)		
Cerebral cortex	p=0.344 (-1.972, 0.546)	p=0.991 (-1.234, 0.964)	p=0.668 (-1.517, 0.682)	p=0.969 (-1.286, 0.913)	
Mean $\pm$ SE	0.938 $\pm$ 0.938	0.167 $\pm$ 0.167	0.833 $\pm$ 0.833	0.250 $\pm$ 0.250	0.000 $\pm$ 0.000
Number	2	3	3	3	3

Table 3.26. Comparison of CD8$^+$ cell infiltration of different brain areas 21 days following trypanosome infection

Mice were infected with *T.b.brucei* GVR/C1.6 and killed 21 days later. The number of CD8$^+$ cells infiltrating the meninges, corpus callosum, external capsule and cerebral cortex was assessed and expressed as the number of cells per mm^2 of tissue. The figures in the body of the table demonstrate the comparisons, in terms of statistical significance, between the brain areas shown in the row and column headings. The p-values and 95% confidence intervals for differences are based on analysis using the logarithmic transformation [log(x + 1)] of the cell counts. The mean cell count $\pm$ the standard error and the number of animals per group are also shown.

	CD8$^+$ cell infiltration at 28 days post-infection				
	Meninges	Corpus callosum	External capsule	Caudate putamen	Cerebral cortex
Corpus callosum	p=0.008 (-2.255, -0.380)				
External capsule	p=0.050 (-1.872, 0.003)	p=0.638 (-0.555, 1.319)			
Caudate putamen	p=0.002 (-2.560, -0.685)	p=0.789 (-1.243, 0.632)	p=0.174 (-1.625, 0.249)		
Cerebral cortex	p=0.002 (-2.560, -0.685)	p=0.789 (-1.243, 0.632)	p=0.174 (-1.625, 0.249)	p=1.000 (-0.937, 0.937)	
Mean ± SE	4.440 ± 1.290	0.417 ± 0.300	1.250 ± 0.722	0.000 ± 0.000	0.000 ± 0.000
Number	3	3	3	3	3

Table 3.27. Comparison of CD8$^+$ cell infiltration of different brain areas 28 days following trypanosome infection

Mice were infected with *T.b.brucei* GVR/C1.6 and killed 28 days later. The number of CD8$^+$ cells infiltrating the meninges, corpus callosum, external capsule and cerebral cortex was assessed and expressed as the number of cells per mm^2 of tissue. The figures in the body of the table demonstrate the comparisons, in terms of statistical significance, between the brain areas shown in the row and column headings. The p-values and 95% confidence intervals for differences are based on analysis using the logarithmic transformation [log(x + 1)] of the cell counts. The mean cell count ± the standard error and the number of animals per group are also shown. Figures detailed in red highlight groups showing significant differences, figures detailed in blue show groups with differences of borderline significance.

	CD8$^+$ cell infiltration at 7 days after induction of late-stage CNS response				
	Meninges	Corpus callosum	External capsule	Caudate putamen	Cerebral cortex
Corpus callosum	p=0.468 (-3.777, 2.200)				
External capsule	p=1.000 (-3.832, 3.884)	p=0.598 (-3.044, 1.672)			
Caudate putamen	p=0.181 (-4.476, 1.501)	p=0.538 (-3.687, 2.289)	p=0.267 (-5.371, 2.345)		
Cerebral cortex	p=0.307 (-5.240, 2.476)	p=0.768 (-4.452, 3.264)	p=0.342 (-5.634, 2.818)	p=0.999 (-3.753, 3.963)	
Mean ± SE	17.080 ± 7.720	7.630 ± 2.620	12.287 ± 0.000	3.094 ± 0.281	2.250 ± 0.000
Number	3	2	1	2	1

Table 3.28. Comparison of CD8$^+$ cell infiltration of different brain areas 7 days following the induction of the late-stage CNS response

Mice were infected with *T.b.brucei* GVR/C1.6, treated with diminazene aceturate (40mg/kg i.p.) on day 21 post-infection and killed 7 days later. The number of CD8$^+$ cells infiltrating the meninges, corpus callosum, external capsule and cerebral cortex was assessed and expressed as the number of cells per mm^2 of tissue. The figures in the body of the table demonstrate the comparisons, in terms of statistical significance, between the brain areas shown in the row and column headings. The p-values and 95% confidence intervals for differences are based on analysis using the logarithmic transformation [log(x + 1)] of the cell counts. The mean cell count ± the standard error and the number of animals per group are also shown.

	$CD8^+$ cell infiltration at 14 days after induction of late-stage CNS response				
	Meninges	Corpus callosum	External capsule	Caudate putamen	Cerebral cortex
Corpus callosum	p=0.203 (-1.400, 0.206)				
External capsule	p=0.334 (-1.312, 0.295)	p=0.997 (-0.715, 0.892)			
Caudate putamen	p<0.0001 (-3.115, -1.508)	p=0.0001 (-2.518, -0.911)	p<0.0001 (-2.607, -1.000)		
Cerebral cortex	p<0.0001 (-3.151, -1.544)	p=0.0001 (-2.554, -0.947)	p<0.0001 (-2.643, -1.036)	p=0.999 (-0.839, 0.767)	
Mean ± SE	38.950 ± 2.870	22.020 ± 3.790	23.630 ± 3.210	3.710 ± 1.440	3.100 ± 0.816
Number	5	5	5	5	5

Table 3.29. Comparison of $CD8^+$ cell infiltration of different brain areas 14 days following the induction of the late-stage CNS response

Mice were infected with *T.b.brucei* GVR/C1.6, treated with diminazene aceturate (40mg/kg i.p.) on day 21 post-infection and killed 14 days later.

Mice were infected with *T.b.brucei* GVR/C1.6 and killed 14 days later. The number of $CD8^+$ cells infiltrating the meninges, corpus callosum, external capsule and cerebral cortex was assessed and expressed as the number of cells per mm^2 of tissue. The figures in the body of the table demonstrate the comparisons, in terms of statistical significance, between the brain areas shown in the row and column headings. The p-values and 95% confidence intervals for differences are based on analysis using the logarithmic transformation [log(x + 1)] of the cell counts. The mean cell count ± the standard error and the number of animals per group are also shown. Figures detailed in red highlight groups showing significant differences.

	$CD8^+$ cell infiltration at 7 days after induction of the PTRE				
	Meninges	Corpus callosum	External capsule	Caudate putamen	Cerebral cortex
Corpus callosum	p=0.007 (-1.683, -0.251)				
External capsule	p=0.009 (-1.646, -0.213)	p=0.999 (-0.679, 0.754)			
Caudate putamen	p<0.0001 (-3.034, -1.602)	p=0.0005 (-2.068, -0.635)	p=0.0004 (-2.105, -0.672)		
Cerebral cortex	p<0.0001 (-3.406, -1.974)	p=0.0001 (-2.440, -1.007)	p<0.0001 (-2.477, -1.044)	p=0.493 (-1.088, 0.344)	
Mean ± SE	32.690 ± 4.790	11.740 ± 1.690	12.030 ± 1.180	2.453 ± 0.736	1.328 ± 0.465
Number	4	4	4	4	4

Table 3.30. Comparison of $CD8^+$ cell infiltration of different brain areas 7 days following induction of the PTRE

Mice were infected with *T.b.brucei* GVR/C1.6 and treated with diminazene aceturate (40mg/kg i.p.) on day 21 post-infection. On relapse to parasitaemia the mice were given a second dose of diminazene aceturate to induce a severe meningoencephalitis similar to that seen in patients that have died from the PTRE. The animals were killed 7 days following administration of the drug. The number of $CD8^+$ cells infiltrating the meninges, corpus callosum, external capsule and cerebral cortex was assessed and expressed as the number of cells per mm^2 of tissue. The figures in the body of the table demonstrate the comparisons, in terms of statistical significance, between the brain areas shown in the row and column headings. The p-values and 95% confidence intervals for differences are based on analysis using the logarithmic transformation [log(x + 1)] of the cell counts. The mean cell count ± the standard error and the number of animals per group are also shown. Figures detailed in red highlight groups showing significant differences.

	$CD8^+$ cell infiltration at 14 days after induction of the PTRE				
	Meninges	Corpus callosum	External capsule	Caudate putamen	Cerebral cortex
Corpus callosum	p=0.919 (-1.740, 1.212)				
External capsule	p=0.829 (-1.820, 1.132)	p=0.999 (-1.556, 1.397)			
Caudate putamen	p=0.073 (-2.787, 0.165)	p=0.141 (-2.523, 0.429)	p=0.175 (-2.444, 0.509)		
Cerebral cortex	p=0.035 (-3.120, -0.167)	p=0.062 (-2.856, 0.096)	p=0.075 (-2.776, 0.176)	p=0.843 (-1.809, 1.144)	
Mean ± SE	36.400 ± 10.100	27.540 ± 7.110	25.000 ± 5.000	10.440 ± 6.060	5.969 ± 0.469
Number	2	2	2	2	2

Table 3.31. Comparison of $CD8^+$ cell infiltration of different brain areas 14 days following trypanosome infection

Mice were infected with *T.b.brucei* GVR/C1.6 and treated with diminazene aceturate (40mg/kg i.p.) on day 21 post-infection. On relapse to parasitaemia the mice were given a second dose of diminazene aceturate to induce a severe meningoencephalitis similar to that seen in patients that have died from the PTRE. The animals were killed 14 days following administration of the drug. The number of $CD8^+$ cells infiltrating the meninges, corpus callosum, external capsule and cerebral cortex was assessed and expressed as the number of cells per mm^2 of tissue. The figures in the body of the table demonstrate the comparisons, in terms of statistical significance, between the brain areas shown in the row and column headings. The p-values and 95% confidence intervals for differences are based on analysis using the logarithmic transformation [log(x + 1)] of the cell counts. The mean cell count ± the standard error and the number of animals per group are also shown.

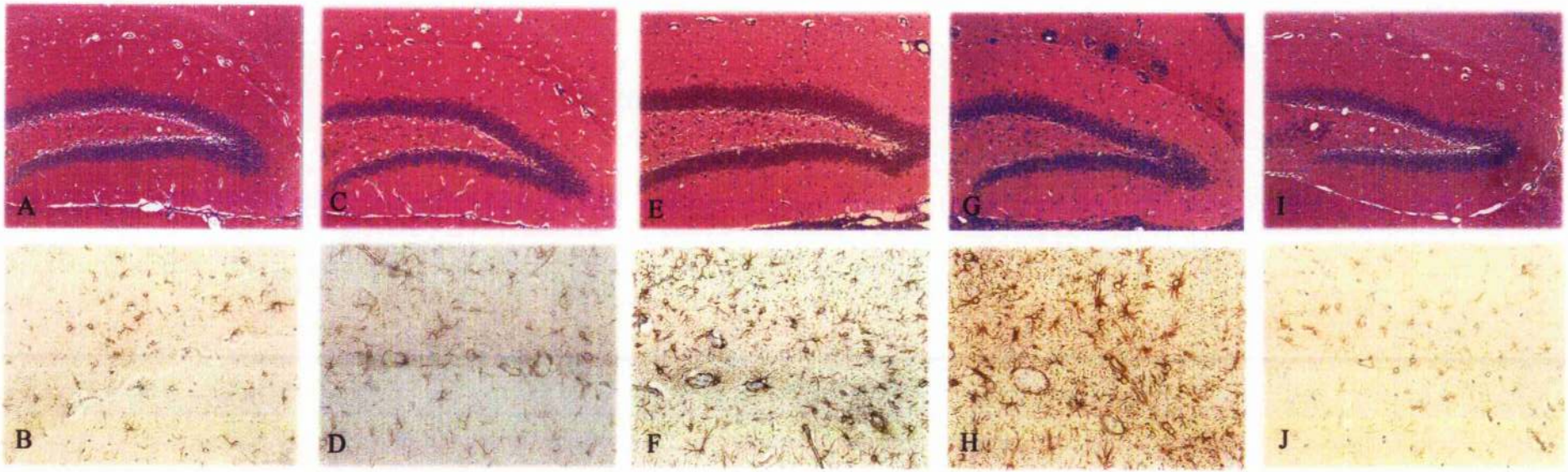

Figure 3.1. CNS inflammatory response to trypanosome infection and subcurative drug treatment.

Cornonal sections through the hippocampal region of the brain prepared from trypanosome-infected mice. Animals killed at 14 days post-infection (A&B) show a slight rise in inflammatory cell number in the ventricle and blood vessels (A) as well as an increase in astrocyte activation (B) compared with that seen in uninfected mice (I&J). The severity of the inflammatory response continues to rise in mice killed on day 28 post-infection (C&D). In mice killed 14 days after induction of the late-CNS stage of the disease (E&F), by administration of diminazene aceturate on day 21 post-infection, perivascular cuffs surround the vessels in the hippocampus and inflammatory cells are present in the ventricle (E). Many reactive astrocytes are also present (F). The severity of the inflammatory response is further increased in mice killed 14 days after the induction of the PTRE, by treatment with a second dose of diminazene aceturate following relapse to parasitaemia (G&H). Large perivascular cuffs are present and inflammatory cells can be seen infiltrating the neuropil (G). Numerous, large, highly stellated astrocytes are also present at this point in the disease (H). In comparison, uninfected mice show no perivascular cuffing and the ventricle appears free from inflammatory cells (I). Only mininal astrocyte staining can be seen (J). Panels A,C,E,G & I, H&E, X150; panels B,D,F,H & J, GFAP, X300.

3.4. Discussion

Histopathological assessment of brain sections, prepared from trypanosome-infected mice killed at various stages throughout the course of the disease process, showed a developing meningoencephalitis with activation of astrocytes and infiltration of a range of inflammatory cells. The inflammatory cell infiltration seemed to proceed in an ordered sequential pattern throughout the meninges, corpus callosum, external capsule, caudate putamen and cerebral cortex. The inflammatory cells initially appeared to infiltrate the meninges closely followed by the corpus callosum and the external capsule. As the severity of the reaction increased the cells moved deeper into the brain parenchyma and could be detected in the caudate putamen. The cerebral cortex appeared to be the final area of the brain to be infiltrated by the inflammatory cells. $CD4^+$ cells were detected in larger numbers than $CD8^+$cells and, in general, preceded the appearance of the $CD8^+$ cells. Macrophages were found in mounting numbers and diffused throughout the brain tissue as the severity of the inflammatory reaction increase. This augmentation of the macrophage population was found until the late-CNS stage of the infection was reached, at which point their numbers appeared to plateaux. B-cells and plasma cells were only detected during the late-CNS stage of the disease and in the post-treatment reactive encephalopathy (PTRE) and were not seen during the acute or early-CNS stage of the infection.

Following infection no pathological changes were observed in the CNS of the mice until 14 days after the animals had been infected with the parasites. At this stage only very mild inflammatory changes were apparent with the initiation of astrocyte activation and the appearance of a few $CD4^+$ and $CD8^+$ cells in the meninges. The occasional $CD4^+$ cell was also found in the corpus callosum at this point. As the disease progressed into the early-CNS stage, the $CD4^+$ and $CD8^+$ cells became more numerous and the severity of the overall inflammatory reaction was significantly greater than that found during the acute stage of the disease. By day 28 post-infection, $CD4^+$ cells could be detected in the caudate putamen together with the occasional macrophage. No $CD8^+$ cells were present in this brain region at this time in the infection. Apart from the detection of an infrequent $CD4^+$ cell in the cerebral cortex at day 21 post-infection this area appeared to remain generally free from inflammatory changes throughout the acute and early-CNS stage of the disease. Astrocyte activation, characterised by an increase in cell number and intensity of GFAP staining, became more widespread as the infection progressed.

When the severity of the CNS reaction was exacerbated, by treating the mice with a subcurative diminazene aceturate treatment to mirror the late-CNS stage of the infection, a substantial increase in the number of inflammatory cells was found. Furthermore, $CD4^+$ cells, $CD8^+$ cells and macrophages were all detected in the cerebral cortex at this time. B-cells were also apparent following exacerbation of the reaction; however, they were largely confined to the meninges, ventricles and perivascular cuffs. On induction of the PTRE a moderate increase in the severity of the inflammatory reaction was found. Although this was accompanied by an overall rise in the numbers of $CD4^+$ and $CD8^-$ cells present, this was not a significant increase compared with the cell numbers found during the late-CNS stage of the disease. In fact, a slight decrease in the T-cell populations, compared with those seen 14 days after induction of the late-CNS stage, was detected 7 days following the onset of the PTRE. This is also true of the macrophage population since this appeared to stabilise following the induction of the late-CNS stage of the disease and did not continue to increase on further exacerbation of the CNS reaction. This suggests that the increased level of B-cell infiltration and the appearance of numerous plasma cells seen during the PTRE may help to account for the increase in the severity of the neuroinflammatory response found at this stage of the disease.

In the mouse model of human African trypanosomiasis used in this investigation the parasites have been shown to become established within the CNS between 14 and 21 days after the mice have become infected (Jennings, Whitelaw, Holmes, Chizyuka *et al.*, 1979). T-cells were not detected in uninfected animals or mice killed on day 7 post-infection. The first signs of CNS inflammation, including astrocyte activation and T-cell infiltration, were detected in mice killed on day 14 post-infection. Therefore, the initiation of the inflammatory reaction occurs before the parasites have invaded the brain tissue. The primary signal for induction of this reaction remains unclear. Since astrocytic foot-processes are in close proximity with the endothelial cells forming the blood-brain barrier (BBB) it is possible that these cells detect the presence of soluble factors, produced either directly by the trypanosomes or by the developing inflammatory response in the peripheral system, that induce the astrocytes to adopt an activated conformation. Following activation astrocytes have been shown to be capable of expressing cellular adhesion molecules and a range of inflammatory mediators (Shrikant and Benveniste, 1996) that could help facilitate the subsequent infiltration of inflammatory cells into the CNS. If the initiation of the reaction takes place in this manner, it is possible that the activated astrocytes control the initial development of the early CNS inflammatory reaction seen following trypanosome infection.

The activation of the astrocytic population is not the only possible scenario that would result in the development of the neuroinflammatory reaction. It is known that naïve T-cells do not cross the BBB and are excluded from the brain tissue. This has been demonstrated by the lack of a T-cell response to allogenic tissue or pathogens when the material is delivered directly into the brain parenchyma (Aloisi, Ria, and Adorini, 2000). However, once T-cells have become primed by the presence of specific antigens in the peripheral system they can cross the BBB and enter the CNS for the purpose of immune surveillance. This phenomenon has been shown in the development of experimental allergic encephalomyelitis (EAE), the animal model of multiple sclerosis (MS), seen following the transfer of T-cells activated against myelin basic protein into the bloodstream of normal healthy animals. In contrast, transfer of naïve T-cells does not result in the generation of EAE in the healthy recipients (Wekerle *et al.*, 1986). Although this infiltration of the CNS by activated T-cells does occur, the numbers of T-cells entering the brain is vastly reduced compared with that found in non-CNS tissue (Hickey, 2001). Following trypanosome infection, T-cells in the periphery will become activated through the presence of the parasite antigens, allowing their subsequent entry into the CNS and this may explain the presence of the occasional $CD4^+$ cell in the corpus callosum detected during the acute stage of the reaction.

The regulation of T-cell recruitment is not strictly controlled in all brain areas as a substantial T-cell and monocytic response is found in the meninges, cerebral ventricles and choroid plexus when allogenic tissue or pathogens are placed within the cerebral ventricles (Aloisi *et al.*, 2000). This may be a result of the presence of a weaker BBB in these areas, in which the tight junctions between the endothelial cells exhibit a lower electrical resistance compared to that created by the endothelial cells forming the BBB surrounding the brain microvessels (Zhang and Tuomanen, 1999). The cellular infiltration pattern associated with trypanosome infection seems to follow this precedent since the appearance of inflammatory cells was first detected in the meninges and ventricles. It is unclear whether the appearance of activated astrocytes or the infiltration of inflammatory cells occurs first in the brain following trypanosome infection. Therefore, it is feasible that the presence of the activated inflammatory cells, rather than the induction of astrocyte activation, controls the development of the CNS inflammation seen during the acute and early-CNS stage of the reaction and may be responsible for the initial activation of the astrocytic population.

Following parasite invasion of the CNS the severity of the response increased significantly and a corresponding rise in the number of inflammatory cells was seen. The introduction

of parasite antigen within the brain tissue could augment this inflammatory response and stimulate the clonal expansion of the individual T-cells already patrolling the CNS compartment. This could result in a further exacerbation of the inflammation since the primed T-cells would become fully activated and secrete additional inflammatory mediators including cytokines and chemokines. On induction of the late-CNS stage of the disease a more severe neuroinflammatory response was seen with increased numbers of T-cells and macrophages. B-cells were detected for the first time in brain sections prepared from animals exhibiting this stage of the infection. The ability of B-cells to enter the normal CNS for the purposes of immune surveillance has not been demonstrated unequivocally. However, following the initiation of an immune response within the CNS the presence of B-cells in the brain is not uncommon and oligoclonal bands can be found in the cerebrospinal fluid (CSF). This indicates that under inflammatory conditions B-cells can enter the CNS, clonally expand and differentiate into antibody secreting plasma cells (Hickey, 2001). Human African trypanosomiasis is characterised by a non-specific polyclonal B-cell expansion and elevated levels of IgM in the serum that are most pronounced in the early-stages of the disease. During the CNS-stage of the infection, increased IgM levels are found in the CSF. The detection of elevated IgM levels in the CSF is used as a valuable indicator that the disease has progressed beyond the peripheral compartments and is manifest in the CNS (Greenwood and Whittle, 1980). The presence of IgM in the CSF could reflect the infiltration of the CNS by B-cells and their subsequent differentiation into antibody secreting plasma cells. The discovery of B-cells in the CNS in the mouse model of HAT used in this study substantiates this hypothesis. Following the induction of the PTRE numerous B-cells and plasma cells were seen in the CNS. The presence of B-cells, $CD4^+$ cells and specific parasite antigen within the brain at this time could permit the proliferation and differentiation of the B-cells into antibody producing plasma cells, in a $CD4^+$ cell-dependent manner. Whether the increased number of B-cells is the result of this type of clonal expansion or due to the influx of additional B-cells from the periphery remains to be elucidated and are not mutually exclusive.

Probably the most methodically investigated inflammatory disease affecting the brain is MS. MS is an inflammatory condition of the CNS white matter and the disease patterns found in MS brain are simulated in EAE. This model has indicated a significant role for autoreactive $CD4^+$ T-cells in the generation of the CNS inflammatory reaction. In EAE these $CD4^+$ cells are directed against CNS antigens such as myelin basic protein (MBP) or proteolipid protein (PLP) and are consequently involved in the demyelination associated with the disease pathogenesis. Moreover, the condition can be induced in normal animals following passive transfer of autoreactive T-cells taken from an affected animal, further

demonstrating the importance of this cell type in the development of the disease state (Bright and Sriram, 2001). Such autoreactive T-cells have also been demonstrated in patients with MS. It appears that these cells become activated in the periphery, by an unknown mechanism, allowing their entry to the CNS. Once in the brain, the cells recognise specific antigen presented by local APC's or glial cells leading to cellular proliferation and disease progression. However, there are some anomalies between the inflammatory reaction seen in the animal model and that of MS patients. The lesions found in EAE are composed largely of $CD4^+$ cells whereas $CD8^+$ cells generally predominate in MS lesions (Bauer, Rauschka, and Lassmann, 2001; Gay, Drye, Dick, and Esiri, 1997). This may explain why the disease can be ameliorated in EAE by administration of anti-$CD4^+$ antibody, but the treatment does not result in the resolution of the condition in patients suffering from MS despite an overall reduction in the total number of $CD4^+$ cells in the peripheral blood (Bright and Sriram, 2001). It is possible that such anomalies also exist between the murine model of human African trypanosomiasis and the disease pathogenesis seen in patients. This seems unlikely, however, as the CNS inflammation induced in the model results from the initial infection with trypanosomes, as is the case in the human disease. The causes and precipitating factors in the development of MS remain unknown. Although there is strong evidence indicating that the CNS inflammation is the consequence of an autoimmune disease directed against CNS myelin or oligodendrocytes, the possibility of the existence of a causative agent for the disease has yet to be discounted unequivocally (Bright and Sriram, 2001; Keegan and Noseworthy, 2002). Therefore, in the animal model of MS the disease is initiated by an artificial means that may be distinct from the instigating factors of the CNS inflammatory reaction seen in human cases of MS and could alter the course of the disease.

In contrast to trypanosome induced CNS inflammation where $CD4^+$ cells predominate in all of the brain areas studied, $CD8^+$ cells are more numerous in the brain parenchyma in MS (Gay *et al.*, 1997; Woodroofe, Bellamy, Feldmann, Davison *et al.*, 1986). In MS the $CD8^+$ cells infiltrate the brain parenchyma while the $CD4^+$ cells remain largely confined to the meninges and perivascular cuffs (Gay *et al.*, 1997). In trypanosome-induced neuroinflammation both T-cell subsets diffuse throughout the brain tissue, the appearance of the $CD4^+$ cells in the parenchyma precedes the infiltration of the $CD8^+$ cells and the number of $CD4^+$ cells in each region outweighs the $CD8^+$ cell population. Multiple sclerosis is characterised by the presence of focal demyelination in association with T-cell and macrophage infiltration. The presence of inflammatory cells leads to axonal damage and deteriorated neuronal function (Bar-Or, Oliveira, Anderson, and Hafler, 1999). As the reaction progresses, the inflammatory lesions develop into a plaque or scar associated with

activated astrocytes and microglial cells (Meinl, Aloisi, Ertl, Weber *et al.*, 1994). In trypanosome-induced CNS inflammation little neuronal damage (Fink and Schmidt, 1979; Morrison *et al.*, 1983) has been detected despite the severity of the meningoencephalitic reaction. Some occurrence of demyelination, with no concomitant neuronal damage, has been reported in cases of human trypanosome infections (Cegielski and Durack, 1997), although this demyelination was not apparent in the mouse model used in this investigation (personal communication, Prof. I. Griffiths, University of Glasgow Veterinary School)

The contrasting T-cell infiltration patterns seen between these conditions may help to account for the extensive differences in the neuropathological outcomes resulting from the two disease states. $CD8^+$ cells are responsible for the elimination of intracellular pathogens such as viruses and certain bacteria and parasites. When activated the $CD8^+$ cells recognise specific pathogen derived peptides, displayed on the surface of the infected cell, in conjunction with MHC class I molecules. Since virtually all cells in the body are capable of expressing MHC class I molecules, in conditions where an autoimmune mechanism is suspected, any cell expressing the autoantigen could become the target for $CD8^+$ cell mediated cytotoxicity. This could result in major tissue damage through the induction of apoptotic pathways by the $CD8^+$ cells, either via receptor mediated cytotoxicity involving the interaction of Fas-ligand and Fas-receptor or through the release of cytotoxic granules, containing perforin and granzymes, by the $CD8^+$ cell. Once apoptosis has been induced in the target cell, the $CD8^+$ cell disengages from the target and can recycle to kill numerous cells displaying the specific antigen in conjunction with MHC class I molecules. The cellular debris resulting from the destruction of the target cell then attracts macrophages to the site, which rapidly clear the cell fragments by phagocytosis. This pattern of tissue damage and inflammatory cell infiltration appears to outline the disease process found in MS (Bar-Or *et al.*, 1999). Further evidence to support a role for $CD8^+$ cells in the development of the neurological symptoms associated with MS comes from studies using a MS model, based of infection with Theiler's murine encephalomyelitis virus (Murray, McGavern, Lin, Njenga *et al.*, 1998). In these investigations, $CD8^+$ and MHC class I molecule deficient mice developed the characteristic demyelination seen in MS but did not display the neurological impairment associated with the disease. When perforin and MHC class II molecule knockout mice were employed the neurological effects were restored in the animals thereby implicating perforin release by $CD8^+$ cells as the most likely cause of the neurological symptoms.

In trypanosome infections tissue damage within the CNS is not commonly found despite the development of a severe meningoencephalitic reaction. This may reflect the reversal of

the $CD4^+/CD8^+$ cell populations seen in the trypanosome-infected mice in this study since fewer cytotoxic $CD8^+$ cells are found and $CD4^+$ cells predominate in the inflammatory reaction both in the meninges and the parenchyma. In contrast to $CD8^+$ cells, $CD4^+$ cells are not generally responsible for the induction of cellular cytotoxicity. The main function of $CD4^+$ cells is to help or induce an inflammatory response through the production of inflammatory mediators such as cytokines and chemokines. Furthermore, in order to trigger an immune response, primed $CD4^+$ cells must encounter their specific antigen presented in conjunction with MHC class II molecules. These MHC class II molecules, unlike the MHC class I molecules, cannot be expressed by all cell types and are generally only exhibited by professional antigen presenting cells such as macrophages, dendritic cells and B-cells. Other cell types, including astrocytes and microglia, can be induced to express these molecules following stimulation with certain molecules such as interferon-γ (IFN-γ) (Keegan and Noseworthy, 2002). Once activated the $CD4^+$ cells proliferate and secrete cytokines that influence the course of the inflammatory response. The range of cytokines produced by the $CD4^+$ cell is dependent on many overlapping factors that remain to be fully elucidated. In some circumstances the $CD4^+$ cells will express cytokines such as IL-2 IFN-γ, TNF-α and lymphotoxin that can enhance macrophage functions and induce opsinization and complement fixation as well as stimulate $CD8^+$ cell activation. $CD4^+$ cells producing this range of cytokines are known as Th1 cells and are important in the removal of intracellular pathogens due to their augmentation of the cell mediated immune response. On the other hand, $CD4^+$ cells can express cytokines including IL-4, IL-5, IL-6 and IL-10, and are known as Th2 cells. This range of cytokines stimulates B-cell proliferation and antibody production and therefore favours a humoral rather than a cell mediated immune response (Mosmann and Sad, 1996). The $CD4^+$ cells present in MS and EAE seem to follow the Th1 paradigm (Karpus and Ransohoff, 1998), and may therefore enhance the activation of the predominant $CD8^+$ cells and macrophages inadvertently leading to additional tissue damage. The situation in the murine model of trypanosome infection differs from that seen in MS since the most abundant T-cells belong to the $CD4^+$ T-cell subset. In addition, the cytokine profile expressed in the brain during the CNS-stage of trypanosomiasis does not easily conform to a Th1 or Th2 type response since mRNA transcripts for IL-1α, IL-6, TNF-α, IL-4, and IFN-γ have all been detected (Hunter, Gow, Kennedy, Jennings *et al.*, 1991; Hunter, Jennings, Kennedy, and Murray, 1992a). However, the cellular source of these inflammatory mediators has yet to be identified.

Plasma cells have been reported to be present in MS lesions, however it is thought that the B-cells in this condition do not cross the intact BBB and only enter the CNS following

disruption of the barrier by the disease process (Keegan and Noseworthy, 2002; Woodroofe *et al.*, 1986). This is perhaps also the case in the development of the CNS reaction associated with trypanosome infection. In this study no B-cells were detected in the brains of infected animals until the late-CNS stage of the disease when the CNS inflammatory response was significantly more severe than that seen during the acute and early-CNS stage of the reaction. The ability of B-cells to enter the CNS only at this point in the development of the CNS response could reflect some impairment of the BBB due to the on-going inflammatory reaction. Although damage to the BBB is a widely accepted consequence of the development of the CNS reaction, conflicting evidence exists regarding the breakdown of the BBB in this condition. In a study using fluorescent dye penetration of the CNS as an indication of BBB damage, severe impairment of the barrier was detected in rats at 40 days post-infection with *T.b.brucei* GVR35/C1.3 (Philip *et al.*, 1994). However, the results of experiments investigating the effects of trypanosome infection on the BBB tight junction proteins occludin and zonula occludens 1, showed that *T.b.brucei* could penetrate the rat CNS while causing no loss of the tight junction proteins (Mulenga *et al.*, 2001). Therefore, the degree of impairment to the BBB resulting from trypanosome infection remains controversial.

The importance of T-cells in the development of a number of additional CNS inflammatory conditions has also been highlighted. Perhaps the most severe complication of infection with *Plasmodium falciparum* is the development of cerebral malaria. The neuropathology found in post-mortem examinations of brain tissue prepared from patients who have died from cerebral malaria is characterised by the congestion of the cerebral microvessels with parasitised red blood cells. Haemorrhages, the deposition of malarial pigment and oedema are also commonly found. In addition, damage to the BBB can occur and a reduction in the expression of the tight junction proteins zonula occludens 1, occludin and vinculin has been found. The invasion of the CNS by inflammatory cells is an inconsistent finding (Medana, Chaudhri, Chan-Ling, and Hunt, 2001). However, T-cells have been shown to play a key role in the generation of cerebral malaria in animal models of the disease (Medana *et al.*, 2001; Yanex, Manning, Cooley, Weidanz *et al.*, 1996). The contribution of T-cells to this reaction was demonstrated in studies that showed that athymic mice do not succumb to disease. Further work demonstrated that the action of the $CD4^+$cells was important in the induction of the neuropathology since depletion of this T-cell subset protected the mice from the disease (Grau and Lou, 1995). A Th1 mediated response has been implicated as the pathway used by the $CD4^+$ cells in the development of cerebral malaria since knockout mice that could not synthesis IL-2 or IFN-

γ failed to acquire the condition whereas IL-4 and IL-10 knockout mice succumbed to cerebral malaria (Yanex *et al.*, 1996). In addition a requirement for functional $CD8^+$ cells in the development of the condition has also been shown using β_2-microglobulin knockout mice that do not express functional $CD8^+$ receptors and in mice where the $CD8^+$ cell population has been depleted using monoclonal antibodies to specifically remove the $CD8^+$ cells. In these experiments no cerebral malaria developed in the mice following elimination of the $CD8^+$ cells (Yanex *et al.*, 1996). The presence of B-cells does not seem to be a prerequisite for the development of cerebral malaria and the condition was found in B-cell deficient mice (Yanex *et al.*, 1996).

Toxoplasma gondii is a protozoan parasite that can cause toxoplasmic encephalitis. Normally the development of the encephalitic response is inhibited by the host's immune system and the infection is generally asymptomatic and the parasites lie dormant in the form of cysts within the brain. These cysts cause little or no inflammatory reaction in the CNS. In immunocompromised patients a reactivation of the parasites occurs resulting in the development of encephalitis (Gazzinelli, Xu, Hieny, Cheever *et al.*, 1992). Investigations, using a mouse model of toxoplasmosis, to discover the components of the immune response responsible for controlling the disease have shown that both $CD4^+$ cells and $CD8^+$ cells act in a synergistic manner to maintain the quiescent nature of the infection. Removal of either $CD4^+$or $CD8^+$ cells did not result in the reactivation of the response. However, when both cell types were depleted simultaneously necrotic lesions were found in the brain tissue following rupture of the parasitic cysts. A similar result was found when the mice were treated with anti-IFN-γ monoclonal antibody or a combination of anti-IFN-γ and anti-$CD4^+$ antibodies. These findings suggest that the presence of IFN-γ is crucial in the control of the parasitic infection and that the presence of $CD4^+$ cells is not necessary for the development of neuropathological response seen following reactivation of the infection (Gazzinelli *et al.*, 1992). Both $CD4^+$ cells and $CD8^+$ cells can produce IFN-γ and this may explain why it is necessary to remove the T-cell subsets simultaneously to reactivate the infection. The finding that the pathological reaction develops following removal of the $CD4^+$ cells, in conjunction with the IFN-γ, suggests that the development of the necrosis and neuroinflammation may be the result of activation of the $CD8^+$ cell population.

The development of the meningoencephalitis associated with trypanosome-infection and subcurative drug treatment involves the infiltration of the meninges, ventricles, perivascular cuffs and brain parenchyma by inflammatory cells and a widespread

astrogliosis. The first sign of the initiation of the CNS inflammatory response was the identification of activated astrocytes in the hippocampus and the presence of a few infiltrating T-cells. The appearance of these inflammatory changes could not be temporally distinguished and therefore the initiating or controlling elements for the generation of the reaction remain unclear. An interesting point to note is the abundance of $CD4^+$ cells found in the brains of the mice following trypanosome infection and sub-curative drug treatment. In previous investigations of trypanosome infection using a rat model of the disease, a key role for $CD8^-$ cell was postulated in the provision of an environment favourable for trypanosome proliferation (Bakheit, Olsson, Van Der Meide, and Kristensson, 1990; Olsson, Bakhiet, Edlund, Hojeberg *et al.*, 1991). These experiments demonstrated that the parasites produced a factor, subsequently termed trypanosome-derived T-lymphocyte triggering factor (TLTF), which could stimulate the production of IFN-γ by the $CD8^-$ cells. The IFN-γ was taken up by the parasites and acted as a growth factor. The CNS is considered a hostile location for parasite growth due to the relatively nutrient depleted environment (Enanga, Burchmore, Stewart, and Barrett, 2002). As the parasite has a means to alter the surrounding milieu to provide a more favourable atmosphere it seems odd that $CD4^+$ cells, rather than $CD8^+$ cells were the most abundant T-cell subset detected. The TLTF phenomenon may however prove to be species specific as no effect on parasite growth was noted when the trypanosomes were treated with human IFN-γ and no IFN-γ production was induced when human $CD8^+$ cells were stimulated with TLTF (Olsson *et al.*, 1991).

The pattern of inflammatory cell infiltration found in this model follows a pattern that would be expected in the immune response to extracellular parasites. In this scenario, the predominance of $CD4^+$ cells would control the reaction, enhance macrophage activity and stimulate B-cell differentiation and antibody production leading to the removal of the parasites. In addition, several of the inflammatory mediators produced by these cells, including, IL-1α and IL-6 have been shown to have neuroprotective capabilities (Hirano, 1994; Lenzlinger, Morganti-Kossmann, Laurer, and McIntosh, 2001; Stoll, Jander, and Schroeter, 2000). The reduced number of $CD8^+$ cells present together with the general absence of polymorphonuclear granulocytes may help to prevent the occurrence of any bystander damage caused to the brain tissue as a result of cell mediated cytotoxicity or the release of toxic enzymes by these groups of inflammatory cells.

Now that the inflammatory cell infiltration pattern occurring as a result of trypanosome infection and subcurative drug treatment has been elucidated it would be of great interest to

further dissect this response, in order to outline the roles of the various cell types in more detail. Future studies employing mice deficient in specific lymphocyte subsets or the use antibody depletion techniques to inhibit individual inflammatory cell types would highlight whether these cells play a predominantly damaging or protective role in the meningoencephalitic response. This knowledge would highlight the most suitable target cells types for novel drug intervention strategies to prevent or ameliorate the devastating adverse CNS reaction that at the present time results from chemotherapy of the disease.

CHAPTER 4

CYTOKINE AND CHEMOKINE RESPONSES IN A TRYPANOSOME-INDUCED CNS INFLAMMATORY REACTION

4.1. Introduction

Trypanosome infection is associated with the development of a severe inflammatory reaction within the CNS. The generation of such an inflammatory response is often governed by the presence of cytokines and chemokines. The participation of cytokines and chemokines in the pathogenesis of human African trypanosomiasis and the development of the CNS inflammatory reaction is unequivocal. However, the exact role played by these inflammatory mediators remains to be fully elucidated. In this Chapter the expression patterns of the cytokines IL-1α, IL-6 and TNF-α, together with the chemokines RANTES, MIP-1α and MCP-1 within the CNS, will be investigated following trypanosome infection and subcurative trypanocidal drug treatment. These mediators have been chosen for study as they are known to be induced following trypanosome infection and they can be expressed in brain tissue. Moreover, these cytokines and chemokines would be likely to generate an inflammatory reaction comparable to the response found in the CNS following trypanosome infection. This introduction will familiarise the reader with cytokines and chemokines as well as describe the roles of the particular inflammatory molecules, chosen for further study, within the CNS and the peripheral system. A review of the knowledge already available with regard to the cytokines and chemokines associated with trypanosome infection is also included.

4.1.1. What are cytokines and chemokines?

4.1.1.1. Cytokines

Cytokines are peptide or glycoprotein molecules, ranging in size from approximately 6 to 60 kilodaltons (kD) although more typically 15 to 30kD. They are produced by many different cell types in response to a multitude of diverse stimuli and over 100 cytokines have now been identified (Rothwell and Luheshi, 2000). These stimuli include infectious agents such as bacteria, viruses, fungi and parasites; mechanical injury; and toxic stimuli as well as the cytokines themselves (Fitzgerald, O'Neill, Gearing, and Callard, 2001). While cytokines and polypeptide hormones share many common features, the existence of multiple cell types, each capable of synthesising a variety of cytokines, rather than the presence of an endocrine gland responsible for the production of specific hormones, is one of the main differences between these mediators (Clemens, 1991).

Cytokine molecules are excreted by cells or expressed on the cell surface. They can influence the behaviour of cells in both an autocrine and a paracrine fashion by binding to specific receptors and initiating a variety of intracellular signal transduction pathways that eventually result in gene activation. Their effects are generally local, however, they can act systemically in an endocrine like manner. Cytokines are an extremely diverse group of molecules that elicit a wide range of effects. Most share some structural and functional features (Oppenheim and Saklatvala, 1993). Cytokines are all typically small protein molecules, although some are modified by the addition of carbohydrate side-chains before secretion and are therefore glycoproteins.

4.1.1.1.1. Control of cytokine production and action

Under normal circumstances cytokine production is tightly controlled, being induced or suppressed by the presence of external specific stimuli. Their half-life in the bloodstream or other extracellular fluids is generally short and they are potent at concentrations as low as 10^{-10} to 10^{-13} M (Clemens, 1991). Some cytokines are synthesized before they are required and sequestered in various forms within the body to provide a rapidly available source on stimulation. Cytokines such as TGF-β and GM-CSF can be stored in cytoplasmic granules, TNF-α and IL-1β may be integrated into the cell membrane and TGF-β and MIP-1β can be complexed with cell surface binding proteins or the extracellular matrix. The majority of cytokines however are rapidly produced through gene expression in response to the appropriate stimulation of the cell and are not pre-manufactured.

Many cytokines require further processing following production to create the free or active moiety. Some can be synthesised as the biologically active molecule, produced in the form of an integral membrane protein that has to be cleaved from the membrane to release the active cytokine molecule. Alternatively, cytokines can be synthesised in a larger, biologically inactive, precursor form that is later enzymatically processed to give the active molecule. The production and activity of the cytokines IL-1α and TNF-α can be controlled using both of these mechanisms.

Soluble binding proteins that complex with cytokines in the blood and tissue fluids have been described. Some of these binding molecules are highly specific, including, those present for IL-1α, TNF-α and IL-6, and are similar to cytokine cell surface membrane receptors. Other cytokine binding proteins, such as α_2-macroglobulin, have more general

binding properties, and will bind with several cytokine molecules. The soluble binding proteins may act in a variety of ways. Once bound to their target they can extend the half-life or, by effectively removing the molecule from the circulation, promote further production of the specific cytokine. It is also possible that this complex of binding protein and cytokine may form a biologically active molecule that can further stimulate specific receptors. This scenario is known to occur in IL-6 pathways. Conversely the binding proteins may control the effects of the cytokine by preventing the cytokine from binding with and thereby further stimulating the cell surface receptors (Fitzgerald *et al.*, 2001).

4.1.1.1.2. Cytokine function

It is impossible to assign a single or clearly defined role to individual cytokines as most have multiple, overlapping biological activities with many cellular targets. This provides a system where there is significant redundancy in the actions of these mediators, which can allow alternative pathways to supersede in instances where the optimal route of action may have become damaged or inhibited. Furthermore cytokines can effectively stimulate the production of other cytokines, and cytokine receptors, as well as regulate their own secretion. Complex cascades of cytokines that can interact with each other in both a synergistic and antagonist fashion therefore control many essential processes in the body. Cellular renewal and wound healing as well as both cellular and humoral immune responses against invading pathogens are mediated by the interaction of a range of these molecules.

4.1.1.1.2.1. Th1 and Th2 cytokines

One useful basis that assists in unravelling the highly complex interactions of the various cytokine functions in the immune response is the existence of what has been termed Th1 and Th2 cytokines. These cytokines are in general produced by different subgroups of the T-helper cell population and support either cell mediated immunity or antibody-mediated, humoral, immune reactions. The antibody-mediated type of response is favoured by Th2 cytokines such as IL-4, IL-5, IL-6, IL-10 and IL-13. These cytokines promote B-cell functions and induce the preferential production of IgE and IgA by the antibody-producing cells as well as enhance eosinophil and mast cell functions.

The Th1 and Th2 groups of cytokines not only promote different immune pathways but also hinder the development of the opposite response. The presence of the Th1 cytokine IFN-γ inhibits the production of Th2 cytokines, while the Th-2 cytokines IL-10, IL-4 and

IL-13 inhibit the production of Th-1 cytokines. The factors determining whether an immune reaction will be biased towards a Th1 or Th2 response are as yet unclear. It appears that many interconnecting determinants such as the nature of the antigen inducing the response, the co-stimulatory signal received by the T-cell, the nature of the cytokine milieu present at the induction of the reaction, as well as genetic make up of the responding animal all influence the final outcome of the response. The polarization of the cytokine response to either Th1 or Th2 can contribute to the pathogenesis of immune-mediated diseases. Th1 cytokines have been shown to contribute to the development of organ specific autoimmune diseases while Th2 cytokines are concerned with the generation of allergic disorders (Fitzgerald *et al.*, 2001).

4.1.1.2. Chemokines

Chemokines, although members of the cytokine superfamily, have a distinct identity with their own discrete actions. The majority of chemokines have been discovered using molecular cloning techniques and based on these findings it has been estimated that there could be 40-50 human chemokines. As the name suggests, chemokines have a chemotactic effect on cells and their migratory influence over cells of the immune system is perhaps their best-characterised function. Unlike other chemotactic mediators such as formyl peptides and complement factors, chemokines deliver migratory signals to highly specific cellular targets (Vaddi, Keller, and Newton, 1997). This is not the only function of chemokines since certain members of the group play an important role in angiogenesis and neovascularisation while others influence haematopoiesis (Rollins, 1997).

4.1.1.2.1. Chemokine families

Chemokines are generally small peptide molecules that range from 8 to 12kD in size and are, in the main, defined by the presence of four cysteine molecules that are expressed in highly conserved locations in the structure of the molecule. The chemokines can be divided into four families depending on the positioning of the conserved cysteine molecules. The CC (or β) chemokines express two adjacent cysteine residues towards the N-terminal of the molecule. In CXC (or α) chemokines, the two N-terminal cysteines are separated by a single amino acid, while the cysteines in CX_3C (or δ) chemokines are separated by three amino acid molecules. Fractalkine is the only known member of the CX_3C group of chemokines. The two remaining cysteines in each of these three chemokine families are located at conserved sites further downstream in the structure of

the molecule. The fourth chemokine family has, at present, only two known members, lymphotactin and single cysteine motif-1 (SCM-1). These molecules are of the correct size for chemokines and have a powerful chemotactic action on T-cells but they are structurally different from the other members since they expresses only two cysteine molecules. The positioning of these amino acids matches the location of the second and the fourth cysteine molecule in the conventional chemokine structure. Lymphotactin and SCM-1, have been classified as belonging to a separate group known as the C (or γ) chemokine family (Rollins, 1997; Vaddi *et al.*, 1997). A schematic representation of these structural similarities is detailed in Figure 4.1.

In general CXC chemokines induce migration of neutrophils, eosinophils and basophils while CC chemokines target monocytes and lymphocytes. There are exceptions to this broad rule since the CXC chemokines IL-8, IP-10 (γ-interferon inducible protein-10) and MGSA (melanoma growth stimulatory activity) are attractive to T-cells while the CC chemokines MCP (monocyte chemoattractant protein)-1, MCP-3, RANTES (regulated on activation, normal T-cell expressed and secreted) and MIP (macrophage inflammatory protein)-1α are chemotactic to basophils (Vaddi *et al.*, 1997).

4.1.1.2.2. How are chemokines chemotactic?

The transmigration of immune cells from the bloodstream into the tissue is a complex process requiring a number of coordinated steps that must be performed in sequential order. One theory suggests that the leucocytes roll along the vascular endothelium forming loose interactions with the cellular adhesion molecules until they reach an area with high concentrations of chemokines bound to the membrane or presented on cell surface molecules. In this immobilised state the chemokines are thought to interact with the leucocytes to increase their integrin affinities and strengthen their adhesiveness with the membrane. In addition, the chemokine leucocyte interactions induce changes in the cytoskeleton of the inflammatory cells that facilitate their subsequent diapedesis through the membrane. However, to permit chemokines to exert an attractive effect, the target cells of the chemokines must express cell surface receptors that are not only capable of detecting the presence of the chemokine but also are able to perceive changes in the concentration of particular chemokines in the microenvironment. This allows the chemokines to direct the movement of specific immune cell types by forming a concentration gradient with the cells migrating towards increasing intensities of the chemokine. Extravasated leucocytes are

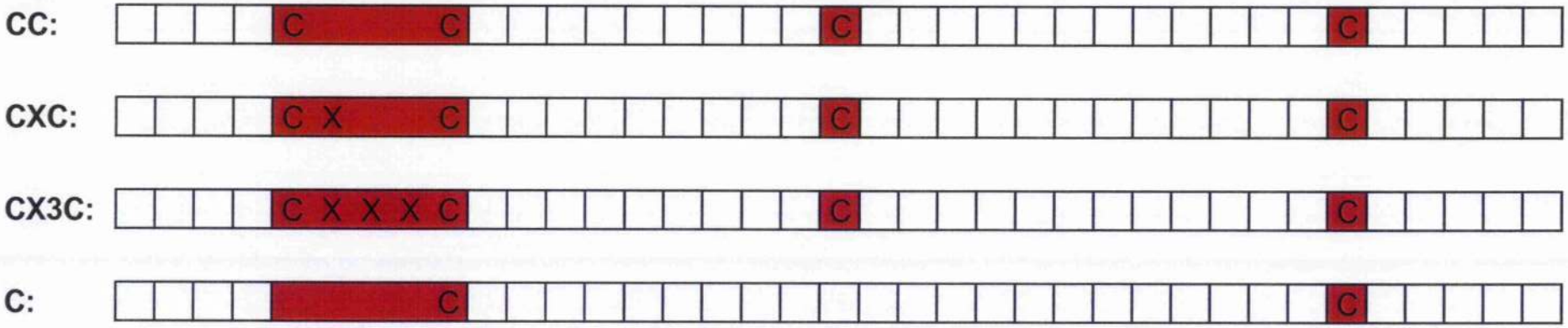

Fig 4.1. Classification of chemokine families according to structure. C indicates the position of a cysteine molecule; X indicates the position of any amino acid other that cysteine within the conserved region; red boxes indicate areas of conserved amino acid sequence; empty boxes indicate the additional amino acids that make up the complete chemokine molecule; gaps between the amino acids indicate spaces in the alignment.

thought to follow such concentration gradients and establish in areas of high chemokine density elaborated by cells at inflammatory foci (Rollins, 1997; Vaddi *et al.*, 1997).

4.1.1.2.3. Chemokine receptors

Chemokine receptors are integral membrane glycoproteins that are on average 350 amino acids long with a calculated molecular weigh of approximately 40kD. Structurally the molecules consist of seven α-helices that traverse the cell membrane. The N-terminal of the glycoprotein molecule lies on the external surface of the membrane while the C-terminal occupies the cytoplasmic side of the membrane. The receptors are coupled with GTP-binding proteins on the cytoplasmic side of the membrane and therefore belong to the G-protein coupled receptor superfamily of proteins. Triggering of these receptors leads to signal transduction with subsequent influx of calcium ions and phosphatidyl inositol turnover.

There is an apparent promiscuity in the use of chemokine receptors since chemokines can signal via multiple receptor types and each receptor type is capable of binding several different chemokines. However, it appears that in general these receptors will bind either CC or CXC group chemokines but not both types. There are eleven known CC chemokine receptors (CCR1-11) and five described CXC chemokine receptors (CXCR1-5) as well as one CX_3C receptor (CX_3CR1) and one receptor for C family chemokines (XCR1). In addition the Duffy blood group antigen has been shown to bind chemokines belonging to both CC and CXC families and has been termed the Duffy antigen receptor for chemokines (DARC) (Bajetto, Bonavia, Barbero, Florio *et al.*, 2001; Rollins, 1997).

4.1.2. Cytokines and chemokines in the CNS

A wide variety of both cytokines and chemokines have been recognized in the CNS where they have been shown to act as crucial mediators in the host immune response and in neuronal and glial functions. Some of these mediators are not only produced following induction of an inflammatory reaction but are manufactured within the normal CNS in response to neuotransmitters and neuropeptides. These constitutively expressed cytokines and chemokines play key roles in regulating glial functions and affect neuronal survival (Hesselgesser and Horuk, 1999; Szelenyi, 2001).

Since an immense number of cytokines and chemokines have been demonstrated to influence normal brain functions, as well as the immune response within the CNS, this study will concentrate on the actions of three cytokines, IL-1, IL-6 and TNF-α and three chemokines MIP-1α, MCP-1α and RANTES which have been shown previously to be induced following trypanosome infection. Their general functions together with their roles in normal and pathophysiological CNS as well as their functions in the immune response are discussed below.

4.1.2.1. Interleukin-1

Interleukin 1 (IL-1) was originally described as a monocyte-derived compound and was given various names including lymphocyte-activating factor (LAF), endogenous pyrogen (EP), leucocyte endogenous mediator (LEM), monocyte cell factor (MCF) and catabolin (Fitzgerald *et al.*, 2001; Oppenheim and Saklatvala, 1993). There are two forms of IL-1, IL-1α and IL-1β, these show only approximately 20% homology and are derived from two distinct genes. Although these molecules appear to be dissimilar, they bind to the same receptors and have largely analogous if not identical biological properties.

IL-1 binds to two different forms of IL-1 receptor, the 80 kDa type I receptor (CDw121a) and the 68 kDa type II receptor (CDw121b) both of which can bind either IL-1α or IL-1β. The type I receptor requires the binding of IL-1 and an accessory protein before signal transduction is initiated while the smaller type II receptor lacks an intracellular domain and therefore binding of the ligand to this receptor does not initiate the intracellular signalling pathways (Rothwell and Luheshi, 2000). The IL-1 type I and type II receptors are both transmembrane glycoprotein molecules found widely distributed on many cell types, including, T-cells, B-cells, monocytes, NK-cells, neutrophils, eosinophils, basophils, dendritic cells, endothelial cells, and neural cells. As well as IL-1α and IL-1β, a third member of the IL-1 type family, IL-1 receptor antagonist (IL-1ra), exists. IL-1ra is a highly selective receptor antagonist that competes mainly with IL-1β in binding with the IL-1 type I receptor. If IL-1ra binds with this receptor it does not induce subsequent signal transduction as it fails to accommodate the accessory protein. IL-1ra binding with the IL-1 type I receptor therefore blocks all actions of IL-1α and IL-1β and as such acts as an endogenous inhibitor of the cytokines (Fitzgerald *et al.*, 2001; Rothwell and Luheshi, 2000).

IL-1α, IL-1β and IL-1ra are produced as precursor molecules. IL-1α and IL-1ra are biologically active in this pro-form however IL-1β requires enzymatic cleaving to release the active moiety. The enzyme responsible for this reaction, and therefore indirectly the production of functional IL-β, is caspase 1 or IL-1β converting enzyme (ICE) and was the first member of the caspase family of cysteine proteases to be identified (Rothwell and Luheshi, 2000). This enzyme appears to be cell surface associated and is under the control of cell membrane inhibitors. Cleavage of the IL-1β precursor by ICE releases the 17 kDa mature cytokine together with 14 kDa and 17.5 kDa fragments from the cell. In contrast IL-1α shows biological activity in both its pro- and mature forms (Dinarello, 1998). However, the actions of IL-1α are for the most part produced by the membrane bound form of the molecule. This fixed positioning of the mature IL-1α may allow direct signalling of the target cell to occur in a highly precise manner as well as result in an extremely high concentration of the cytokine in exactly focussed areas (Dinarello, 1998).

A wide variety of different cell types have been shown to secrete IL-1. These cell types include monocytes, macrophages, T-cells, B-cells, NK-cells, smooth muscle fibres, as well as vascular endothelial cells, astrocytes and microglia. To match this extensive list of IL-1 sources, IL-1 can also act on a broad spectrum of target cells such as B-cells, T-cells and monocytes/macrophages among others. *In vivo* IL-1 can induce several responses including hypotension, fever, appetite suppression, neutrophilia, the development of systemic shock and the acute phase response as well as inducing local inflammatory reactions (Fitzgerald *et al.*, 2001; Martiney, Cuff, Litwak, and Berman, 1998).

Low levels of IL-1α, IL-1β, IL-1ra as well as the accessory protein necessary for effective signal transduction can be synthesised by resident brain cells and can be found at low levels in the normal healthy CNS. IL-1 has been shown to be biological activity at concentrations as low as in the femto-molar range. The exact source of these molecules in the brain and the pathways involved in the control of their production remain uncertain. Microglia, astrocytes, oligodendrocytes, neurones and vascular endothelial cells have all been shown to express IL-1 (Rothwell and Luheshi, 2000). In addition, IL-1α, IL-1β and IL-1ra can enter the brain from the periphery by crossing the BBB using a saturable transport system (Kastin, Pan, Maness, and Banks, 1999). In the normal CNS endogenously produced IL-1 has been demonstrated to play a role in the regulation of sleep patterns since IL-1ra decreases the slow wave sleep irrespective of the presence of infection (Opp and Krueger, 1991) and IL-1 type I receptor knockout mice show a reduced sleep period compared with wild-type mice (Krueger, Fang, Taishi, Chen *et al.*, 1998).

In inflammatory reactions IL-1 is first and foremost a pro-inflammatory cytokine that is produced in response to injury, immunological challenge or infection. Local production of IL-1 can lead to the migration of inflammatory cells to this site, possibly through the induction of chemokine synthesis by monocytes, fibroblasts and endothelial cells amongst others. Under many circumstances the production of the cytokine IL-6 is under direct control of IL-1, since mice given an intramuscular injection of turpentine fail to express IL-6 when the actions of IL-1 are blocked by concurrent administration of anti-IL-1 antibodies (Dinarello, 1998). Following infection or injury either within or outside the CNS, IL-1 production is induced in the brain tissue resulting in several reactions associated with the host defence response including fever, hypophagia, somnolence, neuroendocrine alterations and 'sickness behaviour' (Kennedy and Karpus, 1999; Konsman, Parnet, and Dantzer, 2002). The signals that induce this IL-1 production remain equivocal although several mediators have been implicated, including, circulating IL-6 and direct neuronal stimulation. In addition to these neuroimmune responses evidence suggests that IL-1, in particular IL-1β, plays a key role in conditions where acute neuronal degeneration is found. In mice, conditions that result in severe neuronal loss such as, ischaemia, hypoxia and excitotoxic and traumatic insult, induce the rapid production of IL-1. Furthermore, IL-1ra, when administered to rodents after induction of this type of injury, attenuates oedema and glial activation as well as improves subsequent neurological function. This raises speculation regarding the benefits of administration of this antagonist to alleviate neurodegenerative responses following injury in the human CNS (Rothwell and Luheshi, 2000). The neurotoxic effect of IL-1 may be dependent on the presence of other mediators since, in the absence of inducible nitric oxide sythetase (iNOS), IL-β exerts a protective effect on neurons following hypoxia and excitotoxic injury (Stoll *et al.*, 2000).

The pyrogenic effect of IL-1 results from the action of the cytokine, in conjunction with additional mediators such as IL-6, on particular areas within the hypothalamus. More specifically, IL-1 acts by decreasing the firing rate of the warm-sensitive cells and increasing that of the cold sensitive neurones in the preoptic anterior hypothalamus. This effectively produces a rise in the body temperature. Injection of IL-1ra into various areas of the rat brain leads to a reduction in the fever induced by peripheral injection of LPS further indicating a key role for IL-1 in the generation of the pyrogenic response. In addition to the induction of fever, IL-1 stimulation of the ventromedial hypothalamas appears to control appetite suppression whereas IL-1 actions in the paraventricular nuclei seem to mediate the activation of the hypothalamic-pituitary-adrenal (HPA) axis and

subsequent release of corticosteriods (Rothwell and Luheshi, 2000; Tilders, DeRijk, Van Dam, Vincent *et al.*, 1994).

4.1.2.2. Interleukin-6

Interleukin-6 (IL-6) is a 21-28 kDa glycoprotein molecule comprised of four anti-parallel α-helices with two long and two short loop connections. Both the C-terminus and the N-terminus appear to play a critical role in the function of the IL-6 molecule (Hirano, 1998). This cytokine was first reported in 1985 and was originally described as a substance with anti-viral properties and named IFN-β_2. The anti-viral function of IL-6 was later attributed to the ability of the cytokine to induce the secretion of IFN-α/β. IL-6 was also known by a variety of other names including IL-1-inducible 26 kDA protein, hepatocyte stimulating factor, cytotoxic T-cell differentiation factor, B-cell differentiation factor (BCDF) and B-cell stimulatory factor 2 (BSF-2). This reflected the wide variety of functions originally attributed to IL-6 (Fitzgerald *et al.*, 2001; Oppenheim and Saklatvala, 1993).

Functional IL-6 receptors are a complex of two transmembrane glycoproteins; gp130, a 130 kDa molecule (CD130), and a smaller 80 kDa IL-6 binding protein, IL-6R, (CD126). The larger gp130 molecule forms the signal transduction unit of the receptor and at least three different pathways including JAK/STAT, Ras/Raf and the Src-family of kinases can be activated on receptor binding. Soluble, blood borne forms of both of these subunits exist. The soluble form of the 80 kDa molecule, sIL-6R, is thought to arise via both proteolytic processing and alternative splicing. The pathways leading to the production of soluble gp130 remain unclear, however, two alternative splice variants lacking the transmembrane portion of the molecule have been reported (Diamant, Rienecck, Mechti, Zhang *et al.*, 1997). The soluble gp130 molecules appear to function as down-regulators of IL-6 activity and do not elicit signal transduction within cells. On the other hand sIL-6R binds with circulating IL-6 and extends the half-life of the cytokine and forms a signal transducing complex by binding with cell surface gp130.

Like IL-1, IL-6 is a highly multi-functional cytokine that is produced by a wide range of cells, including, T-cells, B-cells, macrophages, fibroblasts, keratinocytes, endothelial cells, cerebral cortex neurons, astrocytes and microglia (Marz, Cheng, Gadient, Patterson *et al.*, 1998; Oppenheim and Saklatvala, 1993). Many stimuli have been shown to induce production of IL-6. Following stimulation by mitogens or specific antigens, T-cells can be induced to secrete IL-6 and LPS enhances IL-6 production in macrophages and fibroblasts.

This enhanced IL-6 production can be abrogated by glucocorticoids. Other cytokines including IL-1 and TNF have also been shown to induce the expression of IL-6, whereas, IL-4 and IL-13 appear to inhibit IL-6 production by monocytes (Hirano, 1998). IL-6 has been described as a cytokine with both pro- and anti-inflammatory properties and, as suggested by the plethora of previous names, IL-6 exerts a bewildering range of effects on a wide variety of target cells. Following stimulation with appropriate antigen, B-cells differentiate into antibody-secreting plasma cells. This cellular transformation occurs under the influence of various mediators and IL-6 has been found to a play key role in the induction of the synthesis of secretory immunoglobin (Hirano, 1998). IL-6 is also an integral mediator in the activation, growth and differentiation of T-cells. Another central role of IL-6 is the induction of the acute phase reaction in the liver in response to injury and infection (Clemens, 1991).

In addition to these classical immunological roles, IL-6 has been shown to induce the development of PC12 cells into neural cells and can support the survival of neurons in tissue culture (Hirano, 1998). However, transgenic mice over-expressing IL-6 exhibit an acute neurodegenerative pathology (Campbell, Abraham, Masliah, Kemper *et al.*, 1993). Like IL-1, IL-6 has been implicated in mediating the HPA axis and can stimulate the discharge of ACTH. IL-6 can also induce the release of anterior pituitary hormones such as prolactin releasing hormone (PRL), leutenising hormone (LH) and growth hormone (GH) and cells in the anterior pituitary can spontaneously produce IL-6 itself. IL-6 can act as a growth factor for a variety of cell types, including, plasmacytoma, myeloma, hybridoma, renal cell carcinoma and Kaposi's sarcoma. In contrast, breast carcinoma, ovarian carcinoma and myeloleukaemic cell lines show growth retardation in the presence of IL-6 (Hirano, 1998).

4.1.2.3. Tumour necrosis factor-α

Tumour necrosis factor-α (TNF-α) was discovered in 1975 as a factor, induced by bacterial endotoxin, that exhibited potent anti-tumour activity (Beutler and Cerami, 1989; Carswell, Old, Kassel, Green *et al.*, 1975). Subsequently the integral role of TNF-α in immune regulation and inflammatory reactions was uncovered. TNF-α has also been known as cachectin, macrophage cytotoxin, necrosin, cytotoxin, haemorrhagic factor, macrophage cytotoxic factor and differentiation-inducing factor (Fitzgerald *et al.*, 2001). Human TNF-α is a non-glycosylated polypeptide whereas murine TNF-α is N-glycosylated. The cytokine can exist as either a 26 kDa membrane bound protein or a 17

kDa soluble molecule produced by proteolytic cleavage of a precursor molecule by the metalloprotease enzyme TNF-α converting enzyme (TACE or ADAM17) (McDermott, 2001). Both of these forms of the cytokine are biologically active although the soluble molecule is reputedly more potent than its membrane bound counterpart (Decoster, Vanhaesebroeck, Vandenabeele, Grooten *et al.*, 1995). Again the name of this cytokine can be misleading as it reflects the history of the molecule's discovery and although TNF-α can cause the regression of some types of tumour it also has a wide variety of other functions.

There are two different receptors for TNF-α; the TNF type I receptor (TNFRI) (CD 120a) and the TNF type II receptor (TNFRII) (CD120b). TNFRI is a 55 kDa transmembrane glycoprotein expressed by a wide range of mammalian cells where as TNFRII is a 75 kDa transmembrane glycoprotein predominately expressed by leucocytes and endothelial cells. Stimulation of the TNFRI can lead to cellular apoptosis via a cascade of signalling events culminating in the induction of caspase 2 or 8 enzyme activation within the cell. Apoptosis is not the only outcome associated with TNFRI binding since NF-κB can also be activated following TNFRI stimulation. This diverts the apoptotic pathways and leads to the induction of pro-inflammatory cytokine expression (Fitzgerald *et al.*, 2001). The function of TNFRII remains equivocal with the main physiological effects of TNF-α apparently being mediated though TNFRI. Since this receptor lacks a death domain its signalling pathways will differ from TNFRI. TNFRII appears to be involved in binding with membrane bound TNF-α rather than the free form of the cytokine. A role for TNFRII in the transfer of soluble TNF-α to the TNFRI has also been suggested (Fitzgerald *et al.*, 2001; McDermott, 2001). Soluble forms of both TNFRI and TNFRII exist and are though to result by enzymatic cleavage of the membrane bound receptor. These soluble receptors are known to block the activity of TNF-α, however, the pathways that result in the shedding of these receptors remain unclear (McDermott, 2001).

TNF-α, like IL-1α and IL-6, can be secreted by a vast array of cell types such as macrophages, monocytes, T-cells, B-cells, astrocytes, microglia and neurons among others (Allan and Rothwell, 2001; Fitzgerald *et al.*, 2001; Lieberman, Pitha, Shin, and Shin, 1989). TNF-α production by these cells can be induced by many different stimuli, including, LPS as well as the presence of other cytokines such as TNF-α itself, IL-1, IL-6, interferons and colony stimulating factors. Additional molecules including immune complexes and Substance P can also induce expression of this cytokine (Nair and Schwartz, 1995). TNF-α shows a wide spectrum of biological activities and together with

IL-1α and IL-6, plays an integral role in both the innate and adaptive immune response. This cytokine can increase the phagocytic properties of cells such as macrophages and neutrophils, thereby improving innate immunity. In addition TNF-α can augment the adaptive immune response to particular pathogens by enhancing the proliferation of T-cells induced by specific stimuli.

TNF-α was named due to its cytotoxic effects on specific tumours. Regression of the tumours can be initiated either by a direct cytotoxic action of the cytokine on the cancer cells or by TNF-α's ability to increase the capacity of NK-cells and macrophages to kill these abnormal cells. TNF-α production can also lead to the destruction of the vascular tissue supplying the tumour resulting in tissue necrosis of the isolated growth. Another striking effect of this cytokine is the induction of a debilitating combination of responses, including, weight loss, malnutrition and anaemia collectively termed cachexia. This is thought to result, in part, through the ability of TNF-α to inhibit lipoprotein lipase and other enzymes required for the storage of fat in adipose tissue (Beutler, Greenwald, Hulmes, Chang *et al.*, 1985). Also fundamental to the development of cachexia is the onset of anorexia or a reduced appetite induced by TNF-α in experimental animals (Clemens, 1991).

As well as these actions, TNF-α has been implicated in the pathogenesis of a variety of autoimmune conditions including rheumatoid arthritis, Crohn's disease, systemic lupus erythematosus, and multiple sclerosis. Furthermore, a role for TNF-α has been suggested in the development of infectious diseases such as cerebral malaria, septic shock, and chronic hepatitis (McDermott, 2001).

Within the normal brain TNF-α has recently been demonstrated to enhance synaptic activity by increasing the surface expression of α-amino-3-hydroxyl-5-methyl-4-isoxazolepropionic acid (AMPA) receptors and is therefore continually required to maintain the synaptic strength at excitatory synapses (Beattie, Stellwagen, Morishita, Bresnahan *et al.*, 2002). TNF-α can be expressed by many resident CNS cells, including, microglia, astrocytes and neurons (Pan, Zadina, Harlan, Weber *et al.*, 1997). Many of the actions of TNF-α in the CNS mirror those previously described for IL-1, such as, the induction of fever and sickness behaviour (Beattie *et al.*, 2002; Konsman *et al.*, 2002). In addition to TNF-α created locally within the CNS, a transport system to carry the cytokine across the BBB also exists allowing systemically produced TNF-α to enter the brain (Gutierrez, Banks, and Kastin, 1993). This transport system has been shown to be

upregulated following compressive injury to the spinal cord (Pan, Kastin, Bell, and Olson, 1999).

TNF-α appears to have a dual role within the inflamed or injured CNS. This cytokine can affect the BBB resulting in leucocyte infiltration and cerebral oedema and as previously stated can induce cellular apoptosis. It is therefore not surprising to find that inhibition of TNF-α activity results in enhanced motor function recovery following traumatic brain injury indicating a detrimental role for the cytokine. In contrast, transgenic mice lacking TNF-α receptors have been shown to be more vulnerable to traumatic brain injury suggesting a beneficial function for TNF-α. Furthermore, transgenic mice unable to express TNF-α protein show a better neurological motor score than their wild-type counterparts. This beneficial effect of the removal of TNF-α is short-lived since wild-type animals recover from the initial injury more quickly than the TNF-α knockout animals. This indicated a bimodal effect of TNF-α in the injured brain where its initial effects may be detrimental but the presence of the cytokine at later time points following injury is beneficial to the recovery of the animal (Lenzlinger *et al.*, 2001).

4.1.2.4. RANTES

Regulated on activation, normal T-cell expressed and secreted (RANTES), a CC chemokine, also known as TY-5 or SIS-δ, is an 8 kDa protein molecule. Under the new classification nomenclature RANTES is known as CCL5 (Zlotnik and Yoshie, 2000). The chemokine was identified originally in 1988 as a transcript that was expressed in T-cells but not B-cells following stimulation with mitogens or antigens (Schall, 1994). Chemokines bind to multiple receptors and RANTES mediates its action by binding to CCR1, CCR3, CCR4, CCR5 or DARC (Appay and Rowland-Jones, 2001; Schall, 1994). The chemokine has numerous target cells and can recruit T-cells, monocytes, basophils, eosinophils, NK-cells, dendritic cells and mast cells to sites of inflammation. Recently, interest has focused on RANTES due to its ability, in concert with two additional chemokine molecules, MIP-1α and MIP-1β, to inhibit the replication of HIV (Appay and Rowland-Jones, 2001). Aggregates of RANTES that form on the cell surface *in vitro* have been shown to be potent leucocyte activators and show similar effects to those seen following mitogen stimulation. It therefore appears that the effects of RANTES are dichotymous. At low concentrations RANTES acts in a monomeric or dimeric form and directly stimulates specific chemokine receptors. At high concentrations RANTES molecules can form aggregates that can interact with cell-surface glycosaminoglycans

(GAGs) resulting in mitogen like activation of the cell. The suppressive effects of RANTES on HIV infection, although not fully characterised, appear to be dependent on the presence of the GAG molecules on the target cell surface (Appay and Rowland-Jones, 2001).

RANTES can be secreted by many cell types, including, T-cells, monocytes, mesangial cells, eosinophils, microglia and astrocytes but is predominantly produced by $CD8^+$ T-cells, epithelial cells, fibroblasts, and platelets. The upregulation of RANTES production has been found in a wide variety of inflammatory conditions such as transplant rejection, atherosclerosis, arthritis, asthma, delayed type hypersensitivity reactions and glomerulonephritis. RANTES has also been implicated in the pathogenesis of several inflammatory CNS disorders such as multiple sclerosis, Alzheimer's disease, stroke and cerebral lupus. In addition, a role for RANTES in the development of non-inflammatory CNS diseases, including, motor neuron disease and axonal neuropathies has been suggested (Appay and Rowland-Jones, 2001; De Groot and Woodroofe, 2001). RANTES has also been shown to induce the migration of dorsal root ganglia *in vitro* and to encourage the differentiation of these cells into the nonciceptive phenotype subset. This indicates that RANTES may have an important function in the development and maintenance of the normal brain (Bajetto *et al.*, 2001)

4.1.2.5. Monocyte chemoattractant protein-1

Monocyte chemoattractant protein-1 (MCP-1) belongs to the CC family of chemokines and is a small protein molecule of approximately 8-12 kDa (Vaddi *et al.*, 1997). The molecule was first isolated from conditioned tissue culture fluid taken from baboon aortic smooth muscle cells as a factor that could attract monocytes but not neutrophils (Rollins, 1997). MCP-1 has various alternative names including monocyte chemotactic and activating factor (MCAF), lymphocyte-derived chemotactic factor (LDCF), glioma derived chemotactic factor (GDCF), tumour derived chemotactic factor (TDCF), smooth muscle cell derived chemotactic factor (SMC-CF) and JE gene product (Vaddi *et al.*, 1997). Under the new nomenclature system MCP-1 is called CCL2 (Zlotnik and Yoshie, 2000). This chemokine will bind with a variety of chemokine receptors such as CCR2, CCR9 and CCR11 (Bajetto *et al.*, 2001) and has numerous target cells, including, monocytes, haematopoietic precursors, T-cells, basophils, eosinophils, mast cells, NK-cells, cardiac myocytes and microglia (Vaddi *et al.*, 1997).

MCP-1 is a powerful monocyte chemoattractant and induces the expression of the prerequisite integrin molecules necessary for cellular chemotaxis. In *in vitro* transendothelial migration assays MCP-1 has been shown to attract activated $CD4^+$ and $CD8^+$ memory cells but not B-cells or NK-cells. In contrast, in assay systems that do not incorporate endothelial cells MCP-1 does show some attraction for NK-cells and T-cells (Rollins, 1997). MCP-1 has been shown to provoke the migration of astrocytes *in vitro* (Bajetto *et al.*, 2001). In addition to these migratory inducing effects MCP-1 can stimulate NK-cells and $CD8^+$ cytotoxic cells to degranulate and induces the release of histamine by basophils (Schall, 1994). A possible role for MCP-1 in the prevention of tumour growth has been suggested by findings that implantation of tumourigenic cells, engineered to express MCP-1, fail to induce tumours in recipient mice. The mechanisms involved in this anti-tumour effect are unknown although an increased number of monocytes and macrophages were detected at the site of implantation. Sarcoma clones expressing MCP-1 also showed a reduction in growth that was proportional to the levels of MCP-1 produced by the cells (Schall, 1994). In a variety of inflammatory models, transgenic mice in which the MCP-1 gene has been specifically disrupted show defects in the recruitment of monocytes and macrophages to the sites of inflammation. An accumulation of monocytes has been described in the pancreas and brain following genetic manipulation of pancreatic islet cells and oligodendrocytes, respectively, to over express MCP-1. These monocyte infiltrates show few signs of activation suggesting that although MCP-1 is a powerful monocyte chemoattractant it has little ability to induce further activation of these cells (Asensio and Campbell, 2001).

A wide variety of cell types can produce MCP-1. These include monocytes and macrophages, endothelial cells, smooth muscle cells, cardiac myocytes and epithelial cells (Vaddi *et al.*, 1997). Both astrocytes and microglia can be induced to produce MCP-1 and this chemokine is known to be expressed constitutively within the CNS (Asensio and Campbell, 2001). The function of MCP-1 in the normal physiology of the CNS remains unclear. Transgenic mice over-expressing MCP-1 under the control of the myelin basic protein promoter show a marked monocytic infiltrate in the CNS. Furthermore, the expression of a variety of chemokines including MCP-1 has been associated with the progression of EAE and administration of MCP-1 neutralising antibodies to EAE animals prevents relapse of the disease. In MS and EAE, the astrocytes have been the most commonly reported cell type expressing MCP-1 (De Groot and Woodroofe, 2001). An increase in the expression of MCP-1 has also been reported following experimental ischaemia and sterile traumatic brain injury. In Alzheimer's disease, MCP-1 has been

demonstrated in mature senile plaques and reactive microglia suggesting a possible role for this chemokine in the pathogenesis of this disease (Bajetto *et al.*, 2001).

4.1.2.6. Macrophage Inflammatory Protein-1α

Macrophage inflammatory protein-1α (MIP-1α) is an 8-12 kDa protein molecule belonging to the CC-family of chemokines. This molecule has also been called GOS19, LD78, pAT464, TY5 and SISα (Vaddi *et al.*, 1997). Following the new guidelines for chemokine nomenclature MIP-1α should now be termed CCL3 (Zlotnik and Yoshie, 2000). This chemokine was originally purified from a LPS-stimulated murine macrophage cell line in tissue culture and was termed 'macrophage inflammatory protein'. MIP-1α mediates its action by binding to CCR1, CCR4 and CCR5, and has a range of target cells including T-cells, B-cells, monocytes, neutrophils, eosinophils, basophils, mast cells, NK-cells and astrocytes (Rollins, 1997; Schall, 1994; Vaddi *et al.*, 1997). In addition to the wide range of possible target cells MIP-1α can be produced an array of tissue sources including fibroblasts, monocytes, lymphocytes, neutrophils, eosinophils, smooth muscle cells, mast cells, platelets, bone marrow stromal cells, microglial cells, astrocytes and epithelial cells (Vaddi *et al.*, 1997).

MIP-1α has been shown to be a powerful monocyte chemoattractant and activating factor, although it is less effective than MCP-1 in this task. In *in vitro* studies that do not involve endothelial cells MIP-1α attracts principally $CD8^+$ T-cells, whereas, in transendothelial assays both $CD4^+$ and $CD8^+$ T-cells are attracted by this chemokine (Rollins, 1997). MIP-1α has been shown to be chemotactic for B-cells. Eosinophils are not only attracted by MIP-1α but also show a modest level of activation following stimulation with this chemokine (Schall, 1994). Further to these chemoattractant effects, MIP-1α appears to enhance the adhesive properties of T-cells for endothelial cells.

Within the CNS, MIP-1α production appears to be associated with several disease states. Expression of nominal levels of MIP-1α has been demonstrated in unstimulated cultured microglia suggesting that this chemokine may be present in the normal physiological brain (Bajetto *et al.*, 2001). In studies examining the pathogenesis of MS, using the animal model of EAE, treatment with anti-MIP-1α antibodies inhibited the development of acute disease (Glabinski and Ransohoff, 1999b) while, as stated above, treatment with anti-MCP-1 antibodies prevented relapse of the condition. It has therefore been hypothesised that MIP-1α controls the recruitment of mononuclear cells during acute EAE whereas

MCP-1 directs the mononuclear cell infiltration during relapsing disease (Bajetto *et al.*, 2001). In samples prepared from human cases of MS, MIP-1α was found in inflammatory cells associated with active MS plaques (Glabinski and Ransohoff, 1999b). Increased levels of MIP-1α, correlating with leucocyte and protein concentrations, have been reported in the CSF of patients exhibiting several inflammatory conditions, including, MS following relapse, Behcet's disease and HTLV-1 associated myelopathy (Glabinski and Ransohoff, 1999a). Unlike RANTES and MCP-1, MIP-1α fails to induce the migration of dorsal root ganglia in tissue culture systems, although, astrocyte recruitment was observed in *in vitro* scenarios following MIP-1α treatment (Bajetto *et al.*, 2001). A role for this chemokine in the development of Alzheimer's disease has been suggested by findings that amyloid β peptide stimulates MIP-1α production by human monocytes. If this mechanism occurs *in vivo* the presence of the chemokine could account for the recruitment of macrophages and astrocytes resulting in the accumulation of these cells within the senile plaques (Bajetto *et al.*, 2001). MIP-1α may also mediate pyrogenic responses in the host since injection of the chemokine directly into the anterior hypothalamic pre-optic area results in the induction of a slow onset monophasic fever that persists for a considerable period of time (Bajetto *et al.*, 2001). In addition, injection of MIP-1α into this area of the brain can result in appetite suppression and a reduced food intake in rats (Vaddi *et al.*, 1997).

4.1.3. CNS cytokines and chemokines; helpful or harmful?

As can be seen from the above data, cytokines and chemokines play pivotal roles in both the autocrine and paracrine regulatory processes that arise in response to injury or infection and in some instances mediate aspects of normal physiological reactions. Whether the actions of these molecules within the CNS result in beneficial or detrimental changes appears to be largely dependent on the individual circumstances surrounding each incident. As previously stated both IL-1α and TNF-α play key roles in the regulation of the sleep-wake cycle and the levels of these cytokines within brain seem to follow diurnal patterns (Krueger, Obal, Fang, Kubota *et al.*, 2001). A rise in the levels of IL-1α mRNA transcripts have been detected in the hypothalamus following restraint and nociceptive stimulation, suggesting a role for the molecule in the development of the phsyco-emotional stress reaction under non-inflammatory conditions (Tringali, Dello, Preziosi, and Navarra, 2000). If these mediators were absent from the CNS several normal physiological

processes could be severely impaired. The presence of these molecules in the intact CNS is therefore, not only beneficial to the organism but required for facilitating normal brain functions.

The non-specific indications of infection, including, fever, malaise, lassitude, appetite suppression and depression are collectively termed 'sickness behaviour'. The data presented above clearly indicate that this phenomenon is largely mediated by the effect of cytokines such as IL-1α, TNF-α and IL-6 within the CNS. These symptoms are often considered to be of little importance and are generally regarded by doctors as an uncomfortable but unavoidable result of infection. However, if these criteria are considered in the context of the organism's reaction to the infection it becomes apparent that each component plays an important role in a highly organised scheme to systematically fight the infection. The induction of fever benefits the infected organism as it encourages the proliferation of immune cells while providing an environment that is unfavourable for bacterial or viral growth. This rise in body temperature is accompanied by a decrease in the plasma levels of minerals such as zinc and iron that are required by dividing micro-organisms. The general malaise and lassitude associated with sickness behaviour encourages the infected individual to rest thereby reducing the energy expenditure associated with everyday tasks. This is advantageous since the metabolic cost of fever increases proportionally with the rise in body temperature and there is little provision for unnecessary activities. Finally the changes in food intake resulting form infections alter the food preferences of the sick individual in favour of high carbohydrate and low fat food items. Although initially this may seem strange, as fatty foods possess a higher calorific value that carbohydrates, increased cytokine levels result in lipolysis and hypertriglyceridaemia in the organism and consequently, under these circumstances, increased lipid intake would prove detrimental to the recovery of the host (Kennedy and Karpus, 1999). Therefore, the unpleasant symptoms, initiated by cytokine effects within the CNS and collectively termed 'sickness behaviour,' produce a motivational behaviour pattern with an overall beneficial effect on the organism's ability to successfully fight infection and recovery to health.

In many cases animal models have been used to study the cytokine profiles produced in the CNS under various disease conditions. In the EAE animal model of MS, the CNS lesions are characterised by the presence of T-cells, B-cells, plasma cells and macrophages which leave the blood and infiltrate the brain tissue in response to the presence of chemokine molecules, including, MCP-1, MIP-1α and RANTES, expressed within the CNS (Godiska, Chantry, Dietsch, and Gray, 1995). The expression of pro-inflammatory cytokines,

including, IL-1α, TNF-α and IL-6 induce the upregulation of adhesion molecules such as ICAM-1 and VCAM-1 thereby facilitating the extravasion of the inflammatory cells into the brain (Merrill and Benveniste, 1996). In numerous instances a positive correlation exists between the degree of cellular infiltration and the loss of oligodendrocytes and axonal demyelination found in the CNS lesions seen in MS patients suggesting that the inflammatory process forms a key step in the pathogenesis of the disease (Kivisakk, Trebst, Eckstein, Kerza-Kwiatecki *et al.*, 2001). The effect of cytokine and chemokine production in MS would appear to be detrimental to the well being of the affected animal, however, the presence of IL-6, in combination with additional growth factors, has been shown to induce the differentiation of oligodendrocyte precursors into mature functional myelinating cells and stimulate oligodendrocyte migration and survival (Merrill and Benveniste, 1996). Consequently, in this scenario, the production of IL-6 would result in changes within the CNS that would prove largely beneficial to the amelioration of the disease. Nevertheless, the production of cytokine and chemokine inflammatory mediators in MS and EAE appears, overall, to precipitate the development of the disease and as such can be considered as harmful to the organism.

The picture found following focal brain ischaemia and traumatic brain injury, cannot be so clearly defined and there is conflicting data regarding the effects of cytokines in these conditions. For instance, one study found that intracerebroventricular administration of TNF-α prior to middle cerebral artery occlusion resulted in an increase in the size of the ensuing infarct. Whereas a second study showed that TNF-α administration prior to focal cerebral ischaemia had protective effects against subsequent damage. These findings were corroborated in transgenic animals lacking TNF-α receptors, where an increase in infarct size was detected following ischaemic brain injury, again indicating a neuroprotective action for TNF-α (Stoll *et al.*, 2000). More conflicting data have been generated from the use of TNF-α deficient mice. Following traumatic brain injury, the lack of TNF-α initially appears to be advantageous to the animals since they show less severe neurological damage but, since these animals do not recover from the injury as efficiently as wild-type mice, this beneficial effect of the removal of TNF-α is short lived (Lenzlinger *et al.*, 2001).

Transgenic animals over-expressing specific cytokines within the brain have also been developed. These models highlight how the effects of cytokine production within the CNS can contrast markedly depending on the site of the expression, and the particular cells targeted. In animals producing excess IL-6 in astrocytes, under the control of the GFAP promoter, the presence of surplus cytokine has been linked with cognitive impairment,

astrocytosis, BBB deficiencies, vascular abnormalities, neurodegeneration and subsequent neurological disease. However, when IL-6 production is limited to the neuronal population by utilising the neuron-specific endolase promoter, no overt neuronal, vascular or behavioural changes are seen although the animals still exhibit a strong astrocytic reaction. In IL-6 knockout mice a reduction in the astrocytic reaction is seen leading to an increase in neuronal cell loss following injury. Therefore, in the case of IL-6 at least, the production of the cytokine seem to result in both beneficial and damaging outcomes since the cytokine promotes an inflammatory reaction but simultaneously enhances neuronal survival (Lenzlinger *et al.*, 2001).

It would appear that the exact nature and severity of the CNS damage, as well as the precise location and timing of cytokine expression, may prove decisive in determining whether the overall outcome of cytokine production within the brain will be detrimental or beneficial to the organism. Moreover, it is clearly imperative that these divergent findings are carefully considered when novel chemotherapeutic regimens involving either the depletion or addition of cytokines are devised.

4.1.4. Cytokines and chemokines in trypanosomiasis

Although a role for cytokines and chemokines in the pathogenesis of human African trypanosomiasis is beyond question there is a paucity of information with regard to the profiles of these important inflammatory agents during the course of the disease. The first experimental indication, that factors mediating the development of the disease were produced following trypanosome infection, was discovered just after the turn of the century in 1912. In these experiments, Laveran showed that blood taken from trypanosome-infected rabbits and injected into mice, following destruction of the parasites, induced hypothermia, convulsive movements, fatigue and death. From these findings Laveran concluded that the destruction of the parasites had released a 'trypanotoxin' into the rabbit blood that was responsible for the pathological effects seen in the mice. Almost 70 years later, the mediator induced by the 'trypanotoxin' was shown to be cachectin or TNF (Lucas, Magez, Songa, Darji *et al.*, 1993).

TNF-α production has also been suggested to lead to the immunosuppression associated with trypanosome-infection, either by a direct mechanism or an indirect pathway involving IFN-γ production. Evidence for this comes from animal experiments using neutralising

antibodies against the two cytokines. When IFN-γ was removed, the reactivity of the T-cells in the lymph nodes and macrophages was restored. Similarly, treatment of trypanosome-infected animals with anti-TNF-α monoclonal antibodies re-established the proliferative T-cell response in the lymph nodes. It therefore appears that these two cytokines are integrally involved in the development of trypanosome-elicited immunosuppression (Lucas *et al.*, 1993). In addition to an immunosuppressive role, TNF-α has also been shown to have a direct action on trypanosomes with the cytokine exerting a trypanolytic effect *in vitro* and reducing the parasite load *in vivo* (Lucas *et al.*, 1993; Magez, Lucas, Darji, Songa *et al.*, 1993). This effect of TNF-α on the development of the parasitaemia is reflected in late-stage human infections where the number of blood borne trypanosomes is extremely low while the levels of TNF-α in the serum are high (Okomo-Assoumou, Daulouede, Lemesre, N'Zila-Mouanda *et al.*, 1995).

A role for TNF-α in the development of the neuropathological response associated with trypanosome infection and chemotherapy has also been suggested (Hunter *et al.*, 1991). In this study mRNA transcripts for TNF-α could be consistently detected in the nucleic acid extracted from the brains of *T.b.brucei*-infected mice following induction of a meningoencephalitic response by subcurative trypanocidal drug treatment. More recent investigations examining *T.b.brucei*-infections in TNF-α knockout mice confirmed the involvement of TNF-α in both the development of the parasitaemia and the control of the pathological response to trypanosome infection (Magez, Radwanska, Beschin, Sekikawa *et al.*, 1999). This work demonstrated that pathological features of the disease, including, immunosuppression and sensitivity to LPS, were greatly reduced in TNF-α knockout mice compared to wildtype animals. This decrease in immunopathological response was not the result of a reduction in parasite load since the peak levels of parasitaemia were found to be strongly increased in the knockout mice. This finding concurs with those described above indicating a reduction in parasite load due to the presence of TNF-α. In TNF-α knockout mice TNF-α is not present; therefore, one factor that plays a role in controlling the growth of the parasite population has been removed leading to an increase in the levels of parasitaemia.

An upregulation in the production of TNF-α and IL-6 transcripts was also demonstrated (Eckersall, Gow, McComb, Bradley *et al.*, 2001), in the liver and brain of *T.b.brucei*-infected mice both during the early stages of the disease, from 7 days post-infection, and following the induction of the PTRE by subcurative trypanocidal drug treatment. Using the same model system, expression of IL-1α, IL-4, TNF-α, MIP-1, IL-6 and IFN-γ was

detected in nucleic acid extracted from the brains of *T.b.brucei*-infected mice following induction of the meningoencephalitis. IL-2 transcripts were not detected in these animals (Hunter *et al.*, 1991). The early induction of MIP-2, MIP-1α, RANTES, and MCP-1 within the CNS was also investigated in a *T.b.brucei* rat model of trypanosomiasis (Sharafeldin, Eltayeb, Pashenkov, and Bakhiet, 2000). These studies showed an upregulation in the number of cells in the rat brain expressing MIP-2, MIP-1α and RANTES only 6 hours following infection of the animal. By 12 hours post-infection an increase in MCP-1 positive cells was also found. Immunocytochemistry double staining procedures demonstrated that the resident brain astrocytes and microglia as well as infiltrating inflammatory cells were the cellular source of these chemokines. This increase in the expression of chemokines within the rat brain occurred very quickly following infection, at a time well before the trypanosomes are thought to have entered the CNS compartment, indicating that their expression may be induced by an indirect stimulus rather that the direct effect of the parasite within the CNS. The ability of human astrocytes and neurons to express the chemokines IL-8, MIP-1α, MIP-1β, MCP-1 and RANTES has been demonstrated in dissociated cell cultures prepared from first trimester forebrain (Bakhiet, Mousa, Seiger, and Andersson, 2002). Following stimulation of these cultures with either trypanosome-derived lymphocyte triggering factor, a novel compound produced by trypanosomes (described more fully below) or with LPS, an upregulation in the expression of each of IL-8, MIP-1α, MIP-1β, MCP-1 and RANTES was detected using immunocytochemistry and *in situ* hybridsation. In contrast, when the cultures were stimulated with trypanosome VSG, no increase in chemokine expression was found.

4.1.4.1. Trypanosome-derived lymphocyte triggering factor

Further evidence linking cytokines to the pathogenesis and disease development of African trypanosomiasis was indicated by experiments carried out in the early 1990's (Bakheit *et al.*, 1990). In these experiments *T.b.brucei*-infection in rats was shown to induce a rapid and marked increase in splenic IFN-γ. The removal of $CD8^+$ cells prevented this induction of IFN-γ production, checked parasite growth and increased the survival rates in the experimental animals. The presence of a trypanosome-derived mediator with a specific action on a subset of lymphocytes was elucidated using a two-chambered tissue culture system that allows diffusion of soluble factors between the compartments. These experiments suggested that lymphocytes, specifically $CD8^+$ T-cells, were induced to express IFN-γ by a soluble factor produced by the trypanosomes that could diffuse through

the membrane separating the two compartments. This IFN-γ also moved through the barrier and was subsequently taken up by the parasites increasing their growth rate. This growth modulating effect of IFN-γ on the parasite was found to be species dependent since no increase in parasite growth rate was noted following treatment with human IFN-γ or stimulation of human $CD8^+$ cells by *T.b.brucei* (Olsson *et al.*, 1991). The parasite-derived signalling molecule was termed trypanosome-derived lymphocyte triggering factor (TLTF) and has subsequently been cloned and sequenced (Vaidya, Bakhiet, Hill, Olsson *et al.*, 1997). More recently this factor has been further characterised and TLTF has now been shown to be derived from trypanosome cytoskeletal proteins that play a key role in cellular motility, cell trafficking of proteins and cell division (Hill, Hutchings, Grandgenett, and Donelson, 2000).

4.1.4.2. Cytokines and differential susceptibility to trypanosomiasis

Within several species of animal, individual strains have been shown to display an innate resistance to trypanosomiasis and are more capable of controlling the development of parasitaemia, survive longer following infection and show a reduction in the immunosuppression associated with the disease. Cattle breeds indigenous to West Africa such as the N'dama and the West African Shorthorn show a degree of tolerance to trypanosome infections while other breeds including European cattle and *Bos indicus* (Boran) cattle are more susceptible to the disease (Murray *et al.*, 1984). This differential susceptibility to infection is found between strains of mice, *e.g.*, C57BL/6 mice show a degree of resistance to infection while BALB/c mice are highly susceptible (Kaushik, Uzonna, Zhang, Gordon *et al.*, 2000). The genetic basis for these differences has yet to be defined definitively and is thought to involve a variety of genes. The differential ability of each strain to produce cytokines has been implicated as one possible factor influencing resistance to trypanosome infection. Bone marrow-derived macrophages prepared from resistant C57BL/6 mice and stimulated with whole cell extracts of *T.b.brucei* or *T.congolense* have been shown to produce significantly higher levels of TNF-α and IL-12 than those from susceptible BALB/c animals implicating these cytokines in the ability of C57BL/6 mice to resist trypanosome infection. Furthermore bone marrow derived macrophages prepared from BALB/c mice expressed significantly higher concentrations of IL-6 and IL-10 suggesting that production of these cytokines enhances susceptibility of the mice to the disease (Kaushik, Uzonna, Radzioch, Gordon *et al.*, 1999; Kaushik *et al.*, 2000).

The cytokine IFN-γ has also been suggested to play a role in determining the tolerance of specific breeds or strains of animal to trypanosome infection. C57BL/6 mice are normally more resistant to trypanosome infection and produce a strong Th1 profile of cytokines in response. IFN-γ knockout C57BL/6 mice infected with *T.b.rhodesiense* were found to have lost their innate resistance to the parasite. This finding suggests that the presence of the IFN-γ within the Th1 response is critical in establishing the resistance of the animal to trypanosomes (Hertz, Filutowicz, and Mansfield, 1998). In contrast to these results higher plasma levels of IFN-γ have been found in susceptible BALB/c mice compared with C57BL/6 mice following infection with *T.congolense* (Uzonna, Kaushik, Gordon, and Tabel, 1998). When anti-IFN-γ antibodies were given to these *T.congolense*-infected BALB/c animals the mice displayed a more resistant phenotype with lowered parasitaemia and increase survival periods suggesting that IFN-γ results in the animal being more susceptible to trypanosome infection. Suppression of parasite growth and an increase in survival times has also been demonstrated following the depletion of IFN-γ in *T.b.brucei*-infected mice (Bakhiet, Olsson, Ljungdahl, Hojeberg *et al.*, 1996). This increased resistance to trypanosome infections was found irrespective of the normal level of susceptibility of the mouse to infection. Therefore, the role of IFN-γ in the ability of animals to resists trypanosome infection remains controversial.

The cytokine profiles produced as a result of *T.congolense* infection in trypanotolerant N'dama cattle and susceptible Boran cattle have also been studied in cultures of peripheral blood mononuclear cells prepared from groups of each breed of infected animal. In these experiments, differences in the expression pattern of IL-4 and IL-6 were found throughout the course of infection. Trypanosome-resistant N'dama cattle expressed a higher level of IL-4 than Boran cattle, while Boran cattle appear to produce more IL-6 than their trypanotolerant counterparts. These profiles suggest a protective role for IL-4 and a disease-enhancing function for IL-6 (Mertens, Taylor, Muriuki, and Rocchi, 1999). Further evidence to indicate that IL-4 may play a role in controlling the development of trypanosomiasis can be seen in the results of studies investigating the expression of IL-4 in wildtype BALB/c, BALB/c nude and SCID mice. These experiments demonstrated that BALB/c and BALB/c nude mice could control the development of parasitaemia following *T.b.gambiense* infection to varying degrees, with BALB/c nude animals showing a higher parasitaemia than BALB/c mice. In contrast, SCID mice that do not have functional T- or B-cells were highly susceptible to the disease. When the $CD4^+$ T-cell population in BALB/c animals was depleted by anti-$CD4^+$ antibody administration, levels of parasitaemia were similar to those seen in the nude mice indicating a role for $CD4^+$ T-cells

in the reaction. Administration of anti-IL-4 antibodies to *T.b.gambiense*-infected BALB/c mice increased the periods of parasitaemia suggesting a role for this cytokine in the control of the trypanosome infection (Inoue, Inoue, Kuriki, Yamaguchi *et al.*, 1999). A significantly higher expression of IL-4 was also shown in spleen mononuclear cells prepared from trypanotolerant C57BL/6 mice when stimulated with TLTF, compared with those prepared from susceptible C3H/He mice, again suggesting a protective role for IL-4 (Bakhiet *et al.*, 1996).

It is apparent from the evidence presented above that cytokines and chemokines play a complex and significant role in the development and control of trypanosome infections not only in humans but also in their other animal hosts. A clearer understanding of the expression pattern of these mediators following infection may denote the beneficial and detrimental effects associated with their production and facilitate improved drug targeting for treatment of the disease. In this chapter the expression of the cytokines IL-1α, IL-6 and TNF-α as well as the chemokines RANTES, MIP-1α and MCP-1 will be investigated within the CNS during each phase of the disease from the early-stage, through the CNS-stage, to the development of the PTRE. These cytokines have been chosen since they have previously been shown to be induced during trypanosome infections and their expression has also been reported in brain tissue. Furthermore, the different functions of the selected mediators indicate that they would be highly likely to induce and control a CNS inflammatory reaction of a similar nature to that associated with trypanosome infection and subcurative chemotherapy. The induction and expression of these molecules will be investigated at various time points throughout the course of the disease using both molecular and histological techniques. The results of these experiments will provide a profile of the expression of these mediators as the infection progresses and may indicate possible chemotherapeutic targets and feasible intervention time points.

4.2. Materials and methods

The main aim of the following section of this thesis was to determine the expression patterns of specific cytokines and chemokines, induced within the CNS by trypanosome infection and subsequent subcurative drug treatment. The mouse model of human African trypanosomiasis, previously described in Chapter 2, was used to investigate the expression profiles of the cytokines IL-1α, TNF-α and IL-6 and the chemokines MIP-1α, MCP-1 and RANTES at each stage of the infection and following the induction of the PTRE. The expression of these inflammatory mediators was examined using a variety of techniques including; the reverse-transcriptase polymerase chain reaction (RT-PCR) to determine the time course and expression levels of specific mRNA species, immunocytochemistry, to identify the presence of the protein within tissue sections and *in-situ* techniques to demonstrate the cellular source of the molecules.

4.2.1. Animals, infections and treatments

Female CD-1 mice (Charles River Breeding Laboratories) weighing 28-35g were infected with $2x10^4$ *T.b.brucei* parasites of cloned stabilate GVR35/C1.6 as previously described. Each stage in the development of the disease from the early acute infection to the post-treatment reactive encephalopathy was induced in the animals. To emulate the development of CNS reaction during the early stage of the disease animals were killed at 7 and 14 days following the infection, while those killed at days 21 and 28 post-infection were used to mirror the situation found during the early CNS stage of the disease when, the parasites are known to have invaded the CNS compartment. Additional infected mice were treated on day 21 post-infection with a subcurative dose (40mg/kg i.p.) of the trypanocidal drug diminazene aceturate. This drug treatment clears the parasites from the peripheral compartments but cannot cross the blood-brain barrier to kill the trypanosomes present in the CNS. This induces a more severe inflammatory reaction within the brain of the infected mice. Groups of these treated mice were killed at 7 and 14 days following the drug treatment. The pathology exhibited in the brains of these mice mimics that of patients with late-stage sleeping sickness. Further subcuratively treated mice were allowed to progress until they relapsed to parasitaemia, at which time they were given a second subcurative dose of diminazene aceturate and killed 7 and 14 days following the treatment. This regimen induces an extremely severe CNS inflammatory reaction in the infected animals, similar to that found in patients who have died of the PTRE. The complete mouse model is described in detail in Chapter 2 of this thesis.

The experimental model was performed in duplicate. On each occasion the various severities of CNS-reaction were induced in separate groups of mice. Each of these individual treatment groups comprised six animals and each group was included in triplicate in the experimental design. This allowed samples to be taken for section preparation from both frozen and paraffin blocks, permitting histological and immunocytochemical assessment, while the remaining sample was used for extraction of RNA allowing subsequent RT-PCR analyses. The various samples were prepared as previously described in Chapter 2.

4.2.2. RT-PCR analyses

The temporal expression patterns of the cytokines IL-1α, IL-6 and TNF-α together with the chemokines MIP-1α, MCP-1 and RANTES were investigated using the RT-PCR procedure described in Chapter 2. These studies were performed prior to immunocytochemistry or *in-situ* techniques to determine the treatment regimens that induce the expression of the inflammatory mediators and thereby indicate which CNS tissue sections to examine in order to ascertain the cellular source of the material.

4.2.3. Immunocytochemistry

The technique of immunocytochemistry (ICC) is described in detail in Chapter 2 of this thesis. A list of antibodies employed in the cytokine staining procedures is detailed in Table 4.1. In an effort to stain the cytokine proteins successfully, a variety of alterations to the standard approach were employed. These modifications are described in below.

4.2.3.1. Fixation of cryostat sections

The cryostat sections produced from frozen brain blocks were prepared from unfixed material. Therefore, in an attempt to achieve successful staining of cytokines within the tissue, as well as unfixed sections, a range of different fixative protocols were used prior to ICC staining. The various fixation methods included treatment of the tissue sections with one of the following procedures;

- cold acetone for 20 minutes

Primary Antibody	Monoclonal/Polyclonal	Host Species	Source	Dilution	Secondary antibody
Anti murine IL-1α	Polyclonal	Rabbit	Genzyme	1:10 – 1:200	Goat anti-Rabbit IgG
Anti murine IL-1α	Polyclonal	Goat	R&D systems	1:10 – 1:200	Rabbit anti Goat IgG
Anti murine IL-6	Monoclonal	Rat	Genzyme	1:10 – 1:200	Rabbit anti-Rat IgG
Anti murine IL-6	Polyclonal	Goat	R&D systems	1:10 – 1:200	Rabbit anti Goat IgG
Anti murine IL-6	Monoclonal	Rat	Pharmingen	1:10 – 1:100	Rabbit anti-Rat IgG
Anti murine TNF-α	Polyclonal	Rabbit	Genzyme	1:10 – 1:200	Goat anti-Rabbit IgG
Anti murine TNF-α	Polyclonal	Goat	R&D systems	1:10 – 1:200	Rabbit anti Goat IgG
Anti murine TNF-α	Monoclonal	Rat	Pharmingen	1:10 – 1:100	Rabbit anti-Rat IgG
Anti murine TNF-α	Polyclonal	Rabbit	Serotec	1:10 – 1:200	Goat anti-Rabbit IgG
Anti murine TNF-α	Monoclonal	Rat	Gifted	1:10 – 1:50	Rabbit anti-Rat IgG

Table 4.1. Antibodies employed for immunohistochemical analyses of cytokines. The listed antibodies were used to demonstrate particular cytokine proteins in tissue sections. The antibody specificities are given together with the source of the reagent. The antibody listed as 'gifted' was kindly donated by Dr. Christopher Hunter, University of Pennsylvania, Philadelphia, USA. The range of dilutions used for the primary antibodies are detailed. Both paraffin and cryostat sections were emloyed in the procedure. All secondary antibodies were biotinylated, used at a dilution of 1:200 and purchased from Vector® Laboratories, Peterborough, UK.

- cold 4% paraformaldehyde[A1] for 5 minutes
- Bouin's fixative[A1]
- Lana's Fix [A1] for 30 seconds at -20^0C followed by acetone for 30 seconds at -20^0C

Acetone treatment, paraformaldehyde and Bouin's fixative are well recognised, established methods for the fixation of frozen sections (Polak and Van Noorden, 1986). Lana's fix, followed by acetone treatment, was personally recommended by Prof. Krister Kristensson, Karolinska Institute, Stockholm, Sweden.

4.2.3.2. Antigen retrieval techniques

Formalin fixation followed by paraffin embedding is the most commonly used technique for histological examination of tissues. Tissue treated in this manner yields sections with superior preservation and morphology than that of frozen blocks or alternatively fixed material and it is therefore the preferred method of producing sections for all forms of subsequent histological analyses. Unfortunately, formalin treatment, and the process of paraffin wax embedding, commonly result in alterations to, or masking of, the antigens present within the tissue thereby preventing the use of such material for many ICC applications. The mechanisms that lead to these chemical changes in the tissues remain largely unknown. However, the development of 'antigen retrieval' techniques has overcome some of the difficulties associated with the use of these sections in ICC.

The initial attempts to improve the immunoreactivity of formalin fixed tissue antigens involved digestion of the tissue sections with proteolytic enzymes prior to staining. These enzymes help to expose antigens that have become hidden within the tissue due to the protein cross-linking caused by the formalin fixation. In essence the proteolytic enzymes digest some of bonds revealing the concealed antibodies. Enzymes used in these antigen retrieval techniques include trypsin, pepsin and pronase. Although enzyme digestion proved successful in the unmasking of many antigens it failed to yield acceptable immuno-staining of numerous additional important antigens (Van Noorden, 1986). Therefore, the search continued for a simple technique that could be used effectively to retrieve these targets.

[A1] The formulation for this solution is described in Appendix 1.

An entirely new approach to this problem was adopted that relied on a wet heat pre-treatment system to restore the antigen within the section (Shi, Cote, and Taylor, 2001). This restoration of the target molecule resulted in these methods being termed 'antigen retrieval' techniques. Initially this heating procedure was performed in water but as the technique developed it became apparent that the pH of the solution as well as the temperature had a major influence on the effectiveness of the technique. Consequently buffers and commercially prepared retrieval solutions replaced the water in this system. Although this heat-induced antigen retrieval technique is now widely used in pathology the mechanisms resulting in the restoration of the antigenic site remain unknown and the technique is still not applicable to every antigen.

Due to the superior morphology found in paraffin sections both proteolytic enzyme digestion and wet heat antigen retrieval techniques were used in this study. These techniques were applied to help demonstrate cytokine staining in formalin fixed paraffin embedded tissue sections of trypanosome infected mouse brain.

4.2.3.2.1. Proteolytic enzyme digestion

Proteolytic enzyme treatment was carried out on formalin fixed paraffin embedded sections using either a 0.1% trypsin or a 0.4% pepsin solution. Trypsin digestion was performed in a solution of 0.1% calcium chloride adjusted to pH 7.8 with 0.1M sodium hydroxide while pepsin digestion was used in a solution of 0.1% hydrochloric acid. In both cases the sections for digestion were deparaffinised in three changes of xylene and rehydrated through graded alcohols. The endogenous peroxidase activity was then quenched by a 20 minute incubation in 0.5% hydrogen peroxide in phosphate buffered saline[A1] (PBS) followed by a 5 minute rinse in running tap water as previously describe. The slides were then placed in proteolytic enzyme buffer pre-warmed to 37^0C and allowed to equilibrate for 5 minutes before being transferred to the complete enzyme solution. The sections were allowed to digest at 37^0C for various time periods ranging from 5 to 15 minutes. Rinsing the slides in cold running tap water for 5 minutes then stopped the reaction (Van Noorden, 1986). The remainder of the ICC staining procedure was then performed as described in Chapter 2.

[A1] The formulation for this solution is described in Appendix 1.

4.2.3.2.2. Wet-heat antigen retrieval

Antigen retrieval by incubation of formalin fixed paraffin embedded sections in hot buffer solutions was also performed to achieve successful ICC staining of cytokines. Two approaches to this technique were followed. The first strategy utilised 0.01M citrate buffer pH 6.0 [A1] while the second used a commercially prepared retrieval solution, Serotec tissue unmasking fluid (STUF) (Serotec Ltd, Oxford, UK).

4.2.3.2.2.1. Citrate buffer antigen retrieval protocol

Two different approaches were followed in the use of this antigen retrieval technique. These procedures are detailed below.

- 600ml of 0.01M citrate buffer pH 6.0 [A1] were placed into a large heat-proof staining dish. Deparaffinsed, rehydrated sections were then placed into the buffer and the fluid level was marked on the outside of the container. The slides were then microwaved at full power (700W) for a total of 20 minutes. The fluid level was checked at 5 minute intervals and restored to the marked volume with fresh buffer. Following the heating period the slides were allowed to cool in the buffer for a further 20 minutes. The sections were then rinsed in three changes of cold distilled water, each wash lasting for a 5 minute period. This was followed by a 5 minute wash in PBS [A1]. The endogenous peroxidase activity was then quenched and the standard ICC protocol followed as previously described.

- 250ml of 0.01M citrate buffer pH 6.0 were added to a heat-proof staining dish containing deparaffinised, rehydrated slides. This was then microwaved at full power (700W) for 5 minutes. The slides were then transferred to fresh buffer and microwaved for a further 5 minute period at medium power. Again the slides were transferred to fresh buffer and microwaved for a final 5 minutes at low power. On completion the slides were removed from the microwave and placed into PBS at room temperature and allowed to equilibrate for 5 minutes. The endogenous peroxidase activity was then quenched and the standard ICC procedure followed as previously described.

[A1] The formulation for this solution is described in Appendix 1.

4.2.3.2.2.2. Sertoc tissue unmasking fluid (STUF)

STUF is a commercially prepared antigen retrieval solution supplied as a x3 concentrate. The solution can be used to reactivate hidden epitopes in formalin fixed paraffin embedded sections or to enhance the performance of ICC staining in paraffin or cryostat sections. Before use the STUF concentrate was diluted 1:3 with distilled water and placed in a waterbath at 90^0C to pre-warm in a suitable staining dish. Deparaffinised, rehydrated sections or cryostat sections were then incubated in the hot STUF for 10 minutes in the 90^0C waterbath. The staining dish was then removed from the waterbath and allowed to cool for 15 minutes. Following the cooling period the slides were rinsed in two changes of distilled water followed by two changes of PBS. All washes were performed at room temperature and lasted for 5 minutes each. The endogenous peroxidase activity was then quenched and the standard ICC procedure followed as previously described.

4.2.3.3. Tissue permeablisation

In some cases, permeablisation of tissue sections is recommended prior to immunostaining. This allows entry of the antibodies into the cell through the cell surface membrane, thereby permitting staining of intracellular components. This permeablisation procedure was performed on both cryostat and formalin fixed, paraffin embedded sections to facilitate the staining of intracellular cytokines. Two permeabilisation techniques were employed and are described below

- Saponin introduces pores in the cell membrane without appearing to damage the morphology. It accomplishes this by penetrating the plasma membrane at cholesterol groups, resulting in a reversible permeabilisation of the membrane. To achieve this permeabilisation and allow the antibodies to penetrate the cell, 0.1% saponin was included in the buffer at each of the wash stages and in the antibody diluent in the standard ICC protocol. It is important that saponin is included at each stage of this procedure as it could be washed out of the section leading to the loss of the cellular permeability. Saponin was not included in the final washes, prior to the visualisation step.

- The non-ionic detergent Triton X-100 is often used in biochemical applications to solubilize proteins. In ICC procedures 0.01% Triton X-100 can be incorporated into the wash buffers used during the staining protocol. This permeabilises the cell membrane and allows the antibodies to bind with

intracellular targets. Triton X-100 was included in each wash stage during the antibody phase of the staining technique but was omitted from the final washes prior the visualisation of the bound antibody.

4.2.4. *In situ techniques*

In-situ procedures have developed from nucleic acid hybridisation techniques and can be used to detect and localise mRNA transcripts within tissue sections. This ability, to identify particular mRNA species within tissue sections, allows the cellular source of the individual proteins to be determined. *In-situ* procedures were performed to identify the cell types responsible for cytokine production within the CNS following trypanosome infection and subcurative drug treatment in our mouse model. There are a variety of different *in-situ* approaches that can be followed; these are described in more detail below.

4.2.4.1. *In-situ* hybridisation

In-situ hybridisation (ISH) can be used to visualise specific genes and mRNA sequences within intact cells. The procedure was developed in 1969 by two groups of researchers working independently (John, Birnstiel, and Jones, 1969; Pardue and Gall, 1969). The technique involves the use of probes designed specifically to bind with particular nucleic acid sequences in the tissue section. These probes can be labelled with various reporter molecules *e.g.* radioisotopes, fluorescence, digoxigenin or biotin. At the end of the procedure the reporter molecules allow the presence of the bound probe to be visualised and the location of the target sequences to be determined within the tissue section or cell preparation (Leitch, Schwarzacher, Jackson, and Leitch, 1994; Polak and McGee, 1991).

In this study, ISH was adopted to identify the cell types expressing mRNA transcripts for the cytokines IL-1α, IL-6 and TNF-α. The ISH procedure was performed using a commercially prepared "*in-situ* workstation" (British Bio-technology Products Ltd., Oxon. UK). The protocol supplied with this kit was employed. Both cryostat and formalin fixed paraffin wax embedded sections were used. Since the target sequence to be detected was composed of mRNA, the precautions detailed in Chapter 2, with regard to the handling of the sample to prevent the degradation of the nucleic acid were strictly followed. These precautions included, wearing disposable gloves throughout the procedure, where possible, all glassware, equipment and solutions were di-ethyl-pyrocarbonate (DEPC) treated and

autoclaved to denature any contaminating RNase, and disposable RNase free filter tips were used during all the pipetting stages of the techinique.

4.2.4.1.1 ISH of murine CNS sections

Formalin fixed, paraffin wax embedded sections were dewaxed, rehydrated through graded alcohols and rinsed for 5 minutes in DEPC water. The sections were then washed in 2 x salt sodium citrate buffer[A1] (SSC) followed by a 5-minute rinse in DEPC water[A1]. To allow the probe to gain access to the mRNA target within the cells, the sections were permeablised by protease digestion, for 60 minutes at 37^{0}C, with proteinase K. The enzyme was used at various concentrations ranging from 5µg/ml to 60µg/ml and was diluted in proteinase K diluent, containing, 50mM EDTA and 100mM TRIS, pH8.0. Following proteinase K digestion the sections were rinsed in PBS for 1 minute and then post-fixed in 4% paraformaldehyde for 20 minutes at 4^{0}C. This post-fixing step terminates any residual proteinase K activity and prevents the subsequent diffusion or loss of mRNA target from the permeabilised section. Before the hybridisation step, any non-specific binding sites within the tissue section were blocked to prevent background staining. This was acheived by incubating the section in prehybridisation solution. This solution is identical to the buffer used during the hybridisation stage without the addition of the specific probe. While the slides were post-fixing in the paraformaldehyde the prehybridisation solution was placed in a waterbath at 37^{0}C with periodic agitation to pre-warm. This process dissolves any residual salt precipitates that may have formed in the buffer during storage and the mixing ensures that the reagents are distributed homogenously throughout the viscous solution.

The prehybridisation / hybridisation solution provided in the kit contained 0.6M salt, 30% formamide, and 150µg/ml sonicated salmon sperm DNA. The specificity of the hybidisation is controlled by the stringency of the conditions used. The stringency of the conditions is dictated by two main factors, the salt concentration in the buffer and the temperature at which the hybridisation is performed. Low salt concentrations and high temperatures constitute highly stringent conditions and will only permit the formation of nucleic acid duplexes with extremely high homology. High salt concentrations and low temperatures provide low stringency conditions. Under these circumstances non-specific interactions between non-homologous strands can occur. Unfortunately, high temperature are detrimental to the morphology of the tissue, therefore formamide is added to the

[A1] The formulation for this solution is described in Appendix 1.

prehydridisation / hybridisation solution. Formamide disrupts the hydrogen bonds between the nucleic acid strands and destabilises non-homologous duplex formations thereby reducing non-specific binding of the probe. Consequently, the inclusion of the formamide allows the use of lower temperatures which, in turn, help to preserve the tissue sections during the procedure.

Following the post-fixation stage, the sections were drained and rinsed in DEPC water to eliminate the residual paraformaldehyde. The excess fluid was then removed by wiping carefully around the tissue section with a clean paper tissue. Each section was placed on a staining rack and 300µl of pre-warmed hybridisation buffer applied over the section. The slides were then transferred to a humidity chamber and incubated at 37^0C for 60 minutes.

During the prehybridisation step the hybridisation solution was prepared by the addition of the specific probes. The probes used were commercially prepared by R&D systems Europe Ltd. (R&D systems Europe Ltd., Oxon., UK). They consisted of cocktails of oligonucleotides complementary to specific regions of the target mRNA sequences. All the oligonucleotides were single stranded, ranged from 28 to 30 bases in length and were modified at both the 5' and 3' ends by the addition of a digoxigenin reporter molecule. The probe cocktails consisted of an equimolar mixture, of the exon specific probes, and were supplied as 50ng/µl solutions. The probe cocktail used to detect IL-1α mRNA contained oligonucleotides specifically designed to bind with regions in exons 5, 6 and 7 of the murine mRNA sequence. The IL-6 cocktail consisted of four oligonucleotides that bind with regions in exons 2, 3, 4 and 5 of the murine IL-6 mRNA sequence while the probe used for the detection of TNFα expression was designed to bind specifically with four regions, one from exon 3 and three individual areas from exon 4, of the murine TNFα mRNA molecule. The recommended working concentration for oligonucleotide probes of approximately 30 bases is 200ng/ml, although a wide range of concentrations has been employed. To achieve successful ISH staining in this study the probe cocktails were added to the hybridisation buffer to give final concentrations between 200ng/ml and 5,000ng/ml. The complete hybridisation buffer was mixed gently but thoroughly to ensure an even distribution of the probe mix. The solution was then placed at 37^0C until required.

On completion of the prehybridisation stage, the sections were removed from the humidity chamber, the solution was drained from the slide and the excess liquid wiped carefully from around the section using a clean paper tissue. 20µl of the complete hydridisation buffer was then applied to each section and covered with a clean glass coverslip. Any air

bubbles present in the hybridisation solution were removed by gentle tapping of the coverslip. The section were then returned to the humidity chamber and incubated at 37^{0}C overnight.

Following hybridisation, it is necessary to remove all the non-specifically bound oliginucleotides while retaining those that have bound with their specific target sequence. To achieve this, the sections were removed from the humidity chamber and washed in a series of post-hybridisation washes of increasing stringency. The first wash in this procedure was comprised of a solution containing 4 x SSC pre-heated to 37^{0}C. This provides an environment with similar stringency conditions to those used during the hybridisation stage and will therefore remove only excess and extremely loosely bound probe. On removal from the humidity chamber, the slides were immediately placed into this wash solution. The coverslips were not removed from the slides before being placed in the solution as they float off of the section during the wash procedure. Manual removal of the coverslips can result in unnecessary damage to the delicate tissue section. The sections were allowed to rinse in this solution for 5 minutes before transfer to the second wash solution. This buffer was slightly more stringent than the first and contained 2 x SSC, however, the procedure was performed at room temperature. The sections were incubated in this solution for 20 minutes, transferred to fresh 2 x SCC and the incubation repeated. Following the second wash in 2 x SSC at room temperature, the slides were transferred to fresh 2 x SSC. This wash was performed at 37^{0}C for 20 minutes to increase the stringency slightly. As before, this wash stage was performed in duplicate. The wash conditions followed in this procedure were designed to be of low stringency. This was to ensure that specifically bound probe was not removed together with non-specifically bound oligonucleotides. Once a signal has been detected using the technique the stringency of the post-hybridisation washes can be increased as appropriate. This increase in stringency can be achieved by, reducing the salt concentration of the washes, increasing the wash temperatures and the inclusion of formamide in the solutions. Following completion of the post-hybridisation washes any probe remaining bound to the section can be detected using an immunocytochemical detection procedure, similar to that described for ICC. The procedure for visualising the digoxigenin reporter molecule is described below.

A similar protocol was employed using cryostat sections as an alternative to formalin fixed paraffin embedded samples. In this scenario the sections were fixed in 4% paraformaldehyde at 4^{0}C for 20 minutes and then rinsed in DEPC water. The procedure detailed above was then followed, beginning with the proteinase K digestion step.

4.2.4.1.1.1 ISH control sections

The inclusion of control sections in any histochemical techniques, particularly those designed to detect nucleic acid sequences, is essential to exclude the possibility of misleading or false positive results. Control slides for ISH consist of both positive and negative control sections. In this case the positive control slides were prepared from the brain of a trypanosome-infected mouse following a double diminazene aceturate treatment. This treatment regimen has been shown, by RT-PCR analyses, to induce the expression of the cytokines of interest and therefore should provide a good source of the target mRNA within the tissue sections.

It is possible that the reagents used in the tissue pre-treatment stages, or in the hybridisation solution itself, may react non-specifically with elements in the tissue section resulting in background staining that could be interpreted as a positive reaction. Consequently, it is essential to include a negative control section in each ISH run. This negative control is treated in an identical manner to the test section but has no probe added to the hybridisation solution. If positive staining is detected in this slide then it must be due to background noise. A second variety of negative control is also recommended. This involves treatment of the tissue section with RNase prior to the hybridisation step. This will degrade the mRNA in the section and eliminate the nucleic acid target sequence. This form of negative control was not included in this study due to the possible risk of contamination of the test sections, or samples destined for RT-PCR analyses, by the RNase enzyme.

4.2.4.1.2. Visualising the digoxigenin reporter molecule

The location of the digoxigenin reporter molecule in the tissue sections was demonstrated using an anti-digoxigenin antibody labelled with alkaline phosphatase. This anti-digoxigenin antibody was purchased from Boehringer Mannheim (Boerhinger Mannheim UK, East Sussex, UK) and comprised the Fab fragments of anti-digoxigenin sheep IgG. During the detection procedure various Tris buffer solutions were used. These are detailed below.

Buffer 1; 100mM Tris, 150mM sodium chloride, pH7.5.

Buffer 2; 100mM Tris, 100mM sodium chloride, 50mM magnesium chloride, pH9.5

Buffer 3; 10mM Tris, 1mM EDTA, pH8.0

Before the antibody was applied to the sections the slides were washed for 1 minute in buffer 1. Non-specific binding of the antibody was then prevented by incubating the sections, for 30 minutes at room temperature, in a blocking solution containing 2% normal sheep serum and 0.3% triton X-100 diluted in buffer 1. Following the blocking stage, the solution was drained from the slides and the excess wiped carefully from around the section using a clean paper tissue. The anti-digoxigenin antibody, diluted at 1:500 in the blocking solution, was then applied to the sections and allowed to incubate for 2 hours at room temperature. After 2 hours the slides were washed in two, 10 minute, changes of buffer 1. After the second wash, buffer 1 was replaced with buffer 2 and the slides were washed for a further 2 minutes.

A stock substrate solution containing 18.75mg/ml of nitro blue tetrazolium chloride (NBT) and 9.4mg/ml of 5-bromo-4chloro-3indolyl phosphate (BCIP) was purchased from Boehringer Mannheim (Boerhinger Mannheim UK, East Sussex, UK). This was used to prepare the substrate solution required for the detection of the alkaline phosphatase label conjugated to the anti-digoxigenin antibody. The working substrate solution was prepared by the addition of 200µl of NBT/BCIP stock to 10ml of buffer 2. To quench any endogenous alkaline phosphatase activity, 100µl of 1M levamisole was added to the substrate solution.

After 2 minutes, buffer 2 was drained from the slides and the excess removed by wiping around the section with a clean paper tissue. The slides were placed in a humidity chamber and the working substrate solution was applied to the sections. The slides were placed in a dark environment and reaction allowed to proceed at room temperature. After an initial 30-minute incubation time, the colour development was monitored by periodic microscopic examination of the sections. A positive reaction can be seen by the presence of a dark blue/black reaction product in the section. If no satisfactory staining became apparent the colour development was allowed to continue overnight. On completion, the reaction was stopped by washing the slides in buffer 3 for 5 minutes. The sections were then counterstained with neutral red to emphasize any blue/black staining and to ease subsequent histological examination. Since the end product of the alkaline phosphatase NBT/BCIP reaction is alcohol soluble, the slides were mounted in Aquamount®, an aqueous mounting medium that does not require dehydration and clearing of the sections before its use.

4.2.4.2. *In-situ* reverse-transcriptase polymerase chain reaction

In-situ reverse-transcriptase polymerase chain reaction (IS-RT-PCR) is a technique that can be used to amplify specific mRNA sequences within tissue sections to allow their subsequent detection . This amplification of specific nucleic acid target sequences helps to circumvent the problems associated with the detection of low copy number mRNA species using conventional ISH. The procedure utilises the RT-PCR reaction as described in Chapter 2. However, in IS-RT-PCR the nucleic acid target sequences are not extracted from the sample but are amplified *in-situ* within the tissue section thus allowing the cells responsible for the production of the nucleic acid to be identified.

IS-RT-PCR can take two forms, direct and indirect IS-RT-PCR. In this study both forms of this procedure were utilised to ascertain the source of the cytokines IL-1α, IL-6 and TNFα, within the murine CNS following trypanosome infection and subcurative drug treatment.

4.2.4.2.1. Direct IS-RT-PCR

Direct IS-RT-PCR uses the technique of RT-PCR to amplify specific mRNA sequences in tissue sections without the need for prior extraction of the nucleic acid. During the PCR procedure a nucleotide, labelled with a reporter molecule, such as, digoxigenin, biotin or fluorescein, is incorporated directly into the resulting amplicon. This reporter molecule can then be detected in the section and the location of the mRNA target determined (Embelton, 1998).

To perform IS-RT-PCR the following protocol was followed. Formalin fixed paraffin embedded sections were cut and mounted three per slide. This allows the inclusion of control sections on each individual slide as shown in Figure 4.2. Two sets of slides from each tissue block were included in each IS-RT-PCR run. The sections were dewaxed, rehydrated through graded alcohols and then rinsed in PBS. To obtain the optimal permeablisation of the tissue, one set of slides was incubated overnight with 20μg/ml proteinase K at room temperature. The second set of slides was treated for 90 minutes with 40μg/ml proteinase K at 37^0C. Following the enzyme treatment the sections were rinsed in PBS, supplemented with 0.1M glycine, to stop the digestion process. The slides

were then dehydrated through graded alcohols and stored until ready to continue the protocol.

When performing IS-RT-PCR there is a danger that genomic DNA within the section will be amplified during the PCR stage of the procedure. Since the amplification procedure is performed in the tissue section, the PCR products of mRNA and genomic DNA cannot be differentiated by assessing the size of the amplicon. Therefore, to eliminate the risk of generating false positive results, it is necessary to treat the test sections with DNase to degrade the genomic DNA. This DNase treatment also helps to prevent the generation of false positive results due to incorporation of the labelled nucleotide into genomic DNA sequences by the cellular DNA repair mechanisms. The test section and the negative control section on each slide (Fig.4.2) were therefore treated with 10U of DNase, diluted in a buffer containing 100mM sodium acetate and 5mM magnesium sulphate. The enzyme was applied to the sections and allowed to digest overnight at room temperature. The third section on the slide was not treated with DNase and served as a positive control. The sections were dehydrated following DNase digestion.

As with tissue sections it is necessary to convert the mRNA in the tissue sections to cDNA, using reverse transcriptase, before the PCR stage can be performed. The reverse transcriptase reaction was performed on only the test section on each slide (Fig. 4.2). The cDNA was generated in a 50µl reaction volume. The solution comprised 1X 1st strand buffer (5mM Tris pH8.3, 75mM potassium chloride and 3mM magnesium chloride), 600U M-MLV reverse transcriptase, 10mM dithiothreitol (GIBCO BRL®), 1.25mM dNTP's, 30U RNase inhibitor and 2ug random hexamers (Hybaid, UK). The reverse transcriptase mix was applied to the sections and the slides were incubated for 30 minutes at 42^{0}C. The sections were then rinsed for 5 minutes in 50mM Tris pH8.0 and dehydrated through graded alcohols prior to the PCR.

To perform the PCR a master mix containing 1X PCR buffer (20mM Tris pH8.55, 16mM ammonium sulphate and 1.5mM magnesium chloride), 6U *Taq* DNA polymerase (Hybaid, UK) 1ng 3'primer, 1ng 5'primer, 10mM digoxigenin-11-dUTP (Boehringer Mannheim UK, East Sussex, UK), 50mM dNTP's and 2% BSA (Sigma). The reaction volume allocated for each section was 50µl. The primers used in this study were designed to amplify IL-1α, IL-6 and TNF-α. These primers were identical to those used in the procedure described in Chapter 2 for tube PCR and their nucleotide sequence is detailed in Table 2.3. The concentration of each reagent used in IS-RT-PCR is much higher than that used for tube PCR. This is due to the presence of inhibitors within the tissue section that

Figure 4.2

are absent in extracted nucleic acid samples. Thermo-cycling blocks designed by both Perkin-Elmer and Hybaid were used in the IS-RT-PCR procedure. Each block has specific requirements to seal the PCR mix with the tissue section. Therefore, the master mix was applied to the sections and the slides were assembled according to the manufactures recommendations before being placed onto the thermo-cycling block. To help achieve successful IS-RT-PCR staining a range of cycling parameters were used in this procedure. During the initial denaturation step the slides were heated to 94^0C for 5 minutes. This was followed by a short denaturing step of 94^0C for 15 seconds to 3 minutes, an annealing step of 60^0C for 30 seconds to 4 minutes and an extension step of 72^0C for 1 minute 30 seconds to 5 minutes. This profile was repeated for between 10 and 35 cycles. A final extension step of 72^0C for 10 minutes was performed at the end of the cycling procedure. Following the PCR procedure the slides were removed from the cycling block and washed for 10 minutes at room temperature in PBS to remove the excess PCR mix. The digoxigenin-11-dUTP labelled PCR product was then detected using the visualisation procedure described above.

4.2.4.2.2. Indirect IS-RT-PCR

Indirect IS-RT-PCR, utilises a combination of RT-PCR and ISH techniques. The target mRNA is first converted to cDNA and then amplified within the tissue section. No labelled nucleotides are employed in indirect IS-RT-PCR, therefore, the product of this RT-PCR reaction is detected with the use of specific probes through the ISH procedure (O'Leary, 1998).

The protocol used for indirect IS-RT-PCR largely followed that described for direct IS-RT-PCR. However, after the reverse transcriptase reaction the sections were post-fixed in 0.4% paraformaldehyde for 20 minutes at 4^0C before dehydration. The PCR master mix also differed from that used in the direct method as no digoxigenin-11-dUTP was added to the mix. On completion of the PCR cycling the section were post fixed in 0.4% paraformaldehyde for 20 minutes at 4^0C to prevent loss of the amplicons, then rinsed in PBS and dehydrated.

A hybridisation buffer comprising 2 x SSC, 5% dextran sulphate and 0.2% dried milk powder was prepared. To this, a specific oligonucleotide probe, labelled with either biotin or digoxigenin, was added to a final concentration of 10pmol/100µl. In this study oligonucleotide probes, labelled with either biotin or digoxigenin, designed specifically to

bind with the PCR product of IL-1α amplification were employed. The nucleotide sequence of this IL-1α specific probe was as follows:

5'-CTC TTC TTC AGA ATC TTC CCG TTG CTT GAC-3'

The complete hybridisation buffer was applied and the slides heated to 95^0C for 5 minutes to denature the double stranded PCR amplicons in the tissue sections. The slides were then incubated overnight at 42^0C to allow the probe to hybridise with the target sequence. Following the hybridisation the sections were rinsed in 4 x SSC for 10 minutes, followed by two 20 minute washes in 2 x SCC. All post-hybridisation washes were performed at room temperature.

The visualisation procedures employed following the hybridisation depended on the reporter molecule used to label the probe. A biotin label was detected using the standard ABC protocol detailed in the ICC procedure described in Chapter 2 while a digoxigenin label was detected using the visualisation procedure described above.

4.2.5. Statistical analyses

Statistical analyses were performed on the data generated from the assessment of the level of cytokine and chemokine transcription in the murine CNS following trypanosome infection and subcurative drug treatment. Differences in the expression levels of these inflammatory mediators were investigated using a visual assessment scale to grade the intensity of the resulting PCR band following amplification (Figure 2.11). The data produced using this scoring system were analysed using non-parametric statistical tests. Significant differences in the expression levels of these mediators across the groups of mice were detected using the Kruskal-Wallis test. This was then followed by Dunn's test, a pairwise comparison procedure for non-parametric data, to highlight differences between the median values from individual groups. All statistical tests were performed using the proprietary statistical software packages, Minitab version 13 and Sigmastat 2.03.

4.3. Results

4.3.1. Kinetics of cytokine and chemokine expression

The RT-PCR analyses of nucleic acid extracted from murine CNS tissue following trypanosome infection and subcurative drug treatment was employed to detect any variations in the levels of cytokine mRNA expression that occur during the course of the disease. Significant changes in the levels of the transcripts for these inflammatory agents were detected through formal statistical analyses of the data generated from assessing the intensity of the resultant PCR bands when examined on a 2% agarose gel stained with ethidium bromide. Such alterations in cytokine and chemokine expression may indicate that these important mediators play a central role in the disease pathogenesis. This information could help to establish novel drug targets to help prevent the development of the CNS-inflammatory response associated with trypanosome infection.

4.3.1.1. Observational differences and trends in cytokine expression

Pictures of the PCR products obtained on amplification of pooled mRNA from animals in each treatment regimen are shown in Figures 4.3-4.9. Although six mice were included in each group at the outset of the experiment, due to death or euthanasia of the mice prior to the endpoint of the experiment, or unsatisfactory RNA extraction the number of animals comprising each analysis group are listed in Figures 4.10-4.15. Before any comparisons were made regarding the levels of cytokine expression in the mice the quality of the mRNA was checked by amplification of the mRNA of the housekeeping gene β-actin. This resulted in bands of a similar intensity (Fig. 4.3) indicating that differences in the banding pattern for subsequent analyses would be the result of variations in the amount of target transcript present in the initial sample and would therefore provide an indication of the transcription levels of the cytokine or chemokine being examined.

The broad interpretation of the RT-PCR results indicated that cytokines such as IL-α and TNF-α were expressed in the brains of normal uninfected mice and continued to be present following infection. IL-6 mRNA transcripts were never detected in uninfected animals but

were always present by 7 days post-infection. The chemokines MIP-1α, MCP-1 and RANTES were also expressed in uninfected animals and throughout the course of the infection.

The gel staining pattern found on examination of IL-1α expression (Fig. 4.4) shows that the expression of this cytokine appears to rise from 14 days post-infection through to 28 days post-infection. Following the administration of a subcurative diminazene aceturate dose, to exacerbate the CNS inflammatory response, the levels of transcript dropped slightly compared with mice killed at 28 days post-infection. This level was also observed in mice 7 days following the induction of a severe meningoencephalitis by treatment with a second dose of diminazene aceturate. However, by 14 days after the second diminazene aceturate the levels of IL-1α mRNA found were similar to those seen in animals killed at 28 days post-infection. Moderate levels of IL-1α transcription were found to be constitutively expressed in uninfected animals.

In contrast to IL-1α, no IL-6 expression was seen in uninfected mice (Fig. 4.5). Transcripts for this cytokine were found in mice by 7 days post-infection and this remained relatively constant through to day 21 post-infection. A slight increase in the intensity of the PCR band was seen in animals at day 28 post-infection compared to those killed during the earlier stages of disease. Seven days after the exacerbation of the CNS inflammation, by administration of a single dose of diminazene aceturate, the level of IL-6 found was similar to that seen in the early infection and this dropped slightly more by 14 days after the drug treatment. This pattern was not echoed in mice in which the severe meningoencephalitic reaction had been induced and more intense PCR bands were detected in these mice.

Transcripts for TNF-α were detected in animals at similar levels on days 7 and 14 post-infection (Fig. 4.6). The intensity of the resultant PCR bands was higher when the RT-PCR was performed on mice killed at the later time points of days 21 and 28 post-infection. A similar level of expression was found in animals killed 7 days after receiving a single dose of diminazene aceturate. However, this level had dropped by day 14 post-diminazene aceturate and only very weak PCR bands were found. Low levels of TNF-α transcription were also seen in uninfected animals.

When the expression of MCP-1 was investigated weakly staining bands were found in uninfected mice (Fig. 4.7). By 7-days post-infection the intensity of this band had

increased a little and appeared to strengthen slightly further as the degree of the neuroinflammation became more severe. This was not true for mice killed 14 days after the administration of a second diminazene aceturate dose. Although this treatment regimen induces a severe meningoencephalitis the intensity of the band seen following the amplification MCP-1 transcripts, was lower than in other groups in which the CNS reaction had been induced and was similar to that found 7 days after the mice had been infected.

Transcripts for MIP-1α were found in uninfected mice and the intensity of PCR bands increased only slightly following infection (Fig. 4.8). In animals killed at 21 and 28 days post-infection, a further moderate rise in the expression levels was seen. Following exacerbation of the CNS response no gross changes in the intensity of the staining pattern were found. Animals killed 7 days following the administration of a second dose of diminazene aceturate once more showed higher levels of MIP-1α expression. However, by 14 days after this drug treatment the intensity of the resulting band had dropped to levels comparable with those seen in uninfected mice.

RANTES transcription was detected in uninfected animals (Fig. 4.9). The intensity of the PCR band was increased following infection and this remained at largely similar levels through to day 28 post-infection. When the animals were given a single dose of diminazene aceturate the level of RANTES transcription appeared to rise at 7 days after the drug treatment and fall again by 14 days following the diminazene aceturate. A similar pattern of expression was found when the extremely severe meningoencephalitic reaction was induced by treating the infected mice with a second dose of diminazene aceturate. This regimen again initially resulted in an increase in the transcription of RANTES that appeared to reduce by 14 days after the diminazene aceturate treatment.

4.3.1.2. Statistical analyses of RT-PCR results

Significant alterations in the expression levels on IL-1α, IL-6, TNF-α, MCP-1, MIP-1α and RANTES were detected on statistical analyses of the results of the interpretation of the banding patterns as seen on a 2% agarose gel stained with ethidium bromide after RT-PCR analysis. The data were generated by assigning a numerical grading score describing the intensity of staining of the PCR reaction product from each individual mouse. In all cases p-values of less than 0.05 were considered to indicate a significant change in the level of specific cytokine or chemokine transcription. Treatment groups where significant

differences in these expression levels were detected are listed in Table 4.2. Summary data for each cytokine or chemokine in the individual and combined experiments, together with graphs depicting trends in the expression patterns are described in Figures 4.10-4.15.

No significant differences were found in the expression levels of IL-1α within the CNS throughout the progression of the neuroinflammatory reaction. Uninfected animals showed a median PCR value on 2.75. These levels were slightly reduced (median 2.00) in mice killed at 7 and 14 days after infection with *T.b.brucei* GVR35/C1.6. By 21 days post-infection this had increased to a median value 2.5 and a further rise was seen on day 28 post-infection (median 3.00). Following treatment with a single diminazene aceturate dose the level of IL-1α expression returned to that seen at 7 and 14 days post-infection (median 2.00). This increased slightly when the mice were killed 7 days after a second diminazene aceturate treatment (median 2.25) and increased further by 14 days after administration this drug treatment (median 3.00) (Fig. 4.10).

When the expression of IL-6 was examined significant differences in the levels of transcription were detected between the various treatment groups. Transcripts were never detected in any of the uninfected animals and returned a median PCR value of 0.00. By 7 days post-infection expression of IL-6 was found (median 1.00). This expression level remained relatively stable in animals killed on day 14 post-infection (median 0.75) and 21 days post-infection (median 1.00) and a slight increase in the PCR banding intensity was detected in animals killed on day 28 post-infection (median 1.50). Significant differences were found in the expression of IL-6 between animals killed on days 21 and 28 post-infection and the uninfected control mice. Mice treated with a single diminazene aceturate dose also returned a median PCR value (median 1.00) that was significantly different to the uninfected animals. However, by 14 days after the drug treatment this expression level had dropped to a median value of 0.05 and this was no-longer different to that seen in the uninfected mice. An increase in the transcription of IL-6 was found in animals killed 7 days following treatment with a second dose of diminazene aceturate. These animals returned a median PCR value of 1.75 and this had increased further by 14 days after the drug treatment (median 2.00). Both groups of mice treated with two doses of diminazene aceturate showed significantly increased levels of IL-6 transcription compared to uninfected control animals (Fig. 4.11).

TNF-α expression was detected in uninfected mice and a median PCR value of 0.75 was found. By 7 and 14 days post-infection this expression had increased (median 1.25) but this could not be considered significant. A further rise in the expression of this cytokine

was seen in animals killed at 21 days post-infection (median 2.50) and 28 days post-infection (median 3.00). The increased level of transcription found in mice killed on day 28 post-infection was significantly different to the levels seen in control animals. Animals killed 7 days following the administration of a single diminazene aceturate treatment returned a median PCR value of 2.5 this dropped dramatically in animals killed at day 14 after drug treatment (median 0.00). The level of TNF-α transcription found in this group of mice was significantly lower than that seen in mice killed at 28 days post-infection and 7 days after a single diminazene aceturate treatment. Animals treated with a second diminazene aceturate treatment and killed 7 days later returned a median PCR value of 2.75. This was considered significantly higher than that found 14 days after a single diminazene aceturate dose. When the period between diminazene aceturate administration and termination of the mice was extended to 14 days a slight drop in the transcription level for TNF-α was found (median 1.00) (Fig. 4.12).

Low levels of MCP-1 expression were seen in uninfected mice and these animals returned a median PCR value of 0.50. By 7 and 14 days after infection this median had increase to 2.00. A further increase was noted on day 21 post-infection (median 2.50) but this had dropped back down slightly by day 28 post-infection (median 2.25). The levels of MCP-1 transcription seen in these groups of infected animals was not considered significantly different to that found in the uninfected mice. The median PCR value found in mice 7 days after a single diminazene aceturate dose was 2.5. This figure was significantly higher than that found in the uninfected mice. By 14 days post-diminazene aceturate the expression level was again slightly higher than that seen after 7 days post drug treatment. A rise in the transcription level of MCP-1 was seen in mice killed 7 days after receiving a second diminazene aceturate treatment. These animals returned a median PCR value of 3.00; this was significantly higher than the expression level seen in uninfected mice. A reduction in the level of MCP-1 transcription was found in mice killed 14 days after treatment with a second dose of diminazene aceturate (median 1.75) (Fig.4.13).

The expression of MIP-1α in the uninfected mouse brain returned a median PCR value of 1.50. In animals killed at 7 days post-infection this had increased to 2.5 and remained at this grade through to day 14 post-infection. On days 21 and 28 post-infection the levels of MIP-1α expression continued to rise and gave median PCR values of 3.00 and 3.50 respectively. The transcription level, seen animals killed at 28 days post-infection, was significantly higher than that found in uninfected animals. Treatment of the infected mice with a single diminazene aceturate dose resulted in a reduction in the transcription of this

chemokine. Mice killed 7 days after receiving the drug showed a median level of 3.00, which dropped still further in mice killed 14 days after diminazene aceturate treatment (median 2.00). When the infected animals were treated with a second dose of diminazene aceturate, the expression levels returned to those seen in mice killed on day 28 post-infection (median 3.50). This was again significantly higher than the levels seen in uninfected mice. On day 14 after the second diminazene aceturate treatment the expression of MIP-1α was reduced to levels comparable with those seen in uninfected animals (median 1.50) (Fig.4.14).

The chemokine RANTES was found to be expressed in uninfected mice. These animals returned a median PCR value of 1.50. This level increased following infection and a median of 3.00 was found in groups of mice killed at 7, 14, 21 and 28 days post-infection. Groups of animals killed at 14 and 28 days after infection were considered to express higher levels of RANTES than uninfected mice. When animals were treated with a single dose of diminazene aceturate the transcription of RANTES was further increased (median 4.00), however this was reduced by 14 days after drug treatment (median 2.50). Seven days following administration of a second dose of diminazene aceturate the median expression levels return to 4.00. This was significantly higher than the median PCR value found in uninfected animals. A reduction in this median PCR value was found in mice killed on day 14 after receiving the second diminazene aceturate treatment (median 2.75) (Fig.4.15).

4.3.2. Immunocytochemistry

Immunocytochemistry (ICC) was performed to determine the location of cytokine proteins within the CNS of trypanosome-infected mice following various drug regimens. Before this technique was performed, the presence of the mRNA transcripts for these inflammatory mediators had been shown in nucleic acid extracted from the CNS of trypanosome-infected animals killed on day 7 post-infection and in all subsequent samples. This strongly suggests that the protein product of this mRNA should also be found in the CNS of these mice.

A wide range of ICC protocols were used to try and achieve staining of the cytokine proteins. However, none of these techniques proved successful in this study. Despite the use of antibodies from multiple different clones no cytokine protein could be detected using the standard ICC technique with either cryostat or paraffin embedded tissue sections.

Therefore, a variety of tissue permeablisation and antibody retrieval techniques were attempted. Unfortunately none of these methods produced successful staining results.

4.3.3. *In-situ techniques*

4.3.3.1. *In-situ* hybridisation

This investigation attempted to use ISH to localise mRNA transcripts from IL-1α, IL-6 and TNF-α. Sections stained using this procedure, including the negative control slide, either showed high levels of background staining that was indistinguishable from true staining or no staining at all. A range of alterations to the technique described in the Materials and Methods section were instigated in an effort to achieve successful staining using ISH. These modifications included, varying the concentration of proteinase K and the duration of the digestion used to permeablise the tissue, altering the concentration of the probe, raising the hybridisation temperature to 42^0C and changing the stringency of the post-hybridisation washes. The technique was also tried using cryostat sections however, the frozen material was extremely fragile and often floated off of the slide during the lengthy procedure and no improvements in the staining patterns were found. None of these modifications were successful and the use of ISH to localise the mRNA sequences failed. Since this failure could have been the result of low copy numbers of the mRNA transcripts the IS-RT-PCR procedure was performed.

4.3.3.2. IS-RT-PCR

Both direct and indirect IS-RT-PCR techniques were employed in this study. Initial investigations using this technique were performed by means of the Perkin Elmer GeneAmp *in-situ* PCR System 1000 thermocycler while later trials used the Hybaid OmniSlide System.

The production of the misleading staining patterns and floating sections was common to both IS-RT-PCR machines. However, each platform had its own additional drawbacks. The Perkin Elmer machine is of a similar basic format to a regular Perkin Elmer PCR thermocyler in design, however the heating block is designed as a series of vertical plates that the slides are placed between, on their edge, before being tightly clamped into place. The block will only hold a total of 10 slides. Many slides did not survive the thermocycling stage when using this system and broke during the procedure. The

assemblage of the slides for use in this machine is also cumbersome. The PCR mix was sealed onto the surface of the slide by applying a specially designed gasket, held in place by a metal clip. Due to the size of the resulting assemblage some doubt existed as to the accuracy of the temperatures reached in the section during the temperature cycling procedure.

Similar problems with regard to the generation of false positive staining patterns were found when IS-RT-PCR was transferred to the OmniSlide System. This system is a flat bed thermocycler with a novel racking system that allows up to 20 slides to be processed in one run. No clamping mechanisms are required and therefore no breakage of slides was encountered when using this machine. Using this system the slides are placed, section uppermost, onto a flat thermocycling block. The PCR mix is sealed onto the sections by the use of specially designed self-adhesive foam frames and plastic coverslips. This system is simple to assemble and is available in a range of sizes to suit every section. However, problems with regard to maintaining the integrity of the seal during the temperature cycling procedure were evident as the PCR mixture was found to have evaporated from many of the slides following the amplification stage.

The first IS-RT-PCR technique attempted was a direct labelling procedure where digoxigenin labelled dUTP was incorporated directly into the PCR product during the amplification reaction. The main problems with this technique were the production of strongly positive areas within the negative control section, no staining at all and the section floating from the slide during the procedure. No sections stained using this technique yielded interpretable results.

As the generation of false positive staining is a recognised difficulty in direct IS-RT-PCR an indirect approach was attempted. Again severe problems with the section floating from the slide during the procedure were encountered. In sections that managed to survive the lengthy procedure positive staining was once more detected on the negative control slides. Despite discussions regarding the technique with an expert in the commercial sector, who provides an IS-RT-PCR staining service, these difficulties could not be resolved and no meaningful results were gained through the use of this technique.

IL-1α	IL-6	TNF-α	MCP-1	MIP-1α	RANTES
		Experiment 1			
14DPDD vs 7DPI	14DPDD vs UIC 7DPDD vs UIC 28DPI vs UIC	28DPI vs 7DPI 28DPI vs 14DPD	NDD	NDD	NDD
		Experiment 2			
NDD	7DPD vsUIC 28DPI vs UIC	7DPDD vs UIC 7DPDD vs 14DPI 21DPI vs UIC 7DPD vs UIC	7DPDD vs UIC	7DPDD vs UIC 28DPI vs UIC 7DPD vs UIC	7DPD vs UIC
		Experiments 1&2			
NDD	14DPDD vs UIC 7DPDD vs UIC 28DPI vs UIC 7DPD vs UIC 21DPI vs UIC	7DPDD vs 14DPD 28DPI vs 14DPD 7DPD vs 14DPD	7DPDD vs UIC 7DPD vs UIC	7DPDD vs UIC 28DPI vs UIC	7DPDD vs UIC 7DPD vs UIC 28DPI vs UIC 14DPI vs UIC

Table 4.2. Assessment of differential cytokine and chemokine expression in the mouse brain following trypanosome infection and subcurative drug treatment.

Following RT-PCR analyses the intensity of the resulting PCR band, as seen on a 2% agarose gel stained with ethidium bromide, was taken as an indication of the quantity of the target sequence present in the initial sample and was graded on a scale of 0 to 4, where 0 indicated no band and 4 indicated an extremely intense PCR band. The data generated from these tests were analysed to determine if there were significant differences ($p<0.05$) in the expression levels of the cytokines IL-α, IL-6 and TNF-α and the chemokines MCP-1, MIP-1α and RANTES at various time points following trypanosome-infection (7DPI, 7 days post-infection; 14DPI, 14 days post-infection; 21 DPI, 21 days post-infection, 28DPI, 28 days post-infection; UIC, uninfected control) and subcurative drug treatment regimens (7DPD, 7days post-diminazene aceturate; 14DPD, 14 days post-diminazene aceturate; 7DPDD, 7 days post-second diminazene aceturate; 14 DPDD, 14 days post-second diminazene aceturate). The analyses of the data from experiment 1 and 2 as well as the combined data from both experiments are shown. Only groups determined to be significantly different to each other are listed. NDD, no differences detected.

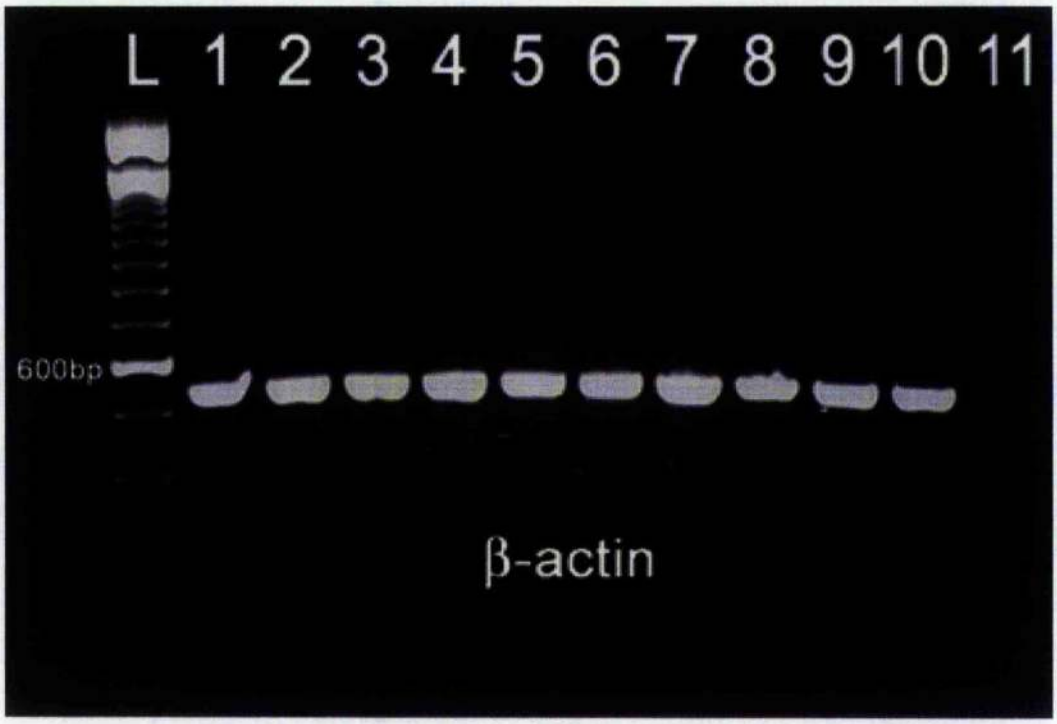

Figure 4.3. β-actin check gel for groups of animals used to investigate the time-course of cytokine and chemokine expression in trypanosome infection.

To ensure the mRNA extracted from each group of mice was of similar quality, amplification of the mRNA for the housekeeping gene β-actin was carried out. RT-PCR was performed on material extracted from the CNS of mice infected with *T.b.brucei* GVR35/C1.6 and killed 7 (lane 1), 14 (lane 2), 21 (lane 3) and 28 (lane 4) days later. Groups of mice were treated on day 21 post-infection with diminazene aceturate (40mg/kg i.p.) to exacerbate the CNS inflammatory response. These animals were killed 7 (lane 5) and 14 (lane 6) days following the drug treatment. To induce a severe meningoencephalitis some mice were allowed to relapse to parasitaemia following the initial diminazene aceturate treatment. These mice were given a second dose of diminazene aceturate and killed 7 (lane 7) and 14 days (lane 8) after the administration of the drug. Amplification of material from uninfected control mice (lane 9), a known positive (lane 10) and a negative control where water was substituted for template (lane 11) are also shown. The banding pattern seen is similar for each group of mice thereby permitting comparisons to be made, with regard to the levels of cytokine and chemokine expression, between the different groups of mice using the RT-PCR techique.

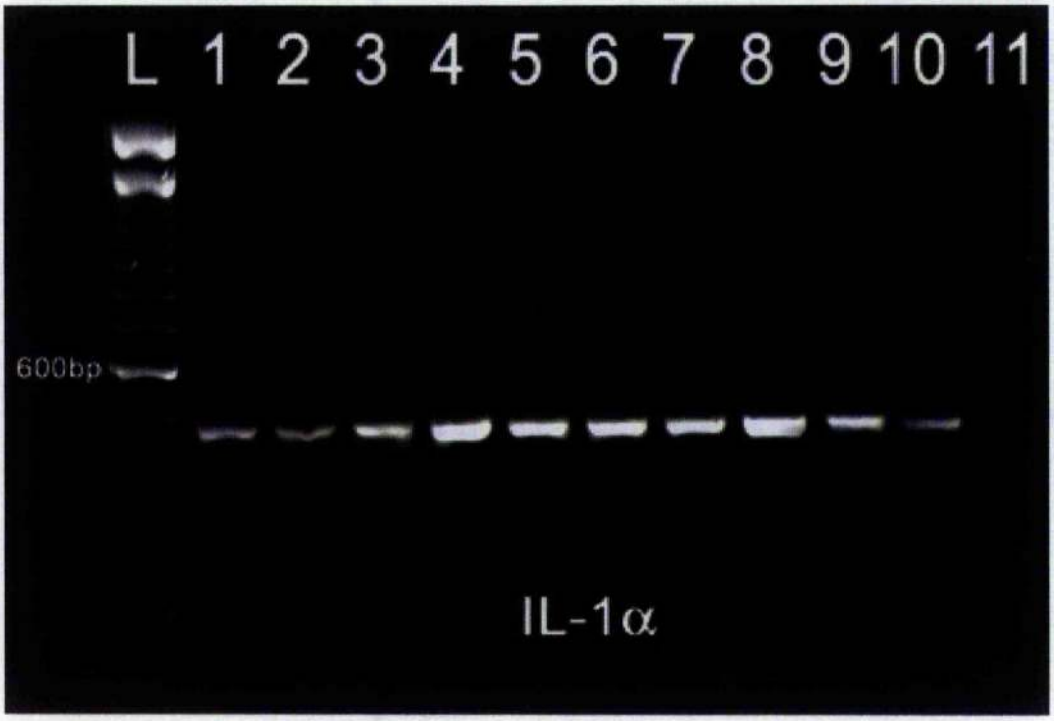

Figure 4.4. IL-1α transcription pattern through the various stages of trypanosome-infection.

RT-PCR was performed, to detect IL-1α expression on the mRNA extracted from mice infected with *T.b.brucei* GVR35/C1.6 and killed 7 (lane 1), 14 (lane 2), 21 (lane 3) and 28 (lane 4) days later. Groups of mice were treated on day 21 post-infection with diminazene aceturate (40mg/kg i.p.) to exacerbate the CNS inflammatory response. These animals were killed 7 (lane 5) and 14 (lane 6) days following the drug treatment. To induce a severe meningoencephalitis some mice were allowed to relapse to parasitaemia following the initial diminazene aceturate treatment. These mice were given a second dose of diminazene aceturate and killed 7 (lane 7) and 14 days (lane 8) after the administration of the drug. Amplification of material from uninfected control mice (lane 9), a known positive (lane 10) and a negative control where water was substituted for template (lane 11) are also shown. A slight increase in the intensity of the staining can be seen in animals from 14 – 28 days post-infection (lanes 2-4) with the highest level of expression found on day 28 post-infection (lane 4) and 14 days following a second diminazene aceturate treatment (lane 8). Bands of moderate intensity are present in material from uninfected mice (lane 9).

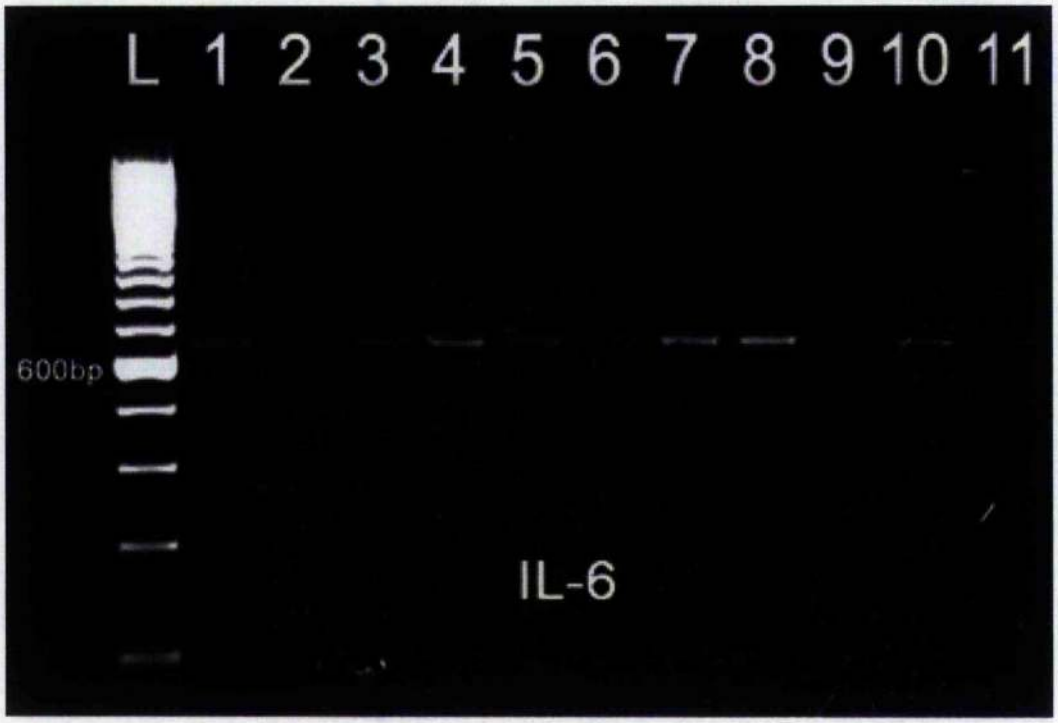

Figure 4.5. IL-6 transcription pattern through the various stages of trypanosome-infection.

RT-PCR was performed, to detect IL-6 expression on the mRNA extracted from mice infected with *T.b.brucei* GVR35/C1.6 and killed 7 (lane 1), 14 (lane 2), 21 (lane 3) and 28 (lane 4) days later. Groups of mice were treated on day 21 post-infection with diminazene aceturate (40mg/kg i.p.) to exacerbate the CNS inflammatory response. These animals were killed 7 (lane 5) and 14 (lane 6) days following the drug treatment. To induce a severe meningoencephalitis some mice were allowed to relapse to parasitaemia following the initial diminazene aceturate treatment. These mice were given a second dose of diminazene aceturate and killed 7 (lane 7) and 14 days (lane 8) after the administration of the drug. Amplification of material from uninfected control mice (lane 9), a known positive (lane 10) and a negative control where water was substituted for template (lane 11) are also shown. No IL-6 expression was seen in uninfected mice (lane 9). By 7 days post-infection (lane 1) IL-6 transcripts were detected and increased through day 28 post-infection (lane 4). Following a single diminazene aceturate treatment the intensity of the amplicon bands reduced (lanes 5 & 6). More intensely staining PCR products are seen in mice killed after the induction of a severe meningoencephalitis (lanes 7 & 8).

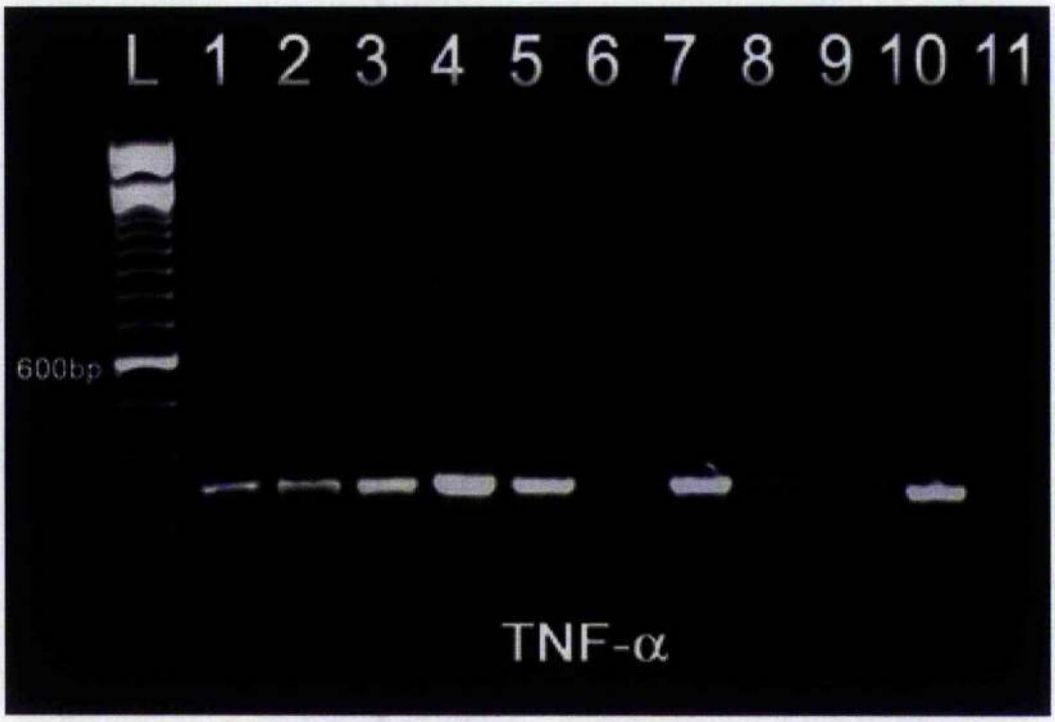

Figure 4.6. TNF-α transcription pattern through the various stages of trypanosome-infection.

RT-PCR was performed, to detect TNF-α expression on the mRNA extracted from mice infected with *T.b.brucei* GVR35/C1.6 and killed 7 (lane 1), 14 (lane 2), 21 (lane 3) and 28 (lane 4) days later. Groups of mice were treated on day 21 post-infection with diminazene aceturate (40mg/kg i.p.) to exacerbate the CNS inflammatory response. These animals were killed 7 (lane 5) and 14 (lane 6) days following the drug treatment. To induce a severe meningoencephalitis some mice were allowed to relapse to parasitaemia following the initial diminazene aceturate treatment. These mice were given a second dose of diminazene aceturate and killed 7 (lane 7) and 14 days (lane 8) after the administration of the drug. Amplification of material from uninfected control mice (lane 9), a known positive (lane 10) and a negative control where water was substituted for template (lane 11) are also shown. An increased intensity of staining can be seen in animals killed on day 21 (lane 3) and 28 (lane 4) post-infection. Raised TNF-α expression levels were also found in mice killed 7 days after a single diminazene aceturate treatment (lane5) and 7 days following the second diminazene aceturate treatment (lane 7). This increase was not sustained in mice killed at 14 days after administration of either drug dose (lanes 6 & 8). Transcripts for TNF-α were detected in uninfected mice (lane 9).

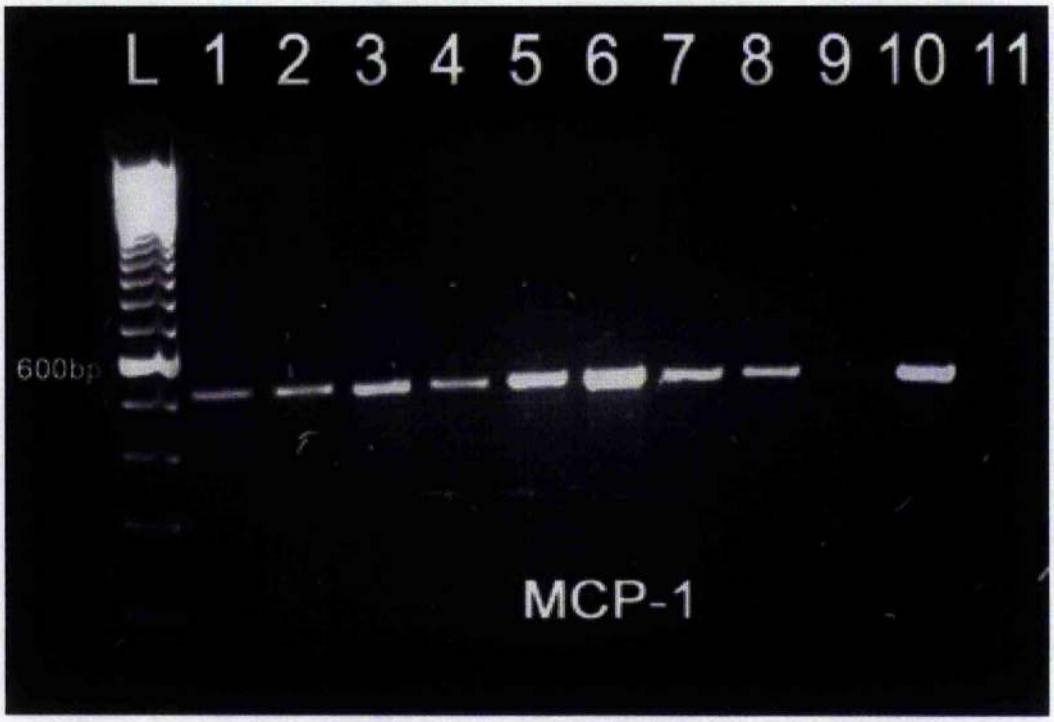

Figure 4.7. MCP-1 transcription pattern through the various stages of trypanosome-infection.

RT-PCR was performed, to detect MCP-1 expression on the mRNA extracted from mice infected with *T.b.brucei* GVR35/C1.6 and killed 7 (lane 1), 14 (lane 2), 21 (lane 3) and 28 (lane 4) days later. Groups of mice were treated on day 21 post-infection with diminazene aceturate (40mg/kg i.p.) to exacerbate the CNS inflammatory response. These animals were killed 7 (lane 5) and 14 (lane 6) days following the drug treatment. To induce a severe meningoencephalitis some mice were allowed to relapse to parasitaemia following the initial diminazene aceturate treatment. These mice were given a second dose of diminazene aceturate and killed 7 (lane 7) and 14 days (lane 8) after the administration of the drug. Amplification of material from uninfected control mice (lane 9), a known positive (lane 10) and a negative control where water was substituted for template (lane 11) are also shown. Uninfected animals showed an extremely low expression level of MCP-1, which was difficult to capture on film (lane 9). Expression increased following trypanosome infection (lanes 1-4) and after a single diminazene aceturate treatment (lanes 5 & 6). Moderate band intensities were found in animals killed following a second diminazene aceturate treatment (lanes 7 & 8).

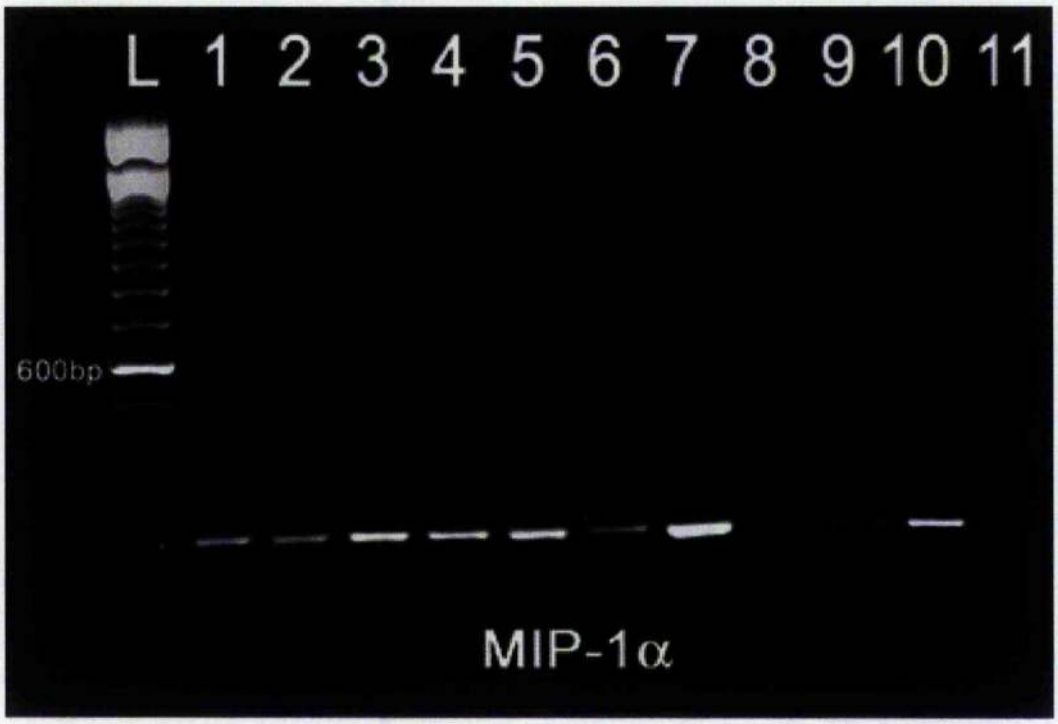

Figure 4.8. MIP-1α transcription pattern through the various stages of trypanosome-infection.

RT-PCR was performed, to detect MIP-1α expression on the mRNA extracted from mice infected with *T.b.brucei* GVR35/C1.6 and killed 7 (lane 1), 14 (lane 2), 21 (lane 3) and 28 (lane 4) days later. Groups of mice were treated on day 21 post-infection with diminazene aceturate (40mg/kg i.p.) to exacerbate the CNS inflammatory response. These animals were killed 7 (lane 5) and 14 (lane 6) days following the drug treatment. To induce a severe meningoencephalitis some mice were allowed to relapse to parasitaemia following the initial diminazene aceturate treatment. These mice were given a second dose of diminazene aceturate and killed 7 (lane 7) and 14 days (lane 8) after the administration of the drug. Amplification of material from uninfected control mice (lane 9), a known positive (lane 10) and a negative control where water was substituted for template (lane 11) are also shown. Transcripts for MIP-1α were detected in uninfected mice (lane 9). An increase in the intensity of the resulting bands was found at 7 and 14 days post-infection (lanes 1 & 2 respectively) and again on days 21 and 28 post-infection (lane 3 & 4). This level of transcription remained relatively stable following a single diminazene aceturate treatment (lanes 5 and 6). A more intense band was found 7 days following a second diminazene aceturate treatment (lane 7). This was reduced by 14 days ater the drug treatment (lane 8).

Figure 4.9. RANTES transcription pattern through the various stages of trypanosome-infection.

RT-PCR was performed, to detect RANTES expression on the mRNA extracted from mice infected with *T.b.brucei* GVR35/C1.6 and killed 7 (lane 1), 14 (lane 2), 21 (lane 3) and 28 (lane 4) days later. Groups of mice were treated on day 21 post-infection with diminazene aceturate (40mg/kg i.p.) to exacerbate the CNS inflammatory response. These animals were killed 7 (lane 5) and 14 (lane 6) days following the drug treatment. To induce a severe meningoencephalitis some mice were allowed to relapse to parasitaemia following the initial diminazene aceturate treatment. These mice were given a second dose of diminazene aceturate and killed 7 (lane 7) and 14 days (lane 8) after the administration of the drug. Amplification of material from uninfected control mice (lane 9), a known positive (lane 10) and a negative control where water was substituted for template (lane 11) are also shown. Transcripts of RANTES were detected in uninfected animals (lane 9) and increased in intensity following infection (lanes 1-4). Treatment with diminazene aceturate appeared to increase the expression levels further in animals killed 7 days after administration of either one or two doses of the drug (lanes 5 & 7). This level had reduced slightly when the interval between drug treatment and termination was extended to 14 days (lanes 6 & 8).

	Treatment Groups								
	UIC	7DPI	14DPI	21DPI	28DPI	7DPD	14DPD	7DPDD	14DPDD
					Experiment 1				
Median	2.00	1.00	1.50	3.00	3.00	2.00	2.00	2.50	3.00
Upper quartile	2.25	1.00	2.00	3.00	3.00	2.00	2.25	3.00	3.00
Lower quartile	2.00	0.75	1.00	1.75	1.75	1.75	1.00	2.00	3.00
Maximum	3.00	1.00	2.00	3.00	3.00	2.00	3.00	3.00	3.00
Minimum	2.00	0.00	1.00	1.00	1.00	1.00	1.00	2.00	3.00
Number	6	6	6	6	6	6	6	4	3
					Experiment 2				
Median	3.25	3.00	2.25	3.25	3.25	3.25	NA	2.00	NA
Upper quartile	3.50	3.00	3.125	3.50	3.50	3.5	NA	2.875	NA
Lower quartile	2.875	3.00	1.00	2.75	2.75	2.375	NA	1.50	NA
Maximum	3.50	3.00	3.500	3.5	3.5	3.5	NA	3.00	NA
Minimum	2.50	3.00	1.00	2.00	2.0	2.0	NA	1.50	NA
Number	6	6	6	6	6	6	NA	4	NA
					Experiments 1 & 2				
Median	2.75	2.00	2.00	2.5	3.00	2.00	2.00	2.25	3.00
Upper quartile	3.375	3.00	2.375	3.375	3.375	3.375	2.25	3.00	3.00
Lower quartile	2.00	1.00	1.00	2.00	2.25	2.00	1.00	1.625	3.00
Maximum	3.50	3.00	3.50	4.00	3.50	3.50	3.00	3.00	3.00
Minimum	2.00	0.00	1.00	2.00	1.00	1.00	1.00	1.50	3.00
Number	12	12	12	12	12	12	6	8	3

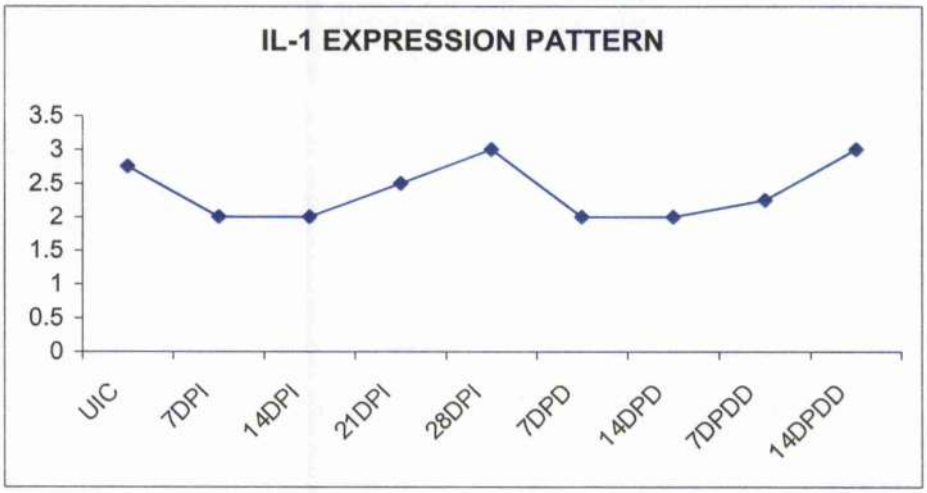

Figure 4.10. Summary statistics for IL-1α

The expression level of IL-1α in mouse brain was assessed at various time points following trypanosome infection (7DPI, 7 days post-infection; 14DPI, 14 days post-infection; 21 DPI, 21 days post-infection, 28DPI, 28 days post-infection) and subcurative drug treatments (7DPD, 7days post-diminazene aceturate; 14DPD, 14 days post-diminazene aceturate; 7DPDD, 7 days post-second diminazene aceturate; 14 DPDD, 14 days post-second diminazene aceturate). Samples from uninfected control (UIC) mice were also assessed. Following RT-PCR analyses the intensity of the resulting PCR band, as seen on a 2% agarose gel stained with ethidium bromide, was taken as an indication of the quantity of IL-1α mRNA present in the initial sample. The intensity of staining was graded on a scale of 0 to 4, where 0 indicated no band and 4 indicated an extremely intense PCR band. Summary statistics are given for each group of animals and the medians of the combined results from experiments 1 and 2 are plotted to indicate any expression trends. NA, not assessed.

	Treatment Groups								
	UIC	7DPI	14DPI	21DPI	28DPI	7DPD	14DPD	7DPDD	14DPDD
					Experiment 1				
Median	0.00	1.00	1.25	1.00	1.25	1.00	0.50	2.00	2.00
Upper quartile	0.00	1.00	1.625	1.50	3.00	1.00	1.00	2.00	2.00
Lower quartile	0.00	0.50	0.50	0.41	0.375	0.50	0.00	1.625	2.00
Maximum	0.00	1.00	2.00	1.50	3.00	1.00	1.00	2.00	2.00
Minimum	0.00	0.50	0.50	0.125	0.00	0.50	0.00	1.50	2.00
Number	6	6	6	6	6	6	6	4	3
					Experiment 2				
Median	0.00	0.75	0.50	1.25	1.25	2.25	NA	1.00	NA
Upper quartile	0.00	1.00	1.125	1.625	1.50	2.50	NA	1.75	NA
Lower quartile	0.00	0.188	0.00	0.875	1.00	1.75	NA	1.00	NA
Maximum	0.00	1.00	1.50	2.00	1.50	2.50	NA	2.00	NA
Minimum	0.00	0.00	0.00	0.50	1.00	1.00	NA	1.00	NA
Number	6	6	6	6	6	6	NA	4	NA
					Experiments 1&2				
Median	0.00	1.00	0.75	1.00	1.50	1.00	0.50	1.75	2.00
Upper quartile	0.00	1.00	1.50	1.5	2.75	2.375	1.00	2.00	2.00
Lower quartile	0.00	0.50	0.125	0.625	1.00	1.00	0.00	1.00	2.00
Maximum	0.00	1.00	2.00	2.00	3.00	2.50	1.00	2.00	2.00
Minimum	0.00	0.00	0.00	0.125	0.00	0.50	0.00	1.00	2.00
Number	12	12	12	12	12	12	6	8	3

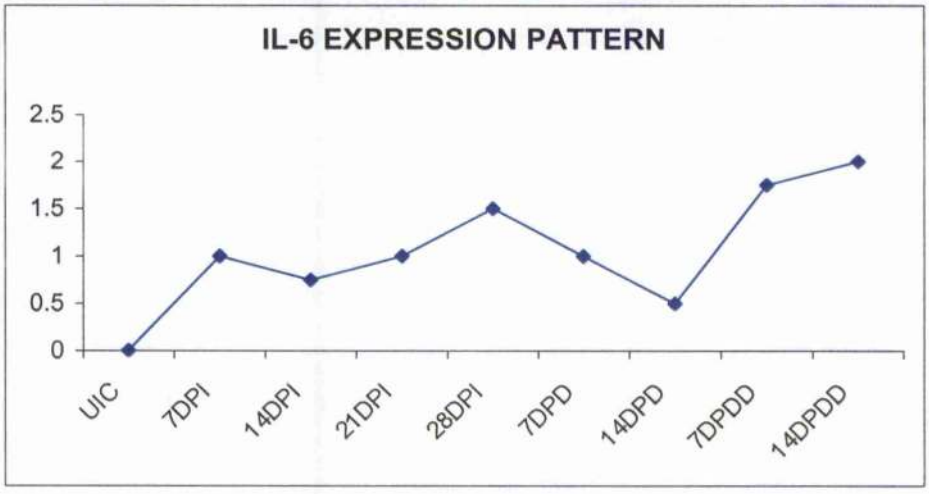

Figure 4.11. Summary statistics for IL-6

The expression level of IL-6 in mouse brain was assessed at various time points following trypanosome infection (7DPI, 7 days post-infection; 14DPI, 14 days post-infection; 21 DPI, 21 days post-infection, 28DPI, 28 days post-infection) and subcurative drug treatments (7DPD, 7days post-diminazene aceturate; 14DPD, 14 days post-diminazene aceturate; 7DPDD, 7 days post-second diminazene aceturate; 14 DPDD, 14 days post-second diminazene aceturate). Samples from uninfected control (UIC) mice were also assessed. Following RT-PCR analyses the intensity of the resulting PCR band, as seen on a 2% agarose gel stained with ethidium bromide, was taken as an indication of the quantity of IL-6 mRNA present in the initial sample. The intensity of staining was graded on a scale of 0 to 4, where 0 indicated no band and 4 indicated an extremely intense PCR band. Summary statistics are given for each group of animals and the medians of the combined results from experiments 1 and 2 are plotted to indicate any expression trends. NA, not assessed.

	Treatment Groups								
	UIC	7DPI	14DPI	21DPI	28DPI	7DPD	14DPD	7DPDD	14DPDD
	Experiment 1								
Median	0.50	0.00	1.00	0.75	2.50	1.00	0.00	1.25	1.00
Upper quartile	0.50	0.50	2.00	1.25	3.00	2.00	0.625	1.875	1.00
Lower quartile	0.375	0.00	0.00	0.00	0.875	0.875	0.00	1.00	1.00
Maximum	0.50	0.50	3.00	2.00	3.00	2.00	1.00	2.00	1.00
Minimum	0.00	0.00	0.00	0.00	0.50	0.50	0.00	1.00	1.00
Number	6	6	6	6	6	6	6	4	3
	Experiment 2								
Median	1.00	2.25	1.75	3.5	3.25	3.5	NA	3.75	NA
Upper quartile	1.50	3.125	2.625	4.00	3.50	3.50	NA	4.00	NA
Lower quartile	1.00	2.00	1.25	3.375	2.50	3.375	NA	3.50	NA
Maximum	1.50	3.50	3.00	4.00	3.50	3.50	NA	4.00	NA
Minimum	1.00	2.00	0.50	3.00	2.50	3.00	NA	3.50	NA
Number	6	6	6	6	6	6	NA	4	NA
	Experiments 1&2								
Median	0.75	1.25	1.25	2.50	3.00	2.50	0.00	2.75	1.00
Upper quartile	1.00	2.375	2.00	3.50	3.375	3.50	0.625	3.875	1.00
Lower quartile	0.50	0.00	0.50	0.625	2.125	1.00	0.00	1.125	1.00
Maximum	1.50	3.50	3.00	4.00	3.50	3.50	1.00	4.00	1.00
Minimum	0.00	0.00	0.00	0.00	0.50	0.50	0.00	1.00	1.00
Number	12	12	12	12	12	12	6	8	3

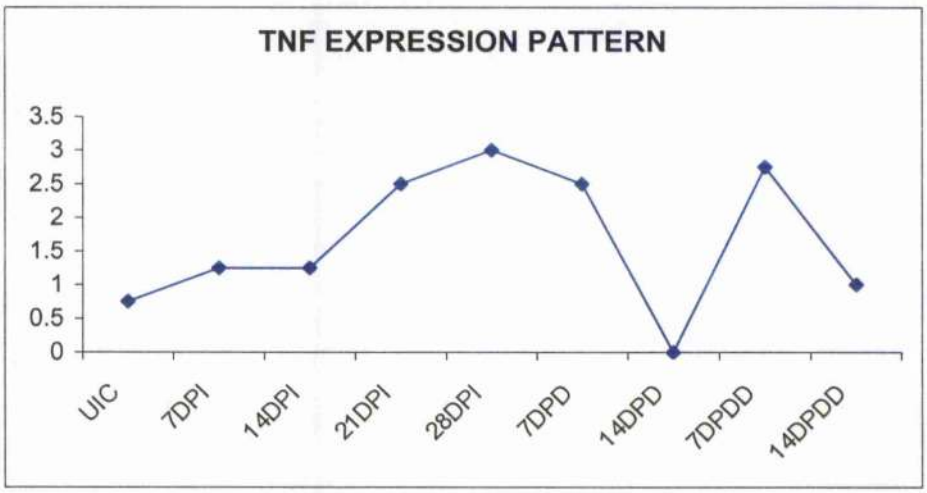

Figure 4.12. Summary statistics for TNF-α

The expression level of TNF-α in mouse brain was assessed at various time points following trypanosome infection (7DPI, 7 days post-infection; 14DPI, 14 days post-infection; 21 DPI, 21 days post-infection, 28DPI, 28 days post-infection) and subcurative drug treatments (7DPD, 7days post-diminazene aceturate; 14DPD, 14 days post-diminazene aceturate; 7DPDD, 7 days post-second diminazene aceturate; 14 DPDD, 14 days post-second diminazene aceturate). Samples from uninfected control (UIC) mice were also assessed. Following RT-PCR analyses the intensity of the resulting PCR band, as seen on a 2% agarose gel stained with ethidium bromide, was taken as an indication of the quantity of TNF-α mRNA present in the initial sample. The intensity of staining was graded on a scale of 0 to 4, where 0 indicated no band and 4 indicated an extremely intense PCR band. Summary statistics are given for each group of animals and the medians of the combined results from experiments 1 and 2 are plotted to indicate any expression trends. NA, not assessed.

	Treatment Groups								
	UIC	7DPI	14DPI	21DPI	28DPI	7DPD	14DPD	7DPDD	14DPDD
	Experiment 1								
Median	0.50	1.50	2.00	2.50	2.25	2.50	2.75	2.75	1.75
Upper quartile	1.00	2.00	2.00	3.00	*	3.00	*	*	*
Lower quartile	0.00	1.00	2.00	2.50	*	2.00	*	*	*
Maximum	1.00	2.00	2.00	3.00	3.00	3.00	3.00	3.00	2.00
Minimum	0.00	1.00	2.00	2.50	1.50	2.00	2.50	2.50	1.50
Number	5	3	3	3	2	3	2	2	2
	Experiment 2								
Median	0.75	2.50	1.25	2.00	2.25	2.75	NA	3.00	NA
Upper quartile	1.00	3.00	2.625	3.50	3.50	3.00	NA	3.00	NA
Lower quartile	0.438	1.875	1.00	0.75	1.50	2.25	NA	3.00	NA
Maximum	1.00	3.00	3.00	3.50	3.50	3.00	NA	3.00	NA
Minimum	0.25	1.50	1.00	0.00	1.50	1.50	NA	3.00	NA
Number	6	6	6	6	6	6	NA	4	NA
	Experiments 1&2								
Median	0.50	2.00	2.00	2.50	2.25	2.50	2.75	3.00	1.75
Upper quartile	1.00	2.75	2.25	3.25	3.375	3.00	*	3.00	*
Lower quartile	0.25	1.50	1.00	1.25	1.50	2.25	*	2.872	*
Maximum	1.00	3.00	3.00	3.50	3.50	3.00	3.00	3.00	2.00
Minimum	0.00	1.00	1.00	0.00	1.50	1.50	2.50	2.50	1.50
Number	11	9	9	9	8	9	2	6	2

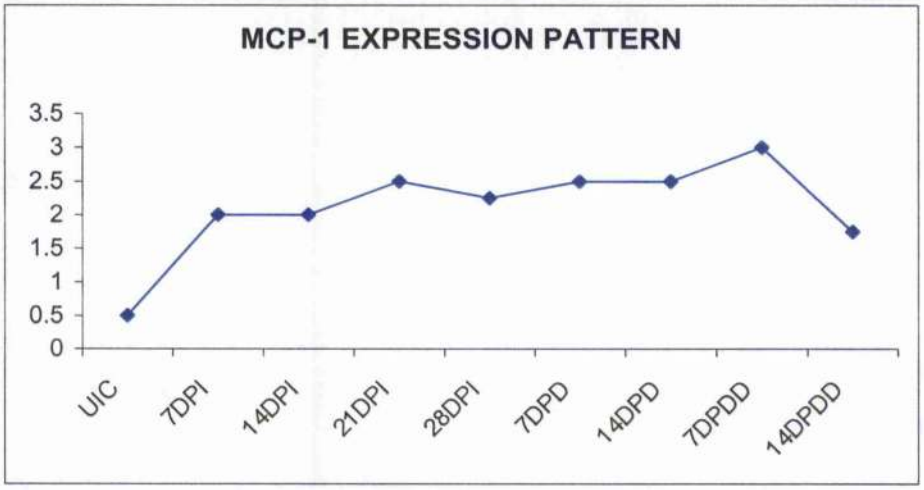

Figure 4.13. Summary statistics for MCP-1

The expression level of MCP-1 in mouse brain was assessed at various time points following trypanosome infection (7DPI, 7 days post-infection; 14DPI, 14 days post-infection; 21 DPI, 21 days post-infection, 28DPI, 28 days post-infection) and subcurative drug treatments (7DPD, 7days post-diminazene aceturate; 14DPD, 14 days post-diminazene aceturate; 7DPDD, 7 days post-second diminazene aceturate; 14 DPDD, 14 days post-second diminazene aceturate). Samples from uninfected control (UIC) mice were also assessed. Following RT-PCR analyses the intensity of the resulting PCR band, as seen on a 2% agarose gel stained with ethidium bromide, was taken as an indication of the quantity of MCP-1 mRNA present in the initial sample. The intensity of staining was graded on a scale of 0 to 4, where 0 indicated no band and 4 indicated an extremely intense PCR band. Summary statistics are given for each group of animals and the medians of the combined results from experiments 1 and 2 are plotted to indicate any expression trends. NA, not assessed; * too few data points.

	Treatment Groups								
	UIC	7DPI	14DPI	21DPI	28DPI	7DPD	14DPD	7DPDD	14DPDD
					Experiment 1				
Median	1.00	2.00	1.50	1.50	2.00	1.50	2.00	2.25	1.50
Upper quartile	1.50	2.00	2.00	2.00	*	1.50	3.00	*	*
Lower quartile	0.00	2.00	1.50	1.50	*	1.00	1.50	*	*
Maximum	1.50	2.00	2.00	2.00	2.00	1.50	3.00	3.00	2.00
Minimum	0.00	2.00	1.50	1.50	2.00	1.00	1.50	1.50	1.00
Number	5	3	3	3	2	3	3	2	2
					Experiment 2				
Median	1.50	3.00	3.00	3.00	3.50	3.250	NA	3.50	NA
Upper quartile	2.00	3.125	3.00	3.00	3.50	3.50	NA	3.50	NA
Lower quartile	1.375	2.375	2.50	2.875	3.375	3.00	NA	3.50	NA
Maximum	2.00	3.50	3.00	3.00	3.50	3.50	NA	3.50	NA
Minimum	3.50	1.00	2.00	2.50	2.50	3.00	NA	3.00	NA
Number	6	6	6	6	6	6	NA	4	NA
					Experiments 1&2				
Median	1.50	2.50	2.50	3.00	3.50	3.00	2.00	3.50	1.50
Upper quartile	1.50	3.00	3.00	3.00	3.50	3.50	3.00	3.50	*
Lower quartile	1.00	2.00	1.75	1.75	2.25	1.50	1.50	2.625	*
Maximum	2.00	3.50	3.00	3.00	3.50	3.50	3.00	3.50	2.00
Minimum	0.00	2.00	1.50	1.50	2.00	1.00	1.50	1.50	1.00
Number	11	9	9	9	8	9	3	6	2

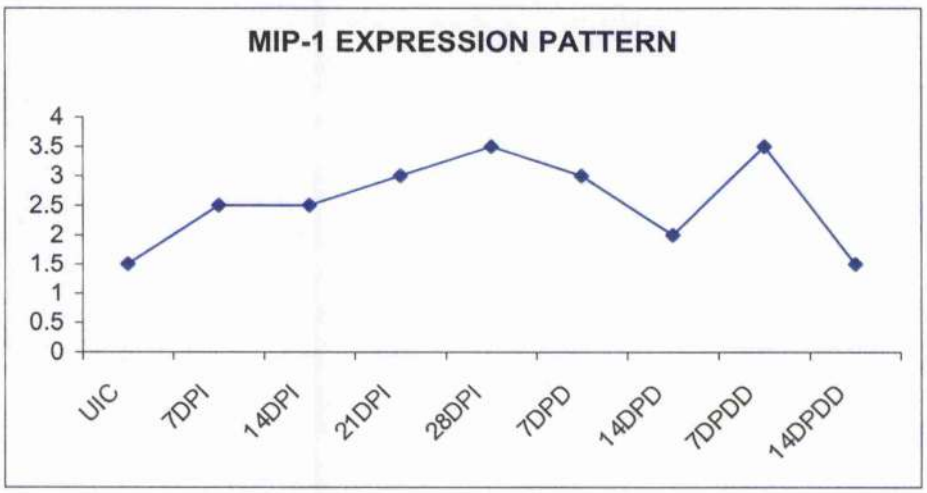

Figure 4.14. Summary statistics for MIP-1α

The expression level of MIP-1α in mouse brain was assessed at various time points following trypanosome infection (7DPI, 7 days post-infection; 14DPI, 14 days post-infection; 21 DPI, 21 days post-infection, 28DPI, 28 days post-infection) and subcurative drug treatments (7DPD, 7days post-diminazene aceturate; 14DPD, 14 days post-diminazene aceturate; 7DPDD, 7 days post-second diminazene aceturate; 14 DPDD, 14 days post-second diminazene aceturate). Samples from uninfected control (UIC) mice were also assessed. Following RT-PCR analyses the intensity of the resulting PCR band, as seen on a 2% agarose gel stained with ethidium bromide, was taken as an indication of the quantity of MIP-1α mRNA present in the initial sample. The intensity of staining was graded on a scale of 0 to 4, where 0 indicated no band and 4 indicated an extremely intense PCR band. Summary statistics are given for each group of animals and the medians of the combined results from experiments 1 and 2 are plotted to indicate any expression trends. NA, not assessed; * too few data points.

	Treatment Groups								
	UIC	7DPI	14DPI	21DPI	28DPI	7DPD	14DPD	7DPDD	14DPDD
	Experiment 1								
Median	1.00	1.50	2.50	3.00	2.75	2.00	2.50	2.50	2.75
Upper quartile	2.00	3.00	3.00	3.00	*	3.00	3.00	*	*
Lower quartile	0.75	1.50	2.50	2.50	*	1.50	2.00	*	*
Maximum	3.00	3.00	3.00	3.00	3.00	3.00	3.00	3.00	3.00
Minimum	0.50	1.50	2.50	2.50	2.50	1.50	2.00	2.00	2.50
Number	5	3	3	3	2	3	3	2	2
	Experiment 2								
Median	1.50	3.00	3.50	3.00	3.25	4.00	NA	4.00	NA
Upper quartile	2.00	3.00	3.50	3.00	3.50	4.00	NA	4.00	NA
Lower quartile	1.50	3.00	3.00	3.00	3.00	4.00	NA	4.00	NA
Maximum	2.00	3.00	3.50	3.00	3.50	4.00	NA	4.00	NA
Minimum	1.50	3.00	3.00	3.00	3.00	4.00	NA	4.00	NA
Number	6	6	6	6	6	6	NA	4	NA
	Experiments 1&2								
Median	1.50	3.00	3.00	3.00	3.00	4.00	2.50	4.00	2.75
Upper quartile	2.00	3.00	3.50	3.00	3.50	4.00	3.00	4.00	*
Lower quartile	1.00	2.25	2.75	3.00	3.00	2.50	2.00	2.75	*
Maximum	3.00	3.00	3.50	3.00	3.50	4.00	3.00	4.00	3.00
Minimum	0.50	1.50	2.50	2.50	2.50	1.50	2.00	2.00	2.50
Number	11	9	9	9	8	9	3	6	2

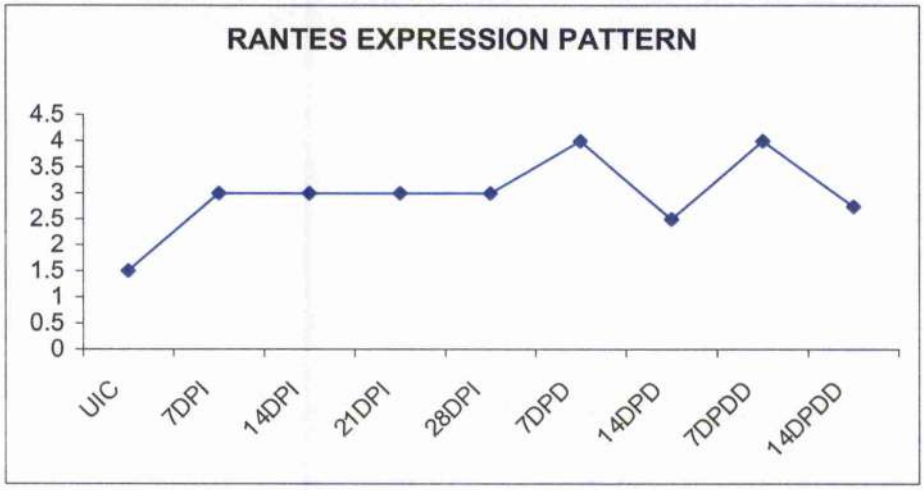

Figure 4.15. Summary statistics for RANTES

The expression level of RANTES in mouse brain was assessed at various time points following trypanosome infection (7DPI, 7 days post-infection; 14DPI, 14 days post-infection; 21 DPI, 21 days post-infection, 28DPI, 28 days post-infection) and subcurative drug treatments (7DPD, 7days post-diminazene aceturate; 14DPD, 14 days post-diminazene aceturate; 7DPDD, 7 days post-second diminazene aceturate; 14 DPDD, 14 days post-second diminazene aceturate). Samples from uninfected control (UIC) mice were also assessed. Following RT-PCR analyses the intensity of the resulting PCR band, as seen on a 2% agarose gel stained with ethidium bromide, was taken as an indication of the quantity of RANTES mRNA present in the initial sample. The intensity of staining was graded on a scale of 0 to 4, where 0 indicated no band and 4 indicated an extremely intense PCR band. Summary statistics are given for each group of animals and the medians of the combined results from experiments 1 and 2 are plotted to indicate any expression trends. NA, not assessed; * too few data points.

4.4. Discussion

The investigations performed in the present study clearly demonstrate variations in the expression levels of the inflammatory mediators IL-1α, IL-6, TNF-α, MCP-1, MIP-1α and RANTES within the CNS following trypanosome infection and during the development of the associated neuroinflammatory reaction. Initially following infection elevated levels of transcription of IL-6, TNF-α, MCP-1, MIP-1α and RANTES were detected and the expression of these mediators, with the exception of RANTES, continued to rise as the infection progressed. IL-1α transcription was found at a reduced level compared to uninfected mice immediately following infection although this did increase as the infection progressed. On exacerbation of the CNS inflammatory reaction by the administration of a single diminazene aceturate treatment, a more varied cytokine and chemokine response was found. Levels of IL-1α, IL-6, TNF-α and MIP-1α dropped following diminazene aceturate treatment while MCP-1 remained relatively stable. This trend was continued in animals killed 14 days following administration of the diminazene aceturate. RANTES expression increased following drug treatment and remained at this level in animals killed at the later time-point. Subsequent to the induction of a severe meningoencephalitis, by treatment of the relapsed mice with a second dose of diminazene aceturate, a mixed response in the transcription of the cytokines and chemokines was again seen. In this scenario IL-1α, IL-6, TNF-α, MCP-1 and MIP-1α all showed an increase in their transcription levels while RANTES expression was reduced. IL-1α and IL-6 transcription continued to increase in animals killed 14 days after being given the second diminazene aceturate treatment but levels of TNF-α, MCP-1 and MIP-1α fell at this stage. In contrast, RANTES transcription was reduced immediately following the second diminazene aceturate treatment and was increased in animals killed at the 14-day post-treatment time-point.

In the mouse model of human African trypanosomiasis (HAT) used in this study, the parasites become established within the CNS between day 14 and day 21 post-infection (Jennings *et al.*, 1979). Only the beginnings of an extremely mild CNS inflammatory response can be detected on histological examination of brain sections prepared from animals killed during the acute stage of the infection (Chapter 3). Despite the lack of overt neuropathological changes, an elevated level of transcription, compared to that found in uninfected animals, was detected for all of the cytokines and chemokines assessed with the exception of IL-1α. The early induction of chemokine expression within the CNS has

been described following trypanosome infection in rats (Sharafeldin *et al.*, 2000). In this study increased expression of MIP-1α and RANTES was detected 6 hours after infection and MCP-1 expression was upregulated by 12 hours after infection. Since parasites have not become established within the CNS at this point they cannot be directly responsible for the initiation of the inflammatory response. The presence of chemotactic molecules such as, MCP-1, MIP-1α and RANTES, which attract lymphocytes and monocytes, could account for the early infiltration of the brain by inflammatory cells seen on day 14 post-infection.

The peripheral levels of the cytokines and chemokines were not assessed in this investigation. However, raised levels of IL-1α, IL-6 and TNF-α have been detected in the liver of mice 7 days after infection with *T.b.brucei* GVR35/ C1.3 in a previous study utilising this model of HAT (Eckersall *et al.*, 2001). A rapid increase in the serum TNF-α levels has also been described in mice following the injection of *T.b.brucei* soluble extracts (Magez *et al.*, 1993). This elevation in serum TNF-α was detected within 72 hours of administering the injection. It is possible that in this investigation the initial induction of the expression of these pro-inflammatory molecules within the CNS, found at day 7 and 14 post-infection, was indirectly triggered by increased levels of the cytokines and chemokines in the blood and peripheral tissues due to the presence of the parasites. This enhanced expression of cytokines within the CNS is known to occur during infections that do not necessarily directly affect the brain tissue resulting in the initiation of sickness behaviour (Konsman *et al.*, 2002). Resident brain cells including, astrocytes, microglia and neurons as well as the endothelial cells of the BBB can produce these cytokines (Fitzgerald *et al.*, 2001). However, the early signs of astrocyte activation found in sections prepared from mice 14 days after infection (Chapter 3) implicate these cells as the likely source of the cytokines. A correlation between astrocyte activation and the production of cytokines has been suggested previously (Hunter *et al.*, 1992a). In this study the expression of IL-1α, TNF-α, MIP-1α, IL-6 and IFN-γ was investigated in the brains of mice infected with *T.b.brucei*. IL-1α was constitutively expressed in the brains of all mice but in contrast to the findings of the present study, expression of the remaining cytokines was not detected until day 21 post-infection. The discrepancy between these results could be due to the differences in the methodology adopted to perform the RT-PCR. In Hunter's paper new cDNA was synthesised for each cytokine investigated using the 3'-primer as the starting sequence for the reverse transcriptase enzyme. This may lead to variations in the quality of the cDNA generated for the individual molecules and alter the sensitivity of the subsequent PCR assay. In the current investigation random primers were employed to

synthesise a complete pool of cDNA that could be used in each of the individual PCR assays. This would eliminate variation due to the presence of low levels of target mRNA in the original sample and those caused by differences in the quality of the resulting cDNA due to primer disparity.

The passage of IL-1α, IL-6, TNF-α and MIP-1β through the BBB has been described (Pan and Kastin, 1999). Therefore, it is feasible that these inflammatory agents could be transported into the brain tissue and directly stimulate local expression within the CNS. In addition, cytokine molecules are known to mediate their own production and that of MCP-1, MIP-1α and RANTES. Consequently, their presence within the CNS could initiate the rise in chemokine synthesis detected during the acute stage of trypanosome infection. A rise in cytokine levels within the CNS, as a result of transport across the BBB, would not be detected using the methodology employed in this study as the levels of specific mRNA transcripts and not the protein end products were assessed.

The general levels of cytokine and chemokine expression within the CNS remained largely constant following trypanosome infection until day 21 post-infection when the expression of IL-1α, IL-6, TNF-α, MCP-1, and MIP-1α began to increase. This rise in cytokine and chemokine transcription coincides with the invasion of the CNS by the parasites and is associated with an increased neuroinflammatory reaction akin to the early CNS-stage seen in human infections. A further rise in the expression levels of IL-1α, IL-6, TNF-α and MIP-1α was seen when the inflammatory reaction was allowed to progress until day 28 post-infection while MCP-1 expression dropped slightly. RANTES transcription remained at a constant level, higher than that found in uninfected mice, following trypanosome infection and throughout the development of the early CNS response. The elevated expression levels of the cytokines and chemokines were accompanied by a further augmentation of the CNS-inflammatory response (Chapter 3).

The administration of a single dose of diminazene aceturate, to exacerbate the neuroinflammatory reaction and mirror the pathology found during the late-CNS stage of HAT, resulted in a more varied cytokine and chemokine response. The levels of IL-1α, IL-6, TNF-α and MIP-1α were reduced compared to those seen at 28 days post-infection and continued to fall in mice killed at 14 days following the drug treatment. In contrast, transcription of MCP-1 remained similar to that found at 28 days post-infection and increased slightly in animals killed at 14 days post diminazene aceturate administration. RANTES expression increased in animals killed 7 days after diminazene aceturate

treatment and remained at the same level in mice killed at 14 days following administration of the drug. The drop in the transcription of IL-1α and IL-6 seen within the CNS following diminazene aceturate treatment of trypanosome-infected mice has been reported previously in a study investigating the expression of IL-6, IL-1α and TNF-α in the liver and CNS and comparing this expression pattern with the levels of the acute phase proteins haptoglobin and serum amyloid A in the serum (Eckersall *et al.*, 2001).

The findings from both studies are enigmatic and do not immediately correlate with the increased CNS inflammation that is associated with this diminazene aceturate treatment regimen. If the levels of these inflammatory agents within the CNS are being controlled by the presence of factors in the periphery, it is possible that, due to the clearance of the trypanosomes following the diminazene aceturate treatment, the inflammatory reaction out-with the CNS could be down regulated resulting in a reduction in the production of a number of cytokines and chemokines within the CNS. However, the persistent presence of the trypanosomes within the brain may stimulate the increased expression of RANTES and MCP-1 while maintaining the lowered degree of expression of the other mediators. The presence of these cytokines and chemokines could induce the continued migration of already activated inflammatory cells into the CNS from the periphery resulting in the augmentation of the neuroinflammatory reaction seen at this stage of the infection.

The situation found in mice following the induction of the severe post-treatment reactive meningoencephalopathy (PTRE) was complex and did not mimic the pattern seen during the late-stage of the CNS infection. Treatment of trypanosome infected mice with a second dose of diminazene aceturate resulted in an up-regulation of the transcription of IL-1α, IL-6, TNF-α, MCP-1 and MIP-1α, 7 days following administration of the drug. At this point the expression of RANTES was reduced compared to that found in mice killed after a single diminazene aceturate treatment. This pattern of cytokine and chemokine expression was not maintained in animals killed at 14 days after administration of the diminazene aceturate. In these animals IL-1α and IL-6 levels continued to rise while a reduction in the levels of TNF-α, MCP-1 and MIP-1α, and an increase in the expression of RANTES, was detected. The initial rise in chemokine expression detected following a second diminazene aceturate treatment may be responsible for the increase in the level of inflammatory cell infiltration associated with this treatment regimen. Numerous B-cells and plasma cells are found in the inflammatory infiltrate at this time. MIP-1α has been shown to be a B-cell chemoattractant (Schall, Bacon, Camp, Kaspari *et al.*, 1993) and IL-6 plays a key role in the differentiation of B-cells into antibody secreting plasma cells

(Hirano, 1998). Although the PTRE is characterised by an extremely severe meningoencephalitis, it has been shown that very little neuronal damage occurs (Fink and Schmidt, 1979; Morrison *et al.*, 1983). Since there is evidence that both IL-1 and IL-6 can fulfil a neuro-protective role in CNS inflammatory reactions (Hirano, 1998; Lenzlinger *et al.*, 2001; Stoll *et al.*, 2000), this sparing of the neuronal elements could be the result the continued increase in expression of these cytokines seen in animals killed at the later time-point.

The presence of cytokines and chemokines within the CNS has been implicated in the pathogenesis of a range of CNS disorders with a variety of aetiologies. Early cytokine and chemokine expression has been detected in experimental autoimmune encephalomyelitis (EAE), the animal model of multiple sclerosis (MS), where distinct patterns of expression have been associated with each phase of the disease. The acute stage of EAE is associated with increased expression of mRNA for a number of pro-inflammatory cytokines, including IL-1α and IL-6. Levels of IL-6 mRNA were found to decrease when the clinical disease stabilised and the animals moved into the recovery or chronic stage of EAE but levels of IL-1α expression remained elevated (Eng, Ghirnikar, and Lee, 1996). In contrast to these findings, investigation of IL-6 expression using immunocytochemistry and *in situ* hybridisation demonstrated only low levels of IL-6 during the acute stage of the disease and found higher levels of the cytokine in the protracted relapsing phase of the condition (Diab, Zhu, Xiao, Mustafa *et al.*, 1997).

The temporal demarcation of specific roles for particular inflammatory mediators is perhaps most clearly demonstrated in the pattern of chemokine expression associated with the various stages in EAE progression. The expression of MCP-1, MIP-1α and RANTES mRNA has been detected in the spinal cord in murine EAE before the onset of clinical symptoms and remains elevated throughout the clinical course of the acute disease (Godiska *et al.*, 1995; Martiney *et al.*, 1998). Treatment of the animals with anti-MIP-1α, but not anti-MCP-1 antibodies, prevented the onset of acute clinical EAE (Karpus and Ransohoff, 1998). The converse of this situation was seen in the treatment of relapsing EAE where administration of anti-MCP-1 antibodies, but not anti-MIP-1α decreased the clinical severity of the response (Kennedy, Strieter, Kunkel, Lukacs *et al.*, 1998). These findings strongly suggest that MIP-1α plays a key role in the initiation of the acute stage of EAE while MCP-1 mediates the relapsing stage of the disease. Administration of anti-RANTES antibodies did not appear to effect the progression of the clinical disease irrespective of the timing of the treatment. The cytokine TNF-α appears to be involved in

the pathogenesis of EAE during the chronic stage of the disease. Administration of TNF-α augments EAE in rats by prolonging the condition and inducing relapses. The detrimental effects of TNF-α in chronic EAE have been confirmed in studies that demonstrated a prevention or amelioration of the condition following blockade of the TNFR1 receptor (Klinkert, Kojima, Lesslauer, Rinner *et al.*, 1997)

Another well recognised CNS disease of non-infectious origin is Alzheimer's disease. The most commonly described features associated with the condition are the presence of reactive astrocytes and microglia, the extracellular deposition of β-amyloid protein forming senile plaques, neurofilbrillary tangles and neuronal cell death (Hull, Lieb, and Fiebich, 2002). In a transgenic murine model of Alzheimer's disease, in which the animals express human β-amyloid precursor protein, elevated levels of the pro-inflammatory molecules; IL-1α, IL-6, TNF-α and MCP-1 have been detected in astrocytes and microglia in close proximity to senile plaques. Sub-populations of reactive astrocytes have also been shown to express TGF-β and IL-10 indicating that both pro and anti-inflammatory pathways are activated in this disease (Apelt and Schliebs, 2001; Sly, Krzesicki, Brashler, Buhl *et al.*, 2001).

Cytokine and chemokine expression has also been demonstrated in CNS inflammatory diseases resulting from viral infections. Subacute sclerosing panencephalitis is a fatal form of encephalitis, caused by defective measles virus replication in the neurons and glial cells, which results in diffuse pathological changes within the CNS. Cytokines including TNF-α, IL-1β, IL-6, TNF-β and IFN-γ have been found associated with the mononuclear cells infiltrating the brain in sections prepared from patients that have died from the condition (Nagano, Nakamura, Yoshioka, Onodera *et al.*, 1994). Lymphocytic choriomeningitis virus (LCMV)-infection is a fatal disease characterised by the infiltration of the meninges, choroid plexus and ependymal membranes by lymphocytes and macrophages. Increased levels of TNF-α, IL-1α, IL-1β and IL-6 mRNA were detected in the brains of mice inoculated with this virus early after infection. Mice infected in this manner develop convulsive seizures 6-8 days after infection that culminate in death. The expression of these molecules increased as the disease progressed. High levels of INF-γ expression were found late in the infection and correlated with the onset of clinical disease (Campbell, Hobbs, Kemper, and Oldstone, 1994). The expression of several chemokines has also been demonstrated in the CNS during the course of LCMV-infection. mRNA transcripts for IP-10, RANTES, MCP-1, MCP-3 and MIP-1β were detected 3 days after the infection, this was followed by late the appearance of MIP-1α on day 6 post-infection (Asensio and

Campbell, 1997). Perhaps the most topical of viral diseases that results in CNS involvement is HIV. The most severe manifestation of HIV-infection is the development of HIV-associated dementia (HAD) or AIDS dementia complex (ADC). This is characterised by the presence of microglial nodules, multinucleated giant cells and diffuse astrocytic and microglial activation (Zhao, Kim, Morgello, and Lee, 2001) Perivascular cuffing is present with macrophages and T-lymphocytes comprising the majority of the cells in the infiltrate. The occasional B-cell is also found among the inflammatory cells (Tyor, Glass, Griffin, Becker *et al.*, 1992). Increased IL-1, TNF-α, IL-6 expression (Tyor *et al.*, 1992) and elevated levels of MIP-1α, MIP-1β, MCP-1 and RANTES (Rausch and Davis, 2001) have been detected in brain samples from autopsy tissue taken from the HIV patients.

Malaria results from infection with the protozoan parasites of *Plasmodium spp.* A severe complication of *Plasmodium falciparum* infection is the development of cerebral malaria. The condition is characterised by congestion of the cerebral microvessels with parasitized red blood cells leading to haemorrhage and oedema. The degree of inflammatory cell infiltration of the brain in this condition is inconsistent although T-lymphocytes and macrophages have been identified. Several cytokines have been detected in brain tissue generated from the murine model of cerebral malaria including the expression of TNF-α and IL-1β. It is interesting to note that IL-6 was not detected in the CNS of these infected mice (Medana *et al.*, 2001). *Toxoplasma gondii* is another protozoan parasite that can infect humans. Under normal circumstances the infection is controlled by the host's immune system and results in an asymptomatic infection. Once infected with *T.gondii* the parasite forms latent cysts within the CNS of the host that persist through the life-time of the animal. These cysts provoke little or no inflammatory response within the CNS. However, in patients with a compromised immune system these cysts can reactivate resulting in a neuroinflammatory reaction and the development of toxoplasmic encephalitis. Due to the increasing numbers of patients with immunodeficiency diseases such as AIDS, and those receiving immunosuppressive therapies, the incidence of toxoplasmic encephalitis is becoming more common. In a mouse model of toxoplasmic encephalits mRNA transcripts for IL-1α, IL-1β, IL-6, TNF-α and MIP-1α were detected within the CNS following infection with the parasite (Hunter, Roberts, Murray, and Alexander, 1992b). These cytokines have been implicated in the development of the neuropathological reaction seen in toxoplasmic encephalitis (Hunter and Remington, 1994; Hunter *et al.*, 1992b).

It is interesting to note, from the information detailed above, that the specific cytokines and chemokines investigated in the present study have been shown to play a role in the pathogenesis of many CNS conditions with varied aetiologies. It would appear that the neuropathogenesis of the CNS inflammatory reaction found in the acute stage of trypanosome-infection is also mediated by the presence of pro-inflammatory cytokines and chemokines including, IL-1α, IL-6, TNF-α, MCP-1, MIP-1α and RANTES. During the acute stage of the infection the factor instigating the increase in expression of these inflammatory mediators remains unclear as this could be the end result of a range of initiating pathways that may act independently, or in a concerted manner, to stimulate the production of the cytokines and chemokines within the CNS. The patterns of expression found in the later stages of the CNS inflammation are more difficult to interpret. It is important to remember that cytokines and chemokines rarely act as individual entities and they often act in either a synergistic or an inhibitory manner. Within the CNS this situation becomes more complex as these mediators often have dual roles acting as both inflammatory mediators and regulators of normal physiological functions. In addition, as the neuroinflammatory process develops it is possible that the integrity of the BBB becomes compromised allowing components normally confined to the peripheral system to enter the CNS and further exacerbate the inflammatory reaction (Philip *et al.*, 1994). However, this breakdown of the BBB has not been unequivocally confirmed following trypanosome infection since no damage to the BBB was detected in a rat model of chronic *T.b.brucei*-infection (Mulenga *et al.*, 2001).

It is important to consider that the approach used in the present investigation detects the mRNA transcription products that will ultimately produce the final cytokine and chemokine molecules. The presence of these transcripts does not necessarily indicate that the proteins will be manufacture. This would also have been true of any information gained from *in-situ* RT-PCR (IS-RT-PCR) or *in situ* hybridisation staining of these murine brain sections although additional data indicating the cellular source of the mRNA molecules would have been available. Failure to detect the mRNA in the tissue sections was most likely due to the degradation or loss of the transcripts at some point during the either the processing of the tissue for section preparation or the performance of the lengthy staining procedures.

It is unfortunate that the immunocytochemistry (ICC) technique used in this investigation failed to provide positive staining profiles. Although a variety of different primary antibodies were employed, together with alterations in the ICC protocol, no staining of cytokines was achieved in the tissue sections. Many reasons exist for the inability to detect

cytokines using this method. Alteration to the conformation of the cytokine by the fixation techniques employed leading to changes in the antigenic site recognised by the antibody would prevent the molecule from being detected by the antibody. If cytokines are rapidly excreted from the cell following synthesis then they could easily be lost from the tissue during the processing and staining procedures. Therefore, failure to detect these molecules is not uncommon and cytokine staining using ICC procedures has been described as "somewhat of an art" (Whiteside, 2002).

Changes in ICC staining patterns may have indicated whether the upregulation in cytokine and chemokine transcription correlated with an increase in the detection of the protein end products. This coupled with the cellular source of the transcripts would have provided a strong indication of the cell types involved in mediating the development of the CNS inflammatory response seen following trypanosome infection and subcurative drug treatment. Although we can deduce that cytokines and chemokines play a role in mediating the neuroinflammation the actual function of the individual molecules within the brain cannot be determined from the findings gained from the present study. This information could only be ascertained by neutralising the individual molecules either through the use of specific antibodies or gene knockout mice. This approach would present its own series of problems. The use of neutralising antibodies or knockout mice may result in the removal of the mediators from the peripheral system as well as the CNS. This would not help to elucidate the role of centrally synthesised cytokines and chemokines in the control of the reaction. Furthermore, in antibody neutralising experiments the efficacy of the technique in removing the inflammatory mediators from the CNS would be questionable since the ability of the antibody to penetrate the BBB would be difficult to establish. The pleiotropic nature of the cytokine and chemokine network allows many different pathways to reach the same end result and therefore a great deal of redundancy is built into the system. This type of structure would be difficult to study using traditional knockout mice as these animals could circumvent the lack of a single cytokine by upregulation or synthesis of an alternative mediator. We have previously encountered this phenomenon in the use of knockout mice (Chapter 6) (Kennedy, Rodgers, Bradley, Hunt *et al.*, 2003).

Without information detailing the specific roles of the individual inflammatory mediators it would be difficult to determine the feasibility of cytokine or chemokine therapy as a novel treatment to reduce or prevent the onset of the CNS inflammation associated with trypanosome-infection and subcurative drug treatment. If cytokines such as IL-1 and IL-6 are acting in a neuro-protective manner in the late-stage of this disease, then their removal

may not only reduce the level of inflammatory cell infiltration, but also, ultimately, increase the amount of neuronal damage resulting from the inflammatory response. This paradoxical effect of lowered inflammation and increased neuronal damage has previously been encountered in the treatment of trypanosome-induced neuroinflammation following the administration of aspirin in a rat model of the disease (Quan, Mhlanga, Whiteside, Kristensson *et al.*, 2000). Further research to dissect the functions of these mediators in this condition is therefore required before novel chemotherapeutic approaches involving the manipulation of cytokine levels can be perused.

CHAPTER 5

THE ACTION OF EFLORNITHINE IN TRYPANOSOME-INDUCED CNS INFLAMMATION

5.1. Introduction

Eflornithine, otherwise known as DL-α-difluoromethylornithine or DFMO, was originally developed in the 1970's, by Merrell Dow Pharmaceuticals, as a potential anti-cancer agent and is the most recently licensed drug in the battle against CNS-stage human African trypanosomiasis. The potential application of this drug in the treatment of trypanosome-infections was indicated by the dramatic results of efficacy studies using eflornithine treatment in a murine model of the disease (Bacchi, Nathan, Hutner, McCann *et al.*, 1980) and clinical trials soon followed. In this introduction the existing knowledge with regard to the mechanism of action of eflornithine, its efficacy as an anti-cancer drug and its use in CNS inflammatory conditions will are considered. In addition, the story of the rise and fall of eflornithine in the chemotherapy of human African trypanosomiasis, since its initial application in the treatment of this disease, will be outlined.

5.1.1. Polyamines and eflornithine

Polyamines such as putrescine, spermidine and spermine are organic poly-cations that play important roles in many cellular functions, including, maintenance, proliferation, differentiation, neoplastic transformation, apoptosis and anti-angiogenesis (Zou, Vlastos, Yang, Wang *et al.*, 2002). The mechanisms used by the polyamines to fulfil these roles remain unclear. It is known that they associate with nucleic acids, cause conformational changes in DNA and interact with proteins and cellular organelles (Zou *et al.*, 2002). Inhibition of ornithine decarboxylase (ODC), the enzyme that performs the rate-limiting step in the polyamine biosynthesis pathway, rapidly depletes cells of these compounds. Cells that have become depleted of polyamines proliferate extremely slowly. However, if an exogenous source of polyamine is provided this growth inhibition is quickly reversed and the cells return to their normal growth-rates. The requirement of dividing cells for polyamines has been exploited in the search for novel anti-cancer drugs and has led to the development of compounds that specifically inhibit ODC. One compound arising from this research was eflornithine.

5.1.2. Eflornithine as an anti-cancer agent

In many tumours and rapidly dividing cells, ODC expression is known to be upregulated. Eflornithine is a highly specific, irreversible inhibitor of ODC and as such prevents the *de*

novo synthesis of polyamines thereby reducing or preventing cellular proliferation. Eflornithine has been shown to possess anti-tumour and anti-metastatic qualities in the treatment of several types of carcinoma development. Many cases of colonic neoplasms are associated with an increased polyamine content in the affected mucosa compared with normal mucosa. In patients with a history of colonic adenoma, treatment with low doses, 0.20-0.40gm/m^2, of orally administered eflornithine resulted in a decrease in the polyamine content in the mucosa (Gwyn and Sinicrope, 2002). Eflornithine has also been employed in a topical form in a randomised placebo-controlled study investigating the progression of actinic keratoses, the pre-malignant precursor cells, of squamous cell carcinoma in skin biopsy specimens (Einspahr, Nelson, Saboda, Warneke *et al.*, 2002). In this study application of eflornithine significantly reduced the numbers of these precursors and lowered the polyamine content. An increase in the expression of ODC has also been suggested as an independent adverse prognostic factor in the overall survival of human breast cancer (Manni, Washington, Griffith, Verderame *et al.*, 2002). In an *in vivo* murine study, administration of 2% eflornithine in the animals' drinking water reduced the growth rate of highly aggressive implanted human breast cancer cell lines and resulted in a significant reduction in the occurrence of lung metastasis in these mice (Manni *et al.*, 2002).

Unfortunately early trials of eflornithine, using oral doses of 10g or more per day were often associated with a host of adverse side effects including, diarrhoea, nausea, emesis, abdominal pain and anorexia. Occasionally bilateral hearing impairment and thrombocytopenia were encountered. These reactions were generally reversible on cessation of the drug treatment. In addition the eflornithine treatment commonly did not produce the anti-tumour response that was hoped for (Schechter, Barlow, and Sjoerdsma, 1987). This led to use of the drug being largely abandoned. The discovery that lower doses of the drug can elicit favourable outcomes in the treatment of colonic neoplasms, without the onset of adverse clinical signs, and that combination chemotherapy regimens, utilising eflornithine and non-steroidal anti-inflammatory drugs (NSAID's) increases the efficacy of the treatment has re-stimulated interest in eflornithine as an potential anti-cancer agent. Many of these combination therapy approaches are currently under clinical trials for the treatment and prevention of various forms of intestinal neoplasm (Gwyn and Sinicrope, 2002)

5.1.3. Eflornithine in non-cancer related conditions

The spread of AIDS in the human population has led to an increase in the number of cases of opportunistic infections including *Pneumocystis carinii* pneumonia. This disease is characterised by fever, dry cough, weight loss, progressive dyspnoea and tachypnoea leading to respiratory failure. This infection is now one of the most common causes of death in patients with AIDS. The currently recommended treatment protocols for *Pneumocystis carinii* pneumonia in AIDS patients are less than satisfactory and a high incidence of allergic or toxic reactions is seen. Eflornithine treatment has been given to these patients on a compassionate basis when the accepted regimens have failed to resolve the infection or become intolerable, with a success rate of approximately 74% (Schechter *et al.,* 1987). Another opportunistic infection that commonly occurs in AIDS is *Cryptosporidium* resulting in severe intestinal symptoms. Initial trials of eflornithine in the treatment of this infection gave inconclusive results and further studies are necessary to determine the value of this treatment.

Eflornithine has shown potential in the treatment of malaria. In *in vitro* culture systems of *Plasmodium falciparum*, eflornithine at a concentration of 5mM or higher was shown to reduce the ability of the parasite to divide (Bacchi and McCann, 1987). The ability of eflornithine to induce protection against subsequent malarial infections has been demonstrated in a murine model of *Plasmodium berghei*-infection (Gillet, Bone, Lowa, Charlier *et al.*, 1986). When mice were inoculated with these parasites during a course eflornithine treatment, administered as a 1% solution in their drinking water, 55% of the animals developed a protective immunity against subsequent parasitic challenge that endured for a period of up to six months. This percentage was increased to 60% when the mice were given a concurrent course of chloroquine to help prevent the development of a lethal parasitaemia following the initial infection.

5.1.4. Eflornithine in brain injury

In the gerbil brain, transient ischaemic brain injury results in an increase in the expression of ODC and polyamines which are thought to play important roles in the resulting oedema and neuronal cell loss (Kindy, Hu, and Dempsey, 1994). Gerbils, pretreated with eflornithine 30 minutes prior to the induction of the ischaemia and reperfusion injury, showed a dose dependent reduction in the levels of ODC and putrescine in the damaged tissue. In addition, this treatment prevented the development of the neuronal cell loss that

is associated with brain injuries of this type. The attenuation of the damage was not found when concurrent treatment with putrescine was administered. The findings are in contrast to those seen in a rat model of transient cerebral ischaemia (Lukkarinen, Kauppinen, Grohn, Oja *et al.*, 1998). In this model of transient ischaemic brain injury was induced in transgenic rats over-expressing ODC. In animals treated with 2% eflornithine in their drinking water, from one week before the induction of the ischaemia, a significant increase in the number of stroke lesions was found compared with non-treated rats. An increase in the degree of oedema was also found in the eflornithine-treated rats. These results were confirmed in another rat model of forebrain ischaemia where the presence of ODC activation was shown to play a pivotal role in the survival of neurons following ischaemic damage (Zoli, Zini, Grimaldi, Biagini *et al.*, 1993). The value of eflornithine treatment following stroke in the human situation therefore remains equivocal.

Studies have also been performed to investigate the effect of polyamines on astrogliosis. In a rat model of mechanical brain injury a marked decrease in the resulting astrocyte activation was seen in animals treated with eflornithine (Zini, Zoli, Grimaldi, Merlo Pich *et al.*, 1990). This effect was prevented when an exogenous source of putrescine was provided in the eflornithine-treated animals. The suppression of astrocyte activation by eflornithine was also seen in another rat model of astrogliosis (Jeglinski, Skup, Zaremba, and Oderfeld-Nowak, 1996). In this model astrocyte activation was induced by transection of the lateral fimbria. Treatment of these rats with eflornithine treatment dramatically reduced the resulting astroglial reaction compared with non-operated control animals. In contrast, when astrocyte activation was induced by neurotoxic insult by 1-methyl-4-phenyl-1,2,3,6-tetrahydropyridine treatment, eflornithine administration had no effect on the degree of astrogliosis (O'Callaghan and Seidler, 1992). The effects of eflornithine on the development of astrocytic reactions therefore appear to vary dramatically with the injury type.

5.1.5. Cosmetic applications for eflornithine

Following the unfavourable outcomes seen during the initial trials of eflornithine as an anti-cancer agent, continued production of the drug became largely abandoned by the pharmaceutical companies despite its dramatic effects in the treatment of human African trypanosomiasis (discussed below). Recently a new interest in eflornithine has arisen due to the discovery of an alternative use for the drug as a depilatory (Wickware, 2002). This depilatory effect of eflornithine is thought to result from the inhibition of ODC in the hair

follicles leading to a reduction in hair growth. A decrease in facial hirsutism was reported in 58% of patients treated with a topically applied eflornithine cream (Balfour and McClellan, 2001). The current course of topical treatment entails the application of a 13.9% eflornithine cream twice daily for a period of 24 weeks. The depilatory effect may last for up to eight weeks following treatment before a repeat course of the eflornithine cream is necessary. This finding opened the market for eflornithine sales to the affluent nations of the world and the cost of a month's course of treatment with eflornithine cream is estimated to be approximately $50 to the pharmacist (Shenenberger and Utecht, 2002).

5.1.5.1. Benefits of a commercially viable eflornithine application

The development of eflornithine as a depilatory instigated the continued manufacture of the drug by the pharmaceutical companies as a commercially viable product. The eflornithine cream is now produced by Bristol-Myers Squibb and Gillette, who advertise the product under the trade name Vaniqa®, and is available for use in the USA. Licensing applications have also been submitted to allow the international marketing of the product (Balfour and McClellan, 2001). The existence of these affluent consumers inadvertently led to development of a partnership between WHO in collaboration with Médecins Sans Frontières (MSF), and Aventis (formerly Hoechst Marion Roussell Inc.), who hold the patent rights for the manufacture of eflornithine, and Bristol-Myers Squibb together with Dow Chemicals Co, Akorn Manufacturing Inc. to produce and donate 60,000 doses of eflornithine for use in the treatment of human African trypanosomiasis. This supply should last until approximately June 2004. Currently, discussions between Bristol-Myers Squibb and WHO/MSF are in progress to try and secure the continued manufacture of eflornithine after 2004. The main stumbling block again appears to be related to the final charge for the drug since synthesis of this fluorinated compound is resource intensive and highly corrosive to the manufacturing plant. The final outcome of these talks is awaited although it is known that MSF would like to agree on a pre-arranged price of $10 per dose, this is half the cost of purchasing the drug in 1997 before the advent of the alternative market (WHO, 2001b).

5.1.6. Eflornithine treatment of African trypanosomiasis

5.1.6.1. Polyamines and ODC in African trypanosomes

In the blood stream form of *T.b.brucei* putrescine and spermidine, constitute the main pool of polyamines produced by ODC. Spermine was not detected in these parasites (Bacchi, 1981). The ability of eflornithine to inhibit trypanosome ODC over mammalian ODC does not arise from a unique sensitivity of the parasitic enzyme to the drug but is the result of two basic differences between the mammalian cells and the parasites. In both cell types all three polyamines are taken up if an exogenous source of the compounds is provided. However, uptake of the polyamines is 100 fold slower in the parasites compared with uptake by mammalian cells (Bacchi and McCann, 1987). In addition, the turnover of ODC within the trypanosome occurs more slowly than that seen in mammalian cells resulting in a prolonged period of ODC inactivity following eflornithine treatment (Ghoda, Phillips, Bass, Wang *et al.*, 1990).

During normal metabolic processes, and in the immune response to infection, cells produce reactive oxygen species. These molecules can result in oxidant damage to the cells; therefore, in order to avoid injury, both mammalian cells and trypanosomes must be able to remove these harmful molecules. In mammalian cells, this balance is maintained by the enzyme catalase, in conjunction with glutathione reductase and glutathione. In this system reduced glutathione (GSH), acts as a carrier for the free radicals resulting from the degradation of hydrogen peroxide or the superoxide anion, producing oxidised glutathione (GS-SG) (Bacchi and McCann, 1987; Van Bogaert and Haemers, 1989).

$$2GSH + R\text{-}O\text{-}OH \longrightarrow GS\text{-}SG + H_2O + ROH$$

The regeneration of reduced glutathione is catalysed by the enzyme glutathione reductase using the reduced form of nicotimadine adenine dinucleotide phosphate (NADPH) as an electron donor. The electrons from the molecule are transferred by glutathione reductase to GS-SG thereby regenerating the two molecules of GSH.

$$GS\text{-}SG + NADPH + H^+ \longrightarrow 2GSH + NADP^+$$

However, in trypanosomes this pathway is not complete as glutathione reductase is not present. Therefore an alternative mechanism involving a two-step process is followed to recycle the GSH. In this pathway the GS-SG is reduced by the transfer of electrons from a molecule known as trypanothione. In the first step of the process trypanothione disulphide [$T(S)_2$] is reduced to dihydrotrypanothione [$T(SH)_2$] by the enzyme trypanothione reductase in a NADPH dependent manner. This enzyme is largely similar to glutathione reductase but is specific for trypanothione and will not react with glutathione.

$$T(S)_2 + NADPH + H^+ \longrightarrow T(SH)_2 + NADP^+$$

In the second stage of the reaction, the $T(SH)_2$ donates the additional electron to the GS-SG molecule in a non-enzymatic exchange.

$$GS\text{-}SG + T(SH)_2 \longrightarrow 2GSH + T(S)_2$$

This reaction regenerates the reduced form of glutathione and allows the molecule to continue scavenging for reactive oxygen species thereby maintaining the redox balance within the parasite.

The trypanothione molecule is synthesised from the polyamine spermidine and is dependent on the presence of this compound for its production. Thus, drugs that inhibit the polyamine biosynthesis pathway, such as eflornithine, would have a profound effect on the ability of the trypanosome to maintain a steady redox state. The fundamental difference between these pathways in mammalian cells and trypanosomes, together with the slow ODC turnover and uptake of exogenous polyamine, makes the parasites more vulnerable to attack by eflornithine than the cells of their mammalian host thus, indicating ODC as a logical target for anti-trypanosomal drugs (Bacchi and McCann, 1987; Van Bogaert and Haemers, 1989).

5.1.6.2. Eflornithine studies in experimental infections

The use of eflornithine to treat *in vivo* trypanosome infections was first demonstrated using a mouse model of the disease (Bacchi *et al.*, 1980). In this study mice were infected with *T.b.brucei* and treated with a range of doses of eflornithine, administered either in the animals drinking water or by intubation. In untreated mice, infected in this manner, the survival time is approximately 5 days. The treatment regimes were given during the early stage of the disease, beginning 24 hours post-infection. The chemotherapy was considered

to be curative if the mice survived for a period exceeding 35 days. To confirm the cured status and ensure that no parasites were sequestered within the CNS of these animals, their brain was homogenised and transferred to uninfected animals. These recipient mice were monitored for a further 30-day period for the development of the disease. Successful cures were found in animals treated with 1% eflornithine in their drinking water for three days with an estimated eflornithine intake of 150mg. The administration of the drug in the drinking water was a more effective method of eflornithine dosing than intubation. This is most likely the result of the short half-life of eflornithine in rodents. Therefore, more frequent intake of the drug results in more efficacious treatment schedules (Bacchi *et al.*, 1980).

In further experiments the effect of eflornithine treatment, supplied as a 4% solution in the drinking water, on the trypanosomes during the course of infection in *T.b.brucei*-infected rat was studied (Bacchi, Garofalo, Mockenhaupt, McCann *et al.*, 1983). Parasites isolated from infected rats, following 36 hours of eflornithine treatment, displayed a short stumpy conformation and showed additional morphological changes. Many of these trypanosomes had several nuclei and kinetoplasts and the cytoplasm appeared granular. In contrast, parasites prepared from non-drug treated animals had a long slender shape with the presence of only an occasional stumpy form. No morphological abnormalities were noted in these parasites. Treatment of infected rats with 4% eflornithine in their drinking water for periods longer than 36 hours resulted in a rapid clearance of the trypanosomes from the bloodstream and the effect of longer exposure times of the trypanosome to the drug could not be determined. These morphological changes, induced in the trypanosomes by eflornithine, were confirmed in experiments investigating the effect of the drug on the parasite in both *in vivo* and *in vitro* scenarios (Giffin, McCann, Bitonti, and Bacchi, 1986). In these experiments *T.b.brucei* parasites were either maintained in tissue culture and exposed to 50μM or 100μM eflornithine or used to infect rats that were subsequently treated with 4% eflornithine in their drinking water. Trypanosomes exposed to eflornithine in either situation displayed a short stumpy conformation and alterations to their nuclear morphology.

5.1.6.2.1. Innate resistance to eflornithine treatment

The differential susceptibility of various trypanosome strains to eflornithine treatment has also been investigated in experimental murine infections (Bacchi, Nathan, Livingston, Valladares *et al.*, 1990). These studies employed one strain of *T.b.brucei* as a reference strain, two strains of *T.b.rhodesiense* supplied from the American Type Culture Collection

(ATCC) and 14 *T.b.rhodesiense* strains, originally isolated from human blood or cerebrospinal fluid, supplied from the Kenyan Trypanosomiasis Research Institute (KETRI) strain bank. In the *T.b.brucei* infections 2% eflornithine in drinking water for a period of 3 days resulted in a cure rate of higher than 80%. If the treatment period was extended to 6 or 9 days then a 100% cure rate was obtained. Five of the *T.b.rhodesiense* isolates from KETRI showed a response to eflornithine treatment similar to that seen in the *T.b.brucei* strain. Six other KETRI isolates and the two ATCC strains were more resistant to eflornithine and a dose regimen of 4% eflornithine for 9 days had to be employed to cure the infections. The remaining three KETRI isolates were refractory to eflornithine treatment. Even when the animals infected with these strains were treated with higher doses of the drug the infections could not be cured although longer survival times were achieved following eflornithine chemotherapy. It would therefore appear that certain *T.b.rhodesiense* infections show an innate resistance to eflornithine treatment since these isolates had not previously been exposed to the drug.

Combination therapy approaches to try and circumvent the innate resistance of specific *T.b.rhodesiense* strains to eflornithine treatment were employed (Bacchi, Nathan, Yarlett, Goldberg *et al.*, 1994). In these studied eflornithine resistant strains of *T.b.rhodesiense* that were also refractory, or moderately resistant, to melarsan oxide, were used to infect mice. It was found that cures could be obtained by administering a regimen of eflornithine plus suramin or eflornithine plus melarsan oxide. These drugs when given as monotherapies were ineffectual in the treatment of the infection. The results from these experiments suggest that eflornithine treatment, in combination with other trypanocidal drugs, may be useful in the treatment of melarsoprol refractory disease even where the parasites have shown innate resistance to eflornithine therapy.

The potentiation of arsenical drugs such as melarsan oxide and melarsoprol had been demonstrated previously in a *T.b.brucei* murine model of CNS-stage disease (Jennings, 1988a; Jennings, 1988b). Here it was shown that combining eflornithine and melarsoprol treatment protocols resulted in a five-fold increase in the efficacy of the treatment regimen compared with melarsoprol monotherapy. These studies also indicated that use of a combination therapy approach could allow reduced dosages of melarsoprol and shorter treatment periods to be employed while still successfully curing the infection.

5.1.6.3. Eflornithine trials in human trypanosome infections

Shortly after the discovery that eflornithine could be used to cure experimental trypanosome infections (Bacchi *et al.,* 1980) human trials using the drug were instigated. The first field trial of eflornithine was carried out in the Sudan using an orally administered form of eflornithine (Van Nieuwenhove *et al.,* 1985). Based on the geographical location and the clinical course of the disease, the patients in this study were considered to be infected with *T.b.gambiense*. Twenty patients were included in the trial, 18 of these patients were diagnosed with late-stage infections and two were treated during the early stage of the disease. Sixteen of the 18 late-stage patients presented with melarsoprol refractory infections while the remaining two late-stage patients had received no previous treatments for the infection.

The first patient was treated with eflornithine in 1981 and was given an oral dose of 258mg/kg/day for a period of 44 days. This patient was diagnosed with late-stage disease and had received no previous trypanocidal therapy. Unfortunately this man showed evidence of a relapsed infection 10 weeks following cessation of the eflornithine treatment. The patient was placed on a course of intravenous melarsoprol that he did not complete. The occurrence of a relapsed infection in this patient prompted the investigators to increase the dosage of eflornithine to 400mg/kg/day administered as four separate doses at six-hour intervals for the treatment of the melarsoprol refractory infections. The second patient who had not been previously treated with any trypanocidal drugs was given 266mg/kg/day for a 37-day period. Although the course was not complete at this time point the patient left the hospital due to the fear of his imminent lumbar puncture. On follow up at 23 months after cessation of the eflornithine treatment the patient appeared to be free from infection. Of the remaining 16 patients with late-stage melarsoprol refractory infections, 13 completed the eflornithine course of 400mg/kg/day. Only two of these patients developed a relapsed infection. The two patients treated with either 218mg/kg/day or 203mg/kg/day eflornithine during the early stage of the infection were also successfully cured of the disease. The follow up period on the patients involved in this trial ranged from 3-23 months. The drug was generally well tolerated and adverse reactions did not precipitate cessation of the chemotherapy. The adverse side effects of oral eflornithine were reported as gastrointestinal complaints and occasional anaemia. These reactions dissipated on completion of the treatment course. This initial trial indicated that eflornithine was a

highly effective and relatively non-toxic drug useful for the treatment of all stages of HAT, including, melarsoprol refractory infection.

In another trial 14 patients with late-stage *T.b.gambiense* infection in the Cote D'Ivoire were studied (Doua, Boa, Schechter, Miezan *et al.*, 1987). Twelve of these cases were considered to be refractory to melarsoprol treatment and the remaining two patients had not received previous trypanocidal therapy. The patients were given a course of eflornithine consisting of 400mg/kg/day administered intravenously for 14 days followed by 300mg/kg/day given orally for 21-28 days. This regimen rapidly cleared the parasites from the body fluids and resulted in a rapid reversal of the clinical signs and symptoms of the diseases. Again, diarrhoea, abdominal pain and anaemia were the most common side effects of the drug although these adverse reactions quickly disappeared on withdrawal of the eflornithine. All of the treated patients appeared to be cured of the infection and in four of the cases followed for 2 years no relapses were recorded. The high success of this regimen indicates that a combined intravenous and oral approach is more efficacious than eflornithine administered purely using the oral route. A synergism between eflornithine and melarsoprol has also been demonstrated in the treatment of *T.b.gambiense* infections (Simarro and Asumu, 1996). In this case conventional trypanocidal treatment regimens and eflornithine monotherapy failed to cure the disease. However, when the patient was treated with a combination of melarsoprol and eflornithine the infection was successfully resolved.

The initial success of eflornithine treatment for *T.b.gambiense* infections was unfortunately not mirrored in the treatment of *T.b.rhodesiense* infections. Initial studies on three cases of melarsoprol refractory *T.b.rhodesiense* infection gave disappointing results and all three cases given eflornithine at 400mg/kg/day subsequently relapsed (Bales, Jr., Harrison, Mbwabi, and Schecter, 1989). More promising results have been reported when eflornithine has been used in combination with suramin to treat *T.b.rhodesiense* infections (Clerinx, Taelman, Bogaerts, and Vervoort, 1998; Taelman *et al.*, 1996). In these studies intravenous suramin was given together with either 400 or 800mg/kg/day of intravenous eflornithine for a 14-21 day period. This was followed by eflornithine administered orally at a dosage of 300mg/kg/day for 10-21 days. All patients responded well to the chemotherapy and all patients treated with these regimens appeared to be cured of the infection. Due to the equivocal results gained from eflornithine treatment of *T.b.rhodesiense* infection only scarce documentation is available regarding the use of the drug for this form of HAT. This is unfortunate as eflornithine remains the only available drug for the treatment of melarsoprol refractory late-stage infections and initial trials

combining eflornithine with other conventional trypanocidal drugs have proved encouraging.

5.1.7. Additional pharmacological actions of eflornithine

A study investigating the effect of eflornithine treatment on the CNS inflammation associated with subcurative drug treatment of late-stage trypanosome infections and the development of the post treatment reactive encephalopathy (PTRE) in experimental murine infections produced interesting results (Jennings *et al.*, 1997). This study utilised a strain of *T.b.brucei* that was resistant to the effect of eflornithine and continued to divide normally even in the presence of curative levels of the drug. Various groups of mice were infected with these eflornithine resistant trypanosomes and the infection allowed to progress naturally. At 14 days post-infection one group of mice was given 2% eflornithine in their drinking water. This treatment was continued for a 14-day period. On day 21 post-infection, halfway through the eflornithine course, the mice were treated with a subcurative dose of diminazene aceturate. This treatment induces a CNS inflammatory reaction in the infected animals that becomes apparent by 7 days after the diminazene aceturate treatment. Groups of mice were killed at 7 and 14 days after the subcurative drug administration. Their brain tissue was examined histologically for neuropathological changes and compared with non-eflornithine treated mice subjected to a similar regimen. Using this model, eflornithine treatment was shown to prevent the development of the neuroinflammatory response associated with subcurative drug treatment of late-stage infections.

A second group of mice were infected and treated with diminazene aceturate on day 21 post-infection. The CNS inflammation was allowed to develop for a 7-day period and then the mice were given the 14-day eflornithine regimen. On completion of the course of chemotherapy the animals were killed and the brains examined for inflammatory changes. The brains of these animals showed a dramatic reduction in the severity of the neuroinflammation compared with mice that had not received eflornithine. These findings indicated that eflornithine treatment could ameliorate an established CNS inflammatory reaction.

This murine model was also used to investigate the effects of eflornithine treatment on the extremely severe CNS inflammatory reaction that can occur in human cases of the disease

following melarsoprol treatment. This PTRE was induced in infected mice by treating the animals on day 21 post-infection with diminazene aceturate to instigate the CNS inflammatory changes. When these animals relapsed to parasitaemia they were given a second diminazene aceturate treatment. This regimen further exacerbates the CNS inflammation resulting in an extremely severe meningoencephalitis similar to that found in the PTRE. If animals treated in this manner were given a 14-day course of eflornithine as described above, beginning 7 days after the second diminazene aceturate treatment, the severity of resulting CNS pathology was substantially reduced compared to animals not given eflornithine. This indicates that eflornithine treatment can ameliorate not only moderate CNS inflammatory reactions but also the extremely severe meningoencephalitis that is characteristic of the PTRE.

The ability of eflornithine to prevent the development of CNS inflammation and to ameliorate established neuroinflammatory reactions appears to be independent of the drugs trypanostatic action since an eflornithine resistant trypanosome stabilate was used in these infections. Furthermore, the effect of eflornithine on ODC was shown to be only partially responsible for this anti-inflammatory action since concurrent administration of putrescine with the eflornithine course only partially restored the CNS inflammatory response.

From the data presented in the study detailed above there appears to be a pharmacological action of eflornithine in addition to its ability to inhibit ODC. This was also suggested by the dramatic clinical improvement seen in comatose sleeping sickness patients treated with eflornithine even when it failed to resolve the infection. This finding resulted in eflornithine being nicknamed "the resurrection" drug (WHO, 1990). In this chapter the effect of eflornithine on the development and amelioration of the CNS inflammatory reaction associated with trypanosome infection and treatment will be further investigated. It is possible that treatment with eflornithine inhibits the production of pro-inflammatory mediators thereby decreasing the severity of the resulting CNS reaction. Therefore, the expression of the cytokines, IL-1α, IL-6 and TNF-α as well as the chemokines MIP-1α, MCP-1 and RANTES will be examined in the presence and absence of eflornithine chemotherapy. As previously stated, these mediators have been shown to be play a role in the pathogenesis of trypanosomiasis and are known to be present within the CNS. The effect of eflornithine treatment on the severity of the CNS inflammatory response will also be examined.

5.2. Materials and methods

Eflornithine chemotherapy can both prevent and ameliorate the CNS inflammatory reaction associated with trypanosome infection and subcurative drug treatment. Studies previously performed in our laboratory have indicated that eflornithine may possess pharmacological actions in addition to the inhibition of ornithine decarboxylase (ODC) (Jennings *et al.*, 1997). Since the mRNA transcripts for the inflammatory mediators IL-1α, IL-6, TNF-α, MIP-1α, MCP-1 and RANTES are present in the brains of trypanosome-infected animals it is possible that eflornithine mediates its anti-inflammatory action by inhibiting the production of one or more of these inflammatory agents. Therefore, the effect of eflornithine treatment on the severity of the neuroinflammatory reaction and the transcription of IL-1α, IL-6, TNF-α, MIP-1α, MCP-1 and RANTES was studied using our murine model of trypanosomiasis.

5.2.1. Parasites

In order to differentiate between the anti-inflammatory effects arising directly as a result of the chemotherapy and those that would occur due to the elimination of the parasitaemia normally associated with eflornithine treatment, trypanosomes that were resistant to the effects of the drug were used in these experiments. These parasites were developed in Glasgow University Veterinary School, by Dr Frank W Jennings and continue to divide when exposed to normally curative levels of eflornithine. The procedure used to create the eflornithine resistant trypanosomes is outlined schematically in Figure 5.1.

To generate these drug resistant trypanosomes six mice were infected with the normal working stabilate of *T.b.brucei* GVR35/C1.3 and housed under a 2-hour light 4-hour dark regimen. The infection was allowed to progress until day 21 post-infection when the mice were given a 14-day course of 2% eflornithine administered in their drinking water. When one of the six mice relapsed to parasitaemia the animal was killed and exsanguinated by cardiac puncture. The parasitaemic blood was then used to infect a further group of six mice. In addition, an intermediate trypanosome stabilate was prepared by infecting two irradiated mice, allowing the parasitaemia to develop and then storing the parasitaemic blood in liquid nitrogen. The whole procedure of infection, eflornithine treatment, relapse and exsanguination was repeated for a further seven rounds. Intermediate stabilates were prepared throughout the process in case the 'resistant' trypanosome was lost at any time. Following the final infection series the mice were treated on day 21 post-infection with 4%

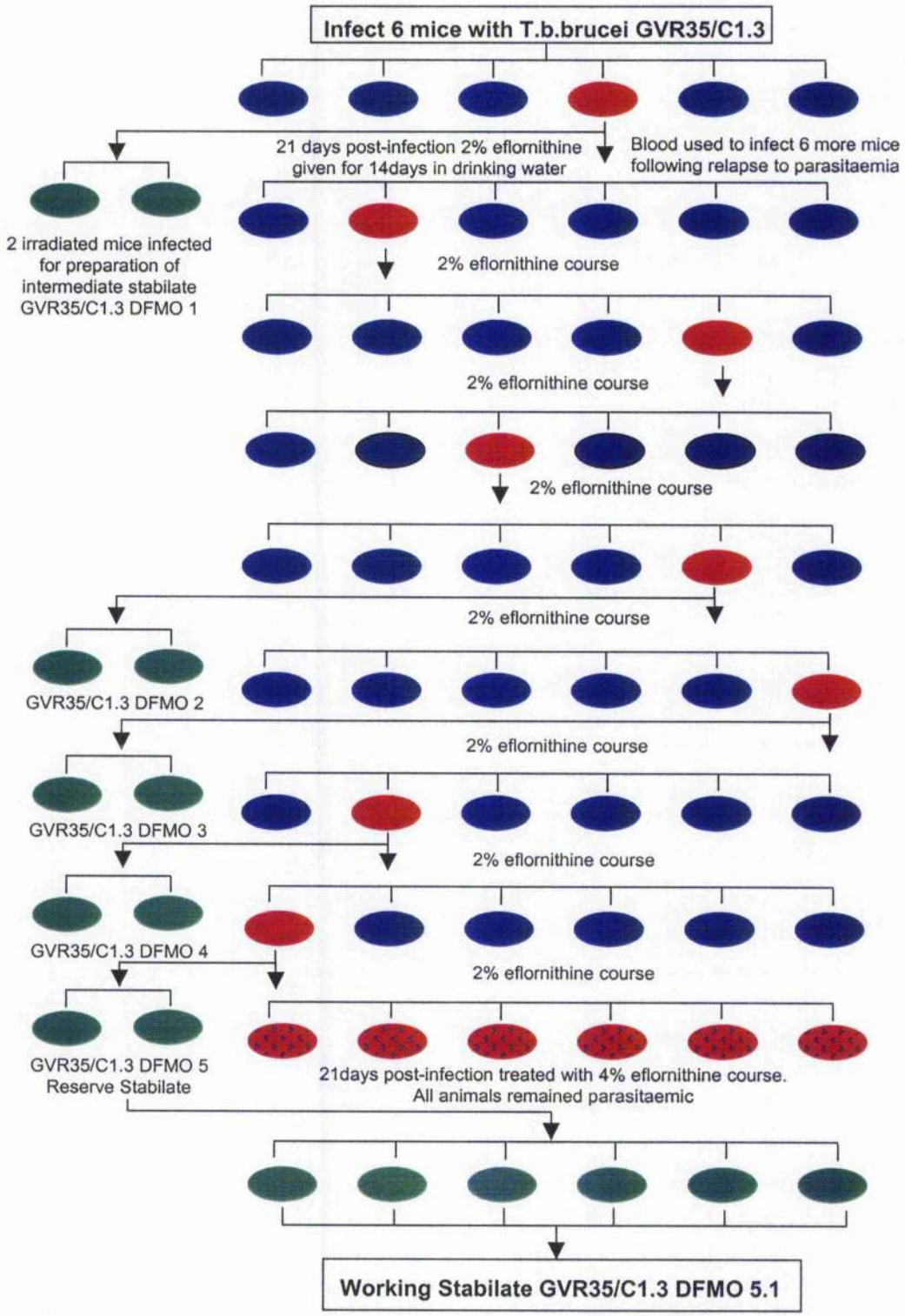

Figure 5.1. Production of eflornithine resistant *T.b.brucei* GVR 35/C1.3 DFMO 5.1
An initial group of mice were infected with *T.b.brucei* GVR35/C1.3. At 21 days post-infection the animals were given 2% eflornithine in their drinking water *ad libitum* for 14 days. When one of these mice relapsed to parasitaemia (red oval) the blood was used to infect 6 more mice. The procedure was repeated a further seven times. Animals were maintained under a 2-hour light 4-hour dark regimen. Following the final round of infections the mice remained parasitaemic through treatment with double the normal dose of eflornithine (red oval with blue chevrons). These parasites were considered to be eflornithine resistant and a working stabilate was prepared from the reserve. Intermediate stabilates were prepared, by infecting irradiated mice (green oval), at intervals throughout the process in case the parasite was 'lost'. Working stabilates are prepared from the reserve stabilate as required. The current working stabilate is GVR35/C1.3 DFMO 5.2.

eflornithine in their drinking water. This treatment had no effect on the trypanosomes and the animals remained parasitaemic. This parasite was considered to be resistant to eflornithine and was stored in liquid nitrogen as stabilate GVR35/DFMO5. Working stabilates were prepared from this original reserve stabilate as required. The current working stabilate is GVR35/DFMO5.2

5.2.2. Animals infection and treatments

The mouse model of human African trypanosomiasis, as detailed in Chapter 2, was used to mirror the CNS-stage of human African trypanosomiasis and the post-treatment reactive encephalopathy (PTRE). The animals were infected with $2x10^4$ *T.b.brucei* parasites of cloned stabilate GVR35/DFMO5.2 and the treatment regimens outlined in Figure 5.2 followed. Six mice were included in each experimental group. Due to death or euthanasia of the mie before the endpoint of the experiment the number of animals comprising the analysis groups are detailed in Tables 5.2-5.3 (neuropathology) and Figures 5.12-5.17 and Figures 5.25-5.30 (cytokine and chemokine expression).

5.2.2.1. Prevention of the CNS inflammatory response

In this experimental regimen infected mice were given a course of eflornithine, administered as a 2% solution in their drinking water beginning on day 14 post-infection. The drug was available *ad libitum* and the mice were housed under a 2 hour light / 4 hour dark lighting regimen. This is known to encourage a more frequent drinking pattern in the mice and therefore regulates the intake of the eflornithine. The drug was administered in this fashion for a 14-day period. On day 21 post-infection the mice were treated with diminazene aceturate (40mg/kg i.p.) to induce a CNS inflammatory response. On day 28 post-infection the eflornithine treatment was withdrawn and the mice were killed. At each termination point the animals were killed by cardiac perfusion with sterile saline while under terminal anaesthesia and their brains extracted and processed for histopathological examination or RNA extraction.

5.2.2.2. Amelioration of an established meningoencephalitis

In this experimental design infected animals were treated on day 21 post-infection with diminazene aceturate (40mg/kg i.p.). The parasitaemia in the animals was monitored on a

Experimental groups:

Prevention of the CNS inflammatory response

Amelioration of an existing post-treatment reactive encephalopathy

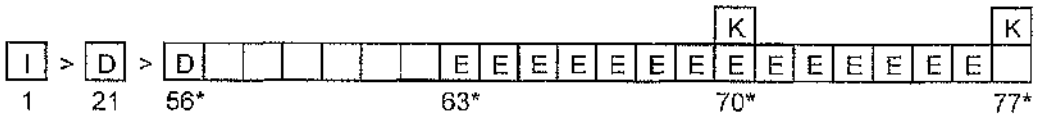

Control groups:

Infected non-eflornithine treated

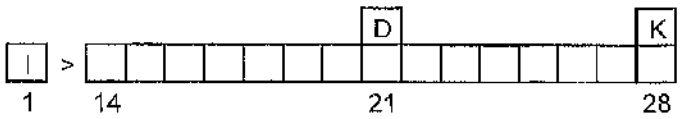

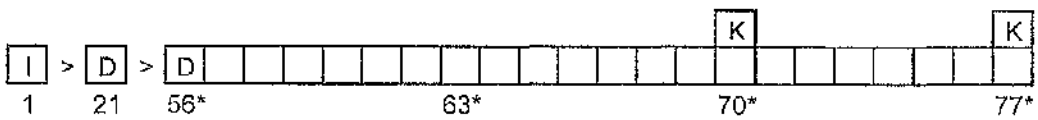

Uninfected drug treated

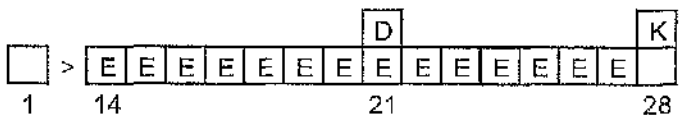

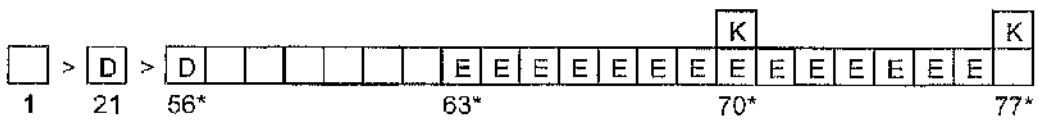

Figure 5.2. Schematic representation of the treatment regimens utilised to determine the effects of eflornithine treatment. In this model experimental groups of mice were infected (I) with $2x10^4$ *T.b.brucei* parasites of cloned stabilate GVR35/C1.6/DFMO5. Animals were administered diminazene aceturate (D) and eflornithine (E) as indicated. The regimens were terminated when the mice were killed (K). The number of days post-infection is shown below the treatment regimen. The interval between the initial diminazene aceturate treatment and the second injection of the drug is dependent on the length of time taken by the animals to relapse to parasitaemia. Therefore, the time points marked * are approximate dates and vary slightly with each experiment.

weekly basis by examining wet blood films prepared from tail snips. When more than 50% of the mice had relapsed to parasitaemia the animals were given a second diminazene aceturate treatment. This regimen induces an extremely severe meningoencephalitis in the

mice, similar to than found in patients that have died of the PTRE, which is apparent by 7 days following the diminazene aceturate treatment. The mice were given a course of eflornithine as described above beginning 7 days after the second diminazene aceturate injection. Groups of mice were sacrificed, after receiving 7 and 14 days of eflornithine chemotherapy.

5.2.2.3. Control animals

In parallel with the experimental regimens, groups of infected animals were treated in an identical manner to the groups described above, barring the administration of eflornithine. In addition uninfected mice were treated with the drug regimens described to ensure that these protocols did not induce changes in the CNS in the absence of trypanosome infection.

5.2.3. Neuropathological assessment

Although it is known that eflornithine treatment can both prevent and ameliorate the CNS inflammatory reaction associated with trypanosome infection (Jennings *et al.*, 1997), this anti-inflammatory effect has never been determined using a quantifiable system. Therefore, the severity of the neuroinflammatory reaction resulting from each treatment regimen was assessed using the neuropathological grading scale described in Chapter 2 and in Table 2.1. Again, haematoxylin and eosin stained brain sections were scored, by two individual assessors, in a blinded fashion.

5.2.3.1.Astrocyte activation

The gross level of astrocyte activation found in each of these groups of mice was assessed using immunocytochemistry (ICC) as described in Chapter 2 to detect glial fibrillary acidic protein (GFAP). GFAP is a major intermediate filament protein peculiar to astrocytes and is therefore an ideal marker to identify this cell type. Formalin fixed paraffin sections were stained with a polyclonal anti-GFAP antibody (Table 2.2) raised in rabbits. This was subsequently detected by the addition of a biotinylated swine anti-rabbit antibody followed

by the avidin-biotin peroxidase complex. Positively labelled cells were visualised using diaminobenzidine (DAB) as the chromogen. The sections were counterstained with haematoxylin to distinguish the nuclei and to facilitate spatial orientation within the section during subsequent histopathological examination.

5.2.4. RT-PCR analyses

To determine the effect of eflornithine treatment on the transcription pattern of the cytokines IL-1α, IL-6 and TNF-α and the chemokines MIP-1α, MCP-1 and RANTES the nucleic acid extraction procedure and the semi-quantitative RT-PCR technique described in Chapter 2 was followed.

5.2.5. Statistical analyses

Statistical analyses were performed on the data generated from the assessment of the severity of the neuropathological response and the levels of cytokine and chemokine transcription.

The severities of the neuropathological reactions were compared, between groups of mice given various treatment regimens, using the average of independent assessor scores. The severity of the reaction was measured in sections prepared from each individual animal. A Wilcoxon signed rank test was employed to show that each assessor had applied the neuropathological grading scale uniformly. Data generated from grading the CNS inflammatory response were analysed using parametric statistical tests. In particular, the general linear model procedure was used to implement a randomised block analysis of variance design. This procedure tested for differences in the mean neuropathological responses among groups of mice.

Differences in the expression levels of cytokine and chemokines were investigated using a visual assessment scale to grade the intensity of the bands resulting from amplification of the individual inflammatory agents in nucleic acid extracted from the CNS of each mouse. The data generated from this scoring system were analysed using non-parametric statistical tests. Significant differences across the groups of animals were detected using the Kuskal-Wallis test. This was followed by Dunn's test, a pairwise comparisons procedure for non-parametric data, to highlight differences between the median values from individual groups.

All tests were undertaken using the proprietary statistical software packages; Minitab version 13 and Sigmastat 2.03. Tests returning p-values of less 0.05 were considered significant.

5.3. Results

5.3.1. Assessment of the severity of the meningoencephalitis

5.3.1.1. Prevention of the neuroinflammatory response

Histopathological examination of brain sections prepared from mice infected with eflornithine resistant *T.b.brucei* showed only a slight reduction in the severity of the meningoencephalitis when treated with a 14-day course of eflornithine beginning 7 days prior to the induction of the CNS reaction, by subcurative diminazene aceturate treatment, compared to similarly infected and treated animals that did not receive eflornithine (Fig. 5.3). The inflammatory changes seen in non-eflornithine treated animals were characterised by the presence of a few inflammatory cells in the meninges and ventricles, and occasional perivascular cuffing of the blood vessels. The inflammatory cells were mainly macrophages and lymphocytes. Sections prepared from the brains of uninfected animals treated with a course of eflornithine showed only very mild signs of inflammatory changes with a few inflammatory cells in the meninges and ventricles.

When the GFAP content of the sections prepared from infected mice not treated with eflornithine was examined, activated astrocytes were detected mainly in area displaying signs of inflammatory cell infiltration such as close to the meninges and surrounding any small perivascular cuffs that were present. These cells stained intensely with GFAP and displayed numerous intricate cellular processes. In animals receiving eflornithine fewer astrocytes were detected and these stained less intensely and displayed a more simple morphology that the cells found in non-eflornithine treated mice (Fig. 5.3, GFAP positive cells show brown staining pattern).

A summary of the results of the statistical analyses of the data generated from the assessment of the severity of the neuroinflammation by applying the criteria outlined in the neuropathology grading scale (Table 2.1) is shown in Table 5.1. The results of a Wilcoxon signed rank test indicated that each individual assessor had applied the scale in a consistant manner. Therefore, an average of the two grading scores was used in the analyses. General linear model analysis of the combined data from three experiments showed no significant differences ($p=0.066$) between the results gained from each individual

experiment. This indicates that the regimens used produced consistent neuropathological changes in each individual experimental run. A significant difference ($p<0.001$) was detected in the severity of the neuroinflammatory response between the three treatment regimens analysed. Here both the infected group receiving eflornithine and the infected mice that were not given eflornithine showed a significantly ($p<0.0001$) higher neuroinflammatory response than the uninfected drug treated animals. These groups returned a neuropathology grading score of 1.028 ± 0.118 (mean $\pm$ standard error) and 1.375 ± 0.110 respectively while the uninfected mice showed no pathological changes (0.00 ± 0.00). Although the severity of the response found in the eflornithine treated group was slightly lower than that seen in non-eflornithine treated mice this reduction was not statistically significant ($p=0.100$).

5.3.1.2. Amelioration of an established meningoencephalitis

A severe meningoencephalitis was found in sections prepared from the brains of mice infected with eflornithine resistant *T.b.brucei* and killed following a second diminazene aceturate treatment (Fig. 5.4). The inflammatory reaction seen in these animals was characterised by the presence of a severe meningitis, perivascular cuffing of most blood vessels, large numbers of inflammatory cells in the ventricles and a moderate to severe encephalitis. The inflammatory cells were composed of macrophages, lymphocytes and plasma cells. A 7-day course of eflornithine resulted in only a slight reduction in the severity of the neuroinflammation compared to mice that did not receive eflornithine while a 14-day course of the drug produced a more marked decrease in the neuroinflammatory response (Fig. 5.4). Animals receiving this 14-day eflornithine treatment showed only a moderate meningitis, with perivascular cuffing of some blood vessels. Inflammatory cells were not seen in the neuropil of mice treated in this manner. No inflammatory changes were found in the brains of the uninfected drug treated animals.

Numerous intensely staining and highly stellate astrocytes were detected in the sections prepared from infected animals following the induction of a severe meningoencephalitic reaction. The astrocytes were particularly prominent in the hippocampus and surrounding the ventricles and perivascular cuffs. Following 14 days of eflornithine treatment there was a reduction in the number of astrocytes detected and the staining pattern displayed was less intense. The astrocytes seen following eflornithine treatment appeared smaller and

showed fewer cellular processes (Fig. 5.4, GFAP positive cells show brown staining pattern).

Analysis of variance using a randomised block design was carried out on the data generated from assessing the severity of the neuroinflammatory reaction. A summary of the results of this analysis is shown in Table 5.2. Since a Wilcoxon signed rank test showed no difference in the grading method employed by the individual assessors the average of the two scores was used in the analysis procedures. The results of the statistical testing showed that the severity of the response seen in infected animals following a 7-day course of eflornithine (2.950 $\pm$ 0.130) was only slightly reduced compared with identically treated mice that were not given eflornithine (3.156 $\pm$ 0.170). This reduction was not statistically significant ($p=0.873$). In contrast the severity of the neuropathological response seen in animals given a 14-day eflornithine course (2.271 $\pm$ 0.129) was significantly reduced ($p<0.0001$) compared with infected animals given a similar course of treatment but no eflornithine (3.348 $\pm$ 0.066). The extension of the eflornithine treatment period to 14 days also resulted in a significant reduction ($p=0.0004$) in the neuropathological reaction compared with that seen in mice given only a 7-day course of the drug.

5.3.2. The effect of eflornithine on cytokine expression

To determine whether eflornithine altered the transcription of the cytokines IL-1α, IL-6, TNF-α or the chemokines MCP-1, MIP-1α or RANTES, RT-PCR analyses were performed on the RNA extracted from the brain tissue of *T.b.brucei* GVR35/C1.3 DFMO 5.2 -infected mice in the presence or absence of eflornithine treatment. mRNA from uninfected mice and uninfected drug treated mice was also analysed for the expression of these mediators.

5.3.2.1. Prevention of the neuroinflammatory response

The effect of eflornithine treatment on the development of a CNS inflammatory reaction was investigated by treating infected mice with eflornithine before the induction of the inflammatory reaction, by subcurative drug treatment with diminazene aceturate, and analysing the cytokine response. This was compared with infected non-eflornithine treated mice, uninfected mice and uninfected drug treated animals.

Before any comparisons were made regarding the levels of cytokine expression between the various treatment groups the quality of the mRNA from each group was assessed by the amplification of mRNA of the housekeeping gene β-actin. The banding pattern, seen on a 2% agarose gel stained with ethidium bromide, resulting from the amplification of pooled mRNA samples from animals in each treatment group is shown in Figure 5.5. All subsequent PCR photographs in this Chapter have been prepared using the PCR products resulting from this amalgamated mRNA sample. The intensity of the PCR bands found following β-actin amplification was similar in each group indicating that the quality of the starting material was comparable and therefore differences in the resulting PCR band intensities would reflect differences in the levels of expression of the target sequence in subsequent cytokine analyses rather than poor quality mRNA.

The banding pattern of IL-1α expression, resulting from amplification of pooled mRNA from the individual animals forming each treatment group, shows that mice constitutively express this cytokine within the CNS. Infection with trypanosomes appears to increase this expression level and eflornithine treatment produces a reduction in the levels of IL-1α compared to non-eflornithine treated infected mice (Figure 5.6). When IL-6 was investigated no expression was found in the CNS of uninfected mice but was detected both eflornithine treated and non-treated infected animals. The expression of IL-6 following eflornithine was reduced compared to non-treated mice and the band, although present, was not captured efficiently on the gel photograph (Figure 5.7). Analysis of TNF-α expression showed that TNF-α mRNA was present following infection and induction of the CNS inflammatory response and this level did not appear to be altered by eflornithine treatment. No expression of TNF-α was detected in either uninfected or uninfected drug treated groups (Figure 5.8).

The banding pattern from MCP-1 RT-PCR analyses showed only a very low level of expression in both uninfected groups of mice. This was again difficult to capture in a photographic image. The expression level of this chemokine was increased in the infected groups and was not further altered by eflornithine treatment (Figure 5.9). All groups of mice showed MIP-1α expression. The strongest band resulted from amplification of material from infected, non-eflornithine treated mice and a slight reduction in this expression level was found following eflornithine treatment. Uninfected mice produced much lower levels of MIP-1α (Figure 5.10). RANTES mRNA was detected in the brains of mice from all treatment groups although both the infected non-eflornithine treated and

the infected eflornithine treated regimens resulted in much higher levels of RANTES expression (Figure 5.11).

No significant change in the levels of cytokine or chemokine expression were found between uninfected mice and uninfected animals treated with diminazene aceturate and eflornithine suggesting that these drugs do not alter the transcription of these mediators under normal conditions.

5.3.2.1.1. Statistical analysis

Alterations in the expression of the cytokines IL-1α, IL-6 and TNF-α and the chemokines MCP-1, MIP-1α and RANTES were detected in mouse brain, between eflornithine treated animals, non-eflornithine treated animals and control mice. To allow statistical analyses to be performed on the RT-PCR findings the intensity of the band resulting from the amplification of these mediators, from mRNA extracted from each individual animal, was assigned a numerical score as described in Chapter 2. In all cases, analyses resulting in p-values of less than 0.05 were considered to indicate a significant alteration in the expression levels of the specified cytokine or chemokine. Treatment groups where significant alterations in the expression of these inflammatory mediators were detected are detailed in Table 5.3. Summary data for each cytokine and treatment regimen, together with graphs depicting trends in their expression levels are described in Figures 5.12-5.17.

Animals infected with *T.b.brucei* GVR35/C1.3 DFMO 5.2 and treated subcuratively with diminazene aceturate gave an IL-1α median value of 2.5. This was significantly higher than that found in either uninfected control mice (median 1.50) or infected animals treated with eflornithine (median 1.50). The levels of IL-1α were not different between uninfected mice and infected animals treated with eflornithine (Figure 5.12). A reduction in the expression of IL-6 was also found in infected mice treated with eflornithine (median 0.25). This level of expression was significantly lower than that seen in infected mice that were not given eflornithine (median 0.5), but was not altered from the uninfected mice (median 0.00). IL-6 expression in the non-eflornithine treated mice was significantly higher than in uninfected mice (Figure 5.13). No difference was found in the expression of TNF-α in eflornithine treated mice (median 1.00) when compared to infected animals that did not receive the drug (median 1.00) and both of these treatment groups showed significantly higher levels of TNF-α expression than uninfected mice (median 0.00) (Figure 5.14). The same pattern was found in the expression of MCP-1 where both groups

of infected mice returned a median value of 1.5. This was significantly higher than that seen in uninfected animals (median 0.125) (Figure 5.15). No significant differences were detected between any of the treatment groups in the expression of MIP-1α. Here the lowest levels of expression were found in the uninfected mice (median 0.50) and the highest was detected in the infected, non-eflornithine treated animals (median 1.50). The infected eflornithine treated group showed a median PCR value of 1.00. In the case of RANTES the highest levels of expression were found in infected eflornithine treated mice (median 3.00) with a lower level seen in non-eflornithine treated infected animals (median 2.00). Although a higher level was found in the eflornithine treated mice the difference between the two groups was not significant. Both of the infected groups of mice showed significantly higher levels of RANTES expression than that seen in uninfected mice (median 0.75) (Figure 5.17).

5.3.2.2. Amelioration of an existing meningoencephalitis

The effect of eflornithine treatment on cytokine expression in the amelioration of a meningoencephalitis was investigated using the RT-PCR technique. Infected animals, treated with two doses of diminazene aceturate to induce a severe meningoencephalitis, were treated with either a 7 or 14-day course 2% eflornithine in their drinking water beginning 7 days after the second diminazene aceturate dose. The cytokine response in these mice was compared to those found in infected animals treated with an identical diminazene aceturate regimen but given no eflornithine, uninfected animals given both diminazene aceturate and eflornithine and normal uninfected animals.

Prior to RT-PCR analyses for assessing cytokine and chemokine expression the mRNA extracted from each group of mice was checked for quality by amplification of β-actin transcripts. The resulting PCR products produced bands of a similar intensity when seen on an ethidium bromide stained, 2% agarose gel. A photograph of the gel resulting from amplification of the pooled mRNA from individual animals in each treatment group is shown in Figure 5.18. This indicated that any alteration in the intensity of the bands present following cytokine or chemokine RT-PCR would be the result of differences in the levels of the specific mRNA in the extracted sample.

As previously seen in chapter 4 of this thesis, RT-PCR analyses revealed that IL-1α was constitutively expressed in uninfected mice. This expression was upregulated in all groups of infected animals irrespective of eflornithine treatment (Figure 5.19). As before no IL-6

bands were detected following amplification of mRNA from uninfected mice but were found in all infected groups with the infected non-eflornithine treated animals showing a slightly more intense PCR band than the eflornithine treated group (Figure 5.20). TNF-α mRNA was found in all groups of animals with weaker bands present in the uninfected groups and more intense PCR bands in the infected animals (Figure 5.21).

When the expression of MCP-1 was examined an increase in band intensity was noted in the infected mice compared to the uninfected animals (Figure 5.22). RT-PCR analyses for MIP-1α detected weak PCR bands in uninfected mice. The strongest expression of MIP-1α was found in infected non-eflornithine treated mice while 7 or 14 days of eflornithine treatment appeared to result in a slight reduction in the strength of this band (Figure 5.23). Expression of the chemokine RANTES was detected by the presence of PCR bands in material amplified from all groups of mice. The intensity of the bands was higher in the infected groups of mice compare to the uninfected animals.

No appreciable alterations in the expression of the cytokines and chemokines examined were detected between uninfected mice and uninfected animals treated with diminazene aceturate and eflornithine. This suggests that the these drugs have no effect on cytokine or chemokine transcription in the normal CNS.

5.3.2.2.1. Statistical analysis

The effect of eflornithine treatment on cytokine and chemokine expression when administered after a severe post-treatment reactive encephalopathy (PTRE) had been induced was analysed in a similar manner to that described above. Treatment groups where significant differences were detected are listed in Table 5.4. Summary statistics for the expression of each cytokine and chemokine, in all experimental regimens, as well as plots of the median expression levels are detailed in Figures 5.25-5.30.

When the levels of IL-1α expression were studied in the amelioration of a severe meningoencephalitis no differences were detected between any of the treatment groups. Infected animals treated with a double diminazene aceturate treatment to induce the PTRE prior to a 7-day course of eflornithine showed a median PCR value of 2.75. The same expression level (median 2.75) was seen in identically treated mice that were not given eflornithine. A slightly higher level of IL-1α expression (median 3.00) was seen after a 14-day course of eflornithine while the median remained at 2.75 in infected animals given a similar course of treatment but no eflornithine. No treatment regimens resulted in a

significant alteration, to level of IL-1α expression, from that found in uninfected control mice (median 2.00) (Figure 5.25).

No IL-6 expression was detected in the uninfected group of animals (median 0.00) whereas both groups infected mice, treated with two diminazene aceturate treatments, showed a significant elevation in IL-6 levels, compared with uninfected animals, with median values of 1.00 and 1.25. Eflornithine treatment of these infected mice did not result in any significant changes in IL-6 expression and animals receiving either a 7 or 14-day course of the drug returned a median PCR value of 1.00 (Figure 5.26).

Both groups of infected non-eflornithine treated mice expressed TNF-α. The level of TNF-α found in these mice (median 1.25, 1.75 respectively) was not statistically different to that seen in the uninfected group of animals (median 0.125). The administration of either a 7 or 14-day eflornithine course to infected, diminazene aceturate treated mice resulted in an increase in the expression of TNF-α (median 2.00, 2.00 respectively). Although this was not statistically higher than the expression seen in the infected non-eflornithine treated mice it was significantly higher that of the uninfected animals (Figure 5.27).

No significant differences were detected, between any of the treatment groups, in the expression levels of MCP-1. Infected animals given a 7-day course of eflornithine showed a median PCR value of 1.75 this was slightly higher when the course of treatment was extended to 14 days (median 2.00). Uninfected mice gave the lowest levels of expression (median 1.00) while the infected groups of animals that were not given eflornithine showed only a small increase in MCP-1 expression (median 1.25, 1.50 respectively) (Figure 5.28).

Uninfected mice expressed low levels of MIP-1α (median 0.375) this was significantly increased in infected non-eflornithine treated groups (median 2.75, 2.00 respectively). There a slight decrease in the level of this chemokine following a 7 days eflornithine course (median 1.00) and a 14-day eflornithine treatment period (median 1.50). The levels found in the eflornithine treated mice were not significantly reduced from those seen in animals that were not given eflornithine. However the reduction in the expression level resulted in no significant difference being detected between the eflornithine treated groups and the uninfected controls (Figure 5.29).

Infected animals given 7-days of eflornithine showed the highest levels of RANTES expression (median 3.00). This was significantly different to the expression of RANTES

found in the uninfected mice (median 1.50). When the eflornithine treatment was extended to 14-days a slightly lowered expression level was seen (median 1.50). The infected groups of animals not given eflornithine gave intermediated median PCR values of 1.75 and 2.00 respectively. The expression seen in these groups was not significantly altered from the levels found in any of the other treatment regimens (Figure 5.30).

	Infected + eflornithine	Infected - eflornithine	Uninfected, drug treated
Infected - eflornithine	p=0.100 (-0.046, 0.645)		
Uninfected, drug treated	p<0.0001 (-1.572, -0.732)	p<0.0001 (-1.881, -1.022)	
Mean ± Standard Error	1.028 ± 0.118	1.375 ± 0.110	0.00 ± 0.00
Number	18	14	9

Table 5.1. The effect of eflornithine treatment on the development of a CNS inflammatory reaction.

The neuropathological response scores were measured in groups of mice housed under three different treatment regimens. These groups comprised; mice infected with *T.b.brucei* GVR35/DFMO5.2, an eflornithine resistant trypanosome, given a 14-day course of 2% eflornithine in their drinking water beginning on day 14 post-infection and treated with diminazene aceturate (40mg/kg i.p.) on day 21 post infection to induce a CNS inflammatory response (infected + eflornithine); mice infected with *T.b.brucei* GVR35/DFMO5.2 and treated with diminazene aceturate (40mg/kg i.p.) on day 21 post infection (infected - eflornithine) and uninfected animals given a 14-day course of 2% eflornithine in their drinking water beginning on day 14 of the experiment and treated with diminazene aceturate (40mg/kg i.p.) on day 21 of the procedure (uninfected, drug treated). All animals were sacrifice on day 28 of the experiment and their brains processed for histopathological examination. The mean score and standard error, together with the number of animals, are shown for each group. The figures in the body of the table demonstrate the comparisons, in terms of statistical significance, between the groups shown in the row and column headings. The 95% confidence intervals for the differences between the group means are given along with the p-values. Figures detailed in red highlight groups showing significant differences.

	Infected, 7 days eflornithine	Infected, 14 days eflornithine	Infected, no eflornithine control 1	Infected, no eflornithine control 2	Uninfected, drug treated
Infected, 14 days eflornithine	p=0.0004 (-1.114, -0.253)				
Infected, no eflornithine control 1	p=0.773 (-2.90, 0.691)	p=0.0001 (0.373, 1.396)			
Infected, no eflornithine control 2	p=0.181 (-0.102, 0.879)	p<0.0001 (0.560, 1.583)	p=0.873 (-0.368, 0.743)		
Uninfected, drug treated	p<0.0001 (-3.253, -2.358)	p<0.0001 (-2.592, -1.652)	p<0.0001 (-3.543, -2.469)	p<0.0001 (-3.731, -2.657)	
Mean ± Standard Error	2.950 ± 0.130	2.271 ± 0.129	3.156 ± 0.170	3.348 ± 0.066	0.083 ± 0.064
Number	15	12	8	7	12

Table 5.2. The effect of eflornithine treatment on an established meningoencephalitis

The neuropathological response scores were measured in groups of mice housed under five different treatment regimens. These groups comprised; mice infected with *T.b.brucei* GVR35/DFMO5.2, an eflornithine resistant trypanosome, given a 7-day course of 2% eflornithine in their drinking water beginning 7 days after a second diminazene aceturate (40mg/kg i.p.) to induce a severe CNS inflammatory reaction (infected, 7 days eflornithine); mice infected with *T.b.brucei* GVR35/DFMO5.2 given a 14-day course of 2% eflornithine beginning 7 days after a second diminazene aceturate (infected, 14 days eflornithine); mice infected with *T.b.brucei* GVR35/ DFMO5.2 and killed 14 days after the administration of a second diminazene aceturate treatment (infected, no eflornithine control 1); mice infected with *T.b.brucei* GVR35/DFMO5.2 and killed 21 days after the administration of a second diminazene aceturate treatment (infected, no eflornithine control 2) and uninfected animals treated with both diminazene aceturate and eflornithine (uninfected, drug treated). The mean score and standard error, together with the number of animals, are shown for each group. The figures in the body of the table demonstrate the comparisons, in terms of statistical significance, between the groups shown in the row and column headings. The 95% confidence intervals for the differences between the group means are given along with the p-values. Figures detailed in red highlight groups showing significant differences.

IL-1α	IL-6	TNF-α	MCP-1	MIP-1α	RANTES
Experiment 1					
NDD	I-E vs UIC	I+E vs UIC	I+E vs UIC	I-E vs UIC	NDD
Experiment 2					
NDD	NDD	NDD	NDD	NDD	NDD
Experiments 1 & 2					
I-E vs UIC	I-E vs UIC	I-E vs UIC	I+E vs UIC	NDD	I+E vs UIC
I-E vs I+E	I-E vs I+E	I+E vs UIC	I-E vs UIC		I-E vs UIC

Table 5.3. Assessment of differential cytokine and chemokine expression in the brain of trypanosome infected mice in the presence and absence of eflornithine treatment.

Following RT-PCR analyses the intensity of the resulting PCR band, as seen on a 2% agarose gel stained with ethidium bromide, was taken as an indication of the quantity of target sequence present in the initial sample. This was graded on a scale of 0 to 4 where 0 indicated no band and 4 indicated an extremely intense PCR band. The data generated from these tests were analysed to determine if there were significant differences ($p<0.05$) in the expression of the cytokines IL-1α, IL-6 and TNFα and the chemokines MCP-1, MIP-1α and RANTES between; mice infected with *T.b.brucei* GVR35/C1.3 DFMO 5.2 given a 14-day course of 2% eflornithine in their drinking water beginning on day 14 post-infection and treated with diminazene aceturate (40mg/kg i.p.) on day 21 post-infection (I+E); mice infected with *T.b.brucei* GVR35/C1.3 DFMO 5.2 and treated on day 21 post-infection with diminazene aceturate (40mg/kg i.p.) (I-E); and uninfected animals given a 14-day course of 2% eflornithine in their drinking water beginning on day 14 of the experiment and treated with diminazene aceturate (40mg/kg i.p.) on day 21 of the procedure (UIC). All animals were killed on day 28 of the experiment. The analyses of the data from experiment 1 and 2 as well as the combined data from both experiments are shown. Only groups determined to be significantly different to each other are listed. NDD, no differences detected.

IL-1α	IL-6	TNF-α	MCP-1	MIP-1α	RANTES
		Experiment 1			
NDD	NDD	NDD	NDD	NDD	NDD
		Experiment 2			
NDD	I+E7 vs UIC	NDD	NDD	NDD	NDD
		Experiment 3			
NDD	NDD	NDD	NDD	NDD	NDD
		Experiments 1, 2 & 3			
NDD	I-E2 vs UIC I+E7 vs UIC I-E1 vs UIC I+E14 vs UIC	I+E14 vs UIC I+E7 vs UIC	NDD	I-E1 vs UIC I-E2 vs UIC	I+E7 vs UIC

Table 5.4. Assessment of the effect of eflornithine on differential cytokine and chemokine expression in the brain of trypanosome infected mice with an established meningoencephalitis.

Following RT-PCR analyses the intensity of the resulting PCR band, as seen on a 2% agarose gel stained with ethidium bromide, was taken as an indication of the quantity of target sequence present in the initial sample. This was graded on a scale of 0 to 4 where 0 indicated no band and 4 indicated an extremely intense PCR band. The data generated from these tests were analysed to determine if there were significant differences ($p<0.05$) in the expression of the cytokines IL-1α, IL-6 and TNFα and the chemokines MCP-1, MIP-1α and RANTES between; mice infected with *T.b.brucei* GVR35/C1.3 DFMO 5.2 treated with diminazene aceturate (40mg/kg i.p.) on day 21 post-infection , re-treated on relapse to parasitaemia and given a 7-day (I+E7) or 14 day (I+E14) course of 2% eflornithine in their drinking water beginning 7 days after the second diminazene aceturate treatment; mice infected with *T.b.brucei* GVR35/C1.3 DFMO 5.2 and treated on day 21 post-infection with diminazene aceturate (40mg/kg i.p.), retreated on relapse to parasitaemia and killed 14 (I-E1) or 21 (I-E2) days later ; and uninfected animals and treated with both diminazene aceturate and eflornithine in parallel with the experimental groups (UIC). The analyses of the data from experiment 1 and 2 as well as the combined data from both experiments are shown. Only groups determined to be significantly different to each other are listed. NDD, no differences detected.

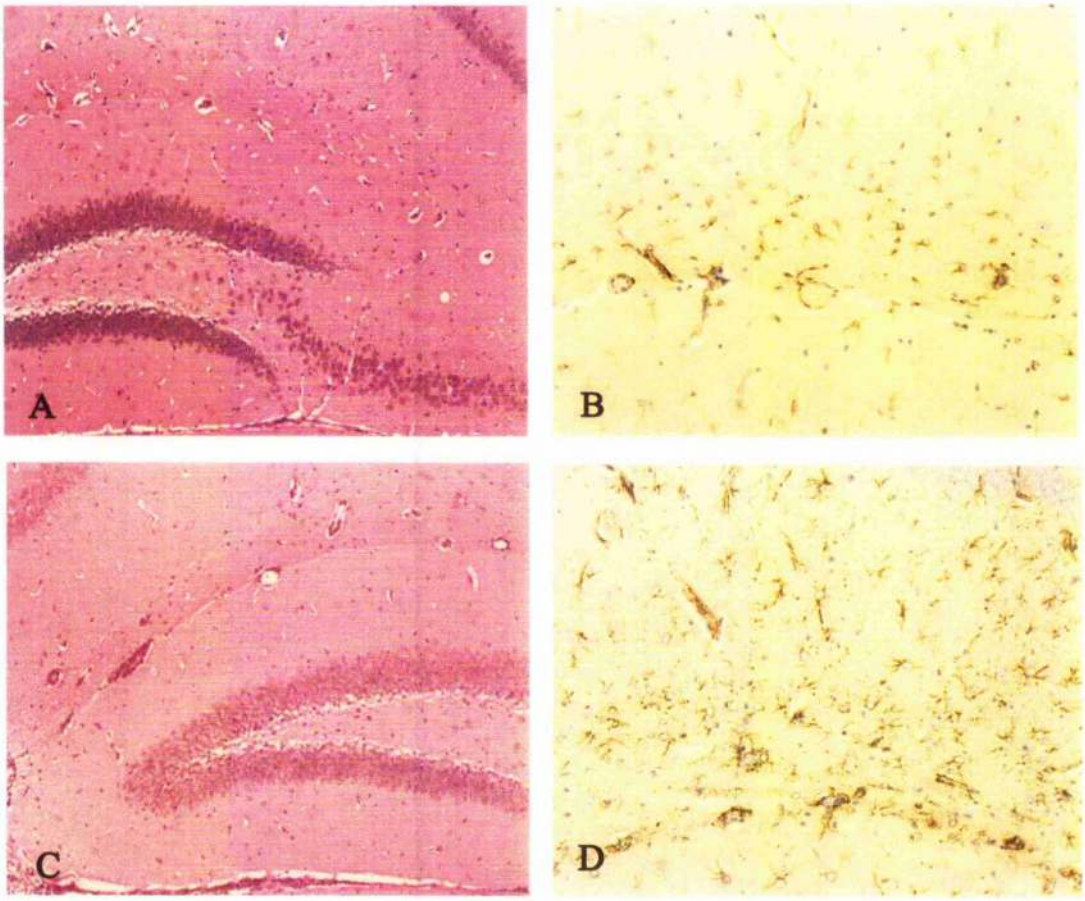

Figure 5.3. Prevention of the CNS-inflammatory reaction by eflornithine treatment.

Coronal sections through the hippocampal region of the brain prepared from trypanosome-infected mice treated on day 21 post-infection with diminazene aceturate. The mice were either treated (A&B) or not treated (C&D) with a 14 day course of eflornithine beginning on day 14 post-infection. The figure demonstrates the reduction in inflammatory cell infiltration, characterised by fewer cells in the ventricle and perivascular cuffs (A) and the down-regulation of astrocyte activation (B) that results from eflornithine treatment compared with non-eflornithine treated mice (C&D). Panels A&C, H&E, X150; panels B&D, GFAP, X300.

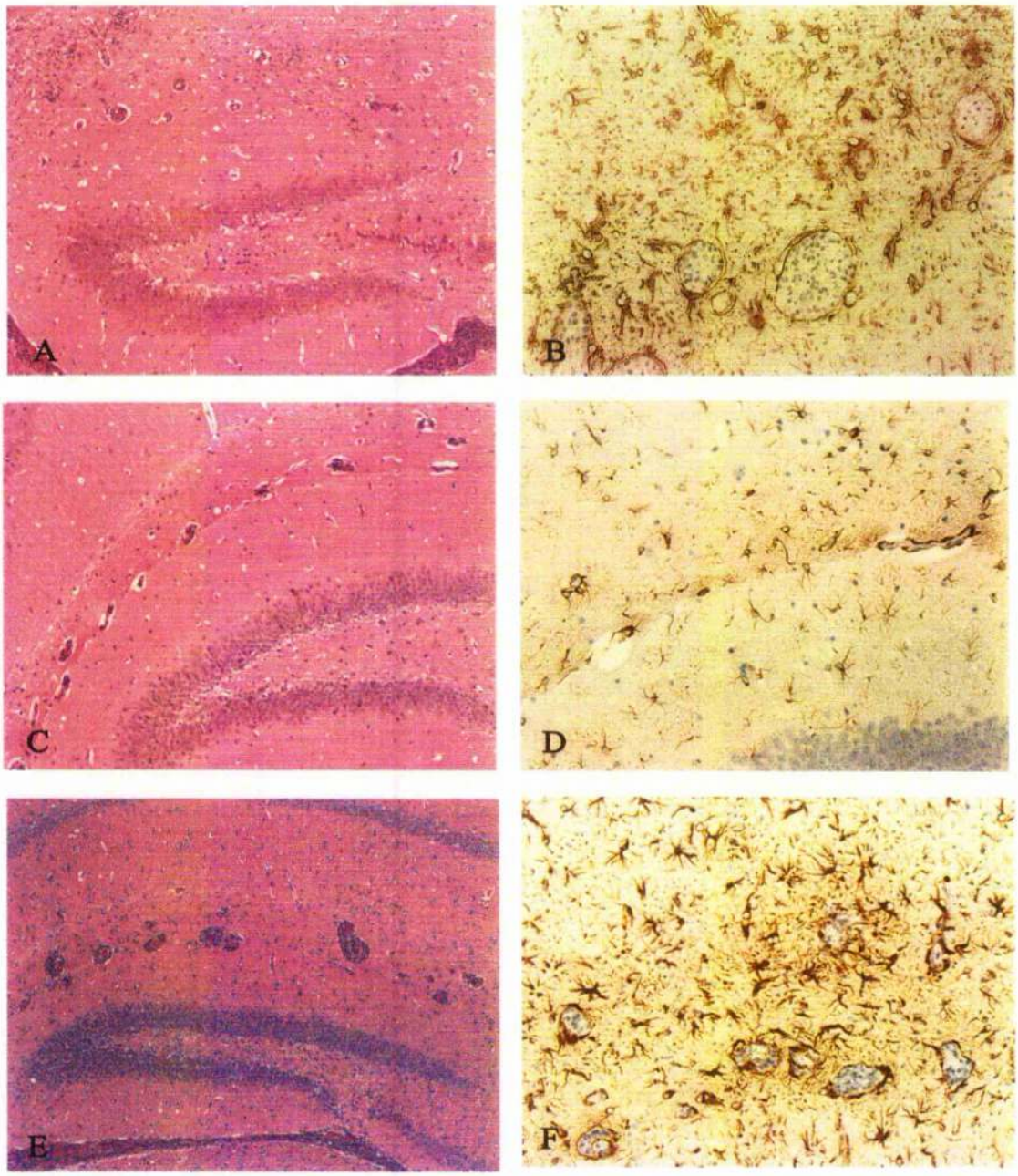

Figure 5.4. Amelioration of an established meningoencephalitis by eflornithine treatment.

Coronal sections through the hippocampal region of the brain prepared from trypanosome-infected mice treated on day 21 post-infection with diminazene aceturate and given a second dose of the drug following relapse to parasitaemia. Mice were given a course of eflornithine, beginning 7 days after administration of the second diminazene aceturate treatment, for a period of 7 (A&B) or 14 (C&D) days. Additional animals did not receive eflornithine treatment (E&F). The figure shows the dose dependent anti-inflammatory effect of eflornithine treatment. Animals given a 7 day course of the drug show a reduction in inflammatory cell infiltration (A) and astrocyte activation (B) compared with non-eflornithine treated mice (E&F). Following a 14 day course of eflornithine the inflammatory reaction in further reduced with fewer cells in the perivascular cuffs, a resolution of the encephalitis (C) and a dramatic reduction in astrocyte activation (D). Panels A, C & E, H&E, X150; panels B, D & F, GFAP, X300.

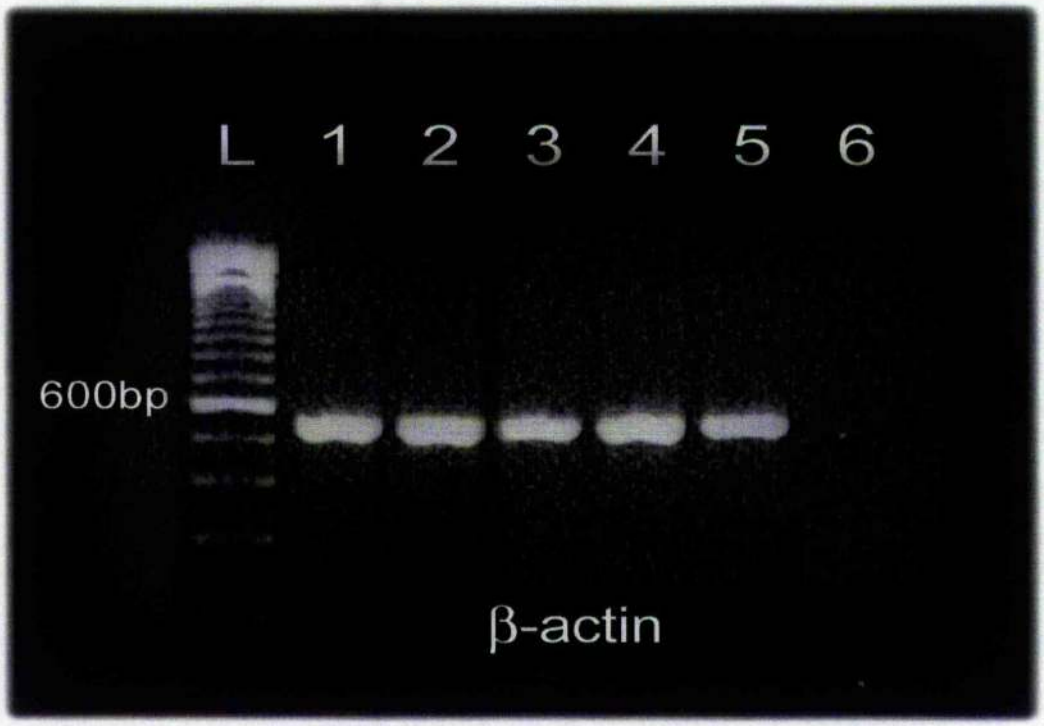

Figure 5.5. β-actin check gel for groups of animals used to study the development of a CNS inflammatory reaction.

To ensure that the mRNA extracted from each group of animals was of a similar quality, amplification of the mRNA of housekeeping gene β-actin was carried out. RT-PCR was performed on the mRNA extracted from; mice infected with *T.b.brucei* GVR35/C1.3 DFMO 5.2 and treated on day 21 post-infection with diminazene aceturate (40mg/kg i.p.) to induce a CNS inflammatory reaction (lane 1); infected animals given a 14-day course of 2% eflornithine in their drinking water beginning at day 14 post-infection and treated with diminazene aceturate on day 21 post-infection (lane 2); normal uninfected mice (lane 3); and uninfected mice treated with diminazene aceturate and eflornithine (lane 4). All animals were killed on day 28 of the experimental procedure. A known positive control (lane 5) and negative control consisting of water in place of template (lane 6) were also included in the RT-PCR reaction. All band are of a similar intensity thus allowing comparisons to be made with regard to the expression levels of the cytokines and chemokines using RT-PCR analyses.

Figure 5.6. The effect of eflornithine on IL-1α expression in the development of a CNS inflammatory reaction.

RT-PCR was performed to detect IL-1α expression, on the mRNA extracted from; mice infected with *T.b.brucei* GVR35/C1.3 DFMO 5.2 and treated on day 21 post-infection with diminazene aceturate (40mg/kg i.p.) to induce a CNS inflammatory reaction (lane 1); infected animals given a 14-day course of 2% eflornithine in their drinking water beginning at day 14 post-infection and treated with diminazene aceturate on day 21 post-infection (lane 2); normal uninfected mice (lane 3); and uninfected mice treated with diminazene aceturate and eflornithine (lane 4). All animals were killed on day 28 of the experimental procedure. A known positive control (lane 5) and negative control consisting of water in place of template (lane 6) were also included in the RT-PCR reaction. IL-α expression was detected in all groups of mice. Lane 1 shows the strongest PCR band and results from the amplification of mRNA from infected, non-eflornithine treated mice. Uninfected animals express IL-1α (lanes 3 & 4) at a much lower level. While infected eflornithine treated mice express IL-1α at an intermediated level (lane 2).

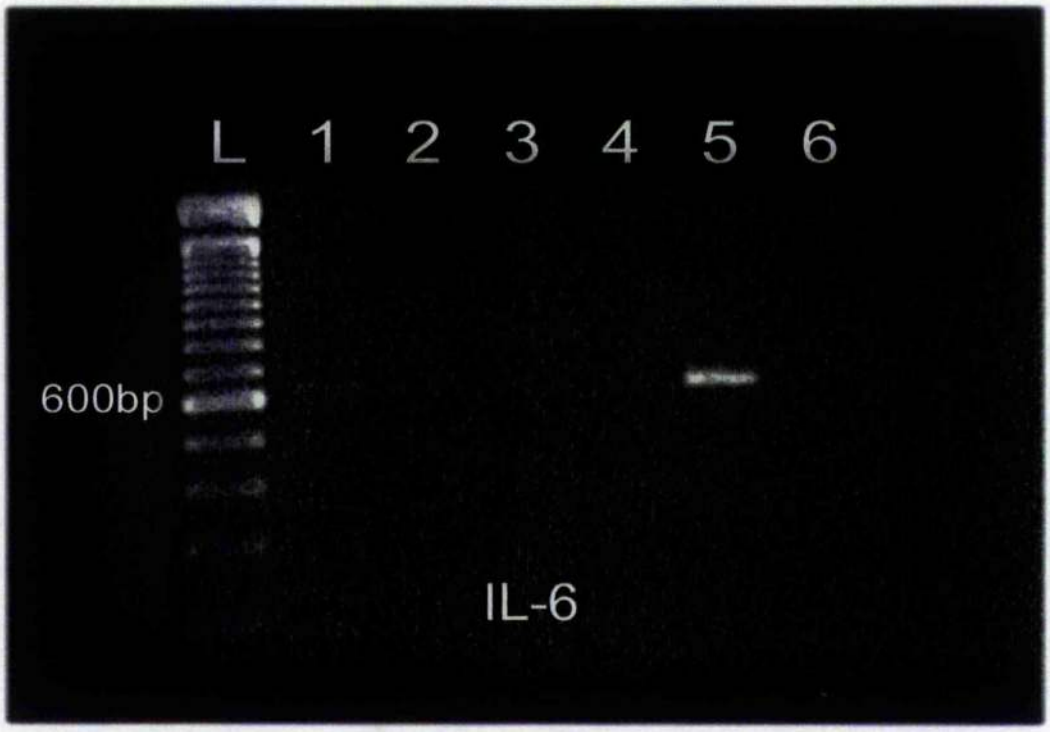

Figure 5.7. The effect of eflornithine on IL-6 expression in the development of a CNS inflammatory reaction.

RT-PCR was performed to detect IL-6 expression, on the mRNA extracted from; mice infected with *T.b.brucei* GVR35/C1.3 DFMO 5.2 and treated on day 21 post-infection with diminazene aceturate (40mg/kg i.p.) to induce a CNS inflammatory reaction (lane 1); infected animals given a 14-day course of 2% eflornithine in their drinking water beginning at day 14 post-infection and treated with diminazene aceturate on day 21 post-infection (lane 2); normal uninfected mice (lane 3); and uninfected mice treated with diminazene aceturate and eflornithine (lane 4). All animals were killed on day 28 of the experimental procedure. A known positive control (lane 5) and negative control consisting of water in place of template (lane 6) were also included in the RT-PCR reaction. The PCR bands resulting from the amplification of mRNA from infected, non-eflornithine treated mice can be seen in lane 1. A much weaker band, was present in the animals treated with eflornithine, although this image was difficult to capture (lane 2). No IL-6 expression was seen in uninfected mice (lanes 3 & 4).

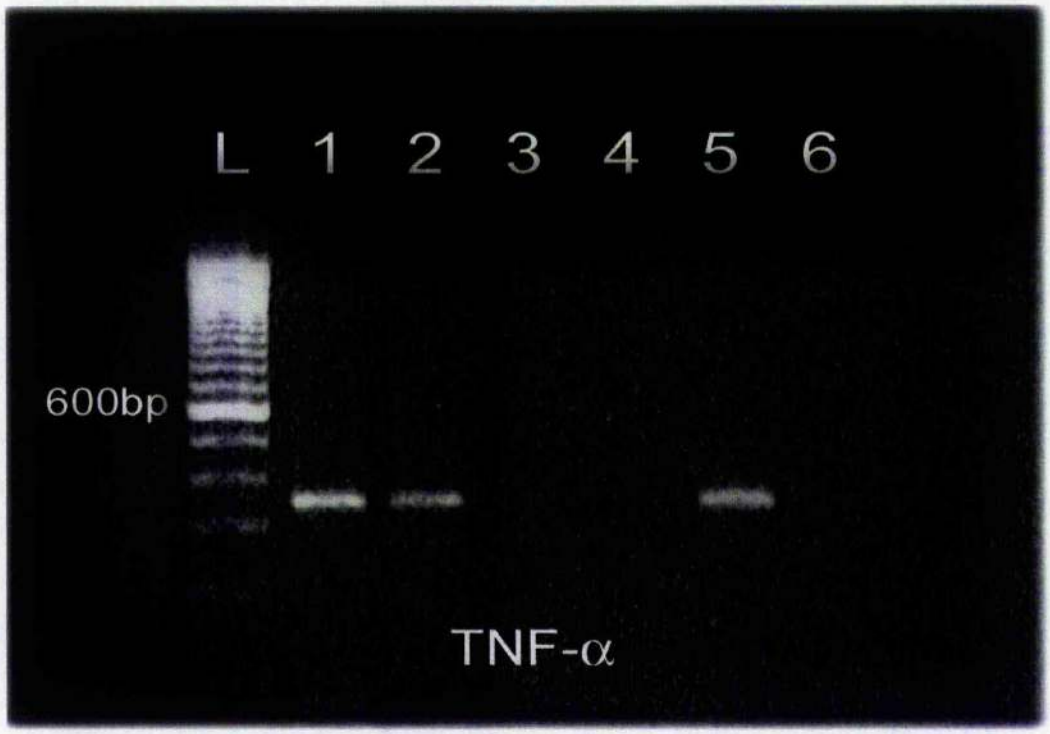

Figure 5.8. The effect of eflornithine on TNF-α expression in the development of a CNS inflammatory reaction.

RT-PCR was performed to detect TNF-α expression, on the mRNA extracted from; mice infected with *T.b.brucei* GVR35/C1.3 DFMO 5.2 and treated on day 21 post-infection with diminazene aceturate (40mg/kg i.p.) to induce a CNS inflammatory reaction (lane 1); infected animals given a 14-day course of 2% eflornithine in their drinking water beginning at day 14 post-infection and treated with diminazene aceturate on day 21 post-infection (lane 2); normal uninfected mice (lane 3); and uninfected mice treated with diminazene aceturate and eflornithine (lane 4). All animals were killed on day 28 of the experimental procedure. A known positive control (lane 5) and negative control consisting of water in place of template (lane 6) were also included in the RT-PCR reaction. The PCR bands resulting from the amplification of mRNA from infected, non-eflornithine treated mice and infected animals given eflornithine are of similar intensity (lanes 1 & 2 respectively). While, uninfected animals show no TNF-α (lanes 3 & 4) expression.

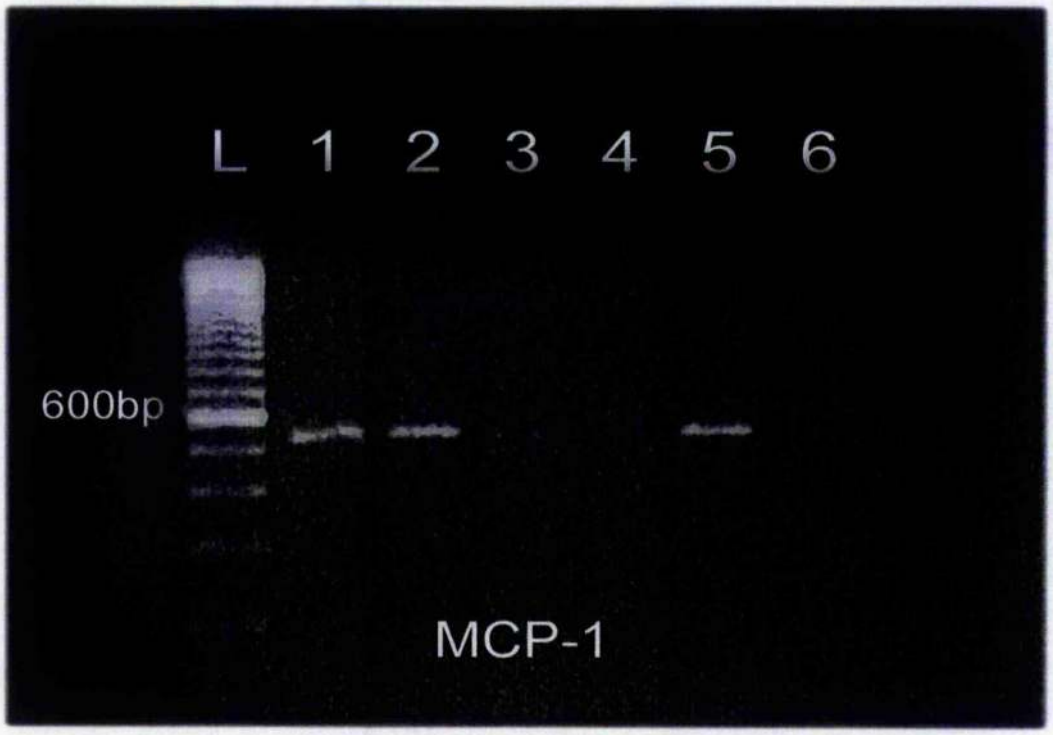

Figure 5.9. The effect of eflornithine on MCP-1 expression in the development of a CNS inflammatory reaction.

RT-PCR was performed to detect MCP-1 expression, on the mRNA extracted from; mice infected with *T.b.brucei* GVR35/C1.3 DFMO 5.2 and treated on day 21 post-infection with diminazene aceturate (40mg/kg i.p.) to induce a CNS inflammatory reaction (lane 1); infected animals given a 14-day course of 2% eflornithine in their drinking water beginning at day 14 post-infection and treated with diminazene aceturate on day 21 post-infection (lane 2); normal uninfected mice (lane 3); and uninfected mice treated with diminazene aceturate and eflornithine (lane 4). All animals were killed on day 28 of the experimental procedure. A known positive control (lane 5) and negative control consisting of water in place of template (lane 6) were also included in the RT-PCR reaction. MCP-1 expression was detected in all groups of mice. The PCR bands resulting from the amplification of mRNA from infected, non-eflornithine treated mice and infected animals given eflornithine are of similar intensity (lanes 1 & 2 respectively). While, uninfected animals showed only an extremely low level of MCP-1 expression, that was difficult to capture on film (lanes 3 & 4).

Figure 5.10. The effect of eflornithine on MIP-1α expression in the development of a CNS inflammatory reaction.

RT-PCR was performed to detect MIP-1α expression, on the mRNA extracted from; mice infected with *T.b.brucei* GVR35/C1.3 DFMO 5.2 and treated on day 21 post-infection with diminazene aceturate (40mg/kg i.p.) to induce a CNS inflammatory reaction (lane 1); infected animals given a 14-day course of 2% eflornithine in their drinking water beginning at day 14 post-infection and treated with diminazene aceturate on day 21 post-infection (lane 2); normal uninfected mice (lane 3); and uninfected mice treated with diminazene aceturate and eflornithine (lane 4). All animals were killed on day 28 of the experimental procedure. A known positive control (lane 5) and negative control consisting of water in place of template (lane 6) were also included in the RT-PCR reaction. MIP-1α expression was detected in all groups of mice. The PCR band resulting from the amplification of mRNA from infected, non-eflornithine treated mice was of the strongest intensity (lane 1). Eflornithine treatment of uninfected mice resulted in a less intense PCR band (lane 2) while uninfected animals expressed MIP-1α at a much lower level (lanes 3 & 4).

Figure 5.11. The effect of eflornithine on RANTES expression in the development of a CNS inflammatory reaction.

RT-PCR was performed to detect RANTES expression, on the mRNA extracted from; mice infected with *T.b.brucei* GVR35/C1.3 DFMO 5.2 and treated on day 21 post-infection with diminazene aceturate (40mg/kg i.p.) to induce a CNS inflammatory reaction (lane 1); infected animals given a 14-day course of 2% eflornithine in their drinking water beginning at day 14 post-infection and treated with diminazene aceturate on day 21 post-infection (lane 2); normal uninfected mice (lane 3); and uninfected mice treated with diminazene aceturate and eflornithine (lane 4). All animals were killed on day 28 of the experimental procedure. A known positive control (lane 5) and negative control consisting of water in place of template (lane 6) were also included in the RT-PCR reaction. RANTES expression was detected in all groups of mice. Both the infected non-eflornithine treated (lane 1) and the infected eflornithine treated (lane 2) group of mice show much higher levels of RANTES expression than the uninfected animals (lane 3 & 4).

	Treatment Groups		
	Infected + eflornithine	Infected - eflornithine	Uninfected, drug treated
		Experiment 1	
Median	1.75	3.00	1.50
Upper quartile	3.00	3.00	1.50
Lower quartile	1.00	3.00	1.50
Maximum	3.00	3.00	1.50
Minimum	1.00	1.50	1.50
Number	6	3	3
		Experiment 2	
Median	1.00	2.50	1.00
Upper quartile	1.50	2.625	*
Lower quartile	1.00	2.00	*
Maximum	1.50	3.00	1.00
Minimum	1.00	2.00	1.00
Number	5	6	1
		Experiments 1 & 2	
Median	1.50	2.50	1.50
Upper quartile	2.00	3.00	1.50
Lower quartile	1.00	2.25	1.125
Maximum	3.00	3.00	1.50
Minimum	1.00	2.00	1.00
Number	11	9	4

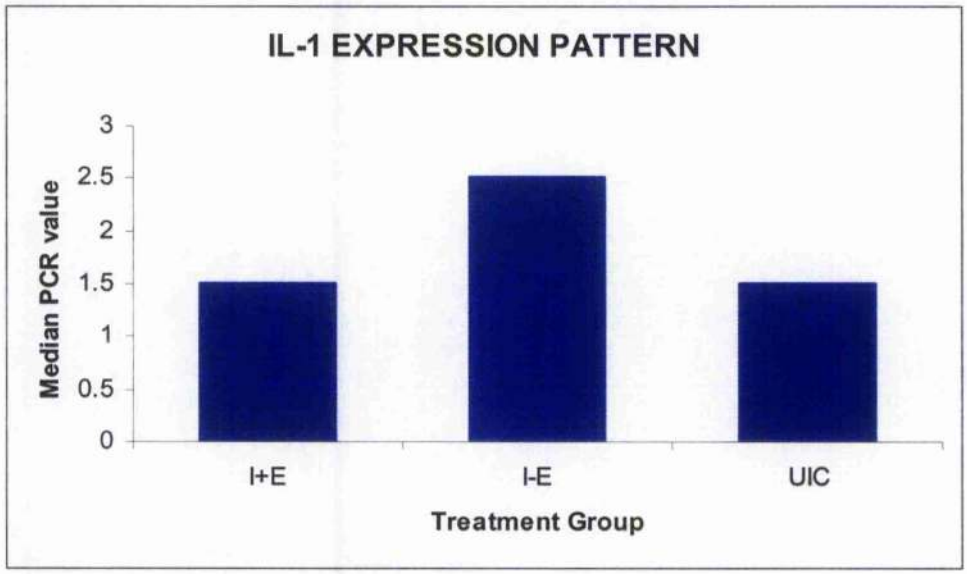

Figure 5.12. Summary statistics for IL-1α

The expression level of IL-1α in mouse brain was assessed in 3 groups of mice; infected with *T.b.brucei* GVR35/C1.3 DFMO 5.2 given a 14-day course of 2% eflornithine in their drinking water beginning on day 14 post-infection and treated with diminazene aceturate (40mg/kg i.p.) on day 21 post-infection (I+E); infected with *T.b.brucei* GVR35/C1.3 DFMO 5.2 and treated on day 21 post-infection with diminazene aceturate (40mg/kg i.p.) (I-E); and uninfected animals given a 14-day course of 2% eflornithine in their drinking water beginning on day 14 of the experiment and treated with diminazene aceturate (40mg/kg i.p.) on day 21 of the procedure (UIC). All animals were killed on day 28 of the experiment. Following RT-PCR analyses the intensity of the resulting PCR band, as seen on a 2% agarose gel stained with ethidium bromide, was taken as an indication of the quantity of IL-1α mRNA present in the initial sample. This was graded on a scale of 0 to 4 where 0 indicated no band and 4 indicated an extremely intense PCR band. The analyses of the data from experiment 1 and 2 as well as the combined data from both experiments are shown. Summary statistics are given for each group of animals and the medians of the combined results from experiments 1 and 2 are plotted to indicate any expression trends. * too few data points.

	Treatment Groups		
	Infected + eflornithine	Infected - eflornithine	Uninfected, drug treated
		Experiment 1	
Median	0.125	0.50	0.00
Upper quartile	0.25	0.50	0.00
Lower quartile	0.00	0.50	0.00
Maximum	0.25	0.50	0.00
Minimum	0.00	0.50	0.00
Number	6	3	3
		Experiment 2	
Median	0.50	1.00	0.00
Upper quartile	0.50	2.25	*
Lower quartile	0.25	0.50	*
Maximum	0.50	3.00	0.00
Minimum	0.25	0.50	0.00
Number	5	6	1
		Experiments 1 & 2	
Median	0.25	0.50	0.00
Upper quartile	0.50	1.50	0.00
Lower quartile	0.00	0.50	0.00
Maximum	0.50	3.00	0.00
Minimum	0.00	0.50	0.00
Number	11	9	4

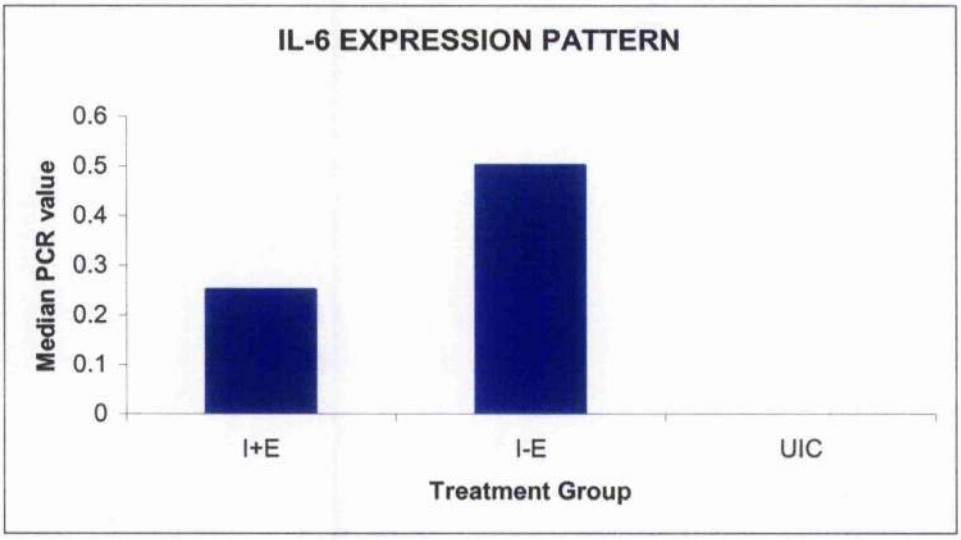

Figure 5.13. Summary statistics for IL-6

The expression level of IL-6 in mouse brain was assessed in 3 groups of mice; infected with *T.b.brucei* GVR35/C1.3 DFMO 5.2 given a 14-day course of 2% eflornithine in their drinking water beginning on day 14 post-infection and treated with diminazene aceturate (40mg/kg i.p.) on day 21 post-infection (I+E); infected with *T.b.brucei* GVR35/C1.3 DFMO 5.2 and treated on day 21 post-infection with diminazene aceturate (40mg/kg i.p.) (I-E); and uninfected animals given a 14-day course of 2% eflornithine in their drinking water beginning on day 14 of the experiment and treated with diminazene aceturate (40mg/kg i.p.) on day 21 of the procedure (UIC). All animals were killed on day 28 of the experiment. Following RT-PCR analyses the intensity of the resulting PCR band, as seen on a 2% agarose gel stained with ethidium bromide, was taken as an indication of the quantity of IL-6 mRNA present in the initial sample. This was graded on a scale of 0 to 4 where 0 indicated no band and 4 indicated an extremely intense PCR band. The analyses of the data from experiment 1 and 2 as well as the combined data from both experiments are shown. Summary statistics are given for each group of animals and the medians of the combined results from experiments 1 and 2 are plotted to indicate any expression trends. * too few data points.

	Treatment Groups		
	Infected + eflornithine	Infected - eflornithine	Uninfected, drug treated
		Experiment 1	
Median	1.50	0.50	0.00
Upper quartile	2.00	1.00	0.00
Lower quartile	0.875	0.50	0.00
Maximum	2.00	1.00	0.00
Minimum	0.50	0.00	0.00
Number	6	3	3
		Experiment 2	
Median	0.50	1.75	0.00
Upper quartile	0.75	3.00	*
Lower quartile	0.375	1.00	*
Maximum	1.00	3.00	0
Minimum	0.25	1.00	0
Number	5	6	1
		Experiments 1 & 2	
Median	1.00	1.00	0.00
Upper quartile	2.00	2.50	0.00
Lower quartile	0.50	0.75	0.00
Maximum	2.00	3.00	0.00
Minimum	0.25	0.50	3.00
Number	11	9	4

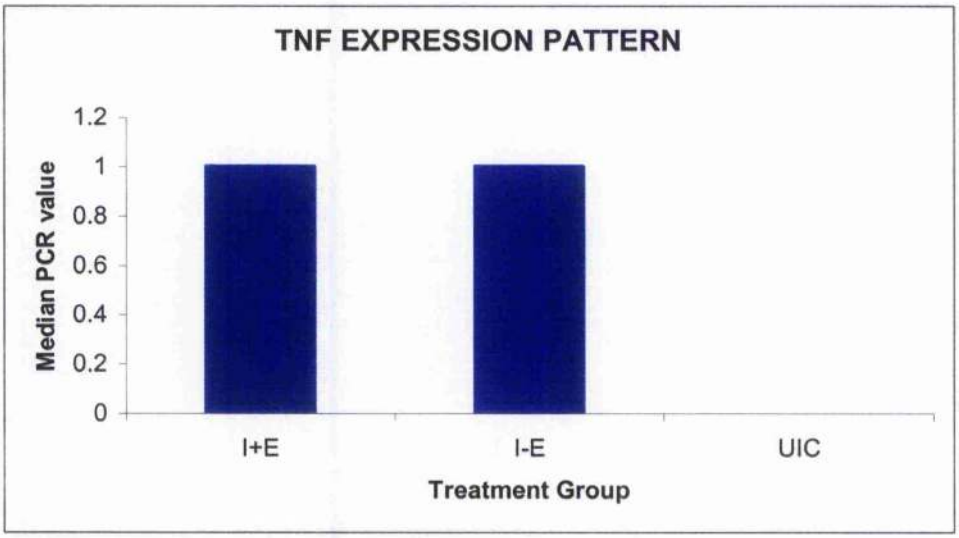

Figure 5.14. Summary statistics for TNF-α

The expression level of TNF-α in mouse brain was assessed in 3 groups of mice; infected with *T.b.brucei* GVR35/C1.3 DFMO 5.2 given a 14-day course of 2% eflornithine in their drinking water beginning on day 14 post-infection and treated with diminazene aceturate (40mg/kg i.p.) on day 21 post-infection (I+E); infected with *T.b.brucei* GVR35/C1.3 DFMO 5.2 and treated on day 21 post-infection with diminazene aceturate (40mg/kg i.p.) (I-E); and uninfected animals given a 14-day course of 2% eflornithine in their drinking water beginning on day 14 of the experiment and treated with diminazene aceturate (40mg/kg i.p.) on day 21 of the procedure (UIC). All animals were killed on day 28 of the experiment. Following RT-PCR analyses the intensity of the resulting PCR band, as seen on a 2% agarose gel stained with ethidium bromide, was taken as an indication of the quantity of TNF-α mRNA present in the initial sample. This was graded on a scale of 0 to 4 where 0 indicated no band and 4 indicated an extremely intense PCR band. The analyses of the data from experiment 1 and 2 as well as the combined data from both experiments are shown. Summary statistics are given for each group of animals and the medians of the combined results from experiments 1 and 2 are plotted to indicate any expression trends. * too few data points.

	Treatment Groups		
	Infected + eflornithine	Infected - eflornithine	Uninfected, drug treated
		Experiment 1	
Median	2.00	1.50	0.25
Upper quartile	2.625	2.00	0.50
Lower quartile	1.00	1.00	0.50
Maximum	3.00	2.00	0.50
Minimum	1.00	1.00	0.00
Number	6	3	3
		Experiment 2	
Median	1.50	1.25	0
Upper quartile	1.50	1.625	*
Lower quartile	0.75	0.875	*
Maximum	1.50	2.00	0
Minimum	0.50	0.50	0
Number	5	6	1
		Experiments 1 & 2	
Median	1.50	1.50	0.125
Upper quartile	2.00	1.75	0.438
Lower quartile	1.00	1.00	0.00
Maximum	3.00	2.00	0.50
Minimum	0.50	0.50	0.00
Number	11	9	4

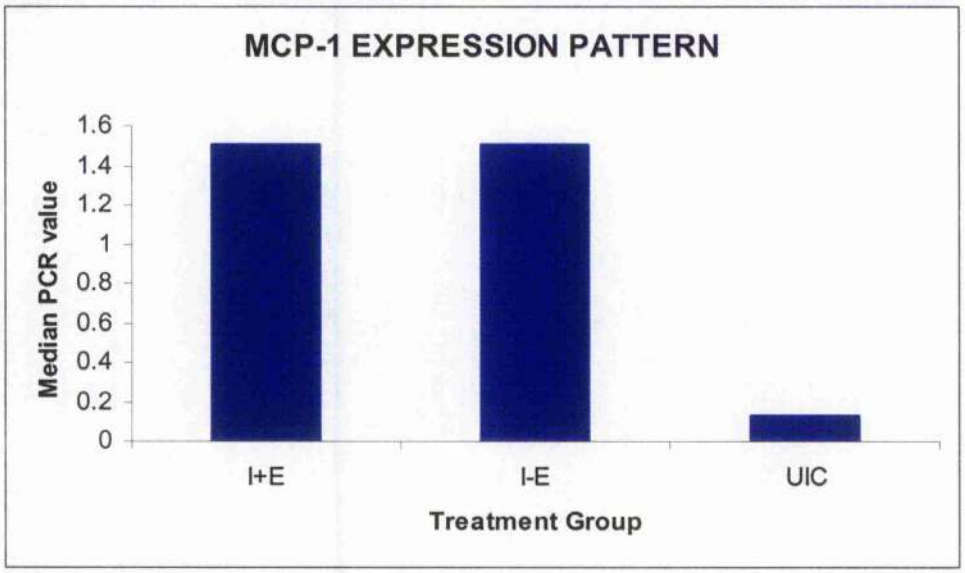

Figure 5.15. Summary statistics for MCP-1

The expression level of MCP-1 in mouse brain was assessed in 3 groups of mice; infected with *T.b.brucei* GVR35/C1.3 DFMO 5.2 given a 14-day course of 2% eflornithine in their drinking water beginning on day 14 post-infection and treated with diminazene aceturate (40mg/kg i.p.) on day 21 post-infection (I+E); infected with *T.b.brucei* GVR35/C1.3 DFMO 5.2 and treated on day 21 post-infection with diminazene aceturate (40mg/kg i.p.) (I-E); and uninfected animals given a 14-day course of 2% eflornithine in their drinking water beginning on day 14 of the experiment and treated with diminazene aceturate (40mg/kg i.p.) on day 21 of the procedure (UIC). All animals were killed on day 28 of the experiment. Following RT-PCR analyses the intensity of the resulting PCR band, as seen on a 2% agarose gel stained with ethidium bromide, was taken as an indication of the quantity of MCP-1 mRNA present in the initial sample. This was graded on a scale of 0 to 4 where 0 indicated no band and 4 indicated an extremely intense PCR band. The analyses of the data from experiment 1 and 2 as well as the combined data from both experiments are shown. Summary statistics are given for each group of animals and the medians of the combined results from experiments 1 and 2 are plotted to indicate any expression trends. * too few data points.

	Treatment Groups		
	Infected + eflornithine	Infected - eflornithine	Uninfected, drug treated
		Experiment 1	
Median	1.00	1.50	1.00
Upper quartile	1.50	2.00	2.00
Lower quartile	0.875	1.50	0.00
Maximum	1.50	2.00	2.00
Minimum	0.50	1.50	0.00
Number	6	3	3
		Experiment 2	
Median	1.50	2.00	0.00
Upper quartile	1.75	3.00	*
Lower quartile	0.75	1.50	*
Maximum	2.00	3.00	0
Minimum	0.50	1.50	0
Number	5	6	1
		Experiments 1 & 2	
Median	1.00	1.50	0.50
Upper quartile	1.50	2.75	1.75
Lower quartile	1.00	1.50	0.00
Maximum	2.00	3.00	2.00
Minimum	0.50	1.50	0.00
Number	11	9	4

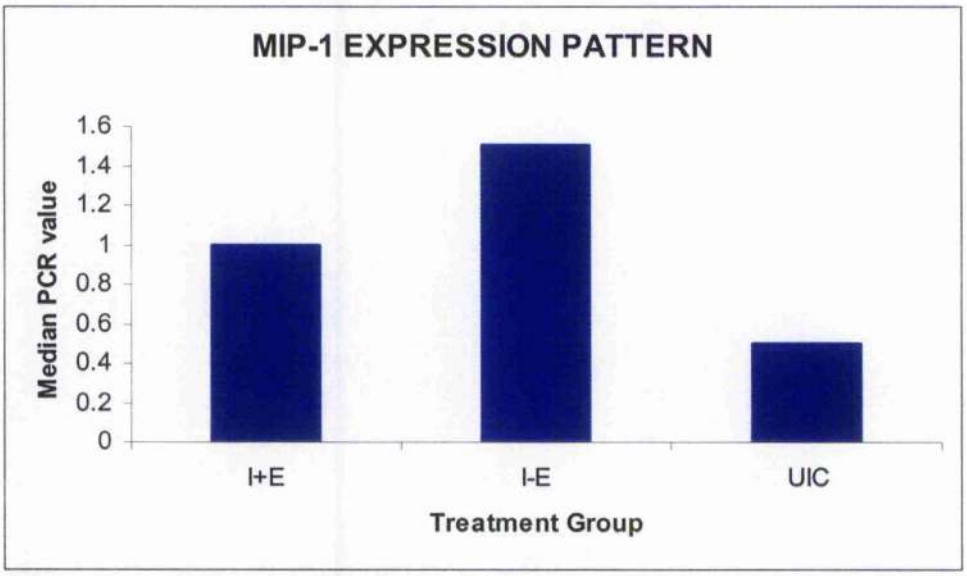

Figure 5.16. Summary statistics for MIP-1α

The expression level of MIP-1α in mouse brain was assessed in 3 groups of mice; infected with *T.b.brucei* GVR35/C1.3 DFMO 5.2 given a 14-day course of 2% eflornithine in their drinking water beginning on day 14 post-infection and treated with diminazene aceturate (40mg/kg i.p.) on day 21 post-infection (I+E); infected with *T.b.brucei* GVR35/C1.3 DFMO 5.2 and treated on day 21 post-infection with diminazene aceturate (40mg/kg i.p.) (I-E); and uninfected animals given a 14-day course of 2% eflornithine in their drinking water beginning on day 14 of the experiment and treated with diminazene aceturate (40mg/kg i.p.) on day 21 of the procedure (UIC). All animals were killed on day 28 of the experiment. Following RT-PCR analyses the intensity of the resulting PCR band, as seen on a 2% agarose gel stained with ethidium bromide, was taken as an indication of the quantity of MIP-1α mRNA present in the initial sample. This was graded on a scale of 0 to 4 where 0 indicated no band and 4 indicated an extremely intense PCR band. The analyses of the data from experiment 1 and 2 as well as the combined data from both experiments are shown. Summary statistics are given for each group of animals and the medians of the combined results from experiments 1 and 2 are plotted to indicate any expression trends. * too few data points.

	Treatment Groups		
	Infected + eflornithine	Infected - eflornithine	Uninfected, drug treated
		Experiment 1	
Median	1.50	2.50	1.00
Upper quartile	1.625	2.50	1.00
Lower quartile	1.00	1.50	0.00
Maximum	1.00	1.50	0.00
Minimum	1.00	1.50	0.00
Number	6	3	3
		Experiment 2	
Median	3.00	3.00	0.50
Upper quartile	3.00	3.00	*
Lower quartile	3.00	2.875	*
Maximum	3.00	3.00	0.50
Minimum	3.00	2.05	0.50
Number	5	6	1
		Experiments 1 & 2	
Median	2.00	3.00	0.75
Upper quartile	3.00	3.00	1.00
Lower quartile	1.50	2.50	0.125
Maximum	3.00	3.00	1.00
Minimum	1.00	1.50	0.00
Number	11	9	4

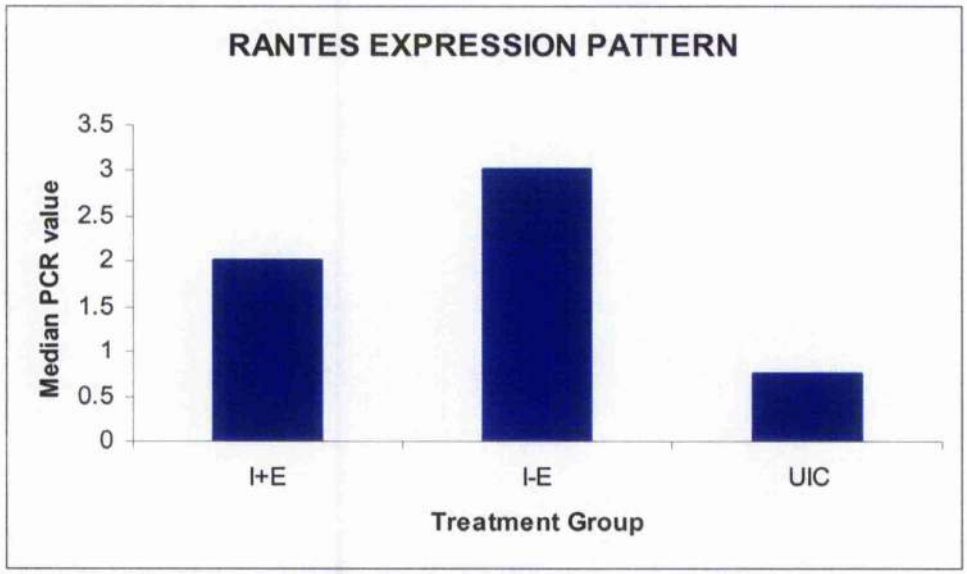

Figure 5.17. Summary statistics for RANTES

The expression level of RANTES in mouse brain was assessed in 3 groups of mice; infected with *T.b.brucei* GVR35/C1.3 DFMO 5.2 given a 14-day course of 2% eflornithine in their drinking water beginning on day 14 post-infection and treated with diminazene aceturate (40mg/kg i.p.) on day 21 post-infection (I+E); infected with *T.b.brucei* GVR35/C1.3 DFMO 5.2 and treated on day 21 post-infection with diminazene aceturate (40mg/kg i.p.) (I-E); and uninfected animals given a 14-day course of 2% eflornithine in their drinking water beginning on day 14 of the experiment and treated with diminazene aceturate (40mg/kg i.p.) on day 21 of the procedure (UIC). All animals were killed on day 28 of the experiment. Following RT-PCR analyses the intensity of the resulting PCR band, as seen on a 2% agarose gel stained with ethidium bromide, was taken as an indication of the quantity of RANTES mRNA present in the initial sample. This was graded on a scale of 0 to 4 where 0 indicated no band and 4 indicated an extremely intense PCR band. The analyses of the data from experiment 1 and 2 as well as the combined data from both experiments are shown. Summary statistics are given for each group of animals and the medians of the combined results from experiments 1 and 2 are plotted to indicate any expression trends. * too few data points.

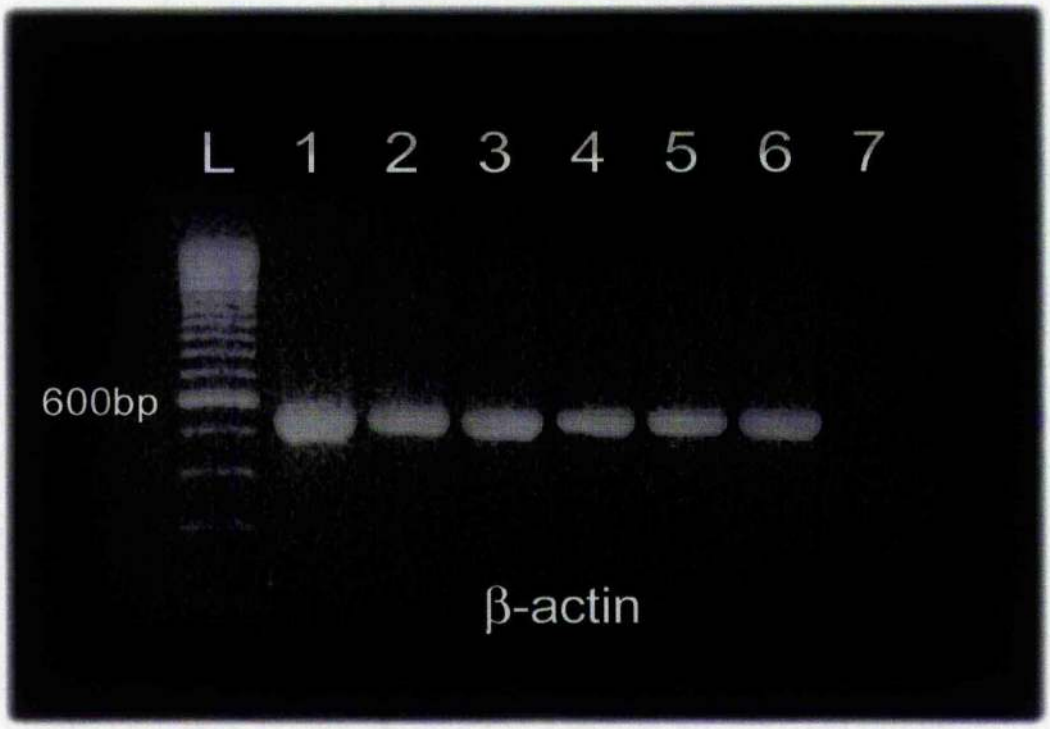

Figure 5.18. β-actin check gel for groups of animals used to study the effect of eflornithine in the amelioration of a meningoencephalitis.

To ensure the mRNA extracted from each group of animals was of similar quality, amplification of the mRNA for housekeeping gene β-actin was carried out. RT-PCR analyses was performed on the mRNA extracted from; mice infected with *T.b.brucei* GVR35/C1.3 DFMO 5.2 treated with diminazene aceturate on day 21 post-infection and again on relapse to parasitaemia and killed either 14 or 21 days later (lane 1); infected animals treated with two diminazene aceturate doses and given a 7-day course of 2% eflornithine in their drinking water beginning 7 days after the administration of the second diminazene aceturate (lane 2); infected animals treated with two diminazene aceturate doses and given a14-day course of eflornithine beginning 7 days after the administration of the second diminazene aceturate (lane 3); normal uninfected animals (lane 4); and uninfected animals treated with diminazene aceturate and eflornithine (lane 5). A known positive control (lane 6) and a negative control consisting of water in place of template (lane 7) were also included in the RT-PCR reaction. All bands are of a similar intensity thus allowing comparisons to be made with regard to the levels of cytokine and chemkine expression using the RT-PCR technique.

Figure 5.19. The effect of eflornithine treatment on the expression of IL-1α in the amelioration of a meningoencephalitic reaction.

RT-PCR was performed, to detect IL-1α expression, on the mRNA extracted from; mice infected with *T.b.brucei* GVR35/C1.3 DFMO 5.2 treated with diminazene aceturate on day 21 post-infection and again on relapse to parasitaemia and killed either 14 or 21 days later (lane 1); infected animals treated with two diminazene aceturate doses and given a 7-day course of 2% eflornithine in their drinking water beginning 7 days after the administration of the second diminazene aceturate (lane 2); infected animals treated with two diminazene aceturate doses and given a14-day course of eflornithine beginning 7 days after the administration of the second diminazene aceturate (lane 3); normal uninfected animals (lane 4); and uninfected animals treated with diminazene aceturate and eflornithine (lane 5). A known positive control (lane 6) and a negative control consisting of water in place of template (lane 7) were also included in the RT-PCR reaction. IL-1α expression was detected in all groups of animals. The infected groups of mice (lanes 1-3) showed similar expression levels regardless of treatment regimen.

Figure 5.20. The effect of eflornithine treatment on the expression of IL-6 in the amelioration of a meningoencephalitic reaction.

RT-PCR was performed, to detect IL-6 expression, on the mRNA extracted from; mice infected with *T.b.brucei* GVR35/C1.3 DFMO 5.2 treated with diminazene aceturate on day 21 post-infection and again on relapse to parasitaemia and killed either 14 or 21 days later (lane 1); infected animals treated with two diminazene aceturate doses and given a 7-day course of 2% eflornithine in their drinking water beginning 7 days after the administration of the second diminazene aceturate (lane 2); infected animals treated with two diminazene aceturate doses and given a14-day course of eflornithine beginning 7 days after the administration of the second diminazene aceturate (lane 3); normal uninfected animals (lane 4); and uninfected animals treated with diminazene aceturate and eflornithine (lane 5). A known positive control (lane 6) and a negative control consisting of water in place of template (lane 7) were also included in the RT-PCR reaction. No IL-6 expression was detected in uninfected animals (lanes 4 & 5). Infected non-eflornithine treated mice (lane 1) show a slightly stronger PCR band than either of the eflornithine treated groups of animals (lanes 2 & 3).

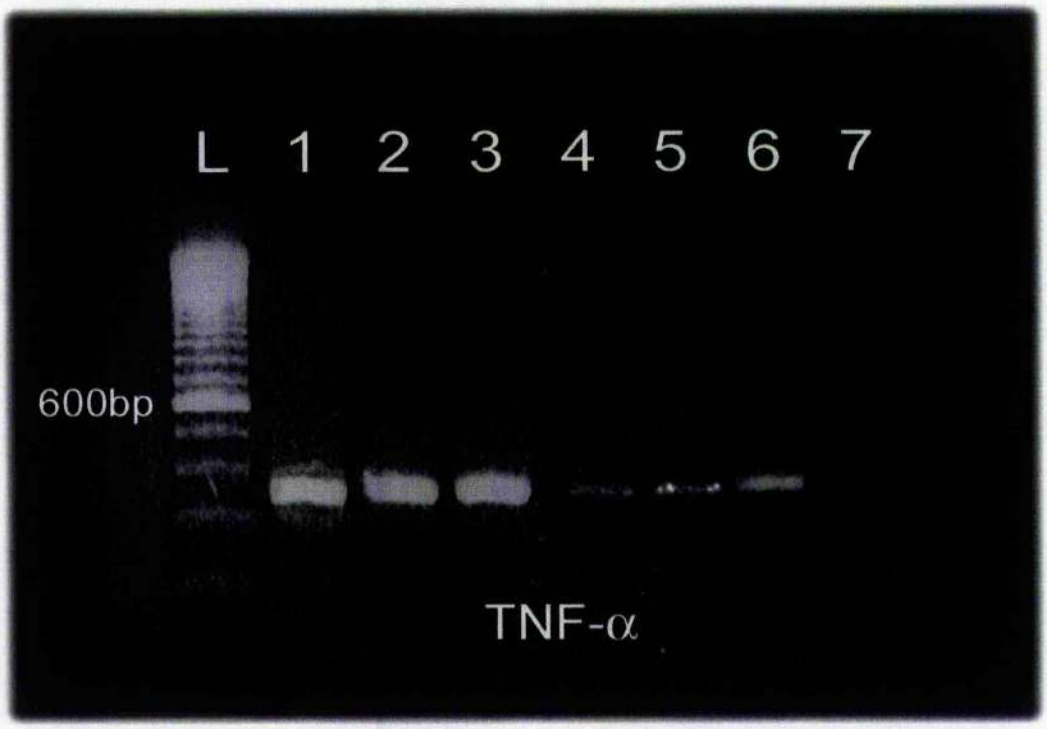

Figure 5.21. The effect of eflornithine treatment on the expression of TNF-α in the amelioration of a meningoencephalitic reaction.

RT-PCR was performed, to detect TNF-α expression, on the mRNA extracted from; mice infected with *T.b.brucei* GVR35/C1.3 DFMO 5.2 treated with diminazene aceturate on day 21 post-infection and again on relapse to parasitaemia and killed either 14 or 21 days later (lane 1); infected animals treated with two diminazene aceturate doses and given a 7-day course of 2% eflornithine in their drinking water beginning 7 days after the administration of the second diminazene aceturate (lane 2); infected animals treated with two diminazene aceturate doses and given a14-day course of eflornithine beginning 7 days after the administration of the second diminazene aceturate (lane 3); normal uninfected animals (lane 4); and uninfected animals treated with diminazene aceturate and eflornithine (lane 5). A known positive control (lane 6) and a negative control consisting of water in place of template (lane 7) were also included in the RT-PCR reaction. Similar levels of TNF-α expression were seen in all groups of infected mice (lanes 1-3). TNF-α expression was detected in uninfected animals although at a much lower level (lanes 4 & 5).

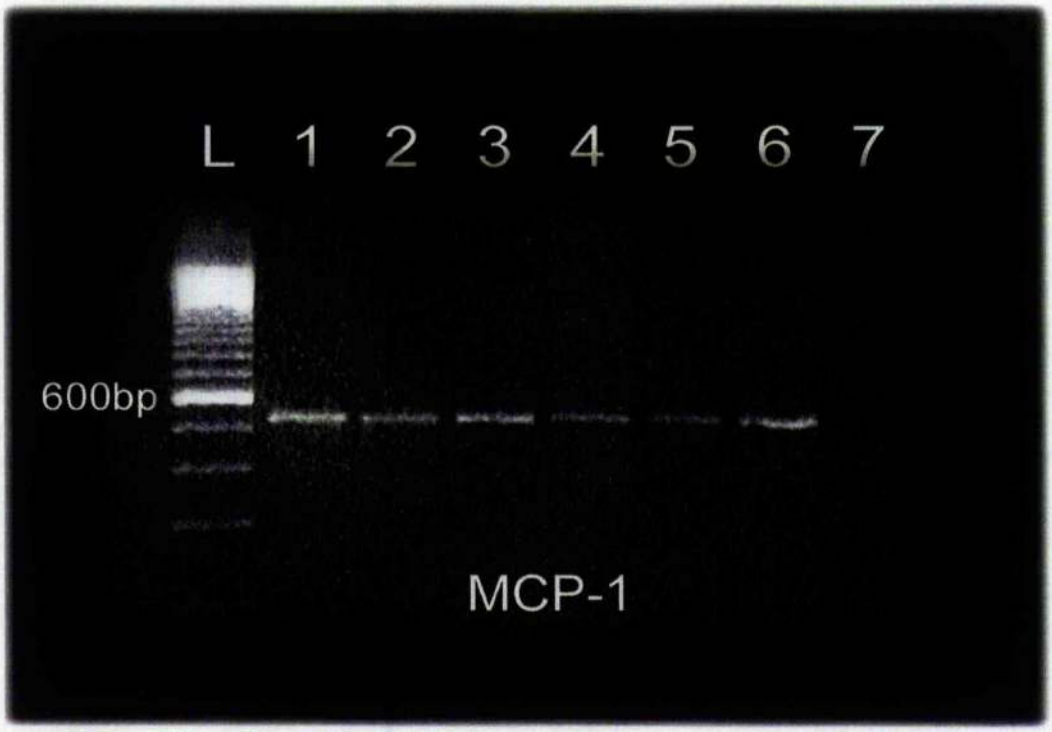

Figure 5.22. The effect of eflornithine treatment on the expression of MCP-1 in the amelioration of a meningoencephalitic reaction.

RT-PCR was performed, to detect MCP-1 expression, on the mRNA extracted from; mice infected with *T.b.brucei* GVR35/C1.3 DFMO 5.2 treated with diminazene aceturate on day 21 post-infection and again on relapse to parasitaemia and killed either 14 or 21 days later (lane 1); infected animals treated with two diminazene aceturate doses and given a 7-day course of 2% eflornithine in their drinking water beginning 7 days after the administration of the second diminazene aceturate (lane 2); infected animals treated with two diminazene aceturate doses and given a14-day course of eflornithine beginning 7 days after the administration of the second diminazene aceturate (lane 3); normal uninfected animals (lane 4); and uninfected animals treated with diminazene aceturate and eflornithine (lane 5). A known positive control (lane 6) and a negative control consisting of water in place of template (lane 7) were also included in the RT-PCR reaction. MCP-1 expression was detected in all animals. No differences in the expression levels were seen between the infected non-eflornithine (lane 1) and the infected eflornithine treated groups (lanes 2 & 3). Uninfected animals showed the lowest levels of MCP-1 expression (lanes 4 & 5).

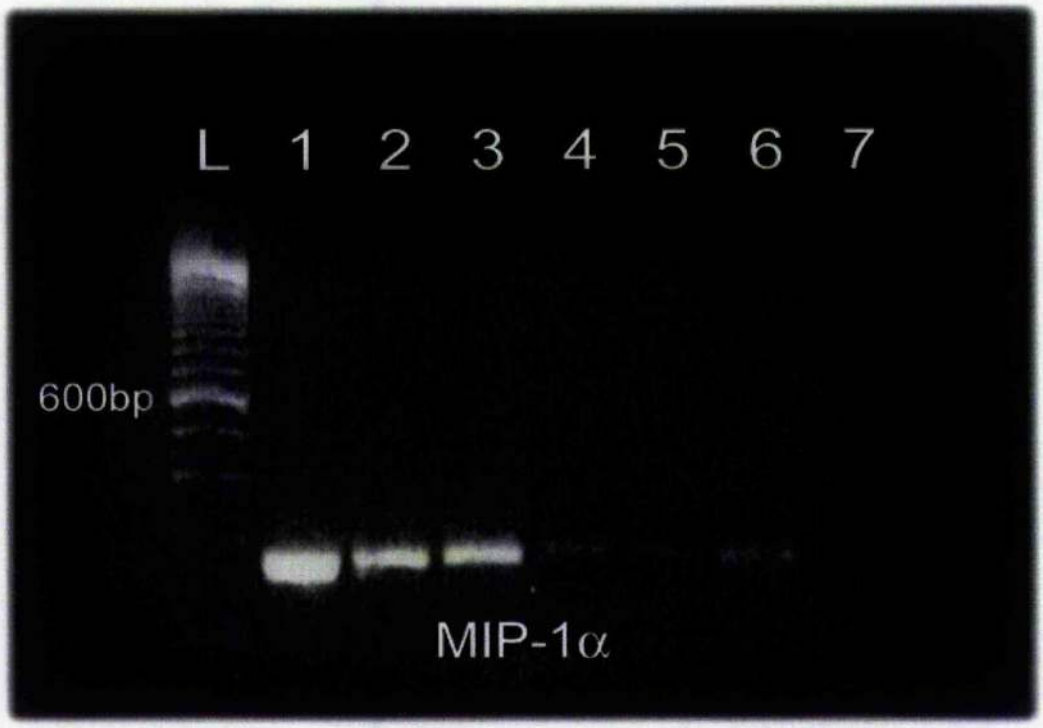

Figure 5.23. The effect of eflornithine treatment on the expression of MIP-1α in the amelioration of a meningoencephalitic reaction.

RT-PCR was performed, to detect MIP-1α expression, on the mRNA extracted from; mice infected with *T.b.brucei* GVR35/C1.3 DFMO 5.2 treated with diminazene aceturate on day 21 post-infection and again on relapse to parasitaemia and killed either 14 or 21 days later (lane 1); infected animals treated with two diminazene aceturate doses and given a 7-day course of 2% eflornithine in their drinking water beginning 7 days after the administration of the second diminazene aceturate (lane 2); infected animals treated with two diminazene aceturate doses and given a14-day course of eflornithine beginning 7 days after the administration of the second diminazene aceturate (lane 3); normal uninfected animals (lane 4); and uninfected animals treated with diminazene aceturate and eflornithine (lane 5). A known positive control (lane 6) and a negative control consisting of water in place of template (lane 7) were also included in the RT-PCR reaction. MIP-1α was detected in all groups of mice. Uninfected animals (lanes 4 & 5) showed the weakest bands whereas infected non-eflornithine treated mice expressed higher levels of the chemokine (lane 1). Eflornithine treatment of infected mice resulted in a slight decrease in the intensity of MIP-1α expression (lanes 2 & 3).

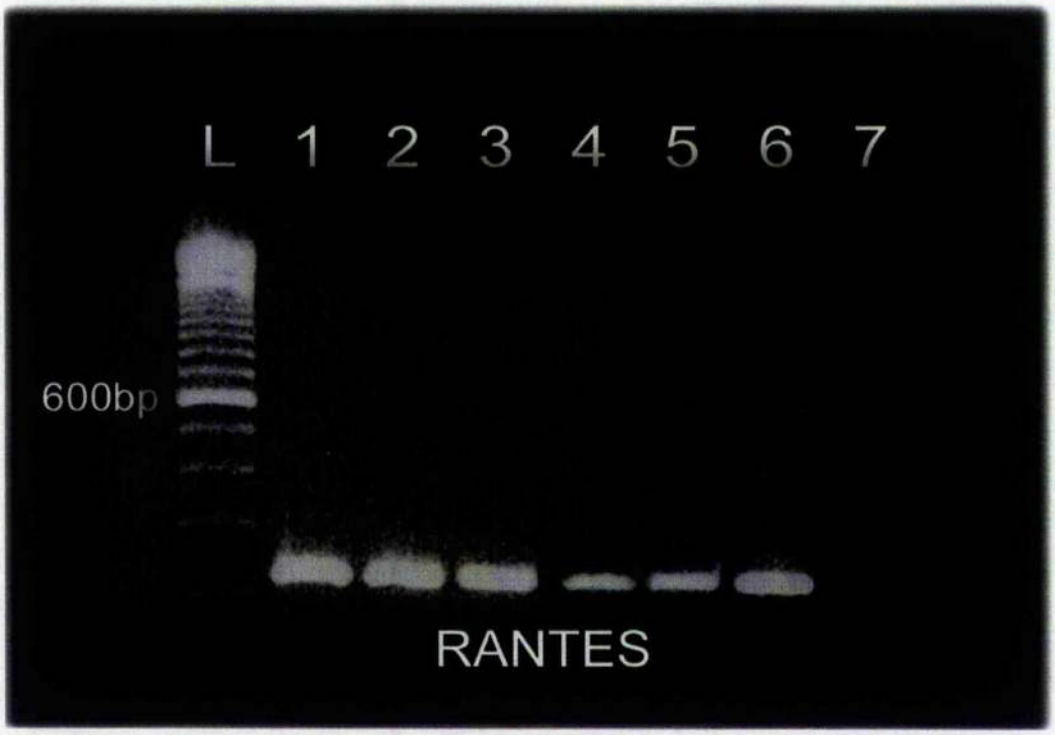

Figure 5.24. The effect of eflornithine treatment on the expression of RANTES in the amelioration of a meningoencephalitic reaction.

RT-PCR was performed, to detect RANTES expression, on the mRNA extracted from; mice infected with *T.b.brucei* GVR35/C1.3 DFMO 5.2 treated with diminazene aceturate on day 21 post-infection and again on relapse to parasitaemia and killed either 14 or 21 days later (lane 1); infected animals treated with two diminazene aceturate doses and given a 7-day course of 2% eflornithine in their drinking water beginning 7 days after the administration of the second diminazene aceturate (lane 2); infected animals treated with two diminazene aceturate doses and given a14-day course of eflornithine beginning 7 days after the administration of the second diminazene aceturate (lane 3); normal uninfected animals (lane 4); and uninfected animals treated with diminazene aceturate and eflornithine (lane 5). A known positive control (lane 6) and a negative control consisting of water in place of template (lane 7) were also included in the RT-PCR reaction. RANTES was expressed in samples from all groups of mice. Higher levels of RANTES mRNA were found in infected mice (lanes 1-3) compared with uninfected animals (lanes 4 & 5).

	I+E7	I+E14	I-E1	I-E2	UIC
			Experiment 1		
Median	3.00	2.00	2.00	2.25	2.75
Upper quartile	3.00	3.00	*	*	3.00
Lower quartile	1.25	1.75	*	*	1.75
Maximum	3.00	3.00	2.00	3.00	3.00
Minimum	1.00	1.50	2.00	1.50	1.00
Number	5	5	1	2	6
			Experiment 2		
Median	2.25	3.00	2.50	2.75	1.75
Upper quartile	2.875	3.00	*	*	2.00
Lower quartile	2.00	2.25	*	*	1.50
Maximum	3.00	3.00	3.00	3.00	2.00
Minimum	2.00	2.00	2.00	2.50	1.50
Number	4	4	2	2	4
			Experiment 3		
Median	3.00	3.00	3.00	2.75	NA
Upper quartile	3.00	3.00	3.00	3.00	NA
Lower quartile	2.50	2.00	2.50	2.125	NA
Maximum	3.00	3.00	3.00	3.00	NA
Minimum	2.50	2.00	2.50	2.00	NA
Number	3	3	3	4	NA
			Experiments 1, 2 & 3		
Median	2.75	3.00	2.75	2.75	2.00
Upper quartile	3.00	3.00	3.00	3.00	3.00
Lower quartile	2.00	2.00	2.00	2.125	1.50
Maximum	3.00	3.00	3.00	3.00	3.00
Minimum	1.00	1.50	2.00	1.50	1.00
Number	12	12	6	8	10

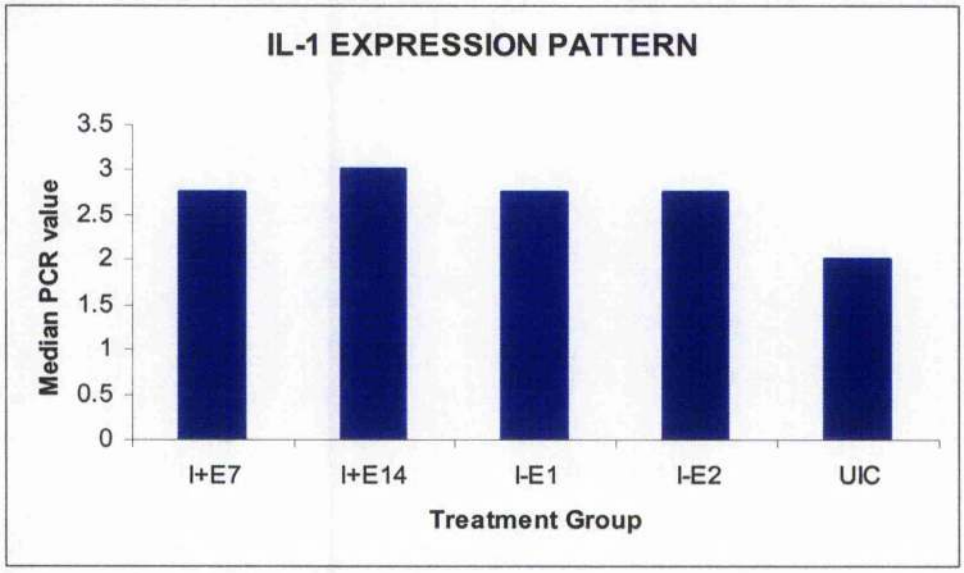

Figure 5.25. Summary statistics for IL-1α

The expression level of IL-1α in mouse brain was assessed in 5 groups of mice; infected with *T.b.brucei* GVR 35/C1.3 DFMO 5.2 and treated on day 21 post-infection with diminazene aceturate (40mg/kg i.p.) and again on relapse to parasitaemia given, a 7 (I+E7) or 14 (I+E14) day course of 2% eflornithine in their drinking water beginning 7-days after the second diminazene aceturate treatment; infected animals treated with both doses of diminazene aceturate and killed 14 (I-E1) or 21 (I-E2) days later; and uninfected animals treated with diminazene aceturate and eflornithine (UIC). Following RT-PCR analyses the intensity of the resultant PCR band was graded on a scale of 0 to 4 where 0 indicated no band and 4 indicated an extremely intense band. The analyses of the data from the 3 individual experiments as well as the combined results are shown. Summary statistics are given for each group of animals and the medians of the combined results plotted to indicate any expression trends. NA; not assessed, * too few data points.

	I+E7	I+E14	I-E1	I-E2	UIC
			Experiment 1		
Median	1.00	1.00	1.00	0.625	0.00
Upper quartile	1.00	1.00	*	*	0.00
Lower quartile	0.25	0.375	*	*	0.00
Maximum	1.00	1.00	1.00	1.00	0.00
Minimum	0.00	0.25	1.00	0.25	0.00
Number	5	5	1	2	6
			Experiment 2		
Median	2.00	1.75	1.50	2.00	0.00
Upper quartile	2.00	2.00	*	*	0.00
Lower quartile	1.625	1.50	*	*	0.00
Maximum	2.00	2.00	2.00	2.50	0.00
Minimum	1.50	1.50	1.00	1.50	0.00
Number	4	4	2	2	4
			Experiment 3		
Median	1.00	1.00	0.50	1.50	NA
Upper quartile	2.50	2.00	2.50	2.75	NA
Lower quartile	0.50	0.50	0.50	0.625	NA
Maximum	2.50	2.00	2.50	3.00	NA
Minimum	0.50	0.50	0.50	0.50	NA
Number	3	3	3	4	NA
			Experiments 1, 2 & 3		
Median	1.00	1.00	1.00	1.25	0.00
Upper quartile	2.00	1.875	2.125	2.375	0.00
Lower quartile	0.625	0.625	0.50	0.625	0.00
Maximum	2.50	2.00	2.50	3.00	0.00
Minimum	0.00	0.25	0.50	0.25	0.00
Number	12	12	6	8	10

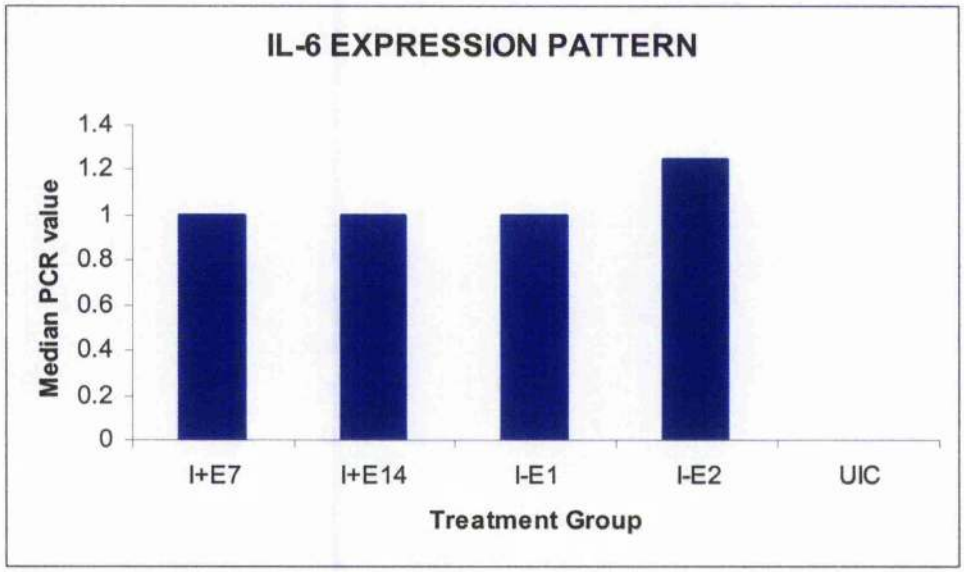

Figure 5.26. Summary statistics for IL-6

The expression level of IL-6 in mouse brain was assessed in 5 groups of mice; infected with *T.b.brucei* GVR 35/C1.3 DFMO 5.2 and treated on day 21 post-infection with diminazene aceturate (40mg/kg i.p.) and again on relapse to parasitaemia given, a 7 (I+E7) or 14 (I+E14) day course of 2% eflornithine in their drinking water beginning 7-days after the second diminazene aceturate treatment; infected animals treated with both doses of diminazene aceturate and killed 14 (I-E1) or 21 (I-E2) days later; and uninfected animals treated with diminazene aceturate and eflornithine (UIC). Following RT-PCR analyses the intensity of the resultant PCR band was graded on a scale of 0 to 4 where 0 indicated no band and 4 indicated an extremely intense band. The analyses of the data from the 3 individual experiments as well as the combined results are shown. Summary statistics are given for each group of animals and the medians of the combined results plotted to indicate any expression trends. NA; not assessed, * too few data points.

	I+E7	I+E14	I-E1	I-E2	UIC
			Experiment 1		
Median	1.50	2.00	3.00	1.00	0.00
Upper quartile	3.00	2.250	*	*	0.125
Lower quartile	0.50	1.25	*	*	0.00
Maximum	3.00	2.50	3.00	2.00	0.50
Minimum	0.00	0.50	3.00	0.00	0.00
Number	5	5	1	2	6
			Experiment 2		
Median	2.00	2.00	1.25	1.75	0.50
Upper quartile	2.375	2.00	*	*	0.50
Lower quartile	2.00	1.625	*	*	0.3125
Maximum	2.50	2.00	1.50	2.00	0.50
Minimum	2.00	1.50	1.00	1.50	0.25
Number	4	4	2	2	4
			Experiment 3		
Median	1.00	1.00	1.00	1.50	NA
Upper quartile	2.00	3.00	2.00	3.00	NA
Lower quartile	1.00	1.00	0.00	0.00	NA
Maximum	2.00	3.00	2.00	3.00	NA
Minimum	1.00	1.00	0.00	0.00	NA
Number	3	3	3	4	NA
			Experiments 1, 2 & 3		
Median	2.00	2.00	1.250	1.75	0.125
Upper quartile	2.375	2.00	2.25	2.75	0.50
Lower quartile	1.00	1.125	0.75	0.00	0.00
Maximum	3.00	3.00	3.00	3.00	0.50
Minimum	0.00	0.50	0.00	0.00	0.00
Number	12	12	6	8	10

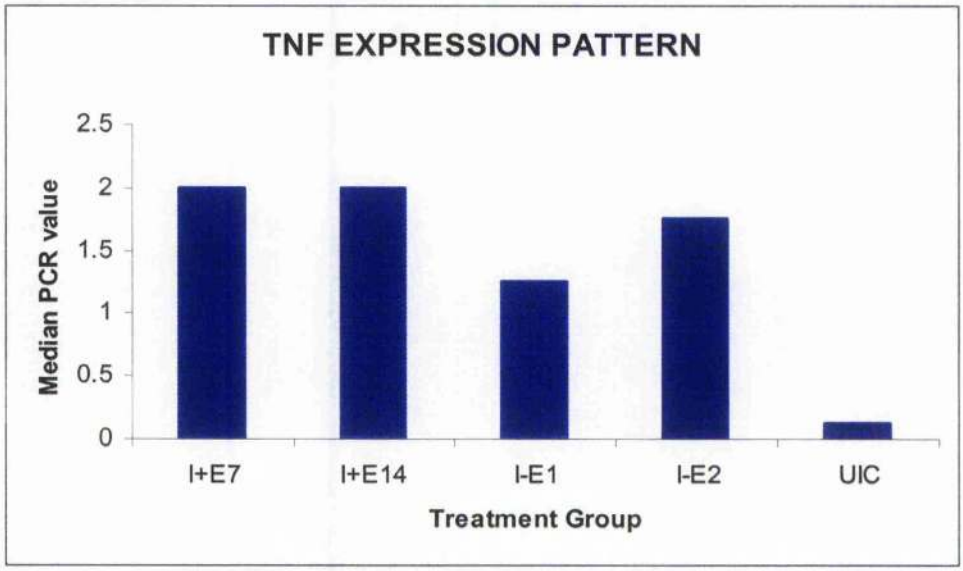

Figure 5.27. Summary statistics for TNF-α

The expression level of IL-6 in mouse brain was assessed in 5 groups of mice; infected with *T.b.brucei* GVR 35/C1.3 DFMO 5.2 and treated on day 21 post-infection with diminazene aceturate (40mg/kg i.p.) and again on relapse to parasitaemia given, a 7 (I+E7) or 14 (I+E14) day course of 2% eflornithine in their drinking water beginning 7-days after the second diminazene aceturate treatment; infected animals treated with both doses of diminazene aceturate and killed 14 (I-E1) or 21 (I-E2) days later; and uninfected animals treated with diminazene aceturate and eflornithine (UIC). Following RT-PCR analyses the intensity of the resultant PCR band was graded on a scale of 0 to 4 where 0 indicated no band and 4 indicated an extremely intense band. The analyses of the data from the 3 individual experiments as well as the combined results are shown. Summary statistics are given for each group of animals and the medians of the combined results plotted to indicate any expression trends. NA; not assessed, * too few data points.

	I+E7	I+E14	I-E1	I-E2	UIC
			Experiment 1		
Median	2.00	2.00	3.00	0.875	0.625
Upper quartile	2.50	2.25	*	*	1.25
Lower quartile	1.00	1.75	*	*	0.00
Maximum	3.00	2.50	3.00	1.50	2.00
Minimum	0.00	1.50	3.00	0.25	0.00
Number	5	5	1	2	6
			Experiment 2		
Median	1.25	2.25	1.25	1.50	1.50
Upper quartile	1.50	2.875	*	*	2.00
Lower quartile	1.00	2.00	*	*	1.00
Maximum	1.50	3.00	1.50	1.50	2.00
Minimum	1.00	2.00	1.00	1.50	1.00
Number	4	4	2	2	4
			Experiment 3		
Median	2.00	1.00	0.25	1.25	NA
Upper quartile	2.00	2.50	3.00	2.875	NA
Lower quartile	1.00	1.00	0.00	0.00	NA
Maximum	2.00	2.50	3.00	3.00	NA
Minimum	1.00	1.00	0.00	0.00	NA
Number	3	3	3	4	NA
			Experiments 1, 2 & 3		
Median	1.75	2.00	1.25	1.50	1.00
Upper quartile	2.00	2.50	3.00	2.25	2.00
Lower quartile	1.00	1.625	1.888	0.063	0.188
Maximum	3.00	3.00	3.00	3.00	2.00
Minimum	0.00	1.00	0.00	0.00	0.00
Number	12	12	6	8	10

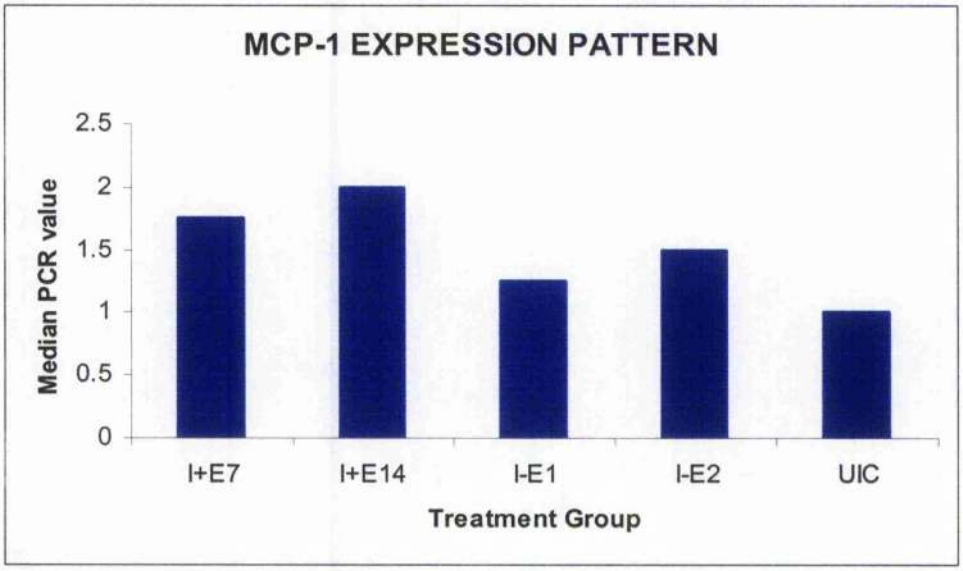

Figure 5.28. Summary statistics for MCP-1
The expression level of MCP-1 in mouse brain was assessed in 5 groups of mice; infected with *T.b.brucei* GVR 35/C1.3 DFMO 5.2 and treated on day 21 post-infection with diminazene aceturate (40mg/kg i.p.) and again on relapse to parasitaemia given, a 7 (I+E7) or 14 (I+E14) day course of 2% eflornithine in their drinking water beginning 7-days after the second diminazene aceturate treatment; infected animals treated with both doses of diminazene aceturate and killed 14 (I-E1) or 21 (I-E2) days later; and uninfected animals treated with diminazene aceturate and eflornithine (UIC). Following RT-PCR analyses the intensity of the resultant PCR band was graded on a scale of 0 to 4 where 0 indicated no band and 4 indicated an extremely intense band. The analyses of the data from the 3 individual experiments as well as the combined results are shown. Summary statistics are given for each group of animals and the medians of the combined results plotted to indicate any expression trends. NA; not assessed, * too few data points.

	Experiment 1				
	I+E7	I+E14	I-E1	I-E2	UIC
Median	1.00	0.50	3.00	1.75	0.125
Upper quartile	1.00	1.50	*	*	*
Lower quartile	0.50	0.25	*	*	*
Maximum	1.00	2.00	3.00	2.00	0.25
Minimum	0.00	0.00	3.00	1.50	0.00
Number	5	5	1	2	2
	Experiment 2				
Median	1.25	2.00	3.00	3.00	0.75
Upper quartile	1.875	2.50	*	*	1.375
Lower quartile	0.625	0.75	*	*	0.313
Maximum	2.00	2.50	3.00	3.00	1.50
Minimum	0.50	0.50	3.00	3.00	0.25
Number	4	4	2	2	4
	Experiment 3				
Median	3.00	1.50	2.00	2.00	NA
Upper quartile	3.00	2.50	2.50	2.375	NA
Lower quartile	2.50	1.50	1.50	1.625	NA
Maximum	3.00	2.50	2.50	2.50	NA
Minimum	2.50	1.50	1.50	1.50	NA
Number	3	3	3	4	NA
	Experiments 1, 2 & 3				
Median	1.00	1.50	2.75	2.00	0.375
Upper quartile	2.375	2.375	3.00	2.875	1.125
Lower quartile	1.00	0.50	1.875	1.625	0.188
Maximum	3.00	2.50	3.00	3.00	1.50
Minimum	0.00	0.00	1.50	1.50	0.00
Number	12	12	6	8	6

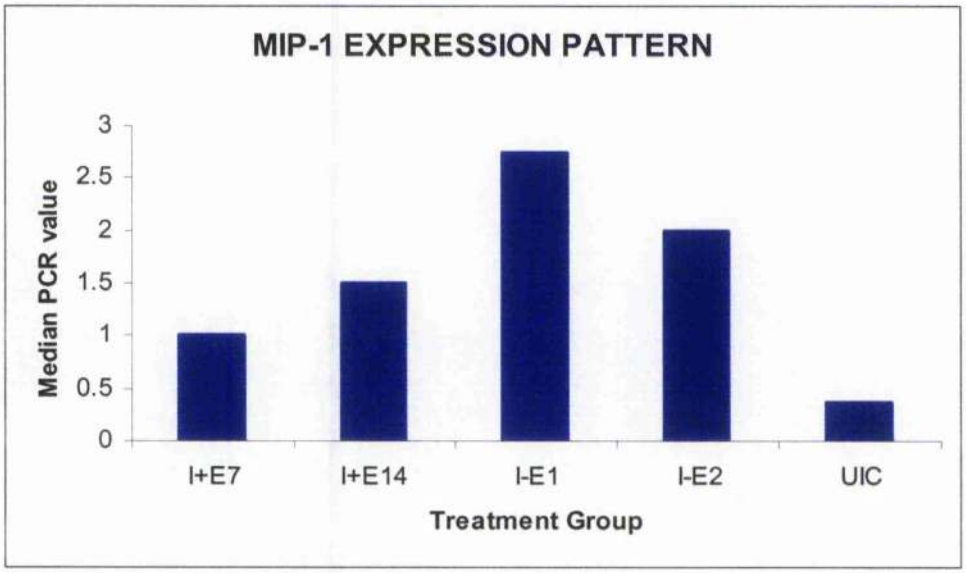

Figure 5.29. Summary statistics for MIP-α
The expression level of MIP-1α in mouse brain was assessed in 5 groups of mice; infected with *T.b.brucei* GVR 35/C1.3 DFMO 5.2 and treated on day 21 post-infection with diminazene aceturate (40mg/kg i.p.) and again on relapse to parasitaemia given, a 7 (I+E7) or 14 (I+E14) day course of 2% eflornithine in their drinking water beginning 7-days after the second diminazene aceturate treatment; infected animals treated with both doses of diminazene aceturate and killed 14 (I-E1) or 21 (I-E2) days later; and uninfected animals treated with diminazene aceturate and eflornithine (UIC). Following RT-PCR analyses the intensity of the resultant PCR band was graded on a scale of 0 to 4 where 0 indicated no band and 4 indicated an extremely intense band. The analyses of the data from the 3 individual experiments as well as the combined results are shown. Summary statistics are given for each group of animals and the medians of the combined results plotted to indicate any expression trends. NA; not assessed, * too few data points.

	I+E7	I+E14	I-E1	I-E2	UIC
			Experiment 1		
Median	3.00	3.00	2.00	2.00	1.50
Upper quartile	3.00	3.00	*	*	1.75
Lower quartile	2.25	2.25	*	*	1.00
Maximum	3.00	3.00	2.00	3.00	2.50
Minimum	2.00	2.00	2.00	1.00	1.00
Number	5	5	1	2	6
			Experiment 2		
Median	2.50	1.50	1.25	1.50	1.50
Upper quartile	2.875	2.00	*	*	2.00
Lower quartile	2.50	1.00	*	*	1.00
Maximum	3.00	2.00	1.50	1.50	2.00
Minimum	2.50	1.00	1.00	1.50	1.00
Number	4	4	2	2	4
			Experiment 3		
Median	3.00	2.00	3.00	1.50	NA
Upper quartile	3.00	2.50	3.00	2.75	NA
Lower quartile	3.00	2.00	1.00	0.625	NA
Maximum	3.00	2.50	3.00	3.00	NA
Minimum	3.00	2.00	1.00	0.50	NA
Number	3	3	3	4	NA
			Experiments 1, 2 & 3		
Median	3.00	2.00	1.75	1.50	1.50
Upper quartile	3.00	3.00	3.00	2.75	2.00
Lower quartile	2.50	2.00	1.00	1.00	1.00
Maximum	3.00	3.00	3.00	3.00	2.50
Minimum	2.00	1.00	1.00	0.50	1.00
Number	12	12	6	8	10

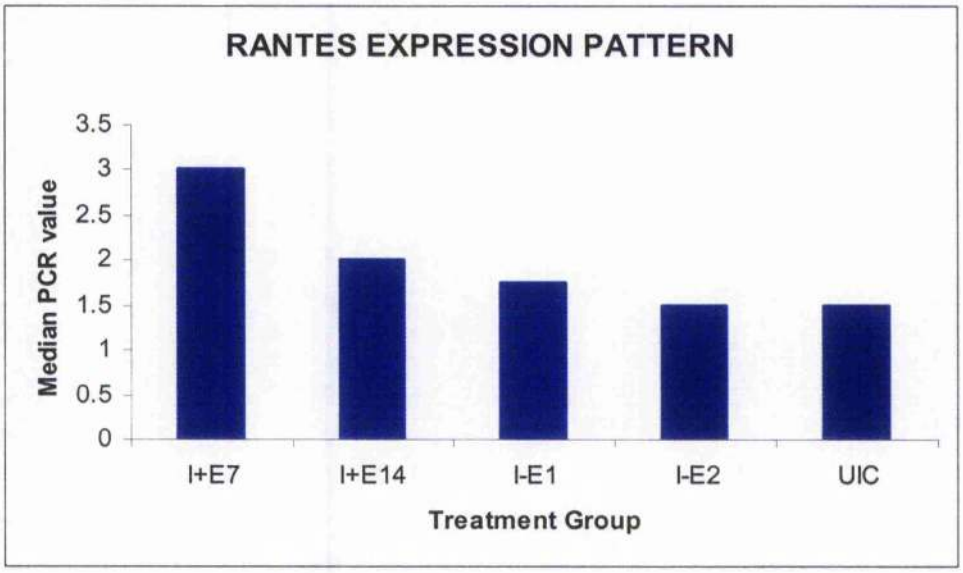

Figure 5.30. Summary statistics for RANTES
The expression level of RANTES in mouse brain was assessed in 5 groups of mice; infected with *T.b.brucei* GVR 35/C1.3 DFMO 5.2 and treated on day 21 post-infection with diminazene aceturate (40mg/kg i.p.) and again on relapse to parasitaemia given, a 7 (I+E7) or 14 (I+E14) day course of 2% eflornithine in their drinking water beginning 7-days after the second diminazene aceturate treatment; infected animals treated with both doses of diminazene aceturate and killed 14 (I-E1) or 21 (I-E2) days later; and uninfected animals treated with diminazene aceturate and eflornithine (UIC). Following RT-PCR analyses the intensity of the resultant PCR band was graded on a scale of 0 to 4 where 0 indicated no band and 4 indicated an extremely intense band. The analyses of the data from the 3 individual experiments as well as the combined results are shown. Summary statistics are given for each group of animals and the medians of the combined results plotted to indicate any expression trends. NA; not assessed, * too few data points.

5.4. Discussion

5.4.1. Eflornithine in the prevention of CNS inflammation

In the current study histological assessment of brain sections prepared from mice infected with eflornithine-resistant *T.b.brucei* showed the presence of mild inflammatory changes characterised by the infiltration of the meninges and ventricle with a few lymphocytes and macrophages and the development of perivascular cuffing around the occasional blood vessel. A reduction in the level of this inflammatory reaction was seen in the brains of mice treated with a course of 2% eflornithine in their drinking water, beginning 7-days prior to the induction of the CNS inflammatory response by subcurative diminazene aceturate treatment. In these animals only a few infiltrating cells were seen and no cuffs were found. A reduction in the degree of astrogliosis was also observed in the mice receiving eflornithine treatment. These findings confirm those published previously (Jennings *et al.*, 1997). In this study eflornithine treatment, when given prior to the exacerbation of the CNS response was shown to reduce the severity of the resultant neuroinflammatory reaction and associated astrogliosis. The findings of both investigations suggest that eflornithine has an anti-inflammatory action that can help to prevent the progress of a CNS inflammatory response irrespective of the effect of the drug on the parasite.

Although this reduction in pathology could be gauged by histological examination, the anti-inflammatory effect was not found to be significant when analysed using statistical methods. This finding could reflect insufficient sensitivity in the grading scale used to score the slides when applied to assess sections displaying only mild inflammatory changes. The changes associated with a very early CNS reaction can be easily identified and a grade of 1 assigned to the section. The point at which this score rises to an intermediate grade 1.5 or a grade 2 is more subjective. This variation would enlarge the standard error of the mean score for these mice and make significant differences harder to detect. Increasing the number of animals included in this investigation and the statistical power of the study may have helped to clarify this point.

Since trypanosome infection can stimulate the production of IL-1α, IL-6 and TNF-α as well as MCP-1, MIP-1α and RANTES, within the CNS (Hunter *et al.*, 1991; Sharafeldin *et*

al., 2000) it would be logical to assume that one possible mechanism by which eflornithine could achieve its anti-inflammatory effect would be through inhibition of the production of these pro-inflammatory agents. In this study a semi-quantitative method of assessing the expression of these cytokines and chemokines, involving the use of RT-PCR analyses to detect specific mRNA transcripts, was employed. The results showed that following eflornithine treatment the transcription of IL-1α and IL-6 was lowered significantly compared with non-eflornithine treated trypanosome infected groups of mice. MIP-1α and RANTES expression was also decreased, but this reduction could not be considered significant. No change in the production of either TNF-α or MCP-1 was detected following eflornithine administration.

IL-1α is a cytokine that is commonly produced in response to injury and immunological challenge. Its plays a primarily pro-inflammatory role in the immune response and its local expression can lead to the migration of inflammatory cells to the site of its production. It is unclear whether this chemotactic action is a direct effect of the cytokine or a secondary effect brought about by the ability of IL-α to stimulate the synthesis of chemokines. The corresponding reduction in the levels of the chemokines MIP-1α and RANTES found in the CNS following eflornithine administration could therefore be a reflection of the alteration in IL-1α expression. Treatment of experimental allergic encephalomyelitis (EAE), the animal model of multiple sclerosis (MS), with anti-MIP-1α antibodies has been shown to shown to inhibit the development of the acute stage of the disease and it has been suggested that this chemokine controls monocyte recruitment during the developmental phase of EAE (Bajetto *et al.,* 2001; Glabinski and Ransohoff, 1999b). Similarly, RANTES is known to attract lymphocytes and monocytes to sites of inflammation (Vaddi *et al.*, 1997) and has been implicated in the pathogenesis of a range of CNS inflammatory disorders including, MS, Alzheimer's disease, stroke and cerebral lupus (Appay and Rowland-Jones, 2001; De Groot and Woodroofe, 2001). Therefore, the reduction in IL-1α levels precipitated by eflornithine treatment could help to diminish the CNS inflammatory response, resulting from trypanosome infection and subcurative drug treatment, by reducing the chemoattractant signal that initiates inflammatory cell migration and infiltration.

The pro-inflammatory properties of IL-1 within the CNS have been demonstrated by investigations administrating the IL-1 receptor antagonist (IL-1ra), a naturally occurring antagonist that blocks the actions of IL-1 by binding non-productively with IL-1 receptors, to mice following induction of cerebral ischaemic injury. Treatment of these animals with

IL-1ra was shown to reduce the levels of oedema and glial cell activation associated with this type of CNS damage. The reduction in astrocyte activation that occurs following eflornithine treatment of trypanosome infected mice, could therefore result from the ability of eflornithine to significantly reduce the production of IL-1α as seen in this study.

IL-1α often controls the synthesis of IL-6 (Dinarello, 1998); it is therefore possible that the reduction in the expression level of IL-6 precipitated by eflornithine treatment is a direct effect of the lowered IL-1α production. On the other hand, since lymphocytes, macrophages and astrocytes are all capable of synthesising IL-6 (Oppenheim and Saklatvala, 1993), the reduction in IL-6 levels seen in the CNS following eflornithine treatment could be the result of the lowered neuroinflammatory reaction. The converse of the above situation has also been documented and under some circumstances IL-α production is mediated by the presence of IL-6. In transgenic mice expressing IL-6 under the control of the GFAP promoter, elevated levels of IL-1α have been detected (Wang, Asensio, and Campbell, 2002). Therefore, the reduction in the synthesis of IL-6 seen following eflornithine treatment could precipitate a corresponding drop in the expression of IL-1α leading to an overall reduction in the severity of the CNS inflammatory reaction. The exact interplay between these two cytokines following eflornithine treatment, resulting in a reduction in the levels of both mediators remains unclear.

Although a significant increase in the expression of the cytokine TNF-α and the chemokine MCP-1 was detected in trypanosome infected animals when compared to uninfected mice no alteration in the production of these mediators was detected following eflornithine treatment. This finding suggests that eflornithine does not mediate the production of either TNF-α or MCP-1 during the development of a CNS-inflammatory response and that in this situation the levels of these inflammatory agents are not directly linked to the expression of IL-1α, IL-6, MIP-1α or RANTES.

5.4.2. Eflornithine in the amelioration of CNS inflammation

In the present study the anti-inflammatory effect of eflornithine treatment was assessed in a semi-quantitative fashion. When the severity of the neuropathological response was graded, following the induction of a severe meningoencephalitis in mice infected with eflornithine resistant trypanosomes, significant differences were found between the groups

given various treatment regimens. Since no gross inflammatory changes were seen in the uninfected groups of animals, all infected groups, including those receiving eflornithine, showed a significantly higher neuropathological response score when compared with these uninfected mice. In the infected groups of mice a 7-day course of eflornithine only slightly reduced the severity of the inflammatory reaction when compared to mice that were not given eflornithine. However, when this course was extended to 14 days, a significant reduction in the severity of the CNS response was found in comparison with all the other infected groups of animals. The reduction in the severity of the neuroinflammatory response was accompanied by a dramatic reduction in the level of astrocyte activation which was more pronounced following the extended treatment schedule. This suggests that the ability of eflornithine to ameliorate the severe meningoencephalitis is a dose dependent response. The findings of this study confirm those previously observed in this model system (Jennings *et al.*, 1997) and measure the efficacy of the anti-inflammatory action of eflornithine in the resolution of a severe neuroinflammatory response in a semi-quantitative manner.

When the expression of IL-α, IL-6, TNF-α, MCP-1, MIP-1α and RANTES was examined no significant differences in the transcript levels in eflornithine-treated verses non-eflornithine treated groups were noted, despite the dramatic decrease in the severity of the CNS inflammation. Unlike the previous experiments, where the preventative effect of eflornithine on the generation of CNS inflammation was examined, IL-1α levels in infected animals appeared to remain only slightly elevated in comparison to those found in the uninfected mice regardless of the drug regimen administered. In a similar fashion, IL-6 expression was not altered by eflornithine treatment during this phase of the disease.

Again in contrast to the effects seen during the developmental phase of the CNS reaction, TNF-α expression seems to increase following eflornithine administration. The expression levels of TNF-α in the eflornithine treated animals were not significantly higher than those seen in the infected non-eflornithine treated mice. However, the increase in the production of this cytokine was substantial enough to make the levels in eflornithine-treated animals significantly higher than those seen in the uninfected mice. Infected mice that were not given eflornithine did not show TNF-α levels that were significantly higher than the uninfected groups. The apparent rise in TNF-α transcription in animals that show a dramatically reduced level of CNS inflammation is anomalous to findings using transgenic mice that over express TNF-α. In these transgenic animals severe neuroinflammatory reactions were seen, characterised by the widespread infiltration of the brain by numerous

inflammatory cells (Wang *et al.,* 2002). However, a dichotomous effect of TNF-α in traumatic CNS damage has been suggested as the initial production of this cytokine following injury appears to have detrimental consequences, whereas, the presence of the cytokine later in the reaction seems to be advantageous and leads to a more rapid recovery (Lenzlinger *et al.,* 2001). Although the meningoencephalitis that develops following trypanosome infection is not the result of traumatic damage, it is possible that the TNF-α production seen following eflornithine administration could have a beneficial effect in these animals.

A minor increase in MCP-1 and RANTES expression was found in infected animals that had received eflornithine treatment. This finding is rather enigmatic since following increased production of these chemotactic mediators a corresponding increase in the numbers of lymphocytes and monocytes into the locale would be expected due to their chemotactic influence on these cells. This would result in an increase in the overall severity of the inflammatory reaction and not a decrease as found in this scenario. When transcripts for MIP-1α were examined a slight drop in the expression of this chemokine was found in infected eflornithine treated mice compared to infected animals not given eflornithine. This drop in expression was not significant and was more marked in mice receiving 7 days of eflornithine rather than the 14-day course.

5.4.3. Potential mechanism of action of eflornithine

As a whole the findings from this investigation indicate that, when eflornithine is administered during the prevention of the development of a neuroinflammatory reaction, the mechanism by which the drug exerts its anti-inflammatory effect is likely to involve the down-regulation of the transcription of IL-1α and IL-6. This could trigger a reduction in the synthesis of MIP-1α and RANTES and instigate an overall dampening of the inflammatory cell infiltration into the CNS. These findings are in contrast to those seen when eflornithine treatment was given to resolve an established meningoencephalitis. Under these circumstances no significant alteration to the level of cytokine or chemokine transcription was detected, indicating that eflornithine treatment does not interfere with the transcription of these inflammatory mediators when given after a CNS inflammatory reaction has become established. However, eflornithine treatment during this stage of the infection still results in a dramatic decrease in the severity of the neuroinflammatory

response. This suggests that a pathway other that inhibition of cytokine or chemokine transcription is altered by eflornithine to resolve the inflammatory CNS lesions at this point.

The temporal expression of cytokine and chemokine species within the CNS has been shown to have differential effects on the development of the disease. In EAE, it is possible to inhibit the acute stages of the disease by treatment with anti-MIP-1α antibodies, whereas, the severity of the relapsing stage of the disease can be reduced by administration of anti-MCP-1 antibodies (Karpus and Kennedy, 1997). Further to these findings it has been suggested that MIP-1α controls monocyte recruitment during the acute stage of the disease but this role is adopted by MCP-1 during the relapsing stage of the condition (Kennedy *et al.*, 1998). It is conceivable that this temporal demarcation of roles also exists in trypanosome-induced CNS inflammation. In this instance IL-1α and IL-6 would be the major initiators of the early CNS reaction; however their roles in the later stages of the disease may have become superseded by other mediators. This situation would not be entirely unexpected due to the increased variety and numbers of additional cells infiltrating the CNS, together with higher levels of cellular activation found in a meningoencephalitic reaction compared with the mild inflammatory situation seen in the early stages. During the developmental phase of the CNS reaction only a few T-lymphocytes and macrophages have entered the brain. These cells are generally confined to the perivascular regions, ventricles and the meninges and no B-lymphocytes or plasma cells are present the CNS at this stage (Chapter 3).

Astrocytes are one of the first cell types to show morphological changes, indicating that they have become activated, during the development of the CNS response. However, these cells become more numerous and display phenotypic changes that indicate an intense state of activation during the meningoencephalitic reaction. In agreement with the findings from this study, a dramatic reduction in the level of astrocyte activation has previously been reported following eflornithine treatment of trypanosome-infected mice when administered prior to the development of the CNS-stage of the disease and following the induction of the PTRE (Jennings *et al.*, 1997). Since IL-1, IL-6, TNF-α, MCP-1, MIP-1 and RANTES can each be synthesised by astrocytic cells (Asensio and Campbell, 2001; Sharafeldin *et al.*, 2000; Szelenyi, 2001) it is possible, particularly during the development of the CNS reaction, that eflornithine acts directly on these cell to down-regulate the synthesis of these agents. This could result in the reduction in the severity of the inflammatory response seen following eflornithine therapy as well as inhibit any autocrine

actions exerted by the cytokines and chemokines that would further exacerbate the astrocytic reaction.

A down-regulation of astrocyte activation has been reported following eflornithine treatment of mechanically induced brain injury in rats (Jeglinski *et al.*, 1996; Zini *et al.*, 1990). This dampening of the astrocytic response was not found following eflornithine treatment when the astrogliosis was induced by administration of the neurotoxicant methyl-phenyl-tetrahydropyridine (MTPT) (O'Callaghan and Seidler, 1992). Following mechanical brain injury, the integrity of the blood-brain barrier (BBB) is compromised allowing the entry of inflammatory cells and other inflammatory mediators that could exacerbate the reactive astrocytosis (Norton, Aquino, Hozumi, Chiu *et al.*, 1992). This is not the case in neurotoxicant injury as the BBB remains intact and therefore inflammatory cells and pro-inflammatory agents do no have free access to the CNS. The contrasting findings of these studies suggest that the astrocytic response may be induced and maintained through different mechanisms depending on the form of the initial insult. The results imply that astrocytic activation follows a pathway that is not directly affected by the presence eflornithine in situations where the BBB remains intact whereas eflornithine appears to play a major role in the dampening of the response in situations where damage to the BBB has occurred.

The extent of any damage caused to the BBB following trypanosome infection remains equivocal at the present time. Several studies have indicated that the integrity of the BBB becomes progressively weakened following trypanosome infection (Pentreath *et al.*, 1994; Philip *et al.*, 1994) while no deterioration of the tight-junctions that form the barrier was detected in another investigation (Mulenga *et al.*, 2001). If the BBB is impaired during the development of the meningoencephalitis the dramatic reduction in astrocyte activation could follow a similar course to that described for mechanical brain injury. This would not be the case during the early developmental stages of the CNS inflammation as the BBB would still be intact. This scenario would be more comparable to that seen following neurotoxicant damage. However, a dampening of the astrocytic response was found during this stage of the inflammatory reaction. This provides further evidence that the reduction in IL-1α and IL-6 expression found in eflornithine-treated mice may have a direct effect on the development of the astrogliosis seen in the early CNS inflammatory response and suggests that this cell type may play a major role in the induction of the CNS response.

Since this investigation was performed using eflornithine-resistant trypanosomes, the parasitaemia within the CNS would not be affected by the eflornithine treatment.

Therefore, the reduction in the severity of the neuroinflammation and the effects seen on cytokine and chemokine transcription are independent of any changes that would be initiated by clearance of the trypanosomes from the CNS. This indicates that eflornithine may be extremely useful as an anti-inflammatory adjunct therapy in the treatment of human disease even in *T.b.rhodesiense* infections where the parasites have shown primary resistance to the drug. The effects of eflornithine treatment on the production of IL-1α and IL-6 may also help to explain the dramatic clinical improvement found in patients treated with the drug. If the production of these two cytokines is lowered within the CNS then the non-specific indications of infection, including, depression, fever, lassitude and appetite suppression, which are induced by these cytokines in conjunction with TNF-α, could be alleviated.

Overall the results from this investigation indicate that there is an urgent requirement to ensure the continued availability of eflornithine for the treatment of trypanosome infections. Further studies are pivotal to determine the exact effect of the drug at each stage in the disease development. The feasibility of using eflornithine as an adjunct therapy for *T.b.rhodesiense*-infections has been demonstrated and field trials, together with additional animal model studies, utilising combination therapy approaches, are now required to determine the most favourable treatment regimens thereby ensuring optimal drug efficacy, economy and safety of the chemotherapy.

CHAPTER 6

SUBSTANCE P AND HUMAN AFRICAN TRYPANOSOMIASIS

6.1. Introduction

6.1.1. Background

6.1.1.1. What is substance P?

Substance P (SP) is an 11-amino acid neuropeptide that is found widely distributed in both the central nervous system and peripheral tissues. Described in 1931 by von Euler and Gaddum, SP was the first neuropeptide to be identified in mammals and was originally extracted from equine brain and intestine (von Euler and Gaddum, 1931). In the early 1970's the amino acid sequence of SP was reported as Arg-Pro-Lys-Pro-Gln-Gln-Phe-Phe-Gly-Leu-Met-NH_2 (Chang, Leeman, and Niall, 1971). It is a member of the tachykinin family of peptides, that also includes neurokinin A (NKA) and neurokinin B (NKB). The tachykinin family is characterised by the carboxy-terminal amino acid sequence Phe-X-Gly-Leu-Met-NH_2 where X is an aromatic or hydrophobic amino acid (McGillis, Organist, and Payan, 1987). In addition to structural similarity, they also exhibit overlapping biological activities, including, contraction of smooth muscle and induction of sub-normal arterial blood pressure. Indeed, the name 'tachykinin' was employed to describe these peptides due to their ability to induce relatively fast smooth muscle contractions (Erspamer and Melchiorri, 1973).

6.1.1.2. Tachykinin nomenclature

At the International Union of Physiological Sciences Satellite Symposium, entitled *Substance P and Neurokinins,* a new nomenclature system was proposed for the tachykinin family and their receptors (Henry, 1987). As the meeting was conducted in Montreal the system was designated the 'Montreal Nomenclature'. In this classification the three endogenous mammalian tachykinins were designated as substance P; neurokinin A, previously referred to as neurokinin α, neuromedin L or substance K; and neurokinin B, previously named neurokinin β or neuromedin K. The receptors were designated as the tachykinin NK1 receptor; previously named SP-P; the tachykinin NK2 receptor, previously called SP-E, SP-K, or NK-A; and the tachykinin NK3 receptor, previously designated SP-E, SP-N, or NK-B. SP is the most potent ligand for the NK1 receptor; NKA shows the highest affinity for the NK2 receptor while NKB prefers the NK3 receptor (Saria, 1999). However, this concept is currently under revision as NKA and NKB also bind to and

stimulate the NK1 receptor with appreciable affinity (Hastrup and Schwartz, 1996). This finding has led to speculation about exact binding mechanism of the ligands to the NK1 receptor. It has been suggested that either the individual ligands bind to differential binding sites on the receptor or that there are two distinct conformations of this receptor. One conformation would act as a general tachykinin receptor and the second would display preferential binding for SP (Maggi and Schwartz, 1997).

6.1.2. Substance P biosynthesis

6.1.2.1. Preprotachykinin A gene

The sequence of the preprotachykinin-A (PPT-A) gene that encodes both SP and neurokinin-A was elucidated in 1984 (Nawa, Kotani, and Nakanishi, 1984). This gene is organised into 7 exons and 3 introns. The coding sequences of exons 2-6 are well conserved between species while there is more variation in the remaining two exons, 1 and 7 (Bonner, Young, and Affolter, 1987). The promoter region that lies immediately in front of exon 1 is also highly conserved. The length of the introns remains similar between species however there is little correlation in the sequence of the bases. The RNA transcribed from the PPT-A gene undergoes differential splicing that results in different mRNAs, an α PPT mRNA that is missing nucleotide regions in exon 6, a β PPT mRNA that includes all 7 exons, and a γ PPT mRNA with nucleotide regions missing from exon 4 (Krause, Chirgwin, Carter, Xu *et al.*, 1987). Exon 3 of the PPT-A gene designates the transcript as capable of producing SP while if exon 6 is included the transcript also codes for NKA (Bonner *et al.*, 1987). Therefore, SP and NKA can be produced from β and γ PPT mRNAs while only SP can be produced from α PPT mRNA (Krause *et al.*, 1987). A fourth splicing variant, δ PPT, has also been identified in the rat (Harmar, Hyde, and Chapman, 1990). A second PPT gene, PPT-B, is responsible for the production of NKB (Pompei, Severini, Costa, Massi *et al.*, 1999)

6.1.2.2. Post-translational processing

The existence of various different mRNA transcripts suggests that the production of tachykinins is controlled at the level of precursor processing. It appears that β PPT mRNA can either produce both SP and NKA in equal amounts or in some cases an N-terminally extended NKA molecule may result through differential proteolytic processing. This

larger than normal NKA molecule is designated as NPK and includes sequence information contained in exons 4 and 5 of the PPT-A gene in addition to exon 6. γ PPT can produce SP, NKA or a shortened form of NPK designated neuropeptide-γ. This attenuated form of NPK is produced from γ PPT since this configuration of the transcript lacks the information encoded by exon 4 that specifies a protein with a potential α-helical conformation whose function remains unknown (Hayes, Shaw, Chakravarthy, and Buchanan, 1993).

SP is synthesised as a biologically inactive, glycine extended, precursor peptide that requires a post-translational carboxy-terminal amidation to produce the active molecule. This process is a two-step procedure involving the sequential action of two separate enzymes. The first enzyme, peptidylglycine α-monooxygenase (PAM), catalyses the formation of a peptidyl-α-hydroxyglycine intermediate molecule. This intermediate is subsequently converted into the α-amidated, biologically active, form of SP by a second enzyme, peptidylamidoglycolate lyase (PGL) (Ogonowski, May, Moore, Barrett *et al.*, 1997). As this amidation process appears to be the rate-limiting step in the production of the active SP molecule the enzymes involved have become prime candidates as pharmacological targets for reducing SP production through the development of specific enzyme inhibitors. One such molecule, 4-phenyl-3-butenoic acid (PBA), a turnover-dependent inactivator of PAM, has been shown to inhibit α-amidation in both cultured bovine epithelial cells (Oldham, Li, Girard, Nerem *et al.*, 1992) and cultured rat thyroid carcinoma cells (Bradbury, Mistry, Roos, and Smyth, 1990). More recently, Ogonowski and colleagues demonstrated that systemic administration of PBA inhibited the acute inflammatory response produced by injection of carrageenan into the hind paws of rats (Ogonowski *et al.*, 1997)

6.1.3. Tachykinin receptors

Binding of tachykinin receptors by ligands or agonists is regulated by guanine nucleotides indicating that the receptors are coupled to G-proteins. In cultures of spinal neurones, it was found that the NK1-agonist complex became internalised following this binding (Mantyh, DeMaster, Malhotra, Ghilardi *et al.*, 1995; Mantyh, Rogers, Honore, Allen *et al.*, 1997). Rapid endocytosis of this receptor was also demonstrated following injection of SP in the rat striatum *in vivo* (Mantyh, Allen, Ghilardi, Rogers *et al.*, 1995). This internalisation of the receptor-ligand complex is characteristic of G-protein coupled receptors (Hunt, 2000). G-protein coupled receptors form a superfamily of proteins

characterised by the presence of seven, transmembrane α-helices. Signalling occurs through interactions with a family of heterotrimeric GTP-binding proteins, referred to as G-proteins (Edwards, Tan, and Limbird, 2000). There appears to be particular amino acids that lie in specific positions within the molecule that are pivotal to the function of the receptor. One example of this can be seen in the positioning of the tyrosine amino acid, located in the inner part of the transmembrane 5 portion of the human NK1 receptor. This molecule appears to be in a crucial position in the G-protein coupling of the receptor. If the amino acid is substituted with an alanine molecule, the binding affinity of the receptor for its ligand remains unaffected; however, the receptor is unable to generate any second messenger response (Quartara and Maggi, 1997).

Stimulation of the NK1 receptor by the binding of SP or a SP agonist leads to the induction of various second messenger systems that can subsequently trigger effector mechanisms that control cellular excitability and function. To date three apparently independent second messenger systems have been reported to be induced following NK1 stimulation. These pathways include; the stimulation of phosphatidyl inositol turnover, via phospholipase C, resulting in both intra- and extra-cellular calcium mobilisation; stimulation of adenylate cyclase leading to cyclic adenosine monophosphate accumulation; and mobilisation of arachidonic acid via phospholipase A2 (Quartara and Maggi, 1997).

There is some evidence to suggest that the upregulation in expression of NK1 mRNA in the dorsal horn of the spinal cord induced by peripheral noxious stimulation is the result of a positive feedback loop involving the activation of the original NK1 receptors (McCarson and Krause, 1996).

6.1.4. Substance P and the NK1 receptor in nervous tissues

6.1.4.1. Distribution in the CNS

Investigations using autoradiography, mapping of NK1 mRNA expression and immunocytochemistry have demonstrated that the NK1 receptor is widely distributed throughout the CNS and the peripheral nervous system.

Within the brain NK1 receptors have been shown in the striatum, the nucleus accumbens, the hippocampus, the lateral nucleus of the hypothalamus, the habenula, the

interpeduncular nucleus, the nucleus of the tractus solitarius, the raphe nuclei and the medulla oblongata (Saria, 1999). Some apparently conflicting information with regard to the distribution of the NK1 receptor and SP itself has also been generated. In the substantia nigra pars reticulata SP immunoreactive nerves have been detected with no apparent receptor presence (Nakaya, Kaneko, Shigemoto, Nakanishi *et al.*, 1994). In the hilus of the dentate gyrus the opposite situation is encountered. Here NK1 receptors are present but the area is apparently devoid of SP-positive fibres (Nakaya *et al.*, 1994). However, it remains unclear whether these mismatches are authentic or artefactual. The possibility also exists that NKA or NKB are the physiological ligands in preference to SP within these mismatched areas (Saria, 1999), or that SP acts at sites distal to its production (Bowden, Baluk, Lefevre, Vigna *et al.*, 1996).

6.1.4.2. SP and NK1 receptors in spinal cord

Substance P is considered to be one of the major mediators of pain and neurogenic inflammation in peripheral tissues, although the precise contribution of SP to this process remains equivocal. SP is synthesised by primary afferent fibres that have their cell bodies in the dorsal root ganglion (DRG). These small diameter, mostly unmyelinated, fibres transport the SP from the DRG to their central and peripheral terminals where it is stored in dense core vesicles. On noxious stimulation SP is thought to be released from these terminals; however, the mechanisms evoking pain behaviour following SP release remain unclear (Basbaum, 1999). The fibres responsible for the synthesis and transport of SP are also responsible for the synthesis of the excitatory amino acid glutamate. On noxious stimulation glutamate is known to be released from these fibres and activate second order neurones in the spinal cord. Some researchers believe that the co-synthesis and release of these two molecules leads to a synergistic effect that enhances the glutamatergic transmission increasing nociceptive processing and pain (Dougherty, Palecek, Zorn, and Willis, 1993; Randic, Hecimovic, and Ryu, 1990). Others refute this hypothesis and claim that SP has little relevance to the production of pain (Bossut, Frenk, and Mayer, 1988). However, the evidence presented in this section strongly supports a role for the tachykinins in pain perception and transmission and provides a framework in which to speculate about the significance and mechanism of action of SP and the tachykinin receptors in this response.

Areas of the spinal cord that express the highest levels of NK1 receptors include the dorsal horns, the intermediolateral nucleus of the thoracic spinal cord and discrete nuclei in the

ventral horns (Nakaya *et al.*, 1994). The surgical loss of sensory fibres has been shown to cause an upregulation of NK1 receptors at discrete sites in the spinal cord. This may indicate that these sites are innervated by primary afferent neurones suggesting that SP and NK1 play a major role in pain perception (Croul, Sverstiuk, Radzievsky, and Murray, 1995; Yashpal, Dam, and Quirion, 1991). Furthermore, there is a distinct biphasic modulation in NK1 receptor expression in the dorsal horns of the spinal cord following adjuvant-induced inflammation of the hind paw in rats as measured by the binding of [^{125}I] Bolton Hunter SP (Stucky, Galeazza, and Seybold, 1993). Acute painful stimuli have been shown to produce a rapid decrease in NK1 receptor binding. This is presumably due to the internalisation of the NK1 receptor-endogenous ligand complex within the neurones of the rat dorsal spinal cord that is associated with the acute pain response (Mantyh *et al.*, 1995). However after 48 hours, the initial decrease in NK1 receptor binding was followed by a widespread increase in [^{125}I] Bolton Hunter SP binding (Stucky *et al.*, 1993). By employing Scatchard analysis the increased level of binding was found to be the result of a 10 fold increase in the affinity of the NK1 receptor for [^{125}I] Bolton Hunter SP and the presence of a low affinity binding site.

Evidence suggesting a significant role for the NK1 receptor in the hyperalgesia that accompanies persistent peripheral inflammation and tissue damage originates from studies employing specific non-peptide NK1 receptor antagonists in decerebrated rats. In these experiments it was found that footpad administration of complete Freund's adjuvant resulted in an increase in the excitability of the flexor reflex in rats. This rise in excitability decreased significantly following administration of the NK1 receptor antagonist RP-67,580 but was unaffected by the inactive enantiomer RP-68,651 (Ma and Woolf, 1997; Parsons, Honda, Jia, Budai *et al.*, 1996).

Further evidence supporting a role for SP in persistent pain became available from additional studies employing the CNS penetrating, non-peptide, non-neurotoxic, NK1 receptor antagonist L-733,060 (Rupniak, Carlson, Boyce, Webb *et al.*, 1996). Injection of formalin into the footpad of conscious gerbils produces a two-phase nociceptive response. The response entails a vigorous licking of the affected paw which peaked during the first 15 minutes immediately following the formalin injection and subsided to a relatively low constant level 20 to 40 minutes after stimulation. The NK1 receptor antagonist was administered by injection into the jugular vein of anaesthetised animals 3 hours prior to the formalin injection. This permitted the entrance of the maximal concentration of the antagonist into the CNS. The treatment was found to inhibit the late phase of the response in a dose dependent manner and block the response completely at a dose of 10mg/kg. No

effect was seen during the early stage, except a minimal reduction in the response in animals that had been given the high dose of antagonist.

The co-administration of a NK1 receptor antagonist and a N-methyl D-aspartate (NMDA) receptor antagonist produces a more potent inhibition of the nociceptive reflex in rats than that seen following administration of the individual antagonists. This suggests a co-operative action between the two receptors in the production of the nociceptive response (Xu, Dalsgaard, and Wiesenfeld-Hallin, 1992). These findings strengthen the theory that the message resulting from activation of the NK1 receptor is a slowly developing long lasting depolarisation while the initial response is the result of the fast synaptic input by excitatory amino acids such as glutamate to second order sensory neurones. Experiments employing NK1 receptor knockout mice have shown that these animals respond normally to acute chemical, thermal and mechanical pain. However, on intraplantar administration of formalin a reduction in the paw licking reaction was noted during the second phase of the response (de Felipe, Herrero, O'Brien, Palmer *et al.*, 1998; Giffin *et al.*, 1986; Wang, 1988). Also a lack of the wind up response whereby increasing the intensity of the stimulus results in a progressive increase in response was absent in the knockout animals (de Felipe *et al.*, 1998; Herrero, Laird, de Felipe, Smith *et al.*, 1997) These data are in agreement with that previously generated from the antagonist administration experiments referred to above.

6.1.4.3. SP and NK1 receptors in astrocytes

Astrocytes are the most numerous glial cell type found in the brain and among other functions play a pivotal role in the brain's reaction to injury. Upon stimulation the astrocytes become activated and participate in immunologic and inflammatory events through the expression of adhesion molecules and the secretion of various cytokines. The human astrocytoma cell lines U-373 MG (Heuillet, Menager, Fardin, Flamand *et al.*, 1993; Lee *et al.*, 1989) and UC11 (Johnson and Johnson, 1992) are known to express functional NK1 receptors. Studies have also demonstrated SP receptors localised to 0-2A progenitor cells and type-2 astrocytes *in vitro* (Marriott and Wilkin, 1993). As astrocytes undergo phenotypical changes in response to injury the phenotypical status of astrocytes in culture remains unclear. It is therefore not known whether normal unstimulated astrocytes *in vivo* express the receptor.

In normal optic nerve, *in vivo*, the astrocytes express very few NK1 receptors but this number increases dramatically in the glial scar formed following transection of the nerve

(Mantyh, Johnson, Boehmer, Catton *et al.*, 1989). A correlation between the extent of NK1 expression in astrocytomas and glioblastomas and the malignancy of the tumour has also been demonstrated (Hennig, Laissue, Horisberger, and Reubi, 1995). Further, it has been suggested that the presence of NK1 receptors may infer an increased growth advantage when present in brain tumours and may be an effective and legitimate chemotherapeutic target in these tumour types (Luo, Sharif, and Sharif, 1996).

In vitro studies employing the human astrocytoma cell line U373 MG cells have shown that SP can induce the production of the proinflammatory cytokine interleukin (IL)-6 (Cadman, Witte, and Lee, 1994; Gitter, Regoli, Howbert, Glasebrook *et al.*, 1994). This induction was inhibited by the simultaneous addition of NK1 receptor antagonists to the culture system. The production of IL-6 is often mediated by the presence of IL-1. To determine if this was the case in this scenario neutralising antibodies were added to remove any endogenous IL-1; however, no change in the production of IL-6 was seen (Gitter *et al.*, 1994). Therefore, the secretion of IL-6 by cultured U373 MG cells appears to be independent of IL-1 induction. In contrast to these findings, the addition of SP alone to rat astrocyte enriched primary cultures was unable to stimulate TNF-α production but caused a dose dependent increase in TNF-α production when added in conjunction with LPS. When IL-1 neutralising antibodies were added the enhanced production returned to the levels observed following stimulation with LPS alone (Luber-Narod, Kage, and Leeman, 1994). This suggests that TNF production by astrocytes may be controlled in part by the presence of IL-1. The apparent discrepancy between the two studies could be the result of primary versus transformed cell lines and the different cytokines being investigated.

Reactive astrocytes, *in vivo*, not only express the NK1 receptor but can also be induced to express SP and SP-immunoreactive astrocytes have been found in post-mortem white matter specimens from 5 patients with multiple sclerosis (MS) (Kostyk, Kowall, and Hauser, 1989). These SP immunoreactive astrocytes were seen around the edges of both inflammatory (active) and non-inflammatory (inactive) MS lesions. Astrocytes expressing SP have also been found in gerbil forebrain following ischaemic, thermal and mechanical injury (Lin, 1995).

6.1.5. SP and NK1 receptors in peripheral tissues

6.1.5.1. The cardiovascular system

SP and NK1 receptors can be found not only in nervous tissue but also on many different cell types in the peripheral tissues.

In the vascular system, immunocytochemistry and autoradiography studies have shown that endothelial cells in large blood vessels and post-capillary venules express NK1 receptors *in vivo* (Greeno, Mantyh, Vercellotti, and Moldow, 1993; Saito, Konishi, Takano, Nonaka *et al.*, 1990). In tissue culture, stimulation of the endothelial cell NK1 receptors induces cellular proliferation and migration. These two processes are central to the development of blood and lymph vessels. In an avascular rabbit cornea, application of SP or NK1 receptor agonists, results in the generation of new vascular tissue (Ziche, Morbidelli, Pacini, Geppetti *et al.*, 1990). This phenomenon has been further demonstrated following co-administration of SP and IL-1α. Doses of these mediators, that do not elicit a response individually, when applied in tandem, result in an intense neovascularisation of implanted sponge material in rats (Fan, Hu, Guard, Gresham *et al.*, 1993; Walsh, Hu, Mapp, Polak *et al.*, 1996). A possible role for the NK1 receptor in tumour growth was also suggested following the discovery of the receptors on the blood vessels in human primary neoplasms (Hennig *et al.*, 1995).

Vasodilation (Maggi, Patacchini, Perretti, Tramontana *et al.*, 1990) and vasoconstriction (Shirahase, Kanda, Kurahashi, Nakamura *et al.*, 1995) of rabbit pulmonary artery and isolated veins (Patacchini and Maggi, 1995) can be induced through stimulation of the NK1 receptors. This ability to control vascular tone indicates that NK1 receptors may be involved not only with the normal regulation of blood pressure but also the early generation of stress induced hypertension. In various salt-dependent hypertensive rat models an increase in blood pressure occurs when the animals are treated with NK1 receptor antagonists. Since the hypertensive effect of the NK1 receptor antagonist was only found in salt-dependent models of hypertension, this suggests that SP could exert an effect on the sodium regulatory mechanisms in the rat (Kohlmann, Jr., Cesaretti, Ginoza, Tavares *et al.*, 1997). The question of whether the blood vessel, endothelial cell NK1 receptors are innervated or stimulated directly by circulating tachykinins remains equivocal (Ferrell, Lockhart, and Karimian, 1997; Maggi *et al.*, 1990).

Another important process that appears to be mediated through the NK1 receptors is the increase in post capillary venular permeability that permits plasma protein extravasion. The use of selective NK1 receptor agonists and antagonists has shown that the NK1 receptor is the major, and perhaps the exclusive, mediator of tachykinin induced plasma protein extravasion. (Eglezos, Giuliani, Viti, and Maggi, 1991). Again this process appears to result from stimulation of the NK1 receptor on endothelial cells. Following stimulation gap formation between the endothelial cells occurs allowing the passage of the plasma proteins (Baluk, Nadel, and McDonald, 1992). However, although the arteries are innervated by many SP-positive fibres this is not true of the post capillary venules; therefore, the reaction seen in these venules may be the result of SP release at distant rather than local sites (Bowden *et al.,* 1996).

In a rat model of cardiomyopathy, induced by magnesium deficiency, increased levels of SP were found in the plasma during the first week of reduced magnesium intake. The resulting elevation of SP levels was followed by increases in the presence of various inflammatory mediators. If the magnesium deficient rats were treated with a NK1 receptor antagonist the increase in SP still occurred, though, there was no concurrent increase in the levels of the inflammatory mediators and no cardiac lesions developed. These findings have been extended to include NK1 receptor activation in the aggravation of cardiac damage resulting from ischaemia-reperfusion injury (Kramer, Phillips, and Weglicki, 1997; Walsh, Weglicki, and Correa-de-Araujo, 1996). However, the results are in contention with those previously reported (Ustinova, Bergren, and Schultz, 1995). These workers found that blockade of the NK1 receptors by administration of a selective antagonist aggravated the post-ischaemic response implying a protective role for the NK1 receptor in the pathogenesis of ischaemic heart disease.

6.1.5.2. The respiratory system

NK1 receptors are found throughout the respiratory system (Walsh, Salmon, Featherstone, Wharton *et al.*, 1994). In the airways of various species, NK1 receptors mediate the tachykinin-induced secretion of mucus by seromucous glands and goblet cells (Rogers, Aursudkij, and Barnes, 1989; Webber, 1989) and the involvement of NK1 receptors in asthma and bronchial hypersensitivity has been demonstrated by employing selective antagonists. Following the inhalation of cigarette smoke, plasma protein extravasion is induced in the guinea-pig trachea and bronchi. This process can be blocked by the administration of a NK1 receptor antagonist (Delay-Goyet and Lundberg, 1991). A

recruitment of leucocytes into the airways was found to occur in parallel with the plasma protein extravasion induced by challenge with hypertonic saline (Baluk, Bertrand, Geppetti, McDonald *et al.*, 1995) or antigen (Kaltreider, Ichikawa, Byrd, Ingram *et al.*, 1997). Again, this inflammatory cell infiltration could be inhibited by administration of a NK1 receptor antagonist. A potentially therapeutic use for NK1 receptor antagonists can be demonstrated from research employing models of asthma. When previously sensitised 'asthmatic' mice were pre-treated with RP-67,580, a NK1 receptor antagonist, before challenge with toluene di-isocyanate, a known cause of occupational asthma, the development of the bronchial hyper-reactivity was inhibited (Scheerens, Buckley, Muis, Van Loveren *et al.*, 1996). The exact cell types involved in this response remain unknown and further research into the role of SP and the NK1 receptor in the pathogenesis of asthma is urgently required.

6.1.5.3. The gastrointestinal system

One of the first properties of SP to be discovered was its ability to cause the smooth muscle of the intestine to contract. NK1 receptors are found at high concentrations in the smooth muscle layers, sub-mucosa, intestinal epithelium and in the ganglia of the enteric plexuses (Sternini, Su, Gamp, and Bunnett, 1995). Definitive evidence that tachykinins, acting through NK1 receptors, are responsible for the non-adrenergic non-cholinergic (NANC) excitation of the circular muscle of the gut has been established by employing selective antagonists (Zagorodnyuk, Santicioli, Turini, and Maggi, 1997). This suggests a key role for NK1 receptors in gut motility. Indeed the activation of NK1 receptors appears to be involved in such processes throughout the intestinal tract including inhibition of colonic motility in response to rectal distension (Julia, Morteau, and Bueno, 1994), stress induced defecation (Ikeda, Miyata, Orita, Kubota *et al.*, 1995) and inhibition of gastric emptying induced by peritoneal irritation (Julia and Bueno, 1997). Various studies, investigating several different species and gut areas including porcine jejunum (Brown, Parsons, and O'Grady, 1992), cat small intestine (Brunsson, Fahrenkrug, Jodal, Sjoqvist *et al.*, 1995) and guinea-pig ileum and colon (Reddix and Cooke, 1992), have also demonstrated the involvement of tachykinins in mediating epithelial ion and water transport (Cooke, Sidhu, Fox, Wang *et al.*, 1997).

The varied roles of SP and the NK1 receptor, ranging from pain and inflammation to gut motility and ion/water regulation, and their wide distribution within the intestine resulted in a number of investigations to determine their role in the pathophysiology of intestinal

inflammatory conditions. In colon specimens taken from human patients with ulcerative colitis and Crohn's disease, a dramatic increase in the expression of NK1 receptors, together with aberrant NK1 receptor expression in areas where it is not usually present, was found (Mantyh, Vigna, Bollinger, Mantyh *et al.*, 1995; Mantyh, Gates, Zimmerman, Welton *et al.*, 1988). In rat intestine SP plays a role in the inflammatory response to *Clostridium difficile* toxin A. This was elucidated by demonstrating that the inflammatory response to toxin A could be inhibited by pre-treating the rats with the NK1 receptor antagonist CP-96,345 (Pothoulakis, Castagliuolo, LaMont, Jaffer *et al.*, 1994). The phenomenon has been further investigated and it appears that the intestinal macrophages in the lamina propria are induced to express and release SP on stimulation with *Clostridium difficile* toxin A instigating an inflammatory reaction in the gut (Castagliuolo, Keates, Qiu, Kelly *et al.*, 1997).

6.1.6. NK1 receptors and SP in inflammatory cells

As a result of the vast quantity of evidence implicating NK1 receptors and SP in the inflammatory response extensive research to elucidate the mechanisms involved in this process has been carried out. It appears that SP has many actions on various cells from the immune system including the stimulation of proliferative responses and the induction of cytokine production. These functions are discussed below.

6.1.6.1. Monocytes

Analysis of normal human monocytes, using flow cytometry, has shown that they contain SP (De Giorgio, Tazzari, Barbara, Stanghellini *et al.*, 1998). These findings were supported by the demonstration of mRNA transcripts for SP in human peripheral blood monocytes (Lai, Douglas, Rappaport, Wu *et al.*, 1998). It appears that monocytes not only produce SP but also respond to its presence. In a study employing cultured human monocyte-derived macrophages the addition of SP to the culture system resulted in an increase in the production of tumour necrosis factor (TNF). If lipopolysaccharide (LPS) was added in conjunction with the SP a synergistic effect was seen and TNF production occurred at higher levels than with either stimulant individually. The stimulatory activity of SP was inhibited by the addition of NK1 receptor antagonists (Lee, Ho, and Douglas, 1994). This potentiation of TNF production by monocytes had been described previously by Lotz and co-workers who had also demonstrated that SP could induce interleukin (IL)–1 and IL-6 production by these cells (Lotz, Vaughan, and Carson, 1988). These findings

were further corroborated when it was shown that preincubation of murine peritoneal macrophages with SP, prior to stimulation with LPS, results in a significant augmentation of the production of the proinflammatory cytokines IL-1, TNF-α and IL-6 (Berman, Chancellor-Freeland, Zhu, and Black, 1996). Further work has shown that a fragment of SP containing the amino acids lying in positions 4-11 can induce TNF production by cultured human peripheral blood derived monocytes or aliquots of whole human blood (Nair and Schwartz, 1995). In addition, the production of the cytokine interferon-γ (IFN-γ) can be induced if monocytes are stimulated with pokeweed mitogen, this stimulation is significantly enhanced by the concurrent addition of SP (Wagner, Fink, Hart, and Dancygier, 1987). These findings suggest that SP could act as a priming agent or primary activation signal in the induction of the cascade of responses that occur during macrophage stimulation

Despite overwhelming evidence that SP elicits many monocyte responses, the ability of SP to bind with high affinity and specificity to human peripheral blood monocytes and macrophages was not reported until 1994 (Lucey, Novak, Polonis, Liu *et al.*, 1994). This group determined that ^{125}I-SP bound to a specific receptor on the monocytes and that this binding occurred within 6 hours of introduction of the labelled SP to the culture system.

6.1.6.2. Polymorphonuclear leucocytes

Flow cytometry has demonstrated that normal human granulocytes contain SP (De Giorgio *et al.*, 1998). Furthermore, SP has been shown to have an effect on polymorphonuclear leucocytes (PMNL). Pre-treatment of cultured human PMNL's with SP resulted in an increase in the respiratory burst produced by these cells in response to stimuli including formyl-methionyl-leucyl-phenylalanine (FMLP), concavalin A (conA) and opsinized zymosan (STZ). However the oxygen burst induced by TNF-α was strongly inhibited by pre-treatment with SP (Serra, Calzetti, Ceska, and Cassatella, 1994). The eosinophils in the liver granulomas that develop in schistosmiasis have been shown, by means of *in situ* hybridisation, to produce SP (Weinstock, Blum, Walder, and Walder, 1988). By employing NK1 receptor antagonists, SP was shown to induce maturation of the B-cells within the schistosome granuloma into antigen secreting cells and also to increase the capacity of the granuloma to produce IFN-γ, IL-4, IL-5 and IL-6 (Blum, Metwali, Cook, Mathew *et al.*, 1993; Blum, Metwali, Elliott, Sandor *et al.*, 1996).

SP and the NK1 receptor have been shown to mediate the adhesion of neutrophils and eosinophils to the endothelial cells of inflamed blood vessels. This adhesion process, controlled by the expression of adhesion molecules on endothelial cells and their complementary ligands on leucocytes, is a necessary step in the transmigration of leucocytes into tissues during an inflammatory reaction. Blockade of the NK1 receptor by administration of the antagonist, CP-96,345 to anaesthetised rats reduced the adherence of both eosinophils and neutrophils in the blood vessels of the tracheal mucosa (Baluk *et al.*, 1995). As SP has been shown to induce the expression of ICAM-1 by cultured human umbilical vein endothelial cells (Nakagawa, Sano, and Iwamoto, 1995) blockade of the NK-1 receptor could prevent this upregulation causing a reduction in cellular adhesiveness.

SP has also been shown to regulate a number of neutrophil functions. The cytotoxic activity of human neutrophils against antibody coated target cells is increased by SP in a dose dependent manner. In addition, pre-treatment of neutrophils with SP results in a rapid increase in FMLP-stimulated superoxide anion production (Wozniak, McLennan, Betts, Murphy *et al.*, 1989). Therefore, SP may play a key role in the control of the cell-mediated immune response to infection by bacteria or parasites.

6.1.6.3. Lymphocytes

Normal lymphocytes have been shown generally to be negative or only weakly positive for SP, with only 10-20% of the cells forming the weakly positive subsets (De Giorgio *et al.*, 1998). However, activated CD4 and CD8 T-cell subsets, and T-cells from leukaemic patients, are strongly labelled with antibodies against SP when analysed using flow cytometry (De Giorgio *et al.*, 1998). The ability of lymphocytes to produce SP has been corroborated in a study employing human peripheral blood isolated lymphocytes stimulated with phytohaemagglutanin (PHA) and IL-2. These cells were shown to contain SP mRNA by nested RT-PCR and SP protein using an enzyme immunoassay method (Lai *et al.*, 1998).

Lymphocytes not only produce SP but also express the SP receptor. This was demonstrated by the ability of T-cells, prepared from murine spleen and Peyers patches, to bind fluorescein labelled SP (Stanisz, Scicchitano, Danzin, Bienenstock *et al.*, 1987). In addition, T-cell functions have been shown to be enhanced by SP. ConA induced proliferation of both spleen and peripheral blood lymphocytes is enhanced by administration of SP. This augmentation was completely inhibited when a NK1 receptor antagonist was added to the tissue culture system at the same time as the SP (Santoni,

Perfumi, Spreghini, Romagnoli *et al.*, 1999). Evidence from a separate study also suggests that T-cells show a chemotactic response to SP that is mediated not only through the NK1 receptor but also through the NK2 receptor (Hood, Cruwys, Urban, and Kidd, 2000). There is also evidence indicating that the adhesiveness of T-cells to endothelial cells is enhanced by SP. This appears to occur through an increased expression of ICAM-1 by the endothelial cells in conjunction with a corresponding increase in the avidity of the LFA-1 ligand on lymphocytes (Vishwanath and Mukherjee, 1996).

SP receptors have also been demonstrated on B-cell populations. Flow cytometry experiments using fluorescein labelled SP and studies using ^{125}I-SP show SP binding to murine B-cells (Stanisz *et al.*, 1987). Immunoglobin secretion by B-cells can be modulated by SP. Laurenzi and co-workers found that the number of IgG secreting cells in cultures of enriched human B-cells stimulated with the polyclonal activator *Staphylococcus aureus* protein A was significantly increased when SP was added to the culture system (Laurenzi, Persson, Dalsgaard, and Ringden, 1989). An *in vivo* experiment investigating the effect of SP in chronic granulomatous inflammation associated with schistosome infection has shown that blockade of the SP receptor leads to a reduction in antibody production by inhibiting the maturation of intragranuloma B-cells. This reduction in IgM production was accompanied by a decrease in IFN-γ, IL-4, IL-5 and IL-6 production by the granuloma and suggests that SP could be affecting a variety of cytokine pathways resulting in B-cell maturation (Blum *et al.*, 1996).

Overall, the effects of SP on lymphocytes appear to be largely stimulatory. Protein, DNA and immunoglobin synthesis by mature T and B-cells is significantly enhanced on stimulation by SP (McGillis *et al.*, 1987). These findings suggests a largely proinflammatory action SP in inflammatory responses.

6.1.7. Substance P and trypanosomiasis

Accumulating evidence implicates SP in the pathogenesis of a wide range of inflammatory conditions. These conditions range from neurological disorders including multiple sclerosis, where SP immunoreactive astrocytes have been demonstrated in the CNS lesions (Barker and Larner, 1992), to systemic diseases such as rheumatoid arthritis, where significantly higher levels of SP were found in serum from arthritic patients compared to healthy controls (Anichini *et al.*, 1997). The involvement of SP has also been demonstrated in parasitic diseases. Sera from patients with Falciparum malaria can induce

the production of SP by cultured human brain microvascular endothelial cells (Chiwakata *et al.*, 1996) and B-cell maturation in schistosome granulomas appears to be controlled by SP produced by granuloma eosinophils (Blum *et al.*, 1996; Weinstock *et al.*, 1988). Mice treated with a SP antagonist show an increased susceptibility to infection with *Salmonella* suggesting a role for SP in possible resistance to bacterial infections. Further evidence for the involvement of SP in bacterial conditions comes from studies investigating the enterotoxic responses of rats to *Clostridium difficile* toxin A. In these experiments pre-treatment of rats with the SP antagonist, CP-96,345, resulted in a reduction in the intestinal response to the enterotoxin (Pothoulakis *et al.*, 1994). In the case of viral infections SP has been shown to modulate the replication of human immunodeficiency virus (HIV). In these studies, treatment of peripheral blood monocyte derived macrophages, infected with HIV *in vitro*, with SP resulted in a 2 to 8 fold increase in the expression of HIV as determined by reverse transcriptase activity (Ho, Cnaan, Li, Zhao *et al.*, 1996)

The ability of SP to modulate this vast range of inflammatory responses of both infectious and non-infectious aetiologies led us to postulate that SP may be involved in the pathogenesis of the meningoencephalitis associated with human African trypanosomiasis. The development of this condition encompasses many of the features of the inflammatory reactions mentioned above. This CNS invasive parasite evokes an elaborate cascade of events, including, astrocyte activation, inflammatory cell infiltration and polyclonal B-cell activation in conjunction with the production of a complex milieu of cytokines and chemokines. SP has previously been implicated in the regulation and control of all of these events. The following chapter will investigate the role of SP in the induction and development of the trypanosome-induced CNS inflammatory reaction found in our mouse model of human African trypanosomiasis.

6.2. Materials and methods

The involvement of SP in the neuropathogenesis of human African trypanosomiasis was investigated using two complementary systems. Initial studies employed the NK1 receptor antagonist RP-67,580 to block the action of SP and the latter experiments used mice in which the NK1 receptor had been genetically ablated. Due to the possible usage of alternative neurokinin receptors by SP in NK1 knockout mice, the neuropathological response was also studied following administration of the NK2 and NK3 receptor antagonists, SR48968 and SR142801 respectively, in these animals. Each of the experimental rationales is detailed individually below.

6.2.1. Administration of the NK1 receptor antagonist

6.2.1.1. RP-67,580 and RP-68,651

The highly selective, non-peptide NK1 receptor antagonist RP-67,580 {2-[1-amino-2-(2-methoxyphenyl)ethyl]-7,7-diphenyl-4-perhydroisoindolone (3aR, 7aR) } was employed in this study. The antagonist was dissolved in isotonic saline and administered to the mice by intraperitoneal injection (i.p.) at a dose rate of 2mg/kg. This treatment inhibits the action of SP by blocking the NK1 receptor. To ensure that any differences found between experimental and control animals were a result of NK1 receptor blockade and not a secondary factor caused by the drug but unrelated to SP, the inactive enantiomer RP-68,651 {3aS, 7aS} was employed in infected control animals. Both the antagonist and the enantiomer were donated by Rhone-Poulenc Rorer (Vitry sur Eine, France)

6.2.1.2. Animals, infections and treatments

6.2.1.2.1. Experiments 1, 2 & 3

Female CD-1 mice (Charles River Breeding Laboratories) weighing 28-35g were infected i.p. with 4 x 10^4 *T.b.brucei* parasites. These parasites belonged to cloned stabilate GVR35/C1.5 previously described in the 'General materials and methods' chapter of this thesis. Parasitaemia was confirmed by weekly examination of blood taken by a tail snip. The infection was allowed to progress until day 28 post-infection when the mice were

treated with the trypanocidal drug diminazene aceturate (Berenil®; Hoechst Pharmaceuticals) at 40mg/kg i.p. to induce a CNS inflammatory reaction. On day 35 post-infection the antagonist was administered. A dose of 2mg/kg i.p. was given to each mouse twice daily. This regimen was continued for a period of 10 days. The animals were sacrificed at the end of this period, their brains excised and processed for histopathology. A total of 26 infected mice were treated with diminazene aceturate and antagonist in these experiments. Experiment 1 involved 6 mice, 11 animals were used in experiment 2 and experiment 3 contained 9 mice.

In parallel with this protocol various control regimens were followed. Control groups included infected mice given diminazene aceturate followed by saline in place of RP-67,580; uninfected mice treated with diminazene aceturate; and uninfected mice given RP-67,580. In experiment 3 the infected saline treated controls were replaced by infected mice treated with the inactive enantiomer RP-68,651.

6.2.1.2.2. Experiment 4

A slightly modified forth experiment was also performed utilising the same basic regimen. In this experiment the animals were infected as before; however, the antagonist therapy was initiated on day 27 post-infection, 1 day prior to the diminazene aceturate treatment. The RP-67,580 was administered as previously described and the treatment continued for 21 days. At the end of this period, on day 49 post-infection the animals were killed and the brains removed for histopathological examination. A total of 9 mice were infected and treated with the antagonist and diminazene aceturate in this experiment. Control groups were included as described above.

6.2.2. Use of NK1 receptor knockout mice

6.2.2.1. Generation of the knockout animals

The genetically altered knockout mice employed in the following experiments were generated using embryonic stem (ES) cells prepared from the inbred 129/Sv mouse strain in which exon 1 of the NK1 receptor gene had been disrupted by targeted homologous recombination using a replacement vector and ultimately re-implanted in a C57BL/6 mouse (de Felipe *et al.*, 1998).

Briefly the procedure involved transfecting the ES cells with a linearised, genetically manipulated genomic DNA fragment known as the targeting vector. In this case the targeting vector consisted of a clone of exon 1 from the NK1 receptor gene, with a cassette containing an internal ribosome entry site and the *lacZ* coding sequence, together with a neomycin resistance gene, inserted into the unique *Stu*I restriction enzyme site. Two copies of the thymidine kinase gene from herpes simplex virus (HSV-TK) were also introduced outside of the homologous region of interest. As the neomycin resistance gene confers resistance to geneticin and the HSV-TK gene confers resistance to gancyclovir, a positive and negative selection strategy could then be employed to detect appropriately transfected clones. Clones resistant to geneticin (positive selection) but sensitive to gancyclovir (negative selection) were selected as successfully transfected cells.

ES cell lines are derived from the inner cell mass of pre-implantation blastocysts. These cells are uncommitted and pluripotent and can therefore form either somatic or germ-line tissues when reintroduced into the blastocyst. The selected ES cell clones were injected into C57BL/6 blastocysts and subsequently reimplanted into the uterus of pseudopregnant foster mothers. The use of ES cells derived from 129/Sv mice facilitates the identification of chimeric animals by the presence of the dominant Agouti coat colour in the offspring. Chimeric males were then mated with C57BL/6 females and transmission of the mutant allele to the pups was determined by Southern blot analysis of DNA extracted from samples of tail tissue. Mice homozygous for the mutation were generated from subsequent matings of animals heterozygous for the disrupted allele. The resultant homozygous mice were healthy, bred normally and did not show impaired maternal behaviour and were therefore used to found the knockout colony (de Felipe *et al.*, 1998).

6.2.2.2. Animals, infections and treatments

Professor Stephen Hunt, gifted the animals used in experiments 1 and 2 below as adult mice, from the MRC Molecular Biology Laboratory, University of Cambridge. Following these initial experiments Prof. Hunt took up a new position at University College London and it became necessary to establish breeding colonies of both knockout and wild-type mice in the Parasitology animal unit at Glasgow University Veterinary School. Following the required quarantine period and prerequisite health screen of pups from the first litters, the breeding animals were transferred to the Parasitology animal unit and the mice used in all subsequent experiments were bred 'in-house'. All animals weighed between 25-35g at the beginning of the experimental procedures.

6.2.2.2.1. Neuroinflammation in NK1 knockout animals

6.2.2.2.1.1. Experiment 1

A total of 14 NK1 receptor knockout mice ($NK1^{-/-}$) and 13 wild-type animals ($NK1^{+/+}$) were infected i.p. with 3 x 10^4 *T.b.brucei* cloned stabilate GVR35/C1.6 as previously described. Parasitaemia was monitored by examination of fresh blood smears. On day 28 post-infection the mice were treated with diminazene aceturate (40mg/kg i.p.) to induce a CNS inflammatory reaction. The experiment was continued until day 40 post-infection when the animals were sacrificed and their brains extracted and processed for histopathology.

In parallel with this regimen uninfected control groups consisting of 5 $NK1^{-/-}$ animals and 6 $NK1^{+/+}$ were included in the design. These mice were treated with diminazene aceturate in the same manner and sacrificed on the same day as the experimental animals. This procedure excludes the possibility of an independent clinical or pathological effect of the drug on the mice in the absence of a trypanosome-infection.

6.2.2.2.1.2. Experiment 2

In experiment 2, 15 $NK1^{-/-}$ and 15 $NK1^{-/+}$ animals were infected as previously described. The infection was allowed to progress naturally until day 21 post-infection when the mice were given diminazene aceturate (40mg/kg i.p). This time point is 7 days earlier than that used in experiment 1. The experiment was terminated at 40 days post-infection when the mice were killed and processed as described above. Again uninfected, diminazene aceturate treated control groups that consisted of 5 $NK1^{-/-}$ and 4 $NK1^{+/+}$ animals were included in the experimental protocol.

The change to the experimental protocol was necessary due to the severity of the reaction encountered in some animals in experiment one. This extreme response necessitated their culling prior to the end point of the experimental regimen.

6.2.2.2.1.3. Experiment 3

This experiment contained 15 $NK1^{-/-}$ and 18 $NK1^{+/+}$ mice. An identical infection and treatment protocol to that outlined in experiment 2 above was followed. However, these animals were maintained under a cycling 2 hours light followed by 4 hours dark regimen.

The control groups in this experiment consisted of 4 $NK1^{-/-}$ and 5 $NK1^{+/+}$ uninfected, diminazene aceturate treated animals. In addition to these mice 5 $NK1^{-/-}$ and 3 $NK1^{+/+}$ animals were included as normal controls. These mice were not infected and did not receive any drug treatments.

6.2.2.2.1.4. Experiment 4

An identical protocol to that detailed for experiment 2 was followed in this experiment. 14 $NK1^{-/-}$ and 15 $NK1^{+/+}$ animals were infected, diminazene aceturate treated and sacrificed at the end of the procedure as described above. Uninfected, diminazene aceturate treated animals were again included as controls. On this occasion 2 $NK1^{-/-}$ and 2 $NK1^{+/+}$ mice were used.

6.2.2.2.2. NK2 and NK3 receptor antagonists

The highly selective, non-peptide NK2 (SR489968) and NK3 (SR142801) receptor antagonists used in this study were kindly gifted by Sanofi Recherche, Montpellier, France. These compounds are currently under clinical trial for the treatment of human CNS disease. The antagonists were dissolved in 0.5ml of DMSO and diluted to 250µg/ml with 0.9% sterile saline. A combined solution containing 250µg/ml NK2 receptor antagonist and 250µg/ml NK3 receptor antagonist was also prepared.

6.2.2.2.2.1. Experiment 5

In this experiment groups of $NK1^{-/-}$ and $NK1^{+/+}$ mice were treated with 25µg of NK2 receptor antagonist, 25µg of NK3 receptor antagonist or a combination containing 25µg of NK2 and 25µg NK3 receptor antagonist. This was administered i.p. in a volume of 0.1ml. The treatment was begun three days prior to trypanosome infection and then daily until sacrifice. The trypanosome-infected groups comprised 7 $NK1^{-/-}$ and 10 $NK1^{+/+}$ animals given NK2 receptor antagonist, 8 $NK1^{-/-}$ and 10 $NK1^{+/+}$ mice treated with NK3 receptor antagonist, 8 $NK1^{-/-}$ and 9 $NK1^{+/+}$ mice given a combination of both antagonists while 6 $NK1^{-/-}$ and 8 $NK1^{+/+}$ mice received no antagonist treatment. All mice were treated with diminazene aceturate (40mg/kg i.p.) on day 21 post-infection. The experiment was concluded on day 40 post-infection when the animals were killed and their brains processed for histopathology.

Control groups of uninfected mice were included in the experimental design. These groups comprised 5 $NK1^{-/-}$ and 4 $NK1^{+/+}$ treated with the NK2 and NK3 receptor antagonist combination followed by diminazene aceturate on day 21 post-infection and 6 $NK1^{-/-}$ and 6 $NK1^{+/+}$ given no antagonist or diminazene aceturate treatment.

6.2.2.3. Clinical Assessment

Throughout the course of the experimental procedures described above the mice were examined independently and the degree of clinical impairment resulting from the treatment regimens assessed. This was determined using a visual assessment scale of 0-6 where 0 indicated a normal healthy mouse and 6 indicated death or euthanasia due to the severity of the reaction. A complete description of this scale is detailed in Table 6.1. As an indicator of the overall clinical performance of the animal throughout the experimental regimens average values were calculated for each mouse over the series of repeat observations. The resulting data was then analysed statistically.

6.2.3. Histopathology

6.2.3.1. Assessing the inflammatory reaction

At necropsy, the brains were removed and fixed in 5% neutral buffered formalin. The tissue was then processed and paraffin wax embedded. Sections were cut from each block at a thickness of 3μm and stained with haematoxylin and eosin for examination by light microscopy. The severity of the neuropathology was graded in a blinded fashion using the grading system detailed in chapter 2. Using this system the severity of the inflammatory reaction is graded on a scale of 0 to 4, where 0 indicates a normal pathology and 4 indicates a severe meningoencephalitis. A detailed account of the criteria used in this assessment scale can be found in Chapter 2, Table 2.1. The inflammatory score for each section was assessed independently by two individuals in a blinded fashion.

The assignation a numerical value to a particular degree of inflammation allowed the results of the pathological assessment to be analysed using appropriate statistical methods.

Animal appearance	Numerical Score
Normal, healthy	0
Slow, sluggish, stary coat	1
Altered gait, reduced co-ordination of hind limbs	2
Flaccid paralysis of one hind limb	3
Atrophy of muscles and hind quarters, complete flaccid paralysis of both hind limbs	4
Moribund	5
Dead / ethanased	6

Table 6.1. Parameters defining the visual assessment scale for the clinical grading scores

6.2.3.2. Assessing astrocyte activation

The level of astrocyte activation in the brain sections was assessed using the indirect immunocytochemistry (ICC) protocol to identify glial fibrillary acidic protein (GFAP). GFAP is a major intermediate filament protein present in differentiated astrocytes. The protocol is detailed in Chapter 2. Briefly, sections were stained using a polyclonal anti-GFAP primary antibody. This was followed by a biotin labelled anti-rabbit IgG and a final addition of a streptavidin-biotin complex labelled with a horseradish peroxidase enzyme. The GFAP positive cells were visualised using the chromogen diaminobenzidine tetra-hydrochloride. This results in the deposition of a brown end product that can be assessed microscopically.

The number of astrocytes stained was determined in a random sample of animals from both experimental approaches. A total of 32 mice, 8 infected mice from both the NK1 receptor antagonist treated and untreated groups and 8 mice from the $NK1^{-/-}$ and $NK1^{+/+}$ groups were assessed. The assessment was carried out by counting the number of astrocytes in 5 random fields in the hippocampal area. An eyepiece graticule was used to standardise the area of the brain counted and each section was assessed on two occasions. Astrocyte activation was not investigated in the NK2 and NK3 receptor antagonist experiment.

6.2.4. Statistical analyses

Comparisons between appropriate groups of animals were undertaken to assess the neurological response, the level of astrocyte activation and the clinical appearance of the mice following infection and induction of a CNS inflammatory reaction by sub-curative drug treatment of trypanosome-infection. The severities of the neuropathological reactions were analysed in both the NK1 receptor antagonist experiments and the experiments employing the NK1 receptor knockout animals. Clinical response scores were analysed in the knockout experiments only. The neuropathological scores for the individual mice were based on the average of the independent assessor scores measured at the end of the experiment. A Wilcoxon signed rank test was employed to ensure that uniformity existed between the assessors scoring methods thus preventing bias results. Clinical response scores were determined using the average score over a series of repeat observations taken during the course of the experiment. Analyses were possible using parametric statistical tests. Comparisons between individual groups in a single experiment were carried out using a two sample t-test while comparisons across experiments were performed using

general linear model procedures and the randomised block analysis of variance. Means and standard errors (S.E.) are shown as summary statistics. The tests were undertaken using a proprietary statistical software package, Minitab version 13, and p-values of less that 0.05 were considered significant.

6.3. Results

6.3.1. The effect of the NK1 receptor antagonist

6.3.1.1. Severity of the meningoencephalitis

The histopathological examination of brain sections prepared from *T.b.brucei*-infected, diminazene aceturate treated, mice from each experiment, showed a severe meningitis and prominent perivascular cuffing associated with most of the blood vessels. In addition, there was a moderate encephalitis with inflammatory cells present in the parenchyma. The inflammatory cell infiltrate comprised mainly lymphocytes, plasma cells and macrophages (Fig. 6.1).

Sections from *T.b.brucei* –infected, diminazene aceturate treated, mice given a course of RP-67,580 showed an overall marked reduction in the severity of the CNS inflammatory reaction compared with saline treated animals. These mice exhibited a moderate meningitis with perivascular cuffing of some vessels and no encephalitis (Fig. 6.1).

A summary of the results of the statistical analyses of the neuropathology grading data is shown in Table 6.2. The results of a Wilcoxon signed rank test demonstrated that the mean of the difference between the pathology scores allocated to each section by the individual assessor was zero. This indicates that the grading scale used to score the sections was uniformly applied by the individual assessors. As the procedures used in experiment 4 were slightly modified from the initial 3 experiments the resulting data were analysed using three different combinations of the data sets. When the results of the initial three identical experiments were combined a significant reduction ($p<0.001$) in the severity of the inflammatory reaction was detected with the antagonist treated mice exhibiting a lower pathology score (2.442 ± 0.176) than the non-treated animals (3.405 ± 0.164). There was no significant difference between the data sets generated form each of the individual experiments ($p<0.252$) and no interaction between the experiment and the scores for each group ($p<0.583$). The neuropathological grades from the antagonist treated animals (2.167 ± 0.441) compared with non-antagonist treated mice (3.0 ± 0.289) in the fourth experiment showed no significant difference ($p=0.14$) when analysed individually. However when this data set was combined with the 3 initial experiments the reduction in the pathological response in the antagonist treated mice (2.371 ± 0.171) remained highly significant ($p<0.001$) when compared to the scores in the non-treated mice (3.283 ± 0.145). Again the

analyses did not detect any difference between the results generated between the experiments ($p<0.275$) and no interaction was found between the experiments and the groups ($p<0.806$).

The inactive enantiomer RP-68,651 had no effect on the severity of the meningoencephalitis induced by subcurative drug treatment following *T.b.brucei* – infection. No significant difference ($p=0.38$) was found between the neuropathology scores of the enantiomer treated group (3.5 ± 0.22) and the saline treated animals (3.3 ± 0.17). This indicates that the reduction in the pathology found following RP-67,580 treatment is a result of the blockade of the NK1 receptor and not attributable to an unrelated secondary action of the antagonist. These data were therefore combined with that from the saline treated animals to form the composite non-antagonist treated control data set represented in Tables 6.2 and 6.3. No pathological changes were found in any of the uninfected control animals given similar drug regimens to the infected animals.

6.3.1.2. Astrocyte activation

A diffuse astrocytosis was seen throughout the brain of infected, diminazene aceturate treated, animals that received saline in place of RP-67,580. Numerous (188.03 ± 5.42), intensely GFAP stained, large reactive astrocytes were evident. These activated astrocytes displayed long and elaborately branched processes and were present particularly in areas of high inflammation (Fig. 6.2, GFAP positive cells show brown staining pattern).

A reduction in this astrocyte activation was seen in infected, diminazene aceturate treated mice following RP-67,580 therapy. In these animals the astrocytes were significantly ($p<0.001$) fewer in number (99.89 ± 3.01) and stained more weakly with GFAP. There was also a reduction in the degree of stellation exhibited by these cells (Fig. 6.2). In addition, the distribution of the activated cells was more limited and appeared to be confined to the corpus callosum, the hippocampus, along the choroid fissure and around the ventricles. The results of statistical analysis of these data are shown in Table 6.3.

6.3.2. The effect of genetic ablation of the NK1 receptor

6.3.2.1. Severity of the meningoencephalitis

The histopathological examination of brain sections from both knockout and wild-type mice showed inflammatory changes characteristic of the post-treatment reactive encephalopathy (PTRE). In general a moderate to severe meningitis was found and perivascular cuffs were apparent. The sections also exhibited a moderate to severe encephalitis with inflammatory cells present in the brain parenchyma. The inflammatory cell infiltrate consisted mainly of lymphocytes, plasma cells and macrophages (Fig. 6.3).

Table 6.4 shows a summary of the statistical analyses of the data generated from assessment of the severity of the neurological response of wild-type and knockout mice to trypanosome-infection. The results of a Wilcoxon signed rank test demonstrated that the mean of the difference between the pathology scores allocated to each section by the individual assessor was zero indicating that the grading scale was uniformly applied. Data from experiments 1 and 3 were analysed individually as the regimen differed slightly to that employed in experiments 2 and 4. Experiments 2 and 4 followed identical protocols and therefore the data were analysed in a combined form. A significant ($p=0.019$) increase in severity of the inflammatory reaction was seen in the brains of the knockout mice (3.173 ± 0.140) compared with wild-type animals (2.538 ± 0.208) in experiment one. This pattern was also found in the pooled data set from experiments 2 and 4 with the $NK1^{-/-}$ animals again showing a significantly ($p=0.003$) higher pathology (3.565 ± 0.092) than the $NK1^{+/+}$ mice (3.008 ± 0.145). When the data set from experiment 1 was combined with that of experiments 2 and 4 a further increase in the level of significance was seen ($p<0.001$) and the inflammatory response in knockout animals remained higher (3.438 ± 0.081) than that seen in wild-type animals (2.866 ± 0.122).

The data generated from experiment 3 however did not match this trend. In this experiment, no significant difference ($p=0.52$) was detected between the CNS grading scores of the $NK1^{-/-}$ mice (2.850 ± 0.204) and the $NK1^{+/+}$ animals (3.028 ± 0.178). In contrast to the other experiments, although the difference is not statistically significant, the pathology grades assigned to the wild-type animals were in fact higher than those seen in the knockout mice. One factor not constant between this and the remaining experiments was the introduction of a 2-hour light and 4 hour dark regimen. Due to the difference in

the environmental conditions during this experiment and the resultant reversal of the pathological findings no analyses were performed on the combined data from all 4 experiments.

Overall, these data indicate that genetic ablation of the NK1 receptor gene results in an increase in the neuropathological response to trypanosome-infection when compared to wild-type mice. An apparent influence on the inflammatory reaction by the photoperiod was also suggested by the result gained from mice maintained under a set light dark regimen.

6.3.2.2. Astrocyte activation

Diffuse astrocyte activation was found throughout the brain sections of both knockout and wild-type animals. When the number of astrocytes present in each group was analysed the resulting counts were not significantly different (p=0.699) between the $NK1^{-/-}$ mice (106.322 $\pm$ 5.62) and the $NK1^{+/+}$ animals (103.38 $\pm$ 4.47). A summary of these statistics is given in Table 6.5. No morphological differences were detected in the appearance of the astrocytes between the two groups of animals and the cells stained intensely with GFAP and displayed long elaborately branched processes (Fig. 6.4, GFAP positive cells show brown staining pattern). This result indicated that any further investigation of astrocyte activation in subsequent experiments using these knockout mice would be of little value.

6.3.2.3. Severity of the clinical response

A summary of the results of statistical analyses of the clinical data is presented in Table 6.6. No significant difference (p=0.230) was detected between the degree of the clinical impairment in wild-type (3.500 $\pm$ 0.384) and knockout (2.792 $\pm$ 0.427) animals from experiment 1. The severity of this reaction was much higher than that found in mice from the other experiments and may reflect the later timing of the diminazene aceturate treatment in this regimen. Analyses of the data from experiments 2 and 4 show that trypanosome-infection in the knockout mice results in a significantly (p=0.047) lower (0.400 $\pm$ 0.113) degree of clinical impairment to that found in the wild-type animals (0.964 $\pm$ 0.270). When the results from experiment 1 were combined with those from experiments 2 and 4 this trend was continued. The $NK1^{-/-}$ animals again showed a significant (p=0.023) reduction in clinical reaction (1.179 $\pm$ 0.232) when compared with $NK1^{+/+}$ mice (1.731 $\pm$ 0.283). The results of the general linear model analysis indicated

that there was a significant difference ($p<0.001$) in the clinical outcomes between the experiment, however there was no significant interaction ($p=0.173$) between the experiment and the genetic status of the animals. This indicates that although the clinical grades do vary between the experiments this has no impact on the differences found between the knockout and wild-type mice. Due to the influence of the later administration of the diminazene aceturate in experiment 1, this finding was in fact to be expected when the pooled data set was analysed.

Analysis of the data generated from experiment 3 did not detect a significant difference ($p=0.28$) between the clinical reaction of the knockout mice (1.856 ± 0.478) when compared to wild-type animals (1.224 ± 0.330). Although the difference between the two means is not significant a reversal of the trend demonstrated in experiments 1, 2 and 4 is suggested. In contrast to the other experiments the knockout animals show a higher level of clinical impairment than that found in the wild-type animals. Again this may reflect the difference in environmental factors during this investigation.

These analyses indicate that disrupting the gene encoding the NK1 receptor results in a significant reduction in the degree of clinical impairment found in these mice following trypanosome challenge and induction of the PTRE. Again the photoperiod appears to be an important environmental factor influencing the clinical outcome of the infection in these animals.

Taken together, the overall results from this series of experiments show that when the knockout animals exhibit a more severe neuropathological response than the wild-type mice they have a healthier clinical appearance. This suggests that these $NK1^{-/-}$ animals demonstrate a disease phenotype where there is an apparent dissociation between the clinical and neuropathological responses.

6.3.3. The effect of NK2 and NK3 receptor antagonists

6.3.3.1. Severity of the meningoencephalitis

Histopathological examination of brain sections prepared from infected wild-type and knockout mice showed inflammatory changes. A moderate to severe meningitis was present and perivascular cuffs were apparent. In some groups a severe

meningoencephalitis was seen with the presence of inflammatory cells in the neuropil. The inflammatory cell infiltrate was characterised by the presence of lymphocytes, plasma cells and macrophages (Fig. 6.5)

As before the severity of the neuroinflammatory response was graded by two independent assessors in a blinded fashion. The results of a Wilcoxon signed rank test on the data generated from this analysis showed that the mean difference between the severity scores allocated by each assessor was zero. This indicated that the grading scale used to assign the neuropathology score had been applied in a uniform manner. During the course of the experimental regimen two $NK1^{+/+}$ mice and one $NK1^{-/-}$ mouse died. Therefore no neuropathology data are available for these animals. Factorial statistical analyses of the data sets indicated a highly significant ($p<0.001$) interaction between the factors examined in the wild-type and knockout groups. Therefore, individual group comparisons were undertaken using a one-factor analysis of variance separately for $NK1^{-/-}$ and $NK1^{+/+}$ mice. The initial results of these tests indicated that the uninfected control groups of mice showed a lower neuropathology score that than the remaining infected groups. This result was to be expected since the animals had not been challenged with trypanosomes and therefore showed normal CNS histology on examination. Consequently, the analyses were repeated comparing only those groups of mice that were infected. The results of these analyses are detailed in Tables 6.7-6.8. Table 6.9 shows a summary of the results of one factor analysis of variance between the wild-type and knockout groups for each treatment regimen.

Statistical analyses of the results in the wild-type animals (Table 6.7) showed that mice treated with the NK3 receptor antagonist developed a significantly ($p=0.0495$) lower neuropathological response (2.950 ± 0.252) than mice given either the NK2 receptor antagonist (3.650 ± 0.113) or those treated with the NK2 and NK3 receptor antagonist combination ($p=0.006$, 3.889 ± 0.060). No treatment regimens significantly altered the severity of the CNS inflammatory reaction from that seen in the untreated wild-type mice (3.250 ± 0.263).

In the knockout animals the data indicate that infected $NK1^{-/-}$ treated with a combination of NK2 and NK3 receptor antagonists displayed a significant ($p=0.035$) reduction in the neuropathological response (2.438 ± 0.290) compared to $NK1^{-/-}$ infected animals that had received no antagonist treatment (3.708 ± 0.187) (Table 6.8). No other significant differences were found between the $NK1^{-/-}$ treatment groups (Table 6.8). $NK1^{-/-}$ animals treated with NK2 receptor antagonist and NK3 receptor antagonist monotherapies also

showed a reduction in the severity of the neuropathological response (2.607 ± 0.308 and 2.688 ± 0.343, respectively) compared to non-treated mice. Although these results follow the downward trend they cannot be considered significant ($p>0.05$).

In comparisons of treatment regimens between the wild-type and knockout mice (Table 6.9) a significantly ($p=0.016$) lower neuropathology score (2.60 ± 0.308) was found in the knockout mice receiving the NK2 receptor antagonist treatment when compared to wild-type animals (3.650 ±0.113) following a similar treatment regimen. No significant difference was found between the response of $NK1^{+/+}$ and $NK1^{-/-}$ animals following NK3 receptor antagonist treatment. However, a significant reduction ($p=0.002$) in the CNS inflammation was found in $NK1^{-/-}$ mice receiving a combination of NK2 and NK3 receptor antagonists (2.438 ± 0.290) compared to $NK1^{+/+}$ animals treated in an identical manner (3.889 ± 0.060).

6.3.3.2. Severity of the clinical response

The factorial design analysis of the clinical data from all groups of animals found no significant ($p=0.298$) interaction between the factors examined in the wild-type and knockout groups. The analysis of all animals indicated a significant ($p=0.009$) difference in the clinical response scores generated by the wild-type and knockout mice. The analysis determined that $NK1^{-/-}$ animals showed a less severe clinical response (0.025 ± 0.01) than their $NK1^{+/+}$ counterparts (0.144 ± 0.032). When the uninfected animals were removed from the analyses the differences between the two groups remained significant ($p=0.002$) with the $NK1^{-/-}$ mice generating a lower clinical response score (0.034 ± 0.013) than the $NK1^{+/+}$ animals (0.180 ± 0.038) (Table 6.10).

One factor analysis of variance was undertaken separately in wild-type and knockout data sets. This confirmed that the treatment regimens had no effect on the clinical responses of the animals in either group ($p=0.122$, $p=0.405$, respectively). In addition, individual regimens were compared for differences in the clinical response between the wild-type and knockout mice. These analyses indicated that $NK1^{-/-}$ mice treated with a combination of NK2 and NK3 receptor antagonists showed a significantly ($p=0.024$) improved clinical response (0.003 ± 0.003) compared to $NK1^{+/+}$ animals (0.224 ± 0.078) receiving a similar treatment regimen (Table 6.11).

Overall these data indicate significant differences in the clinical and neuropathological response of $NK1^{-/-}$ and $NK1^{+/+}$ animals to trypanosome infection and selective NK receptor

antagonist treatments. The results also suggest that alternative receptor usage may influence the neuropathological response in $NK1^{-/-}$ mice since blockade of the NK2 and NK3 receptors resulted in a significant reduction in the neuropathological reaction. However, this phenomenon does not seem to play a role in the development of the clinical picture as this pattern of improvement was not found within the $NK1^{-/-}$ group.

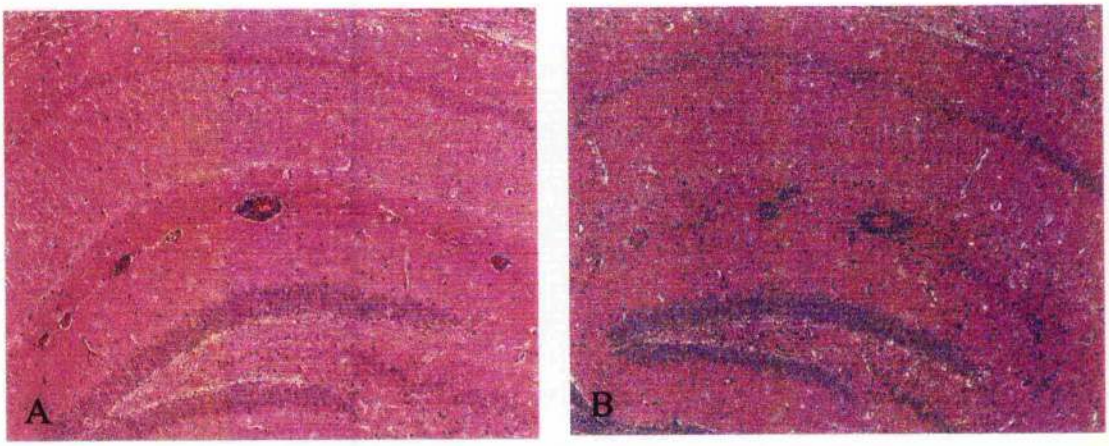

Figure 6.1. The effect of RP-67,580 treatment on the severity of the neuroinflammatory response.

Coronal section through the hippocampal brain region of trypansome-infected mice. Animals treated with the NK1 receptor antagonist for 10 days, beginning 7 days following diminazene aceturate treatment (A) show a reduction in the severit of the neuroinflammation. Fewer inflammatory cells are found in the perivascular cuffs and the degree of encephalitis is reduced compared with mice that did not receive treatment with the antagonist (B). H&E, X150.

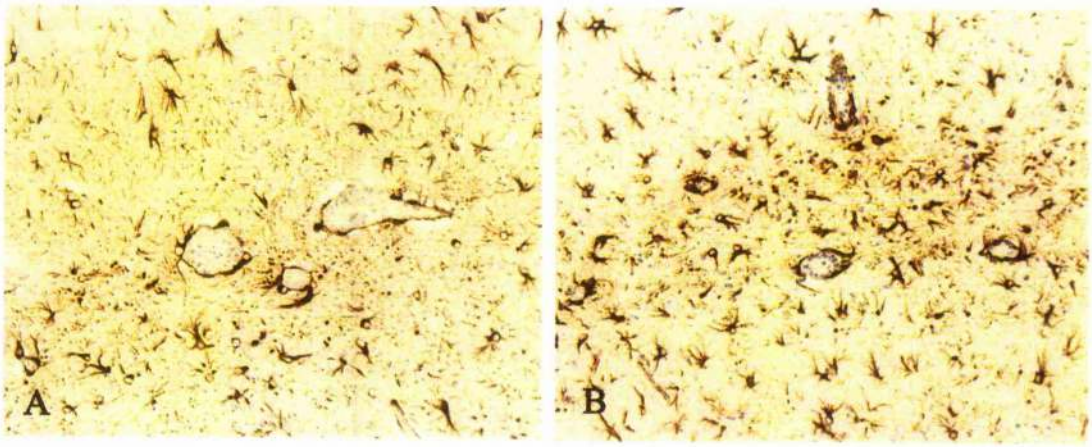

Figure 6.2. The effect of RP-67,580 treatment on astrocyte activation. Cornonal sections through the hippocampal brain region of trypansome-infected mice. Animals treated with the NK1 receptor antagonist for 10 days beginning 7 days following diminazene aceturate treatment (A) show fewer activated astrocytes than mice that were not given RP-67,580 (B). GFAP, X300.

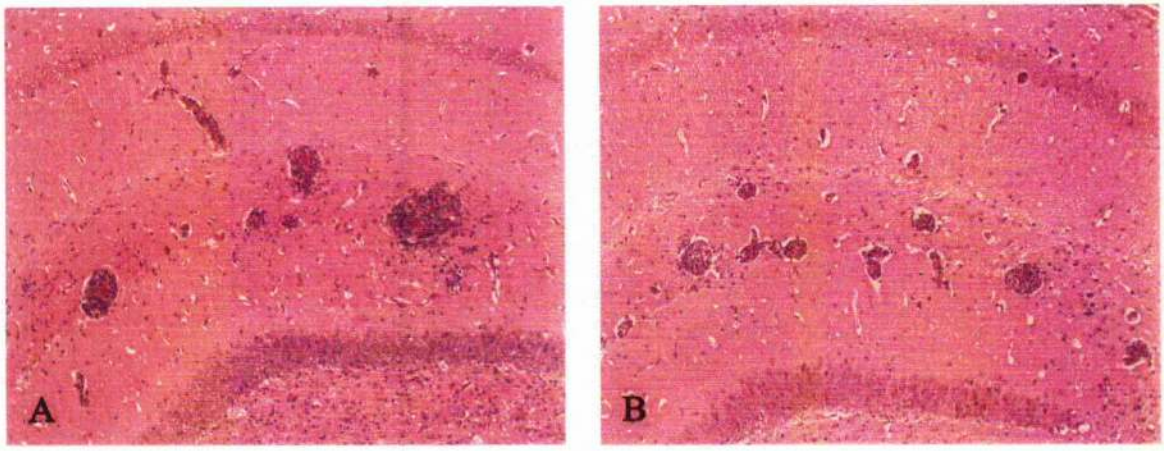

Figure 6.3. The neuroinflammatory reaction in NK1 receptor knockout and wild-type mice.

Coronal sections through the hippocampal brain region of trypanosome-infected mice. NK1 receptor knockout animals (A) show a more severe neuroinflammatory reaction to trypanosome infection and subcurative diminazene aceturate treatment than wild-type mice with functional NK1 receptors (B). The degree of perivascular cuffing and inflammatory cell infiltration of the neuropil is increased in the knockout mice (A) compared to that found in the wild-type animals (B). H&E, X150.

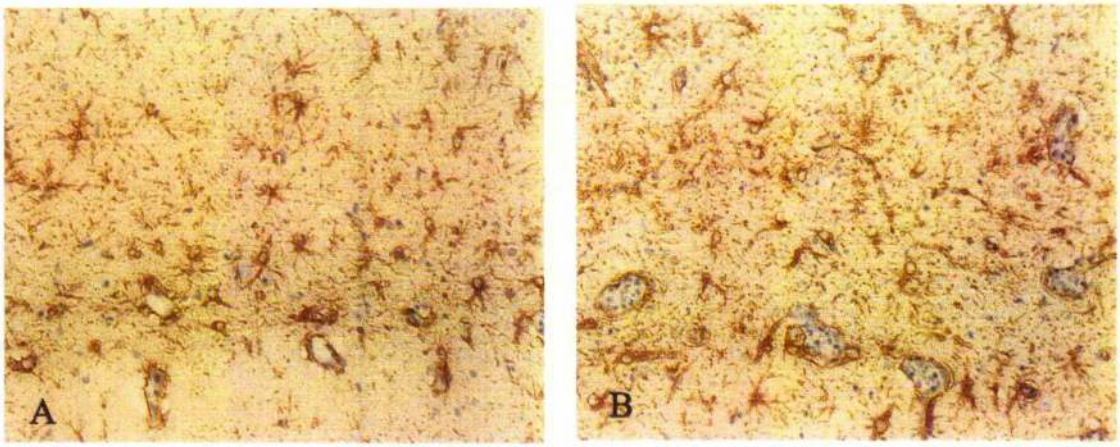

Figure 6.4. The astrocytic reaction in NK1 receptor knockout and wild-type mice.

Coronal sections throuogh the hippocampal brain region of trypanosome-infected mice. NK1 receptor knockout animals (A) and wild-type mice (B) show a similar degree of astrocyte activation following trypansome infection and subcurative drug treatment with diminazene aceturate. GFAP, X300.

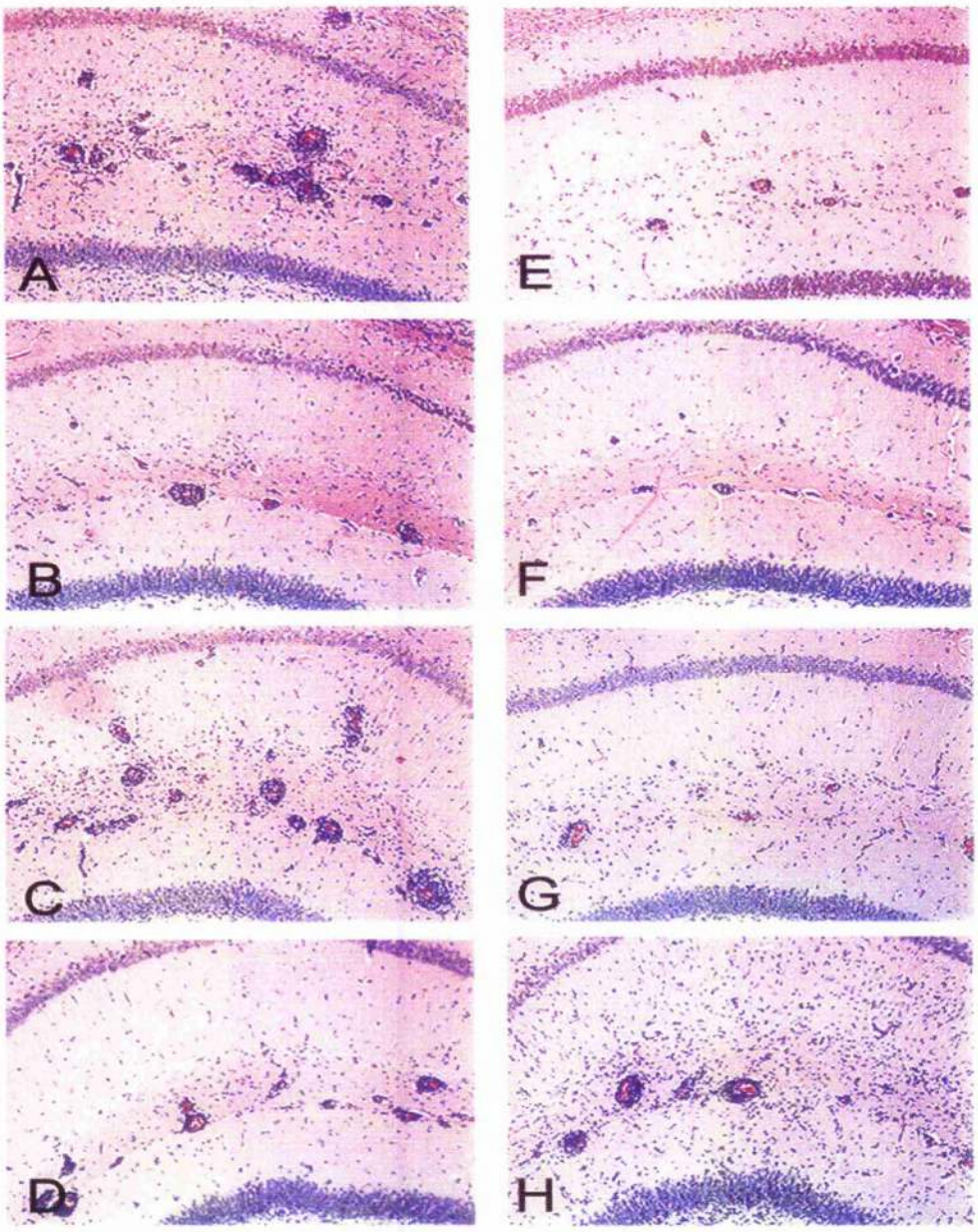

Figure 6.5. The effect of treatment with NK2 and NK3 receptor antagonists on the severity of the neuroinflammatory reaction. Coronal sections through the hippocampal region of NK1+/+ (A-D) and NK1-/- (E-H) mice following various treatment schedules. The figure demonstrates the differences in the neuroinflammatory response between wild-type and knockout animals when treated with the various receptor antagonists. H&E stained sections prepared from NK2 receptor antagonist treated mice (A and E); NK3 receptor antagonist treated mice (B and F); mice treated with a combination of NK2 and NK3 receptor antagonists (C and G); and animals receiving no antagonist treatment (D and H) are shown. The antagonist treatment has resulted in amelioration of the neuroinflammatory response in the NK1-/- mice (E-G) compared with NK1+/+ mice (A-C) following the same antagonist regimen. However, the neuroinflammatory response is more severe in the NK1-/- mice receiving no antagonist treatment (H) than that encountered in similarly treated wild-type animals (D). H&E, X150.

	Neuropathology score		
	Experiments 1, 2 & 3	Experiment 4	Experiments 1, 2 3 & 4
Trypanosome - antagonist	3.405 ± 0.164 (n = 21)	3.0 ± 0.289 (n = 9)	3.283 ± 0.145 (n = 30)
Trypanosome + antagonist	2.442 ± 0.176 (n = 26)	2.167 ± 0.441 (n = 9)	2.371 ± 0.171 (n = 35)
p-value	<0.001	0.140	<0.001

Table 6.2. Assessment of the neuropathological response score to trypanosome-infection in the presence or absence of SP antagonist treatment.

Severity scores were graded on a scale of 0 (low) to 4 (high). Each section was assessed by two independent assessors. Experiments 1, 2 and 3; antagonist given for 10 days beginning 7 days following diminazene aceturate treatment. Experiment 4; antagonist given for 21 days beginning 1 day prior to diminazene aceturate treatment. Data are expressed as mean ± S.E. for each group, n, number of mice in each group. Figures detailed in red highlight groups showing significant differences.

	Astrocyte count
Trypanosome – antagonist	188.03 ± 5.42 (n = 8)
Trypanosome + antagonist	99.89 ± 3.01 (n = 8)
p-value	<0.001

Table 6.3. Assessment of the astrocytic response to trypanosome-infection in the presence or absence of SP antagonist treatment.

Astrocytes were counted in 5 random fields from the hippocampal region of each animal using a graticule to define the area. Each section was assessed on 2 occasions and the average count per animal utilised. Data are expressed as mean ± S.E. for each group, n, number of animals in each group. Figures detailed in red highlight groups showing significant differences.

	Neuropathology score			
	Experiment 1	Experiments 2 & 4	Experiment 1, 2 & 4	Experiment 3
$NK1^{+/+}$	2.538 ± 0.208 (n = 13)	3.008 ± 0.145 (n = 30)	2.866 ± 0.122 (n = 43)	3.028 ± 0.178 (n = 18)
$NK1^{-/-}$	3.173 ± 0.140 (n = 13)	3.565 ± 0.092 (n = 27)	3.438 ± 0.081 (n = 40)	2.850 ± 0.204 (n = 15)
p-value	0.019	0.003	<0.001	0.52

Table 6.4. Assessment of the neurological response scores to trypanosome-infection in $NK1^{+/+}$ and $NK1^{-/-}$ animals.

Severity scores were graded on a scale of 0 (low) to 4 (high). Experiment 1; diminazene aceturate given on day 28 post-infection, experiments 2 & 4; diminazene aceturate given on day 21 post-infection, experiment 3; diminazene aceturate given on day 21 post-infection and animals maintained in 2 hour light / 4 hour dark regimen. Data are expressed as mean ± S.E. for each group, n, number of mice in each group. Figures detailed in red highlight groups showing significant differences.

	Astrocyte count
$NK1^{+/+}$	103.38 ± 4.47 ($n = 8$)
$NK1^{-/-}$	106.32 ± 5.62 ($n = 8$)
p-value	0.699

Table 6.5. Assessment of the astrocytic response to trypanosome-infection in $NK1^{+/+}$ and $NK1^{-/-}$ animals.

Astrocytes were counted in 5 random fields from the hippocampal region of each animal using a graticule to define the area. Each section was assessed on 2 occasions and the average count per animal utilised. Data are expressed as mean $\pm$ S.E. for each group, n, number of animals in each group.

	Clinical score			
	Experiment 1	Experiments 2 & 4	Experiment 1, 2 & 4	Experiment 3
$NK1^{+/+}$	3.500 ± 0.384 (n = 13)	0.964 ± 0.270 (n = 30)	1.731 ± 0.283 (n = 43)	1.224 ± 0.330 (n = 19)
$NK1^{-/-}$	2.792 ± 0.427 (n = 14)	0.400 ± 0.113 (n = 29)	1.179 ± 0.232 (n = 43)	1.856 ± 0.478 (n = 18)
p-value	0.230	0.047	0.023	0.28

Table 6.6. Assessment of the clinical response scores to trypanosome-infection in $NK1^{+/+}$ and $NK1^{-/-}$ animals.

Clinical scores were graded on a scale of 0 (low) to 6 (high). Each mouse was assessed independently using the average over a series of repeat determinations. Experiment 1; diminazene aceturate given on day 28 post-infection, experiments 2 & 4; diminazene aceturate given on day 21 post-infection, experiment 3; diminazene aceturate given on day 21 post-infection and animals maintained in 2 hour light / 4 hour dark regimen. Data are expressed as mean ± S.E. for each group, n, number of mice in each group. Figures detailed in red highlight groups showing significant differences.

	Neuropathology scores of $NK^{+/+}$ mice			
	NK2-RA	NK3-RA	NK2&3-RA	No antagonist
NK3-RA	p=0.049 (-1.380, -0.0003)			
NK2&3-RA	p=0.805 (-0.480, 0.958)	p=0.006 (0.220, 1.658)		
No antagonist	p=0.473 (-1.142, 0.342)	p=0.695 (-0.442, 1.042)	p=0.124 (-1.399, 0.121)	
Mean ± SE	3.650 ± 0.113	2.950 ± 0.252	3.889 ± 0.060	3.250 ± 0.263
Number	10	10	9	8

Table 6.7. Neuroinflammatory response scores of $NK1^{+/+}$ mice following treatment with specific NK receptor antagonists

Neuropathology response scores were measured in trypanosome infected $NK1^{+/+}$ mice following administration of NK2-receptor antagonist (RA), NK3-RA, a combination of both NK2 & 3-RA's or no antagonist treatment. The mean score and standard error (mean ± SE) are shown, together with the number of animals are listed for each group. The 95% confidence intervals for the differences between group means are shown along with the p-values. The figures in the body of the table demonstrate the comparisons, in terms of statistical significance, between the groups shown in the row and column headings. Figures detailed in red highlight groups showing significant differences.

	Neuropathology scores of $NK1^{-/-}$ mice			
	NK2-RA	NK3-RA	NK2&3-RA	No antagonist
NK3-RA	p=0.997 (-1.071, 1.232)			
NK2&3-RA	p=0.977 (-1.321, 0.982)	p=0.925 (-1.362, 0.862)		
No antagonist	p=0.094 (-0.136, 2.338)	p=0.116 (-0.180, 2.222)	p=0.035 (-0.070, -2.472)	
Mean ± SE	2.607 ± 0.308	2.688 ± 0.343	2.438 ± 0.290	3.708 ± 0.187
Number	7	8	8	6

Table 6.8. Neuropathology response scores of $NK1^{-/-}$ mice following treatment with specific NK receptor antagonists

Neuroinflammatory response scores were measured in trypanosome-infected $NK1^{-/-}$ mice following administration of NK2-receptor antagonist (RA), NK3-RA, a combination of both NK2 & 3-RA's or no antagonist treatment. The mean score and standard error (mean ± SE) are shown, together with the number of animals are listed for each group. The 95% confidence intervals for the differences between group means are shown along with the p-values. The figures in the body of the table demonstrate the comparisons, in terms of statistical significance, between the groups shown in the row and column headings. Figures detailed in red highlight groups showing significant differences.

	Neuropathology score			
	NK2 receptor antagonist	NK3 receptor antagonist	NK2 &3 receptor antagonist	No antagonist
$NK1^{+/+}$	3.650 ± 0.113 (*n*=10)	2.950 ± 0.252 (*n*=10)	3.889 ± 0.060 (*n*=9)	3.250 ± 0.263 (*n*=8)
$NK1^{-/-}$	2.607 ± 0.308 (*n*=7)	2.688 ± 0.343 (*n*=8)	2.438 ± 0.290 (*n*=8)	3.708 ± 0.187 (*n*=6)
p-value	0.016	0.548	0.002	0.183

Table 6.9. Assessment of the neuropathological response following treatment with selective NK receptor antagonists.

Assessment of the neuropathological response of $NK1^{+/+}$ and $NK1^{-/-}$ mice to trypanosome infection following treatment with NK2 receptor antagonist, NK3 receptor antagonist, a combination of NK2 and NK3 receptor antagonist or no treatment. Each mouse was assessed by two independent assessors. A severity scale of 0 (low) and 4 (high) was employed. Data are expressed as mean ± standard error and the number of animals (*n*) per group detailed. The statistical test p-values for the differences between group means are also shown. Figures detailed in red highlight groups showing significant differences.

	Clinical response score	
	Uninfected groups included	Uninfected groups omitted
$NK1^{+/+}$	0.144 ± 0.032 (*n*=49)	0.180 ± 0.038 (*n*=39)
$NK1^{-/-}$	0.025 ± 0.01 (*n*=41)	0.034 ± 0.013 (*n*=30)
p-value	0.009	0.002

Table 6.10 Comparison of clinical responses between $NK1^{+/+}$ and $NK1^{-/-}$ mice

The clinical response scores for the wild-type and knockout mice were calculated. The results are shown both including the uninfected animalss and excluding the uninfected animals in each group. Data are expressed as mean ± standard error and the number of animals (*n*) per group detailed. The statistical test p-values for the differences between group means are also shown. Figures detailed in red highlight groups showing significant differences.

	Clinical response score			
	NK2 receptor antagonist	NK3 receptor antagonist	NK2 &3 receptor antagonist	No antagonist
$NK1^{+/+}$	0.248 ± 0.099 (*n*=10)	0.081 ± 0.043 (*n*=10)	0.224 ± 0.078 (*n*=10)	0.168 ± 0.070 (*n*=9)
$NK1^{-/-}$	0.053 ± 0.026 (*n*=8)	0.034 ± 0.028 (*n*=8)	0.003 ± 0.003 (*n*=8)	0.050 ± 0.045 (*n*=6)
p-value	0.107	0.398	0.024	0.234

Table 6.11 Assessment of the clinical response following treatment with specific NK receptor antagonists.

Assessment of the clinical response of $NK1^{+/+}$ and $NK1^{-/-}$ mice to trypanosome infection following treatment with NK2 receptor antagonist, NK3 receptor antagonist, a combination of NK2 and NK3 receptor antagonist or no treatment. A severity scale of 0 (low) and 6 (high) was employed. Data are expressed as mean ± standard error and the number of animals (*n*) per group are detailed. The statistical test p-values for the differences between group means are also shown. Figures detailed in red highlight groups showing significant differences.

6.4. Discussion

6.4.1. Neuropathology

The data from this series of experiments show that blockade of the NK1 receptor by administration of RP-67,580 in trypanosome-infected mice, sub-curatively treated with the trypanocidal drug diminazene aceturate, reduces the severity of the resultant CNS inflammatory reaction. In contrast to these findings, animals in which the NK1 receptor had been genetically ablated exhibited a heightened inflammatory CNS reaction compared to wild-type mice with functional NK1 receptors. Although these results are apparently contradictory they both suggest a role for SP in the generation of the CNS inflammation associated with trypanosome-infection. Further investigations blocking the NK2 and NK3 receptors in the $NK1^{-/-}$ mice suggested that alternative receptor usage may be an important mechanism in the development of the neuropathological changes seen in these animals.

Within the CNS various cells types including endothelial cells, neurones, microglia and astrocytes have been shown to express the NK1 receptor (Kostyk *et al.*, 1989; Lai, Zhan, Campbell, Douglas *et al.*, 2000; Lambert, Lescoulie, Yassine-Diab, Enault *et al.*, 1998; Mantyh *et al.*, 1997). In addition, the NK1 receptor has been demonstrated on many of the cell types present in the inflammatory infiltrate including macrophages and lymphocytes (Lucey *et al.*, 1994; Stanisz *et al.*, 1987). The NK2 receptor is widely distributed in the peripheral nervous system and has also been described in the CNS (Hagan, Beresford, Stables, Dupere *et al.*, 1993; Maggi, 1995). These receptors are especially prevalent in some thalamic nuclei, discrete layers of the frontal cortex and in the hippocampus (Hagan *et al.*, 1993). The CNS is the main, but not exclusive, site of NK3 receptor expression, and these can be found in the cerebral cortex, the solitary nucleus, the interpeduncular nucleus, the habenula and the ventral tegmental area (Maggi, 1995). SP itself can be produced by numerous cell types such as neurones, microglia, astrocytes and endothelial cells within the brain (Kostyk *et al.*, 1989; Lai *et al.*, 2000; Linnik and Moskowitz, 1989; Nakaya *et al.*, 1994) as well as the infiltrating macrophages and lymphocytes (De Giorgio *et al.*, 1998). Therefore, due to the abundance of cell types present in the meningoencephalitic reaction, that can both produce SP and react to its presence, SP could potentially play a central role in the control of this neuroinflammation acting in both an autocrine and paracrine fashion.

It is possible that following activation the astrocytes and microglia within the brain produce SP. This could have a direct chemotactic effect on peripheral T-cells and

monocytes (Hood *et al.*, 2000). In addition, SP could stimulate the brain microvascular endothelial cells to up-regulate adhesion molecule expression (Vishwanath and Mukherjee, 1996). The enhanced expression of ICAM-1 by the endothelial cells together with a corresponding increase in the avidity of the LFA-1 ligand on the lymphocytes, also induced by SP, could facilitate the transmigration of the leucocytes into the brain (Vishwanath and Mukherjee, 1996). In addition to direct effects, SP may elicit the production of pro-inflammatory cytokines by both resident CNS cells and inflammatory cells leading to a cascade of events that result in further exacerbation of the reaction. Indeed the addition of SP in conjunction with LPS to cultures of rat microglia has been shown to induce a fourfold increase in the production of IL-1 by these cells in comparison to LPS stimulation alone (Martin, Anton, Gornbein, Shanahan *et al.*, 1993). However, this enhancement was not found in an earlier study investigating the production of TNF-α by rat microglial cultures. Moreover, through [^{125}I] Bolton Hunter SP binding experiments these investigations indicated that neither resting nor stimulated microglia express detectable SP binding sites (Luber-Narod *et al.*, 1994). In contrast, these receptors have been demonstrated on human foetal microglia (Lai *et al.*, 2000).

Blockade of the NK1 receptor by administration of RP-67,580 could therefore inhibit these inflammatory pathways and subsequently down regulate the intensity of the immune response, suggesting a pro-inflammatory role for SP. As the antagonist was administered by intraperitoneal injection (i.p.) in these experiments this dampening of the inflammation could occur not only within the brain but also in the peripheral systems. It is possible that this overall reduction in the inflammatory response may then be reflected in the CNS as a secondary effect. However, cytokine levels and leucocyte activation states would need to be investigated to confirm this hypothesis.

The reduction in the severity of the inflammatory reaction seen following SP antagonist treatment was not echoed in mice where the action of the NK1 receptor had been blocked by genetic manipulation. In fact, mice that did not express the receptor showed a higher degree of inflammation than the wild-type animals. This finding, although somewhat enigmatic, nevertheless continues to indicate a key role for SP in the control of CNS inflammatory reactions. The level of SP mRNA is known to be increased in these NK1$^{-/-}$ mice and the expression and distribution of the NK2 and NK3 receptors is comparable to the wild-type animals (de Felipe, O'Brien, Palmer, Doyle *et al.*, 1997). It is possible that the heightened SP levels in the knockout mice lead to alternative receptor usage by the neuropeptide in the control of inflammation. A degree of promiscuity between the ligands and their 'preferred' receptor has been suggested by studies investigating discrepancies in

the distribution of the ligands and their receptor. These 'mismatches' between the expression of SP and its receptor in the rat CNS have been demonstrated using immunocytochemistry in both light and electron microscopy studies (Liu, Brown, Jasmin, Maggio *et al.*, 1994). In the guinea pig intestine NK3 receptors are present on specific neurones (Laufer, Wormser, Friedman, Gilon *et al.*, 1985) even though NKB cannot be detected in this area (Too, Cordova, and Maggio, 1989). Since SP and NKA are present in this area it is thought that these tachykinins stimulate the NK3 receptors on these neurones in this scenario, (Too *et al.*, 1989). Moreover, SP has also been shown to induce endothelium-independent contraction of the intrapulmonary arteries in excised rabbit lungs by stimulation of the NK2 receptor rather than via its preferred NK1 receptor (Shirahase *et al.*, 1995).

The investigation utilising specific NK2 and NK3 receptor antagonists in the $NK1^{-/-}$ mice seems to suggest that alternative receptor usage plays and important role in the induction of the neuroinflammatory response in the knockout animals. In $NK1^{-/-}$ mice SP mRNA expression is known to be upregulated (de Felipe *et al.*, 1997). It is possible that, due to this increased production in knockout animals, SP displaces NKA and NKB from the NK2 and NK3 receptors, respectively. Subsequent signalling by SP through these alternative receptors may induce pro-inflammatory mechanisms within the CNS. This would culminate in the increase in the severity of the neuropathological response seen in the knockout mice. The finding that treatment of $NK1^{-/-}$ mice, with specific NK2 and NK3 receptor antagonists, results in a reduction in the severity of the neuropathological reaction substantiates this hypothesis. When a treatment regimen comprising a combination of these NK2 and NK3 receptor antagonists was administered to the knockout animals a statistically significant reduction in the severity of the CNS inflammation was found indicating a synergistic effect of the two antagonists.

The importance of the NK2 receptor in this phenomenon was further highlighted by the results found in the $NK1^{+/+}$ mice. Although none of the antagonist treatment regimens resulted in a significant change in the neuropathological response compared with non-treated mice in the wild-type group, both the NK2 receptor antagonist and combined NK2 and NK3 receptor antagonist treated groups showed a significantly higher neuroinflammatory reaction than the NK3 receptor antagonist treated animals. These findings suggest that in the wild-type mice, the stimulation of the NK2 receptor, normally triggered by NKA, has an anti-inflammatory action, possibly counteracting that of SP signalling through the NK1 receptor. When the NK2 receptor is blocked this counter-regulatory mechanism is inhibited leading to the increase in the severity of the reaction

found in the NK2 receptor antagonist treated and NK2 and NK3 receptor antagonist combination therapy treated $NK1^{+/+}$ mice. Furthermore, both NK2 receptor antagonist and NK2 and NK3 receptor antagonist combination treated groups in the knockout animals showed a significantly lower neuropathological response when compared with their identically treated wild-type counterparts. The role of the NK3 receptor in this reaction remains equivocal since only a slight, non-significant, reduction in the severity of the response was found in NK3 receptor antagonist treated wild-type mice compared to non-treated controls. However, this small difference in the response was enough to highlight the effects of both of the treatments that included the NK2 receptor antagonist.

The existence of non-classical neurokinin receptors in NK1 receptor knockout mice is also conceivable. Such non-classical receptors have been demonstrated in the induction of IL-1 production by microglia in response to SP (Martin *et al.,* 1993). Human monocytes have also been shown to express a non-neurokinin SP receptor that leads to stimulation of MAP kinase on activation (Kavelaars, Broeke, Jeurissen, Kardux *et al.*, 1994). Also, in the bovine adrenal medulla, the N-terminal sequence of SP has been shown to binds to a non-NK1 receptor site (Geraghty, Livett, Rogerson, and Burcher, 1990). It is possible that these non-classical pathways are enhanced in the knockout mice and therefore the inflammatory response would not mimic that found in animals in which the NK1 receptor had been blocked by a specific antagonist especially since the SP mRNA levels are known to be higher in these mice.

The possibility of receptor independent activation is also feasible. There is evidence indicating that SP can integrate itself directly into cell membranes without the presence of a receptor. SP is an amphiphilic molecule with a hydrophilic N-terminus and a hydrophobic tail. The ability of this type of molecule to bind to negatively charged membranes and subsequently insert itself has been demonstrated (Mousli, Bronner, Landry, Bockaert *et al.*, 1990a; Mousli, Bueb, Bronner, Rouot *et al.*, 1990b). Once inserted the molecule adopts a membrane spanning conformation and can activate proteins on the inner side of the membrane. The receptor independent activation of G-proteins by SP has been demonstrated *in vitro*. In this artificial system the addition of SP to the membranes resulted in an increase in the GTPase activity indicating that the G-protein coupled receptor had been successfully stimulated (Mousli *et al.,* 1990a; Mousli *et al.,* 1990b).

The technique used in the production of the NK1 receptor knockout mice employed in these experiments generates animals that lack the gene from the beginning of their

development through to adulthood. This 'permanent' mutation may result in the development of alternative mechanisms in these animals that, in complex systems, allow the blocked pathways to be by-passed. This developmental plasticity may occur through a variety of routes, related proteins may functionally compensate for the absent molecule or differential genetic pathways may be induced. It is also possible that the presence of the defective pathway during the early developmental stages may subsequently compromise functions in the adult animal (Muller, 1999). These theories are substantiated by the indications of alternative receptor usage in the NK2 and NK3 receptor antagonist investigation in the knockout animals and may help to explain the enigmatic results found when the NK1 receptor knockout mice were employed in place of the CD1 animals used in the NK1 receptor antagonist studies.

Recent advances in the field of genetic manipulation have led to the production of transgenic animal with specific mutations whose expression can be controlled in a time or tissue dependent manner. Inactivation of a gene in adulthood could prevent the evolution of the adaptive changes resulting from developmental plasticity witnessed in conventional knockout animals, whereas tissue specific knockout animals would allow the role of genes that exhibit wide spread expression to be defined in individual tissues (Muller, 1999). Either of these conditional gene targeting approaches would be highly applicable to the study of the SP in the induction of CNS inflammation.

6.4.1.1. Astrocytosis

As previously stated astrocytes can be induced to express both the NK1 receptor and its ligand, SP. A significant drop in the number of astrocytes was found in our model following blockade of the NK1 receptor with RP-67,580. This suggests that, during the inflammatory response, there could be an interaction between SP and the astrocytes which culminates in an increase in astrocyte number. The possibility exists that a positive feedback mechanism develops where the astrocytes produce SP that subsequently augments the inflammatory response in these cells by inducing the expression of inflammatory cytokines. Astrocytes *in vitro* have been shown to produce IL-6 when stimulated with SP, and TNF-α production can be upregulated if SP is added to the culture system in conjunction with LPS (Cadman *et al.*, 1994; Gitter *et al.*, 1994; Luber-Narod *et al.*, 1994). Moreover, SP-immunoreactive astrocytes have been demonstrated around the edges of MS lesions suggesting that these cells do produce SP in response to inflammatory situations *in vivo* (Kostyk *et al.*, 1989). However, neither the primary source of the SP nor

the target cells can be determined from these experiments. The resulting down regulation of the astrocyte activation may therefore be due to an indirect effect of the antagonist causing a reduction in cytokine production by other cell types in the inflammatory infiltrate rather than a primary effect on the astrocytes.

When astrocyte numbers were analysed in the NK1 receptor knockout experiments no significant difference was found between the $NK1^{-/-}$ and the $NK1^{+/+}$ mice. Again there are several explanations for this finding including alternative receptor usage or developmental plasticity. However, since the knockout animals develop a more severe CNS inflammatory reaction than the wild-type mice it would be logical to assume that there would be a similar increase in the level of astrocyte activation. Yet this augmentation of the astrocytic response was not seen. It is therefore still possible that the knockout mice do exhibit a reduction in the level of astrocyte activation that is being masked by the corresponding increase in the severity of the neuropathology. If this is in fact the case it would imply that different pathways are being utilised by SP in the induction of inflammatory cell infiltration and the initiation of the activation of the resident CNS astrocytes in these knockout animals.

6.4.2. Clinical Response

The clinical impairment of $NK1^{-/-}$ mice following trypanosome-infection and sub-curative drug treatment was less severe than that seen in wild-type mice. This finding again suggests a role for SP in the development of the pathology associated with trypanosome–infection. However, this clinical improvement was not accompanied by a corresponding decrease in the severity of the neuropathological response, as would be expected, but was associated with a heightened neuroinflammatory reaction in the knockout animals. Thus the NK1 receptor knockout mice exhibit a dissociation between the neuropathological and the clinical response to trypanosome-infection.

This type of dissociation has been reported in inflammatory reactions in the human CNS of patients who have died of HIV infection. Here up to one-third of the patients that exhibited the clinical neurological response of dementia show mild pathological changes within the brain whereas 50% of non-demented cases exhibit these changes (Kennedy, 1993). Several explanations may exist for the paradox. The separation of the clinical from the neuropathological outcome could indicate that independent pathways mediate the induction of each response. In this scenario one of the pathways may be partially inhibited

in the knockout animals while the other remains functional leading to the apparent dissociation of the responses. The differential usage of alternative receptors to induce specific reactions has been suggested by experiments investigating smooth muscle tone and mucus secretion in ferret trachea. In this study the contraction of the smooth muscle in the trachea was attributed to the action of SP and NKA on NK2 or NK3 receptors where as the induction of mucus secretion, lysozyme output and transport of albumin across the tracheal wall was via NK1 receptor stimulation (Webber, 1989). This implies that SP can act through the NK2 and NK3 receptors and that the stimulation of particular neurokinin receptors by the same ligand can induce different outcomes.

As previously stated SP mRNA levels are upregulated in the $NK1^{-/-}$ mice (de Felipe *et al.*, 1997) and a corresponding increase in SP protein could conceivably result in a switch to alternative or non-classical receptor usage by the neuropeptide that may induce the inflammatory reaction in isolation from the clinical response. This hypothesis is further substantiated by the results of NK2 receptor and NK3 receptor blockade in NK1 receptor knockout and wild-type mice. In these studies there were no significant changes to the clinical picture see between the treatment regimens within the two groups of animals. This suggests that alternative receptor usage does not play a role in the development of the clinical response even though this phenomenon was strongly suggested by the results of the neuropathological investigation. When the overall clinical response between the wild-type and knockout groups was examined the $NK1^{-/-}$ mice showed a significantly better clinical response than the $NK1^{+/+}$ animals. This agrees with our initial studies using these animals. While it is reasonable to imagine that any increase in the CNS inflammatory reaction would be detrimental to the mice the possibility that this reaction may be in part beneficial cannot be excluded. This theory of a positive effect of CNS inflammation has been described previously in experiments involving aspirin treatment of *T.b.brucei*-infected rats (Quan *et al.*, 2000). In these studies infected animals given aspirin showed a reduction in the level of CNS inflammation; however, this amelioration of the inflammatory reaction was accompanied by an exacerbation of the neurodegenerative response. Results from the analyses comparing individual treatment regimens between the $NK1^{-/-}$ and $NK1^{+/+}$ mice showed that treatment with a combination of the NK2 and NK3 receptor antagonists induced a significant improvement in the knockout animals. This corresponds with the finding that this treatment regimen significantly reduces the severity of the neuropathological response in the knockout mice compared with both non-antagonist treated knockout mice and identically treated wild-type animals and suggests a beneficial action of reduced CNS inflammation.

Recently, a dissociation between the analgesic effects and the motivational 'reward' effects of opiate administration has been described in the $NK1^{-/-}$ mice (Murtra, Sheasby, Hunt, and de Felipe, 2000). The motivational properties of morphine administration were investigated using a conditioned place preference procedure. In this regimen mice learn to associate the reward of morphine with one of two visually and texturally different compartments. Wild-type mice developed a strong predilection for the compartment where they received morphine yet this preference was not seen in the knockout animals. In addition, these $NK1^{-/-}$ mice showed a significant reduction in the avoidance of naloxone–induced withdrawal from morphine. These findings suggest that the knockout animals have a reduced capacity to detect both the rewards of morphine and the symptoms of its withdrawal. It is unlikely that these behavioural changes are due to a secondary loss of the mu opiate receptor as the animals exhibit classical signs of drug withdrawal and the central analgesic actions of morphine are still present. Therefore, there is an apparent divergence between the opiate-induced motivational and the analgesic pathways in these mice.

6.4.3. Influence of the photoperiod

When trypanosome-infected, sub-curatively drug treated, NK1 receptor knockout mice were maintained under a 2 hour light 4 hour dark regimen the clinical and neuropathological responses were not significantly altered from the wild-type mice. Moreover, the results suggested a reversal of the trend exhibited when the mice were housed under normal 12 hour light 12 hour dark diurnal conditions. These apparently 'aberrant' findings may be the result of the altered light dark ratio under which the mice were maintained.

The eye, as well as the brain, has been described as an 'immuno-privileged' site where under typical conditions a suppression of the normal immune response to antigens occurs. This protects these areas from unwanted, and potentially deleterious, effects of immunological activity. If antigen is introduced into the anterior chamber of the eye an antibody response is induced together with a T-cell mediated suppression of delayed-type hypersensitivity. This altered immune reaction is termed 'anterior chamber-associated immune deviation' (ACAID) and can be modulated by the exposure of the eye to light and dark (Ferguson, Fletcher, Herndon, and Griffith, 1995). A study investigating the role of neuropeptides in this reaction demonstrated that SP was absent or expressed only at very low levels in the eye under normal 12 hour diurnal conditions. However, when mice were housed under a continuous dark regimen the levels of SP increased substantially. This SP

was rapidly released into the aqueous humor of the eye when the mice were reintroduced to light. In the same study the ACAID, in diurnal mice, was inhibited by inoculation of the anterior chamber of the eye with SP at similar concentrations to those detected in the dark reared animals. Following challenge of, SP-treated, immunised animals with antigen the delayed-type hypersensitivity response was not suppressed (Ferguson *et al.*, 1995).

The results from this investigation clearly demonstrate a direct effect of the photoperiod on the levels of SP produced in the eye and a consequential alteration in the immune response. It is possible that a similar mechanism is present within the brain and this would help to explain the anomaly in the experimental results gained following alteration of the photoperiod. If this is the case the raised levels of SP in the wild-type mice may result in an increase in the neuropathological reaction. Furthermore, this subtle change in SP concentrations may not be detected in the knockout animals due to the already high SP levels and the absence of the NK1 receptor. The increased severity of the reaction in the wild-type but not the knockout mice would result in the abolition of any significant difference between the animals and reflect the irregular findings of the anomalous experiment.

6.4.4. SP and human African trypanosomiasis

The results of this study strongly suggest a role for the neuropeptide SP in the induction and control of the CNS inflammatory response associated with sub-curative drug treatment of trypanosome-infection. However, neither the specific cell types involved nor the exact mechanism of action can be ascertained from these experiments. The prevalent expression of this neuropeptide and its receptors, in conjunction with the vast array of possible responses make dissecting the specific mechanisms involved an extremely complex task. The combined results of the experiments utilising the NK1 receptor knockout mice and NK1 receptor knockout mice in conjunction with NK2 and NK3 receptor antagonists strongly suggest an important role for the NK receptors in the development of the neuroinflammatory reaction. Due to the fact that blockade of the individual receptors induces conflicting effects on the neuroinflammation associated with trypanosome infection these experiments indicate that further detailed studies are required to fully investigate the roles of these receptors before any therapeutic regimen employing NK antagonists can be instigated.

Several of the clinical and biochemical features exhibited during the late-stage of sleeping sickness could also result from aberrant SP activity. The increased levels of prostaglandins found in the CSF of late-stage patients could be a consequence of the action of SP as the neuropeptide has been shown to induce the expression of eicosanoids by spinal astrocytes (Marriott, Wilkin, and Wood, 1991). As stated previously, SP plays a central role in the body's response to pain (Basbaum, 1999). Changes in the patients' perception of sensory stimuli occur frequently in sleeping sickness and hyperaesthesia is a commonly reported manifestation in trypanosomiasis cases (Apted, 1970). Another symptom that occurs frequently following trypanosome-infection is an intense generalised pruritus and a role for SP in the pathophysiology of itching has also been suggested (Greaves and Wall, 1996). The combined information regarding the properties of SP and the clinical manifestations present in the late-stage of the disease, together with the results from this series of experiments indicate a central action for the neuropeptide in the pathology of African sleeping sickness.

SP has been implicated as a mediator in a diverse variety of conditions ranging from depression (Kramer, Cutler, Feighner, Shrivastava *et al.*, 1998) and multiple sclerosis (Barker and Larner, 1992) to inflammatory bowel disease (Pothoulakis *et al.*, 1994), emesis (Saria, 1999) and arthritis (Anichini *et al.*, 1997). In the case of depression and emesis compounds have been developed that are currently in clinical trials for the treatment of these conditions (Saria, 1999). It would appear from these studies that administration of NK1 receptor antagonists would be advantageous in treatment of the neuroinflammatory reaction associated with trypanosome infections while NK2 receptor antagonists may prove detrimental to the outcome of the chemotherapy. The role of the NK3 receptor in the development of the neuropathological and clinical response remains unclear. Further detailed studies, to elucidate the exact role of SP in human African trypanosomiasis, are therefore required due to the increasing availability of novel SP related compounds that could potentially be employed in the development of safer and more efficacious treatment regimens for the chemotherapy of this devastating parasitic infection.

CHAPTER 7

GENERAL DISCUSSION AND CONCLUSIONS

7.1. Development of CNS inflammation

The results of the current investigation show that following trypanosome infection an inflammatory reaction develops within the CNS. This inflammatory response is initiated before the parasites have crossed the blood-brain barrier (BBB) and may be the result of inter-related mechanisms involving astrocyte activation, T-cell infiltration and the production of cytokines and chemokines within the CNS (Figure 7.1).

Astrocytes are found in close apposition to the BBB and it is possible that soluble factors present in the blood, produced either directly by the trypanosome or as a result of the developing inflammatory response to the infection outwith the CNS, stimulate the early activation of the astrocyte population. Following activation, astrocytes can produce cytokines and chemokines, as well as cellular adhesion molecules that would enhance the transmigration of T-cells through the BBB to survey the brain tissue for the presence of the parasites. Increased levels of IL-6, TNF-α, MCP-1, MIP-1α and RANTES mRNA were found within the CNS of mice killed at 7 days post-infection. These increases occurred before any influx of inflammatory cells was detected and this suggests that the inflammatory mediators are produced by cells resident within the brain. Activated astrocytes were identified, by increased staining with anti-glial fibrillary acidic protein, on day 14 post-infection, it is therefore possible that activation of this cell population was initiated at an earlier time-point in the course of the disease but was not detected using the staining technique employed. If this is the case the astrocytes could be the cellular source of the cytokines and chemokines. This hypothesis is not inconceivable as production of these inflammatory mediators by astrocytes following trypanosome infection in rats has been demonstrated previously using an immunocytochemistry double-labelling technique (Sharafeldin *et al.*, 2000). It is important to remember that a few macrophages were present in the meninges and blood vessels of both uninfected mice and animals killed at 7 days post-infection. These inflammatory cells could also be the source of the cytokines and chemokines (Fitzgerald *et al.*, 2001; Vaddi *et al.*, 1997). By day 14 post-infection both $CD4^+$ and $CD8^+$ cells were found in the meninges and a few $CD4^+$ cells were seen in the corpus callosum. It is feasible that these cells were initially activated by the presence of trypanosomes in the peripheral tissues and were subsequently attracted to the CNS by the increased levels of chemokines within the brain tissue. MCP-1, MIP-1α and RANTES all have T-cell chemoattractant properties (Vaddi *et al.*, 1997) and their upregulation within the CNS during the acute stage of the infection may explain the early appearance of this cell type in the brain tissue.

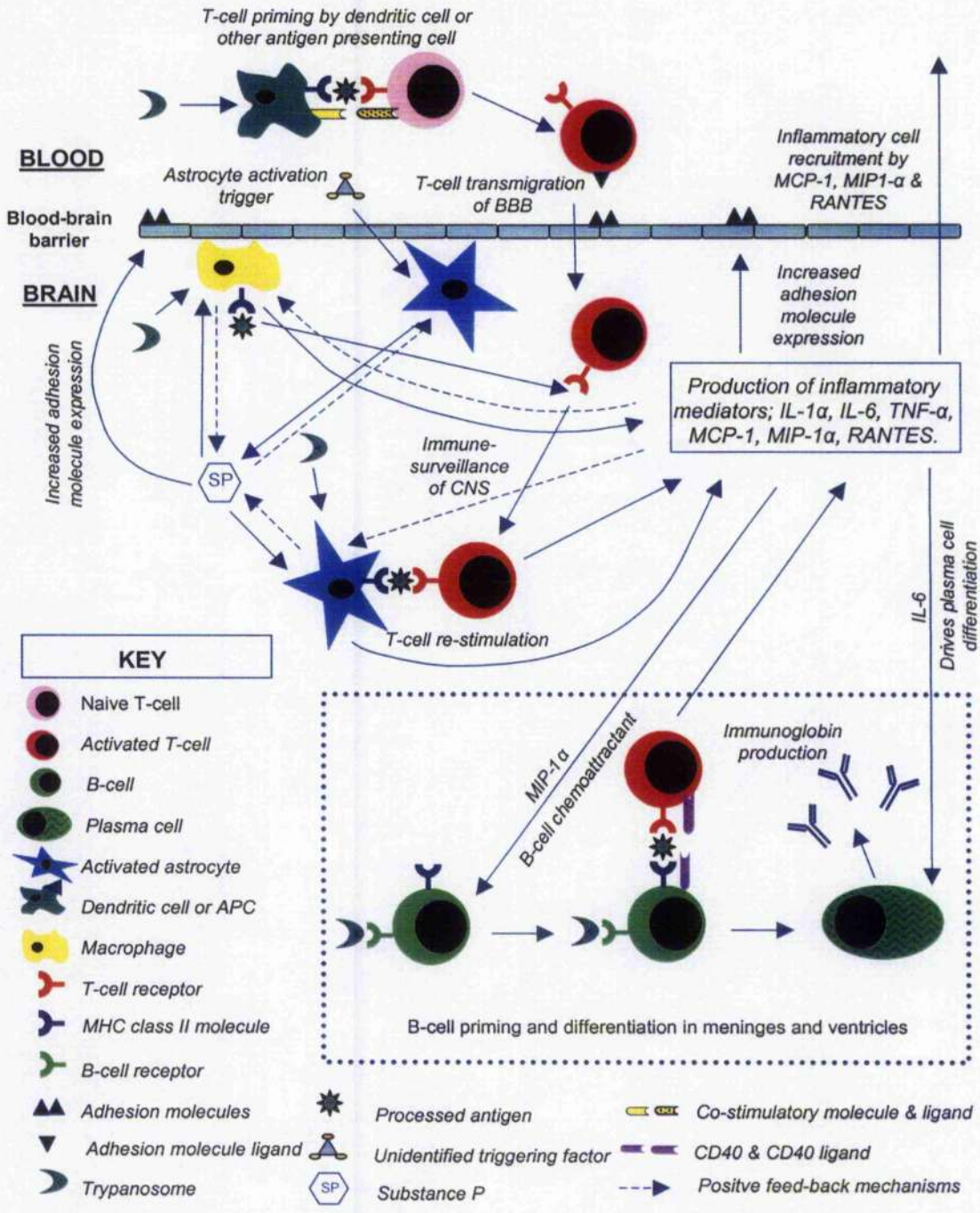

Figure 7.1. Schematic representation of possible inflammatory mechanisms involved in the generation of the post-treatment reactive encephalopathy (PTRE). Following trypanosome infection, astrocytes, in close apposition to the blood-brain barrier, are activated by the presence of parasite derived material or inflammatory mediators in the periphery, inducing the production of cytokines, chemokines and Substance P within the CNS. Many positive feed-back pathways are possible, encouraging the infiltration of T-cells, activated out-with the CNS parenchyma, and macrophages. The majority of infiltrating T-cells belong to the CD4 subset and their effector functions can only be induced by antigen presented in conjunction with major histo-compatability (MHC) class II molecules. These molecules can be expressed by astrocytes, macrophages and B-cells. Once the trypanosomes enter the CNS, the inflammatory reaction is exacerbated as the parasites provide a source of antigen to stimulate the T-cell response. In addition, the parasite antigen induces B-cell activation. The subsequent development of Plasma cells is controlled by the T-cells and the presence of cytokines including IL-6. The cascade of events culminates in the generation of the severe meningoencephalitis associated with the PTRE.

During the early-CNS stage of the infection a significant rise in the severity of the neuroinflammatory reaction within the brain was found, characterised by an increase in the number and spatial distribution of T-cells and macrophages. Astrocyte activation also became more pronounced at this time-point. The worsening of the CNS inflammation was accompanied by an upregulation in the expression of IL-1α, IL-6, TNF-α, MCP-1, and MIP-1α mRNA. An increase in the expression of these cytokines and chemokines could induce enhanced expression of cellular adhesion molecules on the CNS endothelial cells, attract monocytes to the brain from the periphery, and facilitate their subsequent transmigration across the BBB. In the mouse model of human African trypanosomiasis employed in this study the parasites enter the brain between 14 and 21 days post-infection (Jennings *et al.*, 1979). This implies that parasite antigen would be present within the CNS of animals killed at day 21 post-infection. It is possible that the increase in the severity of the overall reaction seen during this stage of the infection results from secondary activation of the infiltrating T-cell population by re-stimulation with the particular parasite antigen specified by their T-cell receptors. This could result in a positive feedback mechanism with the production of additional cytokines and further transmigration of inflammatory cells into the brain. In the case of $CD8^+$ cells the parasite antigen would have to be presented in combination with MHC class I molecules, whereas $CD4^+$ cells only recognise antigen when displayed in conjunction with MHC class II molecules. Resident brain cells such as astrocytes (Wong *et al.*, 1984) and microglia (Nakajima and Kohsaka, 2001) as well as the infiltrating macrophage population can be induced to express both MHC class I and class II molecules. These cell types could therefore play a major role in the exacerbation of the inflammatory reaction ultimately generating the severe meningoencephalitis seen in the post-treatment reactive encephalopathy.

Following subcurative trypanocidal drug treatment with diminazene aceturate, the parasites are cleared from the peripheral tissue, but since the drug does not cross the BBB efficiently parasites can remain sequestered within the CNS. It would be logical to assume that the clearance of the trypanosomes from non-CNS tissue would result in a reduction in the numbers of circulating T-cells activated against specific parasite antigen during the apparently aparasitaemic period. A concurrent decrease in the severity of the reaction within the CNS may also be expected as a consequence of the reduction in T-cell activation. This, however, does not occur and an exacerbation of the neuroinflammatory response, with further astrocyte activation and increased T-cell numbers, is seen following this treatment regimen. Dendritic cells, specialised antigen presenting cells, have been identified in the meninges and choroid plexus of the brain (McMenamin, 1999). It is

possible that during the period of aparasitaemia, the dendritic cells in these regions take up parasite antigen from the trypanosomes in the CNS and transport this to the cervical lymph node to initiate further T-cell activation and CNS infiltration. In addition, it is possible that parasite antigen is carried from the CNS to the lymphatic system in the circulating CSF instigating further immune reactivity (Hickey, 2001). To substantiate this hypothesis the levels of circulating activated T-cells following diminazene aceturate would have to be investigated. Although a rise in the severity of the CNS inflammation was found in the mice at this stage this was not accompanied by a simultaneous rise in the expression of the inflammatory mediators in the brain tissue. Levels of IL-1α, IL-6, TNF-α and MIP-1α expression were reduced immediately following diminazene aceturate treatment compared to mice killed at 28 days post-infection, and MCP-1 expression remained relatively constant. In contrast higher levels of RANTES were detected at this point. RANTES can be produced by a wide variety of cell types, including, T-cells, macrophages, microglia and astrocytes (Vaddi *et al.*, 1997), all of which are present in the CNS by this stage in the neuroinflammatory reaction. RANTES has many target cells and can recruit T-cells, macrophages and dendritic cells to sites of inflammation (Appay and Rowland-Jones, 2001). This could augment the inflammatory response in the brain and result in the exacerbation of the CNS inflammation. Also at this stage in the disease process, B-cells were detected in the CNS. The reduction in the expression of MIP-1α found in the CNS at this point in the infection is surprising, as this chemokine has been shown to attract B-cells to participate in the immune reaction (Schall *et al.*, 1993).

A slight increase in the severity of the CNS inflammation was found in mice exhibiting the PTRE compared to those killed during the late-CNS stage of the infection, and larger numbers of T-cells and B-cells were present in the infiltrate. This was accompanied by an initial increase in the expression of IL-6, TNF-α, MCP-1 and MIP-1α. The expression of IL-1α was only marginally increased and RANTES levels dropped compared to mice killed during the late-CNS stage of the disease. Levels of IL-1α and IL-6 expression continued to rise as the PTRE developed, whereas TNF-α, MCP-1 and MIP-1α expression declined. Following the initial drop in RANTES expression the levels increased to a similar intensity to those found during the late-CNS-stage of the infection, as the PTRE progressed. As well as an increase in the numbers of T-cells present at this time many B-cells and plasma cells were present in the inflammatory infiltrate although these tended to be confined to the meninges, perivascular cuffs and ventricles. The presence of specific antibody is not in general enough to result in the activation of naïve B-cells. B-cells interact with native antigen, recognised by their B-cell surface receptor, which they

internalise and process to display in conjunction with MHC class II molecules. $CD4^+$ cells then interact with the MHC class II molecule:peptide complex, displayed by the B-cell. The presence of co-stimulatory molecules, including ICAM-1, ICAM-3, and CD40 and their respective ligands on each cell enhances this interaction and stimulates the B-cell to enter the cell cycle and proliferate (Roitt *et al.*, 2001). The differentiation of antigen primed B-cells into antibody producing plasma cells occurs under the direction of a range of cytokines including IL-6 (Hirano, 1998). This cytokine was expressed in mice exhibiting the PTRE. This is not always the mechanism used in the activation of B-cells, as there are a few antigens that will cause expansion of the B-cell population with no T-cell intervention. However, the predominance of $CD4^+$ cells in the inflammatory infiltrate, together with the complex cytokine and chemokine milieu, and the subsequent appearance of numerous B-cells and plasma cells suggests that the B-cell activation found at this point in the disease process is controlled in a T-cell dependent manner.

7.2. Substance P in the CNS response

A role for the neuropeptide Substance P (SP), in the generation of the CNS reaction, has also been suggested from the investigations performed in this study. It would appear that this neuropeptide has a largely pro-inflammatory effect since a reduced neuroinflammatory response was found in trypanosome-infected mice following blockade of the NK1 receptor, the preferred receptor for SP, using a specific non-peptide antagonist RP-67,580. Contradictory results were found when transgenic mice, lacking a functional NK1 receptor, were infected with the parasite. These animals showed an increased pathology compared to mice of the same genetic background with normal NK1 receptor function. Further investigations employing the NK1 receptor knockout mice in conjunction with NK2 and NK3 receptor antagonists suggested that these divergent results could be the consequence of alternative receptor usage by SP in the transgenic animals. In addition, in normal wild-type mice, an anti-inflammatory role for usage of the NK2 receptor by its favoured ligand NKA, was indicated by the discovery that inhibition of this receptor by a specific non-peptide NK2 receptor antagonist increased the severity of the neuropathological reaction compared to wild-type mice not treated with the antagonist. This finding suggests that blockade of neuropeptide receptors should be employed with caution in the treatment of neuroinflammatory reactions and NK1 inhibition may be beneficial as an adjunct therapy to the treatment regimens employed in cases of human African trypanosomiasis whereas blockade of the NK2 receptor may have adverse consequences.

SP is known to effect the migration of T-cells (Hood *et al.*, 2000), and can be produced by astrocytes, lymphocytes and macrophages (De Giorgio *et al.*, 1998). These are the main cell types implicated by the current investigation in the generation of the CNS inflammatory reaction associated with trypanosome infection. In addition, SP can induce or enhance the expression of IL-6 by astrocytes (Gitter *et al.*, 1994; Luber-Narod *et al.*, 1994) and IL-1, TNF-α and IL-6 by inflammatory cells (Berman *et al.*, 1996). The ability of this neuropeptide to provoke IL-6 production by astrocytes is of particular interest in this case since expression of this cytokine appears to be upregulated within 7 days of the onset of the infection. The results of this study suggest that the astrocyte population is responsible for the early development of the CNS reaction since activation of this cell type can be detected by 14 days post-infection. Taken together these findings also imply that the astrocytes may be the cellular source of the IL-6 and that this cytokine production could be a consequence of upregulated SP expression. To investigate this hypothesis further it would be useful to determine whether the levels of SP production are enhanced within the CNS following trypanosome infection. Astrocytes not only react to SP but can also express this neuropeptide. It would also be of interest to ascertain the source of this neuropeptide in the CNS of trypanosome-infected mice.

Various theories have been suggested for the development of the PTRE including; parasite persistence within the CNS as a consequence of subcurative chemotherapy (Hunter and Kennedy, 1992; Jennings *et al.*, 1989), the release of parasite antigen within the CNS following chemotherapy (Pepin and Milord, 1991), the toxic nature of the arsenical drugs used to treat late-stage human disease (Hurst, 1959), immune complex deposition (Lambert *et al.*, 1981) and autoimmunity (Poltera, 1980). None of these hypotheses are mutually exclusive. This investigation moves some way towards elucidating the mechanisms generating the CNS inflammatory response by highlighting the prominent role of the astrocytes and $CD4^+$ cells in the reaction. Unfortunately the cellular source of the cytokines and chemokines expressed was not identified and this remains a matter for conjecture. Although, in a rat model of trypanosomiasis, astrocytes and microglia have been implicated as the cells producing these mediators (Sharafeldin *et al.*, 2000). The development of the PTRE in this mouse model of HAT, in the absence of arsenical drug treatment, would suggest that this factor is not a prerequisite for the occurrence of the meningoencephalitis in the human situation. However, use of toxic arsenical-based chemotherapy may still exacerbate the CNS inflammatory reaction. Information from the current investigation indicates that the mechanisms resulting in the development of the severe meningoencephalitis are likely to involve immune-mediated pathways entailing a

combination of the above theories. The pathogenesis of the CNS-inflammatory reaction following trypanosome infection and subcurative trypanocidal drug treatment is complex and involves an intricate interplay between the CNS cells, inflammatory cells, neuropeptides, cytokines and chemokines (Figure 7.1).

7.3 . Mechanism of action of eflornithine

In the present investigation the ability of eflornithine to prevent the development of a neuroinflammatory reaction and to resolve an already established meningoencephalitis was demonstrated. This anti-inflammatory action of eflornithine in preventing and ameliorating the CNS inflammation associated with trypanosome infection and subcurative trypanocidal drug treatment has been reported previously (Jennings *et al.,* 1997); in this study the effects of eflornithine treatment on the severity of the response were not quantified and were purely observational and cytokine and chemokine expression was not examined. The results of these experiments were in agreement with those seen in the present investigation and confirm the value of eflornithine as a prophylactic to preclude the development of the CNS inflammation and in the resolution of an already established meningoencephalitis. It would appear from the results of the current investigation that alteration in the production of cytokines and chemokines, particularly IL-1α and IL-6, may be the mechanism utilised by eflornithine to prevent the development of CNS inflammation. However, this does not seem to be the case in the amelioration of the meningoencephalitis. If the theories raised by the current investigation, regarding the development of the PTRE and the involvement of clonal expansion of the T-cell and B-cell populations within the CNS are correct then the more traditional ornithine decarboxylase (ODC) inhibitory pathway associated with eflornithine treatment could prevent the proliferation of these inflammatory cells. This may play a major role in the resolution of an established CNS reaction. A partial restoration of this proliferative response, may well occur following eflornithine treatment and concurrent putrescine administration resulting in a limited reduction in the severity of the neuropathological reaction, as seen in the earlier study (Jennings *et al.,* 1997).

It is important to remember that the approach used in the present investigation detects changes in the expression level of cytokine and chemokine mRNA. It is possible that eflornithine inhibits the translation of these mRNA transcripts and prevents the production of the active protein molecule. Therefore, alterations in the expression of mRNA may not reflect subsequent changes in the concentration of the cytokines and chemokines in the

tissue studied. For more concrete evidence of the role of these mediators in the mechanism of action of eflornithine their concentrations in the CNS must be investigated.

7.4. Future investigations

The pathways studied and the techniques used in the present investigation are by no means exhaustive. The semi-quantitative method employed in determination of the cytokine and chemokine expression levels in this study has now been superseded by vastly improved techniques. The application of image analysis software to precisely measure the intensity of the PCR amplicons would allow a more accurate interpretation of cytokine and chemokine expression pattern to be made. In addition the data generated using this approach would be more amenable to statistical analysis and would, in all probability, allow the use of more powerful parametric statistical tests rather than the non-parametric procedures employed in the current study. Furthermore, the development of 'real-time PCR' techniques, such as Taqman® or SYBR® Green, provides a method to accurately quantify the level of mRNA in a starting sample. The rationale for these techniques relies on the detection and quantitation of a fluorescent reporter molecule. The signal detected from this reporter molecule increases in direct proportion to the amount of PCR product present in the reaction mix and therefore reflects the concentration of the target sequence in the original sample.

In recent years it has become apparent that cytokines and chemokines do not function as individual entities but instead act in complex cascades and networks. The importance of the balance of pro-inflammatory and counter-inflammatory cytokines as well as the relationship between those which provoke tissue damage and those which protect tissue elements is now appreciated. Within the CNS this situation is complicated further since many of these inflammatory mediators facilitate normal physiological functions, such as the control of sleeping patterns, thermoregulation and appetite control. Although an investigation of the expression profiles of specific cytokine and chemokine elements known to be present within the CNS following trypanosome infection does provide information with regard to the development of the neuroinflammation, it may be of more benefit to study the expression pattern of a much wider range of mediators that could influence the generation of the meningoencephalitic response. With the development of microarray technology this approach is now possible. Using microarrays, the expression of numerous genes can be examined and a snapshot of the gene activity at a given time-point, or following a particular treatment regimen, can be profiled. In this instance valuable

insight would be gained by studying the expression profiles of cytokines, chemokines and neuropeptides within the CNS of mice at various time-points after infection and subcurative trypanocidal drug treatment. By analysing the expression data generated from the microarrays not only the presence or absence of particular mediators could be investigated but also the inter-relationships between the expression patterns of these molecules could be identified. It is possible that the switch from the early-CNS response seen following trypanosome infection to the development of the severe meningoencephalitis reflects an alteration in the balance of pro- and anti-inflammatory mediators rather than a change in an individual agent. The breadth of information gained from microarray studies would therefore substantially enhance the current understanding regarding the delicate equilibrium required to maintain the counter inflammatory profile within the CNS. In addition possible therapeutic strategies to prevent the exacerbation of the CNS inflammatory response, as well as the adverse reactions to melarsoprol chemotherapy, currently encountered in cases of human trypanosome infections, may be highlighted.

7.5. Conclusions

The results gained from the present investigation substantially enhance the currently available knowledge regarding the development of the CNS inflammatory reaction found following trypanosome infection and subcurative drug treatment. The main findings gained from this study are listed below.

- The importance of the astrocytes in the early CNS events that ultimately result in the development of the neuroinflammation has been shown.

- A time-course of inflammatory cell infiltration has been delineated with cellular infiltration of the CNS occurring prior to the detectable invasion of the brain tissue by the trypanosomes.

- The predominance of $CD4^+$ cells in the inflammatory cell infiltrate and the possible mechanisms employed in the augmentation of the inflammatory reaction have been highlighted.

- Alterations in the expression patterns of the cytokines IL-1α, IL-6 and TNF-α as well as the chemokines MIP-1α, MCP-1 and RANTES have been detected throughout the course of the infection.

- Inhibition of the transcription of IL-1α and IL-6 has been indicated as the possible pathway used by eflornithine in the preventing the development of the CNS inflammatory response. However, the mechanism of action of the drug in the amelioration of an established meningoencephalitis remains equivocal.

- A pro-inflammatory role for the neuropeptide Substance P, in the CNS inflammatory reaction has been discovered and the use of NK1 receptor antagonists as an adjunct therapy to decrease the severity of the neuroinflammatory reaction has been suggested.

- In addition to the findings directly related to the development of CNS inflammation occurring as a result of trypanosomiasis, the difficulties of interpreting data gained from the use of transgenic animals in complex systems where redundancy and alternative pathways can be utilised has been highlighted.

In conclusion, it would appear that following trypansome infection an inflammatory reaction is instigated in the CNS quickly after the introduction of the parasite. The factor that initiates this CNS response remains unclear and may be parasite derived or an inflammatory agent produced in response to the infection outwith the CNS. It seems likely that the astrocytes, which are found in close apposition to the BBB, are the primary cell type within the CNS to react to this triggering factor. Once activated the astrocyte population produces an array of cytokines and chemokines, as well as SP, which augment the development of the inflammatory response by recruiting inflammatory cells to the CNS and stimulating further cellular activation. All the elements necessary to propagate the inflammatory reaction are present within the CNS following invasion of the brain by the parasites. As the reaction becomes more severe $CD4^+$ cells become the predominant cell type in the inflammatory infiltrate and may succeed the astocytes in the further development of the inflammation. B-cells and plasma cells increase in number as the response matures. It is probable that these cells are activated and encouraged to proliferate and differentiate within the CNS in response to specific parasite antigen, $CD4^+$ cell stimulation and the provision of the appropriate cytokines in the immediate environment. The complete cascade of events results in the development of the severe

meningoencephalitic response that is characteristic of the PTRE. The trypanostatic drug eflornithine prevents the development of this inflammatory cascade by inhibiting the transcription of IL-1α and IL-6, however, its mechanisim of action in the amelioration of an established meningoecephaltis has yet to be fully elucidated.

As human CNS tissue is accessible only from patients that have died during the late-stage of trypanosome infection or following the development of the PTRE, information regarding the subtle CNS changes that occur early after infection cannot be ascertained from the human population. The availability of the highly reproducible and well-documented murine model of human African trypanosomiasis has therefore provided a means to investigate the events that initiate the inflammatory response and control the development of the subsequent meningoencephalitis. Additional pharmacological actions of the trypanostatic drug eflornithine have been highlighted and the value of the use of this drug in treatment of infections that are not directly susceptible to eflornithine therapy has been demonstrated through the use of this murine model. This information may facilitate the development of new therapeutic approaches to help prevent the devastating adverse effects that are associated with the late-stage of trypanosome infection and subcurative drug treatment. Without this model such knowledge would not be available.

APPENDIX 1

20x SSC (Salt Sodium Citrate)

Sodium chloride	175.3g
Sodium citrate	88.2g

Dissolve the salts in 800ml of distilled water. Adjust the pH to 7.00 and make up the final volume to 1 litre with distilled water. Differing strengths of SSC can be prepared as required by dilution of the x20 stock with distilled water.

2M sodium acetate pH4.0

Sodium acetate (anhydrous)	16.42g
Glacial acetic acid	35ml

Dissolve the sodium acetate in 40ml of distilled H_2O and add the 35ml of acetic acid. Adjust the pH to 4.0 with glacial acetic acid and the final volume to 100ml with distilled H_2O.

0.1M citrate buffer

Solution 1

Tri sodium citrate (di-hydrate)	44.1g

Dissolve salt in 1.5 litres of distilled water

Solution 2

Citric acid (mono-hydrate)	10g

Dissolve salt in 500ml of distilled water

Working Solution

To prepare the buffer solution take 1275ml of tri-sodium citrate (solution 1) and add between 200 and 225 ml of citric acid (solution 2) to give a final pH of 6.0

0.2M phosphate buffer

Solution A

Sodium dihydrogen phosphate	6.24g

Dissolve in 100ml of distilled water

Solution B

Disodium hydrogen phosphate	5.66g

Dissolve in 100ml of distilled water

Working solution

Mix 9.5ml of solution A with 40.5ml of solution B and make to 100mls with distilled water, adjust the pH to 7.4.

4% paraformaldehyde

Paraformaldehyde	1g

Dissolve paraformaldehyde in 10ml of distilled water at 60^0 C with constant stirring. Once dissolved, cool the solution and 12.5ml 0.2M phosphate buffer (see above). Adjust the pH to 7.3 and the total volume to 25ml with distilled water. Store at 4^0 C for up to 24 hours or at -20^0 C for longer periods.

Bouin's fixative

Saturated aqueous picric acid solution	150ml
40% formaldehyde	50ml
Glacial acetic acid	10ml

Mix solutions and store at room temperature

Denaturing Solution

Guanidium thiocyanate	47.5g
Sodium citrate	0.74g

Sarcosyl (N-lauryl-sarcosine)	0.5g
β-mercaptoethanol	0.7ml

Place 50ml sterile H_2O onto a heated stirrer. Slowly add the salts listed above with constant stirring. The reaction is endothermic and requires constant heating to facilitate the dissolution of the salts. Once the salts have dissolved make the volume of the solution up to 90 ml with sterile H_2O and adjust the pH to 7.0. Add the β-mercaptoethanol and adjust the final volume to 100ml with sterile H_2O. The denaturing solution can be stored at 4^0C in the dark for approximately one month.

DEPC water

Di-ethyl-pyro-carbonate (DEPC)	1ml

Add 1ml of DEPC to 999ml of distilled water. This should be performed wearing protective gloves and in the fume cupboard.

LANA's fixative

Sorensen's solution A

Dissolve 17.855g di-sodium hydrogen phosphate di-hydrate in 500ml of distilled water.

Sorensen's solution B

Dissolve 13.8g sodium di-hydrogen phosphate di-hydrate in 500ml of distilled water.

Working fixative solution

Prepare 500 ml of complete Sorensen's solution by adding 360 ml of Sorensen's A and 140ml of Sorensen's B solutions. Add:

40% formaldehyde	108ml
Saturated aqueous picric acid	140ml
Distilled water	252ml

Mix solutions thoroughly and store a 4^0 C until required.

Phosphate Buffered Saline (PBS) for ICC

Di-sodium hydrogen phosphate (anhydrous)	14.8g
Potassium di-hydrogen phosphate (anhydrous)	4.3g
Sodium Chloride	72g

Add salts to 8 litres of distilled water with constant stirring. Adjust the pH to 7.4 and make the total volume up to 10 litres with distilled water.

PCR loading buffer

Bromophenol blue	25mg (0.25%)
Glycerol	3ml (30%)
Distilled H_2O	7ml (70%)

Mix the glycerol and distilled H_2O. Weigh the dye and add to the solution. Mix thoroughly until the bromophenol blue has dissolved.

TBE electrophoresis buffer (x10 stock solution)

Tris base	545g
Boric acid	278g
EDTA (di-sodium salt)	46.5g

Slowly added the salts to approximately 3 litres of distilled H_2O with heat and constant stirring. Once dissolved adjust the pH to 8.3 and the final volume to 5 litres with distilled H_2O.

REFERENCE LIST

Adams, J.H. and Graham, D.I. (1998) Virus and other infections. In: "An introduction to neuropathology." Ed. Adams and Graham. Churchhill Livingstone. Edinburgh. pp94-117.

Adams, J.H., Haller, L., Boa, F.Y., Doua, F., Dago, A., and Konian, K. (1986) Human African trypanosomiasis (T. b. gambiense): a study of 16 fatal cases of sleeping sickness with some observations on acute reactive arsenical encephalopathy. *Neuropathology and Applied Neurobiology* **12**, 81-94.

Allan, S.M. and Rothwell, N.J. (2001) Cytokines and acute neurodegeneration. *Nature Reviews in Neuroscience* **2**, 734-744.

Aloisi, F. (2001) Immune function of microglia. *Glia* **36**, 165-179.

Aloisi, F., Ria, F., and Adorini, L. (2000) Regulation of T-cell responses by CNS antigen-presenting cells: different roles for microglia and astrocytes. *Immunology Today* **21**, 141-147.

Aloisi, F., Ria, F., Penna, G., and Adorini, L. (1998) Microglia are more efficient than astrocytes in antigen processing and in Th1 but not Th2 cell activation. *Journal of Immunology* **160**, 4671-4680.

Anichini, M., Lepori, M., Maddali Bongi, S., Marcsca, M., and Zoppi, M. (1997) Substance P in the serum of patients with rheumatoid arthritis. *Revue du Rhumatisme (Engl.Ed.)* **64**, 18-21.

Antel, J. and Prat, A. (2000) Antigen and superantigen presentation in the human CNS. *Journal of Neuroimmunology* **107**, 118-123.

Apelt, J. and Schliebs, R. (2001) Beta-amyloid-induced glial expression of both pro- and anti-inflammatory cytokines in cerebral cortex of aged transgenic Tg2576 mice with Alzheimer plaque pathology. *Brain Research* **894**, 21-30.

Appay, V. and Rowland-Jones, S.L. (2001) RANTES: a versatile and controversial chemokine. *Trends in Immunology* **22**, 83-87.

Apted, F.I.C. (1970) Clinical manifestations and diagnosis of sleeping sickness. In: "The African Trypanosomiases." Ed. Mulligan. Allen & Urwin. London. pp661-683.

Asensio, V.C. and Campbell, I.L. (2001) Chemokines and viral diseases of the central nervous system. *Advances in Virus Research* **56**, 127-173.

Asensio, V.C. and Campbell, I.L. (1997) Chemokine gene expression in the brains of mice with lymphocytic choriomeningitis. *Journal of Virology* **71**, 7832-7840.

Atouguia, J.M., Jennings, F.W., and Murray, M. (1995) Successful treatment of experimental murine *Trypanosoma brucei* infection with topical melarsoprol gel. *Transactions of the Royal Society of Tropical Medical and Hygiene* **89**, 531-533.

Ausubel,F.M., Brent,R., Kingston,R.E., Moore,D.D., Seidman,J.G., and Smith,J.A. (1987) Current protocols in molecular biology. Ed. Ausubel, Frederick M, Brent, Roger, Kingston, Robert E., Moore, David D., Seidman, J. G., Smith, John A., and Struhl, Kevin. Green Publishing Associates, Inc. and John Wiley & Sons, Inc. USA.

Bacchi, C.J., Nathan, H.C., Hutner, S.H., McCann, P.P., and Sjoerdsma, A. (1980) Polyamine metabolism: A potential therapeutic target in trypanosomes. *Science* **210**, 332-334.

Bacchi, C.J. (1981) Content, synthesis and function of polyamines in trypanosomatids: relationship to chemotherapy. *Journal of Protozoology* **28**, 20-27.

Bacchi, C.J., Garofalo, J., Mockenhaupt, D., McCann, P.P., Diekema, K.A., Pegg, A.E., Nathan, H.C., Mullaney, E.A., Chunosoff, L., Sjoerdsma, A., and Hutner, S.H. (1983) In vivo effects of alpha-difluoromethylornithine on the metabolism and morphology of *trypanosoma brucei brucei*. *Molecular and Biochemical Parasitology* **7**, 209-225.

Bacchi, C.J. and McCann, P.P. (1987) Parastic protozoa and polyamines. In: "Inhibition of polyamine metabolism. Biological significance and basis for new therapies." Ed. McCann, Pegg, and Sjoerdsma. Academic Press. London. pp317-344.

Bacchi, C.J., Nathan, H.C., Livingston, T., Valladares, G., Saric, M., Sayer, P.D., Njogu, A.R., and Clarkson, A.B.Jr. (1990) Differential susceptibility to DL-alpha-difluoromethylornithine in clinical isolates of *trypanosoma brucei rhodesiense*. *Antimicrobial Agents and Chemotherapy* **34**, 1183-1188.

Bacchi, C.J., Nathan, H.C., Yarlett, N., Goldberg, B., McCann, P.P., Sjoerdsma, A., Saric, M., and Clarkson, A.B. (1994) Combination chemotherapy of drug resistant *Trypanosoma brucei rhodesiense* infections in mice using dl-alpha-difluoromethylornithine and standard trypanocides. *Antimicrobial Agents and Chemotherapy* **38**, 563-569.

Bailey, J.W. and Smith, D.H. (1992) The use of the acridine orange QBC technique in the diagnosis of African trypanosomiasis. *Transactions of the Royal Society of Tropical Medical and Hygiene* **86**, 630-

Bailey, J.W. and Smith, D.H. (1994) The quantitative buffy coat for the diagnosis of trypanosomes. *Tropical Doctor* **24**, 54-56.

Bajetto, A., Bonavia, R., Barbero, S., Florio, T., and Schettini, G. (2001) Chemokines and their receptors in the central nervous system. *Frontiers in Neuroendocrinology* **22**, 147-184.

Bakheit, M., Olsson, T., Van Der Meide, P., and Kristensson, K. (1990) Depletion of CD8+ t-cells supresses growth of *Trypanosoma brucei brucei* and interferon-gamma production in infected rats. *Clinical and Experimental Immunology* **81**, 195-199.

Bakhiet, M., Mousa, A., Seiger, A., and Andersson, J. (2002) Constitutive and inflammatory induction of alpha and beta chemokines in human first trimester forebrain astrocytes and neurons. *Molecular Immunology* **38**, 921-929.

Bakhiet, M., Olsson, T., Ljungdahl, A., Hojeberg, Bo., Van der Meide, P., and Kristensson, K. (1996) Induction of interferon-gamma, tranforming growth factor-beta and interleukin-4 in mouse strains with different susceptiblities to *trypanosoma brucei brucei*. *Journal of Interferon and Cytokine Research* **16**, 427-433.

Bales, J.D., Jr., Harrison, S.M., Mbwabi, D.L., and Schecter, P.J. (1989) Treatment of arsenical refractory Rhodesian sleeping sickness in Kenya. *Annals of Tropical Medicine and Parasitolology* **83 Suppl 1**, 111-114.

Balfour, J.A. and McClellan, K. (2001) Topical eflornithine. *American Journal of Clinical Dermatology* **2**, 197-201.

Baluk, P., Bertrand, C., Geppetti, P., McDonald, D.M., and Nadel, J.A. (1995) NK1 receptors mediate leukocyte adhesion in neurogenic inflammation in the rat trachea. *American Journal of Physiology* **268**, L263-L269.

Baluk, P., Nadel, J.A., and McDonald, D.M. (1992) Substance P-immunoreactive sensory axons in the rat respiratory tract: a quantitative study of their distribution and role in neurogenic inflammation. *Journal of Comparative Neurology* **319**, 586-598.

Bancroft, G.J. and Askonas, B.A. (1985) Immunobiology of African trypanosomiasis in laboratory rodents. In: "Immunopathology and Pathogenesis of Trypanosomiasis." Ed. Tizard. CRC Press Inc. Boca Raton, Florida. pp76-101.

Bar-Or, A., Oliveira, E.M., Anderson, D.E., and Hafler, D.A. (1999) Molecular pathogenesis of multiple sclerosis. *Journal of Neuroimmunology* **100**, 252-259.

Barker, R. and Larner, A. (1992) Substance P and multiple sclerosis. *Medical Hypotheses* **37**, 40-43.

Barrett, M.P. (1999) The fall and rise of sleeping sickness. *Lancet* **353**, 1113-1114.

Barron, K.D. (1995) The microglial cell. A historic review. *Journal of the Neurological Sciences* **134(suppl.)**, 57-68.

Basbaum, A.I. (1999) Spinal mechanisms of acute pain. *Regional Anesthesia and Pain Medicine* **24**, 59-67.

Bauer, J., Rauschka, H., and Lassmann, H. (2001) Inflammation in the nervous system: the human perspective. *Glia* **36**, 235-243.

Beattie, E.C., Stellwagen, D., Morishita, W., Bresnahan, J.C., Ha, B.K., Von Zastrow, M., Beattie, M.S., and Malenka, R.C. (2002) Control of synaptic strength by glial TNFalpha. *Science* **295**, 2282-2285.

Bentivoglio, M., Grassi-Zucconi, G., Olsson, T., and Kristensson, K. (1994) *Trypanosoma brucei* and the nervous system. *Trends in Neuroscience* **17**, 325-329.

Berman, A.S., Chancellor-Freeland, C., Zhu, G., and Black, P.H. (1996) Substance p primes murine peritoneal macrophages for augmented proinflammatory cytokine response to lipopolysaccharide. *Neuroimmunomodulation* **3**, 141-149.

Beutler, B. and Cerami, A. (1989) The biology of cachectin/TNF--a primary mediator of the host response. *Annual Reviews in Immunology* **7**, 625-655.

Beutler, B., Greenwald, D., Hulmes, J.D., Chang, M., Pan, Y.C., Mathison, J., Ulevitch, R., and Cerami, A. (1985) Identity of tumour necrosis factor and the macrophage-secreted factor cachectin. *Nature* **316**, 552-554.

Blum, A.M., Metwali, A., Cook, G., Mathew, R.C., Elliott, D., and Weinstock, J.V. (1993) Substance P modulates antigen-induced,IFN-gamma production in murine schistosomiaisis mansoni. *Journal of Immunology* **151**, 225-233.

Blum, A., Metwali, A., Elliott, D., Sandor, M., Lynch, R., and Weinstock, J.V. (1996) Substance P receptor antagonist inhibits murine IgM expression in developing

schistosome granulomas by blocking the terminal differentiatiation of intragranuloma B cells. *Journal of Neuroimmunology* **66**, 1-10.

Bonner, T.I., Young, A.C., and Affolter, H.-U. (1987) Cloning and expression of rat and human tachykinin genes. In: "Substance P and Neurokinins." Ed. Henry, Couture, Cuello, Pelletier, Quirion, and Regoli. Springer-Verlag. New York. pp3-4.

Bossut, D., Frenk, H., and Mayer, D.J. (1988) Is substance P a primary afferent neurotransmitter for nociceptive input? II. Spinalization does not reduce and intrathecal morphine potentiates behavioral responses to substance P. *Brain Research* **455**, 232-239.

Bowden, J.J., Baluk, P., Lefevre, P.M., Vigna, S.R., and McDonald, D.M. (1996) Substance P (NK1) receptor immunoreactivity on endothelial cells of the rat tracheal mucosa. *American Journal of Physiology* **270**, L404-L414.

Bradbury, A.F., Mistry, J., Roos, B.A., and Smyth, D.G. (1990) 4-Phenyl-3-butenoic acid, an in vivo inhibitor of peptidylglycine hydroxylase (peptide amidating enzyme). *European Journal of Biochemistry* **189**, 363-368.

Bright, J.J. and Sriram, S. (2001) Immunotherapy of inflammatory demyelinating diseases of the central nervous system. *Immunologic Research* **23**, 245-252.

Brown, D.R., Parsons, A.M., and O'Grady, S.M. (1992) Substance P produces sodium and bicarbonate secretion in porcine jejunal mucosa through an action on enteric neurons. *The Journal of Pharmacology and Experimental Therapeutics* **261**, 1206-1212.

Bruce,D. (1895) Preliminary report on the tsetse fly disease or nagana in Zululand. Bennett & Davis. Durban.

Bruce,D. (1897) Further report on the tsetse fly disease or nagana in Zululand. Harrison & Sons. London.

Brunsson, I., Fahrenkrug, J., Jodal, M., Sjoqvist, A., and Lundgren, O. (1995) Substance P effects on blood flow, fluid transport and vasoactive intestinal polypeptide release in the feline small intestine. *Journal of Physiology (London)* **483**, 727-734.

Cadman, E.D., Witte, D.G., and Lee, C.-M. (1994) Regulation of the release of interleukin-6 from human astrocytoma cells. *Journal of Neurochemistry* **63**, 980-987.

Campbell, I.L., Abraham, C.R., Masliah, E., Kemper, P., Inglis, J.D., Oldstone, M.B., and Mucke, L. (1993) Neurologic disease induced in transgenic mice by cerebral overexpression of interleukin 6. *Proceedings of the National Academy of Sciences of the USA* **90**, 10061-10065.

Campbell, I.L., Hobbs, M.V., Kemper, P., and Oldstone, M.B.A. (1994) Cerebral expression of multiple cytokine genes in mice with lymphocytic choriomeningitis. *Journal of Immunology* **152**, 716-723.

Carson, M.J., Reilly, C.R., Sutcliffe, J.G. and Lo, D. (1999) Disproportionate recruitment of $CD8^+$ T-cells into the central nervous system by professional antigen-presenting cells. *American Journal of Pathology* **154**, 481-494.

Carswell, E.A., Old, L.J., Kassel, R.L., Green, S., Fiore, N., and Williamson, B. (1975) An endotoxin-induced serum factor that causes necrosis of tumors. *Proceedings of the National Academy of Sciences of the USA* **72**, 3666-3670.

Castagliuolo, I., Keates, A.C., Qiu, B., Kelly, C.P., Nikulasson, S., Leeman, S.E., and Pothoulakis, C. (1997) Increased substance P responses in dorsal root ganglia and intestinal macrophages during Clostridium difficile toxin A enteritis in rats. *Proceedings of the National Academy of Sciences of the USA* **94**, 4788-4793.

Cegielski, J.P. and Durack, D.T. (1997) Trypanosomiasis. In: "Infections of the Central Nervous System." Ed. Scheld, Whitley, and Durack. Lippincott-Raven. Philadelphia. pp807-829.

Chang, M.M., Leeman, S.E., and Niall, H.D. (1971) Amino-acid sequence of substance P. *Nature -New Biology* **232**, 86-87.

Chiwakata, C.B., Hort, G., Hemmer, C.J., and Dietrich, M. (1996) Sera from patients with falciparum malaria induce substance P gene expression in cultured human brain microvascular endothelial cells. *Infection and Immunity* **64**, 5106-5110.

Chomczynski, P. and Sacchi, N. (1987) Single-step method of RNA isolation by acid guanidium thiocyanate-phenol-chloroform extraction. *Analytical Biochemistry* **162**, 156-159.

Clemens,M.J. (1991) Cytokines. Ed. Clemens, M. J. BIOS Scientific Publishers Limited. Oxford.

Clerinx, J., Taelman, H., Bogaerts, J., and Vervoort, T. (1998) Treatment of late stage rhodesiense trypanosomiasis using suramin and eflornithine: report of six cases. *Transactions of the Royal Society of Tropical Medical and Hygiene* **92**, 449-450.

Compston, A. (1993) Inflammation and the brain. *Molecular and Chemical Neuropathology* **19**, 47-64.

Cooke, H.J., Sidhu, M., Fox, P., Wang, Y.Z., and Zimmermann, E.M. (1997) Substance P as a mediator of colonic secretory reflexes. *American Journal of Physiology* **272**, G238-G245.

Croul, S., Sverstiuk, A., Radzievsky, A., and Murray, M. (1995) Modulation of neurotransmitter receptors following unilateral L1-S2 deafferentation: NK1, NK3, NMDA, and 5HT1a receptor binding autoradiography. *Journal of Comparative Neurology* **361**, 633-644.

de Atouguia, J.L.M. (1998) New approaches to the chemotherapy of human African trypanosomiasis; The use of topical formulations in the mouse model. PhD Thesis, Universidade Nova de Lisboa.

de Atouguia, J.L.M. and Kennedy, P.G.E. (2000) Neurological aspects of human African trypanosomiasis. In: "Infectious diseases of the nervous system." Ed. Davies and Kennedy. Butterworth-Heinemann. Oxford. pp321-372.

de Felipe, O'Brien, Palmer, Doyle, Smith, and Hunt (1997) Characterization of the NK1 receptor knockout mouse: Alterations in nociceptive behaviour. *Society for Neuroscience Abstracts* **23**, p 2354.

de Felipe, C., Herrero, J.F., O'Brien, J.A., Palmer, J.A., Doyle, C.A., Smith, A.J.H., Laird, J.M.A., Belmonte, C., Cervero, F., and Hunt, S.P. (1998) Altered nociception,analgiesia and aggression in mice lacking the receptor for substance P. *Nature* **392**, 364-397.

De Giorgio, R., Tazzari, P.L., Barbara, G., Stanghellini, V., and Corinaldesi, R. (1998) Detection of substance P immunoreactivity in human peripheral leukocytes. *Journal of Neuroimmunology* **82**, 175-181.

De Groot, C.J. and Woodroofe, M.N. (2001) The role of chemokines and chemokine receptors in CNS inflammation. *Progress in Brain Research* **132:533-44.**, 533-544.

Decoster, E., Vanhaesebroeck, B., Vandenabeele, P., Grooten, J., and Fiers, W. (1995) Generation and biological characterization of membrane-bound, uncleavable murine tumor necrosis factor. *Journal of Biological Chemistry* **270**, 18473-18478.

Delay-Goyet, P. and Lundberg, J.M. (1991) Cigarette smoke-induced airway oedema is blocked by the NK1 antagonist, CP-96,345. *European Journal of Pharmacology* **203**, 157-158.

Denise, H. and Barrett, M.P. (2001) Uptake and mode of action of drugs used against sleeping sickness. *Biochemical Pharmacology* **61**, 1-5.

Diab, A., Zhu, J., Xiao, B.G., Mustafa, M., and Link, H. (1997) High IL-6 and low IL-10 in the central nervous system are associated with protracted relapsing EAE in DA rats. *Journal of Neuropathology and Experimental Neurology* **56**, 641-650.

Diamant, M., Rieneck, K., Mechti, N., Zhang, X.G., Svenson, M., Bendtzen, K., and Klein, B. (1997) Cloning and expression of an alternatively spliced mRNA encoding a soluble form of the human interleukin-6 signal transducer gp130. *FEBS Lett.* **412**, 379-384.

Dinarello, C.A. (1998) Interleukin-1. In: "The Cytokine Handbook." Ed. Thomson. Academic Press. London. pp35-72.

Dong, Y. and Benveniste, E.N. (2001) Immune function of astrocytes. *Glia* **36**, 180-190.

Doua, F., Boa, F.Y., Schechter, P.J., Miezan, T.E., Diai, D., Sanon, S.R., de Raadt, P., Haegele, K.D., Sjoerdsma, A., and Konian, K. (1987) Treatment of late stage Gambiense trypanosomiasis with alpha-difluoromethylornithine (eflornithine): efficay and tolerance in 14 cases in Cote d'Ivoire. *American Journal of Tropical Medicine and Hygiene* **37**, 525-533.

Dougherty, P.M., Palecek, J., Zorn, S., and Willis, W.D. (1993) Combined application of excitatory amino acids and substance P produces long-lasting changes in responses of primate spinothalamic tract neurons. *Brain Research; Brain Research Reviews* **18**, 227-246.

Eckersall, P.D., Gow, J.W., McComb, C., Bradley, B., Rodgers, J., Murray, M., and Kennedy, P.G. (2001) Cytokines and the acute phase response in post-treatment reactive encephalopathy of *Trypanosoma brucei brucei* infected mice. *Parasitology International* **50**, 15-26.

Edwards, S.W., Tan, C.M., and Limbird, L.E. (2000) Localization of G-protein-coupled receptors in health and disease. *Trends in Pharmacological Science* **21**, 304-308.

Eglezos, A., Giuliani, S., Viti, G., and Maggi, C.A. (1991) Direct evidence that capsaicin-induced plasma protein extravasation is mediated through tachykinin NK1 receptors. *European Journal of Pharmacology* **209**, 277-279.

Einspahr, J.G., Nelson, M.A., Saboda, K., Warneke, J., Bowden, G.T., and Alberts, D.S. (2002) Modulation of biologic endpoints by topical difluoromethylornithine (DFMO), in subjects at high-risk for nonmelanoma skin cancer. *Clinical Cancer Research* **8**, 149-155.

Embelton, M.J. (1998) Reverse transcriptase *in situ* PCR for RNA detection. In: "PCR *In Situ* Hybridization." Ed. Herrington and O'Leary. Oxford University Press. Oxford. pp87-102.

Enanga, B., Burchmore, R.J., Stewart, M.L., and Barrett, M.P. (2002) Sleeping sickness and the brain. *Cellular and Molecular Life Science* **59**, 845-858.

Enanga, B., Keita, M., Chauviere, G., Dumas, M., and Bouteille, B. (1998) Megazol combined with suramin: a chemotherapy regimen which reversed the CNS pathology in a model of human African trypanosomiasis in mice. *Tropical Medicine and International Health* **3**, 736-741.

Eng, L.F., Ghirnikar, R.S., and Lee, Y.L. (1996) Inflammation in EAE: Role of chemokine / cytokine expression by resident and infiltrating cells. *Neurochemical Research* **21**, 511-525.

Eng, L.F., Yu, A.C.H., and Lee, Y.L. (1992) Astrocytic response to injury. *Progress in Brain Research* **94**, 353-365.

Erspamer, V. and Melchiorri, P. (1973) Active polypeptides of the amphibian skin and their synthetic analogues. *Pure Applied Chemistry* **35**, 463-494.

Fan, T.P., Hu, D.E., Guard, S., Gresham, G.A., and Watling, K.J. (1993) Stimulation of angiogenesis by substance P and interleukin-1 in the rat and its inhibition by NK1 or interleukin-1 receptor antagonists. *British Journal of Pharmacology* **110**, 43-49.

Ferguson, T.A., Fletcher, S., Herndon, J., and Griffith, T.S. (1995) Neuropeptides modulate immune deviation induced via the anterior chamber of the eye. *Journal of Immunology* **155**, 1746-1756.

Ferrell, W.R., Lockhart, J.C., and Karimian, S.M. (1997) Tachykinin regulation of basal synovial blood flow. *British Journal of Pharmacology* **121**, 29-34.

Fevre, E.M., Coleman, P.G., Odiit, M., Magona, J.W., Welburn, S.C., and Woolhouse, M.E. (2001) The origins of a new *Trypanosoma brucei rhodesiense* sleeping sickness outbreak in eastern Uganda. *Lancet* **358**, 625-628.

Fink, E. and Schmidt, H. (1979) Meningoencephalitis in chronic *Trypanosoma brucei rhodesiense* infection of the white mouse. *Tropenmedizin und Parasitologie* **30**, 206-211.

Fitzgerald,A.K., O'Neill,L.A.J., Gearing,A.J.H., and Callard,R.E. (2001) The Cytokine Facts Book. Academic Press. London.

Flugel, A. and Bradl, M. (2001) New tools to trace populations of inflammatory cells in the CNS. *Glia* **36**, 125-136.

Gay, F.W., Drye, T.J., Dick, G.W., and Esiri, M.M. (1997) The application of multifactorial cluster analysis in the staging of plaques in early multiple sclerosis. Identification and characterization of the primary demyelinating lesion. *Brain* **120**, 1461-1483.

Gazzinelli, R., Xu, Y., Hieny, S., Cheever, A., and Sher, A. (1992) Simultaneous depletion of CD4+ and CD8+ T lymphocytes is required to reactivate chronic infection with Toxoplasma gondii. *Journal of Immunology* **149**, 175-180.

Geraghty, D.P., Livett, B.G., Rogerson, F.M., and Burcher, E. (1990) A novel substance P binding site in bovine adrenal medulla. *Neuroscience Letters* **112**, 276-281.

Ghoda, L., Phillips, M.A., Bass, K.E., Wang, C.C., and Coffino, P. (1990) Trypanosome ornithine decarboxylase is stable because it lacks sequences found in the carboxyl terminus of the mouse enzyme which target the latter for intracellular degradation. *Journal of Biological Chemistry* **265**, 11823-11826.

Gichuki, C.W., Jennings, F.W., Kennedy, P.G.E., Sommer, I.U., Murray, M., Rodgers, J., and Burke, J.M. (1997) The effect of azathioprine on the neuropathology associated with experimental murine African trypanosomiasis. *Neurological Infections and Epidemiology* **2**, 53-61.

Giffin, B.F., McCann, P.P., Bitonti, A.J., and Bacchi, C.J. (1986) Polyamine depletion following exposure to dl-alpha-difluoromethylornithine both in vivo and in vitro initiates morphological alterations and mitochondrial activation in a monomorphic strain of *Trypanosoma brucei brucei*. *Journal of Protozoology* **33**, 238-243.

Gillet, J., Bone, G., Lowa, P., Charlier, J., Rona, A.M., and Schechter, P.J. (1986) alpha-Difluoromethylornithine induces protective immunity in mice inoculated with *Plasmodium berghei* sporozoites. *Transactions of the Royal Society of Tropical Medical and Hygiene* **80**, 236-239.

Gitter, B.D., Regoli, D., Howbert, J.J., Glasebrook, A.L., and Waters, D.C. (1994) Interleukin-6 secretion from human astrocytoma cells induced by substance P. *Journal of Neuroimmunology* **51**, 101-108.

Glabinski, A.R. and Ransohoff, R.M. (1999a) Chemokines and chemokine receptors in CNS pathology. *Journal of NeuroVirology* **5**, 3-12.

Glabinski, A.R. and Ransohoff, R.M. (1999b) Sentries at the gate: chemokines and the blood-brain barrier. *Journal of NeuroVirology* **5**, 623-634.

Godiska, R., Chantry, D., Dietsch, G.N., and Gray, P.W. (1995) Chemokine expression in murine experimental allergic encephalomyelitis. *Journal of Neuroimmunology* **58**, 167-176.

Goldstein, G.W. and Betz, A.L. (1986) The blood-brain barrier. *Scietific American* **255**, 70-79.

Grau, G.E. and Lou, J.N. (1995) Experimental cerebral malaria: possible new mechanisms in the TNF induced microvascular pathology. *Soz Praventivmed* **40**, 50-57.

Greaves, M.W. and Wall, P.D. (1996) Pathophysiology of itching. *Lancet* **348**, 938-940.

Greeno, E.W., Mantyh, P., Vercellotti, G.M., and Moldow, C.F. (1993) Functional neurokinin 1 receptors for substance P are expressed by human vascular endothelium. *Journal of Experimental Medicine* **177**, 1269-1276.

Greenwood, B.M. and Whittle, H.C. (1980) The pathogenesis of sleeping sickness. *Transactions of the Royal Society of Tropical Medical and Hygiene* **74**, 716-725.

Gutierrez, E.G., Banks, W.A., and Kastin, A.J. (1993) Murine tumor necrosis factor alpha is transported from blood to brain in the mouse. *Journal of Neuroimmunology* **47**, 169-176.

Gwyn, K. and Sinicrope, F.A. (2002) Chemoprevention of colorectal cancer. *American Journal of Gastroenterology* **97**, 13-21.

Hagan, R.M., Beresford, I.J., Stables, J., Dupere, J., Stubbs, C.M., Elliott, P.J., Sheldrick, R.L., Chollet, A., Kawashima, E., McElroy, A.B., and . (1993) Characterisation, CNS distribution and function of NK2 receptors studied using potent NK2 receptor antagonists. *Regulatory Peptides* **46**, 9-19.

Harmar, A.J., Hyde, V., and Chapman, K. (1990) Identification and cDNA sequence of delta-preprotachykinin, a fourth splicing variant of the rat substance P precursor. *FEBS Letters* **275**, 22-24.

Hastrup, H. and Schwartz, T.W. (1996) Septide and neurokinin A are high-affinity ligands on the NK-1 receptor: evidence from homologous versus heterologous binding analysis. *FEBS Letters* **399**, 264-266.

Hayes, R.G., Shaw, C., Chakravarthy, U., and Buchanan, K.D. (1993) Tachykinin-1 gene products in porcine ocular tissues: evidence for transcriptional and post-translational regulation. *Vision Research* **33**, 1477-1480.

Hennig, I.M., Laissue, J.A., Horisberger, U., and Reubi, J.C. (1995) Substance-P receptors in human primary neoplasms: tumoral and vascular localization. *International Journal of Cancer* **61**, 786-792.

Henry, J.L. (1987) Discussions of the nomenclature for tachykinins and tachykinin receptors. In: "Substance P and Neurokinins." Ed. Henry, Couture, Cuello, Pelletier, Quirion, and Regoli. Springer-Verlag. New York. ppxvii-xviii.

Herrero, Laird, de Felipe, Smith, Hunt, and Cervero (1997) Lack of "wind-up" of somatic nociceptive reflexes and persistence of visceral nociception in a NK1 receptor knock-out mouse. *Society for Neuroscience Abstracts* **23**, p 2354.

Hertz, C.J., Filutowicz, H., and Mansfield, J.M. (1998) Resistance to the African trypanosomes is IFN-gamma dependent. *Journal of Immunology* **161**, 6775-6783.

Hesselgesser, J. and Horuk, R. (1999) Chemokine and chemokine receptor expression in the central nervous system. *Journal of NeuroVirology* **5**, 13-26.

Heuillet, E., Menager, J., Fardin, V., Flamand, O., Bock, M., Garret, C., Crespo, A., Fallourd, A.M., and Doble, A. (1993) Characterization of a human NK1 tachykinin receptor in the astrocytoma cell line U 373 MG. *Journal of Neurochemistry* **60**, 868-876.

Hickey, W.F. (2001) Basic principles of immunological surveillance of the normal central nervous system. *Glia* **36**, 118-124.

Hickey, W.F., Hsu, B.L., and Kimura, H. (1991) T-lymphocyte entry into the central nervous system. *Journal of Neuroscience Research* **28**, 254-260.

Hill, K.L., Hutchings, N.R., Grandgenett, P.M., and Donelson, J.E. (2000) T lymphocyte-triggering factor of african trypanosomes is associated with the flagellar fraction of the cytoskeleton and represents a new family of proteins that are present in several divergent eukaryotes. *Journal of Biological Chemistry* **275**, 39369-39378.

Hill, K.L., Hutchings, N.R., Russell, D.G., and Donelson, J.E. (1999) A novel protein targeting domain directs proteins to the anterior cytoplasmic face of the flagellar pocket in African trypanosomes. *Journal of Cell Science* **112**, 3091-3101.

Hirano, T. (1994) Interleukin-6. In: "The Cytokine Handbook." Academic Press. pp145-168.

Hirano, T. (1998) Interleukin-6. In: "The Cytokine Handbook." Ed. Thomson. Academic Press. London. pp197-228.

Ho, W.Z., Cnaan, A., Li, Y.H., Zhao, H., Lee, H.R., Song, L., and Douglas, S.D. (1996) Substance P modulates human immunodeficiency virus replication in human peripheral blood monocyte-derived macrophages. *AIDS Res.Hum.Retroviruses* **12**, 195-198.

Hoare, C.A. (1970) Systematic Description of the Mammalian Trypanosomes of Africa. In: "The African Trypanosomiases." Ed. Mulligan. Allen & Urwin. London. pp24-59.

Hoare, C.A. (1972a) Host Parasite Relationships. In: "The Trypanosomes of Mammals. A Zoological Monograph." Ed. Hoare. Blackwell Scientific Publications. Oxford and Edinburgh. pp107-120.

Hoare, C.A. (1972b) Morphology. In: "The Trypanosomes of Mammals. A Zoological Monograph." Ed. Hoare. Blackwell Scientific Publications. Oxford and Edinburgh. pp6-29.

Hoare, C.A. (1972c) Outline of History. In: "The Trypanosomes of Mammals. A Zoological Monograph." Ed. Hoare. Blackwell Scientific Publications. Oxford and Edinburgh. pp3-5.

Hood, V.C., Cruwys, S.C., Urban, L., and Kidd, B.L. (2000) Differential role of neurokinin receptors in human lymphocyte and monocyte chemotaxis. *Regulatory Peptides* **96**, 17-21.

Hull, M., Lieb, K., and Fiebich, B.L. (2002) Pathways of inflammatory activation in Alzheimer's disease: potential targets for disease modifying drugs. *Current Medical Chemistry* **9**, 83-88.

Hunt, S.P. (2000) Pain control: breaking the circuit. *Trends in Pharmacological Science* **21**, 284-286.

Hunter, C.A., Gow, J.W., Kennedy, P.G., Jennings, F.W., and Murray, M. (1991) Immunopathology of experimental African sleeping sickness: detection of cytokine mRNA in the brains of Trypanosoma brucei brucei-infected mice. *Infection and Immunity* **59**, 4636-4640.

Hunter, C.A., Jennings, F.W., Adams, J.H., Murray, M., and Kennedy, P.G. (1992) Subcurative chemotherapy and fatal post-treatment reactive encephalopathies in African trypanosomiasis. *Lancet* **339**, 956-958.

Hunter, C.A., Jennings, F.W., Kennedy, P.G., and Murray, M. (1992a) Astrocyte activation correlates with cytokine production in central nervous system of *Trypanosoma brucei brucei*-infected mice. *Laboratory Investigation* **67**, 635-642.

Hunter, C.A. and Kennedy, P.G. (1992) Immunopathology in central nervous system human African trypanosomiasis. *Journal of Neuroimmunology* **36**, 91-95.

Hunter, C.A. and Remington, J.S. (1994) Immunopathogenesis of toxoplasmic encephalitis. *The Journal of Infectious Diseases* **170**, 1057-1067.

Hunter, C.A., Roberts, C.W., Murray, M., and Alexander, J. (1992b) Detection of cytokine mRNA in the brains of mice with toxoplasmic encephalitis. *Parasite Immunology* **14**, 405-413.

Hurst, E.W. (1959) The lesions produced in the central nervous system by certain organic arsenical compounds. *Journal of Pathology and Bacteriology* **77**, 523-534.

Ikeda, K., Miyata, K., Orita, A., Kubota, H., Yamada, T., and Tomioka, K. (1995) RP67580, a neurokinin1 receptor antagonist, decreased restraint stress- induced defecation in rat. *Neuroscience Letters* **198**, 103-106.

Inoue, N., Inoue, M., Kuriki, K., Yamaguchi, H., Nagasawa, H., Mikami, T., Fujisaki, K., Suzuki, N., and Hirumi, H. (1999) Interleukin 4 is a crucial cytokine in controlling *Trypanosoma brucei gambiense* infection in mice. *Veterinary Parasitology* **86**, 173-184.

Iten, M., Matovu, E., Brun, R., and Kaminsky, R. (1995) Innate lack of susceptibility of Ugandan *Trypanosoma brucei rhodesiense* to DL-alpha-difluoromethylornithine (DFMO). *Tropical Medicine and Parasitology* **46**, 190-194.

Janeway,C.A. and Travers,P. (1996) Immunobiology; the immune system in health and disease. Ed. Janeway, Charles A. and Traver, Paul. Current Biology Ltd. London.

Jeglinski, W., Skup, M., Zaremba, M., and Oderfeld-Nowak, B. (1996) Difluoromethylornithine counteracts lesion induced astrogliosis in rat hippocampus: enhancement of inhibitory effect by combining treatment with GM1 ganglioside. *Acta Neurobiologiae Experimentalis* **56**, 549-553.

Jenkins, C.G. and Facer, C.A. (1985) Hematology of African Trypanosomiasis. In: "Immunopathology and Pathogenesis of Trypanosomiasis." Ed. Tizard. CRC Press Inc. Boca Raton, Florida. pp13-45.

Jennings, F.W. (1988a) Chemotherapy of trypanosomiasis: the potentiation of melarsoprol by concurrent difluoromethylornithine (DFMO) treatment. *Transactions of the Royal Society of Tropical Medical and Hygiene* **82**, 572-573.

Jennings, F.W. (1988b) The potentiation of arsenicals with difluoromethylornithine (DFMO): experimental studies in murine trypanosomiasis. *Bulletin of the Society of Pathology and Exotics* **81**, 595-607.

Jennings, F.W. (1993) Combination chemotherapy of CNS trypanosomiasis. *Acta Tropica* **54**, 205-213.

Jennings, F.W., Chauviere, G., Viode, C., and Murray, M. (1996) Topical chemotherapy for experimental African trypanosomiasis with cerebral involvement: the use of melarsoprol combined with the 5-nitroimidazole, megazol. *Tropical Medicine and International Health* **1**, 363-366.

Jennings, F.W., Gichuki, C.W., Kennedy, P.G., Rodgers, J., Hunter, C.A., Murray, M., and Burke, J.M. (1997) The role of the polyamine inhibitor eflornithine in the neuropathogenesis of experimental murine African trypanosomiasis. *Neuropathology and Applied Neurobiology* **23**, 225-234.

Jennings, F.W., McNeil, P.E., Ndung'u, J.M., and Murray, M. (1989) Trypanosomiasis and encephalitis: possible aetiology and treatment. *Transactions of the Royal Society of Tropical Medical and Hygiene* **83**, 518-519.

Jennings, F.W., Whitelaw, D.D., Holmes, P.H., Chizyuka, H.G., and Urquhart, G.M. (1979) The brain as a source of relapsing *Trypanosoma brucei* infection in mice after chemotherapy. *International Journal of Parasitology* **9**, 381-384.

John, H.A., Birnstiel, M.L., and Jones, K.W. (1969) RNA-DNA hybrids at the cytological level. *Nature* **223**, 582-587.

Johnson, C.L. and Johnson, C.G. (1992) Characterization of receptors for substance P in human astrocytoma cells: radioligand binding and inositol phosphate formation. *Journal of Neurochemistry* **58**, 471-477.

Julia, V. and Bueno, L. (1997) Tachykininergic mediation of viscerosensitive responses to acute inflammation in rats: role of CGRP. *American Journal of Physiology* **272**, G141-G146.

Julia, V., Morteau, O., and Bueno, L. (1994) Involvement of neurokinin 1 and 2 receptors in viscerosensitive response to rectal distension in rats. *Gastroenterology* **107**, 94-102.

Kaltreider, H.B., Ichikawa, S., Byrd, P.K., Ingram, D.A., Kishiyama, J.L., Sreedharan, S.P., Warnock, M.L., Beck, J.M., and Goetzl, E.J. (1997) Upregulation of neuropeptides and neuropeptide receptors in a murine model of immune inflammation in lung parenchyma. *American Journal of Respiratory Cell and Molecular Biology* **16**, 133-144.

Karpus, W.J. and Kennedy, K.J. (1997) MIP-1alpha and MCP-1 differentially regulate acute and relapsing autoimmune encephalomyelitis as well as Th1/Th2 lymphocyte differentiation. *Journal of Leukocyte Biology* **62**, 681-687.

Karpus, W.J. and Ransohoff, R.M. (1998) Chemokine regulation of experimental autoimmune encephalomyelitis: temporal and spatial expression patterns govern disease pathogenesis. *Journal of Immunology* **161**, 2667-2671.

Kastin, A.J., Pan, W., Maness, L.M., and Banks, W.A. (1999) Peptides crossing the blood-brain barrier: some unusual observations. *Brain Research* **848**, 96-100.

Kaushik, R.S., Uzonna, J.E., Radzioch, D., Gordon, J.R., and Tabel, H. (1999) Innate resistance to experimental *Trypanosoma congolense* infection: differences in IL-10

synthesis by macrophage cell lines from resistant and susceptible inbred mice. *Parasite Immunology* **21**, 119-131.

Kaushik, R.S., Uzonna, J.E., Zhang, Y., Gordon, J.R., and Tabel, H. (2000) Innate resistance to experimental African trypanosomiasis: differences in cytokine (TNF-alpha, IL-6, IL-10 and IL-12) production by bone marrow-derived macrophages from resistant and susceptible mice. *Cytokine* **12**, 1024-1034.

Kavelaars, A., Brocke, D., Jeurissen, F., Kardux, J., Meijer, A., Franklin, R., Gelfand, E.W., and Heijnen, C.J. (1994) Activation of human monocytes via a non-neurokinin substance P receptor that is coupled to Gi protein, calcium, phospholipase D, MAP kinase, and IL-6 production. *Journal of Immunology* **153**, 3691-3699.

Keegan, B.M. and Noseworthy, J.H. (2002) Multiple sclerosis. *Annual Review of Medicine* **53:285-302.**, 285-302.

Kennedy, K.J. and Karpus, W.J. (1999) Role of chemokines in the regulation of Th1/Th2 and autoimmune encephalomyelitis. *Journal of Clinical Immunology* **19**, 273-279.

Kennedy, K.J., Strieter, R.M., Kunkel, S.L., Lukacs, N.W., and Karpus, W.J. (1998) Acute and relapsing experimental autoimmune encephalomyelitis are regulated by differential expression of the CC chemokines macrophage inflammatory protein-1alpha and monocyte chemotactic protein-1. *Journal of Neuroimmunology* **92**, 98-108.

Kennedy, P.G.E. (1993) Overview of HIV in the Nervous System. In: "The Neuropathology of HIV Infection." Ed. Scaravilli. Springer - Verlag Ltd. London. pp259-265.

Kennedy, P.G. (1999) The pathogenesis and modulation of the post-treatment reactive encephalopathy in a mouse model of Human African Trypanosomiasis. *Journal of Neuroimmunology* **100**, 36-41.

Kennedy, P.G., Rodgers, J., Jennings, F.W., Murray, M., Leeman, S.E., and Burke, J.M. (1997) A substance P antagonist, RP-67,580, ameliorates a mouse meningoencephalitic response to *Trypanosoma brucei brucei*. *Proceedings of the National Academy of Sciences of the USA* **94**, 4167-4170.

Kennedy, P.G.E., Rodgers, J., Bradley, B., Hunt, S.P., Gettinby, G., Leeman, S.E., De Felipe, C., and Murray, M. (2003) Clinical and neuroinflammatory responses to meningoencephalitis in substance P receptor knockout mice. *Brain* **In Press**

Kindy, M.S., Hu, Y., and Dempsey, R.J. (1994) Blockade of ornithine decarboxylase enzyme protects against ischemic brain damage. *Journal of Cerebral Blood Flow and Metabolism* **14**, 1040-1045.

Kivisakk, P., Trebst, C., Eckstein, D.J., Kerza-Kwiatecki, A.P., and Ransohoff, R.M. (2001) Chemokine-based therapies for MS: how do we get there from here? *Trends in Immunology* **22** , 591-593.

Kleine (1909) Weitere wisenschaftliche Beobachtungen über die Entwicklung von Trypanosomen in Glossinen. *Deutsche Medizinische Wochenschrift* **21,** p 924.

Kleppe, K., Ohtsuka, E., Kleppe, R., Molineux, I., and Khorana, H.G. (1971) Studies on polynucleotides. XCVI. Repair replications of short synthetic DNA's as catalyzed by DNA polymerases. *Journal of Molecular Biology* **56**, 341-361.

Klinkert, W.E., Kojima, K., Lesslauer, W., Rinner, W., Lassmann, H., and Wekerle, H. (1997) TNF-alpha receptor fusion protein prevents experimental auto-immune encephalomyelitis and demyelination in Lewis rats: an overview. *Journal of Neuroimmunology* **72**, 163-168.

Kohlmann, O., Jr., Cesaretti, M.L., Ginoza, M., Tavares, A., Zanella, M.T., Ribeiro, A.B., Ramos, O.L., Leeman, S.E., Gavras, I., and Gavras, H. (1997) Role of substance P in blood pressure regulation in salt-dependent experimental hypertension. *Hypertension* **29**, 506-509.

Konsman, J.P., Parnet, P., and Dantzer, R. (2002) Cytokine-induced sickness behaviour: mechanisms and implications. *Trends in Neuroscience* **25**, 154-159.

Kostyk, S.K., Kowall, N.W., and Hauser, S.L. (1989) Substance P immunoreactive astrocytes are present in multiple sclerosis plaques. *Brain Research* **504**, 284-288.

Kramer, J.H., Phillips, T.M., and Weglicki, W.B. (1997) Magnesium-deficiency-enhanced post-ischemic myocardial injury is reduced by substance P receptor blockade. *Journal of Molecular and Cellular Cardiology* **29**, 97-110.

Kramer, M.S., Cutler, N., Feighner, J., Shrivastava, R., Carman, J., Sramek, J.J., Reines, S.A., Liu, G., Snavely, D., Wyatt-Knowles, E., Hale, J.J., Mills, S.G., MacCoss, M., Swain, C.J., Harrison, T., Hill, R.G., Hefti, F., Scolnick, E.M., Cascieri, M.A., Chicchi, G.G., Sadowski, S., Williams, A.R., Hewson, L., Smith, D., and Rupniak, N.M. (1998) Distinct mechanism for antidepressant activity by blockade of central substance P receptors. *Science* **281**, 1640-1645.

Krause, J.E., Chirgwin, J.M., Carter, M.S., Xu, Z.S., and Hershey, A.D. (1987) Three rat preprotachykinin mRNAs encode the neuropeptides substance P and neurokinin A. *Proceedings of the National Academy of Sciences of the USA* **84**, 881-885.

Kristjanson, P.M., Swallow, B.M., Rowlands, G.J., Kruska, R.L., and de Leeuw, P.N. (1999) Measuring the costs of African trypanosomiasis, the potential benefits of control and returns to research. *Agricultural Systems* **59**, 79-98.

Krueger, J.M., Fang, J., Taishi, P., Chen, Z., Kushikata, T., and Gardi, J. (1998) Sleep. A physiologic role for IL-1 beta and TNF-alpha. *Annals of the New York Academy of Science* **856**, 148-159.

Krueger, J.M., Obal, F.J., Fang, J., Kubota, T., and Taishi, P. (2001) The role of cytokines in physiological sleep regulation. *Annals of the New York Academy of Science* **933**, 211-221.

Kuzoe, F. (1993) African Trypanosomiasis. In: "Tropical disease research: progress 1991-92. Eleventh programme report of the UNDP/WORLDBANK/WHO Special Programme for Resarch and Training in Tropical Diseases (TDR)." WHO. Geneva. pp57-66.

Lai, J., Zhan, G., Campbell, D.E., Douglas, S.D., and Ho, W. (2000) Detection of substance P and its receptor in human fetal microglia. *Neuroscience* **101**, 1137-1144.

Lai, J.P., Douglas, S.D., Rappaport, E., Wu, J.M., and Ho, W.Z. (1998) Identification of a delta isoform of preprotachykinin mRNA in human mononuclear phagocytes and lymphocytes. *Journal of Neuroimmunology* **91**, 121-128.

Lambert, N., Lescoulie, P.L., Yassine-Diab, B., Enault, G., Mazieres, B., and De Preval, C. (1998) Substance P enhances cytokine-induced vascular cell adhesion molecule-1 (VCAM-1) expression on cultured rheumatoid fibroblast-like synoviocytes. *Clinical and Experimental Immunology* **113**, 269-275.

Lambert, P.H., Berney, M., and Kazyumba, G. (1981) Immune complexes in serum and in cerebrospinal fluid in African trypanosomiasis. Correlation with polyclonal B cell activation and with intracerebral immunoglobulin synthesis. *Journal of Clinical Investigation* **67**, 77-85.

Lassmann, H., Zimprich, F., Rossler, K., and Vass, K. (1991) Inflammation in the nervous system. Basic mechanisms and immunological concepts. *Revue Neurologique* **147**, 763-781.

Laufer, R., Wormser, U., Friedman, Z.Y., Gilon, C., Chorev, M., and Selinger, Z. (1985) Neurokinin B is a preferred agonist for a neuronal substance P receptor and its action is antagonized by enkephalin. *Proceedings of the National Academy of Sciences of the USA* **82**, 7444-7448.

Laurenzi, M.A., Persson, M.A.A., Dalsgaard, C.J., and Ringden, O. (1989) Stimulation of human B lymphocyte differentiation by the neuropeptides Substance P and Neurokinin A. *Scandanavian Journal of Immunology* **30**, 695-701.

Lee, C.-M., Kum, W., Cockram, C.S., Teoh, R., and Young, J.D. (1989) Functional substance P receptors on a human astrocytoma cell line (U-373 MG). *Brain Research* **488**, 328-d331.

Lee, H.-R., Ho, W.-Z., and Douglas, S.D. (1994) Substance P augments tumor necrosis factor release in human monocyte-derived macrophages. *Clinical and Diagnostic Laboratory Immunology* **1**, 419-423.

Leitch,A.R., Schwarzacher,T., Jackson,D., and Leitch,I.J. (1994) *In situ* hybridization: a practical guide. Bios Scientific Publishers Ltd. Oxford.

Lejon, V., Buscher, P., Magnus, E., Moons, A., Wouters, I., and Van Meirvenne, N. (1998) A semi-quantitative ELISA for detection of *Trypanosoma brucei gambiense* specific antibodies in serum and cerebrospinal fluid of sleeping sickness patients. *Acta Tropica* **69**, 151-164.

Lenzlinger, P.M., Morganti-Kossmann, M.C., Laurer, H.L., and McIntosh, T.K. (2001) The duality of the inflammatory response to traumatic brain injury. *Molecular Neurobiology* **24**, 169-181.

Lieberman, A.P., Pitha, P.M., Shin, H.S., and Shin, M.L. (1989) Production of tumor necrosis factor and other cytokines by astrocytes stimulated with lipopolysaccharide or a neurotropic virus. *Proceedings of the National Academy of Sciences of the USA* **86**, 6348-6352.

Lin, R.C.S. (1995) Reactive astrocytes express substance P immunoreactivity in the adult forebrain after injury. *NeuroReport* **7**, 310-312.

Linnik, M.D. and Moskowitz, M.A. (1989) Identification of immunoreactive substance P in human and other mammalian endothelial cells. *Peptides* **10**, 957-962.

Liu, H., Brown, J.L., Jasmin, L., Maggio, J.E., Vigna, S.R., Mantyh, P.W., and Basbaum, A.I. (1994) Synaptic relationship between substance P and the substance P receptor: light and electron microscopic characterization of the mismatch between neuropeptides and their receptors. *Proceedings of the National Academy of Sciences of the USA* **91**, 1009-1013.

Liu, M.K., Cattand, P., Gardiner, I.C., and Pearson, T.W. (1989) Immunodiagnosis of sleeping sickness due to *Trypanosoma brucei gambiense* by detection of antiprocyclic antibodies and trypanosome antigens in patients' sera. *Acta Tropica* **46**, 257-266.

Liu, M.K., Pearson, T.W., Sayer, P.D., Gould, S.S., Waitumbi, J.N., and Njogu, A.R. (1988) Serodiagnosis of African sleeping sickness in vervet monkeys by detection of parasite antigens. *Acta Tropica* **45**, 321-330.

Lotz, M., Vaughan, J.H., and Carson, D.A. (1988) Effect of neuropeptides on production of inflammatory cytokines by human monocytes. *Science* **241**, 1218-1221.

Luber-Narod, J., Kage, R., and Leeman, S.E. (1994) Substance P enhances the secretion of tumor necrosis factor -alpha from neuroglial cells stimulated with lipopolysaccharide. *Journal of Immunology* **152**, 819-824.

Lucas, R., Magez, S., Songa, B., Darji, A., Hamers, R., and de Baetselier, P. (1993) A role for TNF during African trypanosomiasis: involvement in parasite control, immunosuppression and pathology. *Research in Immunology* **144**, 370-376.

Lucey, D.R., Novak, J.M., Polonis, V.R., Liu, Y., and Gartner, S. (1994) Characterization of substance P binding to human monocytes / macrophages. *Clinical and Diagnostic Laboratory Immunology* **1**, 330-335.

Lukkarinen, J.A., Kauppinen, R.A., Grohn, O.H.J., Oja, J.M.E., Sinervirta, R., Jarvinen, A., Alhinen, L.I., and Janne, J. (1998) Neuroprotective role of ornithine decarboxylase activation in transient focal cerebral ischaemia: a study using ornithine decarboxylase overexpressing transgenic rats. *European Journal of Neuroscience* **10**, 2046-2055.

Luo, W., Sharif, T.R., and Sharif, M. (1996) Substance P-induced mitogenesis in human astrocytoma cells correlates with activation of the mitogen-activated protein kinase signaling pathway. *Cancer Research* **56**, 4983-4991.

Ma, Q.P. and Woolf, C.J. (1997) Tachykinin NK1 receptor antagonist RP67580 attenuates progressive hypersensitivity of flexor reflex during experimental inflammation in rats. *European Journal of Pharmacology* **322**, 165-171.

Magez, S., Radwanska, M., Beschin, A., Sekikawa, K., and de Baetselier, P. (1999) Tumor necrosis factor alpha is a key mediator in the regulation of experimental Trypanosoma brucei infections. *Infection and Immunity* **67**, 3128-3132.

Magez, S., Lucas, R., Darji, A., Songa, E.B., Hamers, r., and De Baetselier, P. (1993) Murine tumour necrosis factor plays a protective role during the initial phase of the experimental infection with *Trypanosoma brucei brucei*. *Parasite Immunology* **15**, 635-641.

Maggi, C.A. (1995) The mammalian tachykinin receptors. *General Pharmacology* **26**, 911-944.

Maggi, C.A., Patacchini, R., Perretti, F., Tramontana, M., Manzini, S., Geppetti, P., and Santicioli, P. (1990) Sensory nerves, vascular endothelium and neurogenic relaxation of the guinea-pig isolated pulmonary artery. *Naunyn Schmiedebergs Archives in Pharmacology* **342**, 78-84.

Maggi, C.A. and Schwartz, T.W. (1997) The dual nature of the tachykinin NK1 receptor. *Trends in Pharmacological Science* **18**, 351-355.

Maggioni, C., Carelli, S., Cabibbo, A., Fagioli, C., Fra, A.M., and Sitia, R. (1998) Assembly and secretion of antibodies during B cell development. *Bratisl.Lek.Listy* **99**, 419-425.

Male, D. and Rezaie, P. (2001) Colonisation of the human central nervous system by microglia: the roles of chemokines and vascular adhesion molecules. *Progress in Brain Research* **132:81-93.**, 81-93.

Manni, A., Washington, S., Griffith, J.W., Verderame, M.F., Mauger, D., Demers, L.M., Samant, R.S., and Welch, D.R. (2002) Influence of polyamines on in vitro and in vivo features of aggressive and metastatic behavior by human breast cancer cells. *Clinical and Experimental Metastasis* **19**, 95-105.

Mantyh, C.R., Vigna, S.R., Bollinger, R.R., Mantyh, P.W., Maggio, J.E., and Pappas, T.N. (1995) Differential expression of substance P receptors in patients with Crohn's disease and ulcerative colitis. *Gastroenterology* **109**, 850-860.

Mantyh, C.R., Gates, T.S., Zimmerman, R.P., Welton, M.L., Passaro, E.P., Vigna, S.R., Maggio, J.E., Kruger, L., and Mantyh, P.W. (1988) Receptor binding sites for substance P, but not substance K or neuromedin K, are expressed in high concentrations by arterioles,venules and lymph nodules in surgical specimens obtained from patients with ulcerative colitis and Crohn disease. *Proceedings of the National Academy of Sciences of the USA* **85**, 3235-3239.

Mantyh, P.W., Allen, C.J., Ghilardi, J.R., Rogers, S.D., Mantyh, C.R., Liu, H., Basbaum, A.I., Vigna, S.R., and Maggio, J.E. (1995) Rapid endocytosis of a G protein-coupled receptor: substance P evoked internalization of its receptor in the rat striatum in vivo. *Proceedings of the National Academy of Sciences of the USA* **92**, 2622-2626.

Mantyh, P.W., DeMaster, E., Malhotra, A., Ghilardi, J.R., Rogers, S.D., Mantyh, C.R., Liu, H., Basbaum, A.I., Vigna, S.R., and Maggio, J.E. (1995) Receptor endocytosis and dendrite reshaping in spinal neurons after somatosensory stimulation. *Science* **268**, 1629-1632.

Mantyh, P.W., Rogers, S.D., Honore, P., Allen, B.J., Ghilardi, J.R., Li, J., Daughters, R.S., Lappi, D.A., Wiley, R.G., and Simone, D.A. (1997) Inhibition of hyperalgesia by ablation of lamina I spinal neurons expressing the substance P receptor. *Science* **278**, 275-279.

Mantyh, P.W., Johnson, D.J., Boehmer, C.G., Catton, M.D., Vinters, H.V., Maggio, J.E., Too, H.-P., and Vigna, S.R. (1989) Substance P receptor binding sites are expressed by glia in vivo after neuronal injury. *Proceedings of the National Academy of Sciences of the USA* **86**, 5193-5197.

Marriott, D.R. and Wilkin, G.P. (1993) Substance P receptors on O-2A progenitor cells and type-2 astrocytes in vitro. *Journal of Neurochemistry* **61**, 826-834.

Marriott, D.R., Wilkin, G.P., and Wood, J.N. (1991) Substance P-induced release of prostaglandins from astrocytes: regional specialisation and correlation with phosphoinositol metabolism. *Journal of Neurochemistry* **56**, 259-265.

Martin, F.C., Anton, P.A., Gornbein, J.A., Shanahan, F., and Merrill, J.E. (1993) Production of interleukin-1 by microglia in response to substance P: role for non-classical NK-1 receptor. *Journal of Neuroimmunology* **42**, 53-60.

Martiney, J.A., Cuff, C., Litwak, M., and Berman, J. (1998) Cytokine induced inflammation in the central nervous system revisited. *Neurochemical Research* **23**, 349-359.

Marz, P., Cheng, J.G., Gadient, R.A., Patterson, P.H., Stoyan, T., Otten, U., and Rose-John, S. (1998) Sympathetic neurons can produce and respond to interleukin 6. *Proceedings of the National Academy of Sciences of the USA* **95**, 3251-3256.

Matyszak, M.K. (1998) Inflammation in the CNS: balance between immunological privilege and immune responses. *Progress in Neurobiology* **56**, 19-35.

McCarson, K.E. and Krause, J.E. (1996) The neurokinin-1 receptor antagonist LY306,740 blocks nociception- induced increases in dorsal horn neurokinin-1 receptor gene expression. *Molecular Pharmacology* **50**, 1189-1199.

McDermott, M.F. (2001) TNF and TNFR biology in health and disease. *Cell Molecular Biology* **47**, 619-635.

McGillis, J.P., Organist, M.I., and Payan, D.G. (1987) Substance P and immunoregulation. *Federation Proceedings* **46**, 196-199.

McMenamin, P.G. (1999) Distribution and phenotype of dendritic cells and resident tissue macrophages in the dura mater, leptomeninges, and choroid plexus of the rat brain as demonstrated in wholemount preparations. *Journal of Comparative Neurology* **405**, 553-562.

McNamara, J.J., Bailey, J.W., Smith, D.H., Wakhooli, S., and Godfrey, D.G. (1995) Isolation of *Trypanosoma brucei gambiense* from northern Uganda: evaluation of the kit for in vitro isolation (KIVI) in an epidemic focus. *Transactions of the Royal Society of Tropical Medical and Hygiene* **89**, 388-389.

Medana, I.M., Chaudhri, G., Chan-Ling, T., and Hunt, N.H. (2001) Central nervous system in cerebral malaria: 'Innocent bystander' or active participant in the induction of immunopathology? *Immunology and Cell Biology* **79**, 101-120.

Meinl, E., Aloisi, F., Ertl, B., Weber, F., de Waal Malefyt, R., Wekerle, H., and Hohlfeld, R. (1994) Multiple sclerosis: Immunomodulatory effects of human astrocytes on t cells. *Brain* **117**, 1323-1332.

Merrill, J.E. and Benveniste, E.N. (1996) Cytokines in inflammatory brain lesions:helpful and harmful. *Trends in Neuroscience* **19**, 331-338.

Mertens, B., Taylor, K., Muriuki, C., and Rocchi, M. (1999) Cytokine mRNA profiles in trypanotolerant and trypanosusceptible cattle infected with the protozoan parasite

Trypanosoma congolense: protective role for interleukin-4? *Journal of Interferon and Cytokine Research* **19**, 59-65.

Molyneux, D.H., Pentreath, V., and Doua, F. (1996) African trypanosomiasis in man. In: "Manson's Tropical Diseases." Ed. Cook. W.B.Saunders Company Ltd. London. pp1171-1196.

Montgomery, D.L. (1994) Astrocytes: Form,function and roles in disease. *Veterinary Pathology* **31** , 145-167.

Morrison, W.I., Murray, M., and McIntyre, W.I.M. (1981) Bovine trypanosomiasis. In: "Current Topics in Veterinary Medicine and Animal Science Vol 6." Ed. Ristic and McIntyre. Martinus Nijhoff. pp469-497.

Morrison, W.I., Murray, M., and Sayer, P.D. (1997) The pathogenesis of tissue lesions in *Trypanosoma brucei* infections. In: "Pathogenicity of trypanosomes." Ed. Losos and Chouinard. IDRC No.132e. pp171-177.

Morrison, W.I., Murray, M., Whitelaw, D.D., and Sayer, P.D. (1983) Pathology of infection with *Trypanosoma brucei*: disease syndromes in dogs and cattle resulting from severe tissue damage. *Contributions to Microbiology and Immunology* **7**, 103-119.

Mosmann, T.R. and Sad, S. (1996) The expanding universe of T-cell subsets: Th1, Th2 and more [see comments]. *Immunology Today* **17**, 138-146.

Mousli, M., Bronner, C., Landry, Y., Bockaert, J., and Rouot, B. (1990a) Direct activation of GTP-binding regulatory proteins (G-proteins) by substance P and compound 48/80. *FEBS Lett.* **259**, 260-262.

Mousli, M., Bueb, J.L., Bronner, C., Rouot, B., and Landry, Y. (1990b) G protein activation: a receptor-independent mode of action for cationic amphiphilic neuropeptides and venom peptides. *Trends in Pharmacological Science* **11**, 358-362.

Mucke, L. and Eddleston, M. (1993) Astrocytes in infectious and immune-mediated diseases of the central nervous system. *FASEB J.* **7**, 1226-1232.

Mulenga, C., Mhlanga, J.D., Kristensson, K., and Robertson, B. (2001) *Trypanosoma brucei brucei* crosses the blood-brain barrier while tight junction proteins are preserved in a rat chronic disease model. *Neuropathology and Applied Neurobiology* **27**, 77-85.

Muller, U. (1999) Ten years of gene targeting: targeted mouse mutants, from vector design to phenotype analysis. *Mechanisms of Development* **82**, 3-21.

Mullis, K.B. and Faloona, F.A. (1987) Specific synthesis of DNA in vitro via a polymerase-catalyzed chain reaction. *Methods in Enzymology* **155:335-50.**, 335-350.

Murray, M. (1974) The pathology of African trypanosomiases. *Progress in Immunology* **4**, 181-192.

Murray, M. and Dexter, T.M. (1988) Anaemia in bovine African trypanosomiasis. A review. *Acta Tropica* **45**, 389-432.

Murray, M. and Trail, J.C. (1987) Comparative epidemiology and control of trypanosomes. *International Journal of Parasitology* **17**, 621-627.

Murray, M., Trail, J.C., Davis, C.E., and Black, S.J. (1984) Genetic resistance to African Trypanosomiasis. *The Journal of Infectious Diseases* **149**, 311-319.

Murray, M. and Njogu, A.R. (1989) African trypanosomiasis in wild and domestic ugulates: the problem and its control. *Symposium of Zoology Society of London* **61**, 217-240.

Murray, P.D., McGavern, D.B., Lin, X., Njenga, M.K., Leibowitz, J., Pease, L.R., and Rodriguez, M. (1998) Perforin-dependent neurologic injury in a viral model of multiple sclerosis. *Journal of Neuroscience* **18**, 7306-7314.

Murtra, P., Sheasby, A.M., Hunt, S.P., and de Felipe, C. (2000) Rewarding effects of opiates are absent in mice lacking the receptor for substance P. *Nature* **405**, 180-183.

Nagano, I., Nakamura, S., Yoshioka, M., Onodera, J., Kogure, K., and Itoyama, Y. (1994) Expression of cytokines in brain lesions in subacute sclerosing panencephalitis. *Neurology* **44**, 710-715.

Nair, M.P. and Schwartz, S.A. (1995) Substance P induces tumor necrosis factor in an ex vivo model system. *Cellular Immunology* **166**, 286-290.

Nakagawa, N., Sano, H., and Iwamoto, I. (1995) Substance P induces the expression of intercellular adhesion molecule-1 on vascular endothelial cells and enhances neutrophil transendothelial migration. *Peptides* **16**, 721-725.

Nakajima, K. and Kohsaka, S. (2001) Microglia: activation and their significance in the central nervous system. *Journal of Biochemistry (Tokyo)* **130**, 169-175.

Nakaya, Y., Kaneko, T., Shigemoto, R., Nakanishi, S., and Mizuno, N. (1994) Immunohistochemical localization of substance p receptor in the central nervous system of the adult rat. *Journal of Comparative Neurology* **347**, 249-274.

Nantulya, V.M., Doua, F., and Molisho, S. (1992) Diagnosis of *Trypanosoma brucei gambiense* sleeping sickness using an antigen detection enzyme-linked immunosorbent assay. *Transactions of the Royal Society of Tropical Medical and Hygiene* **86**, 42-45.

Nantulya, V.M., Lindqvist, K.J., Stevenson, P., and Mwangi, E.K. (1992) Application of a monoclonal antibody-based antigen detection enzyme-linked immunosorbent assay (antigen ELISA) for field diagnosis of bovine trypanosomiasis at Nguruman, Kenya. *Annals of Tropical Medicine and Parasitology* **86**, 225-230.

Nawa, H., Kotani, H., and Nakanishi, S. (1984) Tissue-specific generation of two preprotachykinin mRNAs from one gene by alternative RNA splicing. *Nature* **312**, 729-734.

Norton, W.T., Aquino, D.A., Hozumi, I., Chiu, F.C., and Brosnan, C.F. (1992) Quantitative aspects of reactive gliosis: a review. *Neurochemical Research* **17**, 877-885.

O'Callaghan, J.P. and Seidler, F.J. (1992) 1-methyl-4-phenyl-1,2,3,6-tetrahydropyridine (MPTP) induced astogliosis does not require activation of ornithine decarboxylase. *Neuroscience Letters* **148**, 105-108.

O'Leary, J.J. (1998) PCR *in situ* hybridization (PCR ISH). In: "PCR *In Situ* Hybridization." Ed. Herrington and O'Leary. Oxford University Press. Oxford. pp53-86.

Ogonowski, A.A., May, S.W., Moore, A.B., Barrett, L.T., O'Bryant, C.L., and Pollock, S.H. (1997) Antiinflammatory and analgesic activity of an inhibitor of neuropeptide amidation. *The Journal of Pharmacology and Experimental Therapeutics* **280**, 846-853.

Okomo-Assoumou, M.C., Daulouede, S., Lemesre, J.L., N'Zila-Mouanda, A., and Vincendeau, P. (1995) Correlation of high serum levels of tumor necrosis factor-alpha with disease severity in human African trypanosomiasis. *American Journal of Tropical Medicine and Hygiene* **53**, 539-543.

Oldham, C.D., Li, C., Girard, P.R., Nerem, R.M., and May, S.W. (1992) Peptide amidating enzymes are present in cultured endothelial cells. *Biochemical and Biophysical Research Communications* **184**, 323-329.

Olsson, T., Bakhiet, M., Edlund, C., Hojeberg, Bo., Van der Meide, P.H., and Kristensson, K. (1991) Bidirectional activating signals between *Trypanosoma brucei* and CD8+ t-cells: a trypanosome released factor triggers interferon-gamma production that stimulates parasite growth. *European Journal Of Immunology* **21**, 2447-2454.

Opp, M.R. and Krueger, J.M. (1991) Interleukin 1-receptor antagonist blocks interleukin 1-induced sleep and fever. *American Journal of Physiology* **260**, R453-R457.

Oppenheim, J.J. and Saklatvala, J. (1993) Cytokines and their receptors. In: "Clinical Applications of Cytokines." Ed. Oppenheim, Rossio, and Gearing. Oxford University Press. New York. pp3-15.

Ormerod, W.E. (1970) Pathogenesis and pathology of trypanosomiases in man. In: "The African Trypanosomiases." Ed. Mulligan. Allen & Urwin. London. pp587-601.

Pan, W. and Kastin, A.J. (1999) Penetration of neurotrophins and cytokines across the blood-brain/blood- spinal cord barrier. *Advances in Drug Delivery Reviews* **36**, 291-298.

Pan, W., Kastin, A.J., Bell, R.L., and Olson, R.D. (1999) Upregulation of tumor necrosis factor alpha transport across the blood-brain barrier after acute compressive spinal cord injury. *Journal of Neuroscience* **19**, 3649-3655.

Pan, W., Zadina, J.E., Harlan, R.E., Weber, J.T., Banks, W.A., and Kastin, A.J. (1997) Tumor necrosis factor-alpha: a neuromodulator in the CNS. *Neuroscience and Biobehavioural Reviews* **21**, 603-613.

Panet, A. and Khorana, H.G. (1974) Studies on polynucleotides. The linkage of deoxyribopolynucleotide templates to cellulose and its use in their replication. *Journal of Biological Chemistry* **249** , 5213-5221.

Pardue, M.L. and Gall, J.G. (1969) Molecular hybridization of radioactive DNA to the DNA of cytological preparations. *Proceedings of the National Academy of Sciences of the U.S.A* **64**, 600-604.

Parsons, A.M., Honda, C.N., Jia, Y.P., Budai, D., Xu, X.J., Wiesenfeld-Hallin, Z., and Seybold, V.S. (1996) Spinal NK1 receptors contribute to the increased excitability of the nociceptive flexor reflex during persistent peripheral inflammation. *Brain Research* **739**, 263-275.

Patacchini, R. and Maggi, C.A. (1995) Tachykinin NK1 receptors mediate both vasoconstrictor and vasodilator responses in the rabbit isolated jugular vein. *European Journal of Pharmacology* **283**, 233-240.

Pentreath, V.W., Baugh, P.J., and Lavin, D.R. (1994) Sleeping sickness and the central nervous system. *Onderstepoort Journal of Veterinary Research* **6**, 369-377.

Pepin, J. and Milord, F. (1991) African trypanosomiasis and drug-induced encephalopathy: risk factors and pathogenesis. *Transactions of the Royal Society of Tropical Medical and Hygiene* **85**, 222-224.

Pepin, J., Milord, F., Meurice, F., Ethier, L., Loko, L., and Mpia, B. (1992) High-dose nifurtimox for arseno-resistant *Trypanosoma brucei gambiense* sleeping sickness: an open trial in central Zaire. *Transactions of the Royal Society of Tropical Medical and Hygiene* **86**, 254-256.

Pepin, J., Milord, F., Mpia, B., Meurice, F., Ethier, L., DeGroof, D., and Bruneel, H. (1989) An open clinical trial of nifurtimox for arseno-resistant *Trypanosoma brucei gambiense* sleeping sickness in central Zaire. *Transactions of the Royal Society of Tropical Medical and Hygiene* **83**, 514-517.

Philip, K.A., Dascombe, M.J., Fraser, P.A., and Pentreath, V.W. (1994) Blood-brain barrier damage in experimental African trypanosomiasis. *Annals of Tropical Medicine and Parasitology* **88**, 607-616.

Plimmer and Bradford (1895) A preliminary note on the morphology and distribution of the organism found in the tsetse fly disease. *Proceedings of the Royal Society B* **65**, p 274.

Polak,J.M. and McGee,J.O. (1991) *In situ* hybridization; principles and practice. Ed. Polak, J. M. and McGee, James O'D. Oxford University Press. Oxford.

Polak,J.M. and Van Noorden,S. (1986) Immunocytochemistry; modern methods and applications. Ed. Polak, Julia M. and Van Noorden, Susan. John Wright & Sons. Bristol.

Poltera, A.A. (1980) Immunopathological and chemotherapeutic studies in experimental trypanosomiaisis with special reference to the heart and brain. *Transactions of the Royal Society of Tropical Medical and Hygiene* **74**, 706-715.

Poltera, A.A., Hochmann, A., and Lambert, P.H. (1982) *Trypanosoma brucei gambiense:* cerebral immunopathology in mice. *Acta Tropica* **39**, 205-218.

Poltera, A.A., Sayer, P.D., Brighouse, G., Bovell, D., and Rudin, W. (1985) Immunopathological aspects of trypanosomal meningoencephalitis in vervet monkeys after relapse following Berenil treatment. *Transactions of the Royal Society of Tropical Medical and Hygiene* **79**, 527-531.

Pompei, P., Severini, R., Costa, G., Massi, M., Fattoretti, P., and Bertoni-Freddari, C. (1999) In situ hybridization analysis of preprotachykinin-A mRNA levels in young and old rats. *Brain Research; Molecular Brain Research* **64**, 132-136.

Pothoulakis, C., Castagliuolo, I., LaMont, J.T., Jaffer, A., O'Keane, J.C., Snider, R.M., and Leeman, S.E. (1994) CP-96,345, a substance P antagonist inhibits rat intestinal responses to *Clostridium difficile* toxin A but not cholera toxin. *Proceedings of the National Academy of Sciences of the USA* **91**, 947-951.

Prat, A., Biernacki, K., Wosik, K., and Antel, J.P. (2001) Glial cell influence on the human blood-brain barrier. *Glia* **36**, 145-155.

Quan, N., Mhlanga, J.D., Whiteside, M.B., Kristensson, K., and Herkenham, M. (2000) Chronic sodium salicylate treatment exacerbates brain neurodegeneration in rats infected with *Trypanosoma brucei*. *Neuroscience* **96**, 181-194.

Quartara, L. and Maggi, C.A. (1997) The tachykinin NK1 receptor. Part I: ligands and mechanisms of cellular activation. *Neuropeptides* **31**, 537-563.

Randic, M., Hecimovic, H., and Ryu, P.D. (1990) Substance P modulates glutamate-induced currents in acutely isolated rat spinal dorsal horn neurones. *Neuroscience Letters* **117**, 74-80.

Rausch, D.M. and Davis, M.R. (2001) HIV in the CNS: Pathogenic relationships to systemic HIV disease and other CNS diseases. *Journal of NeuroVirology* **7**, 85-96.

Reddix, R.A. and Cooke, H.J. (1992) Neurokinin 1 receptors mediate substance P-induced changes in ion transport in guinea-pig ileum. *Regulatory Peptides* **39**, 215-225.

Risau, W. (1994) Molecular biology of blood-brain barrier ontogenesis and function. *Acta Neurochirurgica* **60(Suppl.)**, 109-112.

Rogers, D.F., Aursudkij, B., and Barnes, P.J. (1989) Effects of tachykinins on mucus secretion in human bronchi in vitro. *European Journal of Pharmacology* **174**, 283-286.

Roitt,I., Brostoff,J., and Male,D. (2001) Immunology. Ed. Roitt, Ivan, Brostoff, Jonathan, and Male, David. Harcourt Publishers Ltd. Edinburgh.

Rollins, B.J. (1997) Chemokines. *Blood* **90**, 909-928.

Ross, C.A. and Sutherland, D.V. (1997) Drug resistance in trypanosomatids. In: "Trypanosomiasis and Leishmaniasis. Biology and Control." Ed. Hide, Mottram, Coombs, and Holmes. CAB International. Oxford. pp259-269.

Rothwell, N.J. and Luheshi, G.N. (2000) Interleukin 1 in the brain: biology, pathology and therapeutic target. *Trends in Neuroscience* **23**, 618-625.

Rupniak, N.M., Carlson, E., Boyce, S., Webb, J.K., and Hill, R.G. (1996) Enantioselective inhibition of the formalin paw late phase by the NK1 receptor antagonist L-733,060 in gerbils. *Pain* **67**, 189-195.

Saito, R., Konishi, H., Takano, Y., Nonaka, S., Sakaguchi, K., Shimohigashi, Y., and Kamiya, H. (1990) Characterization of tachykinin receptors in endothelial cells of porcine artery. *Neuroscience Letters* **110**, 337-342.

Santoni, G., Perfumi, M.C., Spreghini, E., Romagnoli, S., and Piccoli, M. (1999) Neurokinin type-1 receptor antagonist inhibits enhancement of t-cell functions by substance P in normal and neuromanipulated capsaicin-treated rats. *Journal of Neuroimmunology* **93**, 15-25.

Saria, A. (1999) The tachykinin NK1 receptor in the brain: pharmacology and putative functions. *European Journal of Pharmacology* **375**, 51-60.

Schall, T.J., Bacon, K., Camp, R.D., Kaspari, J.W., and Goeddel, D.V. (1993) Human macrophage inflammatory protein alpha (MIP-1 alpha) and MIP-1 beta chemokines attract distinct populations of lymphocytes. *Journal of Experimental Medicine* **177**, 1821-1826.

Schall, T.J. (1994) The Chemokines. In: "The Cytokine Handbook." Academic Press. pp419-460.

Schechter, P.J., Barlow, J.L.R., and Sjoerdsma, A. (1987) Clinical aspects of ornithine decarboxylase with emphasis on therapeutic trials of eflornithine (DFMO) in cancer and protozoal diseases. In: "Inhibition of polyamine metabolism. Biological significance and basis for new therapies." Ed. McCann, Pegg, and Sjoerdsma. Academic Press. London. pp345-364.

Scheerens, H., Buckley, T.L., Muis, T., Van Loveren, H., and Nijkamp, F.P. (1996) The involvement of sensory neuropeptides in toluene diisocyanate- induced tracheal hyperreactivity in the mouse airways. *British Journal of Pharmacology* **119**, 1665-1671.

Schmidt, H. (1983) The pathogenesis of trypanosomiasis of the CNS. Studies on parasitological and neurohistological findings in trypanosoma rhodesiense infected vervet monkeys. *Virchows Arch.A -Pathological Anatomy and Histopathology* **399**, 333-343.

Schneider, A., McNally, K.P., and Agabian, N. (1993) Splicing and 3'-processing of the tyrosine tRNA of Trypanosoma brucei. *J.Biol.Chem.* **268**, 21868-21874.

Schultzberg, M., Ambatsis, M., Samuelsson, E.B., Kristensson, K., and Van Meirvenne, N. (1988) Spread of *Trypanosoma brucei* to the nervous system: early attack on circumventricular organs and sensory ganglia. *Journal of Neuroscience Research* **21**, 56-61.

Serra, M.C., Calzetti, F., Ceska, M., and Cassatella, M.A. (1994) Effect of substance P on superoxide anion and IL-8 production by human PMNL. *Immunology* **82**, 63-69.

Sharafeldin, A., Eltayeb, R., Pashenkov, M., and Bakhiet, M. (2000) Chemokines are produced in the brain early during the course of experimental African trypanosomiasis. *Journal of Neuroimmunology* **103**, 165-170.

Shenenberger, D.W. and Utecht, L.M. (2002) Removal of unwanted facial hair. *American Family Physician* **66** , 1907-1911.

Shi, S.R., Cote, R.J., and Taylor, C.R. (2001) Antigen retrieval techniques: current perspectives. *The Journal of Histochemistry and Cytochemistry* **49**, 931-937.

Shirahase, H., Kanda, M., Kurahashi, K., Nakamura, S., Usui, H., and Shimizu, Y. (1995) Endothelium-dependent contraction in intrapulmonary arteries: mediation by endothelial NK1 receptors and TXA2. *British Journal of Pharmacology* **115**, 1215-1220.

Shrikant, P. and Benveniste, E.N. (1996) The central nervous system as an immunocompetent organ: role of glial cells in antigen presentation. *Journal of Immunology* **157**, 1819-1822.

Simarro, P.P. and Asumu, P.N. (1996) Gambian trypanosomiasis and synergism between melarsoprol and eflornithine: first case report. *Transactions of the Royal Society of Tropical Medical and Hygiene* **90**, 315-

Simpson, L. and Shaw, J. (1989) RNA editing and the mitochondrial cryptogenes of kinetoplastid protozoa. *Cell* **57**, 355-366.

Sjoerdsma, A. and Schechter, P.J. (1999) Eflornithine for African sleeping sickness. *Lancet* **354** , 254-254.

Sly, L.M., Krzesicki, R.F., Brashler, J.R., Buhl, A.E., McKinley, D.D., Carter, D.B., and Chin, J.E. (2001) Endogenous brain cytokine mRNA and inflammatory responses to lipopolysaccharide are elevated in the Tg2576 transgenic mouse model of Alzheimer's disease. *Brain Research Bulletin* **56**, 581-588.

Spector, R. and Johanson, C.E. (1989) The mammalian choroid plexus. *Scientific American* **November**, 48-53.

Stanisz, A.M., Scicchitano, R., Danzin, P., Bienenstock, J., and Payan, D.G. (1987) Distribution of substance P receptors on murine spleen and peyer's patch t and b cells. *Journal of Immunology* **139**, 749-754.

Sternini, C., Su, D., Gamp, P.D., and Bunnett, N.W. (1995) Cellular sites of expression of the neurokinin-1 receptor in the rat gastrointestinal tract. *Journal of Comparative Neurology* **358**, 531-540.

Stoll, G., Jander, S., and Schroeter, M. (2000) Cytokines in CNS disorders: neurotoxicity versus neuroprotection. *Journal of Neural Transmission Supplement* **59**, 81-89.

Streit, W.J. and Kincaid-Colton, C.A. (1995) The brain's immune system. *Scientific American* **November**, 38-43.

Stucky, C.L., Galeazza, M.T., and Seybold, V.S. (1993) Time-dependent changes in Bolton-Hunter-labeled 125I-substance P binding in rat spinal cord following unilateral adjuvant-induced peripheral inflammation. *Neuroscience* **57**, 397-409.

Svendsen, C.N. (2002) Neurobiology: The amazing astrocyte. *Nature* **417**, 29-32.

Szelenyi, J. (2001) Cytokines and the central nervous system. *Brain Research Bulletin* **54**, 329-338.

Taelman, H., Clerinx, J., Bogaerts, J., and Vervoort, T. (1996) Combination treatment with suramin and eflornithine in late stage rhodesian trypanosomiasis: case report. *Transactions of the Royal Society of Tropical Medical and Hygiene* **90**, 572-573.

Tilders, F.J., DeRijk, R.H., Van Dam, A.M., Vincent, V.A., Schotanus, K., and Persoons, J.H. (1994) Activation of the hypothalamus-pituitary-adrenal axis by bacterial endotoxins: routes and intermediate signals. *Psychoneuroendocrinology* **19**, 209-232.

Too, H.P., Cordova, J.L., and Maggio, J.E. (1989) A novel radioimmunoassay for neuromedin K. I. Absence of neuromedin K- like immunoreactivity in guinea pig ileum and urinary bladder. II. Heterogeneity of tachykinins in guinea pig tissues. *Regulatory Peptides* **26**, 93-105.

Tringali, G., Dello, R.C., Preziosi, P., and Navarra, P. (2000) Interleukin-1 in the central nervous system: from physiology to pathology. *Therapie* **55**, 171-175.

Truc, P., Bailey, J.W., Doua, F., Laveissiere, C., and Godfrey, D.G. (1994) A comparison of parasitological methods for the diagnosis of gambian trypanosomiasis in an area of low endemicity in Cote d'Ivoire. *Transactions of the Royal Society of Tropical Medical and Hygiene* **88**, 419-421.

Tuomanen, E. (1996) Entry of pathogens into the central nervous system. *FEMS Microbiology Reviews* **18**, 289-299.

Tyor, W.R., Glass, J.D., Griffin, J.W., Becker, P.S., McArthur, J.C., Bezman, L., and Griffin, D.E. (1992) Cytokine expression in the brain during the acquired immunodeficiency syndrome. *Annals of Neurology* **31**, 349-360.

Ustinova, E.E., Bergren, D., and Schultz, H.D. (1995) Neuropeptide depletion impairs postischemic recovery of the isolated rat heart: role of substance P. *Cardiovascular Research* **30**, 55-63.

Uzonna, J.E., Kaushik, R.S., Gordon, J.R., and Tabel, H. (1998) Experimental murine *Trypanosoma congolense* infections. I. Administration of anti-IFN-gamma antibodies alters trypanosome- susceptible mice to a resistant-like phenotype. *Journal of Immunology* **161**, 5507-5515.

Vaddi,K., Keller,M., and Newton,R.C. (1997) The chemokine facts book. Ed. Vaddi, Krishna, Keller, Margaret, and Newton, Robert C. Academic Press. London.

Vaidya, B.T., Bakhiet, M., Hill, K.L., Olsson, T., Kristensson, K., and Donelson, J.E. (1997) The gene for T lymphocyte triggering factor from African trypanosomes. *Journal of Experimental Medicine* **186**, 433-438.

Van Bogaert, I. and Haemers, A. (1989) Eflornithine: A new drug in the treatment of sleeping sickness. *Pharmaceutisch Weekblad Scientific edition* **11**, 69-75.

Van Nieuwenhove, S., Schechter, P.J., Declercq, J., Bone, G., Burke, J., and Sjoerdsma, A. (1985) Treatment of gambiense sleeping sickness in the Sudan with oral DFMO (DL-alpha-difluoromethylornithine), an inhibitor of ornithine decarboxylase; first field trial. *Transactions of the Royal Society of Tropical Medical and Hygiene* **79**, 692-698.

Van Noorden, S. (1986) Tissue preparation and immunostaining techniques for light microscopy. In: "Immunocytochemistry; modern methods and applications." Ed. Polak and Van Noorden. John Wright & Sons Ltd. Bristol. pp26-53.

Vickerman, K. (1997) Landmarks in Trypanosome Research. In: "Trypanosomiasis and Leishmaniasis; Biology and Control." Ed. Hide, Mottram, Coombs, and Holmes. CAB International. Oxford. pp1-37.

Vishwanath, R. and Mukherjee, R. (1996) Substance P promotes lymphocyte-endothelial cell adhesion preferentially via LFA-1/ICAM-1 interactions. *Journal of Neuroimmunology* **71**, 163-171.

von Euler, U.S. and Gaddum, J.H. (1931) An unidentified depressor substance in certain tissue extracts. *Journal of Physiology (London)* **72**, 74-86.

Wagner, F., Fink, R., Hart, R., and Dancygier, H. (1987) Substance P enhances interferon-gamma production by human peripheral blood mononuclear cells. *Regulatory Peptides* **19**, 355-364.

Wakelin, D. (1996) African trypanosomes. Antigenic variation. In: "Immunity to parasites: How parasitic infections are controlled." Ed. Wakelin. Cambridge University Press. Cambridge. pp83-97.

Walsh, D.A., Hu, D.E., Mapp, P.I., Polak, J.M., Blake, D.R., and Fan, T.P. (1996) Innervation and neurokinin receptors during angiogenesis in the rat sponge granuloma. *Histochemical Journal* **28**, 759-769.

Walsh, D.A., Salmon, M., Featherstone, R., Wharton, J., Church, M.K., and Polak, J.M. (1994) Differences in the distribution and characteristics of tachykinin NK1 binding sites between human and guinea pig lung. *British Journal of Pharmacology* **113**, 1407-1415.

Walsh, R.J., Weglicki, W.B., and Correa-de-Araujo, R. (1996) Distribution of specific substance P binding sites in the heart and adjacent great vessels of the Wistar white rat. *Cell and Tissue Research* **284**, 495-500.

Wang, C.C. (1988) Biochemical approaches to chemotherapy of trypanosomiasis. *Memorias do Insitituto Oswaldo Cruz* **suppl.1 83**, 291-300.

Wang, J., Asensio, V.C., and Campbell, I.L. (2002) Cytokines and chemokines as mediators of protection and injury in the central nervous system assessed in transgenic mice. *Current Topics in Microbiology and Immunology* **265**, 23-48.

Webber, S.E. (1989) Receptors mediating the effects of substance P and neurokinin A on mucus secretion and smooth muscle tone of the ferret trachea: potentiation by an enkephalinase inhibitor. *British Journal of Pharmacology* **98**, 1197-1206.

Weinstock, J.V., Blum, A., Walder, J., and Walder, R. (1988) Eosinophils from granulomas in murine schistosomiasis mansoni produce substance P. *Journal of Immunology* **141**, 961-966.

Wekerle, H., Linington, C., Lassmann, H., and Meyermann, R. (1986) Cellular immune reactivity within the CNS. *Trends in Neurosciences* **9**, 271-277.

Welburn, S.C., Fevre, E., and Coleman, P. (1999) Sleeping sickness rediscovered. *Parasitology Today* **15**, 303-305.

Welburn, S.C., Picozzi, K., Fevre, E.M., Coleman, P.G., Odiit, M., Carrington, M., and Maudlin, I. (2001) Identification of human-infective trypanosomes in animal reservoir of sleeping sickness in Uganda by means of serum-resistance-associated (SRA) gene. *Lancet* **358**, 2017-2019.

Whitelaw, Moulton, Morrison, and Murray (1985) Central nervous system involvement in goats undergoing primary infections with *Trypanosoma brucei* and relapse infections after chemotherapy. *Parasitology* **90**, p 255.

Whiteside, T.L. (2002) Cytokine assays. *BioTechniques* **33**, S4-S15.

WHO (1976) Parallel evaluation of serological tests applied in African trypanosomiasis: a WHO collaborative study. *Bulletin of the World Health Organization* **54**, 141-147.

WHO (1990) Sleeping sickness 'Resurrection' drug approved. *TDR news* **34**,

WHO (1998) Control and surveillance of African trypanosomiaisis. *WHO technical report series, Geneva* **881**, 1-113.

WHO (2000) Public / private partners in sleeping sickness. *TDR news* **61**, 11-11.

WHO (2001a) Human African Trypanosomiasis Treatment and Drug Resistance Network. Report of the Fourth Steering Committee Meeting.

WHO (2001b) New lease of life for the resurrection drug. *TDR news* **64**,

Wickware, P. (2002) Resurrecting the resurrection drug. *Nature Medicine* **8**, 908-909.

Wong, G.H., Bartlett, P.F., Clark-Lewis, I., Battye, F., and Schrader, J.W. (1984) Inducible expression of H-2 and Ia antigens on brain cells. *Nature* **310**, 688-691.

Woo, P.T. (1970) The haematocrit centrifuge technique for the diagnosis of African trypanosomiasis. *Acta Tropica* **27**, 384-386.

Woodroofe, M.N., Bellamy, A.S., Feldmann, M., Davison, A.N., and Cuzner, M.L. (1986) Immunocytochemical characterisation of the immune reaction in the central nervous system in multiple sclerosis. Possible role for microglia in lesion growth. *Journal of the Neurological Sciences* **74**, 135-152.

Wozniak, A., McLennan, G., Betts, W.H., Murphy, G.A., and Scicchitano, R. (1989) Activation of human neutrophils by substance P: effect on FMLP- stimulated oxidative and arachidonic acid metabolism and on antibody- dependent cell-mediated cytotoxicity. *Immunology* **68**, 359-364.

Xu, X.J., Dalsgaard, C.J., and Wiesenfeld-Hallin, Z. (1992) Spinal substance P and N-methyl-D-aspartate receptors are coactivated in the induction of central sensitization of the nociceptive flexor reflex. *Neuroscience* **51**, 641-648.

Yanex, D.M., Manning, D.D., Cooley, A.J., Weidanz, W.P., and van der Heyde, H.C. (1996) Participation of lymphocyte subpopulations in the pathogenesis of experimental murine cerebral malaria. *Journal of Immunology* **157**, 1620-1624.

Yashpal, K., Dam, T.V., and Quirion, R. (1991) Effects of dorsal rhizotomy on neurokinin receptor sub-types in the rat spinal cord: a quantitative autoradiographic study. *Brain Research* **552**, 240-247.

Zagorodnyuk, V., Santicioli, P., Turini, D., and Maggi, C.A. (1997) Tachykinin NK1 and NK2 receptors mediate non-adrenergic non-cholinergic excitatory neuromuscular transmission in the human ileum. *Neuropeptides* **31**, 265-271.

Zhang, J.R. and Tuomanen, E. (1999) Molecular and cellular mechanisms for microbial entry into the CNS. *Journal of NeuroVirology* **5**, 591-603.

Zhao, M.L., Kim, M.O., Morgello, S., and Lee, S.C. (2001) Expression of inducible nitric oxide synthase, interleukin-1 and caspase-1 in HIV-1 encephalitis. *Journal of Neuroimmunology* **115**, 182-191.

Ziche, M., Morbidelli, L., Pacini, M., Geppetti, P., Alessandri, G., and Maggi, C.A. (1990) Substance P stimulates neovascularization in vivo and proliferation of cultured endothelial cells. *Microvascular Research* **40**, 264-278.

Zini, I., Zoli, M., Grimaldi, R., Merlo Pich, E., Biagini, G., Fuxe, K., and Agnati, L.F. (1990) Evidence for a role of neosynthetized putrescine in the increase of glial fibrillary acidic protein immunoreactivity induced by a mechanical lesion in the rat brain. *Neuroscience Letters* **120**, 13-16.

Zlotnik, A. and Yoshie, O. (2000) Chemokines: a new classification system and their role in immunity. *Immunity.* **12**, 121-127.

Zoli, M., Zini, I., Grimaldi, R., Biagini, G., and Agnati, L.F. (1993) Effects of polyamine synthesis blockade on neuronal loss and astroglial reaction after transient forebrain ischemia. *International Journal of Developmental Neuroscience* **11**, 175-187.

Zou, C., Vlastos, A.T., Yang, I.., Wang, J., Nishioka, K., and Follen, M. (2002) Effects of difluoromethylornithine on growth inhibition and apoptosis in human cervical epithelial and cancerous cell lines. *Gynecologic Oncology* **85**, 266-273.